



In this volume are collected the proceedings of the Annual General Meeting of CORILA, held 26th – 28th April 2006 at Palazzo Franchetti, Venice



**SCIENTIFIC RESEARCH
AND SAFEGUARDING OF VENICE
2006**

CORILA
Research Programme 2004 - 2006
2005 Results

Edit by
PIERPAOLO CAMPOSTRINI

© Copyright CORILA. Consorzio per la Gestione del Centro di Coordinamento
delle Ricerche Inerenti il Sistema Lagunare di Venezia

30124 Venezia – Palazzo Franchetti, S. Marco 2847

Tel. +39-041-2402511 – Telefax +39-041-2402512

venezia@corila.it

www.corila.it

INDEX

AREA 1. Economics

RESEARCH LINE 1.2. Cost-benefits analysis of land reclamation of brownfields in the Venice lagoon

The new version of ELGIRA: a support system for knowledge building and evaluation in brownfield redevelopment – 5

D. Patassini, P. Cossettini, E. De Polignol, A. De Mitri, S. De Zorzi, M. Hedorfer, E. Rinaldi

Addressing the problem of contaminated sites remediation: preliminary results from a survey of the Italian public – 19

A. Chiabai, S. Tonin, M. Turvani, A. Alberini

AREA 2. Architecture and cultural heritage

RESEARCH LINE 2.2. Catalogue of Venetian plasters and historical interventions for high water defence

Systems for the protection of single buildings from high tides – 37

M. Piana, F. Restiani

The plaster catalogue: comments on the results of the research – 51

A. Ferrighi

Experimental tests for the study of the structural behaviour of the damaged venetian buildings – 59

P. Faccio, D. Chiffi, A. Vanin

RESEARCH LINE 2.3. Methodologies and technologies for conservation and restoration of historical Venetian building

Studies on behaviour of venetian masonry made of altinella bricks 73

– G. Mirabella Roberti, F. Trovò, M. Bondanelli, S. Cancelliere

Detective constructive dispositions of inward out-of-plumb on venetians dwelling houses external masonries – 89

F. Doglioni, A. Squassina, F. Trovò

From artificial stone to reinforced concrete: a plan for a specialist method for diagnostics – 1016

P. Faccio, G. Bruschi, P. Scaramuzza

From artificial stone to reinforced concrete ii: project for experimental investigation protocol for the characterization of decay phenomena 113

– P. Faccio, G. Bruschi, P. Scaramuzza

From the artificial stone to the reinforced concrete: data system project for diagnostics – M. Pretelli, A. Matteini, I. Daga 123

“A Venezia si perde il senso della verticale”. some meaningful episodes of the historical debate about the nature of the geometrical organization of Venetian buildings – A. Squassina 131

AREA 3. Environmental processes

RESEARCH LINE 3.8. Speciation and flow of pollutants

Micropollutant effects in estuarine organisms (mussels, polychaetes and fish) in the lagoon of Venice, Italy – N. Nesto, S. Romano, G. Campesan, D. Cassin, V. Moschino, M. Mauri, L. Da Ros 157

RESEARCH LINE 3.9. Pollutant flows in the lagoon carried by aerosols and atmospheric fall-out

Aerosol characterization in the Venice lagoon – F. Prodi, F. Belosi, S. Ferrari, G. Santachiara, P. Masia, L. Di Matteo 171

Real time pm2.5 concentration and vertical turbulent flux on the Venice lagoon – D. Contini, A. Donateo, F. Belosi, F. Prodi 183

RESEARCH LINE 3.10. Groundwater flows in the Venice lagoon system

Underground water flow determination in Venice lagoon system by natural isotopic markers and geoelectric tomography. Underground waters monitoring – V. Bassan, V. Bisaglia, E. Conchetto, A. Mazzuccato, A. Vitturi, T. Abbà 199

Monitoring of the saline intrusion with time-variant geo-electric-tomography: test site Casetta (Chioggia, Italy) – R. De Franco, G. Biella, A. Corsi, A. Morrone, G. Boniolo, A. Lozej, G. Saracco, B. Chiozzotto, M. Giada, M. Barbetta, V. Bassan, V. Bisaglia, T. Abbà, A. Mazzuccato, C. Claude, E. Conchetto, G. Gasparetto Stori, A. Mayer, F. Pizzetto, L. Tosi, P. Teatini 207

RESEARCH LINE 3.11. Ecological quality indices, biodiversity and environmental management for lagoon areas

Testing an integrated approach bioindicator for the Venetian lagoon – F. Giomi, M. Beltramini, C. Lanfrit, D. Maruzzo, G. Fusco, L. Perilli, L. Zane, M. Gennari, I. Marino, F. Barbisan, P. M. Bisol 219

Proposal of a new environmental quality index for the macrofouling biocoenosis of hard substrata in the lagoon of Venice – F. Cima, P. Burighel, L. Ballarin 227

A preliminary chemical index for the estimation of the sediment quality in the Venice lagoon: objectives and methodology – C. Micheletti, S. Ciavatta, A. Critto, M. Rando, I. Rumonato, R. Pastres, A. Marcomini 235

RESEARCH LINE 3.12. Trophic chain and primary production in the lagoon metabolism

Picophytoplankton contribution to phytoplankton community in the Venice lagoon – J. Coppola, F. Bernardi Aubry, F. Acri, A. Pugnetti 245

Studies on the spatial and temporal variability of microphytobenthos in the Venice lagoon – C. Facca, A. Sfriso, A. Pugnetti 255

Rapid assessment index to assess the ecological status of transitional environments: the lagoon of Venice as study case - A. Sfriso, C. Facca, M. Tibaldo 261

Carbon partitioning in the plankton community, production and decomposition processes in the lagoon of Venice -A. Valeri, F. Acri, F. Bernardi Aubry, D. Berto, J. Coppola, P. Del Negro, M. Giani, C. Larato, A. Pugnetti 271

RESEARCH LINE 3.14. Erosion and sedimentation processes in the Venice lagoon

Tidal flat – salt marshes transition in the Venice lagoon, Italy - A. Defina, L. Carniello, L. D’Alpaos 283

Morphodynamics of meandering tidal channels – V. Garotta, G. Seminara 297

RESEARCH LINE 3.15. Solid transport and circulation of the upper layers in the inlets and the coastal zone

Time series of suspended particle concentration from the conversion of acoustic backscatter at the Lido inlet – V. Kovačević, V. Defendi, L. Zaggia, F. Costa, F. Arena, F. Simionato, A. Mazzoldi, M. Gačić, C. Amos 315

RESEARCH LINE 3.16. Characteristics of the lagoon underground layer

Preliminary results of the high resolution seismic surveys in the Venice lagoon – G. Brancolini, L. Tosi, L. Baradello, A. Bratus, F. Donda, F. Rizzetto, M. Zecchin 333

Preliminary study of geomorphological features discovered in tidal flats of the Venice lagoon by VHR seismic surveys – L. Tosi, G. Brancolini, L. Baradello, F. Donda, F. Rizzetto, M. Zecchin 347

RESEARCH LINE 3.17. Transport phenomena in the hydrological cycle: model of substances release in lagoon

Mathematical modelling of low-velocity flows in wetlands – A. C. Bixio, M. Cerni 361

RESEARCH LINE 3.18. Residence times and hydrodynamical dispersion in the Venice lagoon

Long term net exchange of sand through Venice inlets: part II - N. Tambroni, G. Seminara 375

AREA 4. Data management

RESEARCH LINE 4.2. Modeling, analysis and environmental data visualization

Spatial on line analytical processing for environmental data – S. Bimonte, A. Tchounikine, T. Ahmed, M. Miquel, R. Laurini 393

INTRODUZIONE

Pierpaolo Campostrini

Direttore di CORILA

Questo libro rappresenta il quinto della serie “La ricerca scientifica e la salvaguardia di Venezia” ed il secondo riferito al Secondo Programma di ricerca del CORILA. Sono incluse in esso tutte le discipline, per offrire al lettore un accesso più facile a documentazione che si trova usualmente distribuita in più riviste scientifiche. Questa collezione costituisce un contributo allo sforzo interdisciplinare che oggi è ritenuto necessario per un completo avanzamento nelle Scienze Ambientali, specialmente per quella parte che è ritenuta urgentemente necessaria per il supporto alle decisioni della Pubblica Amministrazione nelle materie ambientali.

Venezia è un'altra volta un caso paradigmatico, dove la sfida scientifica di produrre una conoscenza più ampia ed approfondita si incontra con la sfida posta alla politica di prendere decisioni lungimiranti, per le quali il tempo di ritorno degli effetti è molto più grande degli intervalli elettorali. Tuttavia, le decisioni politiche sono necessarie e fornire un appropriato supporto scientifico per esse è di straordinaria importanza.

In realtà, pochi politici, per un piccolo numero di questioni, assisteranno direttamente al risultato reale di molte loro scelte controverse, per le quali vengono spesso spese quantità ingenti di pubblico denaro. Questo è vero anche per molti scienziati, che difficilmente assisteranno alla prova diretta dei loro modelli predittivi nel reale laboratorio della Natura. Inoltre, in molti casi, il numero delle variabili (sociali, fisiche, biologiche) coinvolte è così grande che esprimere una relazione diretta di causa-effetto è impossibile: pertanto, sia gli scienziati che i politici, guardando in un futuro ipotetico all'evidente fallimento della loro teoria/decisione, potrebbero dire: “non è colpa mia”.

E' una questione di responsabilità della cosiddetta “classe politica” da un lato e della “comunità scientifica” dall'altro. Attorno le questioni ambientali, in tutto il mondo e a Venezia in particolare, abbiamo assistito ad un sorprendente crescita dell'interesse da parte della pubblica opinione. Tuttavia, il senso di responsabilità sembra non essere cresciuto in pari misura e l'Ambiente è stato largamente usato spesso solo per ottenere consenso politico, avanzando tesi con basi scientifiche deboli, fornite da ricerche poco finanziate, frammentate, che non hanno subito né il giudizio dei pari né altra forma di valutazione. Quella scienza e quella politica si sono aiutate vicendevolmente per coprire le loro mancanze ed i loro errori di fronte alla pubblica opinione.

Con questa serie di libri, il CORILA e gli scienziati che sono autori dei testi qui presentati, stanno cercando di agire in modo differente, dando pubblica evidenza della loro parte di responsabilità. CORILA sta guidando un

Programma di ricerca importante, finanziato dallo Stato Italiano, ovvero dai contribuenti, che coinvolge più di 70 istituzioni scientifiche, anche straniere. Queste istituzioni hanno promesso di fornire risposte scientifiche alle difficili domande presentate nel Programma, derivate dall'esame degli effettivi bisogni delle Pubbliche Amministrazioni coinvolte nella salvaguardia di Venezia. Il Comitato tecnico-scientifico di CORILA, con il supporto di tutta la staff di CORILA, stanno offrendo una valutazione rigorosa dei risultati, realizzando un continuo contatto e scambio di dati con tutti i Gruppi di ricerca coinvolti.

In questo libro, realizzato da tutti i ricercatori coinvolti nel programma di ricerca di CORILA, grazie all'aiuto paziente dell'arch. Enrico Rinaldi della staff di CORILA che ne ha curato la raccolta e l'edizione grafica, sono presentati i risultati intermedi (a fine 2005) del Secondo Programma di Ricerca, disciplina per disciplina. Questi risultati possono essere parziali o provvisori, poiché il Programma sarà completato il prossimo anno. Tuttavia, essi sono qui presentati per una loro possibile ed aperta valutazione, che può avvenire, come sempre nella scienza, nel contesto internazionale più ampio. E noi speriamo di essere giudicati sulla base di questi risultati.

Come dicevamo, è una questione di responsabilità.

FOREWORD

Pierpaolo Campostrini

Director of CORILA

This book represents the fifth of the series “Scientific Research and Safeguarding of Venice”, the second related to the CORILA’s Second Program of research. All the disciplines are included, offering to the readers an easy access to a documentation usually distributed in many scientific journals. This collection is offered also as a contribution for the inter-disciplinary effort that is today considered essential for a comprehensive advance in the Environmental Sciences, especially for that part urgently needed to support the policy decisions by the Public Administrations in the managing of the environment.

Venice is again a paradigmatic case, where the scientific challenge of producing a wider and deeper knowledge meets the political challenge of long-sight decisions, where the return-time of the decisions’ actual effects is much longer than the elections interval. However, political decisions are needed and to provide a sound scientific support for them is of paramount importance.

In fact, few politicians, for a little number of matters, will assist directly to the results of many of their controversial choices, involving often a large use of public money. This is true also for many scientists, who hardly will be able to assist to an overall direct test of their predictive models in the real laboratory of the Nature. In addition, in many cases, the number of variables involved (of social, physical, biological types) is so large that to express a direct cause-effect relationship is impossible: therefore both scientists and politicians, in a far hypothetic future, looking to the evident failure of their theory/decision could say: “it’s not my fault”.

It is a matter of responsibility of the so-called “political class” from one side and of the “scientific community” on the other. Around the environmental matters, all over the world and in Venice in particular, we assisted in the last years to a amazing increase of interest by the public opinion. However, apparently the sense of responsibility did not rise consequently and the Environment has been largely used just to drive political consensus, divulgating theses often with weak scientific bases, provided by researches scarcely funded, fragmented, not peer-reviewed, never evaluated. That science and that politics co-operated in hiding their mistakes in front of the public opinion.

With this book series, CORILA and the scientists who are authors of these papers are trying to act differently, giving public evidence of their part of responsibility. CORILA is managing one important Research Program, funded by the Italian State, i.e. by Italian taxpayers, involving more than 70 scientific Institutions, also out of Italy. These Institutions promised to give scientific answers to the challenging questions included in the Program and derived from the actual needs of Public Administrations involved in the safeguarding of Venice. The Scientific Committee of CORILA and the CORILA’s staff are

offering a rigorous evaluation of the results, providing continuous contacts and data transfers with the Research Groups.

In this book, realised by all the researchers involved in the CORILA program, with the patient help of arch. Enrico Rinaldi of the CORILA's staff, the intermediate results (up to the year 2005) of the Second Research Program are presented, in each discipline. These results may be partial or provisional, as the Program will be completed in the next year. In any case here they are presented, for a possible open evaluation to be made, as always should occur in Science, in the international arena. And we are willing to be judged on the basis of these results.

As we said, it is a matter of responsibility.

INDEX OF AUTHORS

Abbà T., 199, 207
Acri F., 245, 271
Ahmed T., 393
Alberini A., 19
Amos C., 315
Arena F., 315
Ballarin L. 227
Baradello L., 333, 347
Barbetta M., 207
Barbisan F., 219
Bassan V., 199, 207
Belosi F., 171, 183
Beltramini M., 219
Bernardi Aubry F., 245, 271
Berto D., 271
Biella G., 207
Bimonte S., 393
Bisaglia V., 199, 207
Bisol P. M., 219
Bixio A. C., 361
Bondanelli M. , 73
Boniolo G., 207
Brancolini G., 333, 347
Bratus A., 333
Bruschi G., 101, 113
Burighel P., 227
Campesan G., 157
Cancelliere S., 73
Carniello L., 283
Cassin D., 157
Cerni M., 361
Chiabai A., 19
Chiffi D., 59
Chiozzotto B., 207
Ciavatta S., 235
Cima F., 227
Claude C., 207
Conchetto E., 199
Contini D., 183
Coppola J., 245, 271
Corsi A., 207
Cossettini P., 5
Costa F., 315
Critto A., 235
D'Alpaos L., 283
Da Ros L., 157
Daga I., 123
De Franco R., 207
De Mitri A., 5
De Polignol E., 5
De Zorzi S., 5
Defendi V., 315
Defina A., 283
Del Negro P., 271
Di Matteo L., 171
Doglioni F., 89
Donateo A., 183
Donda F., 333, 347
Facca C., 255, 261
Faccio P., 59, 101, 113
Ferrari S., 171
Ferrighi A., 51

- Fusco G., 219
Gačić M., 315
Garotta V., 297
Gasparetto Stori G., 207
Gennari M., 219
Giada M., 207
Giani M., 271
Giomi F., 219
Hedorfer M., 5
Kovačević V., 315
Lanfrit C., 219
Larato C., 271
Laurini R., 393
Lozej A., 207
Maffulli S., 147
Marcomini A., 235
Marescotti L., 147
Marino I., 219
Maruzzo D., 219
Mascione M., 147
Masia P., 171
Matteini A., 123
Mauri M., 157
Mayer A., 207
Mazzoldi A., 315
Mazzuccato A., 199, 207
Micheletti C., 235
Miquel M., 393
Mirabella Roberti G., 73
Morrone A., 207
Moschino V., 157
Nesto N., 157
Pastres R., 235
Patassini D., 5
Perilli L., 219
Piana M., 37
Pretelli M., 123
Prodi F., 171, 183
Pugnetti A., 245, 255, 271
Rando M., 235
Restiani F., 37
Rinaldi E., 5
Rizzetto F., 207, 333, 347
Romano S., 157
Ruminato I., 235
Santachiara G., 171
Saracco G., 207
Scaramuzza P., 101, 113
Seminara G., 297, 375
Sfriso A., 255, 261
Simionato F., 315
Squassina A., 89, 131
Tambroni N., 375
Tchounikine A., 393
Teatini P., 207
Tibaldo M., 261
Tonin S., 19
Tosi L., 207, 333, 347
Trovò F., 73, 89
Turvani M., 19
Valeri A., 271
Vanin A., 59
Vitturi A., 199
Zaggia L., 315
Zane L., 219
Zecchin M., 333, 347

AREA 1
Economics

RESEARCH LINE 1.2

Cost-benefits analysis of land reclamation of brownfields in the Venice lagoon

THE NEW VERSION OF ELGIRA: A SUPPORT SYSTEM FOR KNOWLEDGE BUILDING AND EVALUATION IN BROWNFIELD REDEVELOPMENT

Domenico Patassini¹, Paola Cossetini², Enrico De Polignol³, Antonio De Mitri¹,
Stefania De Zorzi⁴, Markus Hedorfer¹, Enrico Rinaldi⁴

¹Department of Planning, University Iuav of Venice, ²VESTA, Venice Territorial and Environmental Services, ³Venice Municipality, Environment and Territorial Safety Management, ⁴CORILA, Lagoon Research Consortium, Venice

Riassunto

Nel corso del 2005 il sistema ELGIRA è stato sviluppato e testato in due aree contaminate del mega-sito di Porto Marghera (Venezia). Nuove funzioni sono state inserite nel modello logico che individua i meccanismi di interazione tra moduli operativi, ed è stato prodotto un nuovo prototipo. Lo sviluppo ha interessato quattro domini: il data base delle tecnologie di bonifica, la zonizzazione delle aree inquinate e delle tecnologie applicabili, costi e performance delle tecnologie, il modulo REC di valutazione del rischio, merito ambientale e costo.

Sulla base di esperienze locali e internazionali e della letteratura disponibile è stato progettato un database finalizzato alla scelta e all'applicazione di tecnologie a siti inquinati di dimensione medio-piccola. L'archivio dispone di interfaccia web ed è interrogabile con l'aiuto di criteri multipli di estrazione. Il modulo di zonizzazione consente di acquisire le mappe prodotte dal modello di inquinamento, di relazionarle fra loro individuando compresenze e sovrapposizioni spaziali degli inquinanti e di associare le potenziali tecnologie disponibili. Possono essere quindi prodotte le opzioni di bonifica plausibili, ovvero le combinazioni tecnologia-inquinante, dati gli scenari di avvio (limitati ad ipotesi di destinazione d'uso del suolo), vincoli di rischio sanitario e costo, obiettivi di merito ambientale. Il modulo relativo a costi e performance delle tecnologie è stato aggiornato rispetto alla precedente versione: ora è strutturato per singola tecnologia, descritta da una vettore di attributi, importa dal modulo di zonizzazione le informazioni sulle opzioni e sulle aree inquinate, genera le informazioni sulle opzioni per il modulo finale REC (aggiornato) di valutazione del rischio, del merito ambientale e dei costi finanziari dell'intervento.

La nuova versione chiude il 'circuitto cognitivo' e precisa i luoghi d'incontro fra conoscenza di processo e nozioni tecniche di tipo fisico-chimico, ingegneristico, ecologico, economico-sociale e urbanistico.

Abstract

Throughout 2005 the ELGIRA system was further developed and tested in two contaminated areas of the Porto Marghera (Venice) mega-site. New functions were inserted into the logic model - that which identifies the mechanisms of

interaction between operational modules – and a new prototype was produced. The development involved four main modules: the reclaim technologies database, the zoning of polluted areas and applicable technologies, technology costs and performance, the REC module for the evaluation of risk, environmental merit, and cost.

A database was planned, based on local and international experience and available literature, with the aim of enabling the most appropriate choice and application of technologies in small to medium sized brownfields. The archive has a web interface and can be researched with the aid of multiple extraction criteria. The zoning module enables the user to visualize the maps produced by the pollution model, compare and contrast the maps by identifying the simultaneous presence and spatial juxtaposition of polluting substances, and to then link them to the available potential technologies. This enables plausible reclaim options (the combinations of technology and pollutant) taking into account the initial scenarios (limited to hypotheses concerning the destination use of the area), health hazards and cost limitations, and environmental merit objectives. The module concerning technology costs and performance has been updated since the previous version: it is now structured according to single technologies; it is described as a vehicle of attributes, it imports from the zoning module information relating to options and polluted areas, and generates options information for the (updated) REC of risk evaluation, environmental merit, and the financial costs of the operation.

The new version closes thus the 'cognitive circuit', and pinpoints the meeting areas between processing knowledge and technical notions in the physics/chemistry, engineering, ecology, socio-economic and regional planning spheres.

1 Introduction

In 2005 two new operational modules were added to ELGIRA, and another two were updated. The logic model was thus consolidated and the operational model reinforced.

The new database of reclaim technologies, which is available on the web, is simultaneously both a surveying and an operational tool since it offers a full perspective of the feasible technologies and is consultable independently of the system's sequence of operative phasing. Furthermore, it allows for the selecting of technologies according to features of the site and planning limitations. The information is available also for other ELGIRA modules.

The module for zoning of polluted areas and reclaim options enables, starting from the distribution mapping of the substances in the pollution model, the identification of the areas where more than one polluting agent is present. Knowing which reclaim technologies are feasible means that a polluting agent may be matched with a technology, thus achieving the identification of the reclaim options from which to choose the most appropriate. Hereafter the cost-performance modules regarding the technologies and REC become operational. This is the core of the system.

The new structure of the cost-performance module of reclaim technologies, apart from providing the necessary information for each of the technologies in the database (from which it imports the general characteristic data of the technology itself), also generates information regarding the surface areas and volumes to be treated in the pollution and zoning models. The information concerns the creating of the worksite (volume, timing, power consumption, and work surface area) and costs (set-up, site management, accessories, and maintenance). For each reclaim option it is then possible to estimate costs and performance. The latter (cost and performance) may assume various forms: a result, if the reference is to output (realization) or outcome; an impact, but also that of a process (site management, timing, overall dimensions, energetic and financial balance). Performance hence becomes the manifestation of criteria, indicators, or indices.

The updating of the REC module (from version 2 to version 4) improves the use of the available information and the final evaluation, it means we can distinguish between urban and rural application and carry out internally the health risk calculation, which up until now was done externally from the module. The user interface has also been expanded. The new version is currently being adapted to Italian legislative norms and usages via tests in the two research areas – “43 hectares” and “Ex-Sava” – in the Porto Marghera mega-site (which has already been subject to investigation in the first stages of research).

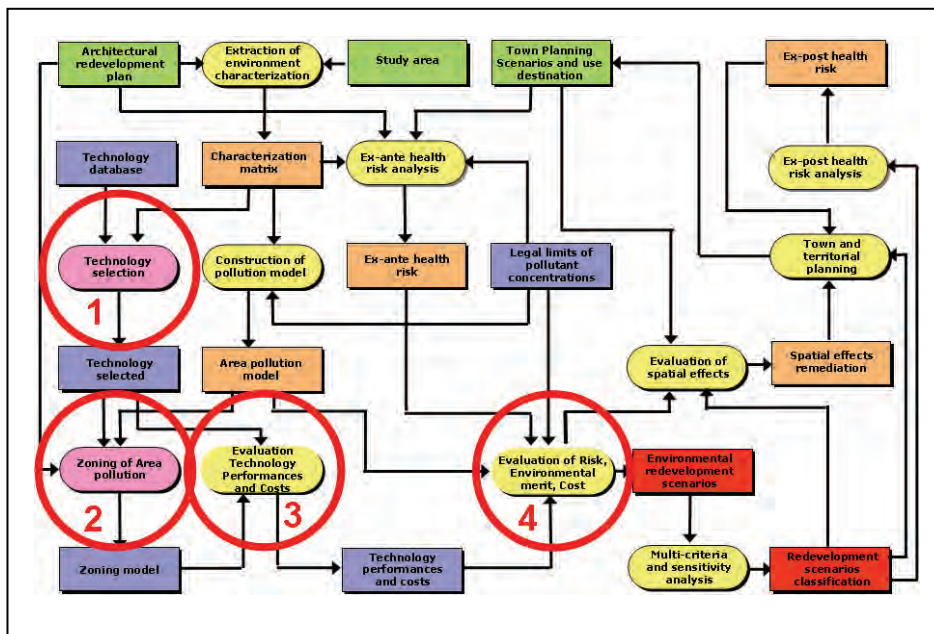


Fig. 1. New modules in the ELGIRA operational plan: 1. Database technologies, 2. Zoning module, 3. Cost and Performance module, 4. REC module.

2 Reclaim technologies database

The archive for reclaim technologies is structured as a relational database with web interface. The intention is to reinforce the knowledge-oriented aspect of the ELGIRA modules rather than the procedural usage.

There are several sources, of which the main one is the Porto Marghera Master Plan. It is here that the feasible technologies are set out with information

regarding characteristics and efficiency (the Master Plan archive was the first operational reference for ELGIRA in the preliminary tests of the procedure). Another source is the bibliographical analyses within industries and publications that concern this particular field; the third source is that of other computer-based archives.

The archive, otherwise called ArTe DB consists of a two-channel interface: one for consultation and the other for the insertion of data. The consultation channel allows the user to search the archive for one or more technologies on the basis of single or multiple parameters, while the insertion channel allows the user to insert new technologies or to update pre-existent data.



Fig. 2. Reclaim techniques archive with web interface

Consultation of the archive produces three types of information: a list of the techniques, simple research, and complex research.

The list of techniques visualises all the plan descriptions. The simple research index allows the user to select techniques on the basis of research criteria: treatment location, treatment type, treatable terrain, state of terrain, costs, and pollutant classing.

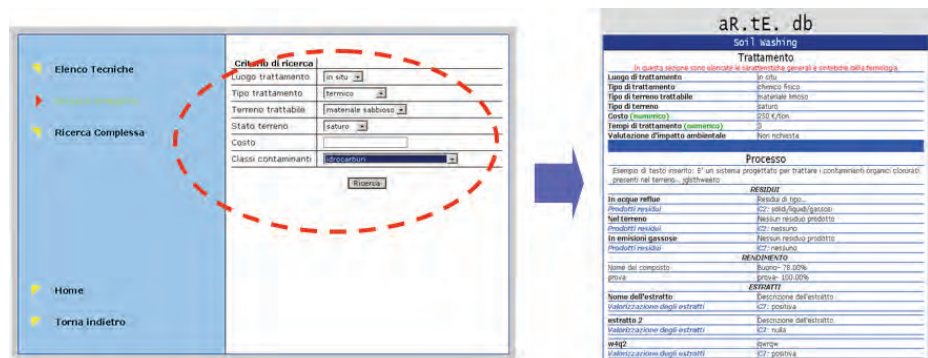


Fig. 3. Consultation of reclaim techniques (simple research).

Complex research comes about through statements; namely, the identification of particular terms in the fields of the various files, and the extraction (download) of the latter.

Each descriptive technologies file is divided into five groups of information type, and for each group parameters and features are available, as indicated below.

Category	Topic	Parameter
Treatment	Treatment	Treatment location
		Type of treatment
		Type of terrain
		Costs
		Timing
		Environmental impact evaluation
Process	Residue	Refluent waters
		Into the terrain
		In gaseous emission
	Costs	Reclaim costs per hectare
		Transport costs
Pollutants	Actions	Compound classes
	Effects	Effects on the pollutants
Performance technology	General information	State of the art Limitations
	Effects on the environment	In water In the terrain In the air
	Environmental conformity	Conformity
	Exposure	Workers, users
		Population
	Availability	Techniques
		Plant engineering
	Competitivity	Technical competitiveness
	Energy balance	Energy balance
	Social acceptability	Social acceptability
	Energy consumption	Natural gas consumption
Oil consumption		
Electricity consumption		

Fig. 4. Parameters and features of reclaim techniques.

Some of the parameters are selective, i.e. they involve the selection of a subset of techniques; others, whereas, are descriptive, and complete the information regarding the technology without, however, conditioning selection.

New technologies or modifications of existing technologies can be achieved by use of the insertion channel. When 'insertion' is selected, an empty form appears, and the various fields can be edited according to specific requirements.

The screenshot shows a web browser window titled 'aR.T.E. db' with the URL 'http://217.133.18.154 - | aR.T.E. db | Scheda tecnica | - Microsoft Internet Explorer'. The main heading is 'soil Washing' and the section is 'Trattamento'. Below this, there is a red note: 'In questa sezione sono elencate le caratteristiche generali e sintetiche della tecnologia'. The form contains several input fields and dropdown menus:

- Luogo di trattamento:** in situ
- Tipo di trattamento:** chimico fisico
- Tipo di terreno trattabile:** materiale limoso
- Tipo di terreno:** saturo
- Costo (numerico):** 250
- Tempi di trattamento (numerico):** 3
- Valutazione d'impatto ambientale:** Richiesta Non richiesta

The 'Processo' section contains a text area with the example: 'Esempio di testo inserito: E' un sistema progettato per trattare i contaminanti organici clorurati presenti nel terreno... jglsthweèto'. The 'RESIDUI' section has three rows:

- In acque reflue:** Si No Residui di tipo...
- Prodotti residui:** CZ: solidi/liquidi/gassosi
- Nel terreno:** Si No Nessun residuo prodotto
- Prodotti residui:** CZ: nessuno
- In emissioni gassose:** Si No Nessun residuo prodotto
- Prodotti residui:** CZ: nessuno

The 'COSTI' section has a text area: 'Descrivere i costi di bonifica'. At the bottom, it says 'Operazione completata' and 'Internet'.

Fig. 5. Technologies archive. Insertion of a new technology

3 Area zoning module and reclaim options

The zoning module enables the representation of the reclaim site including indications as to the polluted areas and feasible reclaim technologies. The terrain pollution model and information gained from the technologies archive are utilized.

The bi-dimensional maps regarding the concentration of each polluting agent are constructed with the terrain pollution model and are used in the zoning module. These are then subjected to thresholding so as to extract significant subsets, and, when necessary, are unified¹. Via these maps, zoning may be defined as a juxtaposition of pollutants. The technologies contained in the archive, chosen according to parameters and possibly later positioned in a multi-criteria ranking scale, are put in relation to the pollutants so as to determine suitable pollutant-technology pairing.

It may be possible to preset for reclaim scenarios for portions of the site, should the geography of the pollutants, redevelopment planning, or particular site management require.

The various phases of the procedure are: thresholding of the pollutant maps, unification of the maps, and zoning – namely, the projection in a single layer of each map along with the relation between zones and reclaim technologies.

The operational processes are as follows:

¹ The maps of polluting agents that may be unified are those referring to pollutants of the same family (for instance, see Ministerial Decree #471/99 and further amendments to Italian legislation)

- The contaminating substances maps supplied by the pollution model are subjected directly to zoning (P1).
- The contaminating substances maps supplied by the pollution model are subjected to thresholding (so as to extract the subset map that contains the highest count of a given threshold²) before the zoning phase (P2).
- The contaminating substances maps supplied by the pollution model may be put together (unifying the contaminating substances in similars³) and then subjected to zoning (P3).
- The whole process calls for the thresholding of the contaminating substances maps supplied by the pollution model, the unifying of the resulting maps, and the zoning of the latter (P4)

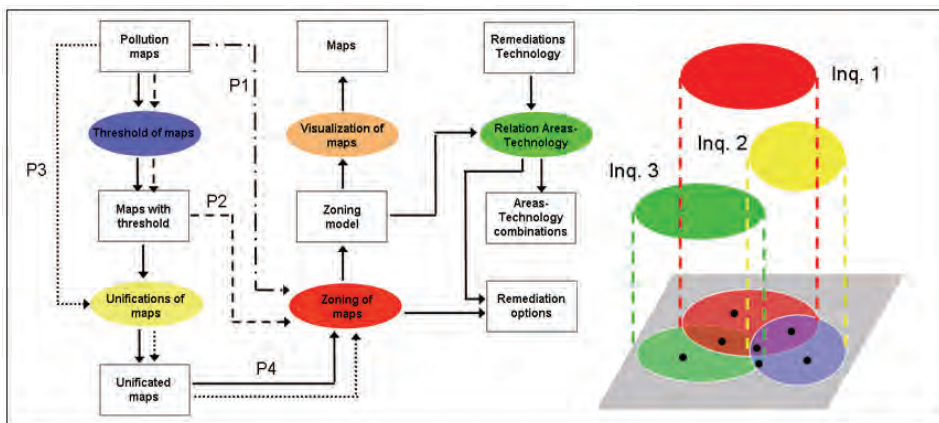


Fig 6. Operational processes for the zoning model (left) and juxtaposition of the polluted areas (right).

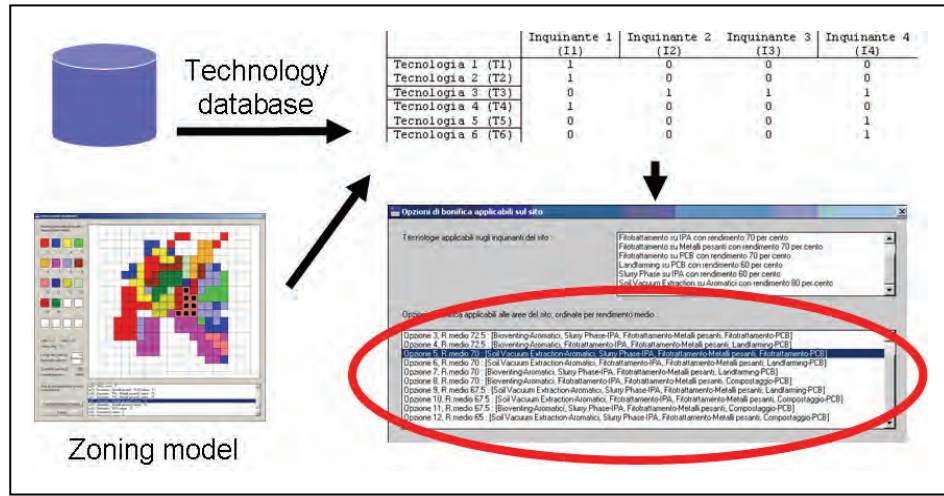
After the zoning phase, the relation between the zoned areas and feasible technologies may be defined for the four operational processes. Zoning of the polluting agents may therefore be put into relation with technologies for a first screening of each area.

It is then finally possible to construct a preliminary set of reclaim options, to be tested at a later date: each of these options consisting of a set of technologies paired with treatable pollutants in the designated area. On the basis of the zoning (areas and pollutants) hitherto created, and the available technologies, all the combinations of technologies-pollutants are then produced, and a description, together with other useful information, are provided for each option.

² For instance, the concentration count of a contaminating substance higher than the acceptability level as defined by law (e.g. for Italy, the Ministerial Decree #471/99 and further amendments).

³ Referring, for instance, to the quoted Ministerial Decree #471/99, and considering that reclaim technologies treat pollutants by 'family' groups, and not singly

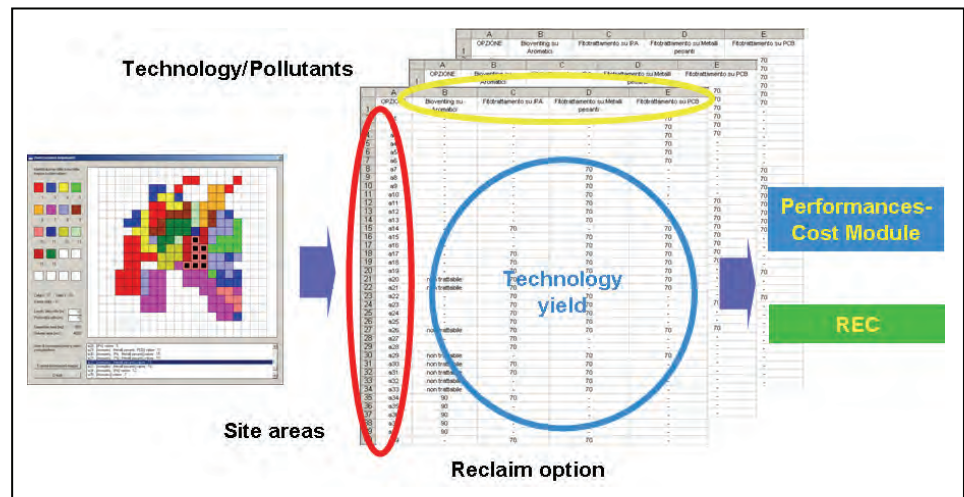
Fig 7. The construction of reclaim options, including information from the technologies archive and the zoning model.



The technological combinations are visualized in a summary window with option information.

Each option is described in a table, the columns of which represent pairs of applications (pollution technology) and the rows, the areas of intervention (according to zoning). The correspondence between areas and technique-pollutant pairs represents a value, such as efficiency. This information then feeds into the cost modules, the options performance and the REC model.

Fig. 8. Description of the reclaim options.



4 Costs and performance of reclaim technologies

This module deals with the process of site-setting (overall volume, timing and times, energetic consumption and work surface area), and the costs (of the starting process, site management, accessories, maintenance) for each single technology.

The module uses information from the technologies archive and from zoning, and is operationally based on two calculation sheets for site-setting and costs and on a worksheet of reclaim options and technologies.

INFORMAZIONI SPECIFICHE SUL PROGETTO							
Superficie totale	mq						
superficie coperta	mq						
Superficie di intervento	mq						
Profondità	m						
Volume da trattare/movimentare	mc	0					
Peso specifico	ton/mc	1.6					
Quantità terreno	ton	0					
Giorni di lavoro/anno	giorni/anno	310					
Ore di lavoro/giorno	h/giorno						
Concentrazione massima per contaminante	mg/kg						
Resa vagliatura	%					dipende dalle caratteristiche del terreno	
Quantità materiale dopo vagliatura	ton	0				non va sommato in caso di applicazione di più di una tecnologia contemporaneamente	
Quantità di suolo escavato e non ripristinato	mc					scavi e fondazioni	
Distanza cava/luogo prod. Terreni ripristino	km						
Peso specifico gasolio	g/mc	0.04					
						Valori da inserire variabili da caso a caso	
n.	Voce	u.m.	n.	Dati	Dati	Risultato	Note
1	Capacità di ridurre la concentrazione delle sostanze inquinanti nel suolo, nelle acque di falda e nelle acque superficiali per ognuna delle sostanze rilevate. Occorre inoltre tenere conto della profondità a cui si trovano le sostanze da trattare.						
	Rendimento	%					Da schede tecnologie
2	Tempi necessari per completare la riduzione delle concentrazioni. La metodologia «RMC» richiede che venga precisato un diagramma tempo-concentrazioni in cui riportare di quanto vengono ridotte le concentrazioni per ogni singolo anno d'esercizio.						
	Pretrattamento (vagliatura)	n linee/ton/h/ore/giornozanni		25	#DIV/0!		Per interventi ex situ
	Trattamento	n linee/ton/h/ore/giornozanni			#DIV/0!		Dati da scheda tecnologia
	Totale				#DIV/0!		si considera il tempo massimo fra i 2 interventi
3	Quantità di suolo (espresso in m ³) escavato e non ripristinato.						
		mc					Dipende dal progetto di ripristino dell'area
4	Quantità di suolo (espresso in m ³) escavato e riutilizzato in altro luogo.						
		mc					Dipende dal progetto di ripristino dell'area e dalla qualità del terreno
5	Quantità di suolo (espresso in t) escavato.						
	Intervento di asportazione	ton					0 per interventi ex situ

Fig. 9. Module for costs and performance of reclaim technologies: site-setting

The site-setting sheet consists of a preliminary section dedicated to specific information regarding the terrain (as with every technology), the data of which then converge with the second section. The resource table contains information on efficiency; concentration reduction times; amount of soil that has been excavated, restored, re-used and shipped; the shipping distances; amount of soil reclaimed (for each processing type); amount of table water treated; consumption of gas, oil and electricity; polluting substances and waste produced by the reclaim process; site surface areas and amount of time in occupancy. Each item of information is reported in unit measures, amounts, other data, and expected results.

The costs sheet consists of a preliminary sheet describing general planning costs as regards the size of the site, and, in the second section, is structured in a similar way to the site-setting sheet, where initial, current, and renewal costs

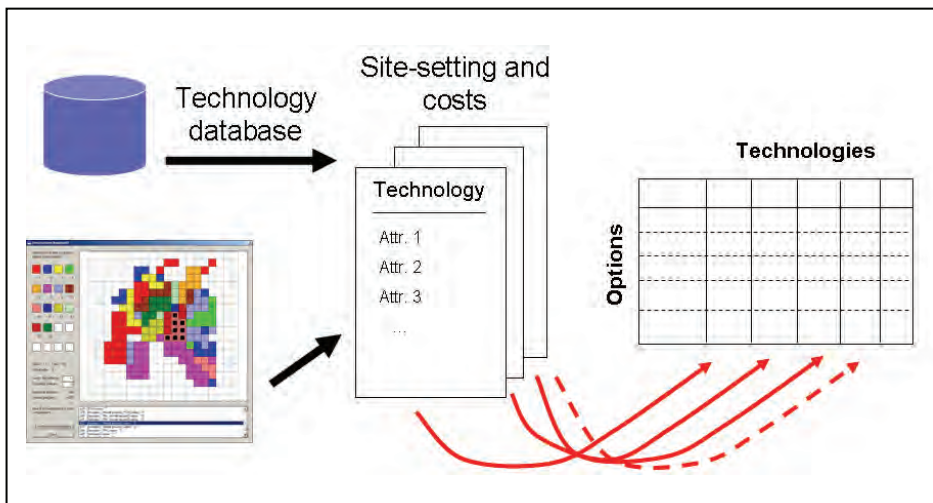


Fig. 11. Module for costs and performance of reclaim technologies. Final summary

5 From REC 2 to REC 4

REC – the evaluation model of the reduction of risk, of environmental merit and of intervention costs regarding reclaim operations in brownfields – was deployed by the research group at the beginning of 2001. In autumn of the same year it was adopted within the framework of the as yet experimental evaluation model ELGIRA. The version at the time was denominated 2, as the second in a series, and referred to the implementation, with no particular modifications, of the first conceptual model in the form of calculation sheets. This first implementation software was produced in the original Flemish edition and also in an edition which was partially translated into English. In 2002 the ELGIRA group carried out an almost complete adaptation of the application to Italian contexts. This adaptation excluded the evaluation criteria for environmental merit, this being deemed at the time too onerous a task, in that it would have involved the interviewing of a group of experts, representatives of the territorial situations (the Italian Republic, the Veneto Region, the Province of Venice, the Porto Marghera Megasite).

After version 2 of REC (whose features have been amply documented in previous papers already published by Corila) a third version was prepared and published by SKB (Stichting Kennisontwikkeling en Kennisoverdracht Bodem, Foundation for the development and transfer of land knowledge) in Gouda, Netherlands. This version, however, has never appeared in the scientific publications circuit of the so-called REC Consortium.

The latest development consists of the finalization of version 4, which in some aspects differs considerably from previous editions. Most importantly, a geographical distinction has been made regarding the nature of the sites to be evaluated: one type being the urban sites, with a maximum surface area of 2 hectares, and the other, the rural sites, with no specified maximum size. The model for the urban sites follows very much the same procedures as seen in versions 2 and 3, minus some errors that were present.

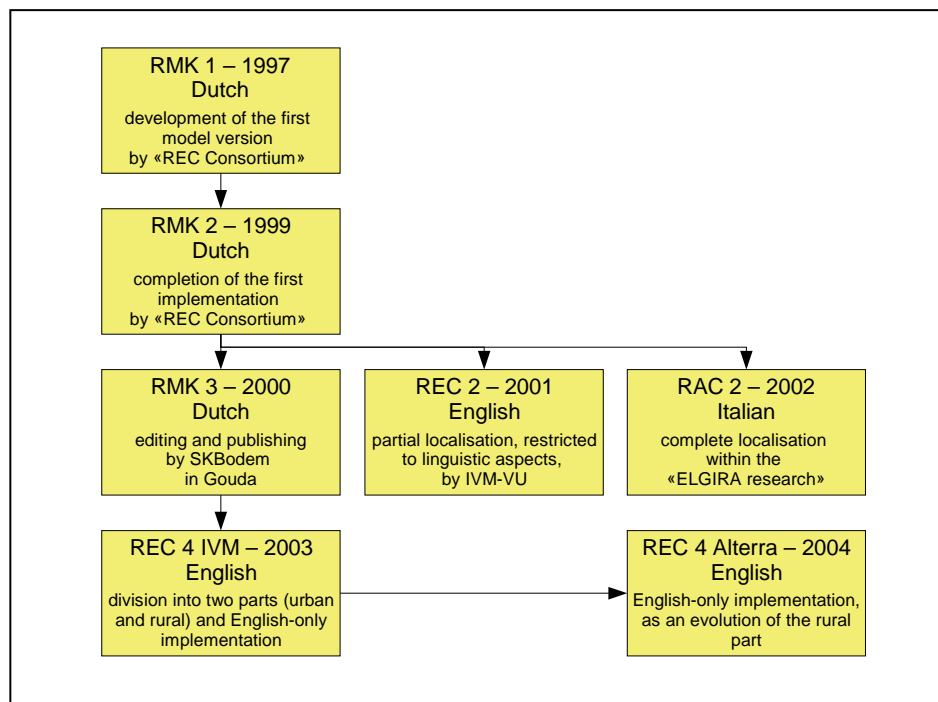


Fig. 12. REC versions.

The distinction is not only geographical, in that mega- and micro- contaminated sites are also distinguished. Generally speaking, the former are the outcome of great industrial, military, and services investment (railways, ports, airports, etc.) and are characterized by their considerable dimensions. The need for reclaim in these cases is easily quantifiable on the basis of data such as environmental characteristics, redevelopment scenarios and morphological readjustment (prevertissement interventions, water drainage, safety implementation). The latter, the micro-sites, are generally distributed within urban territories, and due to the proximity to ongoing residential and commercial usage, require more complex interventions.

Edition 4 of REC regarding the so-called rural sites is characterized by the following innovations: firstly, the evaluation of health risks may now be carried out through a simplified procedure directly from REC, without having to acquire the corresponding risk indices from other software such as HESP, CSOIL, Giuditta, Rome, RBCA, Risk 4, or similar. Secondly, the TAUW relations table, which compared various pollutant concentration counts standardized to the value of HC50 with the risk index, has been made obsolete. Diversification of the terrain according to vegetation has also been introduced. Another innovation is the decision to discontinue the generalized use of the concept of HC50 (the concentration under which 50% of species is in danger of extinction). Furthermore, the notion of presumed density of equivalent targets has been abandoned in favour of the more general concept of critical concentration. This is based (according to the combination of vegetation and substance or family of substances) on the HC50 count in itself, on the LAC count (Landbouw Advies Commissie – the Agricultural Commission within the Ministry for Agriculture, Nature, and Fishing, now obsolete), or else on “critical values for land use” from

other investigations. In the evaluation model for environmental costs (primarily for the zero option), calculation of land loss due to erosion has been introduced. Finally, for potential use with all intervention options, allowance for the reduction of the pollution level caused by lixiviation phenomena and vegetation absorption has been included in the evaluation model for environmental benefit.

Once REC 4 was finalized, the Alterra⁴ Research Institute produced a second, rural edition with even more innovations. The first of these consists of the total revision of the algorithms for the evaluation of health and ecological risks, substituting the simplifications of the first edition with calculation methods that are more coherent with the methods used by the software for risk analysis. The second innovation involves the disuse of the dissolved organic carbon (DOC) concentration parameter in favour of the characterization of terrain properties in the sphere of determination of the phyto-extraction process.

Throughout the ELGIRA research process, version 2 of REC (in the edition for specific use in Italy⁵) was utilized right up until the end of 2005. The final phase of research, therefore, involves the problem of the adaptation of the Italian version of REC to the innovations introduced by the IVM and by Alterra.

This problem poses itself primarily in terms of overall articulation of the Italian usage. In such a context three operational scenarios may be envisaged: a) completely new re-adaptation of the ten calculation sheet models; b) reorganization of the sheets already adapted so as to include the innovations added to version 4; c) the detailing of the calculation sheets and their re-usage in another application platform, or possibly the redefinition of parts of the model algorithms.

References

Alterra, A Decision Support System to quantify cost/benefit relationships of the use of vegetation in the management of heavy metal polluted soils and dredged sediments, 2004, <http://www.alterra-research.nl/pls/portal30/docs/folder/phytodec/index.htm>

Beinat E., van Drunen M A (eds) ,2001, The REC decision support system for comparing soil remediation options. A methodology based on risk reduction, environmental merit and cost, REC Consortium, Amsterdam.

Bonten L.T.C., van Drunen M. A., Japenga J, 2005, REC-model for diffusively

⁴ The Institute is part of the Wageningen UR (Wageningen Universiteit en Researchcentrum, University and Research Centre of Wageningen) and is a recent member of the REC Consortium. It had a prominent role in the development of edition 4.

⁵ It should be remembered here that the adaptation to Italian contexts was carried out by the research group

polluted areas; Decision support system for remediation strategies, including Risk, Environmental merits and Costs, Alterra, Wageningen.

Comune di Venezia, 1996, La pianificazione urbanistica come strumento di politica industriale. La Variante al Prg per Porto Marghera, Urbanistica Quaderni 9.

Comune di Venezia, Direzione Centrale Ambiente e Sicurezza del territorio, 2001, Accordo di programma per la chimica a Porto Marghera. Dpcm 12.02.99. Quadro conoscitivo di riferimento per la redazione del Master Plan per la bonifica delle aree contaminate di Porto Marghera (a cura di E De Polignol, F Zanetti), Venezia.

Fabris E., 2005, "Area Ex-Sava: analisi del rischio eseguita su diversi scenari di bonifica del suolo e sottosuolo", Rapporto interno, Venezia.

Hedorfer M., 2004, Elgira Toolkit 1, Algoritmi di interpolazione verticale delle concentrazioni di inquinanti, rapporto interno.

Karadimitriou N., Deak J., Rethinking brownfields: discourses, networks and space-time relations, Aesop Congress, Vienna, 13-17th, 2005.

Patassini D., Hedorfer M., Rinaldi E., De Polignol E., Cossettini P., Paneghetti C., 2005a, Contextual knowledge generated by a dss for brownfield development- the case of Porto Marghera (Venice), in D. Miller, D. Patassini 2005, Beyond benefit cost analysis. Accounting for non-market values in planning evaluation, Ashgate, Aldershot.

Patassini D., Hedorfer M., Rinaldi E., De Polignol E., Cossettini P., 2005b, ELGIRA: Support System for Knowledge Building and Evaluation in Brownfield Redevelopment, in Scientific Research and Safeguarding of Venice, CORILA Research Programme 2001-03, CORILA.

Patassini D., Hedorfer M., Rinaldi E., De Polignol E., Cossettini P., 2005c, ELGIRA - A Knowledge Support Procedure to reclaim Porto Marghera Brownfields, Environmental Protection of the Lagoon of Venice: An Economic Valuation, Elgar Edward.

Provincia di Venezia, www.provincia.venezia.it/proveco/rifiuti/chimica.

Regione del Veneto, 1999, PALAV. Piano d'area della laguna e dell'area veneziana, Cierre Edizioni, Verona.

Regione del Veneto, Comune di Venezia, 2002, Master Plan delle Bonifiche a Porto Marghera.

Van Drunen M. A., Beinat E., Nijboer M., Okx J. P., Multi-objective decision-making for soilremediation problems, in Land Contamination & Reclamation, 13 (4), 2005: 349-370.

ADDRESSING THE PROBLEM OF CONTAMINATED SITES REMEDIATION: PRELIMINARY RESULTS FROM A SURVEY OF THE ITALIAN PUBLIC

Aline Chiabai¹, Stefania Tonin², Margherita Turvani², Anna Alberini³

¹*FEEM; Venezia* ²*Dipartimento di Pianificazione, Università IUAV di Venezia*

³*Agricultural and Resource Economics Department, University of Maryland*

Riassunto

La bonifica dei siti contaminati è considerata attualmente in molti paesi come una delle politiche ambientali a cui assegnare priorità elevata. Bonificare i siti inquinati permette di realizzare una serie indiscussa di benefici che vanno dalla riduzione dei rischi per la salute umana e per i sistemi ecologici, alla realizzazione di una serie di altri potenziali benefici economici e sociali. E' rilevante inoltre sottolineare che le bonifiche sono operazioni costose sia in termini di denaro che di tempo e, inoltre, gli oneri finanziari sostenuti dai contribuenti al tempo presente permetteranno di ottenere dei benefici quasi esclusivamente nel futuro.

In questo articolo riportiamo i risultati preliminari di un'indagine condotta nel 2005 in Italia in cui si è indagato la conoscenza delle persone riguardo al problema dei siti contaminati e si è ricavata una prima valutazione delle loro preferenze per alcune possibili politiche di bonifica.

Abstract

Contamination released from hazardous waste sites is nowadays one of the key environmental issues. Cleaning up of contaminated sites is important because it reduces risks to human health and ecological systems, and brings a host of potential social and economic benefits. Yet, it is a costly and time consuming effort, with the taxpayers shouldering much of the financial burden, and its benefits are incurred primarily in the future.

In this paper we offer the preliminary results of a survey conducted in 2005 in Italy, where we query people about their awareness of contaminated sites and elicit an assessment of their preferences regarding different remediation policies.

1 Introduction

Contamination released from hazardous waste sites is nowadays one of the key environmental issues. Emissions and discharges of dangerous substances from local sources have negative impacts on the quality of soil and groundwater, and on human health. For these reasons, cleaning up of contaminated sites is considered as an urgent policy for many countries, for the wide range of benefits it could bring to the society, like reduction of human health related

risks, protection of soil and groundwater, and other social and economic benefits. A comprehensive analysis of the benefits of contaminated sites can be found in Tonin (2006). In addition, people are becoming more aware of the possible negative effects that environmental pollution can pose to human health and the ecosystem, as it is evident from the Eurobarometer survey 2006. Six out of ten European citizens consider that it is “very” or “fairly likely” that environmental pollution will damage their health (61%) (Special Eurobarometer, 2006).

The Italian Law defines as contaminated sites those sites with levels of contamination or chemical, physical or biological alteration of soils, sub-soils, surface or ground water that pose a danger to public health or the natural or built environment. The law further dictates that the most egregious contaminated sites be placed on the National Priorities List (NPL), and spells out criteria that must be met for a site to be included in the NPL. Only sites on the NPL qualify for funding for cleanup and oversight from the national government. Although at this time the NPL is comprised of 50 sites, contaminated sites are spread throughout the nation, and are particularly numerous in cities with a strong industrial tradition. Recent estimates peg the total number of potentially contaminated sites in Italy at almost 13,000 (APAT, 2004). About 420 sites on this registry have been already cleaned up—about 8% of the total number of listed contaminated sites (APAT, 2004).

The relevance of environmental and health hazards posed by the existence of contaminated sites in Italy is evident. Notwithstanding the information about people attitudes and knowledge regarding these issues is rather scarce.

In our research we devoted attention to citizens' knowledge and opinion about contaminated sites and cleaning up issues. To this end, in May 2005 we administered a survey to the general public of four Italian cities (Venice, Milan, Bari and Naples) about contaminated sites remediation. The choice of these specific urban areas is related to their proximity to relevant contaminated sites. Porto Marghera, near Venice, is one of the largest contaminated site of national interest in Italy (approximately 3500 hectares) and the most expensive, where main activities are petrochemical and chemical plants. A master planning of remediation works was adopted at the site, envisaging large interventions for the next 20 years. Milan and its surroundings have the highest number of registered contaminated sites, even if they are not all included in the National Priority List. These sites are characterized by a numerous chemical industries and contamination of groundwater (Sesto San Giovanni), uncontrolled dump of industrial wastes, Tetraethyl lead contamination in river sediment (Cerro al Lambro), pharmaceutical and chemical industries, production of solvents and acetates (Piolto-Rodano). Regional plans for appropriate remediation have been developed. In the city of Bari the contaminated site of national interest Fibronit is attributable to the factory's production of asbestos-containing materials for the building industry. The site has been almost completely surrounded throughout the years by residential neighbourhoods. The city council plans to develop residential, commercial, and transport facilities after rehabilitation via complete removal of the hazardous substances. Finally, the

city of Naples is characterized by the contaminated site of Bagnoli-Coroglio, mainly characterized by the industrial area ex Ilva and ex Eternit responsible for asbestos contamination. A remediation plan is being implementing with a defined project of reuse. Other contaminated sites of national interests are Coastal Areas of Domizio Flegreo and Agro Aversano (CE-NA), Areas along the Vesuvian Coast, and Naples: Eastern Area (Legambiente, 2005).

The survey has several research purposes. The first goal is to analyse the degree of knowledge of Italian citizens about contaminated sites and their awareness of related issues. The second goal is to investigate peoples' opinions about remediation policies and their support for alternative instruments for addressing the contaminated site problems. These first two objectives are part of an exploratory research study and the corresponding results about public's preferences for policy instruments are analysed in details in the paper Turvani et al. (2006).

The third goal of the survey is to estimate the monetary benefits of a mortality risk reduction arising from implementation of public remediation programs. In this context, the valuation methodology and the benefits estimates can be found in Alberini et al. (2006).

In this paper we report the descriptive statistics of the Italian survey and the overall results about people knowledge and awareness of contaminated sites, and their opinions about public remediation programs. Detailed analysis of the questionnaire design is reported also in Chiabai et al. (2005).

The remainder of the paper is organized as follows. Section 2 presents the survey. Section 3 presents the descriptive statistics of the sample, the results for public's knowledge and awareness, and the opinions about remediation policies. Section 4 reports the conclusions.

2 The survey

The survey was administered in the four Italian cities (Bari, Milan, Naples and Bari) in May 2005, resulting in 804 completed questionnaires (approximately 200 people in each city). The sample is stratified by age using three broad age groups (25-44, 45-54, 55-65), with an equal number of respondents for each of them, and a roughly equal number of men and women. The questionnaire was self-administered by the respondents using the computer at centralized facilities.

The questionnaire is made up of three main parts. The first part provides information and ask questions about people's awareness of contaminated site and knowledge of environmental remediation and cleanup technologies. We then investigate people's perception of the possible adverse health effects due to exposure to toxic substances and their assessment of the importance to reduce the health risks for human well-being.

In the second part of the questionnaire we want to examine what are respondents' preferences for some environmental remediation strategies and actions. We ask respondents about the usefulness of possible interventions that

Government may implement to address the problem of contaminated sites. Specific questions have been included in order to understand if the public accept programs that offer economic inducement to firms, and if it consider them substitutes of or complements with enforcement-based programs. Furthermore, we examine if people give priority to long-lasting and effective cleaning up even if more expensive, if they support environmental remediation that guarantees ecosystems protection or human health protection, and what they think about remediation which will save human lives only in 30 years from now.

A specific part of the questionnaire is designed to elicit respondents' preference for public cleanup policies intended to reduce the potential risk of mortality for people living in proximity of contaminated sites. Through conjoint choice exercises we asked respondents to compare various remediation plans and to choose the most preferred. The plans differed for number of lives saved, population involved, duration of the benefits, remediation costs, and time lag between the cleanup actions and the benefits in terms of lives saved. A statistical elaboration of the answers to different conjoint choice exercises allow us to infer the willingness to pay for specific remediation programs and to value the monetary benefits of a risk reduction.

3 Results

3.1 Characteristics of the Sample

We have analysed data of our survey for the full sample and for each of the cities in the survey.

Descriptive statistics of the respondents are reported in Table 1, for the full sample and for each town separately. As per our sampling plan, about 50% of our respondents are males. The average age in the full sample is 47 years, which is slightly more than the average age in the Italian population (42.3 years), but is consistent with our sampling plan. Age distribution among the four cities shows the same result.

Analysing the full sample descriptive statistics first, we notice that 49% of the sample has a high-school degree and 13% has a university degree or post graduate education. When attention is restricted to the Italian population of ages 18-65 (the same ages in our samples) these percentages are 32% and 11%. The average household income is €26,784 per year. This figure is comparable to the average household income in Italy, which is about €29,483 per year (Banca d'Italia, 2004). About 73% of the respondents are married or living together, while 19.4% are single and 7.21% are divorced, separated or widowed. The average household size in our sample is 3.25. This is slightly higher than the average in Italy (2.69 people per household). Fifty-two percent of respondents are occupied, 15% are retired and 22% are housewives. Finally, 30% of the respondents have children from 0 to 15 years old.

Variable	Full sample mean	Venice	Milan	Bari	Naples
Male (dummy)	0.50	0.51	0.50	0.50	0.51
Age (years)	47.02	47.3	46.8	48.3	47.3
Married/living together (dummy)	0.73	0.57	0.74	0.85	0.78
CHILDREN 0-15 (dummy)	0.308	0.22	0.21	0.42	0.38
High school degree (dummy)	0.49	0.48	0.61	0.47	0.43
University degree (dummy)	0.13	0.25	0.11	0.06	0.12
Employed	0.52	0.58	0.61	0.42	0.47
Retired	0.15	0.19	0.16	0.15	0.10
Housewives	0.22	0.09	0.16	0.31	0.32
Household size	3.25	3	2.87	3.5	3.6
Household income (euro/yr)	26,784	29,187	34,651	20,850	22,375

Table 1 - Socio-demographic characteristics of the respondents.

Comparing descriptive statistics among cities, some differences emerge. The percentage of married or living together is higher in the city of Milan and Bari, while it is the lowest in Venice. As regards education, the highest percentage of respondents with high-school degree is observed in Milan, while the lowest is observed in Naples. For university degree, Venice registers the highest percentage of graduate or post graduate respondents, and Bari registers the lowest percentage.

The higher rates of employment is observed in Milan (61%), followed by Venice (58%). The two cities of South Italy have the lower rate of employment, and this fact can probably explain the higher presence of housewives in Bari and Naples (31% and 32% respectively). People retired from work are equally distributed over the four cities surveyed, with a lower rate of retirement observed in Naples (10%) and a higher observed in Milan (19%).

Average household size is higher in the two cities of South Italy, than in the North, as well as the percentage of respondents with children from 0 to 15 years old. As expected, the two cities of North Italy (Venice and Milan) register higher average household income, while the two cities of the South (Bari and Naples) have lower income.

3.2 Information about Contaminated Sites

In Italy, the first inventory of contaminated sites includes almost 13,000 potentially contaminated sites, distributed all over the country. All the regions and the main cities are characterised by the presence of contaminated sites with more or less severe pollution and hazardousness. This reality does not imply that Italian citizens know contaminated sites problems and the effects of exposure to contamination on human health and environment. Moreover, direct experience with contaminated sites of people living or working in proximity of contaminated sites, may give rise to attitudes and behaviours that could be very different from those of people with no familiarity with soil problems.

Therefore, we examine respondents' knowledge and awareness of the contaminated sites issue. Table 2 displays the responses about the

respondents' awareness of contaminated site issues, for the full sample and for each city as well. We found that 90% of the respondents has previously heard about contaminated sites. This seems reasonable, since our respondents were selected among the residents of cities with serious contaminated site problems. Knowledge of sites appears to be related to the respondent's educational attainment. For example, 92.49% of the mostly educated respondents (high school diploma or college degree) have heard of contaminated sites, against 85.91% of the less educated respondents. The difference between the two groups is statistically significant at the 1% level.

Variable	Description	Full sample mean	Venice	Milan	Bari	Naples
Heard	whether respondent heard of contaminated site	0.90	0.92	0.97	0.82	0.91
Knowsite	whether respondents is aware of pollution event in site close they live or work	0.43	0.34	0.35	0.41	0.63
Hearboni	whether respondent heard of environmental remediation of contaminated site	0.80	0.82	0.79	0.75	0.85
Knowboni	whether respondent is aware of contaminated sites for which clean-up has been implemented	0.37	0.39	0.38	0.41	0.29

Table 2 - Respondent's awareness of contaminated site issues

Figure 1 shows how the respondent get information about contaminated sites and the related problems, if by newspapers and television ("common media"), and/or by participation to conferences, or neighbourhoods meetings ("social events"). Results show that roughly 77% of the "informed" group obtained their information from the newspapers and television (media), and 28.8% from conferences and neighbourhood meetings, or at school or university (social). The propensity to acquire information from events such as neighbourhood meetings and conferences increases with education and is higher for respondents living in proximity of dumps and abandoned factories. Specifically, 26.48% of the more highly educated respondents (persons with a high school diploma or a college degree) obtain information by participating in these events, against 16.78% of the others—a difference that is statistically significant at the

1% level. Moreover, 36.41% of the respondents living near dumps and 26% of those living near abandoned factories get their information by participating in meetings or conferences, against 18.98% and 20%, respectively, for all others⁶. We do not know whether those respondents who live near waste disposal sites went to meetings and conferences to seek information about these sites, or rather learned that these sites are contaminated because they attended these meetings.

From Table 1 we observe that 43% of our respondents are aware of contaminated sites near their homes or workplaces (knowsite). Eighty percent of the sample has heard of environmental remediation of contaminated sites (hearboni), and 37% is aware of contaminated sites in Italy for which clean-up strategies have been implemented (knowboni).

The questionnaire includes also some questions intended to investigate peoples' concerns about health risks associated with contaminated sites. We found out that the majority of the sample (89%) thinks it is very important to reduce the negative effects to human health caused by exposure to hazardous substances. To understand how respondents perceived health effects potentially caused by environmental contamination, we asked them to consider a list of possible temporary or permanent diseases and to indicate how it is likely to contract one of these diseases for people living in proximity of contaminated sites. Eightyone percent of our sample believes that it is very likely for people living near contaminated sites to develop temporary diseases (allergy, temporary damages to respiratory organs and other organs), almost 66% thinks that it is very likely to contract some kind of health permanent damages (i.e. permanent damages to different organs), and 76% thinks that there is high probability of developing cancer. However, the interpretation of these statistical results needs some cautions because answers were given before providing information and scientific data about the adverse effects of exposure to contamination on human health. To conclude, we find out that respondents who are aware of contaminated sites near their homes or workplaces, consider it more likely that exposure to toxicants at contaminated sites will result in a number of adverse health effects, including allergies, respiratory problems, damage to liver and other organs, and cancer.

⁶ Statistically significant at the 5% level for abandoned factories, and 1% level for dumps.

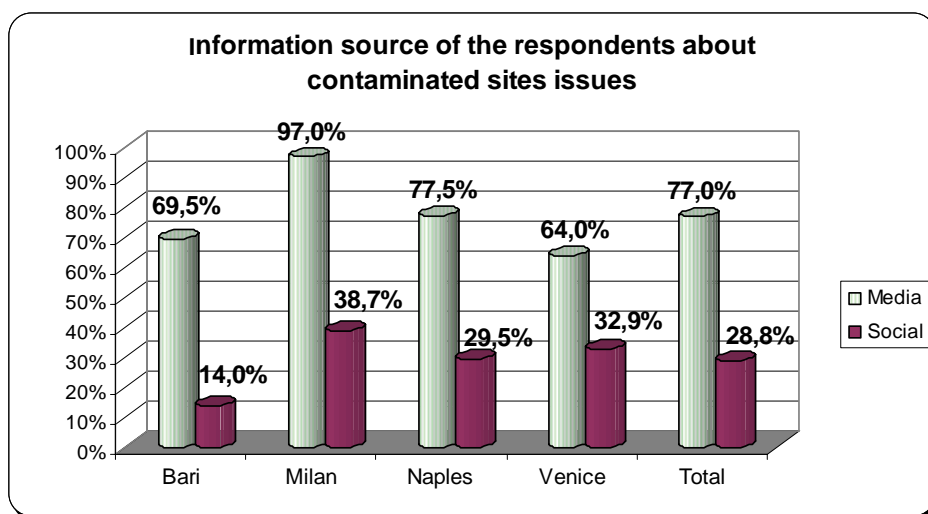


Figure 1 - Information source of the respondents

When analysing these results for each city separately and comparing the corresponding figures, we notice that respondents living in Bari appear to be the less informed (82% of them have previously heard of contaminated sites), while the respondents living in Milan are the more informed (97%). If we focus on the information media, the highest percentage of respondents acquiring information from newspapers and television (media) is observed in Milan, as well as the highest percentage of participation to conferences and meetings (social).

As regards respondents' awareness of pollution event in site near their homes or workplaces (knowsite), the highest percentage is observed in Naples, as it can be seen from Table 2. Accordingly, respondents of Naples attach higher health risks to exposure to hazardous substances of contaminated sites. The highest percentage of respondents who have heard of contaminated sites remediation (hearboni) is registered in Naples and the lowest is registered in Bari. Instead, Naples has the lowest percentage of respondents' aware of contaminated sites cleanups (knowboni), the highest being observed in Bari.

3.3 Public Programs' Priorities

There are various kind of policies that countries have endorsed and applied to address the problem of contaminated sites with different objectives and degree of effectiveness. The common denominator seems to be the attempt to discourage further future contamination and to charge to the responsible parties the entire cost of cleanups. For example, US Superfund legislation, European Directive on Environmental Liability, and Italian legislation aim to support the polluter pays principle and to impose stringent liability rules to responsible parties.

Problems still remain for those sites which have been contaminated by past activities and/or for those whose responsible parties are impossible to find. In these cases, the legislator cannot undertake legal actions and generally the burden of cleaning up costs falls on the shoulder of local or central governments. Consequently, citizens are generally asked to sustain public

initiatives and to contribute to public expenditures for contaminated sites cleanups. However, in many situations people are not well informed or are not necessarily willing to support the public interventions.

In this section we wish to examine respondents' beliefs about priorities for contaminated sites cleanup. For this purpose we showed the respondents several statements, asking to what extent they agree or disagree with them ("Do you agree with the following statements? When deciding about remediation plans, the Government should:..."). We used a Likert scale ranging from 1 ("completely disagree") to 5 ("completely agree"). Results are displayed in Figure 2 for the "completely agree" responses (full sample).

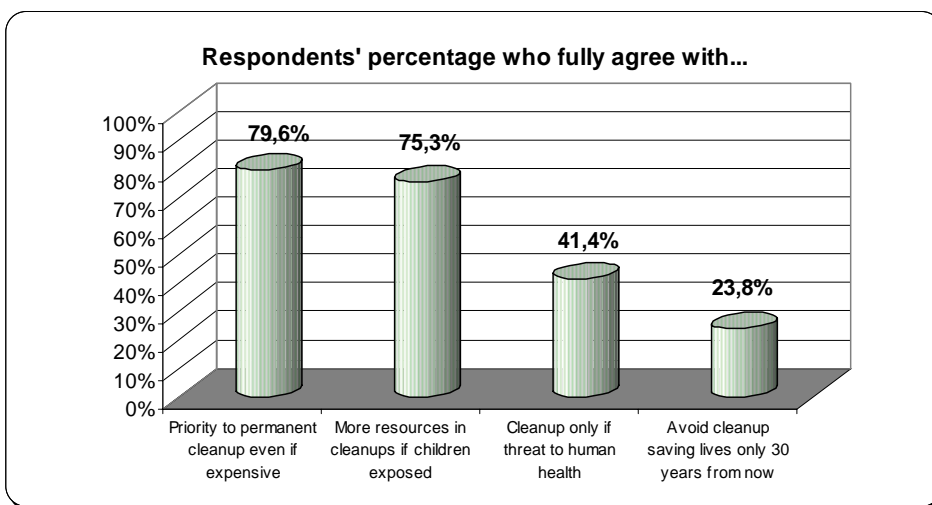


Figure 2 - Respondents' percentage who fully agree with...

Seventy nine percent of the sample fully agrees with giving priority to permanent cleanup and effective remediation plans, even if they cost more. Seventy five percent fully agrees with investing more resources for the cleanup of sites where children are the most exposed. Forty one percent fully agrees with implementing remediation plans only if the contaminated site is a threat for human health. Finally, 23.8% fully agrees in avoiding to invest resources in cleanup which will save lives only 30 years from now.

Figure 3 shows the results separately for the North cities of our sample (Venice and Milan) and for the South cities (Bari and Naples).

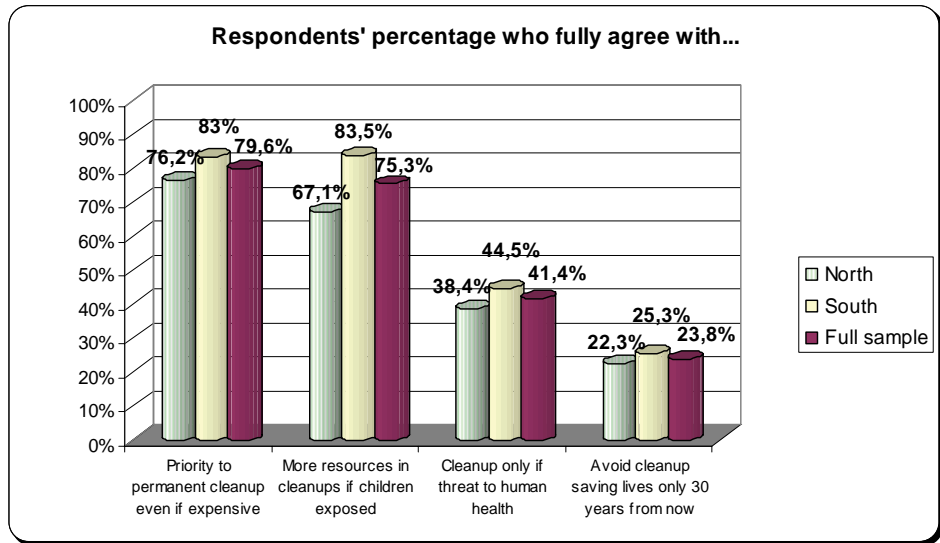


Figure 3 - Respondents' percentage who fully agree with...(North, South and full sample).

Results illustrate in general a higher support for the above stated remediation policy options in the South compared with the North of Italy. The two cities of South Italy show a higher percentage of respondents who fully agree in giving priority for permanent cleanup even if expensive (83%), if compared with North Italy (76.2%). The same applies for investing more resources for the cleanup of sites where children are the most exposed (83.5% in the South versus 67.1% in the North), and for realising cleanups only if the contaminated site is a threat for human health (44.5% in the South versus 38.4% in the North). As regards the last option, avoiding to invest resources in cleanup which save lives only 30 years from now, the difference between North and South is less evident (25.3% in the South versus 22.3% in the North).

People's concern about cleaning up of contaminated sites and their desire to find a solution for them is also confirmed when examining the support given to Government intervention enforcing the remediation of orphan sites. It is noteworthy to remember that the Italian Ministerial Decree N. 471/1999 states that when it is impossible to find the responsible parties or if they cannot afford the cleanups costs, the local territorial competent agency must proceed with the cleanups. People familiarity with these issues has not being investigated so far, and what people think about public intervention is not known.

In our survey, respondents have been asked how much useful they judge the government intervention for cleanup of orphan sites. Responses were recorded using a likert scale ranging from 1 ("slightly useful") to 5 ("very useful"). Results are displayed in

Figure 4, showing that the great majority of respondents (83.6%) consider very useful the public intervention for remediation of orphan sites. The percentage of people indicating a lower support to direct remediation of the Government is very low. In particular, if we consider jointly the last two score categories (4 and 5), we notice that 90% of the sample consider direct remediation of orphan sites more than somewhat useful.

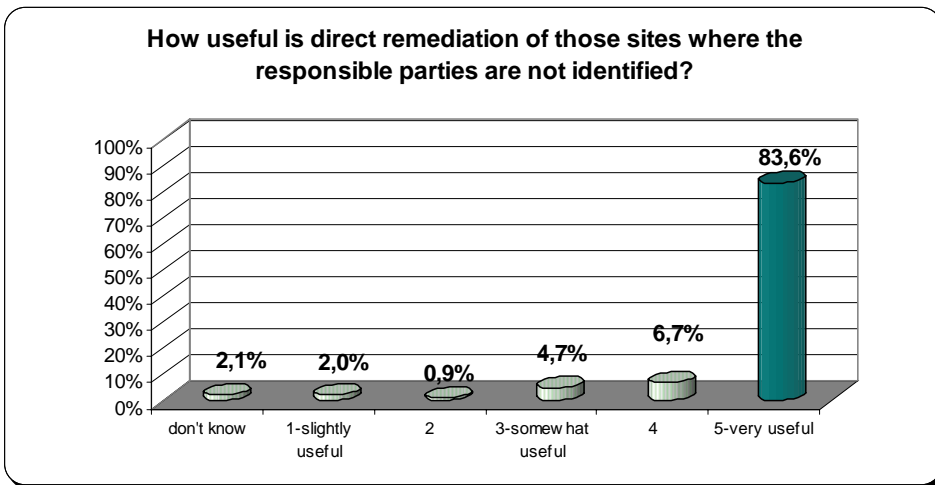


Figure 4 - Respondents' percentage who find very useful direct remediation of orphan sites.

Much more than for other contaminated sites, the remediation of orphan sites implies a direct intervention of government in terms of money and policies. In practice administrations realize that liable parties are difficult to be identified or have not sufficient resources to cover the necessary cleanup costs, implying that they frequently contribute either by providing a public budget to finance major cleanups, or establishing special funds, such as waste taxes collection, loan systems or voluntary agreements with industry. For example, in the US, monies for the Superfund trust account derive from the dedicated tax on petroleum and chemical feedstock. All of these funds should be used for the Superfund process and most should be used for cleaning up orphan sites. A similar initiative could be introduced in Italy to help the national and local government to carry out the major number of remediation actions.

The fact that respondents consider very useful the public intervention for remediation of orphan sites could be also indicative that they are willing to give up part of their income to expedite the remediation of contaminated sites.

We have also analysed the existence of possible geographical differences in the distribution of respondents' responses. The results are showed in Figure 5.

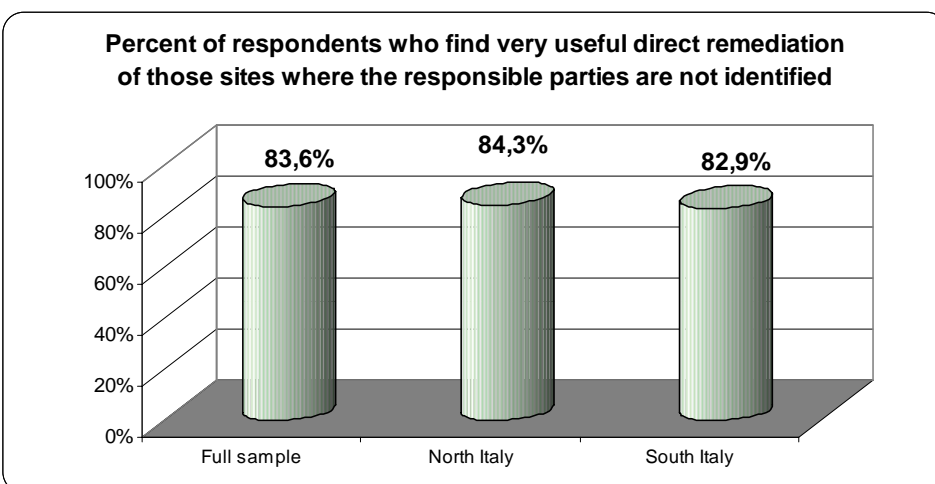


Figure 5 - Respondents' percentage who find very useful direct remediation of orphan sites.

Figure 5 compares the results among the cities of North and South Italy, showing no evident difference. Most of the respondents give support to Government intervention for cleanup of orphan sites, regardless the city of origin.

4 Conclusions

Effective solutions for addressing the problem of contaminated sites are a necessity for many industrialized countries where the legacy of abandoned polluting industrial activities is causing serious problems to human health and to the environment. People opinions regarding these issues has not being investigated in the past and specifically not much is known about preferences for public remediation policies.

In our research, we surveyed residents of four Italian cities (Venice, Milan, Bari and Naples) with serious contaminated site problems to investigate their awareness of the contaminated site problem, their opinion about the effects of contamination on human health and on the environment, and with the purpose of eliciting their preferences for various public programs to remediate contaminated sites.

We have found that people are largely aware of the existence of contaminated sites and that the major source of knowledge are television and newspapers. Only few of our respondents had acquired their information about contaminated sites directly in organized events, such as conferences or civic association or neighbourhood meetings, although the tendency to acquire information from organized events tends to be greater among the more educated respondents and among those living close to waste disposal sites or derelict areas. In this paper we offer an analysis of the scale at national and city level.

Most of our respondents are aware of the existence of contaminated sites near their home or workplace, and 89% think that it is very important to reduce the adverse effects to human health due to toxic substances found at contaminated sites. Taking into account possible public remediation programs, we find that almost 80% of the respondents are in favour of permanent remediation, even if more expensive, and 75% agree with the necessity of investing more resources for environmental cleanups where children are the most exposed. Forty one percent agree with supporting cleanup plans which have an impact on human health. Twenty four percent suggest to avoid remediation plans saving lives only 30 years from now. Our results also show that respondents in the South of Italy support more strongly these policies than the respondents in the North.

We have also found that 83.6% of the respondents are in favour of direct intervention of the public sector to finance remediation of orphan sites, with similar results for North and South Italy. This fact implies a high concern and awareness of our respondents about contaminated sites issues and the strong desire to find a solution also for those sites where the remediation operations could be very difficult without public monies.

References

A. Alberini, S. Tonin, M. Turvani, A. Chiabai, (2006), Paying for Permanence: Public Preferences for Contaminated Site Cleanup, paper presented at SURED 2006, Ascona (Switzerland), 4-9 June, 2006 and at the "Third World Congress of Environmental and Resource Economists, Kyoto (Japan), 3-7 July 2006

Alberini, Anna, Alberto Longo and Marcella Veronesi (2005), "Basic Statistical Models for Conjoint Choice Experiments," in *Valuing Environmental Amenities using Choice Experiments: A Common Sense Guide to Theory and Practice*, Barbara Kanninen (ed.), Springer.

APAT, 2004, *Annuario dei dati ambientali*, ISBN 88-448-0147-7, Roma

Banca d'Italia, (2004), *Rapporto Annuale – La situazione del paese nel 2004*, Rapporti Istituto Nazionale di Statistica, Roma

Case, D. W. (2001), "The Law and Economics of Environmental Information as Regulation," *Environmental Law Reporter* 10774, July

Chiabai, A., A. Alberini, M. Turvani, S. Tonin, (2005), Valuing the benefits of contaminated sites remediation, in *Scientific Research and Safeguarding of Venice*, Research Programme 2004-2006, Volume IV

Eurobarometer (2005), *The attitudes of European citizens towards environment*, Retrieved June, 2006 from http://europa.eu.int/comm/public_opinion/archives/ebs/ebs_217_en.pdf

Legambiente, 2005, "La chimera delle bonifiche".

Perreira, K.M., F.A. Sloan, 2002, Living Healthy and Living Long: Valuing the Nonpecuniary Loss from Disability and Death, *The Journal of Risk and Uncertainty*, Vol. 24(1), pp 5-29.

Special Eurobarometer (2006), *Risk Issues*, Retrieved Retrieved June, 2006 from http://ec.europa.eu/public_opinion/archives/ebs/ebs_238_en.pdf

Tonin, S. (2006), *Measuring the socio-economic benefits of brownfields remediation projects*, Ph.D dissertation, SSAV, Venice, Italy

M. Turvani, A. Chiabai, A Alberini, S. Tonin, (2006), Public Support for Policies Addressing Contaminated Sites: Evidence from a Survey of the Italian Public, paper presented at SURED 2006, Ascona (Switzerland), 4-9 June, 2006 and at the "Third World Congress of Environmental and Resource Economists, Kyoto (Japan), 3-7 July 2006

Viscusi, W.K., W.A. Magat, and J. Huber, 1991, Pricing Environmental Health Risks: Survey Assessments of Risk-Risk and Risk-Dollar Trade-Offs for Chronic Bronchitis, *Journal of Environmental Economics and Management*, Vol. 21(1), pp 91-96.

AREA 2

Architecture and Cultural Heritage

RESEARCH LINE 2.2

Catalogue of Venetian plasters and historical interventions for high water defence

SYSTEMS FOR THE PROTECTION OF SINGLE BUILDINGS FROM HIGH TIDES

Mario Piana¹, Federica Restiani²

¹Dipartimento di Storia dell'Architettura, Università IUAV di Venezia. ²Architetto, Venezia

Riassunto

Dalla seconda metà del XX secolo, certamente sotto lo stimolo dall'aumento progressivo sia della frequenza che della sempre maggiore altezza raggiunta dalle acque alte, e grazie alle nuove disponibilità offerte dalla tecnica sono apparsi sistemi di difesa di singoli edifici dalle invasioni mareali: dalle vasche sottopavimentali in calcestruzzo armato, con risvolti inglobati nelle pareti o adagiati ad esse, a quelle o con giunti elastici di collegamento parete-vasca, fino ai più recenti impianti basati sulla depressione della falda d'acqua superficiale. Si tratta di interventi ancora relativamente contenuti quanto a numero, ma destinati a diffondersi anche dopo la futura regolazione generale delle maree dell'intera laguna, quantomeno negli edifici con pavimentazioni di pianterreno poste ad una quota inferiore ai +100-110 centimetri sul medio mare.

Dopo una ricognizione archivistica dei principali e più interessanti interventi compiuti, seguita da una classificazione delle tipologie riscontrate, sono stati individuati alcuni casi emblematici e particolarmente significativi, ricostruiti nelle loro vicende progettuali e realizzative: dalla cripta di San Marco al chiostro di Sant'Apollonia, al Duomo di San Donato di Murano, al Refettorio d'Estate nel convento dei Frari a San Polo, a Ca' Pesaro.

La comparazione dei diversi sistemi, valutata in relazione alla loro influenza sulle caratteristiche costruttive e sul comportamento strutturale delle fabbriche e alla loro compatibilità con la sostanza materiale e con i valori dell'architettura, consentirà di individuare gli eventuali aggiornamenti tecnologici possibili e di offrire indicazioni metodologiche per i futuri interventi.

Abstract

Since the second half of the XX century, under the stimulus of the progressive increase of both the frequency and the height of the acque alte (high tides), and thanks to the new technical resources available, systems for the protection of buildings from the tides have appeared: from reinforced concrete tanks under the floors, with edges included in the walls or flush against them, to tanks equipped with elastic wall-tank linkage joints, to the most recent plants, whose concept is based on the depression of the surface water table. There have not been many of these interventions as yet, but their numbers shall increase also after the implementation of the future general regulation of the tides in the whole lagoon, at least in buildings whose ground floor lies at a height of less than 100-110 centimetres above the average sea level.

After examining the archives of the main and most interesting actions taken, and after having classified the main types of action found, some exemplary and significant cases were identified and their planning and implementation reconstructed: from St. Mark's crypt to St. Apollonia's cloister, to the Duomo of San Donato di Murano, to the Summer Mess Hall in the Frari convent in San Polo, in Ca' Pesaro.

The comparison between the different systems, assessed with regard to their influence on the building characteristics and structural behaviour and to their compatibility with the material substance and architectural values, shall make it possible to identify the possible technological updates, if any, and to glean methodological directions for future interventions.

1 Foreword

A branch of the Corila research titled Venice, one thousand years of building and the protection from "salt waters" addressed the techniques used until now for the protection of the ground floors of the lagoon's buildings from the tides.

The phenomenon of acque alte (high tides) is not a recent problem: in the past, too, the tide's sovrabondanti (excesses) used to invade, albeit less frequently than they do today, calli, fondamenta and the city's campi, as well as the ground floors of many houses and of public and religious buildings. The inconvenience and problems caused by tidal invasions have been dealt with substantially with a single technique throughout the centuries: by lifting the floors.

In the second half of the XX century, however, under the stimulus of the progressive increase of both the frequency and the height of the acque alte (high tides), and thanks to the new technical resources available, systems for the protection of buildings from the tides have appeared, able to protect effectively single parts of or whole buildings, based on the installation of reinforced concrete tanks under the floors, that are meant to intercept water filtering in from the surrounding ground, associated with the installation of mobile metal gates at the entry of the building – or area – to be protected. More recently, other methods have been perfected and tested, involving the installation, under the floor, of a network of draining pipes connected to extraction pumps, it, too, coupled with temporary mobile gates that produce a localized depression of the surface water table, able to keep the relevant area dry.

2 The underfloor tanks

The first, representative examples of all similar operations carried out until the 1980s were the actions taken in the Sant'Apollonia cloister and in the basilica of San Donato di Murano, were the basis for today's defence techniques were laid, even though, in some cases, only as an hypothesis.

In Sant'Apollonia¹ the restoration works, started in 1967 following a project by Ferdinando Forlati, the Proto (that is, architect) of Saint Mark's Basilica, were carried out by the Zerbo-Francalancia building firm that also elaborated the executive plans of the works².

The underlying aim of the project was to restore the architectural and spatial proportions of the Romanic cloister, that had been altered, besides by two massive buttresses meant to support the cloister's east wall, also by three subsequent elevations of the floor that had hidden the whole skirting board and reached to the base of the double columns. In order to go back to the level of the ancient floor of the cloister, it was decided that the floor height had to be reduced by about 90 cm, going from the current +1.30 cm above average sea level to about + 0.40 cm above average sea level³: a level that would have entailed an almost constant presence of tidal water. Therefore, in order to isolate the cloister area from the lagoon's water, a reinforced concrete, double mesh "basin" was created, crossing the columns' foundations and turning back to reach inside the inside of the perimeter walls. Rainwater, collected in the open area of the courts or coming down from the drainpipes on the roofs of the nearby buildings, collect, through dedicated pipes, in four watertight wells, prepared within the concrete floor slab. The wells, in turn, empty, through other pipes laid below the floor slab, into a main well located in a small court next to the cloister, equipped with a pump that pumps the water into the nearby Rio della Canonica. In order to block the path of waters coming from the openings, the doors opening on the fondamenta and on the rio were equipped with fixed

¹ The origins of the Benedictine complex, that includes the church dedicated to the Saints Phillip and James, the Sant'Apollonia cloister and the monastery, date back to the XII century. In mid-XV century the monks donated the complex to Saint Mark's Ducal Chapel and the Procuratoria de Supra used it as the home of the Primicerio (head of the chapter). After the fall of the Republic, the complex was variously used as court of law, public offices, private residences, until it was acquired by the Saint Mark Procuratoria. At present the complex hosts the Lapidarium, the Diocesan Museum of Sacred Art and the Archives of the patriarchate

² For details on the restoration of the complex, see: Ferdinando FORLATI, *Il restauro del chiostro di S. Apollonia a Venezia*, in "Palladio", year X, n° I-IV, 1970; Jolando FRANCALANCIA, *Il restauro del complesso storico architettonico di S. Apollonia – Venezia*, I.T.E., Lido di Venezia 1970.

³ "si tratta di realizzare un'opera mai prima tentata a Venezia: si doveva cioè riportare la pavimentazione alla quota antica che è assai vicina al medio mare: essa però nel XII° secolo era molto più profonda, in altre parole si dovevano contenere quelle sottopressioni che oggi sono divenute notevolissime" Ferdinando FORLATI, *Il restauro ... cit.*, page 153 ["it is a matter of carrying out a work never before attempted in Venice: restore the flooring to its ancient level, that is quite close to the average sea level: however, in the XII century, such level was much deeper. In other words, it was necessary to find a way of containing those deep pressures, that today are quite high"].

thresholds, with steps, at a height of +1.60 cm above average sea level.

The story concerning the cathedral dedicated to the Saints Mary and Donato of Murano⁴ represents a significant step towards the defence of the individual buildings from the tides: with reference to the date of its realization and to the scope of the project, it can be considered (overlooking some debatable aspects of the intervention, such as the absence of appropriately conducted archaeological diggings) the most important work of the XX century with regard to the defence from acqua alta, not only in terms of the solution that was finally adopted, but also because of all the alternatives that were presented and discussed at the time.

Between 1969 and 1973 the church was the object of several studies aimed at eliminating the frequent floodings this sacred building was subject to. Particular alarm was felt for the preservation of the important XII century mosaic floor (whose level varied between +70 and +80 cm above average sea level), that was considerably ruined by the constant floods that occurred during high tide due to both seepage from the underlying ground and direct invasion through the church's two entries, one of which had a threshold at +1.32 above average sea level.

There were several hypotheses to choose from: a system with a flow-through floor made of two connected large slabs, with the upper one equipped with a vertical joint at the walls and columns, between which a network of drainage pipes connected to extraction pumps lie; a deep external diaphragm around the church, connected to the perimeter walls by a continuous concrete slab; ground waterproofing through electrodirected injections, with planting of shoes around the church, connected with a direct current generator, which would both create a potential drop that would induce the water in the ground to migrate towards the negative poles, where it would be extracted by pumps and at the same time favour the introduction of electrolyte solutions for a progressive waterproofing of the ground.

All of these proposals were discarded, in favour of the adopted solution: a reinforced concrete underfloor tank (Picture 1). In order to enable its construction, the whole mosaic floor had to be detached by dividing it in a lot of small areas, and then replaced at the end of the works (Picture 2). The reinforced concrete mat, divided into plates (for operating reasons linked to the organization of casting, but also in order to cope with thermal dilation and contraction) with copper plate joints, passes below the columns too (which, during the works, were supported by disposable jacks) and folds back to form the vertical, containment walls where it joins the perimeter walls. Seventy 12.5

⁴ SS. Mary and Donato, founded in the VII century, was dedicated to Mary in 999 and to Donato in 1125. Completion of the building in its present form dates back to 1140, the year shown in the mosaic floor.

m-long micropiles have to anchor the concrete mat to the floor, thus contrasting the hydraulic component that is not absorbed by the weight of the built structure.

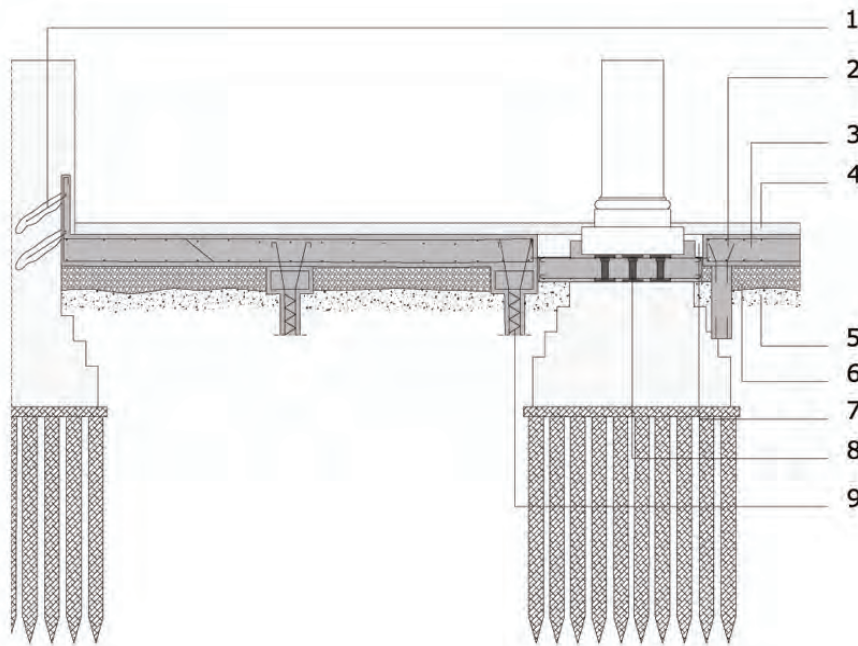


Figure 1- Saints Mary and Donato di Murano Church: diagram representing the underfloor tank (Legend - 1. Wall-slab anchoring, 2. Concrete anchoring micropiles ($l=12.5$ m), 3. Concrete base slab (25 cm), 4. Floor, 5. Ground, 6. Gravel (20 cm), 7. Cement mortar, 8. Disposable jacks, 9. Foundation micropiles).

After these first instances and until the end of the 1980s, the protection of buildings from invading tidal waters was carried out exclusively through the use of underfloor tanks of various shapes and associated with mobile gates at the entries. These are guaranteed effective actions, provided they are well planned and implemented. The underfloor tank forms a continuous structure, generally constituted by a concrete slab that intercepts water seepage from the underground. The pressures the slab is subject to can be contrasted by the slab's own weight and the weight of the slab's permanent loads, or by micropiles that serve the purpose of anchoring it to the ground. In the first instance, the structure is always considerably thick, as its weight must be sufficient to counterbalance the buoyancy, in the second the plate can be thinner, but requires much stronger reinforcing. The choice to create a weight-resistant tank or a micropile-anchored one, in Venice, is linked also to the distance of the works to be realized from the canals. The burden of moving the materials from the boat to the tank's location, an operation that can only be carried out by hand, is a deciding factor: When the worksite is far from the canal, it is often preferable to install a micropile-anchored tank, which requires a more complex technology and greater skill in some phases, but which makes for lower concrete requirements for the slab, thus also limiting the expense.



Figure 2 - Saints Mary and Donato di Murano Church: one phase of the removal of the mosaic flooring

In the last decades of last century, the underfloor tanks have undergone some technical improvements, aimed at solving some drawbacks and incompatibilities involving the buildings and derived from the tanks as they were then built.

Even if the destruction of historical materials of the building, that is always negative and is due to the demolition of the whole base of the building so as to create some space for the vertical edges of the tank, were to be overlooked, the relationship that is created between the underfloor slabs and the building's elements is one of the more delicate and controversial aspects of this kind of work. The underfloor tanks with edges that fall within the perimeter walls and cross the foundations of the inner elements, indeed, imply a radical change in the body of the building: the tanks are invariably built within mat foundations, thus substituting for the foundation structures, either in line or plinth ones, that had supported the building until then. This alteration, that might be seen as negligible, structurally indifferent or even advantageous for the stability of the building, in reality leads to an incongruous and contradictory alteration of the static behaviour of the Venetian building. The whole of the buildings erected in the lagoon are characterized by unique building methods, by a complex of techniques, precautions and singular procedures, that were determined by the uniqueness of the location, that are simply absent from any other mediaeval and modern building complex in the peninsula. Given the scarce quality of the grounds – layers of slime, sand, clay, with extremely limited resistance and completely unable to bear significant loads – the techniques available in the past did not make it possible to avoid the relative settlements of the single walls, that nevertheless have a considerable entity in absolute terms. 20-30 cm settlements between the different walls in the same construction (which would

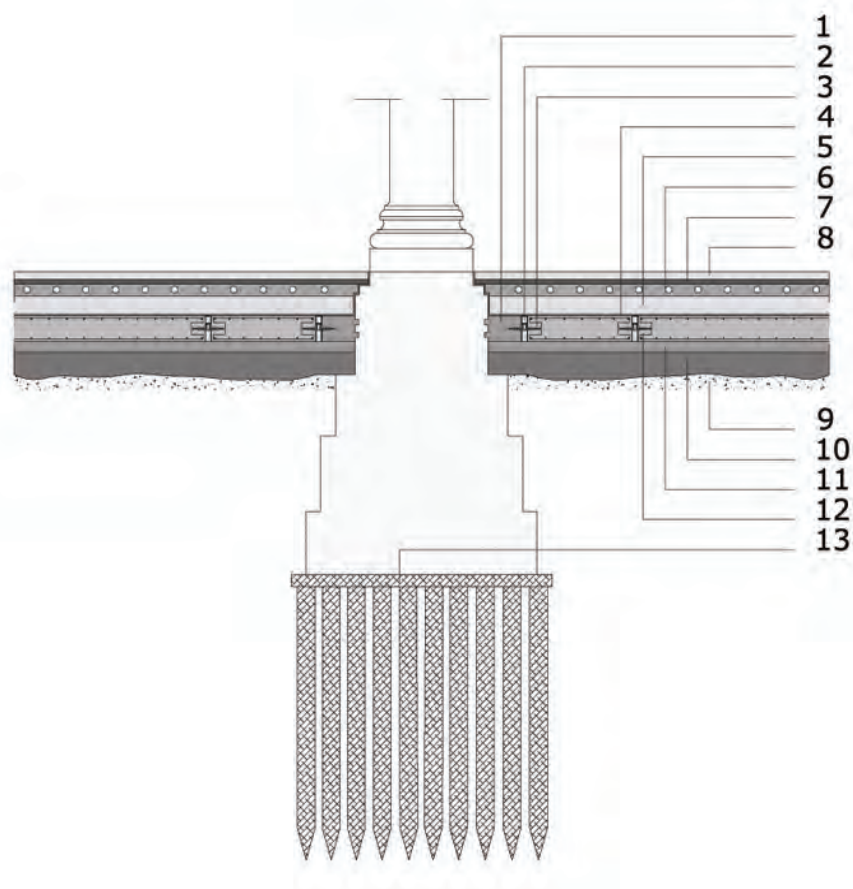
produce dramatic consequences in any other building) are quite common in the city and fall within the physiological limits of a lagoon building. This problem has been studied by generations of Venetian workers, who tackled it by, on the one hand, diversifying the foundations within the same building, calibrating them according to the loads transmitted by the various wall systems, so as to attain an homogeneous settlement, and, on the other hand, by erecting the walls so as to allow the constructs to warp freely, without compromising the general balance of the building. The main ploy used for this purpose was the systematic detachment of the walls. With the exclusion of the perimeter walls, well linked at the corners, every joining between internal partitions and between the internal partitions and the perimeter walls is deliberately absent: the walls can therefore move freely, without creating dangerous tensions and, consequently, fractures.

The alteration of the foundation system of buildings designed and built to withstand significant and differentiated settlements of their walls, consequent to the introduction of underfloor plates that are rigidly connected with the vertical walls cannot but mean an alteration – even though partial – of their very nature.

For these reasons, besides for reasons of greater building simplicity, sometimes the vertical edges of the tanks are built outside the walls, and moulded so as to adhere to the perimeter and internal walls. This system, if adopted with the appropriate precautions, does not entail structural interference with the building. The offsets of the turnups, however, by increasing the thickness at the base of the wall, alter the space in the rooms and are impracticable when there are valuable architectural features decorating the walls (stone portals, plinths or column bases, pillars or responds, etc.) or when the dimensions of the internal passages from one room to another are too small.

Thus, starting from the 1980s, with the works carried out in the Summer Mess Hall in the Frari Convent in San Polo, in some cases elastic joints were preferred to connect the underfloor plates and the perimeter and inner foundations, so as to make the defence works independent and avoid any structural interaction, leaving to the perimeter brick wall the task of blocking the acque alte, preventing them from entering the building.

Figure 3 – Frari Convent in San Polo: diagram representing the underfloor tank with elastic joints installed in the Summer Mess Hall (Legend - 1. Added concrete, 2. Polystyrene, 3. Water-stop joint, 4. Insulation sheath, 5. Laterlite (12 cm), 6. Heating coil (8 cm), 7. Mortar, 8. Floor tiles (4 cm), 9. Ground, 10. Gravel (15 cm), 11. Lean concrete (7 cm), 12. Concrete base slab (16 cm), 13. Foundation planks and piles).



In the big Mess Hall⁵ the underfloor waterproof slab comprises eleven reinforced concrete plates, thin and connected to micropiles that contrast the buoyancy during high tide, joined together, with the perimeter walls and with the columns' foundation plinths through PVC flexible couplings that can withstand

⁵ For further information on the restoration of the Summer Mess Hall, please consult: C. BOZZONI, Refettorio d'Estate dell'ex convento dei Frari, ora Archivio di Stato, in G. CARBONARA (edit.), *Restauro e cemento in architettura*, Roma 1981 pp. 102–105; F. CAVAZZANA ROMANELLI, *Storia e restauri. Il restauro del Refettorio d'Estate nel convento dei Frari a Venezia ora sede dell'Archivio di Stato*, in "Bollettino d'Arte del MBCA", supplemento n° 5, 1983, pp.13–32; M. PIANA, *Lavori di consolidamento e restauro. Il restauro del Refettorio d'Estate nel convento dei Frari a Venezia ora sede dell'Archivio di Stato*, ibidem, pp. 35–42; G. BISCONTIN – G. RIVA – F. ZAGO, *Caratteristiche fisiche, chimiche e meccaniche della struttura muraria*, ibidem, pp. 43–50; P. SCARPA, *Ceramiche veneziane sotto le antiche pavimentazioni soprastanti le volte*, ibidem, pp. 51–53; M. DE MIN, *Vicende del ritrovamento: classificazione, cronologia e tipologia delle ceramiche*, ibidem, pp. 55–59; L. CALOI – P. CASSOLI – M.R. PALOMBO, *Ritrovamento di resti ossei*, ibidem, pp. 60 – 62; M. PIANA, *Il Refettorio d'Estate nel Convento dei Frari*, in *Venti anni di restauri a Venezia*, Roma 1987, pp. 83–91.

movements of the plates against one another and the walls, of several centimetres (Picture 3-4).

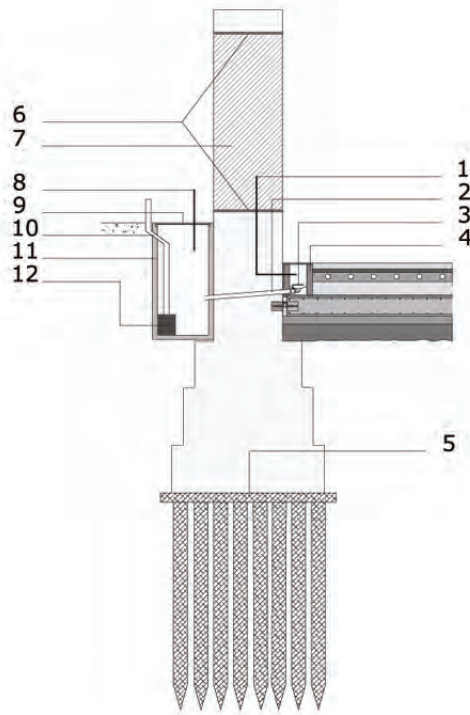


Figure 4 – Frari Convent in San Polo: diagram representing the underfloor tank with elastic joints installed in the Summer Mess Hall (Legend - 1. Lead plate, 2. Reconstructed wall, 3. WATER EXPULSION WELL, 4. Steel cover, 5. Water drainage pipe, 6. Concrete well, 7. Suction pump, 8. WATER COLLECTION WELL, 9. Steel pipe, 10. Ball valve, 11. Bricks).

The tank was completed with a heat-insulating layer, a heating coil that integrates the heating system and the laying of a cotto tiled floor. In order to avoid the water capillary migration and the consequent crystallisation of soluble salts throughout the brickwork inside the perimeter walls, two horizontal barriers were installed, made of lead plates inserted one slightly above the floor level, at about +1.10 above average sea level, the other at +2.00 m above average sea level, that is, at a level highest than the highest tide registered in the XX century. This precautionary measure, taken in order to eliminate any small water seepage from the vertical walls and to counter the risk of acque alte invasion through the three entry doors (quite possible, if the gates are not correctly closed), a perimeter trough was excavated, below the floor, with the appropriate drainage slope, connected through ball valves to two external, waterproof wells. The liquids that might seep inside can therefore be collected through grids next to the doors and the ground joints of the perimeter brickwork, and expelled by primed pumps.

3 The draining systems

The second system used to knockout the tidal invasions, that is, the laying of an underfloor draining system, has been in use only for a couple of decades.

Saccardo, the proto of Saint Mark's basilica from 1881, can be considered a distant pioneer of this method, as he, in order to keep the crypt free from water, installed a rudimentary pumping system⁶. About a century later, the idea was perfected and developed by Mr Francalancia, engineer, as one alternative solution to the intervention that was later carried out in the Church of San Donato di Murano. The system is based on a very simple principle: in the event of high tides, once the access doors have been closed with mobile gates, the drainpipes have been intercepted, water gradually seeping in from the ground inside the building is intercepted by a network of underfloor drainpipes, channelled into appropriate wells and later eliminated through a pumping system. The localized depression of the surface water table obtained by draining water at a lower level than the ground floor level keeps the inside of the building dry.

This system, apparently banal, seemingly requires less onerous works than the installation of underfloor concrete tanks, but it actually entails a considerable body of cautions and operating instructions. In fact, water pumping might, in the long run, give rise to dangerous instability events: in the absence of specific measures, the aspiration of liquids would entail the elimination also of solid particles, with a consequent progressive impoverishment of the ground's mechanical characteristics and foundation collapse. The provided geotextile protections and the general composition of the draining strata, that have the task of intercepting and blocking the solid materials that make up the ground, the dimensions and layout of the draining network, the definition of the number of pumps to be installed must be preceded by an essential prevention campaign, made up of geognostic and hydraulic tests and analyses aiming at, on the one hand, at obtaining every possible information on the composition and characteristics of the ground, and, on the other hand, at developing answers to the tide ranges of surface waters inside the building.

In Ca' Pesaro, first instance of this, with a through-portego flooring at slightly more than 70 centimetres above average sea level, a maximum defence level corresponding to a high tide of +1.70 above average sea level was assumed. The axis of the drainpipes network was set at about 40 centimetres below such flooring, corresponding to a level of + 30 cm above average sea level, with a maximum drop in water level between inside and outside of 1.40 metres.

⁶ With regard to this, please consult: Pietro SACCARDO, *I restauri della Basilica di San Marco nell'ultimo decennio*, Venice 1890, page 25.

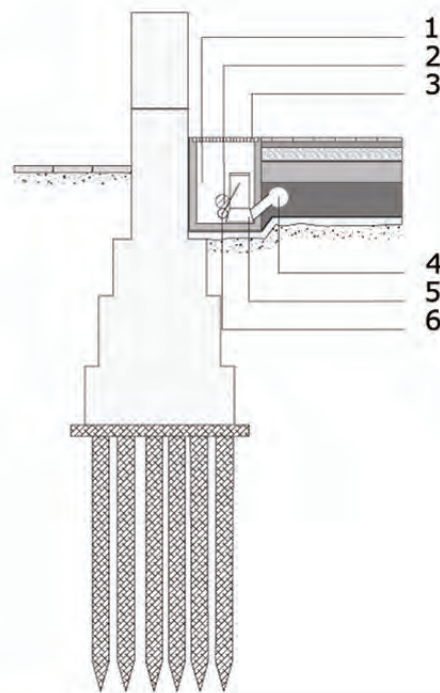


Figure 5 - Cà Pesaro: diagram representing the draining system installed on the building's ground floor (Legend - 1. DETAILS SECTION BB, 2. Concrete well (52x52x66 cm), 3. Water drainpipe (d=10 cm), 4. Grid, 5. PVC drainpipe (d=14 cm), 6. Pump float).

The realisation of this system required, initially, the prior plastering of joints, cracks and discontinuities on the wall faces, together with the implementation of the *scuci-cuci* method of patching on the perimeter walls, so as to create a virtually waterproof diaphragm and obtain the maximum possible reduction of the water flow rate through the vertical walls, followed by removal of the stone floors, sometimes quite complex ones, and of the underlying ground. On a sand bed, a geotextile mat was laid, to avoid transportation of solids due to the infiltration modalities from the outside. Then, the draining stratum was formed, contained within a gravel layer, through laying of a PVC pipes network, where the pipes are dotted with microholes, to allow water to seep in, and protected by a nylon geotextile stocking, and converge into the wells that contain the pumps, equipped with check valves installed within each pump's delivery pipe (Figure 5). The restoration and laying back of floorings were the final phase of the work.

4 Effectiveness and compatibility assessment

The analysis of the works under consideration shows clearly that the choice of defence system to be adopted depends on a variety of factors and that there are several variables to be taken into account, also because of the peculiar construction characteristics of the Venetian buildings, that require a planning approach that takes into account individual peculiarities and structural behaviours of the Lagoon's buildings.

The factors that have the highest impact on the choice of a defence system depend first of all on the building's planimetric system, on its structural layout, on its architectural and formal layout, on the materials used in its building, on its collocation within the city plan, on the relationship with the surrounding buildings

and also on the ground floor levels – and, consequently, on the frequency of the floods that have occurred – on the quality of whole and surrounding grounds, on the configuration of the collection and elimination systems for rain waters and sewage, on the presence of archaeological findings in the area, on the kind of user and use of the building itself. The organization and logistics of the worksite, too, have a sensible influence on the choice to be made, and so do the duration and cost of the intervention.

It is therefore impossible to decide, abstractly, which of the technical solutions described until now is the best one; the current research, however, seems to show that the draining systems evidence a higher degree of compatibility with the construction characteristics of lagoon building. This system, recently experimented with, seems, for the moment, more easily applicable in less critical cases, that is to say, in those situations in which the ground floor floorings seem to be relatively high in level and, therefore, seem to evidence only occasional instances of acqua alta, of floodings that are relatively reduced in scope and duration.

These limitations notwithstanding, however, this type of approach appears to be particularly appropriate if the intrinsic advantages of the system are taken into account, namely, reduced intrusiveness, relative simplicity of realisation and of cost containment.

References

BISCONTIN Guido, RIVA Gianna, ZAGO Franco, 1983. Caratteristiche fisiche, chimiche e meccaniche della struttura muraria, in “Bollettino d’Arte del MBCA”, supple–mento n° 5, 43–50.

BOZZONI Carlo, 1981. Refettorio d’Estate dell’ex convento dei Frari, ora Archivio di Stato, in G. CARBONARA (a cura di), *Restauro e cemento in architettura*, Roma, 102–105.

CALOI Lucia, CASSOLI Pierfrancesco, PALOMBO Maria Rita, 1983, Ritrovamento di resti ossei, in “Bollettino d’Arte del MBCA”, supple–mento n° 5, 60– 62.

CAVAZZANA ROMANELLI Francesca, 1983. Storia e restauri. Il restauro del Refettorio d’Estate nel convento dei Frari a Venezia ora sede dell’Archivio di Stato, in “Bollettino d’Arte del MBCA”, supple–mento n° 5, 13–32.

DE MIN Maurizia, 1983. Vicende del ritrovamento: classificazione, cronologia e tipologia delle ceramiche, in “Bollettino d’Arte del MBCA”, supple–mento n° 5, 55–59.

FORLATI Ferdinando, 1970. Il restauro del chiostro di S. Apollonia a Venezia, in “Palladio. Rivista di storia dell’architettura e restauro”, anno X, n° I-IV, 48-49.

FRANCALANCIA Jolando, 1970. Il restauro del complesso storico architettonico di S. Apollonia – Venezia, I.T.E, Venezia.

PIANA Mario, 1983. Lavori di consolidamento e restauro. Il restauro del

Refettorio d'Estate nel convento dei Frari a Venezia ora sede dell'Archivio di Stato, in "Bollettino d'Arte del MBCA", supplemento n° 5, 35–42.

PIANA Mario, 1987. Il Refettorio d'Estate nel Convento dei Frari, in *Venti anni di restauri a Venezia*, Roma, 83–91.

SACCARDO Pietro, 1890. *I restauri della Basilica di San Marco nell'ultimo decennio*, Venezia.

SCARPA Pietro, 1983. Ceramiche veneziane sotto le antiche pavimentazioni soprastanti le volte, in "Bollettino d'Arte del MBCA", supplemento n° 5, 51–53.

THE PLASTER CATALOGUE: COMMENTS ON THE RESULTS OF THE RESEARCH

Alessandra Ferrighi¹

¹ *Dipartimento di Storia dell'Architettura, Università Iuav di Venezia*

Riassunto

Tracciare un bilancio sulla catalogazione degli intonaci esterni del centro storico della città di Venezia significa inevitabilmente ripercorrere questi anni di ricerca da due angolazioni differenti. Da un lato la formazione dei rilevatori, la predisposizione dei materiali, i sopralluoghi ed il rilievo a tappeto sul campo, l'informatizzazione dei dati, le verifiche e gli aggiustamenti alla struttura delle banche dati. Dall'altro lato l'interpretazione dei dati e la possibilità di renderli fattivamente utilizzabili anche da altri soggetti.

La costruzione dell'abaco degli intonaci storici rilevati consente una precisa lettura delle varietà dei tipi morfologici, pur nella permanenza delle classi individuate secondo una categorizzazione cronotipologica (le quattro classi delle Stabiliture, degli Affreschi, dei Marmorini e degli intonaci della tradizione locale).

Rispetto all'iniziale stato delle conoscenze sono stati rivisitati alcuni intervalli temporali delle classi; sono stati messi in rilievo i dati dei diversi trattamenti delle facciate principali rispetto alle laterali o secondarie; si sono in parte definite le percentuali sulle permanenze degli intonaci storici rispetto alla totalità dei trattamenti sulle superfici esterne. Anche se le conclusioni della ricerca si possono oggi solo tratteggiare, si può già affermare che l'obiettivo iniziale, lo studio e la comprensione del "volto della città storica", è stato pienamente perseguito.

Abstract

Drawing conclusions on the cataloguing of external plasters in Venice's historic centre means, inevitably, reviewing the research of these years from two different points of view. It is necessary to consider, on the one hand, the training of surveyors, the preparation of materials, the inspections and sweeping field surveys, computerised data processing, data bank structure checks and adjustments, and, on the other hand, data interpretation and the possibility of actually making data usable by third parties.

The creation of an abacus of the surveyed historic plasters makes it possible to give a precise reading of the variety of morphological types, always within the various classes, identified according to a chrono-typological categorisation (the four classes of Skim coats, Frescoes, Marmorinos and local traditional plasters).

As against the initial level of knowledge, a review was made of some time intervals with regard to the various classes; data on the different treatments of

the main façades, as compared to the lateral or secondary ones, were highlighted; it has been possible to define, in part, the permanence of historic plasters as a percentage of the total external surface treatments. Even though the results of the research can still only be outlined, it is already possible to maintain that the initial goal, namely, the study and understanding of the “face of the historical city”, has been fully attained.

1 The permanence of materials

There are more than one hundred islands constituting Venice’s historical centre. Of these, only some ten or so were developed in the 19th and 20th centuries, within the context of a productive expansion and modernization of the city – such as the new residential neighbourhoods in S. Elena, Sacca Fisola and the changes linked to the railways, and later, car connection with the mainland. The Giudecca islands’ waterfront itself was developed recently, in comparison with the thousand-year history of building in this Lagoon’s city.

The gothic and modern era city, the one built before the changes that took place since the end of the XVIII century, is characterized by continuous building activities on the city’s real estate. The works also included new developments, of course, but they were mainly concerned with the alteration of existing structures, such as elevations, additions, façade renovations and so on. It is these activities that eventually would give birth to the image of the modern city of Venice. The exterior views of the buildings become the vehicle and support of the finishings, that are stratified layer by successive layer, thus changing the colours and shapes of the urban skin.

This research highlighted the changes in the outer surfaces, that, as any other part of a building, change not because they are substituted, but rather because they adapt: Indeed, they used to lay new plasters over the existing ones, simply by “tapping” them on. It is quite common to find marmorino plasters laid over already plastered walls, with thin finishing layers according to the gothic tradition; or to find simple lime and sand mortars layered over previous, more ancient strata with a similar composition.

Thanks to this tradition, many of the material traces are still preserved today, even though maybe somehow hidden under more recent layers. Catalogue data take into account all the peculiarities of this method of work, by continuous adjustments, and create links between the reports on the layers.

Table 1. Total architectural units on the Historical centre islands included in the research.

Identified AUs (identified AUs and partially identified AUs)	13.674
Unidentifiable AUs	1.572
Total AUs identified in the studied islands	15.246

The study, carried out on more than 15,200 architectural units, includes 10.5% of unidentifiable units. The remaining units, numbering slightly more than 13,600, are the buildings studied by the surveyors (Table 1). For this reason,

the percentage of still visible so-called historical plasters must be related not to the total number of architectural units in the whole of the historic centre, but to the number of units actually included in the study. Such architectural units were studied also at a macroscopic level, to ascertain whether there were historical plasters belonging to the A- Skim coat, B-Fresco, C-Marmorino and D-common plaster classes, included in the XIV-XIX centuries time frame.

Identified AUs	6.028
Partially identified AUs	7.646
Total AUs studied and analysed	13.674

Table 2. Architectural units actually studied

The permanence of materials data must take into account also the percentage of architectural units that were only partially studied, because parts of the external façades abutted onto light wells or private courtyards. Indeed, slightly less than half of these units - 44% - could be completely analysed, while from the remaining 56% those abutting onto private courtyards or onto nearby spaces that were impossible to reach from the public areas (Table 2).

The calculation of the number of still preserved historic plasters cannot overlook these considerations. On the contrary, the type of urban planning and the organization of public areas, or their dimensions, as compared with private open spaces, were factors that strongly influenced the possibility of collecting useful information for the survey. For this very reason the percentages linked to the surveyed units and those linked to units that could not be surveyed change for each sestiere and for each island. The two sestieri – S. Marco and S. Polo – with the highest building density, compared to their area, that include trade buildings and urban sectors formed by the union of buildings without private courtyards or gardens, offered more surveyable fronts, so much so that only 4-5% of their architectural units was impossible to survey, as against 23% in the Giudecca islands, that lower the percentage of the Dorsoduro sestiere from 15 to 12%.

Sestiere	Total AUs	Surveyed AUs	AUs unsurveyed	% of surveyed AUs
Cannaregio	3.730	3.390	340	91 %
Castello	3.624	3.197	427	88 %
Dorsoduro	3.340	2.832	508	85 %
S. Croce	1.455	1.308	147	90 %
S. Marco	1.903	1.818	85	96 %
S. Polo	1.194	1.129	65	95 %
Total	15.246	13.674	1.572	90 %

Table 3. AU divided by sestiere, with the percentage of surveyed AUs

The plasters included into the two general categories of “historic plasters” (XIV-XIX century) and “non-historic” (XX-XXI century) do not constitute the total of external coatings. The class defined as “F-Other” , which includes both stone and brick coatings and coatings that were removed and any other kind of coating, identified on a case by case basis, represents 16% of total coatings. It must be added, however, that they do not always concern the whole façade, but only part of it: often, the brickwork facing is to be found in the lower areas of the building, where the deteriorated part of the masonry was removed, using a scuci-cuci method of patching and subsequently, letting them remain exposed. The same applies to the stone coating that sometimes concerns only the ground floor or the first few floors. In both the abovementioned examples, the façades may present plasters in their upper parts.

Table 4. Plasters divided into the two categories of historic and non historic plasters

Historic plasters (XIV-XIX centuries)	2.745	18%
Plasters (XX- XXI centuries)	12.493	82%
Total	15.238	

There are many buildings whose external surfaces were completely renovated and no longer show any trace of the former treatments. These cases concern mainly the maintenance actions carried out in the last few decades and that led to the complete elimination of the original plasters, the subsequent cleaning of the joints and to a new layer of thick cementitious mortar. The first category (historic plasters) represents only 18% of the total or surveyed plasters (Table 4).

Other remarks can be made in connection with the permanence of data of each class of historic plasters (Graph 1), Traditional plasters, those with lime and sand mortar, prevail, constituting slightly more than half of all historic plasters, both because they are more recent and because they concern residential buildings. The greatest number of buildings, after this, is represented by buildings with Marmorino plasters, that were better preserved thanks to their dissemination throughout the Lagoon city, starting from the second half of the XV century. They represent about 30% of the surveyed buildings and include both single-layer (those created with stone dust or ground cotto, in a single layer) and double layer (that is, with a ground cotto preparatory layer) plasters. The more ancient coatings, the so-called *regalzier*, and the pictorial layers amount to slightly more than 16%. this is quite significant, given the extremely reduced thickness of these coatings and the time in which they were created, even though, in most cases, it is simply a matter of traces. The best preserved ones in this category are located under the porticoes of buildings such as the Palazzo dei Dieci Savi, in Rialto.

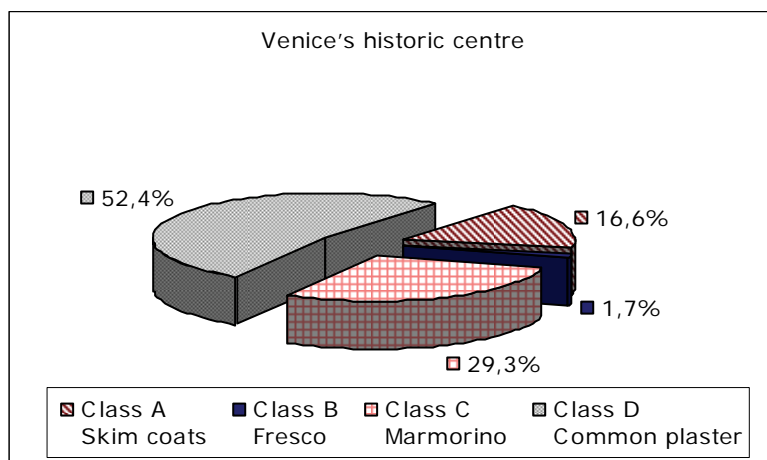


Figure 1. Historic plasters divided by class.

The table on plasters divided by class (Table 5) includes all data concerning the surveyed façades, including all the external coatings. This means that they do not correspond to the architectural units, as, very often, each architectural unit shows the simultaneous presence of several plasters.

Sestiere	Class A Skim coats	Class B Fresco	Class C Marmorino	Class D Common plaster	Total Plasters
Cannaregio	122	10	175	253	560
Castello	106	4	209	501	820
Dorsoduro	40	6	97	198	341
S. Croce	42	2	82	115	241
S. Marco	92	10	144	282	528
S. Polo	54	15	96	90	255
Total	456	47	803	1.439	2.745

Table 5. Historic plasters divided by class and by sestiere.

If data from sample diagrams or from diagrams representing the macroscopic study of historic plaster layers are analysed, percentages drop, because this kind of information is strictly linked to those individual cases that were studied in more detail. As against the total of surveyed units, the architectural units surveyed from a macroscopic point of view that have historic plasters represent about 12%, with a range going from 17.1% in the S. Marco sestiere, to 5.7% in the Giudecca.

Table 6. Sestieri and Aus taken from the plasters database, with the percentage of Aus showing surveyed historic plasters as against the total number of Aus present.

Sestiere	Total AUs	AUs surveyed	AUs with surveyed historic plasters	%
Cannaregio	3.730	3.390	333	9,8 %
Castello	3.624	3.197	375	11,7 %
Dorsoduro	2.351	2.072	202	9,7 %
Dorsoduro – Giudecca	989	760	43	5,7 %
S. Croce	1.455	1.308	169	12,9 %
S. Marco	1.903	1.818	296	16,3 %
S. Polo	1.194	1.129	193	17,1 %
Total	15.246	13.674	1.611	11,8 %

Table 6 includes all the units in the sestieri islands, including also the newly built ones. This number should be reduced by the units that belong to the latter islands, as just mentioned, being always aware of the city borders in the modern era.

In the data analysis, the range of percentages goes from a maximum concentration in the isle of San Zuane Laterano (CS075), with more than 50% of buildings still retaining their historic plasters, to values around 35% in the three isles of San Zuane Grisostomo (CN071), Megio (SC023) and Santa Maria Zobenigo (SM087), to around 25% for other seventeen isles, and, for the remaining isles, from 10% to a total absence of historic plasters, such as in the isle of Ghetto (CN011).

The distribution of historic plasters, notwithstanding the fact that data for the various sestieri are not very homogeneous, is still characterised by elements that unite the six different realities. Excluding from the start any analysis concerning the newly developed islands, it can be said with certainty that the buildings along the Canal Grande, whether they belong to S. Marco, Cannaregio or Dorsoduro, S. Polo or S. Croce were almost all renewed, in terms of façade finishings, repeatedly along the centuries. The same reasoning applies to the buildings abutting onto *campi*, *campielli* or *fondamenta*.

References

DANZI E, FERRIGHI A, PIANA M, CAMPOSTRINI P, DE ZORZI S, RINALDI E, 2005. Research for conservation of the Lagoon Building Culture: catalogue of the External Plasterwork in Venetian buildings, in "Flooding and Environmental Challenges for Venice and its Lagoon. State of Knowledge", Cambridge – UK, 193-198.

DE ZORZI S, FERRIGHI A, PIANA M, RINALDI E, 2004. Catalogue of Venice

External Plasterwork: Web Gis Tools, in "Scientific research and safeguarding of Venice", Venezia, 85-88.

FERRIGHI A, 2002. The plasters data base, in "Scientific research and safeguarding of Venice", Venezia, 97-10.

FERRIGHI A, 2004. The cataloguing of Venetian External Plasters: the progress of Research, in "Scientific research and safeguarding of Venice", Venezia, 79-83.

FERRIGHI A, PIANA M, 2004. Un GIS-Web per la catalogazione degli intonaci esterni veneziani, in www.storiaurbana.it/biennale/Relazioni/B9PIANA.doc

FERRIGHI A, PIANA M, 2007. Conoscere per conservare: il censimento degli intonaci esterni della città di Venezia, in "Conoscere per restaurare", Trento.

PIANA M, DANZI E, 2002. The Catalogue of Venetian External Plasters in Venetian Building, in "Scientific research and safeguarding of Venice", Venezia, 87-95.

PIANA M, DANZI E, 2004. The Catalogue of Venetian External Plasters: Medieval Plasters, in "Scientific research and safeguarding of Venice", Venezia, 65-77.

PIANA M, 2006. Marmorino Plasters in Venice between the XVI and XVIII centuries, in "Scientific research and safeguarding of Venice", Venezia, 71-90.

PIANA M, DANZI E, DE ZORZI S, FERRIGHI A, RINALDI E, 2003. Venezia organismi architettonici storici. Il censimento degli intonaci attraverso tecniche di rilievo e classificazione basata su strumenti GIS e WebGIS, in "Atti del convegno ASITA", Verona, <http://217.58.108.240/cartografia/eventi/7confNazAsita/cd/Pdf/FIN401.pdf>

EXPERIMENTAL TESTS FOR THE STUDY OF THE STRUCTURAL BEHAVIOUR OF THE DAMAGED VENETIAN BUILDINGS

Paolo Faccio¹, Donato Chiffi¹, Alessia Vanin¹

¹ *Dipartimento di Costruzione dell'Architettura, Università IUAV di Venezia*

Riassunto

La continua interazione con l'ambiente lagunare pone seri problemi alla conservazione degli edifici storici Veneziani. L'alterazione dell'originaria consistenza materica degli elementi strutturali comporta sia una modifica dell'immagine architettonica sia una modifica del funzionamento strutturale.

Prove sperimentali sono state svolte su due prototipi semplificati del sistema muro-solaio veneziano realizzati in laboratorio con dimensioni prossime a quelle reali. Nel corso delle prove i prototipi sono stati progressivamente danneggiati per riprodurre il degrado degli elementi strutturali e delle relative connessioni.

E' stato analizzato il comportamento strutturale dei solai in legno e dei paramenti murari sottoposti all'azione di carichi verticali distribuiti e concentrati al crescere del danneggiamento.

Sono qui presentati i risultati dei test sperimentali.

Abstract

The continuous interaction with the aggressive lagoon environment gives serious problems for the preservation of the historical Venetian buildings. Nowadays many buildings show a severe decay of their structures, that often implies not only an alteration of their architectural image, but also a significant modification of their structural behaviour.

Experimental tests were performed on two specimens that reproduced the system masonry walls-Venetian wooden floors without any significant scale effect. During the tests these specimens were progressively damaged, in order to simulate the decay of the structural elements and of their connections. They were loaded with distributed and concentrated vertical loads.

The structural behaviour of the wooden floors and of the masonry walls at the increasing of the damage was investigated.

The results of the experimental tests are here presented.

1 Introduction

It is well known that the building process of the historical Venetian buildings was strictly conditioned by the singular environmental circumstances. The scarce load-bearing capacity of the foundation ground and the interaction with the lagoon water imposed the adoption of specific technical solutions, in order to

preserve the integrity of the structures and to guarantee the efficacy of the structural functioning of the buildings [Piana 1984, 2000].

Despite the efficacy of these technical solutions nowadays many buildings show a severe decay of their structures, partially due to the natural ageing, partially to the modification of the environmental circumstances over the centuries.

In particular the direct contact with the lagoon-water resulting from the increase of the sea level caused the wash of the mortar joints of the brick-walls facing the canals, and sometimes a significant reduction of their thickness. In this way the rising-damp was emphasized, so that the wooden beams of the first floors often show a severe damage of their heads. In some cases also the connection between the orthogonal walls becomes inefficient, because of the oxidization of the tie rods due to the driving rain [Chiffi, Faccio and Vanin, 2006].

All these alterations provoked a progressive modification of the original structural functioning, with possible severe consequences for the complex equilibrium of the buildings [Zuccolo, 1975].

An experimental program was made to evaluate the incidence of the described alterations on the structural safety of the historical Venetian buildings.

This paper presents the first results of experimental tests performed on two specimens, through which we tried to simulate, in simplified way, the condition of the historical Venetian buildings with some of the described problems.

2 Object of the experiments

Two simplified models of the system masonry walls-Venetian wooden floors were defined. The geometrical shape of these specimens was conceived so that they can reproduce the system of the ground and first floor of the historical Venetian buildings preventing any significant scale effect (Fig. 1).

The masonry walls were built using UNI (ITALIAN standard) bricks, with a mortar prepared mixing equal proportion of sand, water and a binder comprising $\frac{3}{4}$ lime and $\frac{1}{4}$ Portland cement 325. The bricks were 25 by 12 by 5.5 centimetres. The mortar joints, made flush with the brick's face, were 1 centimetre thick.

The structure of the first floor was different for the two specimens, in order to reproduce the two types of floors that were more frequently employed in the historical Venetian houses (Fig. 2). In the specimen 1 it was built with wooden beams, on which a simple layer of wooden planks was nailed. In the specimen 2 a layer of "terrazzo" was arranged on the first layer of wooden planks.

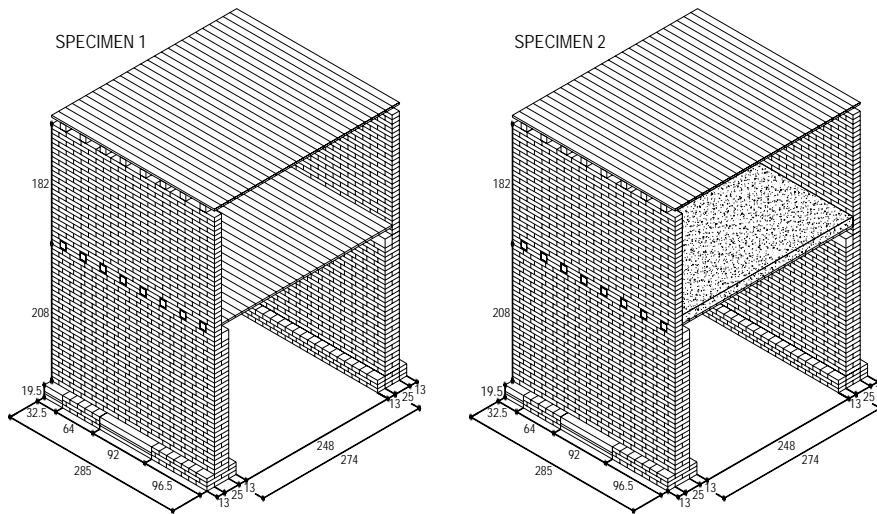


Figure 1. Geometrical shape of the two specimens

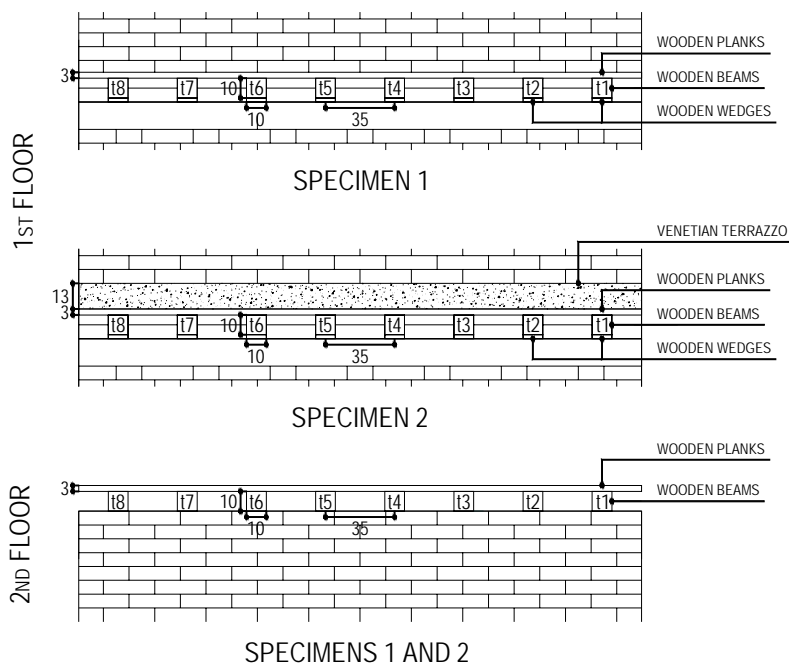


Figure 2. Structure of the floors of the two specimens

It was composed by three layers: the “sottofondo”, 10 centimetres thick, the “coprifondo”, 2 centimetres thick, and the “stabilitura”, only 1 centimetres thick. These layers were built with the composition shown in Table 1 [Crovato, 1989].

Table 1. Composition of the "terrazzo"

Sottofondo		Coprifondo		Stabilitura	
Slaked lime	Crushed bricks and tiles	Slaked lime	Powdered bricks	Slaked lime	Marble chips
kg/m ²	kg/m ²	kg/m ²	kg/m ²	kg/m ²	kg/m ²
40	160	10	30	10	10

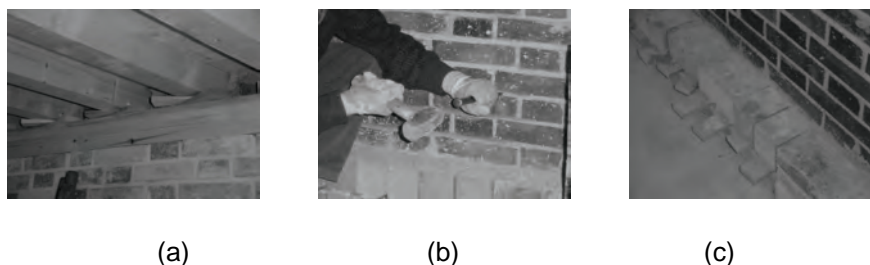
The structure of the second floor was the same for the two specimens. It was built with wooden beams on which a layer of wooden planks was nailed (Fig. 2).

These specimens were conceived so that they can be modified in order to simulate the described alterations of the material consistency of the structural elements and of their connections.

For this reason the beams of the first floor were put on wooden planks with the interposition of some wooden wedges (Fig. 3a). These wedges could be removed in order to simulate the reduction of the contact with the wall, when the rising damp provokes the decay of the heads of the wooden beams. On the contrary the beams of the second floor were simply put on the walls. Moreover one of the two bases of the walls of each specimen was partially built with bricks, partially with wooden planks and parts of wooden beams, with the interposition of wooden wedges under the beginning of the wall (Fig. 3b). These wedges can be removed in order to simulate a sinking of the foundation ground at the centre and at the end of the wall.

In correspondence of the same wall the horizontal and vertical mortar joints of the first seven courses were partially removed at the beginning of the experimental tests for a depth of five or six centimetres (Fig 3c), in order to simulate the wash due to the lagoon water.

Figure 3. Particulars of the structure of the two specimens"



The main goals of the experimental program were:

- the evaluation of the behaviour of the first floor built with and without the layer of terrazzo subjected to distributed and concentrated loads, at varying of the contact area between the heads of the wooden beams

and the wall;

- the evaluation of the distribution of the compression stress at the base of the masonry walls with respect to these changes of the contact area and when some vertical sinkings of the foundation ground appear at the base.

3 Experimental program

The experimental program is articulated into four steps, that were equally performed on the two specimens. The first floor of the two specimens was loaded with distributed and concentrated vertical loads. During the steps the structure of the specimens was progressively modified. The inflection of the beams and the crushing of the masonry wall were measured with continuity.

The steps are synthetically described, specifying for each of these the modifications of the structure of the specimens and the loading conditions:

- 1st step: structure in the original condition, distributed load increased from 1 to 3 kN/m², concentrated force keep equal to 0 kN;
- 2nd step: structure in the original condition, distributed load keep equal to 3 kN/m², concentrated force increased from 0 to 20 kN;
- 3rd step: removal of the two wedges supporting the two central beams of the first floor, distributed load keep equal to 3 kN/m², concentrated force increased from 0 to 20 kN;
- 4th step: Removal of the foundation beams distributed load keep equal to 3 kN/m², concentrated force increased from 0 to 20 kN.

The applied loads, and in particular the concentrated force, are increased until a value that avoids the failure of the wooden beams. On the contrary it is to note that the applied loads are very low in order to produce even a little a damage of the masonry walls.

4 Test set-up

The first floor of both the specimens was loaded with distributed and concentrated loads.

The distributed loads were produced with sacks of sand placed at the top of the first floor.

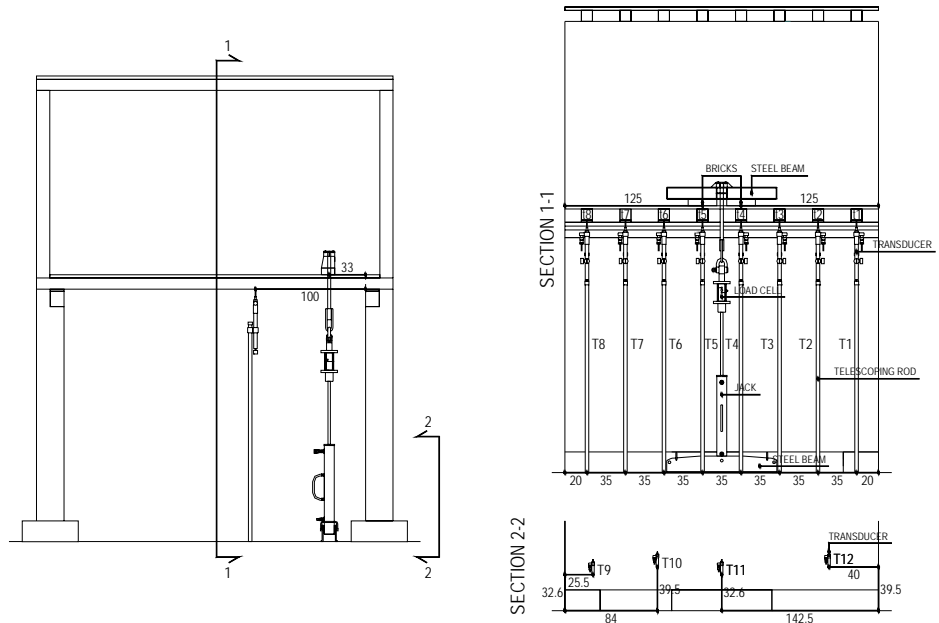
The concentrated load was applied by means of an hydraulic jack, in decentralized position with respect to the vertical axis of the structure (Fig. 4). This jack was fixed at its base to a steel beam connected to the floor of the laboratory with chemical plugs. At the top it crossed the wooden planks of the first floor preliminarily drilled, and it was fixed to a second steel beams. Two bricks were placed between this second steel beam and the top layer of the floor in correspondence of the two central wooden beams, in order to localise the force generated by the jack.

A load cell capable of measuring the applied force was connected to the jack

(Fig. 4).

Eight differential transducers mounted on telescoping rods were placed at the intrados of the first floor, to measure the inflection of the wooden beams. Four differential transducers were placed at the base of the wall, to measure the crushing of the masonry, too (Fig. 4).

Figure 4. Experimental set-up



All the measuring equipment was connected to a data acquisition system, that both controlled the rate of application of the concentrated load and the required loading steps, and also recorded the readings from the measuring instruments evaluating them and converting them into graphs.

5 Experimental results

Given the very limited number of the specimens involved in the tests some considerations must be made with reference to both the purposes of the trial and the validity of the obtained results. The aim of the tests was not to determine precise values for the lowerings of the wooden beams and of the masonry walls at each step, but rather to establish indicative values and behavioural tendencies. The value of the tests is consequently in comparative terms.

5.1 Wooden floors

The comparison of the results obtained in the steps 1 and 2 for the specimen 1 (Fig. 5a,b) shows that the inflection of the central beams increases a lot in consequence of the application of the concentrated load, whereas the lowering of the lateral ones remains practically unchanged.

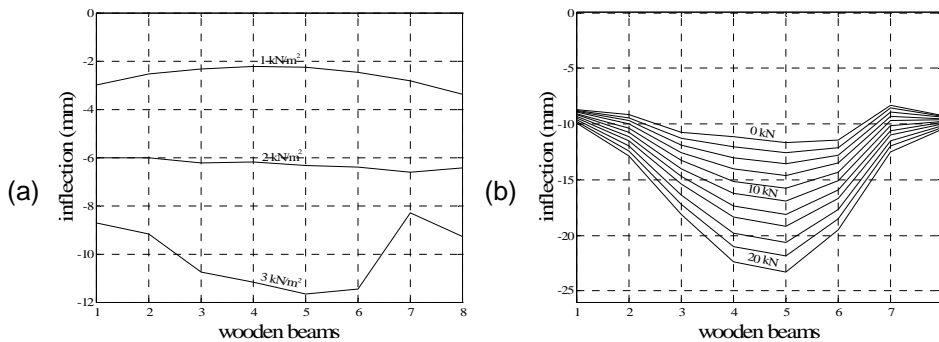


Figure 5. Inflection of the wooden beams of the specimen 1 in the step 1 (a) and 2 (b) at varying of the distributed (step 1) and concentrated loads (step 2)

For example, the inflection of the beam 5 at the step 1 with a distributed load of 3 kN/m² is equal to 11.65 mm, while at the step 2, when both a distributed load of 3 kN/m² and a concentrated load of 20 kN are applied, it is equal to 23.32 mm. Therefore the increase of the inflection in consequence of the application of the concentrated load is equal to 11.67 mm. On the contrary, the inflection of the beam 1 at the step 1 with a distributed load of 3 kN/m² is equal to 8.71 mm, while at the step 2, when both a distributed load of 3 kN/m² and a concentrated load of 20 kN are applied, it is equal to 9.93 mm. Therefore in this case the increase of the inflection in consequence of the application of the concentrated load is equal to 1.22 mm.

The comparison of the results obtained in the steps 1 and 2 for the specimen 2 (Fig. 6a,b) shows that the lowerings of the central and lateral beams are comparable not only for a distributed load, but also for a concentrated load.

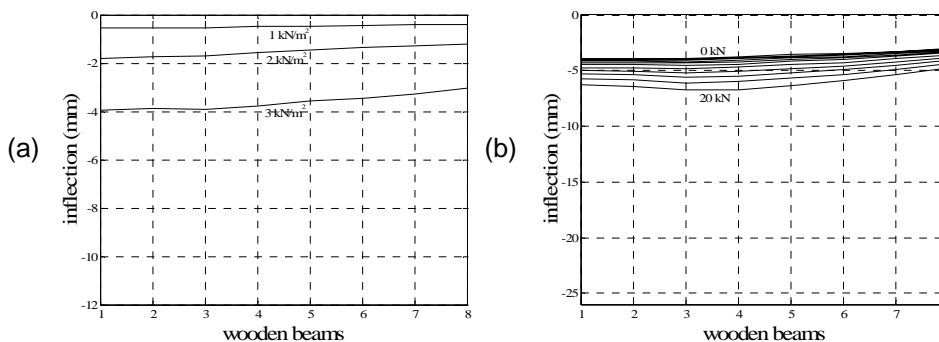


Figure 6. Inflection of the wooden beams of the specimen 2 in the step 1 (a) and 2 (b) at varying of the distributed (step 1) and concentrated loads (step 2).

For example, the inflection of the beams 5 at the step 1 with a distributed load of 3 kN/m² is equal to 3.56 mm, while at the step 2, when both a distributed load of 3 kN/m² and a concentrated load of 20 kN are applied, it is equal to 6.33 mm. Therefore the increase of the inflection in consequence of the application of the concentrated load is equal to 2.77 mm.

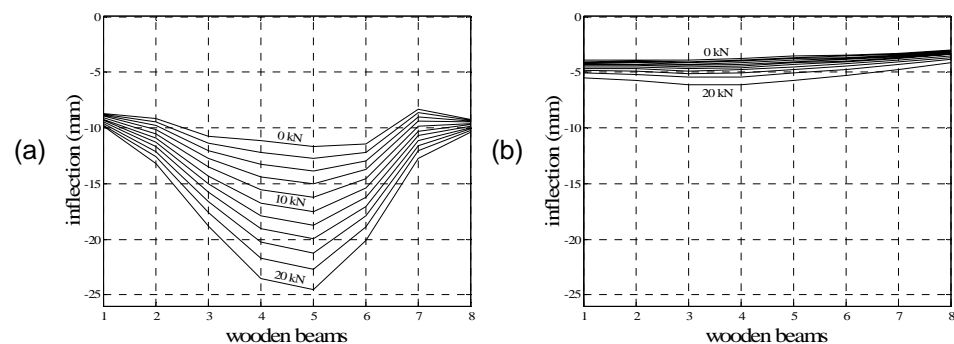
In a similar way the inflection of the beam 1 at the step 1 with the distributed load of 3 kN/m² is equal to 3.95 mm, while at the step 2, when both the distributed load of 3 kN/m² and the concentrated load of 20 kN are applied, it is equal to 6.24 mm. Therefore the increase of the inflection in consequence of the application of the concentrated load is equal to 2.29 mm.

These results indicate that, in the case of the specimen 1, the central beams,

that directly support the concentrated force, cannot benefit of the collaboration of the lateral ones, because the wooden planks are not capable to distribute this load so that all the wooden beams equally contribute to support it. On the opposite, in the case of the specimen 2, the layer of terrazzo permits this distribution along the development of the wooden floor, so that all the wooden beams contribute to the load-bearing function at the same way.

The results obtained for the two specimens at the step 3 (Fig. 7a,b) show that the removal of the wooden wedges supporting the central beams doesn't modify this behaviour of the two floors.

Figure 6. Inflection of the wooden beams of the two specimens in the step 3 for the specimen 1(a) and 2 (b)



In fact the inflection of the central and lateral wooden beams of the specimen 1 at the increasing of the concentrated load is slightly greater than those recorded at the step 2, but the deformed shape of the wooden floor remains the same. The inflection of the central and lateral wooden beams of the specimen 2 is practically unchanged with respect to this recorded at the step 2, so that even in this case the deformed shape of the wooden floor remains the same.

We can conclude that even with a reduction of the contact area of the wooden beams directly loaded from the concentrated load with the wall, no significant variations characterize the functioning of the two floors. In the case of the specimen 1 the existing concentration of the vertical force is only emphasized, while in the case of the specimen 2 the terrazzo continues to ensure the original collaboration among the wooden beams. In second way, the comparison of the inflection values of the wooden beams of the two specimens shows a substantial difference: the values obtained for the specimen 1 are always greater than those obtained for the specimen 2, under the same load conditions.

This fact doesn't seem comprehensible because the two specimens were built with the same geometry and the wooden beams were equally arranged on the two walls. In second way it doesn't seem comprehensible because the weight of the floor of the specimen 2 is greater than that of the floor of the specimen 1, so that even if the external load conditions are the same for the two specimens, the beams of the specimen 2 are more stressed those of the specimen 1.

The experimental values of the inflection of the wooden beams for the specimen 1 show that they can be modelled as double-supported beams, stressed by distributed and concentrated loads.

For example, the experimental value of the inflection of the beam 5 for a distributed load of 3 kN/m² is equal to 11.65 mm, while the theoretical value in the described boundary conditions is equal to 11.60 cm (Young modulus of the wooden beams equal to 13000 N/mm²). This correspondence between the experimental and the theoretical values validates the expressed hypothesis on the boundary conditions, and indicates that the masonry walls at the first floor exert only a weak joint action on the wooden beams.

The same boundary conditions characterize the wooden beams of the specimen 2, because they were equally arranged on the two walls. So we can conclude that the different values of their inflection are probably due to a collaboration of the layer of terrazzo in the load-bearing function of the wooden floor. In other words it behaves not only as a load, but also as a resistant element of the structural section of the wooden floor. This collaboration is not justified from a mechanical connection between the beams and the layer of terrazzo, but its structural effects on the behaviour of the wooden beams are clear.

The experimental value of the lowering of the beam 5 for a distributed load of 3 kN/m² is equal to 3.56 mm. We can suppose that this load is really supported by the wooden beam and by the share of the terrazzo put on its top. The share of the terrazzo increases the inertial properties of the floor, so that the inflection of the floor in correspondence of the beam 5 can be calculated supposing a resistant element, that is a beam, with a section constituted by two not connected parts, one of wood and the other of terrazzo. In this hypothesis the value of the lowering is equal to 4.11 mm (Young modulus of the terrazzo equal to 5000 N/mm²). The two values are rather near, so that the expressed hypothesis can be confirmed.

5.2 Masonry walls

The stresses that derive to the masonry walls in consequence of the applied loads are very small, so that the consequent deformations are very limited. Yet the comparison of the values of the lowerings recorded in the four steps, shown in Tables 2 and 3, permits to appreciate the distribution of the vertical loads transferred from the wooden floor at varying of the contact area with the wooden beams and at varying of the boundary condition of the walls at the base.

	Load	Lowerings for the wall of the specimen 1				Lowerings for the wall of the specimen 2			
		T 9	T 10	T 11	T 12	T 9	T 10	T 11	T 12
	kN/m ²	mm				mm			
Step 1	1	0	0	0	0	0	0	0	0
	2	0	0	0	0	0	0	0	0
	3	0.01	0.01	0.01	0.01	0.01	0.01	0.01	0.01

Table 2. Experimental results for the masonry wall for the step 1

	Load	Lowerings for the wall of the specimen 1				Lowerings for the wall of the specimen 2			
	kN	T 9	T 10	T 11	T 12	T 9	T 10	T 11	T 12
		mm				mm			
Step 2	10	0.01	0.02	0.02	0.02	0.01	0.02	0.02	0.01
	20	0.02	0.02	0.03	0.02	0.02	0.02	0.02	0.02
Step 3	10	0.01	0.02	0.02	0.02	0.01	0.02	0.02	0.01
	20	0.02	0.02	0.03	0.02	0.02	0.02	0.02	0.02
Step 4	10	0.01	0.02	0.02	0.01	0.01	0.02	0.04	0.01
	20	0.01	0.04	0.04	0.01	0.02	0.05	0.06	0.01

Table 3. Experimental results for the masonry wall for the steps 2, 3 and 4

The results obtained for the two specimens in the steps 1 and 2 are coherent with the distribution of the distributed and concentrated loads shown from the discussed lowerings of the wooden beams of the two floors.

In both specimens the lowerings of the wooden beams subjected to a distributed load are very similar, with the only exception of the extreme beams, however stressed by a smaller load in consequence of their position. In same way the recorded lowerings of the masonry walls have the same values, confirming the uniform distribution of the stress also on the base of the masonry walls.

On the contrary when the concentrated force is applied in addition to the distributed load, the lowerings of the wooden beams are different in the two specimens.

The increase of the lowering of the central beams with respect to the lateral ones that characterizes the specimen 1 is confirmed by the distribution of the lowerings of the wall at the base, where the transducer 3, that is positioned in the centre of the base of the wall, records a greater value of the lowering. In same way the uniform lowering of both the central and the lateral beams shown from the specimen 2 is confirmed by the distribution of the lowering of the wall at the base, where all the transducers still record the same value.

This correspondence between the lowerings of the wooden beams and of the masonry walls is shown also for the step 3, when the wedges that supported the central beams were removed.

With respect to the difference of the lowering values recorded for the wooden beams of the two specimens it is to note that no relevant difference exists between the lowering values recorded for the masonry walls. Nevertheless, given the very small values of the lowerings because of the limited load, it is possible that the difference was not appreciable from the transducers.

Finally the results of the step 4 for the two specimens evidence that a significant increase of the lowerings is given from the sinking of the foundation ground, simulated through the removal of the wedges and of the wooden beams at the base of the wall. In both specimens the transducers placed in correspondence of the removals record very big values of the lowerings with respect to those recorded from the other transducers.

Conclusions

Notwithstanding the increase of the loads on the vertical structures of the buildings the experimental results evidence the benefits to the structural functioning of the wooden floors due to the presence of the terrazzo.

On the one hand it permits the distribution of the vertical concentrated loads among the wooden beams of the floor, so that no significant difference appears among their deformations. This behaviour of the terrazzo is valid even when some wooden beams reduce their contact area with the wall, for example in consequence of the decay due to the rising damp. In this case the presence of the terrazzo keeps the functioning of the wooden floor unchanged, and therefore the distribution of the stress on the base of the masonry walls.

On the other hand the terrazzo increases not only the load of the wooden floors, but also its inertial properties, and in so doing it increases the load-bearing capacity of the floor and contains the inflection of the wooden beams.

Both the distribution of the vertical loads on the floors and the sinking of the foundation ground is reflected from the lowerings of the masonry walls at their base. In every case it will be necessary to massively increase the vertical loads or to introduce other modifications on the structural elements, as for example a significant reduction of the transversal section of the walls in order to appreciate the reduction of the structural safety of these.

Numerical models will be realized to make deeper the experimental results.

References

Chiffi D., Faccio P., Vanin A., 2006. Analysis of the structural behaviour of the historical Venetian buildings through theoretical and experimental models: state of the research. In Corila Research Program 2005 results, by P. Campostrini, Venezia.

Crovato A., 1989. I pavimenti alla veneziana. L'altra riva, Venezia.

Piana M., 1984. Accorgimenti costruttivi e sistemi statici dell'architettura veneziana, in "Dietro i palazzi; Tre secoli di architettura minore a Venezia 1492-1803", by G. Gianighian and P. Pavanini, Arsenale Editrice, Venezia.

Piana M., 2000. Note sulle tecniche murarie dei primi secoli dell'edilizia lagunare, in "L'architettura gotica veneziana: atti del Convegno Internazionale di studio. Venezia, 27-29 novembre 1996", by F. Valcanover and W. Wolters, Istituto Veneto di Scienze, Lettere ed Arti, Venezia.

Zuccolo G., 1975. Il restauro statico nell'architettura di Venezia. Istituto Veneto di Scienze Lettere ed Arti, Venezia

RESEARCH LINE 2.3

Methodologies and technologies for conservation and restoration of historical Venetian building

STUDIES ON BEHAVIOUR OF VENETIAN MASONRY MADE OF ALTINELLA BRICKS

Giulio Mirabella Roberti¹, Francesco Trovò¹, Michele Bondanelli¹, Stefano Cancelliere²

¹ *Università Iuav di Venezia, Dipartimento di Storia dell'Architettura*

² *Università Iuav di Venezia, Laboratorio Analisi Materiali Antichi*

Riassunto

In questo lavoro viene dapprima illustrato lo stato delle conoscenze attuali riguardanti un particolare tipo di mattone noto come altinella, caratterizzato da dimensioni molto ridotte, impiegato a Venezia dal XII al XIV secolo. Si sono in particolare evidenziate le informazioni relative al periodo di impiego, alle caratteristiche morfologiche, ai luoghi e alle tecniche di produzione e alla sua diffusione.

L'osservazione diretta di alcuni casi particolari ha quindi consentito di descrivere i modi di apparecchiatura muraria in altinelle ritenuti più diffusi, a cui possono essere associati peculiari vulnerabilità e modi di dissesto.

Sono state condotte osservazioni sull'impasto di circa 50 altinelle in modo da evidenziare alcuni parametri ricorrenti, come il grado di omogeneità e il colore.

Infine le analisi delle sezioni sottili di due campioni di altinelle, provenienti da Ca' Zusto a Santa Croce e da una casa nel sestiere di Castello, mostrano l'eterogeneità dell'impasto e danno informazioni di tipo minero-petrografico, anche in relazione ai processi di cottura, consentendo di associarle alle principali cause dei processi di alterazione materica.

Abstract

In the first part of this paper, the state of the art is recalled about altinella brick, which is a peculiar kind of brick used in Venice from XII to XIV century, with the main characteristic of very small dimensions. Then, some direct observations have been carried out about the blend of 50 different altinella bricks in order to highlight some recurring parameters linked to different degrees of homogeneity and color. Finally, thin section analysis have been performed of two altinella bricks, coming from Ca' Zusto in Santa Croce and from a house in Castello. They show the heterogeneity of the blend and give mineral-petrographic information, connected also to baking process, allowing to associate them to the main causes of the alteration processes.

1 Introduction

Except for lonely cases, historical Venetian buildings are made by bricks, whose constructive tradition lasts almost nine centuries. It is easy to understand that in a so long period the wide variety of bricks employed was the result of different evolutionary processes concerning architectonic, commercial and geographic

aspects. A qualitative observation of the bricks used in a wall allows to outline the correlations with the observed deterioration phenomena. From that point of view, the bricks would be no more classified solely with a dimensional approach: brick dimensions would only become a single parameter in a whole system of characters, including morpho-stylistic (texture, superficial and pointing treatment); archeometric and chemical-physical aspects. Studies conducted on alтинella bricks, started in the '80, are continued in that research with the aim of improving knowledge about the time extent of the usage of alтинella brick and the way these bricks were used. Another target of the research was also to understand how the small dimensions of alтинella brick, the bond adopted as well as the thickness of bedding mortar used in each layer can affect the structural behaviour of that masonry. Starting from the observation of the constitutive blend and from a series of tests, it is possible to describe physical and chemical characteristics of that kind of bricks, in order to detect the origin of the clay, the heterogeneity degree of the blend and the baking temperature used in the oven.

2 Alтинella bricks in Venice: notes from previous studies

The usage of alтинella bricks, which name come from the ancient roman center of Altino, was extremely important for its role in the passage from a wooden architecture to a stony one. This switch was probably triggered and catalyzed by the huge damages due to the XII century's great fires. Their usage is documented across all XIII cent until XIV, when alтинella bricks are associated with Romanic and gothic bricks¹. Alтинella bricks made in Venice are very similar to the roman ones, except for the passage from the roman unit of measure to the vulgar Venetian foot (34,773 cm)².

Until year 1200, in Venice "*There is a clear prevalence of wood (...), the town was a sort of wooden universe except for sporadic cases of buildings made of bricks (...)*". With the usage of clay and the increasing brick production "*the change was so extensive that the proportion was overturned in a period of one or two centuries*"³.

The first explicit reference to the term alтинella was made by Temanza in 1781 in his "*Dissertazione intorno ad una antichissima pianta dell'inclita città di Venezia*". He relates about the catastrophic fires that destroyed a large part of the city during XII century and he describes alтинella bricks with this words:

¹ Dorigo, W. , Venezia Romanica: la formazione della città medioevale fino all'età gotica, Venezia, 2002.

² Dorigo, Op. cit.

³ Piana, M., Note sulle tecniche murarie dei primi secoli dell'edilizia lagunare, in L'architettura gotica veneziana, Valcanover, F., Wolters, W., (a cura di) Atti del seminario dell' Istituto Veneto di scienze lettere ed arti –Venezia, 1996, Venezia, 2000.

“son’elleno di buona terra, ben cotta, ma di piccola mole (...) con siffatti modi dunque nel XII secolo fu murata quasi interamente la città di Venezia, la quale di giorno in giorno sorgeva più nobile e maestosa”⁴.

The first bricks used in Venice were probably taken away from roman buildings and reused, then they were produced in Venice and in the next hinterland. Between 1100 and 1200 there were not many furnaces in Venice, so it is possible that most of the demand for bricks was absorbed by the hinterland furnaces, as can be proved by the information about those acting in Torcello and Mestre from the beginning of XIV century. In Venice there are evidences about the existence of a kiln in San Gregorio since 1197 and in San Rocco. It is also possible that other kilns were active in the sestiere of Castello, which production was aimed to the great building works of the Arsenale. At the end of XIV century there was certainly a considerable number of Venetian kilns.

Giuseppe Tassini⁵, in his “*Curiosità veneziane*” relates that the production of bricks in Venice was strictly regulated by rules concerning brick’s size and shape, production procedures and clay baking techniques. Into “*Capitolari delle arti*”⁶, of 1229 and 1222 it is possible to find laws concernig production (*Capitulare de Fornesariis*) and commerce of bricks and lime (*numeratori e trasportatori*). There was a strict control on brick size, by means of official moulds and patterns that were exposed at Rialto.

Some recent mensio-chronologic studies outlined that the bricks used in Venice during nearly thousand years may range from very small dimensions (15 x 7 x 5 cm) to much bigger size (28 x 14 x 7 cm)⁷.

According to previous researches, the employment of *altinella* bricks began in XI century, but the duration of their use is not clear. In accordance to the study of W. Dorigo an important passage is linked to the famous deliberation of the XL council of Venice Republic in 1368, concerning brick’s prices, where officially the distinction is made among “*lapides cocti ad mensuram parvam*” (*altinella*

⁴ Fontana, V., Appunti sulle malte e i mattoni in uso nei cantieri veneziani del cinquecento da documenti e trattati dell’epoca, in *Il mattone di Venezia*, atti del convegno presso fondazione Cini, Venezia, 1979.

⁵ Tassini, G., *Curiosità veneziane*, ovvero origini delle denominazioni stradali di Venezia, prima edizione, Venezia, 1863.

⁶ Monticolo, G., (a cura di), *I capitolari delle Arti veneziane sottoposte alla Giustizia e poi alla Giustizia vecchia dalle origini al 1330, I capitolari delle Arti veneziane sottoposte alla Giustizia e poi alla Giustizia vecchia dalle origini al 1330*, Venezia, 1896.

⁷ Varosio F., a.a. 2000/2001. Tesi di Laurea in Rilievo e analisi tecnica dei monumenti antichi, relatore Ferrando I., correlatore Varaldo C., Mannoni T., Ricerca per una mensiocronologia dei laterizi a Venezia, Università degli studi di Genova, Facoltà di Lettere e Filosofia, Corso di Laurea in Conservazione di Beni Culturali, indirizzo archeologico, architettonico e per l’ambiente.

bricks) and “*lapides cocti ad mensuram magnam*” (bigger size bricks).

The period between the beginning of XIV century and 1368 was therefore a period of transition in which there is a coexistence of different kind of bricks. *Altinella* bricks were progressively abandoned and at the same time the usage increased of gothic bricks, which size was much bigger.

Studies of ecclesiastic constructions between XI and XIV century⁸ shows a large use of Venetian *altinella* from XI to XIII century. In a first period *altinella* bricks were probably taken from roman pavements, then they were produced in Venice and in the whole Venetian region. At the same time a new unit of measure, the “Venetian foot” (35 cm) started to spread. Bigger size bricks were requested for building foundations and for special works such as bell towers.

In some notarial acts, the thickness of medieval Venetian wall is described in terms of “foot” (2 *altinella* bricks joined by their longer side, 17,5 cm, measure one Venetian foot, 35 cm); and in terms of “one foot and a half” (2 gothic bricks joined for their longer side measure 52 cm, that is one Venetian foot and a half). It is possible that there was a constructional strategy that would make available the use of a thicker masonry, built on gothic bricks, for the walls with structural roles, and a thinner masonry, built by *altinella* bricks, for internal walls.

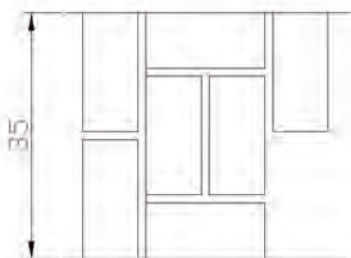


Fig. 1. Scheme of a brickwork made of *altinella* bricks (15 x 7 x 5 cm) with thickness corresponding to one Venetian foot.

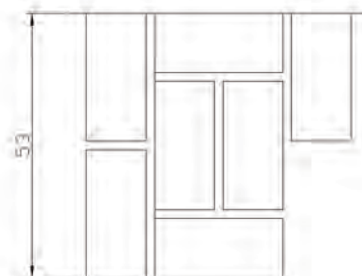


Fig. 2. Scheme of a brickwork made of gothic bricks (26 x 13 x 6 cm) with thickness of 53 cm, corresponding to one Venetian foot and a half. Gothic bricks are compatible with section thickness till 59 cm.

The passage from the dimension of one foot to one foot and a half, keeping and improving the practice of *duabis pietras*, comes with the 26-27 cm gothic bricks. If we admit to associate Venetian foot (35 cm) to the *altinella* masonry (as shown in Figure 1); and one foot and a half (52 cm and later 59) to the gothic bricks masonry (as shown in Figure 2), according to Dorigo, we find a confirmation of the tendency toward the *murus de duabis pietras*, wich is more

⁸ Dorigo, Op. cit.

practical and give a contribution to the progressive abandonment of small size bricks. These bricks needed a longer, and therefore not practical, masonry work, giving a layer thickness of about 69 cm, equivalent to two Venetian feet.

3 Observations on selected cases

Previous studies⁹ are a good starting point that allows us to focus on some not enough explored topics. Variations on size of *altinella* bricks and variation of their arrangement in the masonry layer would request a peculiar mensio-chronologic characterization for that kind of brick. An important aspect to be investigated concern the relationship between length and width of *altinella* bricks: in some cases dimensional relationships among the sides do not comply with the rule-of-thumb saying that the length corresponds to the double of the width plus the mortar joint thickness. So that there is not a clear link between the thickness of the mortar layer and brick dimensions, in a way that is similar to the roman *opus caementitium*.

A detailed analysis of the brickwork would allow to better distinguish at least 3 different characterizations concerning brickwork bond:

- the 3 layers wall, characterized by the presence of a inner core, also made of *altinella* bricks and other material randomly disposed, and two external veneers of *altinella* bricks;
- one layer wall made of *altinella* bricks regularly bonded in the thickness (thickness can vary from 30 cm to 40 cm);
- employment of *altinella* bricks bonded as rowlock or stretcher in partition or boundary walls.

A certain difference in the brickwork bond was probably related to masonry importance and function. Palladio tells about differences in brick dimensions according to their employment: “(...) si fanno maggiori o minori secondo la qualità degli edifici da farli, e secondo che di loro ci vogliamo servire: onde gli antichi fecero i mattoni dei pubblici, e grandi edifici maggiori dei piccoli, e privati”¹⁰.

The ruins of the façade of *Santa Maria dei Servi* church in *Cannaregio* (Fig. 3,4)

⁹ Fazio, G., Hreglich, S., Lazzarini, L., Pirredda U., Verità, M., Le altinelle a Venezia: problemi storici, caratterizzazione chimico fisica, cause di deterioramento, in *Il mattone di Venezia*, atti del convegno, Venezia, 1982.

Zago, F., Biscontin, G., Michelon, G., Riva G., Valle, N., Indagine chimica, fisica e meccanica di murature storiche a Venezia e proposte di risanamento, in *Il mattone di Venezia*, op cit.

Canal, E., Cavazzoni, S., Antichi insediamenti antropici nella Laguna di Venezia: analisi multivariata di tipo “Fuzzy c-means clustering” in *Archeologia e calcolatori*, n 1, 1990

¹⁰ Palladio, A., *I quattro libri dell’architettura*, edizione Hoepli, Milano 1945

show that the masonry thickness is clearly divided in an external veneer of *altinella* bricks regularly bonded and an internal one lacking a regular texture, showing the appearance of a filling.

Similar considerations can be made in the case of the *Tese dell'Isolotto* building in the *Arsenale*, where the wall shows an internal core of *altinella* bricks (Fig. 5 and 6).

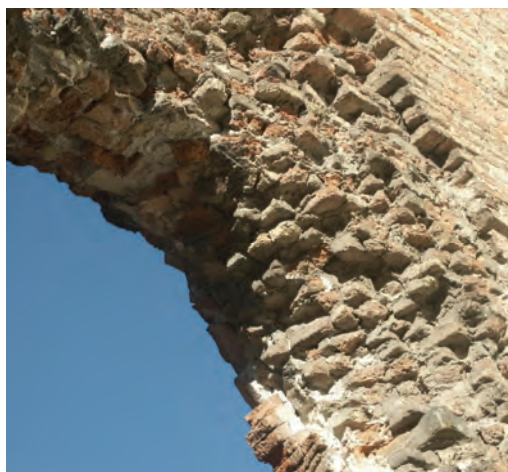


Fig. 3. Santa Maria dei Servi church in Cannaregio: detail of the inner core made of *altinella* bricks.



Fig. 4. Santa Maria dei Servi church in Cannaregio, the brickwork surface.



Fig. 5. Tese dell'Isolotto in the Arsenale, West view, *altinella* brick masonry.



Fig. 6. Detail of the internal part of the wall.

It seems possible (but it should be verified) that some religious buildings such as *Carmini* church (Figs. 7 and 8) have a masonry composed by *altinella* bricks well bonded in the whole depth of the wall, despite its huge thickness.



Fig. 7. The Carmini church in Dorsoduro. Lateral walls are made by altinella bricks with signed pointing on mortar joints.



Fig. 8. Carmini church in Dorsoduro. Specimen of 1 square meter from lateral masonry (by students G.Burello, L.Mares, E.Toniolo, L. Zanmarchi, 2005)

In the remains of the dormitory of the female Cistercian monastery in *San Giacomo in Paludo* island, (Fig. 9-10), dating back to XIII century, the *altinella* brickwork is not used as filling, but is regularly bonded, in a thickness of 45 cm, where the bricks have 18 x 8,5 x 4,5 cm dimensions; they are connected with abundant gray-sandy mortar and disposed in horizontal layers irregularly alternating 2-3 stretcher and one header acting as bond¹¹.

In the same site, some *altinella* masonry can be observed regularly bonded all as headers or all as rowlock¹². This bond may be probably related to a different static role of the wall that should have only an internal delimitative function, considering the low thickness of the section.

¹¹ Gelichi, S., *Archeologia e monasteri nella laguna veneziana: San Giacomo in Paludo, Venezia, 2004*

¹² Gelichi, Op. cit.



Fig. 9. San Giacomo in Paludo Island: altinella brick masonry in archeological ruins of female Cistercian monastery, dating back to XIII century.



Fig. 10. San Giacomo in Paludo Island, altinella brick masonry: detail of brick arrangement.

Altinella bricks employed in civil buildings were probably disposed in a pattern where longer sides (stretchers) might be seen. Proofs of that can be found in the houses in *Crosera San Pantalon* in *Dorsoduro* (Figs.11, 12), or in the side of the palace on *calle Spezier* in *Santa Croce*, or in *Fontego del Megio* on the Grand Canal in *Santa Croce* (Figs.13, 14).

In this kind of brickwork the elements are bonded together into the layer, at least in the boundary walls, in order that the thickness of wall should be at least 34-42 cm (corresponding to 4-5 brick heads of 7.5 cm).



Fig. 11. Houses with altinella brick masonry in Crosera San Pantalon in Dorsoduro.

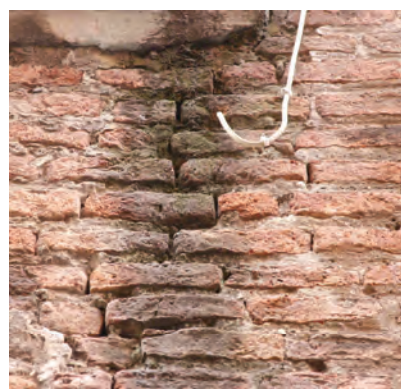


Fig. 12. Houses with altinella brick masonry in crosera San Pantalon in Dorsoduro. Detail showing pointing on mortar joints.



Fig. 13. Fontego del Megio on Grand Canal, in Santa Croce.



Fig. 14. Fontego del Megio on Grand Canal in Santa Croce. Detail showing *altinella* brick masonry and the bedding mortar.

Many examples can be found in the city of masonry in which *altinella* bricks are arranged in a mixed pattern some as rowlock and some as stretcher.

Stratigraphic readings show that this usage of the *altinella* brick can be found in closing walls or in constructional resumption of brickwork. Other cases should be examined more carefully in order to verify if the mixed bond could be connected to the initial constructive phase (house in *calle Sansoni* in *sestiere San Polo*, Figs. 15, 16). The rowlock course of *altinella* brick increase velocity of brickwork but is not suitable due to the lack of concatenation among the elements (Figs. 17, 18). The small size of *altinella* bricks may have caused an important slowdown in construction. This reason may have allowed and preferred a quicker way of laying bricks, particularly where the requirement of masonry strength and effectiveness was considered of minor importance in the building phase.



Fig. 15. House on Raspi Bridge in San Polo. This brickwork is entirely made of *altinella* bricks.



Fig. 16. House on Raspi Bridge in San Polo. Detail of brickwork showing alternated overlapping courses of *altinella* bricks.



Fig. 17. Brickwork with alternated overlapping courses of altinella bricks in Dorsoduro.



Fig. 18. Brickwork with single courses of altinella bricks disposed as rowlock.

4 Observations on the clay blend

The macroscopic analysis of the clay blend in a sample of 50 altinella bricks has taken into account a series of parameters:

- homogeneity/heterogeneity of the blend;
- background color of the blend;
- dimensions, quality and color of inclusions.

From the observations made a wide variety of blend appears. It is often very heterogeneous both in what concern the size of the inclusions and the mineralogical characterization.

The iron components, associated to a red-rosy coloration, characterize clasts that are bigger than the yellowish background blend.

In case of homogeneous, ironed and red colored background, the presence of bigger inclusions can be observed, which color progressively shifts to the dark red and then to black, due to the increasing contents of iron and/or to baking temperature. The presence of calcite, that can be observed by microscope in correspondence to some hollows, is evidence that baking process did not exceed 750 °C. On the other side, the presence of some black nodules of baked clay with strong ceramic-like consistence is connected to an higher baking temperature.

It is frequently observed that constitutive material isn't selected in order to result homogeneous and depurated both in altinella bricks layer both in mixed ones, and is valid for all kind of brickwork too.

The research performed shows a basic mineralogical–petrographic characterization of the blend in altinella bricks coming from two buildings: Ca' Zusto in Santa Croce (sample A) and a house in Castello (sample B); (Fig.19-20). The sample have been studied both with standard method of mineralo-petrographic analysis (microscopic observation of thin sections) and

diffractometric x-ray analysis¹³.



Fig. 19. Ca' Zusto in Santa Croce. Building dating back to XIII century presenting both altinella and gothic bricks.



Fig. 20. House in Rio Terà Seco Marina in Castello. Altinella bricks come from masonry base.



Fig. 21. Brick coming from Ca' Zusto, in Santa Croce. Dimensions are: 15,5 x 7,6 x 5,4 cm.



Fig. 22. Brick coming from house in Rio Terà Seco Marina in Castello. Dimensions are: 18,5 x 9 x 6 cm.

4.1 Sample a1: Ca'Zusto in Santa Croce

It is a white brick (with yellowish blend), made of calcareous clay and used as they were, baked at 750°C, next to the calcite dissociation temperature. That one, in fact appears in thin sections as dissociation residues. The brick contains inclusions of big dimension (5mm) even of carbonatic nature (Fig. 23-24); the presence of so big dimensions of bonhertz is a proof of bad blend processing and of an average sandy framework (less than 20%) coinciding with the detritic fraction of original clays and a leaning sandy component.

¹³ diffractometer Philips Pw 1830, radiation Cn K/Ni Kv and 20 mA

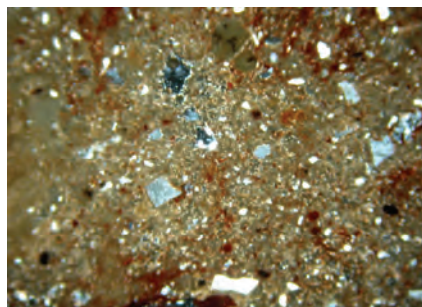


Fig. 23 Micrography of thin section of alтинella coming from Ca' Zusto, in Santa Croce. It is possible to read hiatal texture with clasts of quartz and secondary porosity linked to decomposition of clacite (N+, 66x).

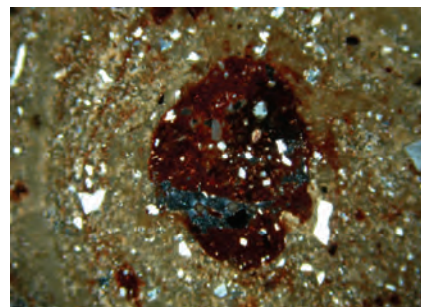


Fig. 24 Micrography of thin section of alтинella coming from Ca' Zusto, in Santa Croce. It is possible to read the presence of a bonhertz clasts as a demonstration of bad blend processing (N+, 66x).

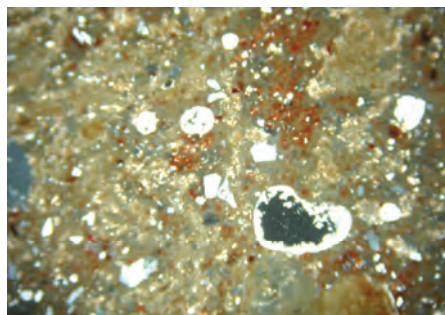


Fig. 25. Micrography of a thin section of alтинella coming from Ca Zusto, in Santa Croce. It is possible to read the hollow made by calcite (N+, 66x) .

The brick shows a fine and hiatal grain and appears to be of carbonatic nature (micritics clasts); it contains an average quantity of sharp and poly-crystalline quartz, chert, pyroxene, plagioclasts and mica. Diffractometric analysis (Fig. 26) confirms the mineralogical composition already seen in the thin section.

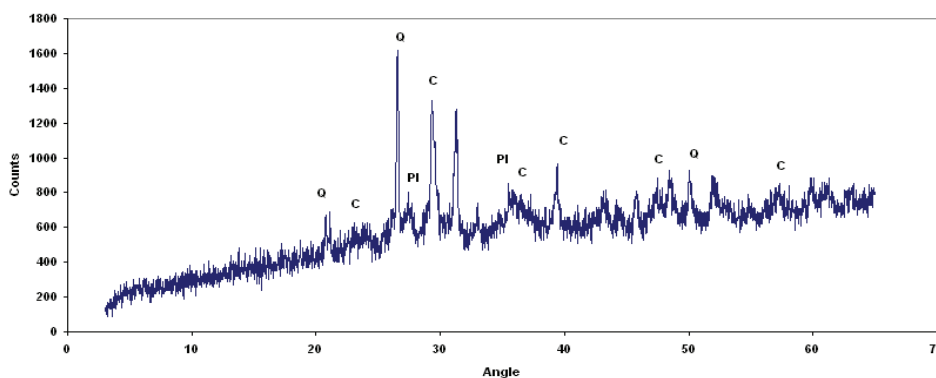


Fig. 26. Dust diffractometric analysis of brick coming from Ca' Zusto, in Santa Croce. C=calcite; Q=quartz; Pl=plagioclasi; Px=pyroxene.

4.2 Sample b1: house in rio terà Seco Marina in Castello

This is a white brick, very similar to sample A1 (Figs. 23, 24). It is characterized by blend with aggregate polarization and with carbonatic bonhertz of different dimensions. (Figs. 27, 28).

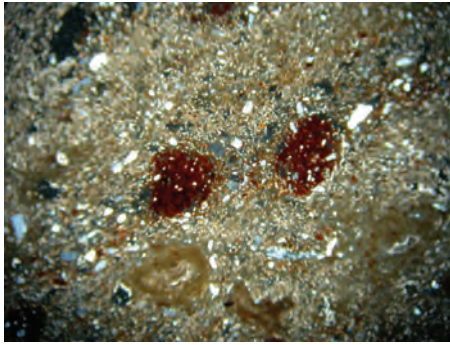


Fig. 27. Micrography of a thin section of alтинella coming from house in Castello. It is possible to read serial texture with clasts of quartz (sharp and nearly sharp) and the presence of two bonhertz and micro-crystalline blend (N+, 66x).

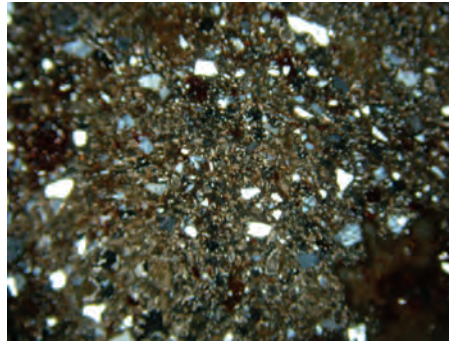


Fig. 28. Micrography of a thin section of alтинella coming from a house in Castello. It is possible to see a serial texture with clasts of quartz (sharp and nearly sharp) and the presence of pieces of stones (N+, 66x).

There are sandy components (quantity: 20 to 30%) with minero-petrographic characters very similar to the sample A1: fine and hiatal grain; composition of quartz (sharp + poly-crystalline ± chert) and calcareous clasts with thermal variation (presence of true phantasms of calcite) and plagioclasis, peaces of granite-looking stones, pyroxene, iron oxide, and mat minerals, sometimes biotite.

Diffractometric analysis (Fig. 29) confirms the results obtained by minero-petrographic microscope observations. The condition of the calcite components demonstrates that the baking temperature was about 750 °C. The porosity of both bricks is due to hollows and shrinkage during drying and subsequent baking phases.

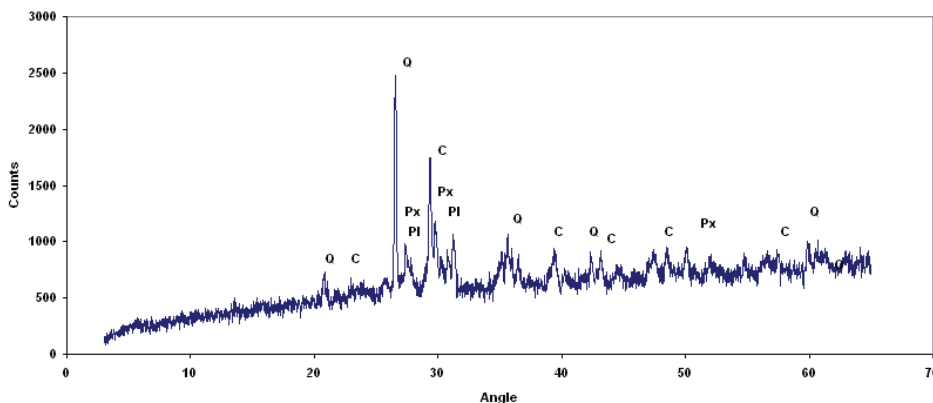


Fig. 29. Dust diffractometric analysis of brick coming from a house in Castello. C=calcite; Q=quartz; Pl= plagioclasio; Px=pyroxene.

The two samples have similar blend characteristics even if they are situated in two different places of the city and have a different dimensions.

5 Some remarks about structural behaviour of Venetian altinella bricks masonry .

Observations deal with:

- masonry texture heterogeneity
- bricks and bedding mortar variations
- ways of brickwork building

Table 1. Results of compression tests on altinella bricks

specimen	length (mm)	width (mm)	height (mm)	strength (Kgf)	strength (N)	N/mm ²
A1.1	43,2	42,6	42,8	3700	36297	19,7
A1.2	41,9	41,5	43,1	3420	33550,2	19,3
A2.1*	41,9	41,8	39,8	2500	24525	14,0
A2.2*	39,9	42,3	40,5	2930	28743,3	17,0
A2.3	39,9	42,5	40,5	3800	37278	22,0
A3.1*	40,3	41,4	43,7	1420	13930,2	8,3
A3.2	39,9	41,6	42,7	2040	20012,4	12,1
A3.3	42,3	42,1	41,3	2010	19718,1	11,1
B1.1	40	41,8	30,3	5200	51012	30,5
B1.2	40,5	42,5	42,5	5750	56407,5	32,8
B2.1	41,1	42,6	42,3	4220	41398,2	23,6
B2.2	40,1	41,8	41,8	3640	35708,4	21,3
B2.3	40	41,8	41,4	2540	24917,4	14,9
B3.3*	42,5	43,3	42,8	3660	35904,6	19,5
B3.4*	39,7	39,1	44,7	3340	32765,4	21,1
B3.6	43,2	38,7	42,4	3110	30509,1	18,2

* endamaged specimen

In the present paper, only the results of a first series of mechanical tests will be shortly presented (Tab. 1), made on the same altinella bricks that were previously analyzed. Generally speaking, it appears that the specimen belonging to group B show a better behaviour of those belonging to group A, that have a lower peak strength: this behaviour has to be related to the differences recognized in the brick composition and baking process.

Conclusions

Venetian masonry are characterized by a strong rising damp process, due to

the constant presence of water and soil characteristics. Salt crystallization process causes diffused erosion phenomena in masonry. The masonry damage increase where the masonry and the bricks are not homogeneous.

In altinella brick masonry the quantity of bedding mortar is higher, because those bricks are smaller. Damage makes masonry weaker.

This problem is more evident in the case of masonry made of three leaves of altinella bricks, but also in case of masonry characterized by several building phases and different kind of bricks

The observations and the analysis that has been conducted in this research have the goal of better understanding the factors that are more important in determining the behaviour of a very particular kind of masonry, but the same method can be applied in the future to others, giving a general tool for masonry analysis that connect historical and archeometric studies with physical-mechanical observations¹⁴.

References

Dorigo, W. , Venezia Romanica: la formazione della città medioevale fino all'età gotica, Venezia, 2002.

Piana, M., Note sulle tecniche murarie dei primi secoli dell'edilizia lagunare, in "L'architettura gotica veneziana", Valcanover, F., Wolters, W. (a cura di) Atti del seminario dell'Istituto Veneto di scienze lettere ed arti –Venezia, 1996, 2000.

Fontana, V., Appunti sulle malte e i mattoni in uso nei cantieri veneziani del cinquecento da documenti e trattati dell'epoca, in "Il mattone di Venezia", atti del convegno presso fondazione Cini, Venezia, 1979.

Tassini, G., Curiosità veneziane, ovvero origini delle denominazioni stradali di Venezia, prima edizione, Venezia, 1863.

Monticolo, G. (a cura di), I capitolari delle Arti veneziane sottoposte alla Giustizia e poi alla Giustizia vecchia dalle origini al 1330, Venezia, 1896.

Varosio F., Ricerca per una mensiocronologia dei laterizi a Venezia, Tesi di Laurea in Rilievo e analisi tecnica dei monumenti antichi, relatore Ferrando I., correlatore Varaldo C., Mannoni T., Università degli studi di Genova, Facoltà di Lettere e Filosofia, Corso di Laurea in Conservazione di Beni Culturali, indirizzo archeologico, architettonico e per l'ambiente, a.a. 2000/2001.

Fazio, G., Hreglich, S., Lazzarini, L., Pirredda U., Verità, M., Le altinelle a Venezia: problemi storici, caratterizzazione chimico fisica, cause di deterioramento, in Il mattone di Venezia, atti del convegno, Venezia, 1982.

¹⁴ Authors contribution: G.M.R. introduction and conclusion and general supervision; F.T. historical and analysis share; S.C. analysis laboratory share.

Zago, F., Biscontin, G., Michelon, G., Riva G., Valle, N., Indagine chimica, fisica e meccanica di murature storiche a Venezia e proposte di risanamento, in *Il mattone di Venezia*, atti del convegno, Venezia, 1982.

Canal, E., Cavazzoni, S., Antichi insediamenti antropici nella Laguna di Venezia: analisi multivariata di tipo "Fuzzy c-means clustering", in *Archeologia e calcolatori*, n 1, 1990.

Gelichi, S., *Archeologia e monasteri nella laguna veneziana: San Giacomo in Paludo*, Venezia, 2004.

Palladio, A., *I quattro libri dell'architettura*, edizione Hoepli, Milano 1945.

DETECTIVE CONSTRUCTIVE DISPOSITIONS OF INWARD OUT-OF-PLUMB ON VENETIANS DWELLING HOUSES EXTERNAL MASONRIES

Francesco Doglioni, Angela Squassina, Francesco Trovò

Dipartimento di Storia dell'Architettura - Università IUAV di Venezia

Riassunto

Nell'ambito dello studio delle forme di dissesto dell'edilizia storica lagunare, la ricerca vuole acquisire elementi per comprendere se i frequenti assetti ad entro-piombo riscontrabili sui fronti siano dovuti ad una volontà costruttiva iniziale o acquisiti a seguito di processi di dissesto. Dopo un esame speditivo di carattere generale, che ha individuato sei diverse configurazioni ad entro piombo, è stato compiuto con diversi strumenti l'esame di dettaglio di due edifici di epoca gotica, analizzando comparativamente le possibilità che l'assetto sia il risultato di una configurazione intenzionale in fase costruttiva, oppure di un processo di dissesto, o della concatenazione di entrambe. La conclusione tratta dall'esame dei due casi è che il loro assetto è in via principale riconducibile alla fase costruttiva iniziale, e pertanto non è da considerare di per sé un fenomeno di dissesto.

Abstract

In the scope of the study of venetian historical building forms of damage, the research wants to acquire some elements in order to understand the frequent lays-out on inward out-of-plumb of building facades.

The question is if they are due to an intentional way of building or to damage processes. Six different way of inward out-of-plumb are recognized during a quickly research.

Afterwards a specific research was carried out in two gothic buildings; the results of this research underline that the lay-out of inward out-of-plumb is generally due to an intentional way of building, so it is not to be considered a way of damage.

1 Introduction to the purposes of the research

In the framework of research program on damage appearance in order to diagnose structural reliability and recognize high vulnerability forewarning signal, it has to know the case history (the anamnesis), in particular damage appearance, highlighted by different crack and deformation patterns, and repair actions in the centuries.

The recognition of characteristic damage appearance and the diagnosis of their

causes, useful for the knowledge of structural damage processes and the estimation of residual resources, bases itself on the knowledge of differential formed during the time as regard to building first structure.

Frequently, damage effects are studied in touch with crack and deformation patterns. The measures of deformations indicate the removal from foreseeable and regular geometry, as a characteristic of a build duly made (verticality and planarity of walls, horizontal position of diaphragms).

Marked deviations from vertical plane can be observed in outside walls of venetian buildings more than in another city. Among these there is the prevalence of the inward out-of-plumb on external out-of-plumb.

The discussion on this theme is very old, as we can read in Angela Squassina test below. One of the subjects of the resarch on Venetian buildings is the detection of the initial configuration of the buildings, in order to verify the origin and the nature of the frequently found inward out-of-plumb, and if and in what proportion it can be referred to an intentional original design or to a subsequent deformation.

The demonstration of intentional original design determines to know the structural framework, the mentality of build, the expectation in order to behaviour, the favourite parts of building where inward out-of-plumb can be found, and its diffusion too.

2 General expeditious observations

At the beginning an extensive expetidius survey of a great area was made, to highlight buildings characterized by a clear inward out-of-plumb.

The consequence is a first classification based on the places in which the inward out-of-plumb is present (wall on "calle", on "fondamenta", on the water), on how many walls of the same building is present, and if its presence is due to damage appearances.

A first significant element is represented by the recognition of six inward out-of-plumb types: continuous inclined one (type a), broken one with an initial vertical part (type b), broken one with an initial external out-of-plumb part and the other inward out-of-plumb (type c). Other types, less frequent, are: vertical till the first floor, then inward out-of-plumb, at the end vertical one (type d), inward out-of-plumb with offset in the external part (type e, compared in only one building) inward out-of-plumb till the first floor, then vertical one (type f).

The types a and b have been studied with more attention. Type c can derive from the type b because of damage effect, type d can be considered a type b raised. Type f has doubt characteristics, generally on buildings with stone pilasters.

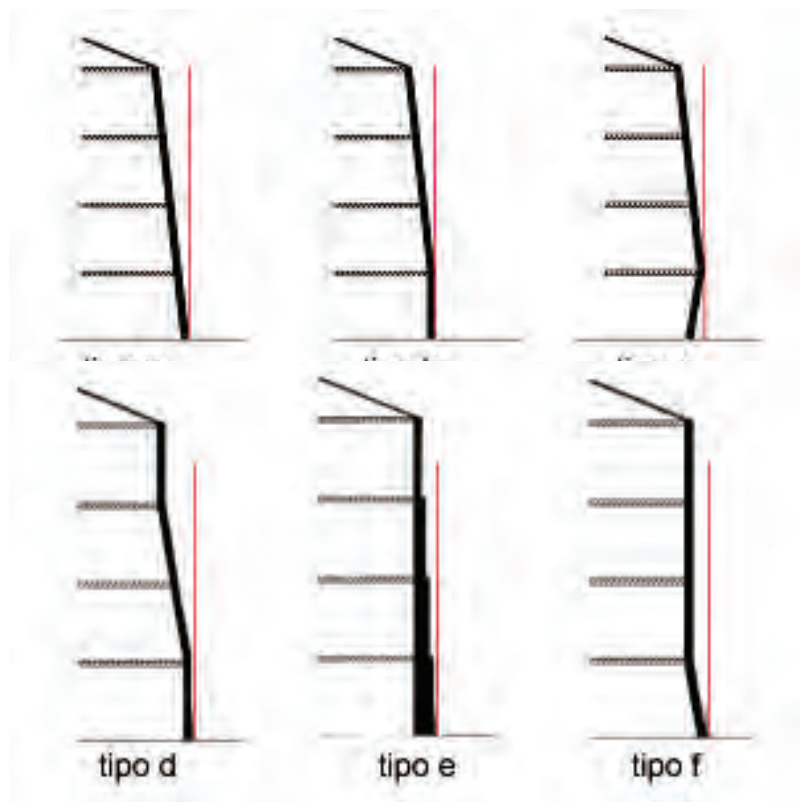


Fig.1 Graphics schemes describing the six types

3 Choices and interpretative reading of case-studies

The first question we want to answer by exempla is if the inward out-of-plumb is an intentional way of building. If it is intentional we could explain the specific physiological and pathological tracings and its different forms of evolutive behaviour. We have analyzed two specific cases because of their requirements:

- high stratigraphic-building readability, that is surfaces in which the initial condition and the following transformations can be verified, included cracks due to damage and their repair actions;
- stone elements belonged to initial building phase, only partially modified, interesting because of stereotomy studies;
- in both cases the inward out-of-plumb is present at least on two walls so that it is less probable the mechanism of whole building rigid rotation.

3.1 *Ca Corner della Frescada*

Ca Corner della Frescada¹ (Dorsoduro, 3911) is a gothic building of the middle of XV secolo². “Quali testimonianze complete di un gusto più simmetrico va

¹ “Bella facciata archiacuta che, passato ai Loredan, fu dimora del doge Pietro Loredan”, 1567-70. (Lorenzetti, Venezia e il suo estuario, 1956, pag. 577)

² Lorenzetti, Venezia e il suo estuario, 1956; Maretto, L'edilizia gotica veneziana, 1959; Arslan, Venezia Gotica, 1970.

citato il palazzo Corner della Frescada con balcone e mezzanino già rinascimentale nella facciata sul rio, una facciata posteriore con quadrifora e sala passante a pianterreno aperta con un grande arco quattrocentesco sulla corte confinante con la calle, nonché un piano ben conservato". (Arslan, Venezia Gotica – L'architettura civile, 1970, pagg.79, 256, 257).

Fig. 2. Up to the left: piece of Venice view by J.De Barbari, 1500.

Fig. 3. In the middle:Ca Corner della Frescada, facade on the canal, 2006.

Fig. 4 .To the right: Palazzo Corner della Frescada, lateral facade, 2006.



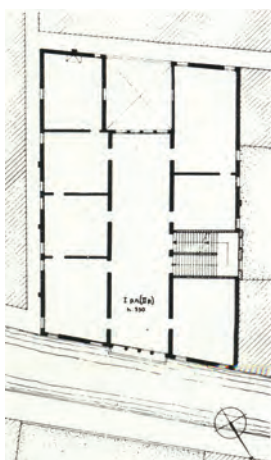
The windows stone element are studied in relation to the morphological evolution of arc during "veneto-bizantina " and gothic period.

" Il motivo dell'arco inflesso semplice, (...), entra nel patrimonio dell'architettura civile veneziana, anche se esso sarà impiegato in misura diremmo sporadica, rispetto all'uso, straordinariamente diffuso, dell'arco inflesso trilobato.

Un caso dubbio – the presence of simple inflected arc- è quello offerto dalla facciata sulla corte del palazzo Corner della Frescada. La quadrifora sulla corte, sorretta da capitelli di tipo trecentesco, lascia cioè in dubbio se si tratti di un'opera coeva alla facciata o di un elemento antico sfruttato nella nuova costruzione (il poggolo è certo della fine del Quattrocento)". (Arslan, Venezia Gotica – L'architettura civile, 1970).

Fig. 5. Up on the left: Palazzo Corner della Frescada, first floor plan, Maretto, P., 1960, pag 106.

Fig. 6. On the right: Palazzo Corner della Frescada, detail of a windowsill, facade on the canal, 2006: look at the prominence on the windowsill.



3.1.1 Geometry descriptions

Ca' Corner della Frescada presents the main wall on the canal, opposite to a secondary facade and an inside court.

Three outlines have been surveyed, two on the main facade (inward out-of-plumb of cm 34 and 38, that is 2 and 3 degrees), one on the lateral wall on the left (inward out-of-plumb of cm 18), on the roof cornice.

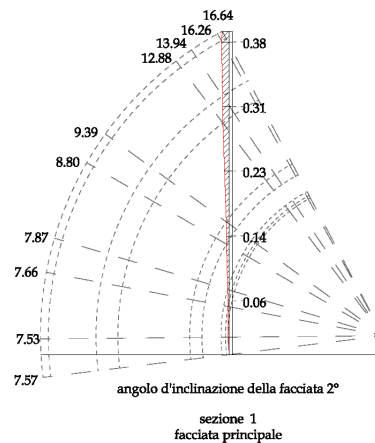


Fig. 7: Palazzo Corner della Frescada, geometrical rise of the facade course on canal (made by students of architecture: A. Levorato, L. Rudko e V. Selvaggio, 2006).

The first floor course has been surveyed and has been resulted plane. For this reason we can exclude that inward out-of-plumb could be due to a mechanism of whole building rigid rotation.

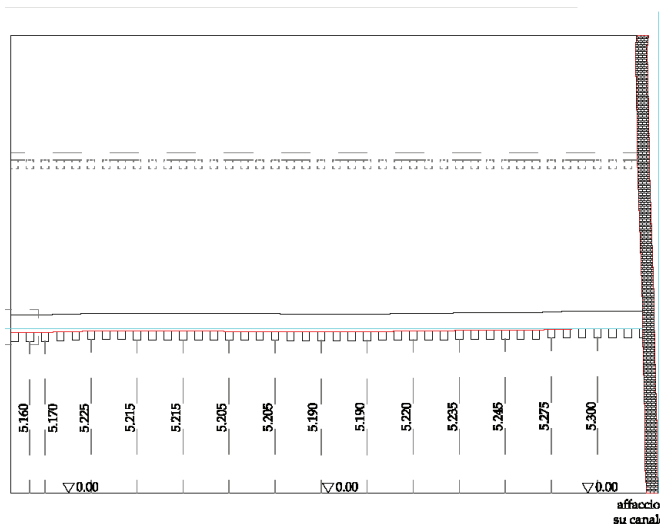


Fig. 8. Palazzo Corner della Frescada, geometrical rise of the first floor course (made by students of architecture: A. Levorato, L. Rudko e V. Selvaggio, 2006)

In the original windowsills of the main facade we have surveyed a particular building contrivance: an inclined prominence, necessary to give to the embrasures a horizontal base to the external inclined course.

Probably the superficial part of the windowsill has been worked during the years because of the rain downflow.

However the superior frieze of the cornice (from lateral point of view) is inclined forward external side, but its height is constant. That is the reason why we can exclude the windowsill prominences are due to probable reduction of surfaces.

The same considerations are not possible as far as the lateral wall is concerned because of the complex re-arrangement of stone elements and numerous interventions on the windows.

The presence of a so shaped windowsill and the planarity of the floor, that excludes any damage, strengthen the hypothesis of the intentional way of building a wall on the canal with the inward out-of-plumb.

Figs. 9-10. Palazzo Corner della Frescada, details of a windowsill with the particular prominence.

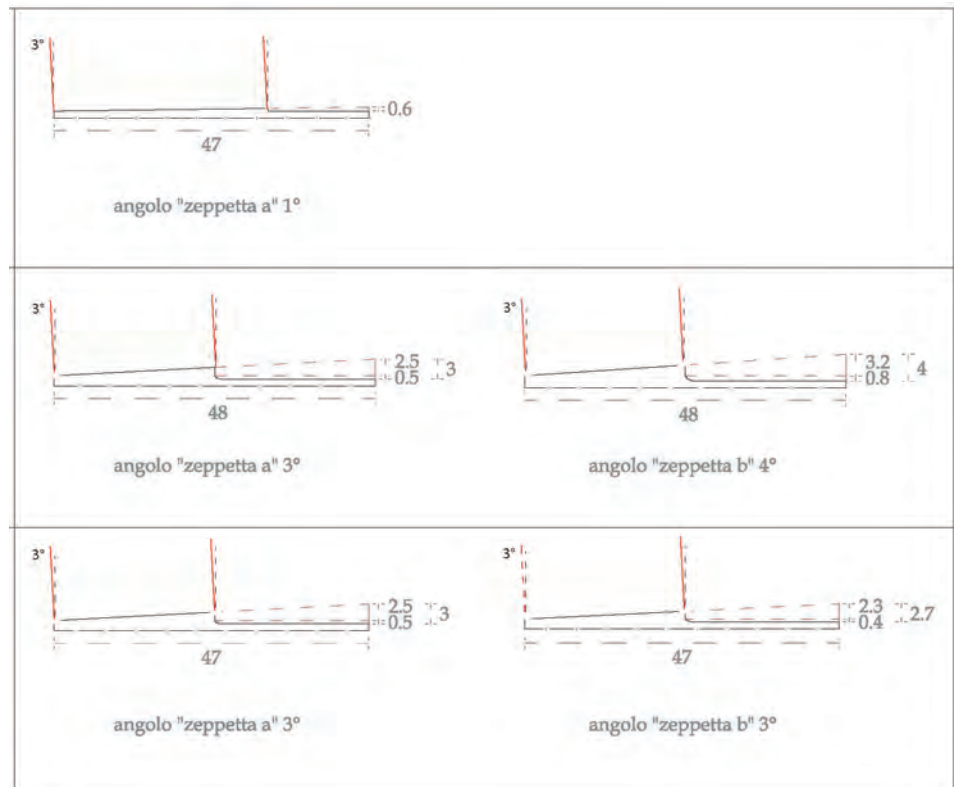


Fig. 11. Palazzo Corner della Frescada, windowsill section (rise made by students of architecture: A. Levorato, L. Rudko e V. Selvaggio, 2006).

3.2 Palazzo Soranzo Pisani

The valuable stone bas-relief of diagonal facade belongs to XIV century (Rizzi)³ or to XV century (Lorenzetti)⁴. It is “*stemma con alto rilievo (metà XIV sec.). Pietra d'Istria, cm. 110 x 220 circa. Al centro scudo gotico bipartito (Soranzo – Pisani) sormontato da busto di angelo benedicente (...).*” (Rizzi, *Scultura esterna a Venezia*, 1987).



Fig. 12. Up on the left: piece of Venice view by J.De Barbari, 1500.

Fig. 13. In the middle: Palazzo Soranzo Pisani, view, 2006

Fig. 14. On the right: Palazzo Soranzo Pisani, detail of the stone element in corrispondence with the edge of the portal.

The stone portal with bas-relief and the angles made by stone elements and bricks belong to the same building period. The bricks are altinella type, compatible with the age of realization of the stone plate.

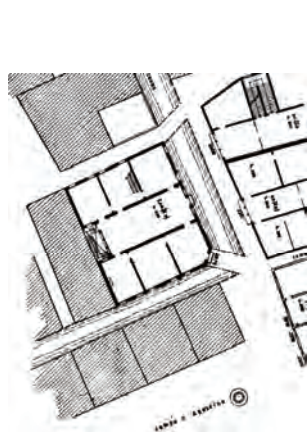


Fig. 15. Up to the left: Palazzo Soranzo Pisani, plant of the first level (P.Maretto, 1960, edizione Filippi Editore, 1978).

Fig. 16. In the middle: Palazzo Soranzo Pisani, view before stone cleaning actions, (Rizzi, edizione Stamperia di Venezia, 1987).

Fig. 17. To the right: Palazzo Soranzo Pisani, view of stone portal in corrispondence with diagonal facade, 2006.

³ Rizzi, *Scultura esterna a Venezia*, 1987

⁴ Cit.

Arslan studied the theme of morphological evolution of arcs in this building; he found here one of the rare gothic simple arcs with three lobes in Venice: “L’arco trilobato semplice si ritrova anche nell’unica finestra gotica rimasta in Palazzo Soranzo Piasani in rio Terà Primo del Parrucchetto, sull’asse di una porta, di cui rimane un notevole bassorilievo riconosciuto come trecentesco.” (Arslan, Venezia Gotica – L’architettura civile, 1970 pag.82).

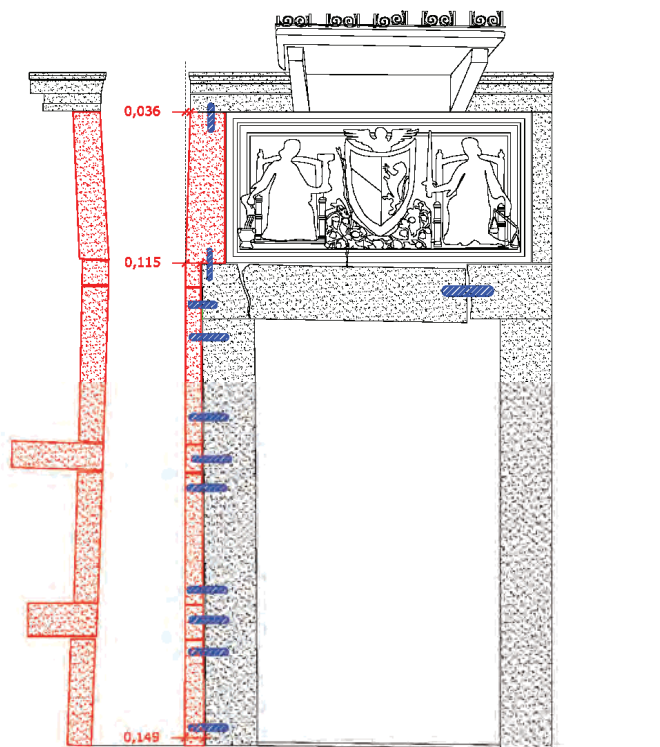


Fig. 18. Palazzo Soranzo Piasani, study of the portal: stone elements's course, that deflects on height, shows the intentionality of trapezoidal geometry of the facade. (reliefs by student of architecture N. Colleoni, M.C. Matzeu, C. Pulino, 2006).

P. Maretto brings the Corner della Frescada typological structure (U type) near to Soranzo Piasani's one: “con la casa Soranzo Piasani a Sant’Agostin, Ca’ Corner della Frescada, una casa a Santa Maria Formosa e poche altre, questi edifici, riferibili agli inizi del ‘400, sono dei singolari esempi di case tripartite organizzate su un rigoroso e ricco asse di simmetria in direzione acqua terra (accesso dal canale – portego – corte – ingresso da terra) secondo un impianto distributivo che potremmo definire ad “U”.” (Maretto, “L’edilizia gotica veneziana”, 1959).

3.2.1 Geometry description

Palazzo Soranzo Piasani presents two walls in marked inward out-of-plumb and one wall (diagonal, between the two other facades) in inward out-of-plumb in the upper part. The measure of inward out-of-plumb changes between 21 cm and 47 cm.

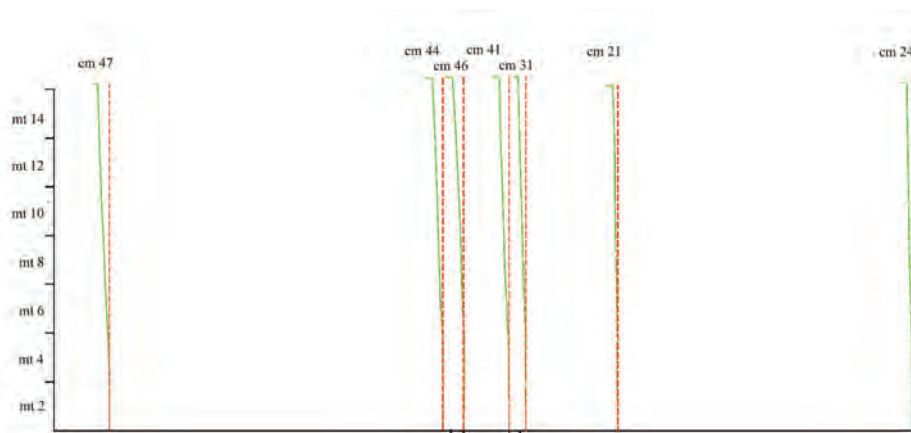


Fig. 19. Palazzo Soranzo Pisani, geometrical rise of the facade course (made by CIRCE-IUAV, arch. F. Guerra, Dott. L. Pilot, arch. S. Mander).

West facade cm. 44-47; central facade cm 41-46; south facade cm 24-31.

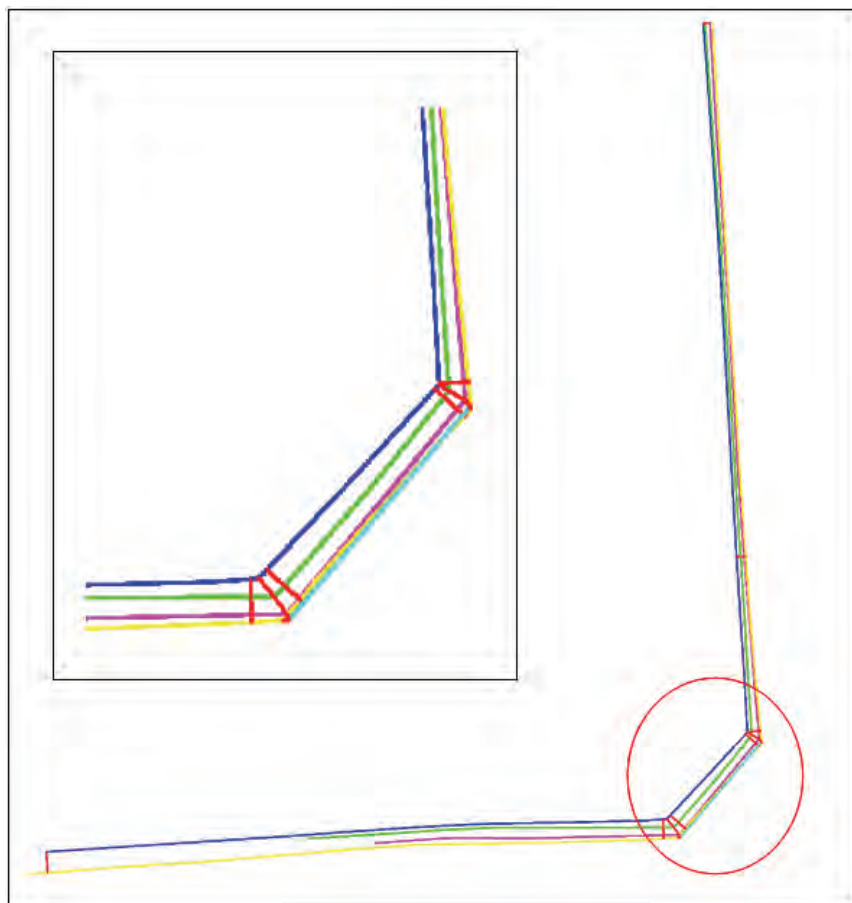


Fig. 20. Palazzo Soranzo Pisani, geometrical superimposition of the facade external course on different height: yellow 0,2 mt to the ground; azure 3,33 mt; violet 5,13 mt; green 10,26 mt; blu 14,5 mt. (made by CIRCE-IUAV, 2006). Up to the left: detail of diagonal facade.

The measurements demonstrate the inward out-of-plumb on three facades, that generate a triangular prism.

The diagonal facade has a marked trapezoidal form (width in correspondence of portal lintel cm 284, in correspondence of roof cornice cm 268) : it excludes that the inward out-of-plumb on three facades could be linked to effects of a mechanism of whole building rigid roto-traslazione.

The amount of cracks present on stone element (about 40 mm) and the incompressive form of the upper masonry demonstrate that the inward out-of-plumb is linked to an initial building.

The marked trapezoidal form of the cornerstone (mm 305 down e mm 282 up), placed laterally to stone plate, and its no re-working character are elements that confirm this thesis.

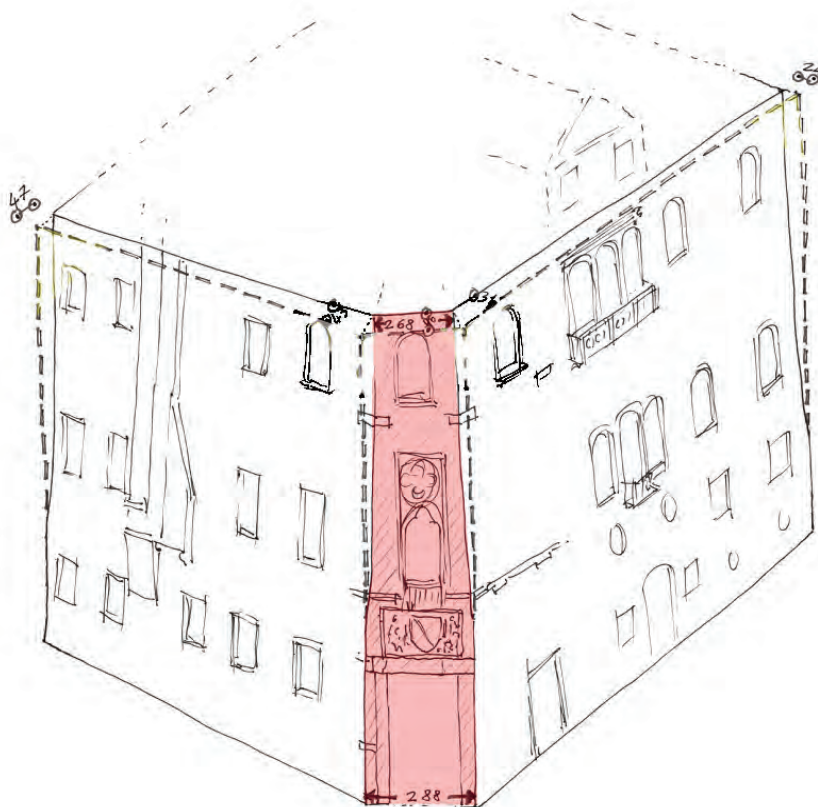


Fig. 21. Palazzo Soranzo Pisani, scheme that puts in evidence the trapezoid form of diagonal facade, linked to the inward out-of-plumb on two other facades, 2006.

The entity and the amount of cracks present on stone element (40 mm) can not justify the great inward out-of-plumb deformations (21–47 cm) of lateral facades.

In the upper part of altinelle' s masonry it is not possible to observe cracks.

These observations and the plant morphology of the building demonstrate that the inward out-of-plumb is linked to an initial building.

The presence of old altinelle' s masonries, of well visible angulars and the execution of stratigraphical analysis, that put in evidence walls continuity and discontinuity, deny following modifications, linked to other assumptions.

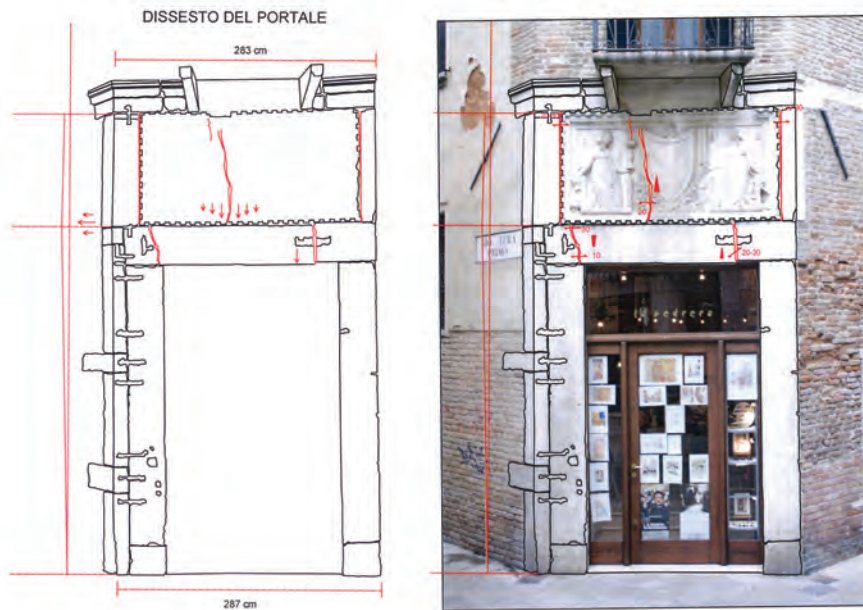


Fig. 22. The survey of crack patterns on portal and stone plate; highlighted some active mechanisms.

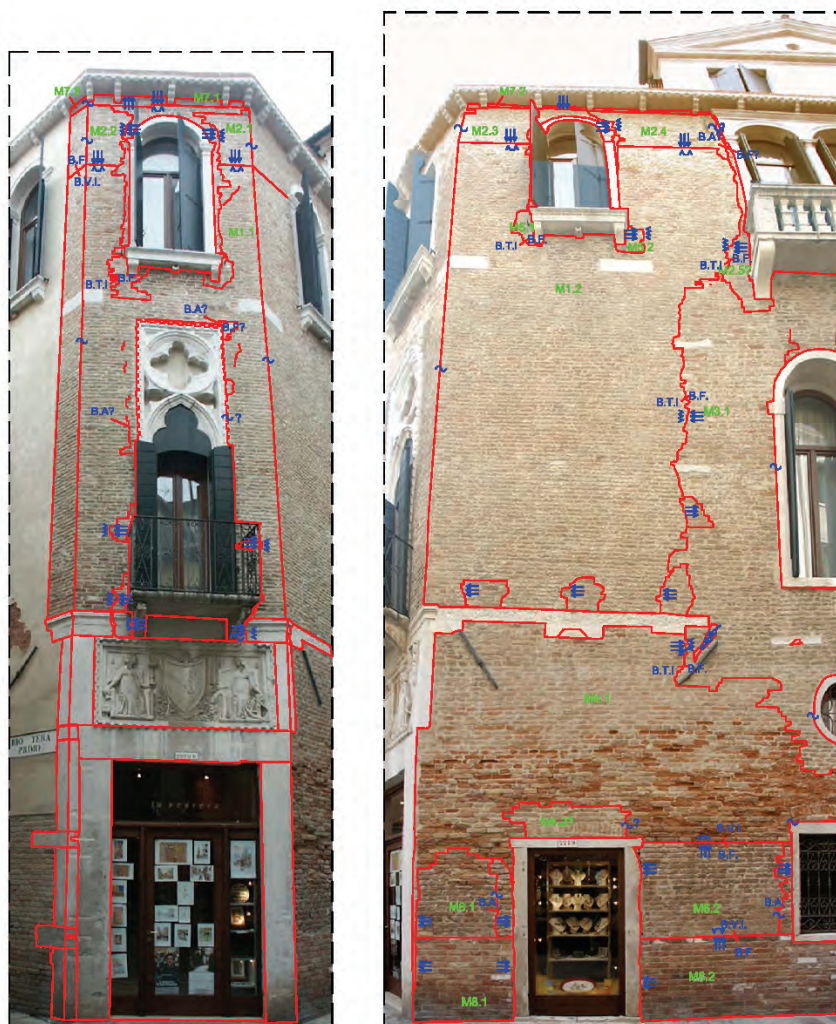


Fig. 23. Palazzo Soranzo Pisani, stratigraphical analysis. M1 is corresponding to altinelle's masonry. The stratigraphical continuity highlighted on edges between diagonal facade and two other lateral, strengthens the unitary building of three walls.

Conclusions

We retain to have argue that the inward out-of-plumb is an intentional building practice through the analysis of these two different buildings, and we can say that it is not a casualty⁵.

At the same time we can exclude it is the result of a deformation due to a structural damage, the last one considered only as a limited component.

We consider necessary both to examin single representative buildings, and to make an extensive census based on significant parametres.

For example the types c is referable to a damage that modifies the types a and b: a typical damage mechanism as pathological consequence of first structure.

However only an "epidemiological" planning out could led to recognize the role and importance of such an element in venetian buildings and in the structural vulnerability.

The appretiation for venetian architecure "building hyperboles": "una nobilissima arte e non puramente (...) scienza geometrica", as Pompeo Molmenti said in 1902, invites to look at venetian buildings in a different way.

Generally writing, the theme of the way of building by venetian builders is open and always interesting, and especially the role in it of the inward out-of-plumb and its link to a specific expectation of building behaviour -the "nature" as Rusconi says . ()

References

E.Arslan, "Venezia Gotica", Milano, 1970

G.Lorenzetti,"Venezia e il suo estuario", Trieste, 1956

P.Maretto," L'edilizia gotica veneziana", Venezia, 1959

P.Maretto, "La casa veneziana nella storia della città dalle origini all'Ottocento, Venezia,1986

A.Rizzi, "Scultura esterna a Venezia", Venezia, 1987

⁵ This consideration meet the historical thesis by the venetian architect Giuseppe Sardi, about an intentional deformation of Palazzo Dario.

FROM ARTIFICIAL STONE TO REINFORCED CONCRETE: A PLAN FOR A SPECIALIST METHOD FOR DIAGNOSTICS

Paolo Faccio¹, Greta Bruschi², Paola Scaramuzza²

¹ *Dipartimento di Costruzione dell'Architettura, Università IUAV di Venezia* ² *Dipartimento di storia dell'architettura, Università IUAV di Venezia*

Riassunto

Lo studio è rivolto all'individuazione dei temi da approfondire nell'ambito tecnico e in quello architettonico, relativamente all'utilizzo del calcestruzzo armato a vista e/o rivestito. La ricerca procede parallelamente alla definizione delle tecniche di rilievo ed indagine, propedeutiche all'analisi degli elementi in calcestruzzo armato e non armato, metodologie sperimentate mediante l'applicazione su alcuni casi studio. In questa fase inoltre si ipotizzano le prime metodologie diagnostiche per l'evidenziazione delle patologie di degrado e dissesto degli elementi analizzati.

Saranno avviate prove sperimentali rivolte alla quantificazione dei fenomeni.

Abstract

The study involves determining the issues, within the technical and the architectural fields, of the use of exposed artificial stone and reinforced concrete and/or as cladding. In parallel this research considers the definition of survey and investigation techniques, preparatory work to the analysis of elements in reinforced and non-reinforced concrete, methodologies tested through their application on some case studies. At this stage the first diagnostic methodologies for the singling out of the pathologies of degeneration and impairment of the elements under analysis are put forward.

1 Introduction

The restoration of concrete in contemporary architecture is double faceted: structural strengthening and preservation of the material. Referring to structural strengthening, if scientific development and technical solutions allow apparently comprehensive answers, the work of conservation exposes the problem of the image of architecture, albeit that the work of conservation is based on the analysis of: the characteristics of the material; the style of alteration and the related causes.

This problem of the image of architecture is present in the field of contemporary architectural restoration and becomes more specific, above all, in regard to adopted construction technologies and to the materials the operators must deal with. The research project intends to define a useful methodology to establish a survey and assessment protocol of the state of construction work conservation,

aimed at defining the conservation project.

Thus the study deals with the ways of analysis and conservation of artificial stone, exposed concrete characterized by specialized surface work and concrete cladding.

The work premise has been developed via a survey system, reading and interpretation of the construction, proposing a methodology specific to graphic return capable of representing both the technological qualities and the degeneration phenomena as well as the diagnostic, conservation and maintenance type operation indications. The necessity to develop experimentation in relation to controlled application of currently used products and techniques is linked to the possibility of carrying out a consideration based on known data and objective in regard to the possibilities offered by the market of reinforced concrete conservation materials used in contemporary architecture. This is also because of the partial and marginal interest shown, mainly by the production companies, in investment in research that deals with these problems, above all considering the aspect of aesthetic assessment of the conservation project results.

2 Case studies

It is possible to find in Venice few interesting elements in exposed concrete which the most significant examples are offered by Carlo Scarpa's buildings, characterized in diverse use of concrete, that presents several textures and surface patterns, and also pathologies of degeneration linked to concrete casting, and also to environment in which are exposed.

Case study 1: Fondazione Querini Stampalia, Venezia

The element is part of the arrangement of the ground floor and garden of Querini Stampalia foundation, realized between 1961-63 (Fig. 1).

*Fig. 1 - Orthogonal-
photographical survey of
the element sampled in
exposed concrete, garden
of Fondazione Querini
Stampalia, Venice*



The exposed concrete element is made by two staggered panels, decorated with a glass mosaic; concrete presents a refined surface working with mix-design enriched by Istria stones, which presents degeneration due to insufficient thickness of coated rebars, in particular toward the palace (Figs. 2, 3, 4).



Figs. 2, 3, 4 - Alterations on surveyed concrete

Study case 2: “Ligabue” building, Venice

“Ligabue” building designed by the arch. De Marzi and realized in 1951, provides to an investigation about the forms of alteration and the methodologies of intervention on coated concrete. Some elements on the roof top has been taken in consideration (Figs. 5, 6).



Fig. 5 - View of roof top of “Ligabue” building

Fig. 6 - Orthogonal - Photographical survey of a decay beam

The problems related to an aesthetic evaluation of the restoration concern coated concrete too. In a particular way if interventions are on structural strengthening. A necessary application of a thick layer of mortar modifies indeed the geometry and the proportions of the architecture (Fig.7)

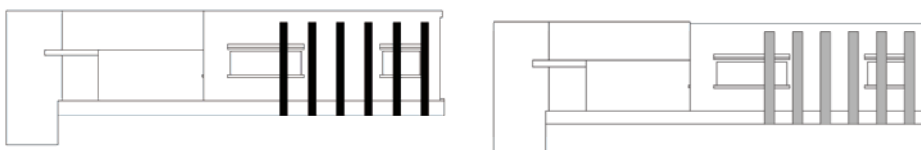


Fig.7 - Simulation of dimensional variation before and after structural intervention

3 Inquiry protocol

The knowledge of the building is necessary for a correct analysis and can be achieved through several depth studies, depending on the accuracy of the survey operation, historic research and experimental inquiries.

During the survey is possible to characterize either geometric or materic element properties, but also describe decay pathologies and alteration.

The aim is to define for every sample a file of analysis made by a double level; a first part which can be defined expeditious, able to provide a geo-referred location of element and a first risk factor (Tab 1).

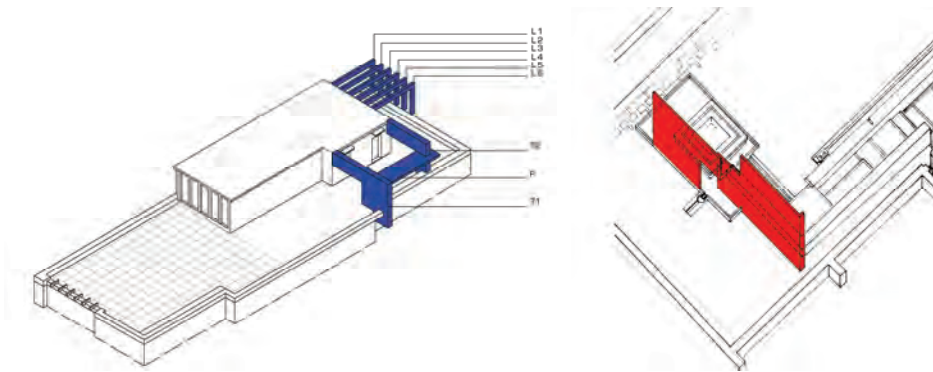
Considering that the concrete behaviour in environment is very changeable, in this first general part of file are described environment characteristics.

Tab 1 - Expeditious file

IDENTIFICATIVO	
1.1 denominazione -natura del bene -periodo di realizzazione 1.2 localizzazione -regione -provincia -comune 1.3 riferimenti catastali -foglio -particella 1.4 confinanti -foglio -particella 1.5 destinazione d'uso	ANAGRAFICO-IDENTIFICATIVO
2 georeferenziazione -coordinate -sistema di riferimento -toponomastica -dati catastali	CARATTERISTICHE GENERALI (1)
LOCALIZZAZIONE	
3.1 caratteristiche geomorfologiche 3.2 profondità dell'acqua 3.3 livello sul medio-mare	CARATTERISTICHE GENERALI (2)
4.1 ambito territoriale 4.2 definizione unità strutturale per gli aggregati edilizi 4.3 caratteristiche ambientali geografiche	CARATTERISTICHE GENERALI (3)
DANNI ESTRINSECI	
5.1 caratteristiche ambientali lagunari -frequenza del fenomeno acqua alta 5.2 caratteristiche ambientali lagunari antropiche -prossimità di un canale soggetto a traffico	CARATTERISTICHE GENERALI (4)
6.1 caratteristiche ambientali antropiche -prossimità di complessi industriali, viabilità primaria 6.2 caratteristiche ambientali atmosferiche -presenza di venti dominanti	CARATTERISTICHE GENERALI (5)

A second analytic part of the file, includes direct and indirect inquiries on the element.

Every file is referred to only one concrete element identified by a code in the considered architecture (Figs. 8, 9).



Figs. 8, 9 - Samples individuation

The file has the aim to give a methodology to surveyed data, either through macroscopic analysis or historic search, including informations like tecnic building but also possible transformations. A specific section of the file is dedicated to description of different kind of concrete casting, with particular attention to the characteristics which could be linked to pathologies of decay like for example thickness or presence of reinforced bars.

The following part has informations related to surface, varying in texture, working tecnic and final treatment, and is linked to photographies and graphic symbologies.

The concrete texture is carefully analyzed as it is strictly connected to decay pathologies depending from physical, chemical or mechanical characteristics, and also because of aesthetic value.

The final file describes the alterations surveyed on the element.

Is it then necessary to link every file to a graphic support able to give geometrical and dimensional informations and also to describe concrete appearance and materical consistence.

Photography can document surfaces in association with survey through photogrammetry.

Photogrammetry technique which can be used is based on strict straightening of photographic digital pictures, using specific softwares.

From photographical survey is possible to extract and select many informations like dimensions and arrangement of formwork benches, able to create complex textures and patterns.

After the geometrical survey follows concrete characterization. This description is based on macroscopic analysis thanks to knowledge of building techniques.

However these informations need to be confirmed by more deepened diagnostic inquiries. For each data is found the type of inquiry that leads to obtain more specific informations.

codice campione				
Q_01				
inquadramento generale				
elemento	caratteristiche di esposizione	collocazione	impegno strutturale	getto
setto	zona inguine ambiente non confinato, esterno non protetto	il terra orientamento fronte principale est	a compressione	armato EA a vista GV spessore medio
descrizione macroscopica				
mix-design	tecnica di posa in opera	texture	lavorazione superficiale	trattamento del profilo
aggregato tondi sabbie fine 0-3 mm sabbie 3-5 mm ghiaie 5-20 mm ghiaie 20-40 mm AT presenza di aggregati sili in pietra d'Istria	calcestruzzo a strati realizzato in strati di altezza variabile CS calcestruzzo vibrato CV	ruvida superficie che presenta irregolarità, aree macroporose e sbocciature TR presenza dell'impronta delle tavole della cassaforma, direzione delle tavole orizzontale TO	disarmo con uso di dicamanti DD superficie non lavorata NL in parte superficie a sasso lavato SL	spigolo vivo PV presenza di tessere vitree PT
colore				
matrice RAL 7038 inerti RAL 9002				

alterazioni riscontrate				
1. fessurazioni	2. ferri di armatura scoperti	3. delaminazioni superficiali del c/c	4. distacchi del c/c	5. tracce di ossidazione
non rilevate	puntuali agli spigoli del setto murario e a contatto con l'acqua della vasca corrosione generale del ferro ruggine porosa spessore del copriferro variabile da 0 a 15 mm	puntuali in corrispondenza del rigonfiamento dei ferri di armatura spessore da 0 a 3 mm il c/c delaminato tende a sfaldarsi	puntuali di spessore variabile da 5 mm a 4-5 cm in corrispondenza dei copriferri espulsi e nella fascia alla base a contatto con l'acqua della vasca, c/c compatto	puntuali per percolamento dai ferri di armatura corrotti macchie di forma irregolare
6. macchie di umidità	7. patine biologiche	A. interventi pregressi	B. indagini diagnostiche	C. note
diffuse su tutta la superficie soprattutto nei mesi invernali macchie di forma irregolare	poco diffuse localizzate alla sommità e alla base del muro macchie di forma irregolare	non rilevati	pachometro, termografia, pull out, prove microscismiche, profondità di carbonatazione, analisi quantitativa dello ione cloro, verifica del potenziale di corrosione	

Figs. 10 e 11 - Particular of analysis file related to sample at sight

In this system of representation photographical survey is completed by graphic symbologies able to describe materials, processing and diagnostics inquiries to be developed.

Observation of the emerging data from the analysis leads to investigate the

decay of the concerning the element.

In this reading phase is necessary to look carefully at material's characteristics as it is possible to define as concrete defects what could be in fact an architect casting design decision .Therefore macro porosity is pointed out as a characteristic not as a form of decay.

Graphically concrete alterations are resumed to eight phenomena, localized and numbered on each front. Also in this case, diagnostics inquiries are fixed to deepen pathology knowledge (Fig. 12).

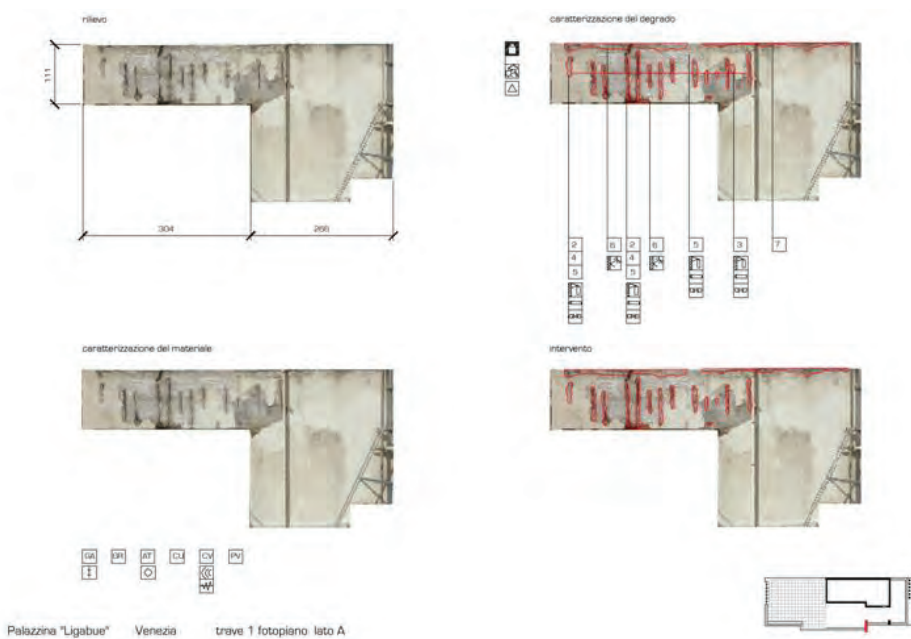
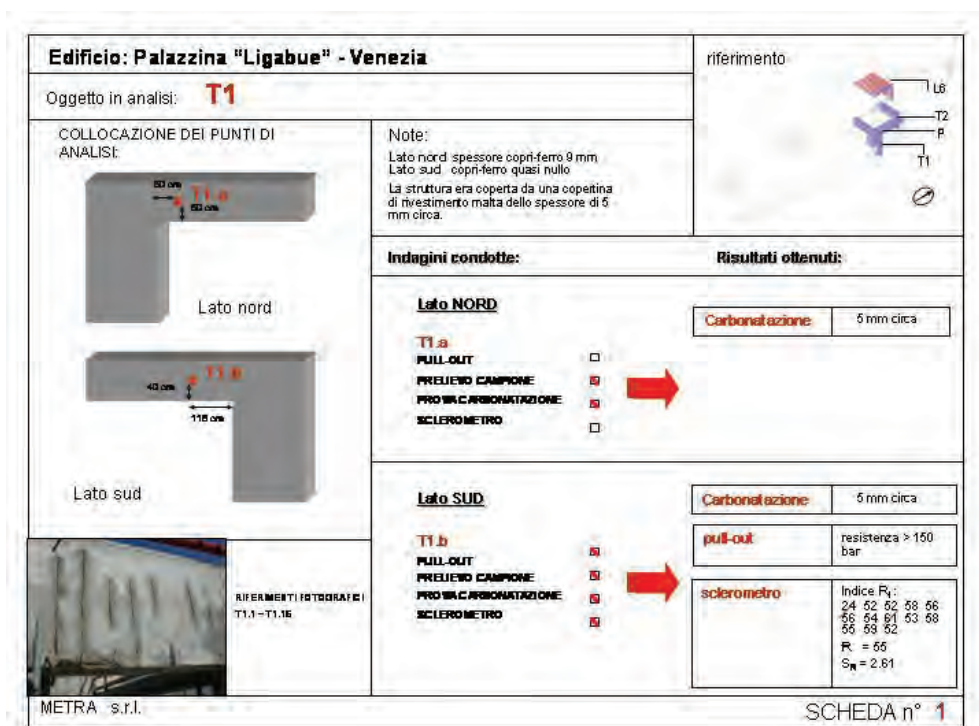


Fig. 12 - Orthogonal-photographical survey necessary to show dimensions, concrete characterization, decay characterization and possible intervention

Photographical survey is moreover able to show the kind of intervention, submitted to a concrete check and defined according currently methodology in preserving deteriorated concrete, by previous efficiency test of most updated solutions.

Thanks to these results coming from diagnostics analysis it is possible to choose the possibility to avoid a direct intervention for a monitoring able to check the decay evolution in time (Figs. 13-14).



Edificio: Palazzina "Ligabue" - Venezia

Risultati dell'analisi chimica dei 4 campioni di cls prelevati

Campione	Fluoruri (%)	Cloruri (%)	Nitriti (%)	Nitrati (%)	Fosfati (%)	Solfati (%)	Ossalati (%)	Potassio (%)	Ammonio (%)	Sodio (%)	Magnesio (%)	Calcio (%)
T1.b	0.045	0.004	0.000	0.018	0.000	0.400	0.000	0.100	0.000	0.028	0.000	0.849
T2.a	0.012	0.020	0.000	2.216	0.000	0.428	0.000	0.027	0.000	0.007	0.000	1.897
P	0.000	0.004	0.000	0.000	0.000	0.074	0.000	0.051	0.000	0.016	0.000	0.642
L6.a	0.014	0.005	0.000	0.000	0.000	0.143	0.000	0.000	0.000	0.000	0.000	2.750

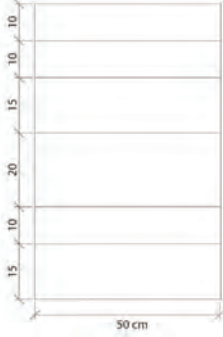
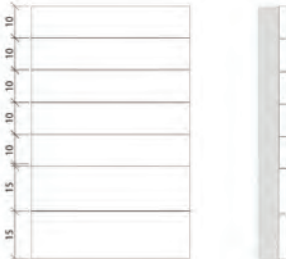
Figs. 13-14 - Results of diagnostics analysis enveloped on roof top of "Ligabue" building

4 Carried out of search: experimental test

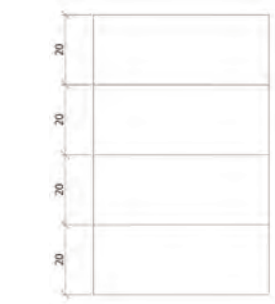
As a first step has been started a test in collaboration with "Centro Formazione Maestranze Edili" and MAC-Degussa in Treviso, which aim is to allow a critical reflection about conservation possibilities in reinforced concrete considering the compatibility between the most updated technological solution available in market resources and the necessity to preserve characteristics of several surveyed surfaces, and at same time qualified workers training able to intervene on these concrete elements.

Four concrete samples of same dimensions have been made with reinforced rebars and different mixing, like surveyed concrete surfaces and so characterized by different textures.

First step is to design suited formwork to reproduce a similar surface of surveyed concrete (Tab. 2).

Campione n. 1			
	<p>cassaforma: tavole in legno sabbiate al fine di evidenziare le venature tavole che presentano il segno del taglio con sega a nastro</p>	<p>mix design 35 Kg cemento 15 Kg ghiaino 30 Kg inerti in pietra d'Istria di granulometria: pietrischetto 5-10 mm 20 Kg sabbia rapporto A/C: 0.6 pezzatura: sabbia 0-3 mm ghiaino 3-5mm ghiaietto 5-20mm ghiaia >20mm</p>	<p>note: il calcestruzzo dovrà essere vibrato con mazzuola la lavorazione superficiale del calcestruzzo a disarmo avvenuto prevederà il "lavaggio" con rimozione della boiacca solo su alcune fasce</p>
Campione n. 2			
	<p>cassaforma: tavole in legno grezzo, non piallate tavole che presentano il segno del taglio con sega a nastro</p>	<p>mix design 35 Kg cemento 15 Kg ghiaino 30 Kg ghiaietto 20 Kg sabbia rapporto A/C: 0.6</p>	<p>note: le tavole dovranno essere separate tra loro, la distanza dovrà essere di circa 5-8 mm in modo tale da permettere la fuoriuscita di biacca tra tavola e tavola</p>

Tab. 2 - Formwork and casting design

<p>Campione n. 3</p> 	<p>cassaforma: tavole in legno grezzo, non piallate che presentano il segno del taglio con sega a nastro</p>	<p>mix design 35 Kg cemento 15 Kg ghiaio 30 Kg ghiaietto 20 Kg sabbia rapporto A/C: 0.6</p>	<p>note: le tavole dovranno essere poste in modo sfalsato rispetto al piano verticale, si possono usare tavole di diverso spessore oppure sovrapponendo in parte tavole dello stesso spessore</p>
<p>Campione n. 4</p> 	<p>cassaforma: tavole in legno senza particolari lavorazioni</p>	<p>mix design n.1 35 Kg cemento 15 Kg ghiaio 30 Kg ghiaietto 20 Kg sabbia rapporto A/C: 0.6 mix design n.2 35 Kg</p>	<p>note: Il getto prevede l'impiego di due impasti caratterizzati da differente granulometria, una più fine e una più grossa da gettare in modo alternato</p>

Tab. 2 - Formwork and casting design

Description of first testing steps:

Figs. 15-17 - Choice of benches (sand-blasted, not planed, cutted with belt saw); building of formworks and reinforcing bars



Figs. 18-20 - Closing formworks, arrangement for casting and choice for mix design





Figs. 21-23 - Casting and vibrating concrete with mallet



Figs. 24-25 - Samples n. 2 - 3 - 4 and particular of sample 3 surface

Conclusions

Choice and analysis of study cases allows to realize a survey model and to take over geometric and materic data of considered elements. In parallel diagnostics inquiries has been done allowing to characterize the nature and the level of concrete alteration.

This step allows to define rules of procedure to realize sperimental test, now in progress, on sample realized in laboratory.

References

- Albani F., Bertolini L., Manera M., Valvassori F., La conservazione dei materiali dell'architettura contemporanea: calcestruzzo armato, pietra e rame in un edificio di Figini Pollini a Milano, in (a cura di) Biscontin G., Driussi G., Scienza e beni culturali XX 2004, Architettura e materiali del novecento. Conservazione, Restauro, Manutenzione, Atti del convegno di studi, Bressanone 13-16 luglio 2004, Arcadia Ricerche, Venezia, 2004
- Andrade C., Alonso C., Misura in situ del grado di corrosione delle armature metalliche, "L'Industria Italiana del Cemento", n. 9, 2001
- Berlucchi N., Catacchio C., Restauro di un'architettura moderna a Venezia: la sede dell'INAIL di Giuseppe Samonà, spunti di riflessione, in (a cura di) Biscontin G., Driussi G., Scienza e beni culturali XX 2004, op.cit
- Businaro E., Consolidamento in opera dello strato superficiale di strutture cementizie, "L'Edilizia", n. 9, 1990
- Calebich E., Problematicità della conservazione dell'architettura diffusa nel novecento: alcuni casi a Venezia, in Pratali Maffei S., Rovello F. (a cura di), Il moderno tra conservazione e trasformazione, Atti del Convegno Internazionale, Trieste, 5-8 dicembre 2005, Editreg, Trieste, 2005

- Coppola L., La diagnosi del degrado delle strutture in calcestruzzo, "L'Industria italiana del cemento", n. 10, 1993
- Coppola L., Criteri di scelta delle malte per il restauro delle strutture in calcestruzzo armato, "L'Industria Italiana del Cemento", n. 1, 2001
- Favero A., Guida ai prodotti per la protezione superficiale dei manufatti in calcestruzzo, "L'Edilizia", n. 3/4, 1999
- Garancini L., Ursella P., Calcestruzzo. I trattamenti per la protezione delle superfici, "L'Edilizia", n. 3/4, 1999
- Hemmons P.H., Vaysburd A.M., Corrosion protection in concrete repair: Myth and reality, "Concrete International", March, 1997
- Lazzari L., Pedefferi P., Protezione catodica, McGraw-Hill, Milano, 2000
- Mailvaganam N.P., Cusson D., Materiale e soluzioni per un restauro durevole delle strutture in calcestruzzo, "L'Industria Italiana del Cemento", n. 12, 1996
- Morano S.G., Il consolidamento e la riparazione di strutture in c.a. con malta a base cementizia, "L'industria Italiana del Cemento", n. 5, 1998
- Nelva R., Vancetti R., Elementi di facciata in cls armato. Valutazioni di durabilità delle reintegrazioni, "Arkos", n.3, 2001
- Nelva R., Vancetti R., Metodi di valutazione della durabilità di tecniche di reintegrazione con malte di elementi di facciata in conglomerato cementizio armato, in (a cura di) Guido Biscontin, Guido Driussi, Scienza e beni culturali XX 2004, op.cit.
- Pastore T., Sistemi di monitoraggio della corrosione di strutture in c.a. , in "L'Edilizia", n. 1/2, 1993
- Pedefferi P., Protezione e ripristino di strutture in c.a. interessate dalla corrosione, "L'Edilizia", n. 1/2, 1992
- Pedefferi P., Bertolini L., La durabilità del calcestruzzo armato, McGraw-Hill, Milano, 2000
- Siviero E., Cantoni R., Forin M., Durabilità delle opere in calcestruzzo, F. Angeli, Milano, 1996

FROM ARTIFICIAL STONE TO REINFORCED CONCRETE II: PROJECT FOR EXPERIMENTAL INVESTIGATION PROTOCOL FOR THE CHARACTERIZATION OF DECAY PHENOMENA

Paolo Faccio¹, Greta Bruschi¹, Paola Scaramuzza¹

¹ *Dipartimento di Costruzione dell'Architettura, Università IUAV di Venezia*

Riassunto

Questa fase della ricerca ha l'obiettivo di sviluppare un adeguato protocollo di indagini sperimentali al fine di caratterizzare e comprendere i processi di degrado che avvengono nei calcestruzzi armati con particolare accento su quelli a facciavista.

L'individuazione dei meccanismi di degrado risulta infatti necessaria alla sperimentazione di prodotti e metodologie da impiegare per migliorare lo stato di conservazione del calcestruzzo.

La sperimentazione prevede l'invecchiamento artificiale di modelli in c.a. di composizione il più possibile simile a quelli rilevati nei casi studio precedentemente trattati e caratterizzati da diverse textures.

I campioni sono stati assoggettati a cicli di invecchiamento naturale e indotti artificialmente, al fine di simulare l'azione di sali solubili di natura marino o provenienti dal suolo, sottoponendoli anche a cicli di gelo-disgelo.

Il monitoraggio costante delle superfici attraverso rilevamenti fotografici, prelievo di campioni per la caratterizzazione dei materiali costitutivi, prove ultrasoniche e sclerometriche, consente di fornire le prime osservazioni in merito.

Parallelamente alla sperimentazione di laboratorio lo studio prosegue organizzando i dati raccolti in fase di rilievo al fine di definire la struttura del sistema esperto per la diagnostica.

Abstract

Aim of this phase of research is the development of a proper protocol for the experiment. It enquires the characterization and understanding of diverse degeneration pathologies for reinforced concrete.

Characterization of decay pathologies is a necessary step for testing technological solutions in order to improve the conservation of concrete.

Experiments are made to foresee artificial ageing of concrete samples made by similar mixing of surveyed ones.

Aged sample, made to simulate salt action, have been underwent to icy-thaw cycles. Surface monitoring through photography, ultrasonic and sclerometric

surveys, allows first results.

At the same time the research goes on organizing surveyed data for the definition of a structure for a specialist diagnostic method.

1 Introduction

The article shows the developing of the research started during summer 2005. The research is focused on the characterization of decay processes and on intervention methodologies for reinforced concrete.

Aim of the research is the development of a proper protocol of experimental investigation for the comprehension of the decay mechanics and for the investigation of the time structure of the decay process. All these data represent a necessary issue for the experimentation of methodologies and for the testing of different products for improve concrete conservation.

Laboratory research has been followed from dott. Monica Favaro (ICIS, CNR, PADOVA), it has involved the studies of the chemical, mechanical and physical characteristics of different test proof, each one specifically prepared, and capable to permit the identification of decay processes and limit values for the revelation of the beginning of any alteration phenomena.

2 Experimental methodology

The results of different surveys have been an important way to identify the complete carbonation of surfaces and to reveal the presence of sulphates, chlorides, nitrates in study cases.

The investigation has brought the specific proof tests to a forced ageing for simulating the decay action of marine soluble salt or salt coming from the soil. Furthermore some concretes, after the soluble test has been put under a process of icy-thaw cycles.

All the operations done during the ageing phase consist in the continuous control of the surface of the tests through the production of images, in the constant monitoring the physical - chemical condition of the surface through the optical microscope and electronic scanning microscope observation, microanalysis, EDS(x rays micro test), dust x rays diffractometry, analysis of different components through EC (ionic chromatography), for monitoring decay transformation of components and qualitatively characterize the possible decay signs, in the study of material solidness with ultrasonic and sclerometric measurement for the mechanical properties variation monitoring of the decay.

Once test proofs and surfaces to investigate are ready, images of the surfaces are taken before ageing process (time 0) and sample are taken for the characterization of the material with IC SL, SS, SEM (electronic scanning microscope), XRD (x rays diffraction).

Not tested surfaces, on the short sides are made waterproof by Fluormet CP to avoid the iron oxidation of could affect the saline solutions.

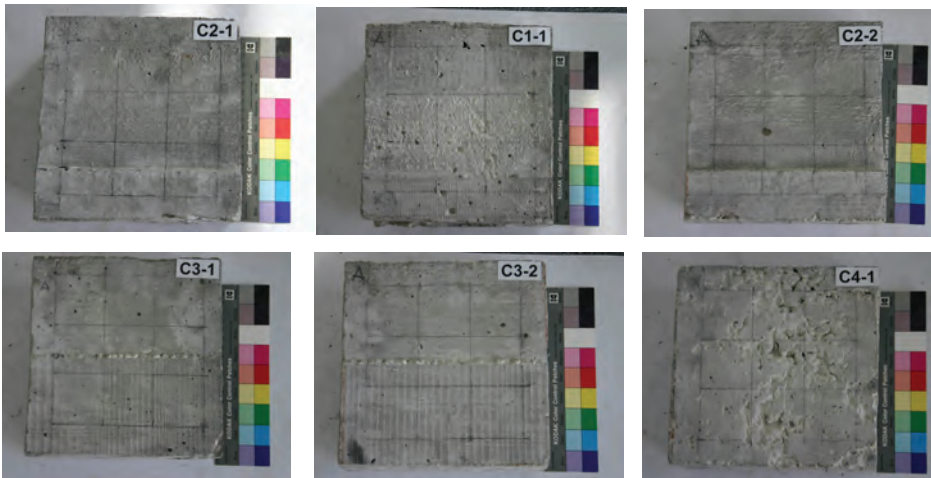


Fig. 1. Test proofs images at time 0.

Images of sample surfaces at $t=0$

sigla campioni		soluzioni saline	invecchiamento nella fase di asciugatura
C1	calcestruzzo Querini	1	Gelo-disgelo camera
C2	calcestruzzo a fasce sfalsate	1 e 2	Ambiente esterno
C3	calcestruzzo a fasce piane	1 e 2	Ambiente esterno
C4	calcestruzzo butterato	1	Gelo-disgelo camera

Tab 1 – Aging project

Soluzioni saline		
1	acqua marina	composizione salina (% w sale/w soluz) NaCl 3.0 MgCl ₂ *6H ₂ O 1.5 Na ₂ SO ₄ *10H ₂ O 1.0
2	suolo	composizione salina (% w sale/w soluz) NaCl 0.1 Na ₂ SO ₄ *10H ₂ O 1.5 MgSO ₄ 1.5 NaNO ₃ 1.0 NaNO ₃ 1.0

Tab 2 – Saline composition

Invecchiamento accelerato		Tempo
Bagno in soluzione salina (acqua marina)	composizione salina (% w sale/w soluz) NaCl 3.0 MgCl ₂ *6H ₂ O 1.5 Na ₂ SO ₄ *10H ₂ O 1.0	3 gg
Camera climatica/gelo disgelo e all'esterno	ASTM C666: -18 a +5°C; ciclo totale: 6h. 1h a +5°C, 2h passaggio da +5 a -18 °C, 1h a -18°C, 2 h passaggio da +5 a -18 °C	2 gg
T = 25°C		2 gg

Tab 3 – Accelerated aging

Ultrasonic survey based on the time measure of the needed time of compression waves to cross the material. They allow to find defects inside solid materials. Moreover, if compared with laboratory tests these surveys allows to indicate the material resistance.



Figs. 2, 3, 4 – Ultrasonic investigation

Sclerometric surveys allows to evaluate on the base on bounce index, the compression resistance of the proof test. They have the limit to investigate only a restricted and superficial area and usually needs other investigation system for data integration.



Figs. 5, 6, 7 – Sclerometric investigation



Fig. 8. Surface sample for analysis IC, XRD, SEM

Fig. 9. Total watering of sample in saline solution, for 4 days in climatic room outside.

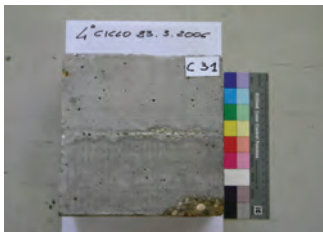
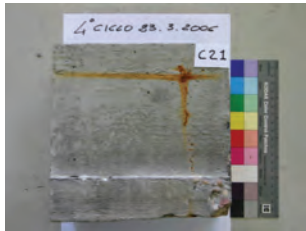


Fig. 10. Surface images after 4th cycle

3 First results after 4 weeks of experiment

Measure of carbonation deepness.

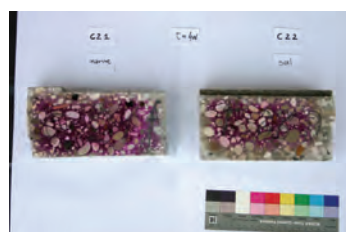
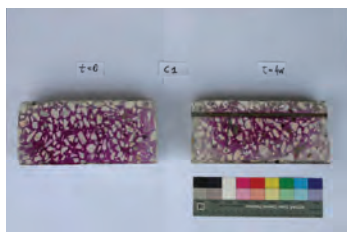


Fig. 11. Concrete 1. Carbonation deepness $T=\text{natural}$ $T=4$ Marine salty solution

Fig. 12. Concrete 2.1 - 2.1. Carbonation deepness with marine and soil salty solution.

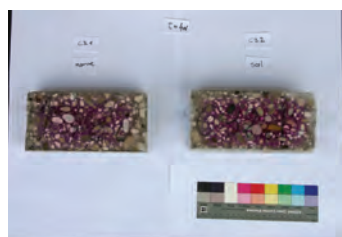


Fig. 13. Concrete 3.1 – 3.2. Carbonation deepness with marine and soil salty solution

Fig. 14. Concrete 4 . Carbonation deepness $T=\text{natural}$ $T=4$ Marine salty solution

Fig. 15. Carbonation surface conditions and saline ageing (Graphics by dott.sa Monica Favaro, (ICIS, CNR, Padova)

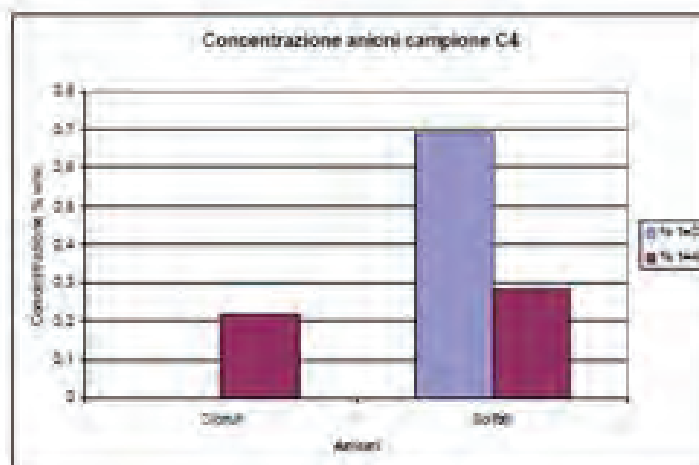
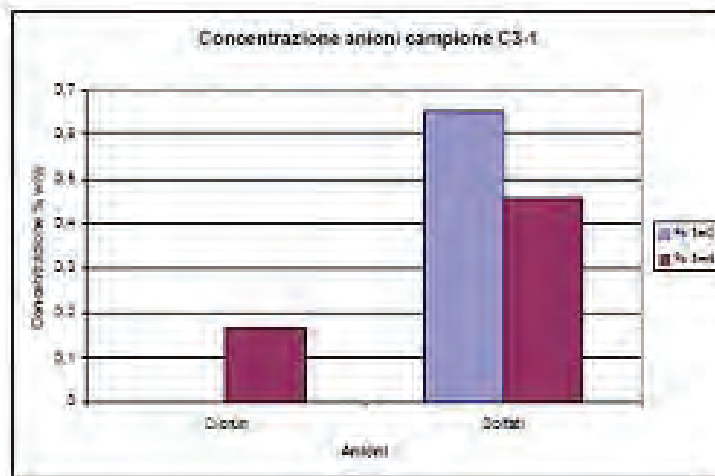
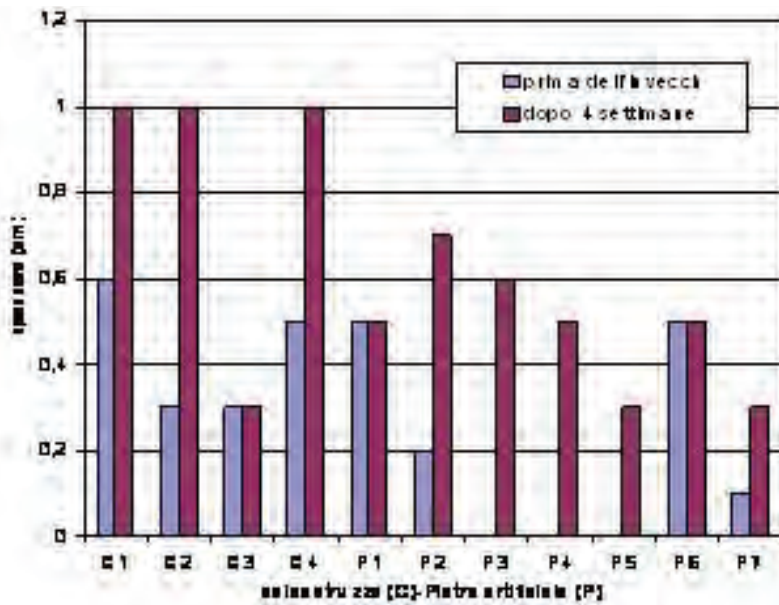


Fig. x. Chloride and sulphate presence after four weeks . After 4 weeks of forced ageing on the surface.

- appearance of minimum chloride quantities.
- contents of soluble sulphates reduces.

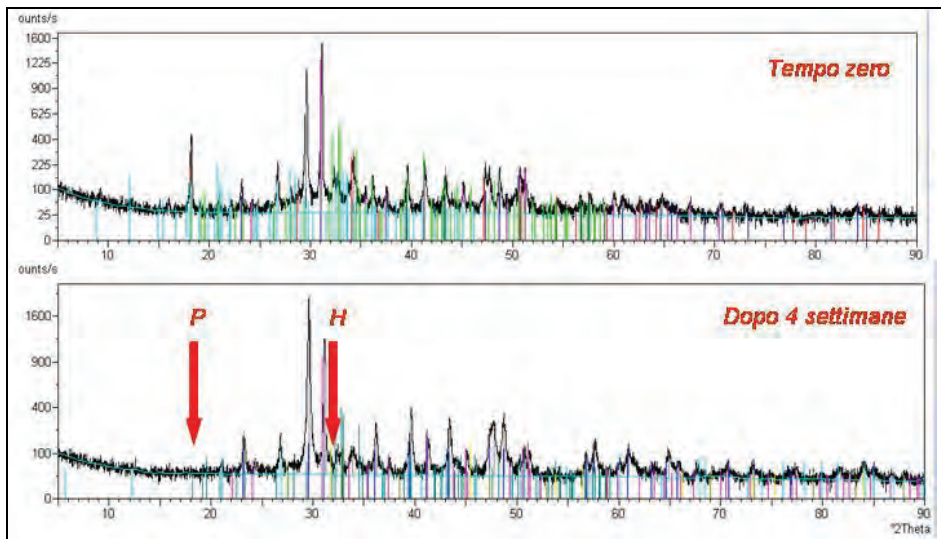


Fig. 17. After 4 weeks of forced ageing on the surface. Portlandit (P) Signal disappears, concrete phase. Halite (H) signal appears, soluble chloride

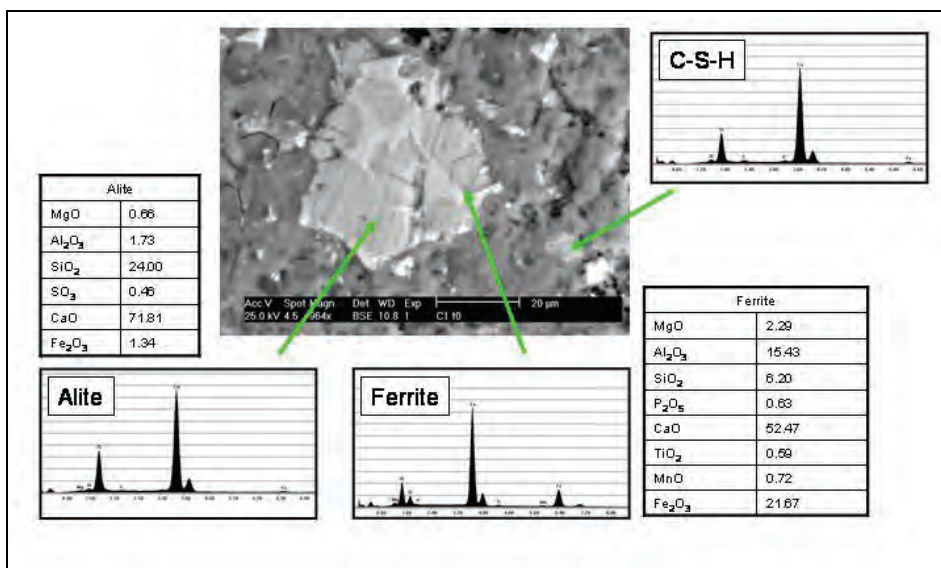


Fig. 18. Observation with electronic microscope and microanalysis EDS
C1 , Querini concrete T=0
Concrete granule, in surface proximity.

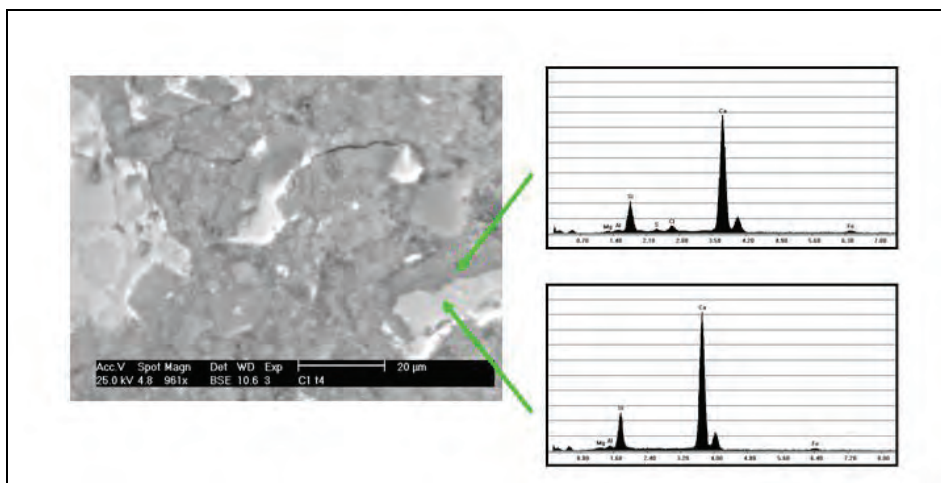


Fig. 19. Observation with electronic microscope and microanalysis EDS
Querini concrete, after 4 weeks of ageing
Concrete granule, in surface proximity, at granule border micro cracks and chloride salt and sulphates are evident.

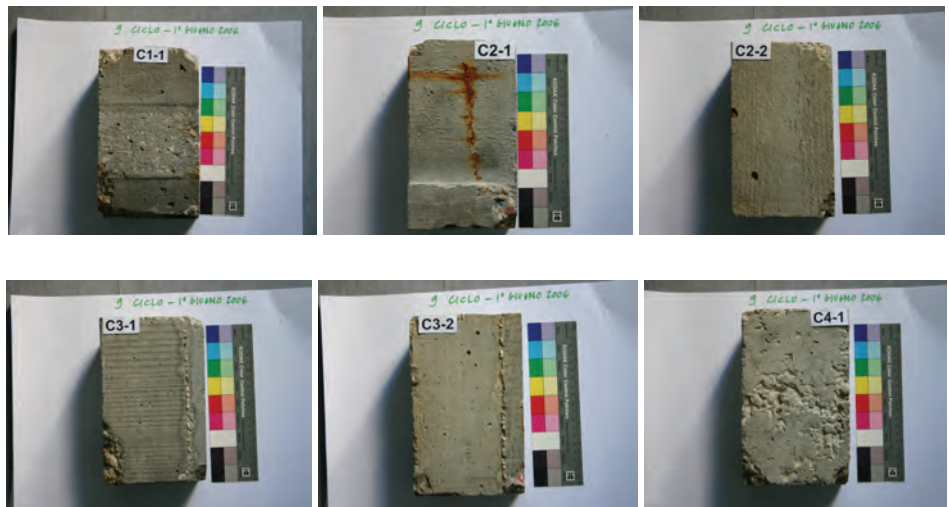


Fig.20. Surface Images after 9th cycle

Fig. 21. Damages after 9th cycle.

Delaminating



cracking and oxidation phenomenon



break up of concrete



porous concrete



Conclusions

Once experimental investigations have concluded and after processing data, research goes on testing products for concrete conservation; the necessity to develop experimentation in relation to controlled application of currently used products and techniques is linked to the possibility of carrying out a consideration based on known data and objective in regard to the possibilities offered by the market of reinforced concrete conservation materials used in contemporary architecture.

References

- Baronio G., Berra M., Bertolini L., Pastore T., Monitoraggio della corrosione di armature in calcestruzzi sottoposti a prove accelerate di degrado, "L'Edilizia", n. 1-2, 1995
- Brunetti G., Tecnologie innovative nella diagnostica del costruito., "L'Edilizia", n. 9, 1992
- Vai A., Finzi F., La carbonatazione in relazione all'ambiente ed al tipo di cemento, Parte I: L'influsso dell'ambiente e del "fattore tecnologico" sulla carbonatazione naturale., "L'Edilizia", n. 10, 1991
- Vai A., Finzi F., La carbonatazione in relazione all'ambiente ed al tipo di cemento, Parte II: L'influsso del tipo di cemento sulla carbonatazione accelerata e su quella naturale., "L'Edilizia", n. 11, 1991
- Vai A., La carbonatazione del calcestruzzo., "L'Edilizia", n. 5, 1992

FROM THE ARTIFICIAL STONE TO THE REINFORCED CONCRETE: DATA SYSTEM PROJECT FOR DIAGNOSTICS

Marco Pretelli¹, Alice Matteini², Isabella Daga²

¹ *Facoltà di Ingegneria, Università del Molise* ² *Dipartimento di Storia dell'Architettura, Università IUAV di Venezia*

Riassunto

La fase attuale di ricerca è finalizzata all'elaborazione e all'interpretazione dei risultati delle prove sperimentali eseguite in situ e in laboratorio con l'obiettivo di definire un percorso metodologico per la diagnostica. I risultati delle indagini di laboratorio effettuate dal LAMA, Laboratorio di Analisi dei Materiali Antichi dello IUAV di Venezia, hanno evidenziato la natura chimico-mineralogica del calcestruzzo e dei fenomeni di degrado avvenuti. La fase sperimentale ha previsto la produzione di 7 campioni di pietra artificiale cementizia, realizzati in collaborazione col Centro di Formazione Maestranze Edili di Mestre, secondo diverse ricette tratte dalla manualistica specialistica dei primi del Novecento. Sulla base dei risultati delle prove di laboratorio è stato sviluppato dall'Istituto di Chimica Inorganica e delle Superfici del CNR di Padova un metodo di invecchiamento artificiale e un protocollo di indagini sperimentali per simulare i processi di degrado che avvengono in situ.

Abstract

The current phase of the research is oriented to define the data processing and the interpretation of the results of the experimental data control, in order to find a diagnostic methodological course. The results of the laboratory research carried out by the LAMA, "Laboratorio di Analisi dei materiali Antichi" of the IUAV Venice University, showed the mineralogical and chemical nature of the concrete and the deterioration phenomena. The experimental data control section provided the production of 7 samples made by artificial stone on the basis of different recipes taken from the specialistic reviews of the early XX century. The samples were realized in collaboration with the "Centro di Formazione Maestranze Edili" of Mestre. On the basis of the results of the laboratory research, the "Istituto di Chimica Inorganica e delle Superfici, CNR" of Padova has defined an artificial ageing method and a protocol for data collection in order to simulate the realistic deterioration.

1 Introduction

The first part of the experimental data control section provided for the production of 7 samples made by artificial stone on the basis of different recipes taken from the specialistic reviews of the early XX century:

- P1 15 Kg Portland, 29 Kg siliceous sand, 56 Kg siliceous gravel

- P2 13 Kg Portland, 30 Kg siliceous sand, 57 Kg siliceous gravel
- P3 18 Kg Portland, 28 Kg siliceous sand, 53 Kg siliceous gravel
- P4 25 Kg Portland, 80 Kg siliceous sand
- P5 30 Kg pigmented cement, 30 Kg white cement, 30 Kg marble powder, coarse salt, 0,1Kg cadmium orange, 0,06Kg cadmium yellow
- P6 30 Kg Portland, 60 Kg Istrian stone, marble powder
- P7 internal core: 12 Kg Portland, 24 Kg siliceous sand
external core: 16 Kg Portland, 30 Kg siliceous sand

The samples were put in wooden formworks sized 1m x 0,2m x 0,2m with a volume of 0,04m³ and were reinforced with 6mm iron rod; after the maturing phase (>28 days), they were unarmored (Fig. 1) and treated with the typical surface finishings of the natural stone, i.e. the “bocciardatura”, the dressing and the muriatic acid washing. Afterwards, the 7 samples were cut in blocks sized 20x20x10 cm (Fig. 2) and the surfaces not interested in search were treated with an hydrophobic substance (Fluormet CP) in order to arrange them for the artificial ageing tests.



Fig. 1 The opening of the wooden formworks



Fig. 2 The cutting of the samples.

2 Artificial ageing tests

Before the artificial ageing tests, photos of the sample's surfaces were collected (Fig. 3) and concrete portions were taken in order to characterize the material through the IC, SL, SS, SEM, XRD analysis.

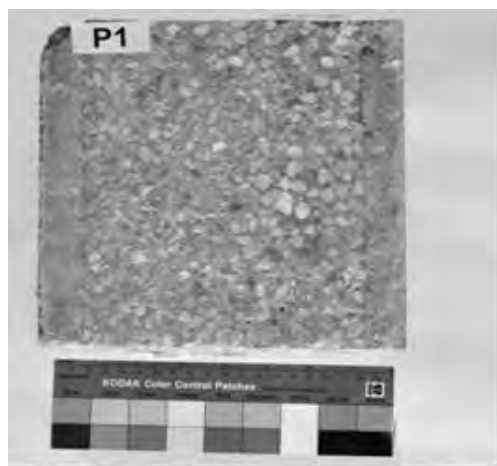


Fig. 3 Photographic relief of the sample P1

The artificial ageing tests provided for the samples imbibition with a saline solution simulating sea water and for the drying of the P1, P2, P3, P5, P7 samples in exterior environment, whereas the P4, P6 were dried in a climatic room (Tab. 1):

Artificial ageing tests		Time
Imbibition with the saline solution	Saline solution (% w salt/w solut)	3 days
	NaCl 3.0	
	MgCl ₂ *6H ₂ O 1.5	
	Na ₂ SO ₄ *10H ₂ O 1.0	
Climatic room/chill-thaw cycles	ASTM C666: -18 a +5°C; cycle: 6h. 1h +5°C, 2h from +5 to -18 °C, 1h -18°C, 2 h from +5 to -18 °C	2 days
T = 25°C		2 days

Tab. 1 Artificial ageing tests

At the end of each cycle, the monitoring of the samples superficial morphology was carried out and the photographic relief of each sample was taken. Moreover, concrete portions were drowed to control the deterioration of the constituent parts and to find out the deterioration markers through the IC, XRD and SEM analysis. Finally, ultrasonic (Fig. 4) and sclerometric tests (Fig. 5) were carried out in order to estimate the mechanical properties variation closely connected with the deterioration.



Fig. 4 Ultrasonic test.



Fig. 5 Sclerometric test.

Among the phenomena of degradation, the most dangerous and diffused concrete deterioration type turns out to be the iron reinforcing rods oxidation, since it could determine the cracking of the conglomerate. This phenomenon may be triggered by the carbonation of the conglomerate because the concrete is no more protective towards the iron rods once it has lost its alkalinity. The constant monitoring of the deepness of the carbonation showed that the phenomenon has increased considerably during 4 weeks (Fig. 6).

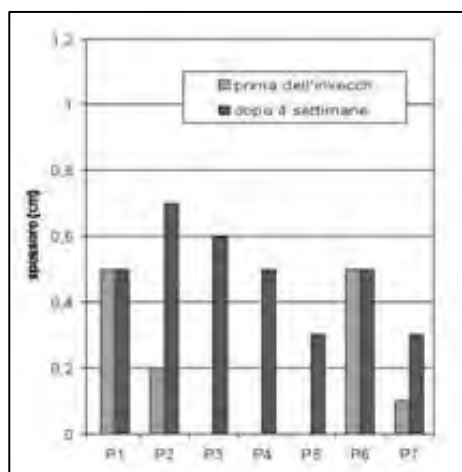


Fig. 6 The progress of carbonation after 4 weeks of artificial ageing tests.

The deepness of the carbonation was determined by means of the phenolphthalein test. A film of the alcoholic solution of phenolphthalein was sprayed on the surface of the sample; the carbonated conglomerate doesn't modify its color, whereas the conglomerate not yet carbonated assumes the typical color of phenolphthalein in an alkaline media (Fig. 7, Fig. 8).

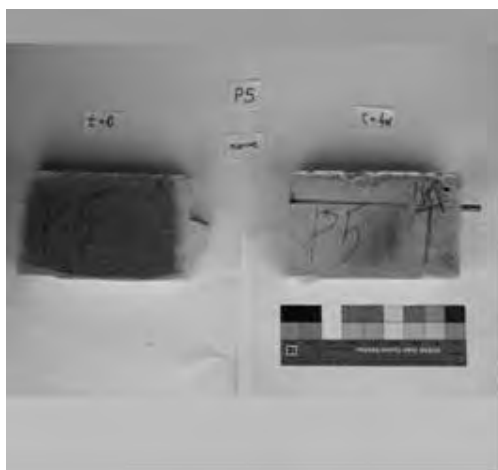


Fig. 7 The phenolphthalein test on sample P5 at the beginning of the experimental data control section ($t=0$) and after 4 weeks ($t=4$).

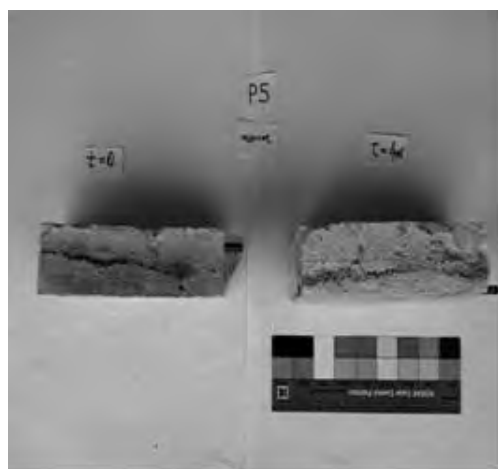


Fig. 8 The phenolphthalein test on sample P5 at the beginning of the experimental data control section ($t=0$) and after 4 weeks ($t=4$).

The trigger of the corrosion reaction may be determined also by means of the critical concentration of chlorides. Its amount was measured through chemical analysis of portions of material, showing that very small quantity of chlorides appeared during 4 weeks.

Fig. 9 The concentration of chlorides in sample P7 after 4 weeks of artificial ageing tests.

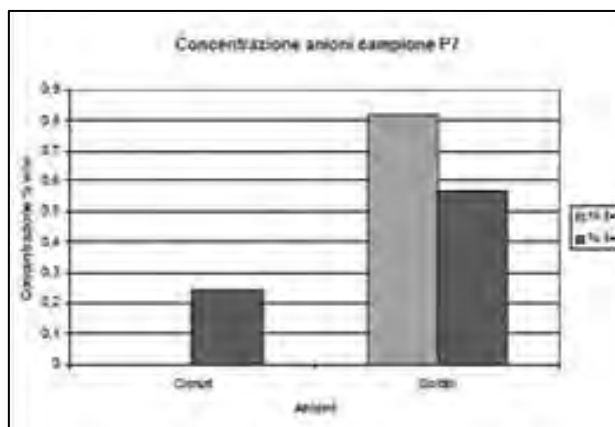
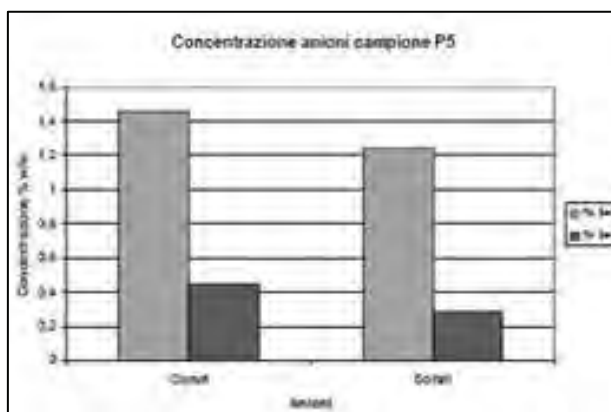


Fig. 10 In sample P5 the concentration of chlorides decreased because of the initial large amount of chloride salt used in setting.



Conclusions

The comprehension of the deterioration phenomenon and the identification of deterioration markers are the basic principles to develop guidelines for the creation of an expert system of diagnostics which allows one to preserve the artificial stone elements.

References

- Bakker R.F.M., 1992. La corrosione dell'acciaio nel calcestruzzo, in "L'Edilizia", VI, 6, 397-402.
- Bertolini L., Gastaldi M., 1999. La corrosione delle armature, in "Nuovo cantiere", XXXIII, 10, 34-39.
- Collepari M., 2000. Durabilità del calcestruzzo, in "L'industria italiana del cemento", 5, 432-441.
- Collepari M., 1992. Durabilità del calcestruzzo: teoria, pratica e prescrizioni di capitolato, parte I: Cause di degrado di tipo chimico, in "L'industria italiana del cemento", 11, 707-724.
- Collepari M., 1993. Durabilità del calcestruzzo: teoria, pratica e prescrizioni di

capitolato, parte III: Calcestruzzo durevole secondo le norme nazionale ed europee, in "L'industria italiana del cemento", 5, 357-370.

Collepari M., 1991. Scienza e tecnologia del calcestruzzo, Milano.

Coppola L., 1993. Durabilità del calcestruzzo: teoria, pratica e prescrizioni di capitolato, parte II: Cause di degrado di tipo fisico e meccanico, in "L'industria italiana del cemento", 3, 199-209.

Macchia C., Ravetta F., 1995. Degrado e ripristino delle strutture in calcestruzzo, Rimini.

Monosi S., Morioni G., Pauri M.G., Cerulli T., 1993. Diagnosi del degrado delle opere in calcestruzzo, in AA.VV., Calcestruzzi antichi e moderni: storia cultura e tecnologia, Atti del convegno di studi di Bressanone 6-9 luglio 1993, Padova.

Neville M.A., 1980. Le proprietà del calcestruzzo, Firenze.

Pedefferri P., 1999. Corrosione e protezione nel calcestruzzo, in "L'Edilizia", XIII, 7-8, 62-67.

Pedefferri P., 1998. La corrosione per vaiolatura o pitting, in "L'Edilizia", XII, 3, 70-73.

Ravatta F., 1996. Il degrado del calcestruzzo. Seconda parte, in "Nuovo cantiere", XXX, 4, 52-54.

Schiessl P., Bakker R.F.M., 1992. La corrosione dell'acciaio nel calcestruzzo, in "L'Edilizia", VI, 11, 687-690.

Treadaway K., 1992. La corrosione dell'acciaio nel calcestruzzo, in "L'Edilizia", VI, 7-8, 473-479.

“A Venezia si perde il senso della verticale”.

**SOME MEANINGFUL EPISODES OF THE
HISTORICAL DEBATE ABOUT THE NATURE OF THE
GEOMETRICAL ORGANIZATION OF VENETIAN
BUILDINGS**

Angela Squassina

Dipartimento di Storia, Iuav Università di Venezia

Riassunto

Le condizioni ambientali di Venezia e le relative influenze sugli assetti architettonici, sono state oggetto di interesse anche nel passato meno recente. I precedenti storici emersi da una breve disanima della pubblicistica ottocentesca e di quella relativa al dibattito sulle condizioni di Palazzo Ducale dopo l'incendio del 1577, hanno sin da allora indotto a ritenere intenzionali alcune di quelle che vengono percepite come deviazioni rispetto ai principi della regolarità e del buon costruire - in particolare gli assetti in entropiano delle facciate.

L'aspirazione di quanti hanno affrontato questo tema sembra essere stata quella di riconoscere in taluni assetti non convenzionali le peculiari configurazioni di un'architettura fortemente condizionata dalla natura del luogo, con l'impegno a delinearne ragioni e modi di comportamento. Una tesi che non è mai stata accolta all'unanimità ma che continua a suscitare gli stessi interrogativi.

Abstract

The influence of environment on Venice architecture has been for a long time the subject of several studies. A short analysis of 18th century technical literature and of some documents concerning Palazzo Ducale burnt in 1577, shows that some kind of geometrical deviations, in comparison to the rules of regular and good building – especially the deflection toward inside of the façades - have been upfront considered as intentional features.

Those ones, who have read on this matter, aim at acknowledging that some of these non-conventional arrangements may be the peculiar shapes of an architecture which is strongly conditional on the nature of the site; and they are working at defining the reasons and behaviour of such peculiarities. There is no universal agreement on this theory, but now-a-days it is still arousing a great interest.

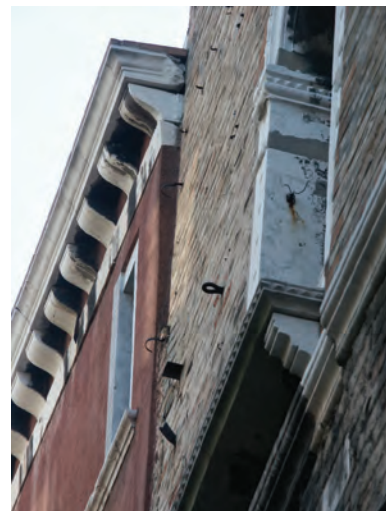
1 Introduction

“Il visitatore, percorso che abbia il magico ed imponente Canal Grande, o vagato per poco attraverso le calli strette tortuose e pittoresche, non dimentica certo le case, i monumenti ed i palazzi contorti e fuori d'appiombo, in lotta con

le regole della statica e quasi atteggiati ad eludere la legge della gravità. Un mio amico giustamente riassume le sue osservazioni dicendo: che a Venezia si perde il senso della verticale.”¹

The character of Venice is a widely handled matter which can be faced according to several reference frames (a literary or scientific manner, rather than an artistic or technical one, etc.), whereby the subject may be differentiating. Besides those tightly architectural and formal facets², the constructive distinctive features due to the peculiar site always drum up³, in addition to the close relation to the water and the resulting structural effects. Within such a complex frame of knowledge, the geometrical structure of Venice architecture is an issue belonging to the wider subject of constructive characters and manners, whereof it is a specification.

A special attention is all along directed to a sort of patchiness which typecasts some buildings, and that was accounted either as a form of structural disorder, or as a constructive mistake, or rather as a corrective solution, along of some changes in the course of works, but also as a specific device.



Figs.1-2 Ca' Corner Zaguri: the deflection toward inside of the gothic palace is emphasized by the contiguous plumbed building.

¹ Max Ongaro, "La principale causa dei danni ai fabbricati di Venezia", in "Monitore Tecnico", n.4 – anno X, Milano, 1904.

² The works of P. Maretto, "L'edilizia gotica veneziana", 1959, E. Trincanato, "Venezia Minore", 1948, E. Arslan, "Venezia Gotica", 1970 are well-known.

³ Among the most recent works we find those ones of F.Doglioni, "Caratteri del costruire i area veneta", IP in "La costruzione del progetto di restauro", Lint, Trieste, 1992; M.Piana "Note sulle tecniche murarie dei primi secoli dell'edilizia lagunare", in F.Valcanover e W.Wolters (a cura), L'architettura gotica veneziana : atti del Convegno internazionale di studio, Venezia, 27-29 novembre 1996, and the graduation thesis of F. Marino, "Notizie sul cantiere e suimodi del costruire nel tardo medioevo a Venezia attraverso lo studio di conti di fabbrica", rel. F. Doglioni, luav, Venezia, aa.1988-89.

An exhaustive research about the historical discussion of this topic implies an high technical mastery of several subject matters, but we can devolve upon some meaningful episodes, although it could be insufficient and requiring further examination, in order to uphold the significance of this enduring argument.

2 Some remarkable literary records

The 16th century discussion about the damages, caused by the fire occurred in 1577 at Palazzo Ducale, is a first opportunity for the most important architects at that time to compare each other and to highlight their own idea about the nature of the geometrical organisation of Venetian buildings.

The main questions of the 16th century debate seem to outcrop in the second half of the 19th century and find their climax after the collapse of the St. Mark bell tower in 1902, when the problem involved the first institutions for the preservation of ancient buildings.

We can ascertain this discussion gains energy every time some harmful event occurs and some new worrying questions about the firmness of the Venetian monuments are posed.

2.1 The 16th century diatribe about the damages due to the fire of 1577 at Palazzo Ducale



Figs.3-4 Palazzo Ducale: some details of the thick wall overarching the open loggia and the tie bars across the porch at the ground floor.

The evaluation of fire damages occurred in 1577 at Palazzo Ducale⁴ involved

⁴ The story of the fire of 1577 is defined by: G. Cadorin, "Pareri di XV architetti e notizie storiche intorno al Palazzo Ducale", Venezia, 1838; G.B. Lorenzi, "Monumenti per servire alla storia del Palazzo Ducale", Venezia, 1869; G.Zorzi, "Il contributo di Andrea Palladio e di Francesco Zamberlan al restauro di Palazzo Ducale di Venezia dopo l'incendio del 20 dicembre 1577" e "Altre due perizie ...", cit., in Atti dell'Istituto Veneto di Scienze, Lettere ed Arti, CXV, 1956-57, pp.11-68 e pp.133-174; G. Lupo, "Principio murario e principio dei concatenamenti: i pareri sul restauro di Palazzo Ducale di Venezia dopo l'incendio del 1577, in "Rassegna di architettura e Urbanistica", Roma, a.32, n.94, 1998.

some of the first architects at that time, who were officially charged of detecting the condition of the palace and describing the intervention suggested.

Because of the architectural and symbolic meaning of the building, the experts introduced their reports as surveys, that is official documents which give the scholars an opportunity to compare the technical approach and mentality of the most skilled minds at that time.

Several works deal with the events occurring in 1577 at Palazzo Ducale, and screening the expert reports, we can find out their idea about those structures, which were felt as a waiver with respect to the constructive regularity.

They were especially inquired for the relief of wall static disorders and for checking the efficiency of the tie bars, in order to understand whether the building was in danger or no.

Some interesting statements about the nature (structural disorders, constructive mistakes, intentional deformation) of those wall-deflections, which were then noticed, are included in the description of walls that were "*parte (...) trovat(e) a piombo, et parte andar un poco fuori et parte andar in dentro.*"⁵

The most part of experts admit the lack of upright walls as a fact not depending on the fire, as "*le cantonade et fazzade non sono mosse più di quello che erano avanti il fuoco.*"⁶

As what concerns the problem of the deflection toward inside of the façades – a feature which every architect detected but only some of them connected to the fire⁷ - in many surveys it was put down to some soil differential partitioning⁸ or it was included among the "*risentimenti (...) per causa del cargo et cadene di ferro arrugginite*", that is a loss of strength of the tie bars⁹.

⁵ G. Zorzi, "Altre due perizie...", cit., pagg.139

⁶ "(...) Bozzetto afferma che (...) gobbe panze et mancamenti (...) non erano stati provocati dall'incendio ma molto prima. (...) Zamberlan afferma che (...) sebbene pendono in dentro (...) questo dice importar poco alla sicurtà sua. (...)", there, pag.139.

⁷ "Giacomo Guberni, proto ai lidi, afferma che i muri hanno patito et per il cascar del coperto et per il foco (...). A sua volta il veronese Francesco Malacrea (...) avendo piombato (...) tutte le muraglie (...) se ben per ora non par che detta muraglia habbi patito, potria però in avvenire scoprire difetto per il carico. ", there.

⁸ "Invece Antonio da Ponte (...) trova che tutte le muraglie hanno patito poco (...) ma il muro del Paradiso (...) venne a calar, et non callando egualmente, ma solo dalla parte verso S. Zorzi, causò la panza in essa muraglia maistra (...)", Cristoforo Sorte (...) afferma di aver veduto li legni grossi di larice (...) essendosi abbrusati vien ad essere dessecurata essa muraglia", there, pagg.141-142.

⁹ "(...) Angelo Marco da Corticelle (...) trovò che le muraglie erano in gran pericolo di cadere, e ciò per causa della travamenta che era marcia.(...) Andrea Palladio (...) trova che le catene di ferro che (...) tengono uniti i volti (...) sono talmente corrose che poco tempo potranno durar che non si

A few of those experts established a relation between the wall deflection toward inside and the typical Venetian way of building, and they said that *“le muraglie che pendono in dentro siano state fatte con questo ordine”*, and hold them as strong enough and *“sicure per mettere il coperto com’era prima.”*¹⁰

The most exhaustive survey belonging to G. A. Rusconi, who recognized a frame of reasons for the structural disorders of Palazzo Ducale and he suggested a strengthening intervention by means of the replacement of every broken tie bar¹¹. Besides, he rejected the recreation of the wall facing S.Giorgio, which was worrying all hands because it was inclined toward inside and partially toward outside¹².

Rusconi, on the contrary, explained this complex outline as the result of a constructive custom: *“Al terzo capitolo rispondo che le muraglie (...) verso S. Giorgio, et la piazza son così grosse nel piede, come nella cima, et danno indentro nella parte di sopra et in fuori in quella di sotto, et le doi altre che sono sopra la corte (...) hanno le condizioni medesime (...) le quali tutte cose furono fatte dal maestro con buonissime ragioni, perché facendo che la parte interiore delle muraglie desse dentro nella fabbrica, (...) bisognava anco che la parte di fuori d’esse desse medesimamente dentro (...) di necessità era bisogno che la fabbrica fosse contratta verso la cima, la qual cosa non solamente da questo fu osservata in questo Palazzo, ma ancora per maggior fortezza e decoro delle fabbriche da Greci, da Latini e da Romani fu posta in consuetudine, et l’esempio di questa cosa fu preso da coloro dal corpo della piramide, el quale per la forma contratta che lui ha è atto a resistere contro il tempo atternamente sopra ogni altro corpo.”*¹³

spezzino (...e) li traviamenti (...) che entrando nel muro delle fazzade le fortificavano incredibilmente (...) abbruggiat(i) nelle teste dove facevano quel buon effetto (...) e quelle non abbruggiate sono marcie (...)”, there., pagg.141-142.

¹⁰ Besides Rusconi, other architects held the wall deflection toward inside as an intentional feature. They were Simone Sorella e Antonio Palmari, who said *“tutte le muraglie sono buonissime (...) sebbene (...) in dentro onze tre in quarto in circa (...) fatte con quest’ordine”*, there, pag.140.

¹¹ Rusconi’s regard for the so-called building vulnerabilities emerges when he suggested *“di legar le muraglie quanto più presto fosse possibile con legni di conveniente grossezza quali fussero almanco sei, posti a traverso di esse muraglie fra li spatii dove si hano da poner le catene, et sicurate in buona maniera sopra di quelle per ogni accidente di terremoto o vento sferzevole.”*, Prima deposizione di Gio. Antonio Rusconi in G. Zorzi, in *“Altre due perizie”*, cit., pag.162.

¹² *“Andrea Palladio dice che (...) la più alta (muraglia) di tutte (...) pende parte in dentro et parte in fuori et ha diverse fisure fatte per la gran furia del foco (...)”*, in G. Zorzi, *“Il contributo di Andrea Palladio e di Francesco Zamberlan al restauro di Palazzo Ducale di Venezia dopo l’incendio del 20 dicembre 1577”*, in *Atti dell’Istituto Veneto di Scienze, Lettere ed Arti*, CXV, 1956-57, p.62.

¹³ G. Zorzi, *“Altre due perizie...”*, cit., pag.167.

Rusconi set up in this way a downright theory about Venice gothic architecture, focused on two main principles: the “contracted form of the facades” and the “principle of concatenation”, whereas the “*catene (...) sono i nervi della fabbrica*” and “*quando le travemente saranno legate insieme sì che siino come d’un pezzo, et fermati con i lor capi nelli estremi muri, (...) qual fortezza si troverebbe fatta con tanti legami come questa, che di sicurtà fusse eguale?*”¹⁴

Rusconi gave evidence to his ideas by demonstrating the mechanisms collapsing such a structure as unlikely, because “*(...) dovendo cadere esso palazzo o bisognerebbe chel trabaltasse, o veramente ch’el muro slamasse da quello(...).*”¹⁵

The discussion arisen from the fire of Palazzo Ducale engendered a kind of strife between the rebuilding promoters and the conservation supporters. But instead of simply putting the figures of Palladio and Rusconi in opposition¹⁶, it would be better to compare - following G. Lupo¹⁷ - the two principles they followed, that is the classical principle of “masonry” and the principle of “concatenations”.

The first one representing the ancient pyramidal system, that is based upon the structural efficiency of the wall mass, so that “*il minore conviene per natural*

¹⁴ Rusconi shew a conservative attitude toward those changes of the original structure, due to some no-more-in-progress static problems: “il rimedio migliore che a queste si potria fare, saria di confermarle in quell’essere con far che le catene che le ritengono (...) fossero ben ferme (...) perché non callando più il muro suddetto non è anco possibili che esse colonne si movino altamente dal loco suo.”, Prima deposizione di Gio. Antonio Rusconi ..., cit., pag.164.

¹⁵ “Quanto al trabaltare dico non esser possibile perché avendo fatto tal resistenza le catene di ferro et di legno (...) bisognerebbe che tal disposizione di muro, la qual dà in dentro nella parte di sopra, desse in fuori et che puoi la istessa parte avesse tanto peso che di gran lunga el superasse tutto il restante, che pesa la fabbrica (...) et (...) movendosi il tutto sforzatamente si verrebbe a trabaltare (...). Quanto puoi il slamar il detto muro, dico similmente essere impossibile (...) se somiglieremo il palazzo alla stadera (...) dovendosi slamar il detto muro bisognerebbe (...) ch’esso (...) bilanciasse (...) il muro della corte, il che non è possibile, che la parte attaccata in corto fusto, possi più che ‘l tutto attaccato in lungo fusto (...)”, Prima deposizione di Gio. Antonio Rusconi ..., cit., pag.170. Questi principi sono efficacemente illustrati da schemi grafici esplicativi in G. Lupo, “Principio murario e principio dei concatenamenti: i pareri sul restauro di Palazzo Ducale di Venezia dopo l’incendio del 1577, in “Rassegna di architettura e Urbanistica”, Roma, a.32, n.94, 1998.

¹⁶ G. Zorzi aims at confuting the thesis – in his opinion spread by Temanza and then handed down – according to which Palladio suggested the demolition of the Palace: “(...) il pensiero dell’architetto vicentino fu ben diverso da quello (del) Sorte e (del) de Grandi (...) Andrea da Valle e Paolo da Ponte, che dopo aver affermato che il Palazzo era deforme e di maniera barbara (...) avevano addirittura proposto di ruinar tutto sino alle fondamenta per rifar una fabbrica di tal fortezza e bellezza che saria la più bella del mondo”!, G. Zorzi “Il contributo ...”, op.cit., pag.48.

¹⁷ G. Lupo. Op.cit.

*necessitate ceder al maggiore*¹⁸. The second principle leading to an architecture made of connected parts working together, that *“portava a concepire la costruzione sempre più come una macchina composta da un insieme di parti dove il problema maggiore era costituito dalla concatenazione degli elementi (...) contemplava la possibilità del movimento delle strutture (...) ricorrendo all'uso delle catene di ferro per ovviare (...) alla mancanza di salde connessioni murarie.”*¹⁹

2.2 “Le principali cause de’ danni ai fabbricati di Venezia”. The resumption of the debate in the 19th century

Ruskin conjured up the incident of fire in 1577 and wrote about it in the chapter of “The Stones of Venice” dedicated to Palazzo Ducale, whence he praised the qualities of Giovanni Rusconi who argued a conservative thesis²⁰.

But again, in the second half of the 19th century, the geometrical organization of Venetian monuments was in dispute among the foremost figures of conservation. The authors turned out to be split up, and dissenting opinions ensue from a short analysis of some writings.

Among them Giacomo Boni’s, who agreed with Ruskin bringing the debate about Venetian constructive peculiarities back to the 16th century. The incident of 1577 fire at Palazzo Ducale reminded Boni the mean authorities at that time had criticized the constructive system of the Palace²¹. This fact brought to his

¹⁸ Palladio said the biggest disorder was due to a thick wall overarching an arcade, G.Zorzi, “Il contributo ...”, cit., pag.65.

¹⁹ G. Lupo, op.cit., pp.26-27: “sul piano teorico sarà il principio dei concatenamenti ad allontanare progressivamente l’architettura dalla natura (...) per farla entrare progressivamente nel dominio delle leggi della meccanica”.

²⁰ “Un altro terribile incendio, chiamato di solito il grande incendio, scoppiò nel 1574 (...) lasciando l’edificio nello stato di un semplice guscio, danneggiato o bruciacchiato dalle fiamme. Si discusse allora nel Gran Consiglio se la rovina dovesse essere abbattuta e al suo posto si dovesse costruire un palazzo interamente nuovo. Furono raccolte le opinioni dei principali architetti di Venezia per sapere se le pareti erano ancora sicure e se v’era la possibilità di ripararle nello stato in cui erano ridotte. Non posso trattenermi dal sentire un certo fanciullesco piacere per la casuale somiglianza del mio nome con quello dell’architetto la cui opinione fu la prima favorevole all’antico edificio: Giovanni Rusconi. Altri, specialmente Palladio, desideravano abbattere il vecchio palazzo e costruirne uno nuovo su progetti propri; ma i migliori architetti di Venezia, e, a sua gloria immortale, soprattutto Francesco Sansovino, difesero energicamente la fabbrica gotica, e vinsero (...).”, J. Ruskin, “Il Palazzo Ducale” in “Le pietre di Venezia”, Torino, 1962, pag.138.

²¹ “Tutti s’accordano nel reputare il Palazzo Ducale primo fra gli edifici civili del XIV secolo (...) eppure trecento anni or sono gli pendeva sopra una sentenza capitale, mossa nell’occasione che l’incendio del 1577 (...).”, G. Boni (non firmato), “L’avvenire dei monumenti in Venezia”, Stab. Litografico di M.Fontana, Venezia, 1882, pagg.9-11.

mind that *“Più che all'ostinazione di chi vegliava al Palazzo Ducale, dobbiamo la sua salvezza al generoso ardimento di Gian Antonio Ruscone. (...) Il Ruscone considerava cosa di poca importanza l'essere i capitelli fessi, perché essendo di assai conveniente grandezza hanno da conservarsi in opera nel modo medesimo come se fossero stati fatti in due pezzi, e finiva coll'attribuire l'inclinazione della muraglia ad artificio originale, simile a quello che ai dì nostri si dimostrò far parte degli accorgimenti statici del greco Ittino nel Partenone. L'essere giunti sino a noi è già una smentita a chi opinasse il contrario.”*²²

Boni's taking office puts him among the supporters of the existence of some kind of constructive intentional patchiness in Venice architecture.

The author lingers on the analysis of architectural forms in his writing “Natura ed arte” and he tells apart “random”, “dubious” and “wilful” shapes, rating the latter with specific architectural and perceptual purpose²³.

Another venetian architect, Giuseppe Sardi, came to the same conclusion, although he produced some hygienic reasons and by a writing in 1904, he argued that Palazzo Dario was provided with an intentional deflection; he suggested to *“riconoscere in tale deviazione un nuovo coefficiente di quella caratteristica originale e singolare che affetta nell'elegante insieme del '500 l'edificio suddetto (...) indagini più profonde (...) proverebbero (...) che il Dario si sia dall'origine costruito a bella posta, e che ragioni utilitarie prevalenti, l'aria e la luce, abbiano consigliato quella smisurata “rastremazione” proprio da (...) quella parte dove presentasi un edificio di epoca anteriore. (...) E' provato quindi: che la parte inferiore (...) poco discosta dalla verticale, che senza aver*

²² There.

²³ “Forme accidentali. L'ondulazioni nel pavimento di S.Marco, si considerano come avvallamenti quando una parte del suo mosaico è rifatta liscia a livello.

Forme dubbie. Dopo aver riedificate verticali le lunette superiori a coronamento rampante nei due fianchi di S.Marco, si lamenta il loro aspetto rigido che dà all'indietro; ed in appresso, a proposito d'una simile lunetta nella facciata maggiore, si scopre che l'inclinazione accusata era stata voluta dall'architetto originale per addolcire l'impressione delle linee a chi le riguarda dal basso, operando in questo come chi sospende inclinato al muro un dipinto.

Forme volute. Vicina abbiamo la Porta della Carta. Essa fino al coronamento a fogliami (...) è perfettamente a piombo, ma la curva inferiore del coronamento risente già una lieve inclinazione, che si fa decisa nel tratto lineare di mezzo; passando da questo alla curva superiore, l'inclinazione si moltiplica ed il muro di sfondo, a cui queste parti sono collegate, si mantiene verticale, né esse hanno traccia alcuna d'aver ceduto.

Ora qui appunto sta la sottigliezza di accorgimento dell'architetto: (...) angoli attualmente esistono nel coronamento, ma per la diversa natura e direzione delle linee nei piani che li formano, l'occhio non riesce a scoprirli e risente invece tutta la dolcezza di forme, che salendo si piegano lievi come cirri d'un tramonto.”, G. Boni, cit., pagg.11-12, voce “forma” in “Natura ed Arte”.

subito una deformazione proporzionale, la facciata presenta ad est un'inclinazione all'angolo di 80 cm circa, ad ovest di 10 cm; inclinazioni confermatemi dal valente costruttore Biondetti, che ebbe gran parte nei restauri (...) che non si spiega una così enorme rastremazione (...) senza pensare allo sviluppo superficiale del tetto, degli impalchi, dei marmi di paramento, delle cornici, degli archi che a ragione dovrebbero aver sofferto una riduzione proporzionale; che dato di ripristinare alla supposta primitiva verticalità l'edificio, converrebbe procurare dei nuovi materiali (...) per colmare i vuoti lasciati dalle differenze (...). Quindi la trovata non è peregrina (...) L'arte in tutti gli antichi monumenti è ingegnosamente e magistralmente applicata, né sono, a mio avviso, commendevoli quelle inclinazioni così fatte per contrapporsi alle gravi spinte dell'interno, né si troverebbe alcun motivo di meravigliarsene, se studiando intimamente le origini delle nostre architetture si vagliassero sempre le ragioni tecniche attraverso alle alte finalità artistiche ed estetiche di quei tempi."²⁴



Figs.5-6 Ca' Dario: view from the Gran Canal with a detail of the slope starting from the first floor.

Pompeo Momenti was like minded as Sardi²⁵ and he pointed out how Venetian

²⁴ G. Sardi, "Sulle principali cause de' danni ai fabbricati di Venezia", in "Cose d'arte" da "La Gazzetta di Venezia", anno CLXXII, n.68, 1904.

²⁵ "Un giovane architetto veneziano, di cui tutti riconoscono il valore, il Sardi, mi faceva osservare che il tetto della scuola della Madonna di Giustizia o di San Girolamo, ora Ateneo Veneto, è artificiosamente deformato, per circa trenta centimetri, a fine di rendere il timpano più libero e snello. E lo stesso Sardi crede le rastremazioni del Palazzo Dario, che tanto falso allarme hanno suscitato, essere state fatte ad arte per aver luce ed aria.", P. Molmenti, "Per i monumenti veneziani", adunanza del 23.11.1902, in "Atti del R. Istituto Veneto di Scienze, Lettere ed Arti", a.a.1902-1903, Tomo LXII, P.II, pagg.71-84.

architects relish “*iperboli costruttive*”, that is constructive boundary conditions: “*Ma certe anomalie, certe asimmetrie, certe inclinazioni bizzarre, certe deformazioni apparenti, erano volute dai costruttori del Rinascimento, i quali erano sopra tutto artisti (...) e consideravano l'architettura come una nobilissima arte e non puramente come una scienza geometrica. (...) Guardate nel Palazzo Ducale il divino controsenso dello svelto e leggero loggiato, che, contro ogni regola, sostiene l'ampia muraglia poderosa; (...). Queste bizzarrie geniali sono subito intese ed amate da chiunque abbia gli occhi aperti alla luce del bello. Ma gli antichi poeti della sesta e dello scalpello si piacevano anche di più strane irregolarità, che possono sembrare deformazioni statiche e destar perfino serie apprensioni ad un osservatore superficiale. (...) a questa antica libertà nell'arte e nella vita io mi sento (...) più vicino (...) che non ai canoni di arte e di convivenza sociale, ben altrimenti complessi e rigidi, creati da età più mature.*”²⁶

On the contrary, Max Ongaro disagreed with Sardi and likewise Boito, he was inclined to impute some irregular features of Venetian architecture to a wrong building system or to some differential soil partitioning, due to a non-homogeneous load allotment.

“*I vecchi costruttori (...) costruivano le fondazioni non troppo larghe, ma consolidate con accurate palafitte o passonate per i muri perimetrali, mentre trascuravano la resistenza di quelle dei muri intermedi; ed in ciò sta l'errore. (...) Sotto l'enorme peso, cedendo le fondazioni dei muri interni molto si più di quelle dei muri di perimetro, si inclinarono le travi dei solai, che rattenute all'esterno da tiranti, fecero alla lor volta inclinare i muri delle facciate ove non di rado si riscontrano fessure orizzontali. Tali strapiombi verso l'interno furono a torto creduti un accorgimento, epperò anche in recenti costruzioni fu data ad arte una esagerata pendenza alle muraglie d'ambito.*”²⁷

Despite Ongaro was sometimes harsh, he engaged for accurate geometrical surveys in order to validate his own position, according to which he said that the deformation in Palazzo Dario were not intentional: “*(...) Le deformazioni del*

²⁶ P. Momenti, cit.: “Sdegnavano essi la regolarità fredda e muta, la rigida simmetria: cercavano dare all'edificio un'anima, un'espressione, curando sopra tutto l'aspetto pittoresco. Dice bene il Castelar: chi vuole esaminare i monumenti veneziani con Vitruvio alla mano (...) con la squadra e il compasso, facendovi uno studio matematico, volendoli rigorosamente conformi alle leggi della statica (...) non vada dinnanzi a quegli edifici, nei quali sfolgora sopra tutto la ricchezza della espressione, ricchezza grande, inverosimile, come sono inverosimili tutte le iperboli (...).”

²⁷ Max Ongaro, “La principale causa dei danni ai fabbricati di Venezia”, in “Monitore Tecnico”, n.4 – anno X, Milano, 1904, pag.9. E a proposito di Palazzo Dario (pag.10): “Questo bizzarro ed elegante edificio tanto contorto da sembrar molle e flessuoso, ha nell'interno una fila di colonne normale alla facciata, che sostengono un muro su cui vanno ad appoggiare le travi dei solai. Le colonne (...) avevano meschinissime fondazioni e sotto il peso sprofondarono, portando quei notevoli strapiombi alle facciate divenuti caratteristici del palazzo.”

*Palazzo Dario non sono né originarie né volute (...) qui l'inclinazione è sempre verso il rivo, le pendenze dei vari membri sono difformi, le cornici anziché seguire una curva sono spezzate, e spesso con inclinazioni opposte, gli archi hanno ceduto e mentre è impossibile coordinare tali fatti ad una regola, tutto si spiega coi cedimenti del muro divisorio interno e del muro che dà sul rivo. Il primo ha prodotto la inclinazione esagerata verso l'interno della facciata (43 centimetri), il secondo lo strapiombo del lato ovest e dell'intero edificio.*²⁸

Ongaro revealed an orderly thought about this topic, and though he set Ca'Dario wall deformations down to some foundation droop, he did not count out a Venetian way of intentional building warping, but only as a borderline case: *"E' bensì vero che in alcuni casi si dava al muro una certa rastremazione ma ciò si usava per lo più nei muri in vivo o con rivestimento di vivo o di marmo ma in origine la parete interna era sempre verticale."*²⁹

While Camillo Boito was inclined to regard some constructive irregular shapes as mistakes, giving venetian builders recognition for being able to mix expertise and negligence³⁰, L. Beltrami kept a neutral position among the others; in *"Le fondazioni del ponte di Rialto"*³¹, the author, writing about the condition of Palazzo dei Camerlenghi at Rialto, identified the presence of two concomitant phenomena, that is both differential partitioning and intentional alterations in the

²⁸ "Strano costruttore sarebbe quello che facesse un lato con una rastremazione di 50 centimetri, mettendo l'altro a strapiombo. (...) Ma non è più logico il pensare che vi sia stato uno scorrimento verso il rio, il quale ha una forte corrente che occasionò più volte guasti alle fondazioni? (...) si vedono i pavimenti convergere verso l'interno dai tre muri perimetrali, cosicché l'avvallamento massimo (...) raggiunge quasi 3 centimetri per metro. (...) (ma) tutto il palazzo pende verso il rivo (...) si può stimare ad occhio che il basamento si inclina verso il rivo di oltre 10 centimetri (...)", Max Ongaro, "Deformazione od originalità del Palazzo Dario", in "Monitore Tecnico", n.4 – anno XI, Milano, 1904, pagg.16-18.

²⁹ Max Ongaro, cit., nota n.3, pag.9.

³⁰ Camillo Boito, recalling a mistake seen in a bridge arch bending in Riva degli Schiavoni: "La magistratura dell'edile è in Venezia più ardua assai che negli altri siti. Altrove basta conoscere i bisogni nuovi e provvedervi con utilità e decoro; qui bisogna essere (...) invasi dallo spirito di Venezia (...) non intendiamo tanto parlare degli abitanti quanto della città materiale, che pianta sui pali di rovere, di larice, di ontano (...). Gli artefici e gli operai veneziani (...) hanno queste due prerogative insieme - una paziente e delicata cura nelle loro opere, e a volte una trascuratezza indolente e spensierata. Guardando i loro lavori si resta meravigliati della sottile precisione, dove il cervello e la mano entrano al pari; ma non di rado si rimane stupiti di una svista (...) che pare incredibile (...)", C. Boito, "Rassegna Artistica. Venezia ne' suoi vecchi edifici", in "Nuova Antologia" n.20/1872, pagg.916-927, pag.919.

³¹ Appendice a "Indagini e studi per la ricostruzione dal marzo al giugno 1903", in Antonio Fradeletto [a cura di], "Il campanile di San Marco riedificato: studi, ricerche, relazioni", Comune di Venezia, 1912, pagg 119-129.

shape, that he called “*ripieghi originari*”: “*Infatti, in una raccolta di memorie professionali del capomastro Biondetti (...) avevo potuto rilevare come il Palazzo dei Camerlenghi – eretto a valle del Ponte (...) – sia fondato sopra uno zatterone (...) ad una distanza di m.1,60 dalla spalla del ponte. E’ bensì vero che quel Palazzo presenta, nell’eleganza delle sue linee architettoniche, alcune deformazioni le quali attestano cedimenti nelle fondazioni, che si potrebbero attribuire alla circostanza dall’esser stata, a così piccola distanza, palificata la robusta spalla del Ponte: ma, oltre che le deviazioni nelle linee architettoniche non sono interamente da attribuire a cedimenti, trattandosi in parte di ripieghi originari, è piuttosto nel risvolto verso il Canal Grande che si possono, in quel Palazzo, constatare degli abbassamenti attribuibili al fatto che, da quella parte, la ripartizione del peso gravante sullo zatterone non ha trovato la zona di terreno uniformemente incassata per resistere al carico (...).*”

The historical debate set up a very complex situation actually reflecting the state of Venetian architecture, wherein the question of constructive irregular shapes is still an open forum in need of deepening.



Fig.7 – Palazzo dei Camerlenghi from Rialto Bridge.

Conclusions

The documents under examination attest a sort of link between the two episodes, both emphasized by explicit references and by the outcropping of the same questions.

If Palladio culturally had to deny the deflection toward inside of front walls as an intentional feature, both Rusconi and other 16th century architects admitted such a constructive device; and it openly appears in 19th century literature, by Sardi, Boni, Molmenti; while Beltrami simply mentioned it and Ongaro regarded it as an exception.

Rusconi identified in his survey the constructive principle of “the contracted form” and described its profile and features, adding something about the fact that this slope usually starts at the level of the first floor, “*questa contrattura non*

cominciava dal piede della fabbrica, ma solamente dal piede delle sale³²; the same thing was seen by Sardi in Palazzo Dario, where the upper part of the facade was leaning toward inside while the ground floor wall was bias, “*la parte inferiore (...) poco discosta dalla verticale.*”³³

We can remark Rusconi’s technical outlook, including the deformations of buildings as physiological behaviours, that is a natural and in some measure foreseeable fact, where Nature and constructive structures can positively team up with. By Rusconi Nature is no firm reference model but it rather embodies the transformation process³⁴.

As for the reasons of such a geometrical deflection toward inside, Rusconi first found some historical precedents and then said it was intended to strengthen and preen the building, so that it could gain “*maggior fortezza e decoro.*”

Later authors are not so in agreement each other, with someone adducing healthy reasons - air and light above all - and someone else bringing formal facets in explanation – Boni’s “*forme intenzionali*” and Molmenti’s “*deformazioni apparenti*”, for instance.

A certain kind of interest arises from the convergence between Sardi and Rusconi, about the deflection toward inside as a safety factor for venetian architecture, so that “*né sono (...) commendevoli quelle inclinazioni così fatte per contrapporsi alle gravi spinte dell’interno*”. Sardi thought that venetian builders were acting in consideration of the most probable damage mechanisms and believed in their awareness. This theory is finding a positive feedback in the present³⁵ and deserves further deepening.

³² “Questa contrattura (...) s’ha mantenuta fin a quest’ora presente nel modo medesimo che la faccie nel cantone (...) che guarda S.Giorgio, il qual cantone si ha conservato dal tempo nel suo primo essere (...) che da dentro dalla fabbrica doi onze et per questa cagion si vede che tutta la fabbrica vien ad essere contratta quattro onze nella cima, et altre tanto dal piede la sii larga, et così viene ad esser più larga quattro onze dal piede che dalla cima (...) per tutto la lunghezza della fabbrica (...)”, G. Zorzi, “Altre due perizie...”, cit., pag.167.

³³ Go to note n.25.

³⁴ “(...) et questa contrattura (...) per due cagioni si ha mutata alquanto la forma; la prima cagione è stata perché (...) la faccia di questa fabbrica (è) fatta con più sottil magistero che quelle di dentro (...) per la qual cosa bisognava che vi fossero dentro più copia di commessure (...) le quali bisognava che non potendo essere serrate dall’arte nel modo che si conveniva, che quest’operatione restasse alla natura, la qual operando et stringendo tutte le parti d’esse, dimostrasse l’effetto del restringimento con qualche segno el qual fu di muover nel mezzo la muraglia facendola prender contrattura diversa da quella che facie il Maestro, et questo si conosce per la muraglia, che da in dentro in quel loco, circa il spatio di quatro onze.”, Prima deposizione ..., op.cit., pp.167-168.

³⁵ “Non è peraltro improbabile che, dando una leggera pendenza verso l’interno alle murature alte,

In summary, the documents in examination keep on calling forth questions and, as if they were single words of the same speech protracting in the course of time, they suggest a new way of looking at the architectures, by going down the "material town", as Boito urged upon. This means a closer touch with the buildings and the possibility of telling "*forme accidentali*" (random shapes) - due to some mistakes or structural damage, and therefore to be contrasted - apart from "*forme intenzionali*"³⁶ (intentional shapes), these ones to be identified and then accepted. But we cannot forget that there may be some hybridization, due to the presence of the two kind of forms and phenomena, such as, for instance, when some settlement requires falling back to corrective devices, as it occurred in the past to several bell towers³⁷.

We should follow Boni's advice for more awareness about architectural forms, especially when restoring a building. In that case some precious features could be lost forever because of a lack of knowledge: "*doppia cagion di guasto ne viene quando si ristaura, perché si distruggono forme che non comprese da noi potrebbero esserlo dai posterì, ed ove queste forme sieno accidentali si interrompe sempre l'armonia dell'assieme.*"³⁸

References

G. Cadorin, "Pareri di XV architetti e notizie storiche intorno al Palazzo Ducale", Venezia, 1838.

C. Boito, "Rassegna Artistica. Venezia ne' suoi vecchi edifici", in "Nuova Antologia n.20/1872, pagg.916-927.

(non firmato) G. Boni, "L'avvenire dei monumenti in Venezia", Stab. Lito-tipografico di M.Fontana, Venezia, 1882.

M. Marasso, "Un'intervista con Giacomo Boni", in "L'Adriatico", 04.09.1902.

si cercasse di orientare in anticipo, verso l'interno, la direzione di eventuali movimenti dei muri portanti causati dai cedimenti delle fondazioni.", G. Lupo, op.cit., pag.24.

³⁶ G. Boni (non firmato), "L'avvenire dei monumenti in Venezia", Stab. Lito-tipografico di M.Fontana, Venezia, 1882.

³⁷ "I campanili di Venezia, fino dai lontani tempi, erano in generale inclinati; e il Sabellico, parlando di quello di S.Giovanni Decollato, scrive: hic, ut plerisque locis, acclivis turris. Gettate le fondamenta e incominciata la costruzione, si notavano molte volte, per la cedevolezza del suolo, taluni spostamenti, a cui l'architetto rimediava senza indugio. Così il campanile dei Greci appare inclinato fino alla cella campanaria, e poi diritto, perché lo spostamento accadde durante la fabbrica.. Le particolari proprietà del sottosuolo di Venezia non certo erano ignote ai nostri antichi costruttori (...).P. Molmenti, "Per i monumenti veneziani", adunanza del 23.11.1902, in "Atti del R. Istituto Veneto di Scienze, Lettere ed Arti", a.a.1902-1903, Tomo LXII, P.II, pag.81.

³⁸ G. Boni, "Natura ed Arte", cit., pag.9.

P. Molmenti, "Per i monumenti veneziani", adunanza del 23.11.1902, in "Atti del R. Istituto Veneto di Scienze, Lettere ed Arti", a.a.1902-1903, Tomo LXII, P.II, pagg.7184.

Max Ongaro, "La principale causa dei danni ai fabbricati di Venezia", in "Monitore Tecnico", n.4 – anno X, Milano, 1904.

Max Ongaro, "Deformazione od originalità del Palazzo Dario", in "Monitore Tecnico", n.4 – anno XI, Milano, 1904.

G. Sardi, "Sulle principali cause de' danni ai fabbricati di Venezia", in "Cose d'arte" da "La Gazzetta di Venezia", anno CLXXII, n.68, 1904.

L. Beltrami, "Le fondazioni del ponte di Rialto", appendice a "Indagini e studi per la ricostruzione dal marzo al giugno 1903", in Antonio Fradeletto [a cura di], "Il campanile di San Marco riedificato: studi, ricerche, relazioni", Comune di Venezia, 1912, pagg119-129.

G.Zorzi, "Il contributo di Andrea Palladio e di Francesco Zamberlan al restauro di Palazzo Ducale di Venezia dopo l'incendio del 20 dicembre 1577", in Atti dell'Istituto Veneto di Scienze, Lettere ed Arti, CXV, 1956-57, pp.11-68;

- "Altre due perizie inedite per il restauro del Palazzo Ducale di Venezia dopo l'incendio del 20 dicembre 1577", in Atti dell'Istituto Veneto di Scienze, Lettere ed Arti, CXV, 1956-57, pp.133-174.

G. Lupo, "Principio murario e principio dei concatenamenti: i pareri sul restauro di Palazzo Ducale di Venezia dopo l'incendio del 157", in "Rassegna di architettura e Urbanistica", Roma, a.32, n.94, 1998.

SIDEV: towards a service based architecture

Luca Marescotti¹, Maria Mascione², Stefano Maffulli³

¹.Professore, Dipartimento BEST, Politecnico di Milano ².Assegnista di ricerca, Dipartimento BEST, Politecnico di Milano ³.Libero professionista

Riassunto

Il progetto del Sistema Informativo dell'Edilizia Veneziana (SIDEV) è il risultato dell'individuazione dei requisiti funzionali, l'analisi dei materiali e delle interazioni tra utenti e sistema. Nei precedenti rapporti si era confermata la convenienza di concepire il SIDEV come un'architettura basata su servizi. Ovvero, un'architettura che permetta di gestire un'attività di ricerca costruita nel tempo da diversi gruppi di lavoro distribuiti territorialmente. Il SIDEV, pur facendo uso di dati geografici, prevede che i gruppi di lavoro inseriscano i dati testuale e descrittivi sugli edifici raccolti nell'ambito della ricerca attraverso un sistema basato sul web. Per le cartografie si è progettato di non replicare alcuna informazione e basarsi su concetti collaudati di erogazione di servizi mappali, usando gli standard del OpenGisConsortium (OGC) WMT e OWS. I vantaggi per CORILA dell'approccio basato su servizi riguardano l'economicità della manutenzione delle basi cartografiche, che invece di essere duplicate, corrette, modificate in ogni luogo, vengono semplicemente usate dalle varie applicazioni a fronte di arricchimenti tematici derivanti dalle attività di ricerca. Quindi le applicazioni non vanno più pensate come sistemi monolitici sviluppati e consegnati in pacchetti onnicomprensivi di dati geografici, allegati e cartografie. SIDEV si appoggia pesantemente su questo modello di architettura in modo da consentire un'elevata scalabilità delle applicazioni e garantire gli esiti migliori alle attività di ricerca.

Abstract

The project of Sistema Informativo dell'Edilizia Veneziana (SIDEV) is the result of the functional analysis of the system, analysis of the materials and interactions between users and the system itself. In our previous reports we confirmed the convenience of planning SIDEV as a service based architecture. That is, an architecture that would allow managing a research activity built over a wide time span and by working groups spread over the territory. Even if SIDEV makes use of geographical data, working groups are asked to insert the descriptive textual data about buildings found during the research activities through a web based interface. SIDEV will not replicate any information that is already available for CORILA, instead it will be based on proven concepts of mapping services, using OpenGisConsortium blessed standards like WMT and OWS. The service based approach for CORILA will guarantee convenient and effective management of cartographic base: instead of duplicating, correcting, modifying maps in each application, these will be simply used by the applications and will be enriched with thematic improvements by all research

activities. The applications will not be designed as monolithic systems, developed and delivered as packages that contain all data, including descriptive textual data, other attachments and cartography. SIDEV is deeply based on this model of architecture that allows a high scalability of applications and best results for the research.

1 Introduction

One of the most important aspect of an effective information system is its capability to allow mutual collaboration of groups of users from different disciplines and their easy sharing of knowledge. An effective information system allows modeling and representing the complexity of real life problems, issues, aspects in a complete multidisciplinary approach. Architectures reside in a natural environment where disciplines like biology, geology, structural engineering and other aspects insist simultaneously therefore information systems must allow scientists not only to gather all information of their own field of interest, but to analyze the more complex relations happening in real life. In practice, it should be possible to ask to the information systems questions like "Is there a connection between tides, average temperatures of the air and degradation of plaster in historical buildings?"

Very often it is possible to gather raw data about many physical aspects of nature because many agencies and companies, public and private, collect them. Possibly this data is also available easily and cheaply, although more often this is not the case. But it is still rare to have access to information in a timely and interoperable form. Interoperability allows to create an open system, from which a variety of data sources can be added on-the-fly from different data providers, displaying new relations between observed phenomena, independently from observation scale.

2 Levels of information: territory, city, insula, building

The design of the SIDEV (Information System for Diagnostic of Venetian Buildings) keeps as a requisite allowing multiple sources of data to be consulted and added. The system allows analysis and representation of data at two scales: from the wider territory to the single building, meanwhile scaling the quantity of information allowed. These levels of detail are complimentary since they allow managing the knowledge in two different directions: from the synthesis (or aggregation) to the analytic datum and viceversa, depending on the level of competence and of intervention. This aspect is the foundation layer for the definition of research criteria of the information system. Aggregation and disaggregation of data depending on the competence level and of intervention is coherently applied to both spatial/geographic data and alphanumeric attributes.

2.1 Level of Territory and Lagoon

For SIDEV the territorial level is basically the one that includes the Lagoon of Venice: all information levels are pertaining to the environmental characteristics of the wider scale. The sources of data for this level are mainly identified in the

Environmental database of Venice Lagoon and Environmental data of CORILA consortium. From these data providers SIDEV can gather information about atmosphere, hydrosphere, lithosphere and biosphere. Another significant source of information come from the results of other work packages of the CORILA research.

2.2 Level of city, insula, building

The local level should be distinguished into three distinct sub-levels that will determine the visual aggregation of different data sets: urban, insula and building. The distinction is only used for visualization purposes, because the database doesn't separate the information in any way: all the built environment is treated as a continuum. So, for the database a building is a kind of atom of the city and atoms can be mixed to form molecules (like the insulae) and bigger parts. The database of the built environment is modeled to allow also describe other architectures, like bridges or gardens, and empty spaces like squares.

Urban level: this is the reference level and shows the data necessary for the definition of the environmental context and urban morphology of Venice, that is the elements that concur to the assessment of the 'artifact' Venice.

Insula level: this level participates to the pre-projectual investigation phase and can give significant contributions to deepen the knowledge on the single artifact. This knowledge helps representing the context and it is very useful to interpret phenomena of degradation and damage that are significant also on urban level. For example, the proximity of other buildings or of waters are elements that request a wider view of the surroundings and they represent rulers for more profound analysis of the building level.

Building level: the conservation's project refers to this level for the specific knowledge of the building. The building can be described in two ways, either the synthesis or the details. The building can be represented as synthesis of its qualitative and quantitative characters, coherently with the level of detail represented. In details, the same data regarding the building are useful for the conservation's project, particularly for the diagnostics. The building is dissected into all its components and the results of the analysis are displayed in all details, together with the precise localization with respect to the elements of the building.

The identification and localization of the building must be semantically coherent with the rest of CORILA databases, so that the different data sources can be effectively mixed. This is one of the levels of interoperability that will also be discussed later.

3 User requirements and use cases

The Unified Modeling Language (UML) has been used to describe the user requirements of the information system, the use case scenario and the structure of the database for the actual work packages. UML has proved an extremely powerful and useful mean to describe with graphical formalisms the complex behaviors of system and of the users. Through the use cases, based on a

description of actions both in text and standardized graphics, it is possible to describe the interactions between the components of the system. To describe the conceptual structure of the database a diagram of classes has been used. The main requirements are organized in three areas:

A. Data entry

Data entry to be done via a web-based user interface

Description of the characteristics of the user interface

B. Data consultation or query

Basic research criteria

Characteristics of user interface and levels of consultation of the system

Scalability of information

Management of documents for analysis as attachments

Consultation of project guidelines, proceedings, norms, specifications

Consultation of metadata

Connection to the expert system VMDS

C. Data visualization

Bilingual user interface (Italian and English)

Different levels of consultation of the system

Visualization of buildings

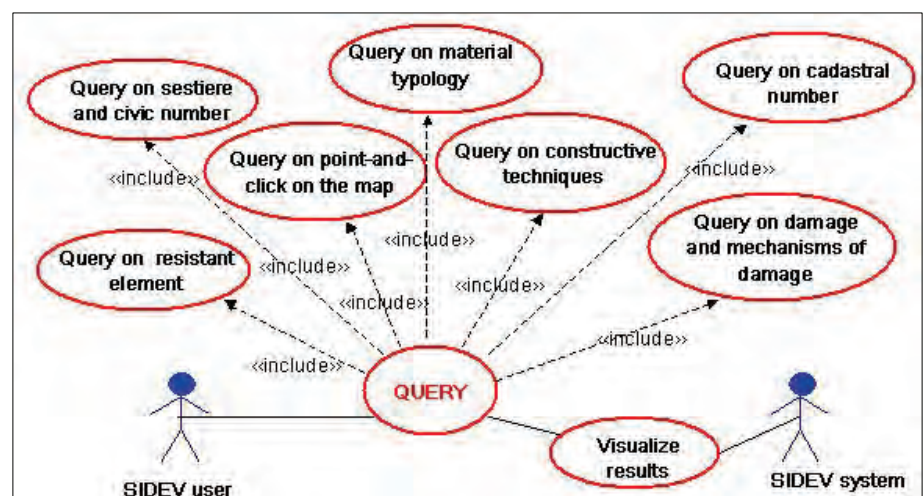


Fig. 1 – Use case about data entry on web.

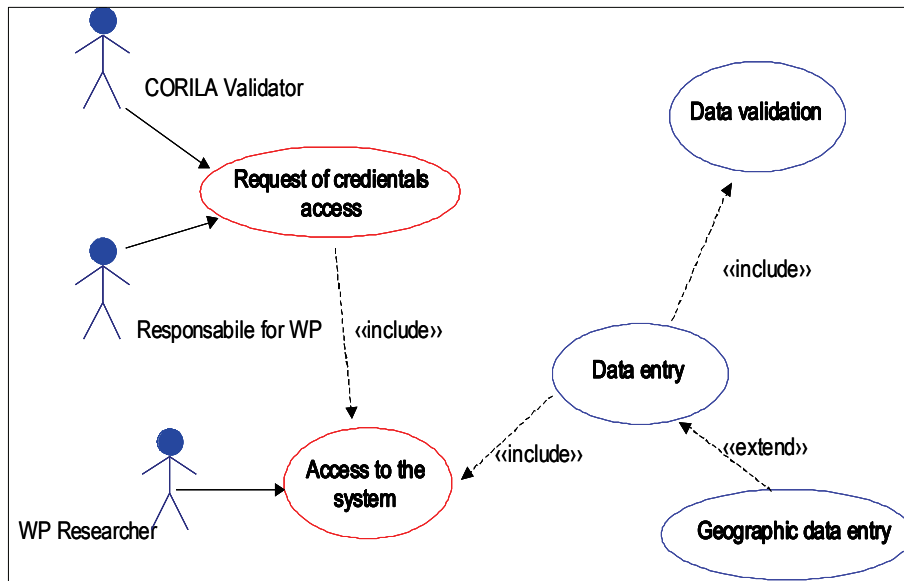


Fig. 2 – Use case about query criterias

4 Interoperability and 'service based architecture'

The term 'standard' has many different meanings but in the technology field a standard is “a set of specifications, that is a set of constraints and requirements that identify globally the external behavior of a product or of a service. External behavior implies that the implementation of the standard is irrelevant so far it adheres to the specifications”. For example, the GSM standard for mobile phones is implemented by all manufacturers of telephones and all network operators and as a result all phones can communicate with all the networks, interoperably.

Interoperability means the ability of Information and Communication Technology systems and of business processes to exchange data and allow sharing of information and knowledge.

Open standards are of extreme importance for SIDEV and in general for all information systems since they allow that information is transported safely and integrally across applications. The standards set by the Open Geospatial Consortium (OGC) and other international bodies (ISO, W3C ecc) allow for transportation of information but in multidisciplinary environments there is more to it than that to keep into consideration.

The semantics of the data is paramount to share descriptions of buildings in a meaningful way between different working groups. The definition of a set of common words and their meaning, thesaurus is the only way to achieve real interoperability between systems and start developing a 'service based system'. The concepts behind SIDEV allow to enter the data only once and use that information often, without having to make copies of it in different applications: using open standards it is possible to take the cartographic layer of the territory from one source, take the city layer from another, then import from different sources also atmospheric data and combine them into one application, together with the data coming from other CORILA researches.

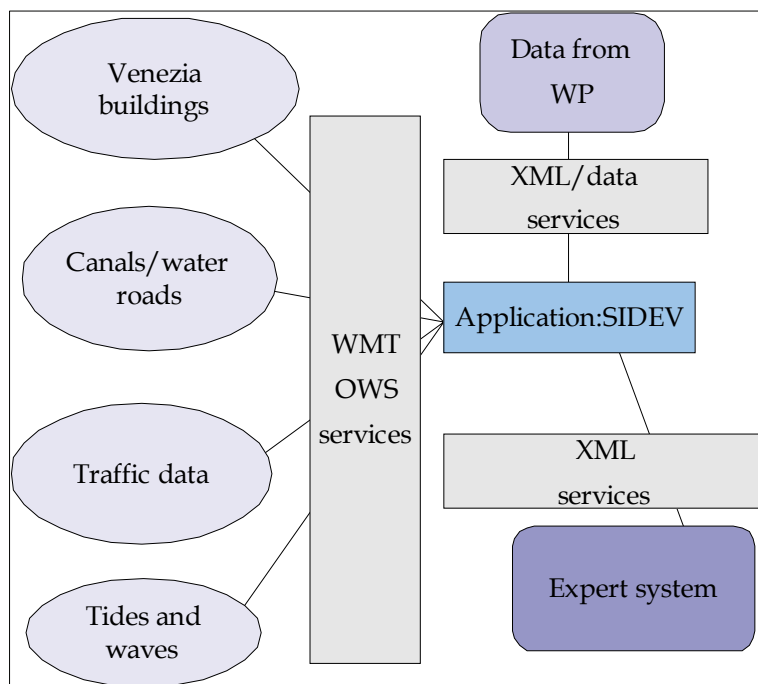


Fig. 3 – Schema for distribution of information and applications between services in SIDEV

Conclusions

An approach to designing information systems that allows flexibility and expandability, with data thought as building blocks glued together by international standards will lead to an architecture that would allow managing a research activity built over a wide time span and by working groups geographically spread. SIDEV is designed not to replicate any information that is already available for CORILA, instead it is based based on proven mapping services, using standards set by Open Geospatial Consortium, like WMS and WFS. The service based approach guarantees convenient and effective management of cartographic base: instead of duplicating, correcting, modifying maps in each application, these will be simply used as served centrally and will be enriched locally with thematisms by all research groups, as needed. The applications are not designed as monolithic systems, developed and delivered as closed packages that contain all data, including descriptive textual data, other attachments and cartography. SIDEV is deeply based on this model of architecture that allows a high scalability of applications and best results for the researches.

AREA 3

Environmental processes

RESEARCH LINE 3.8

Speciation and flow of pollutants

MICROPOLLUTANT EFFECTS IN ESTUARINE ORGANISMS (MUSSELS, POLYCHAETES AND FISH) IN THE LAGOON OF VENICE, ITALY

Nicoletta Nesto¹, Stefania Romano^{2,3}, Giancarlo Campesan¹, Daniele Cassin¹,
Vanessa Moschino¹, Marina Mauri³, Luisa Da Ros¹

¹ Istituto di Scienze Marine, CNR, Venezia, ² Istituto di Scienze Marine, CNR, Bologna,

³ Dipartimento di Biologia Animale, Università di Modena e Reggio Emilia

Riassunto

Lo scopo di questo lavoro è valutare il bioaccumulo e gli effetti di alcuni microinquinanti inorganici (Cd, Cr, Cu, Fe, Mn, Pb e Zn) ed organici (Idrocarburi Policiclici Aromatici, IPA) sulle risposte biologiche di organismi appartenenti al benthos quali mitili (*Mytilus galloprovincialis*), policheti (*Hediste diversicolor*, *Perinereis cultrifera*) e pesci (*Zosterisessor ophiocephalus*).

Esemplari di ciascuna specie sono stati raccolti stagionalmente in due aree lagunari caratterizzate da un diverso impatto antropico: S. Giuliano, prevalentemente influenzata dalla vicina area industriale e Sacca Sessola, situata nelle immediate vicinanze del Centro storico. Negli organismi è stato determinato il contenuto di metalli (Cd, Cr, Cu, Fe, Mn, Pb e Zn) e IPA, e sono stati inoltre valutati alcuni biomarker biochimici, istochimici e fisiologici per valutare sia l'esposizione ambientale a xenobiotici sia i loro effetti: malondialdeide (MDA) e metallotioneine (MT); attività dell'enzima etossiresorufina D-dietilasi (EROD), metaboliti fluorescenti della bile e indici somatici solo nei pesci; latenza dell'enzima N-acetil- β esosaminidasi, contenuto di lipofuscine e lipidi neutri e sopravvivenza in aria solo nei molluschi.

Per quanto riguarda le variazioni stagionali dei metalli, nei mitili e in *H. diversicolor* è stato evidenziato un generale abbassamento delle concentrazioni in estate, in accordo con i trend di MDA e MT. Gli IPA sono risultati generalmente più elevati in estate nei policheti e in primavera nei pesci, meno variabili nei mitili.

Il bioaccumulo dei metalli raggiunge livelli simili nelle due aree, sia relativamente ai mitili (solo Pb e Cd si accumulano maggiormente negli organismi di S. Giuliano), che nel polichete *P.cultrifera* e nei pesci. Il contenuto di IPA è risultato generalmente superiore negli organismi di S. Giuliano, soprattutto durante i periodi riproduttivi. Anche le risposte biologiche sono simili nei mitili di entrambi i siti; per il polichete *P.cultrifera* e per *Z. ophiocephalus* è stata invece rilevata una maggior induzione dei biomarker di esposizione negli organismi di S. Giuliano.

H. diversicolor, specie rinvenuta solo a S. Giuliano, ha mostrato in generale una maggior capacità di bioaccumulo di metalli e livelli più elevati di MDA rispetto a *P. cultrifera* campionata nella stessa area.

L'analisi multivariata, applicata ai dati chimici e biologici per ciascun taxa, ha

messo in evidenza che i campioni di mitili analizzati sono discriminabili in base al fattore stagione, mentre i policheti sono raggruppabili in base al sito di campionamento. Entrambi i fattori, stagione e sito, sono invece risultati importanti per i pesci.

Abstract

This study aims to evaluate the effects of inorganic and organic micropollutants on the biological responses of mussels (*Mytilus galloprovincialis*), polychaetes (*Hediste diversicolor* and *Perinereis cultrifera*) and fish (*Zosterisessor ophiocephalus*).

Metals (Cd, Cr, Cu, Fe, Mn, Pb e Zn) and PAH bioaccumulation and various biomarkers (malondialdehyde MDA and metallothioneins MT; Ethoxyresorufin D-deethylase activity EROD, fluorescent bile metabolites and somatic indices in fish only; latency of N-acetyl- β hexosaminidase, lipofuscin, neutral lipids and survival in air in mussels only) were evaluated in organisms seasonally collected from two different impacted areas: S. Giuliano and Sacca Sessola.

Referring to the seasonal variations, the metal content showed a general summer decrease in mussels and in the polychaete *H. diversicolor*, in agreement with the trends of MDA and MT. PAHs were generally higher in summer in polychaetes, and in spring in fish.

Intraspecific comparisons indicated similar metal bioaccumulation levels in the organisms from both areas, S. Giuliano mussels showing higher Pb and Cd concentrations. PAHs contents were generally higher in the organisms from S. Giuliano, in particular during the reproductive period. Additionally, the results of the biomarkers showed a similar biological response in the mussels of the two sites, and higher induction of exposure biomarkers in the polychaete *P. cultrifera* and in *Z. ophiocephalus* from S. Giuliano.

The species *H. diversicolor*, found in S. Giuliano only, showed generally bioaccumulation capability and MDA levels higher than *P. cultrifera* from the same area.

The multivariate analysis, performed on chemical and biological data, showed how the seasonality is the main factor discriminating the mussels samples, the sampling site resulted the main discriminating factor for the polychaetes, whereas both factors are important in fish.

1 Introduction

Biological effects of xenobiotics on organisms may be related to both toxicity of each compound or mixture and the duration of the exposure, and can be detected throughout the biomarker approach. In an estuarine environment, mussels, polychaetes and fish are specific indicators of different environmental compartments in relation to their habitat and food web position and they exhibit different rates of biotransformation and/or bioaccumulation with respect to various xenobiotics (Porte & Albaigès, 1993; Livingstone, 1998, Scaps et al.,

2002). Pollutants may have sub-lethal effects at different levels of the biological organisation (cellular, organ, individual, community) and the biomarkers include a variety of measures of specific molecular, cellular and physiological responses to contaminant exposure (Bayne et al., 1985). This investigation was carried out with the aim of acquiring improved knowledge on the relationship between bioaccumulation of metals, PAHs, and their effects on the biological response of the mussel *Mytilus gallprovincialis* (filter-feeder), a well known bioindicator of the water column, the ragworms *Perinereis cultrifera* and *Hediste diversicolor* (deposit-feeders), possible indicators of the sediment quality and the grass goby *Zosterisessor ophiocephalus*, (predator, bottom-dwelling) as representative of the lagoon nekton.

At biochemical level, the biological response in all these species was evaluated by determining the contents of malondialdehyde (MDA), a metabolite indicating generic oxidative stress caused by an excess of membrane lipid peroxidation (Gérard-Monnier et al., 1998), and of metallothioneins (MT) which are involved in the detoxification processes of excess amounts of both essential and non-essential trace metals (Viarengo et al., 1997). Moreover, the levels of ethoxyresorufin-D-deethylase (EROD) as a specific enzyme of the mixed-function oxidase system (MFO), able to transform lipophilic xenobiotics to more water soluble compounds (Bucheli & Fent, 1995), and of the fluorescent bile metabolites indicating recent PAHs exposure (Aas et al., 2000) were evaluated in fish.

At cellular level, the accumulation of lipofuscins and neutral lipids were determined in the digestive gland of mussels, as generic response to heavy metals and organic micropollutants, respectively (Viarengo et al., 1990, Viarengo e Canesi, 1991; Regoli, 1992), as well as the measure of the latency of the N-acety- β -hesosaminidase, able to evaluate the fragility of the lysosomal membrane (Moore, 1988).

At physiological level the survival in air test (SOS) was evaluated in mussels as simple but effective test to determine pre-existing stress (Eertman et al., 1993); the liver somatic index (LSI) and the gonad somatic index (GSI) were determined in fish being also considered generic responses to the presence of chemical contamination (Sloof et al., 1983; Corsi et al., 2003).

2 Materials and methods

2.1 Samplings

Samples were seasonally collected during 2005 (April, July and October) from two different impacted areas of the Lagoon of Venice: S. Giuliano (close to the industrial zone of Marghera) and Sacca Sessola (close to the historical centre of Venice).

As regards mussels, a subsample of 50 individuals (4-5 cm) were immediately frozen in liquid nitrogen and stored at -80°C until biomarker analyses, whereas for the chemical analyses a subsample of 30 animals were kept for 24h in aquaria with sea water to purge.

A similar procedure was adopted for polychaetes. A subsample of 15 organisms (3-4 cm) were immediately frozen in liquid nitrogen and stored at -80°C until the biomarker analyses; for chemical analyses, a subsample of 50 individuals were kept for 3 days in aquaria containing quartz sand and sea water to purge sediment particles from intestine. Samples of sediment from each sites were also taken and analyzed for their metal content.

As regard fish, liver, bile and gonad were excised individually from 10 organisms (when possible, 5 males and 5 females) per sample, weighted, immediately frozen in liquid nitrogen and stored at -80°C until biomarkers analyses. Their fillets, frozen at -20°C, were used for chemical analyses.

2.2 Chemical analyses

Total metal concentrations (Cu, Cd, Cr, Fe, Mn, Pb, Zn) were determined with flame and furnace AAS after drying at 60 °C for 12 hours and total HNO₃ bomb digestion in microwave on 4-6 pools of 3 specimens for mussel and polychaetes and 4-5 single individuals for fishes. Metal concentrations in sediments were measured with flame and furnace AAS on original sediment after hot nitric acid extraction under reflux. All results are referred on matrix-dry weight.

PAHs concentrations were determined in the biota samples. Hydrocarbons were Soxhlet-extract for 8 h with n-hexane. The extract was evaporated at 50°C to constant weight for determination of extractable organic matter and after dissolution in 1 cm³ n-hexane, fractionated by chromatography on a alumina/silica gel column. PAH analyses were performed on a Hewlett-Packard 1090A high-performance liquid chromatograph (HPLC) equipped with a reverse-phase column and a Hewlett-Packard 1046A fluorescence detector.

2.3 Biomarkers analyses

The content of MDA and MT were determined spectrophotometrically on 3 pools of digestive gland in mussels, in the all body of pooled polychaetes and in pooled livers of fish according to Gérard-Monnier et al. (1998) and Viarengo et al. (1997), respectively.

The EROD activity was measured fluorometrically in the individual liver tissue of 10 fish, according to the method described by Burke & Mayer (1974), whereas the bile metabolites (1-OH Naphtalene, 3-OH Benzo(a)pyrene, 1-OH pyrene) were evaluated by fixed wavelength fluorescence analysis according to Aas et al. (2000).

Lipofuscins (LF) and neutral lipids (NL) content and the latency of N-acetyl- β -hesosaminidase (LAT) were histochemically determined in the digestive gland of 10 mussels according to the methods reported by Viarengo et al. (1990), Regoli (1992) and Moore (1988), respectively.

Survival in air (expressed as LT50) was determined on 30 mussels according to Eertmann et al. (1993), LSI and GSI were measured in 10 fish according to the method reported by Waring et al. (1996).

2.4 Statistical analyses

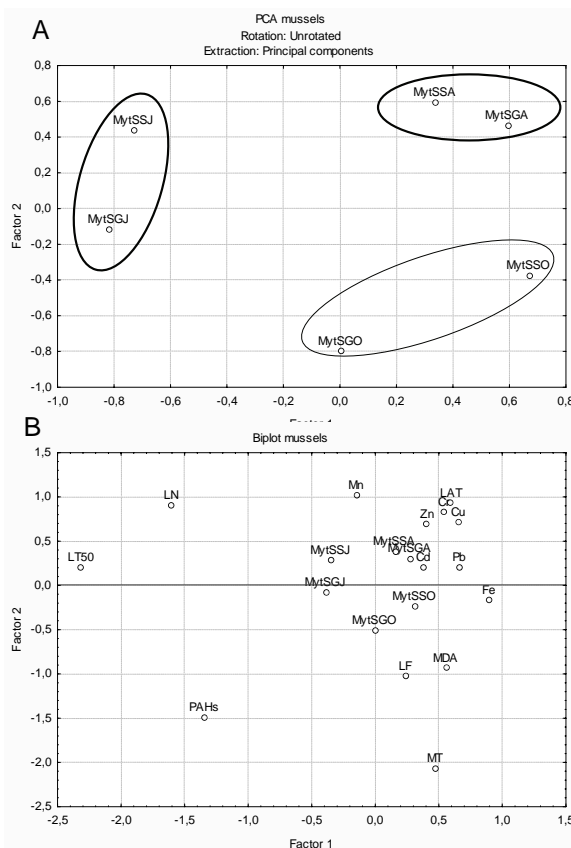
Biological and chemical data were first standardized subtracting the mean and dividing by the standard deviation (Sokal & Rohlf, 1969) then subjected to Principal Component Analysis (PCA).

Metal biota/sediment accumulation factors (BSAFs) were calculated for polychaetes. Biological results of MDA and MT were compared using the non-parametric Kruskal-Wallis test.

3 Results and discussion

Metal concentrations in *M. galloprovincialis* samples resulted lower than a study performed in Lagoon of Venice in 1991-1992 (Pipe et al., 1995); and generally similar to levels already highlighted by more recent studies (Giusti & Zhang, 2002; Mauri & Baraldi, 2003). Mussels from the two sites exhibited comparable metal levels, except for Pb and Cd, higher at S. Giuliano, and showed a parallel decrease of concentrations in July. Ranges for each element (min-max, µg/g d.w.) were: Pb 1.1-4.3, Cd 0.8-6.6, Cr 0.2-2.7, Cu 3.6-10.8, Mn 4.7-11.9, Zn 134.9-260.3, Fe 3.8-234. PAHs concentrations resulted generally higher in samples from S. Giuliano (range 133.4-149.1ng/g) than from Sacca Sessola (64.8-98.6 ng/g). In July the levels of MDA and MT were significantly lower in both stations, following the same seasonal trend of metal concentrations, suggesting the possible use of these biomarkers to assess metal exposure (Amiard et al., 2006; G eret et al., 2002). In general, the biomarker response indicated similar conditions in mussels from the two areas, the level of MT and lipofuscins only revealing a clear worse condition for S. Giuliano mussels in April, just after the reproductive period. The multivariate analysis, performed using the standardized mean values for all chemical and biological data, showed a spatial separation of three groups, identified by the sampling period (Fig. 1A). The first two PCA factors account for 61% of variance. The biplot (Fig. 1B) allowed the simultaneous distribution of stations and parameters. The stations are distributed along the first factor according to an increase of metal concentration (except for Mn, which shows a different pattern) and high values of MDA and LF. Therefore, July samples are distributed far from the metals, as in July the metal concentration values decreased in both sites. On the contrary, the stations are distributed along the second factor mainly according to decreasing values of PAHs and MT.

The concentration of metals in the polychaetes *P. cultrifera* did not reveal either specific seasonal patterns (except for Cd, Cu and Pb which at S. Giuliano tended to decrease in July and to increase in October) or differences between the two sites. Ranges for each element (µg/g d.w.) were: Pb (0.7-1.4), Cd (0-0.8), Cr (0.1-0.4), Cu (20.3-81.2), Mn (7.9-17.7), Zn (112-217), Fe (275-491).



	Factor 1	Factor 2
Pb	0,66568	0,20139
Cd	0,38089	0,20351
Cr	0,54202	0,82765
Cu	0,65542	0,71592
Mn	-0,14678	1,01904
Zn	0,40512	0,69264
Fe	0,8958	-0,16603
PAHs	-1,34022	-1,49884
MDA	0,56039	-0,93379
MT	0,47402	-2,07067
LAT	0,59369	0,92979
LF	0,23877	-1,02612
LN	-1,60616	0,89922
LT50	-2,31865	0,2063

Fig. 1 – PCA analysis performed on standardized mean values of metal and PAHs concentrations and different biomarkers measured in mussels from S. Giuliano (SG) and Sacca Sessola (SS) in April (A), July (J) and October (O).

The Cd and Zn bioaccumulation levels resulted similar to those obtained by Volpi Ghirardini et al. (1999). The BSAF seasonal trends for *P. cultrifera* from S. Giuliano and Sacca Sessola resulted similar, with lower values in S. Giuliano. As the sediments were always more polluted in this site, this may indicate the possible induction of physiological regulation mechanisms where environmental metal availability is enhanced (Tab. 1).

Tab. 1 – BSAF values calculated in samples of *P. cultrifera* collected at S. Giuliano (SG) and Sacca Sessola (SS) in April (A), July (J) and October (O) 2005.

	Pb-BSAF	Cd-BSAF	Cr-BSAF	Cu-BSAF	Mn-BSAF	Zn-BSAF	Fe-BSAF
SS-A	0,17	6,86	0,04	5,46	0,07	4,27	0,00
SS-J	0,03	0,62	0,03	1,47	0,05	2,38	0,01
SS-O	0,07	2,80	0,03	1,75	0,08	1,85	0,07
SG-A	0,05	4,08	0,02	2,15	0,08	4,22	0,02
SG-J	0,01	0,49	0,01	0,45	0,02	0,96	0,01
SG-O	0,04	2,51	0,01	2,20	0,03	1,10	0,03

The PAHs values resulted higher in *P. cultrifera* from S. Giuliano (20.5-167.8 ng/g) in comparison with both *P. cultrifera* from Sacca Sessola (41.7-62.3 ng/g) and *H. diversicolor* from S. Giuliano (35.6-85.3 ng/g). MDA values showed decreasing values between July and October for both stations whereas an opposite trend has been recorded for MT values (Fig. 2-3), being similar to that one exhibited by the metal concentrations (at least for S. Giuliano samples). Samples from S. Giuliano generally revealed a higher induction of both biomarkers. *H. diversicolor* was a more efficient bioaccumulator in comparison with *P. cultrifera*, and often showed higher values of MDA. Only in July, when most of the metal concentrations decreased, the levels resulted comparable in the two species (Fig. 2).

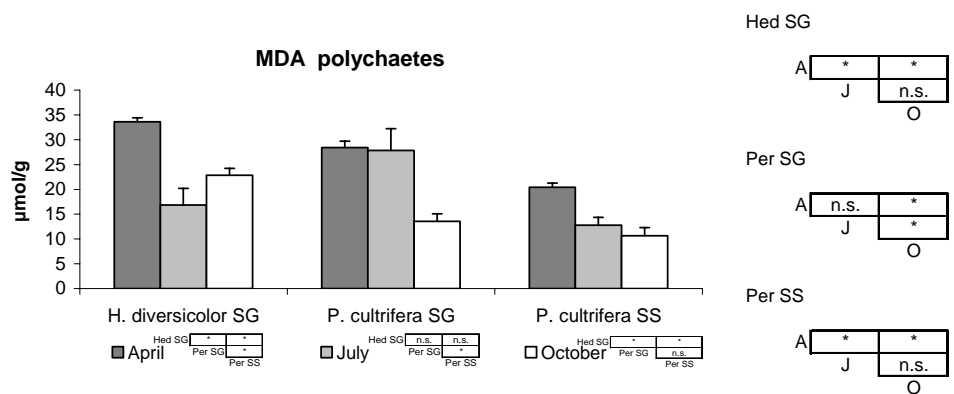


Fig. 2 – Malondialdehyde content (mean ± st. err., n=3 pools) measured in *H. diversicolor* from S. Giuliano and *P. cultrifera* from two sites of the Venice Lagoon.

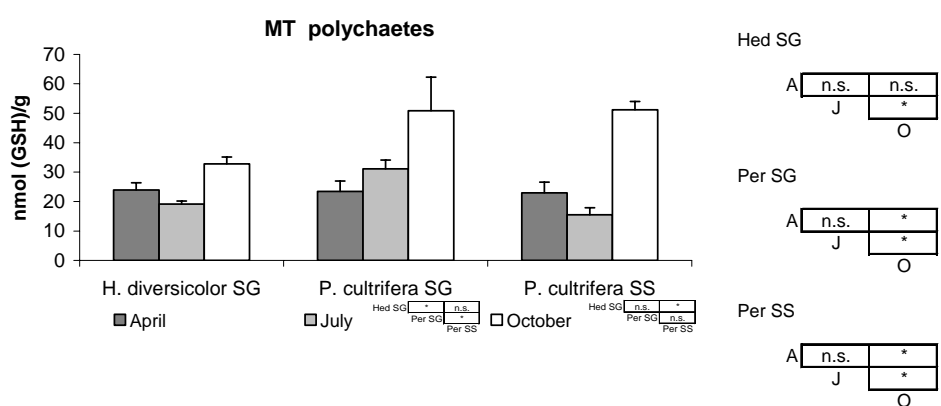


Fig. 3 – Metallothioneins content (mean ± st. err., n=3 pools) measured in *H. diversicolor* from S. Giuliano and *P. cultrifera* from two sites of the Venice Lagoon.

The PCA analyses, performed using the standardized mean values of all chemical (PAHs concentrations and metal BSAFs) and biological data (MDA and MT), showed a spatial separation of three groups, mainly identified by the three polychaete populations (*H. diversicolor* from SG, *P. cultrifera* from SG, and from SS) (Fig. 4A). The first two PCA factors account for 55% of variance. The stations are distributed along the first factor according to increasing of PAHs concentrations as well as Zn-BSAF, Cd-BSAF and Cu-BSAF, whereas along the second factor the stations are discriminated essentially by increasing values of MDA and Cr-BSAF and decreasing values of MT (Fig. 4A,B). Therefore, the group identified as *H. diversicolor* resulted mainly characterized by the highest values of MDA and Cr-BSAF, whereas in general the *P. cultrifera* groups showed similar BSAF values, underling their similar metal regulation capability, and samples from S. Giuliano are discriminated by those from Sacca Sessola mainly by high values of MT.

The bioaccumulation of both inorganic and organic micro-pollutants in fish fillets was lower than previously recorded by Fossato et al. (2000) and no differences were detected between sites and seasons for metals. The ranges of values for each element (µg/g d.w.) were as following: Pb (0-1.8), Cr (0-1.2), Cu 0.9-1.7), Mn (1.8-17.3), Zn (0.8-34.8), Fe (4.9-24.9). Fish exhibited generally a higher content of micro-organic contaminants in spring during their reproductive period and S. Giuliano samples resulted more polluted than Sacca Sessola ones (total PAHs 4.4-40.7 and 4.3-11.6 ng/g, respectively). As a whole, in S. Giuliano samples the levels of micro-organic pollutants correlated with higher induction of EROD, MT as well as higher level of MDA and fluorescent bile metabolites.

Most of these biomarkers showed their typical seasonal trend, i.e. EROD activity is depressed in April during the reproductive period when the presence of estradiol tends to inhibit the activity of this enzyme (Förlin & Andersson, 1984). Also the GSI followed its peculiar physiological change, peaking during reproductive period and lowering in July. Similarly, fluorescent bile metabolites (3-OH Benzo(a)pyrene and 1-OH Pyrene), showed a physiological pattern, their values decreasing from April to July. This last biomarker is highly influenced by the nutritional status of the organism (Brumley et al., 1998), therefore the higher concentrations recorded in April may be due to the lower feeding rates related to the greater reproductive and parental investment in that period (Malavasi et al., 2002). The PCA analysis, performed on standardized biological and chemical data obtained from the April and July samplings, showed a spatial separation of two groups, identified both by the sampling period and the sampling site (Fig. 5A). The first two PCA factors account for 82% of variance. The stations are distributed along the first factor according to decreasing MDA values and increasing Fe, Zn, Cd and 1-OH Naphtalene concentrations, and along the second factor by increasing levels of MT, 3-OH Benzo(a)pyrene, 1-OH Pyrene, PAHs and EROD activity. On the whole, the analysis of the biplot (Fig. 5B) showed that the stations are discriminated along the first axis by seasonality, whereas the chemical contamination is the main discriminant along the second axis.

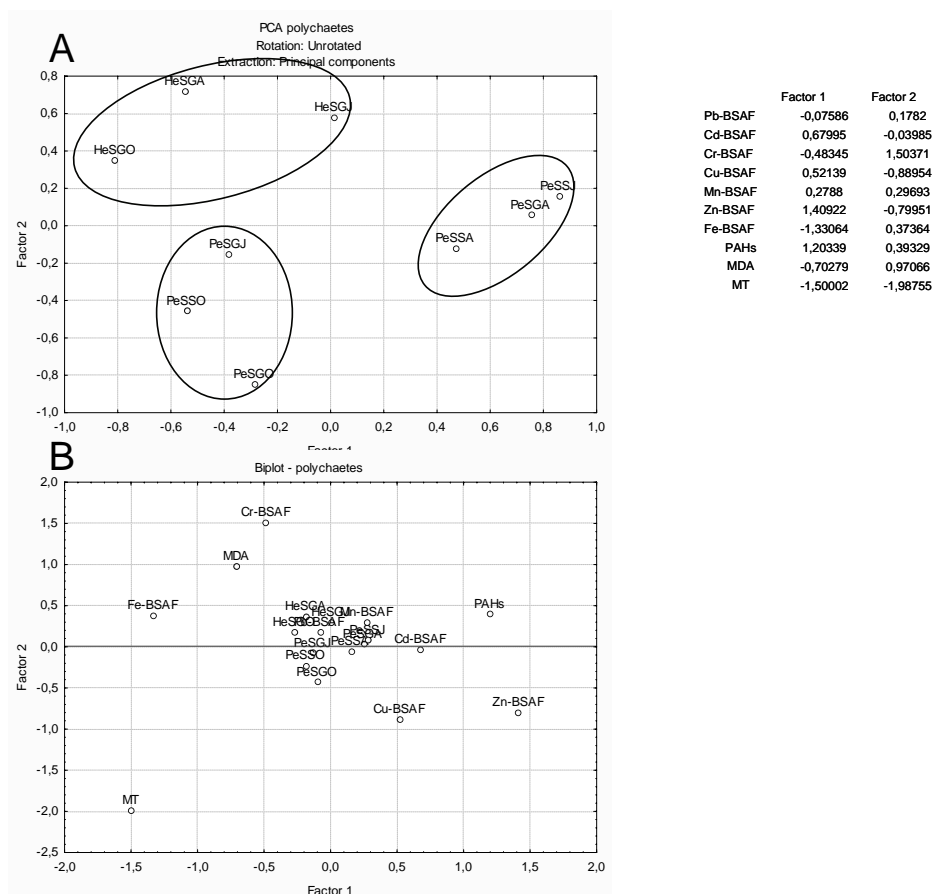


Fig. 4 – PCA analysis performed on standardized mean values of metal BSAF and PAHs concentrations and different biomarkers (MDA and MT) measured in polychaetes (Hed= *H. diversicolor*, Pe= *P. cultrifera*) from S. Giuliano (SG) and Sacca Sessola (SS) in April (A), July (J) and October (O).

Conclusions

In general, the results of the metal concentrations were quite low in the three taxa and similarly between the two sampling sites. No seasonal trend was detected in *P. cultrifera* and *Z. ophiocephalus*, whereas decreasing values were recorded in the metal bioaccumulation in *M. galloprovincialis* and *H. diversicolor* from S. Giuliano in July. Both polychaete species showed the capability to activate regulatory mechanisms when metal sediment concentrations increased.

PAHs concentrations in mussels, polychaetes and fish were always higher in samples from S. Giuliano, especially during the different reproductive periods.

Also the biomarker approach showed a similar condition between mussel samples, MDA and MT following the same seasonal trend of the metal concentrations. Only MT and lipofuscins content evidenced a worse situation at S. Giuliano.

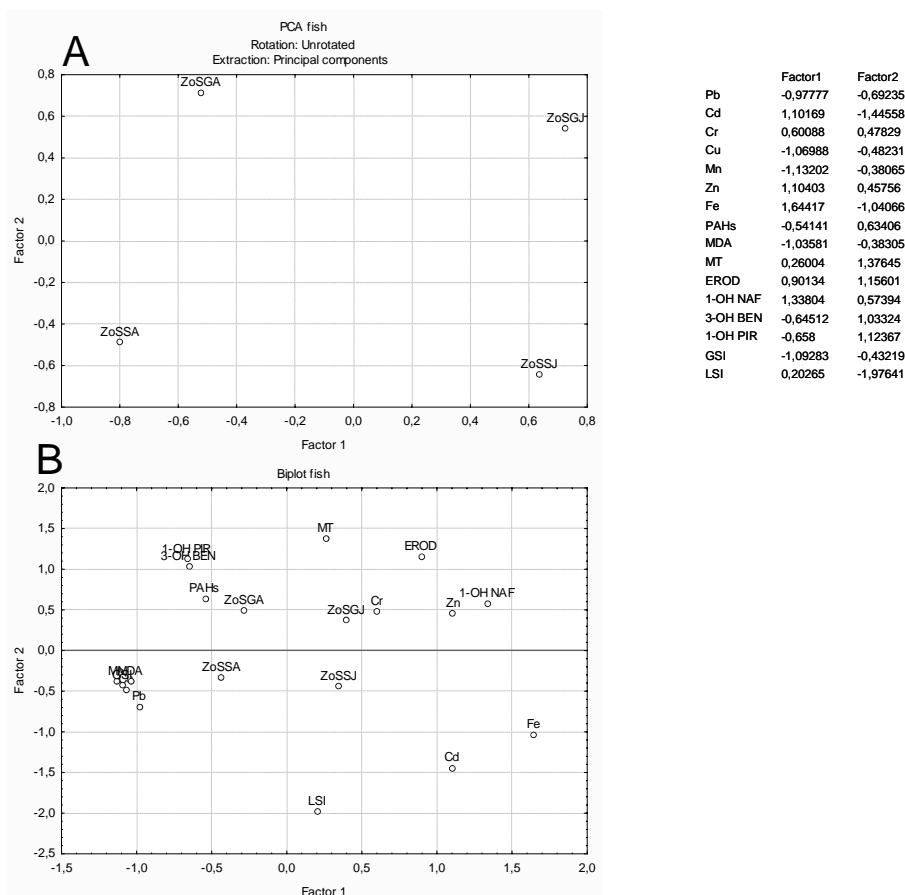


Fig. 5 – PCA analysis performed on standardized mean values of metal and PAHs concentrations and different biomarkers measured in fish from S. Giuliano (SG) and Sacca Sessola (SS) in April (A) and July (J).

On the contrary, the polychaetes *P. cultrifera* from S. Giuliano generally revealed a higher induction of both MDA and MT with respect to Sacca Sessola. *H. diversicolor* was revealed to be a more efficient bioaccumulator and generally showed higher values of MDA in comparison with *P. cultrifera*. Most of the biomarkers applied to *Z. ophiocephalus*, i.e. MDA, MT EROD and

fluorescent bile metabolites, notwithstanding their physiological seasonal trend, demonstrated a worse condition in S. Giuliano samples.

Finally, the multivariate analysis showed how seasonality is the main factor in discriminating the mussels samples, sampling site is the main factor in discriminating the polychaetes, whereas both factors are important in fish.

References

- Amiard J.C., Amiard-Triquet C., Barka S., Pellerin J., Rainbow P.S., 2006. Metallothioneins in aquatic invertebrates: their role in metal detoxification and their use as biomarkers. *Aquatic Toxicology*, 76, 160-202.
- Aas E., Beyer J., Goksoyr A., 2000. Fixed wavelength fluorescence (FF) of bile as a monitoring tool for polyaromatic hydrocarbon exposure in fish: an evaluation of compound specificity, inner filter effect and signal interpretation. *Biomarkers*, 5 (1), 9-23.
- Bayne B.L., Brown D.W., Burns K., Dixon D.R., Ivanovici A., Livingstone D.R., Lowe D.M., Moore M.N., Stebbing A.D.R., Widdows J., 1985. *The Effects of Stress and Pollution on Marine Animals*. Praeger, New York, Philadelphia, Eastbourne U.K., Toronto, 384 p.
- Brumley C.M., Haritos V.S., Ahokas J.T., Holdway D.A., 1998. The effects of exposure duration and feeding status on fish bile metabolites: implications for biomonitoring. *Ecotoxicology and Environmental Safety*, 39, 147-153.
- Bucheli T.D., Fent K., 1995. Induction of cytochrome P450 as a biomarker for environmental contamination in aquatic ecosystems. *Crit. Rev. Environ. Sci. Technol.*, 25, 201-268.
- Burke T.K., Mayer R.T., 1974. Ethoxyresorufine: direct fluorimetric assay of a microsomal O-dealkylation which is preferentially inducible by 3-methylcholanthrene. *Drug. Metab. Dispos*, 2, 583-588.
- Corsi I., Mariottini M., Sensini C., Lancini L., Focardi S., 2003. Cytochrome P450, acetylcholinesterase and gonadal histology for evaluating contaminant exposure levels in fishes from a highly eutrophic brackish ecosystem: the Orbetello Lagoon, Italy. *Marine Pollution Bulletin*, 46, 203-212.
- Eertman R.H.M., Wagenvoort A.J., Hummel H., Smaal A.C., 1993. "Survival in air" of the blue mussel *Mytilus edulis* L. as a sensitive response to pollution-induced environmental stress. *Journal of Experimental Marine Biology and Ecology*, 170, 179-195.
- Förlin L., Andersson T., 1984. Influence of biological and environmental factors on hepatic steroid and xenobiotic metabolism in fish: interaction with PCB and β -naphthoflavone. *Marine Environmental Research*, 14, 47-58.
- Fossato V.U., Campesan G., Craboledda L., Dolci F., Stocco G., 2000. Persistent chemical pollutants in mussels and gobies from the Venice Lagoon. In: *The Venice Lagoon Ecosystem*, Lasserre P., Marzollo A. (eds), UNESCO

421-437.

Gèret F., Jouan A., Turpin V., Bebianno M.J., Cosson R.P., 2002. Influence of metal exposure on metallothionein synthesis and lipid peroxidation in two bivalve molluscs: the oyster (*Crassostrea gigas*) and the mussel (*Mytilus edulis*). *Aquatic Living Resources*, 15, 61-66.

Giusti L., Zhang H., 2002. Heavy metals and arsenic in sediments, mussels, and marine water from Murano (Venice, Italy). *Environmental Geochemistry and Health*, 24, 47-65.

Livingstone D.R., 1998. The fate of organic xenobiotics in aquatic ecosystems: quantitative and qualitative differences in biotransformation by invertebrates and fish. *Comparative Biochemistry and Physiology Part A*, 120, 43-49.

Malavasi S., Coppola J., Pranovi F., Granzotto A., Franco A., Torricelli P., 2002. Habitat riproduttivo di *Zosterisessor ophiocephalus* Pall. (Pisces, Gobiidae) in Laguna di Venezia e osservazioni sulle caratteristiche dei riproduttori. *Lavori Soc. Ven. Sci. Nat. Vol. 27*, 47-56.

Moore M.N., 1988. Cytochemical responses of the lysosomal system and NADPH-ferrihemoprotein reductase in molluscan digestive cells to environmental and experimental exposure to xenobiotics. *Marine Ecology Progress Series*, 46, 81-89.

Pipe R.K., Coles J.A., Thomas M.E., Fossato V.U., Pulsford A.L., 1995. Evidence of environmentally derived immunomodulation in mussels from the Venice Lagoon. *Aquatic Toxicology*, 32, 59-73.

Porte C., Albaigès J., 1993. Bioaccumulation pattern of hydrocarbons and polychlorinated biphenyls in bivalves, crustaceans and fishes. *Archives of Environmental Contamination and Toxicology*, 26, 273-281.

Regoli F., 1992. Lysosomal responses as a sensitive stress index in biomonitoring heavy metal pollution. *Marine Ecology Progress Series*, 84, 63-69.

Scaps P., 2002. A review of the biology, ecology and potential use of the common ragworm *Hediste diversicolor* (O.F. Müller) (Annelida: Polychaeta). *Hydrobiologia*, 470, 203-218.

Sloof, W., Kreijl, C.F., Baars, A.J., 1983. Relative liver weights and xenobiotic-metabolizing enzymes of fish from polluted surface waters in the Netherlands. *Aquatic Toxicology*, 4, 1-14.

Sokal, R.R., Rohlf, F.J., 1969. *Biometry*. Freeman & Company, S Francisco: 776 pp.

Viarengo A., Canesi L., Pertica M., Poli G., Moore M.N., Orunesu M., 1990. Heavy metal effects on lipid peroxidation in the tissue of *Mytilus galloprovincialis* Lam. *Comparative Biochemistry and Physiology*, 97C, 37-42.

Viarengo A., Canesi L., 1991. Mussels as biological indicators of pollution. *Aquaculture*, 94, 225-243.

Volpi Ghirardini A., Cavallini L., Delaney E., Tagliapietra D., Ghetti P.F., Bettiol C., Argese E., 1999. *H. diversicolor*, *N. succinea* and *P. cultrifera* (Polychaeta: Nereididae) as bioaccumulators of cadmium and zinc from sediments: preliminary results in the Venetian Lagoon (Italy). *Toxicological and Environmental Chemistry*, 71, 457-474.

Waring C.P., Stagg R.M., Fretwell K., McLay H.A., Costello M.J., 1996. The impact of sewage sludge exposure on the reproduction of the sand goby, *Pomatoschistus minutus*. *Environmental Pollution*, 93 (1), 17-25.

RESEARCH LINE 3.9

Pollutant flows in the lagoon carried by aerosols and atmospheric fall-out

AEROSOL CHARACTERIZATION IN THE VENICE LAGOON

Franco Prodi, Franco Belosi, Silvia Ferrari, Gianni Santachiara, Paola Masia,
Lorenza Di Matteo

*CNR- Istituto di Scienze dell'Atmosfera e del Clima, Via Gobetti 101, 40129,
Bologna, Italy*

Riassunto

Vengono presentati i risultati della seconda campagna di misure, per la caratterizzazione dell'aerosol atmosferico, effettuata a Mazzorbetto, nella Laguna Nord di Venezia, nel periodo dal 15 Febbraio al 10 marzo 2005.

Nel corso di questa campagna sono state effettuate misure con strumenti in parte utilizzati nella precedente campagna già illustrati nel precedente rapporto, e precisamente: uno spettrometro inerziale INSPEC, uno spettrometro laser (LAS-X, PMS), un misuratore ottico di PM_{2.5} (Mie pDR-1200). Si è inoltre effettuato un campionamento di aerosol con diametro aerodinamico minore di 1 µm su filtro e successivamente si è effettuata l'analisi chimica del materiale depositato, per la frazione inorganica solubile in acqua. Da questa indagine si osserva che, ammettendo che il sodio sia completamente di origine marina, il rapporto Cl/Na⁺ (nel range 1.9–4.9) è in generale maggiore del rapporto nell'acqua marina (1.8 in peso). Si può pertanto concludere che deve essere presente una sorgente non marina di cloro, collegata con attività umana (e.g. processi di combustione). Per quanto riguarda i solfati, il rapporto in massa SO₄²⁻/Na⁺ risulta molto maggiore (range 15-40) del valore nell'acqua del mare (0.25). I valori misurati per i nitrati (nel range 5-12 µg m⁻³) sono maggiori di quelli riportati per aree urbane costiere. La correlazione tra la concentrazione dei nitrati e quella del sodio e calcio è bassa, mentre è elevata la correlazione tra NH₄⁺ e SO₄²⁻+ NO₃⁻ (r² = 0.90). Si deduce quindi che nella frazione PM₁ lo ione NH₄⁺ è prevalentemente sotto forma di nitrato e solfato. Infine dalle analisi sia SEM che PIXE si osserva come gli elementi prevalentemente cristallini (Ca, Mg, Si) sono presenti in percentuale maggiore nella frazione "coarse" e quelli di origine antropica (Ni, As, Zn, Ti) oltre a K e Mn, sono prevalentemente nella frazione "fine". Il Cl si trova sia nella frazione "coarse" che "fine".

Abstract

In this work the results from the second experimental campaign at Mazzorbetto (northern part of the Venice Lagoon), aimed at the aerosol characterization, will be presented. The measurements were carried out from 15th February to 10th March 2005.

Aerosol sampling has been performed mainly by means of the same samplers used in the previous campaign i.e. INSPEC (Inertial Spectrometer), a light scattering (LAS-X, PMS) and a nephelometer (PdR, Mie).

In addition, measurements of PM1 fraction have been carried out by means of cyclone. By assuming that Na is totally from sea source, the observed ratio

Cl-/Na+ (range 1.9–4.9) is higher than the value in the sea water (1.8 weight ratio), therefore it could be inferred a non sea-source for chlorine (i.e. combustion processes from anthropogenic activities). As far as sulphates, the mass ratio SO₄²⁻/Na+ (range 15-40) is much higher as to the sea water value (0.25). The same is true for nitrates (range 12–120 μg m⁻³) compared to coastal urban atmospheres. Strong correlation has been observed between NH₄⁺ and SO₄²⁻ - NO₃⁻ ($r^2 = 0.90$). Therefore in the PM1 fraction the NH₄⁺ ion is mostly in the form of sulphate and nitrate. Finally the SEM and PIXE analysis show elements mainly crustal (Ca, Mg, Si) in the coarse fraction and the anthropogenic elements (Ni, As, Zn, Ti) and K and Mn, mainly in the fine fraction. Chlorine is in the coarse as well in the fine fraction.

1 Introduction

The more important processes responsible of the contamination of the Venice lagoon are the direct injection of industrial effluents in water, sewage from the city and its hinterland, the atmosphere-water exchanges, the inflow of rivers and the water-sediments exchanges, the emission from motorboats. In addition it should be considered the exchange of pollutants between the lagoon and Adriatic sea at any tidal cycle.

In order to evidence the complexity of the system which must be monitored, we note that, if we consider only the pollutant atmosphere-water exchange, there should be taken into account not only dry and wet deposition, but in addition the transfer of aerosol from sea-water to atmosphere during the formation of marine aerosol (bubble bursting, raindrop splashing), the diffusive air-water vapor exchange, etc.

In this work we will continue the study on the chemical and physical characterization of the aerosol, by considering also the PM1 fraction.

2 Experimental set up and methods

The measurements were carried out in Mazzorbetto from 15th February to 10th March 2005. Most of the sampling devices used, lodged in a small wood home, are the same as described elsewhere [Prodi et al., 2005] and they are here only briefly summarised.

The Inertial Spectrometer (INSPEC) samples the aerosol on Nuclepore filters (0.1 μm porosity) and separates the particles on the basis of their aerodynamic size. The INSPEC sampling scheme is shown in Table 1.

Filter Number	Sampling Start	Sampling End	Sampling Time (h)	Sampling Volume (m ³)
2	17/02/05 11.30 am	18/02/05 9.30 am	22 h	0.462
4	01/03/05 06.25 pm	02/03/05 04.15 pm	22 h	0.462
5	02/03/05 06.05 pm	03/03/05 06 pm	24 h	0.504
6	08/03/05 03 pm	09/03/05 01 pm	22 h	0.462
7	09/03/05 01 pm	10/03/05 01 pm	24 h	0.504

Table – 1 Sampling scheme with the INSPEC

After the sampling the filters were analysed at the electronic microscope (SEM interfaced with EDAX - Physics Department, University of Bologna) and with the PIXE - Particle Induced X-ray Emission - Physics Department (University of Florence).

The light particle scattering sampler (Las-X, PMS inc.) measures the size and number concentration of aerosol particles in a limited size range (0.1 – 7.5 µm) by measuring the light scattered by single particles.

In addition sampling of PM1 aerosol fraction was carried out with a low volume sampler (0.7 m³ h⁻¹ flow rate), PM1 sampling inlet (cyclone) and nylon-PTFE filters coupled, in order to collect the particles and the semivolatile fraction (Kerminen et al. 2000; Yao et al., 2005). Each sampling session lasted about 24 h according to the data shown in Table 2.



Fig. 1 – PM1 size cyclone sampler

Table 2 – Sampling scheme for the PM1 fraction

Filter Number	Sampling Start	Sampling End	Sampling Time (h)	Sampling Volume (m ³)
1	23/02/05 01 p.m.	24/02/05 01 p.m.	24	15.90
2	24/02/05 07 p.m.	25/02/05 03 p.m.	20	12.96
3	01/03/05 06:30 p.m.	02/03/05 04 p.m.	21-22	12.77
4	02/03/05 06 p.m.	03/03/05 6 a.m.	12	7.92
5	08/03/05 03 p.m.	09/03/05 01 p.m.	22	14.59
6	09/03/05 01:15 p.m.	10/03/05 01:15 p.m.	24	16.05

The analytical determination was carried out with a ionic chromatograph (Chemistry Department, University of Florence). The aerosol sampled on the filter packs has been extracted by means of an ultrasonic bath in 10 ml of Milli-Q water, filtered through a 0.45 µm porosity membrane filter, and successively injected into the chromatographic column (Dionex DX 120).

The determination of the inorganic cations has been carried out through a a CG12A column followed by the Dionex CS12A. The columns allow the simultaneous assessment of the monovalent and the bivalent species. The analysed ion species have been Cl⁻, NO²⁻, NO³⁻, SO₄²⁻, Na⁺, NH₄⁺, K⁺, Mg²⁺, Ca²⁺. Among the organic compounds only the MSA was analysed by means of a Dionex DX 500 chromatograph with a Dionex AS11 column preceded by a AG11 column.

From the 23rd of February to the 3rd of March, in cooperation with Dr. Snells (ISAC-Rome), measurements with a micro LIDAR (micro Light Detection And Ranging) have been performed. The LIDAR employs a laser as a source of pulsed energy of useful magnitude and suitable short duration; as the transmitted laser energy passes through the atmosphere, the gas molecules and particles encountered cause scattering. A small fraction of this energy is backscattered in the direction of the lidar system and is detected as shown in Fig. 2 (Hinkley, 1976).

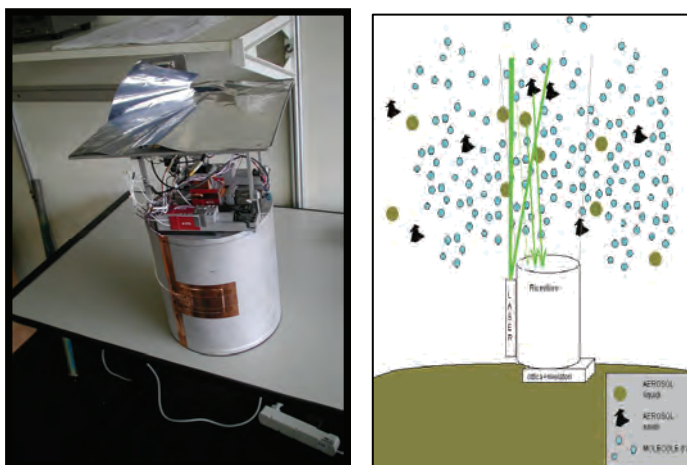


Fig. 2 – The micro LIDAR (on the left) and its working principle (on the right)

3 Results and discussion

In the following the results for each investigation technique will be described together with their comparison.

3.1 PM1 water soluble chemical composition

Table 3 shows the chemical concentration of water soluble inorganic ions obtained from analysis of PM1 aerosol, and Table 4 the ratios Cl^- / Na^+ ; SO_4^{2-} / Na^+ and K^+ / Na^+ . By supposing that the Na is only from the sea-water, it is possible to infer that Cl^- / Na^+ ratio (1.9 – 4.9 range) in the aerosol is generally higher than the ratio in the sea-water (1.8). This means that must be present a non-sea source for Cl (e.g. combustion process).

Species	Filter 1	Filter 2	Filter 3	Filter 4	Filter 5	Filter 6
	Concentration ($\mu g/m^3$)					
Na^+	0.108	0.199	0.066	0.180	0.070	0.088
NH_4^+	3.564	3.019	1.976	3.347	3.073	2.649
K^+	0.357	0.468	0.336	0.383	0.317	0.320
Mg^+	0.022	0.120	0.021	0.065	0.011	0.014
Ca^+	0.071	0.088	0.063	0.240	0.043	0.052
Cl^-	0.378	0.384	0.294	0.621	0.209	0.430
NO_2^-	ND	0.030	ND	0.003	ND	ND
NO_3^-	12.278	9.369	4.987	7.866	10.032	9.452
SO_4^{2-}	4.326	3.022	2.117	4.648	2.957	2.570

Table 3 – Water soluble inorganic ions concentration

Ratio	Filter 1	Filter 2	Filter 3	Filter 4	Filter 5	Filter 6
Cl^- / Na^+	3.5	1.9	4.5	3.5	3.0	4.9
SO_4^{2-} / Na^+	40.1	15.2	32.1	25.8	42.2	29.2
K^+ / Na^+	3.3	2.4	5.1	2.1	4.5	3.6

Table 4 – Investigated ion ratios

As regards to the SO_4^{2-} / Na^+ ratio, which is always higher than the seawater ratio (from 15-40 times), it is clear that most sulphate is not of marine origin. The excess of sulphate, that is nss- SO_4^{2-} , may be calculated from total sulphate using the equation

$$[nss-SO_4^{2-}] = [SO_4^{2-}] - 0.25 [Na^+]$$

where 0.25 is the mass ratio SO_4^{2-} / Na^+ in the sea-water.

Sulphate from sea-salt to total sulphate ratio is about unitary. In non-polluted marine areas a source of nss- SO_4^{2-} is from oxidation of dimethylsulfide (DMS) released by biogenic activity on the marine surface. The oxidation of DMS produces nss- SO_4^{2-} and methane sulphonic acid (MSA). The MSA concentration in our samples is in the range 0.02-0.06 $\mu g m^{-3}$. In conclusion, in

the examined area, nss-SO_4^{2-} comes prevalently from homogeneous and heterogeneous oxidation of SO_2 emitted from industrial plants. Concerning nitrates, present both in the fine and coarse particles, they can derive from photo-oxidation of NO_2 produced from combustion processes, or through reaction of HNO_3 with sea-salt determining a Cl loss. The measured values (5–12 $\mu\text{g m}^{-3}$ range) are higher than those measured in urban coastal areas (Zhuang et al, 1999b) and of sulphate concentrations (2.2 – 4.7 $\mu\text{g m}^{-3}$). Fig. 5 shows that NH_4^+ concentration is well correlated with the sum of SO_4^{2-} and NO_3^- ($r^2 = 0.90$). This indicates that ammonium sulphate and nitrate in the PM1 fraction contribute to a large fraction of these anions.

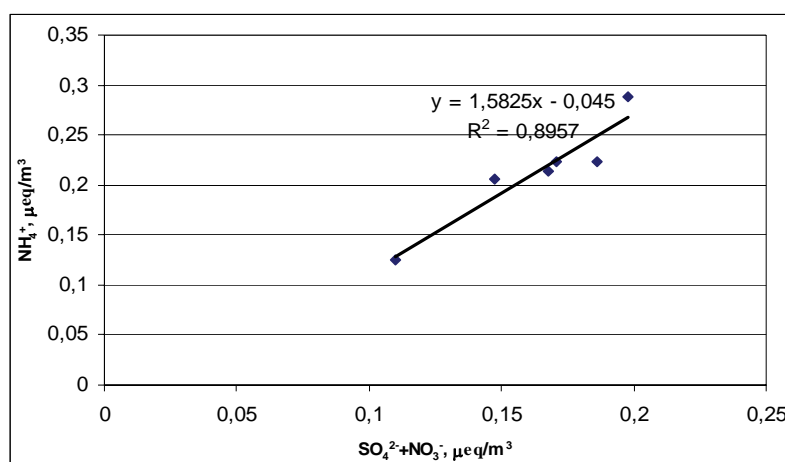


Fig. 5 – Correlation between NH_4^+ and SO_4^{2-} and NO_3^-

Giugliano et al. (2005) measured the Cl^- , NH_4^+ , SO_4^{2-} , NO_3^- concentrations in the PM2.5 fraction, in an urban site (Milan). Cl^- and NO_3^- concentrations are comparable with our results in the PM1 fraction, while NH_4^+ and SO_4^{2-} values are higher in Milan. Concerning the K^+ / Na^+ ratio in PM1 fraction, it is always higher (2-5 range) than sea-water (0.036). This suggests the existence of an anthropogenic source for K.

3.2 Elemental chemical composition of aerosol

Filters sampled with Inertial Spectrometer were analysed with SEM, interfaced with Edax, and with PIXE techniques. In the following only the results of a few filters will be shown.

The elemental analysis obtained from SEM (Filters no.2 and 4) show for both filters the presence of anthropogenic elements (Pb, Ti, Zn, Tl) in the size range 1.5 - 6.6 μm . In addition Na is mainly present in aerosol particles containing crustal element (mixed crystals).

In Table 5 the total concentration (ng m^{-3}) is shown of the considered element (water soluble and insoluble) obtained with PIXE in the size range lower than 6 μm (filters no.4 and 5), and lower than 3.5 μm (filters no.4, 5 and 7). In addition it's reported filter no. 5 of the first campaign (June 2004).

Element	Filter 4 < 3.5 µm	Filter 4 < 6.0 µm	Filter 5 < 3.5 µm	Filter 5 < 6.0 µm	Filter 7 <3.5 µm	Filter 5 < 6 µm
	II campaign					I campaign
Na	110	147	82	164	154	203
Mg	69	157	44	147	46	211
Si	131	328	144	410	177	1497
P	41	90	ND	ND	ND	196
S	673	1121	1328	2415	1630	11254
Cl	13	18	20	20	86	620
K	356	445	295	492	564	198
Ca	242	537	169	563	200	1262
Ti	2	2	2	2	ND	74
Cr	27	77	ND	ND	3	228
Mn	10	12	7	11	4	2
Fe	200	334	76	190	112	334
Ni	3	4	1	1	3	5
Cu	11	19	ND	ND	4	9
Zn	84	112	28	47	45	23
As	3	7	ND	ND	ND	8
Pb	5	10	7	12	20	16

Table 5 – Element concentration from PIXE analysis

By comparing element concentrations, we can note that filter no.5 (sampled during 1st campaign – July 2004) presents S, Cl, Ca, Si, Cr and Fe in concentrations higher with respect to filters of the 2nd campaign. Na concentration in both campaigns is comparable (150-250 ng m⁻³ range).

In Fig. 6 is shown the percentage of mass concentration for each element in the different size range for the Filter n.4.

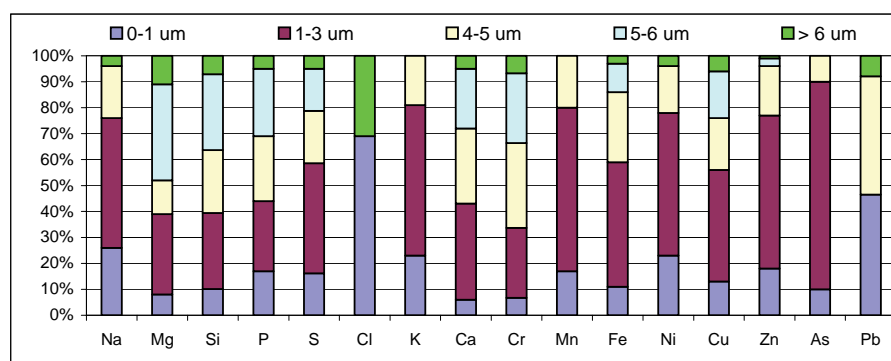


Fig. 6 – Percentage of element mass concentration (Filter n. 4)

Crustal elements (Ca, Mg, Si) are present in higher percentage in the coarse fraction, while anthropogenic elements (Ni, As, Zn, Ti), and also K and Mn, are

prevalently in the fine fraction. Cl is both in the fine and coarse fraction.

We can compare the results obtained from SEM and PIXE with those from soluble fraction of PM1. We will consider filter No.3 (PM1) and Filter n. 4 (INSPEC): The sampling period for both filters is 1/03/2005 – 2/03/2005.

Na concentrations in Filter 4, obtained with PIXE is 147 ng m^{-3} and in Filter 3 obtained with Ionic Chromatograph is 66 ng m^{-3} . From SEM analysis results that Na is present in a percentage of about 15% of particles with diameter $> 1.5 \text{ }\mu\text{m}$ and in mixed crystals containing in addition Si, Ca, S, P, K and Al. In addition we can note that Na is present both in the fine and coarse fraction.

The ratio $\text{Mg}^{2+} / \text{Na}^+$ in filter 3 results 0.32, and in filter no.4 is about 1.1 (sea-water ratio 0.12). Then Mg is prevalently in the coarse fraction and has a source other than sea.

Concerning sulphate, by comparing concentrations of SO_4^{2-} in the PM1 fraction ($2.1 \text{ }\mu\text{g m}^{-3}$) with the S value from PIXE ($1.12 \text{ }\mu\text{g m}^{-3}$, which corresponds to $3.3 \text{ }\mu\text{g m}^{-3}$ of SO_4^{2-}), we can deduce that these compounds is prevalently in the fine fraction. K, found first of all in the fine fraction ($0.336 \text{ }\mu\text{g m}^{-3}$ PM1 and $0.445 \text{ }\mu\text{g m}^{-3}$ as total concentration), should derive from combustion process. As regards to Ca, it is present both in the fine and coarse fraction ($0.063 \text{ }\mu\text{g m}^{-3}$ in the PM1 fraction and $0.537 \text{ }\mu\text{g m}^{-3}$ as total concentration).

3.3 Size distribution and particle number concentration

Fig. 7 shows the particle number concentration obtained from LAS-X measurements. The comparison with the first campaign points out that the particle number concentration in the winter campaign is a factor of 10 higher, according to the real time measurements of mass concentration which bears in evidence higher concentration in winter.

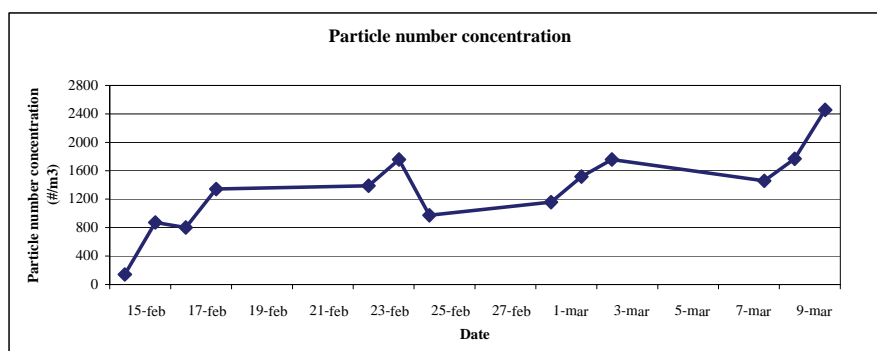


Fig. 7 – Particle number concentration

As it can be seen from Fig. 7, there are several spikes in the particle number concentration pattern. These have been investigated and are in agreement with real time aerosol mass concentration. Moreover the wind direction (from SODAR profile – Ente Zona Industriale, and from the sonic anemometer at Mazzorbetto) is from westerly sectors and is possible that these spikes could come from the more polluted areas of Porto Marghera (industrial area) and

Mestre (traffic area). In the following is shown one of these outcomes (March the 2nd). Fig. 8 shows the spike temporal detail of mass concentration derived from LAS-X measurements, combined with the real time PM2.5 values from PdR, while Fig. 9 shows the wind direction profile.

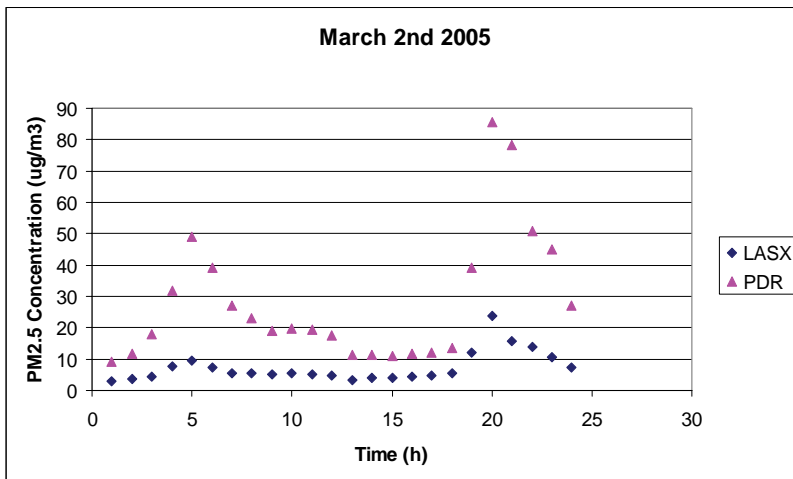


Fig. 8 – LAS-X and PdR temporal aerosol trend

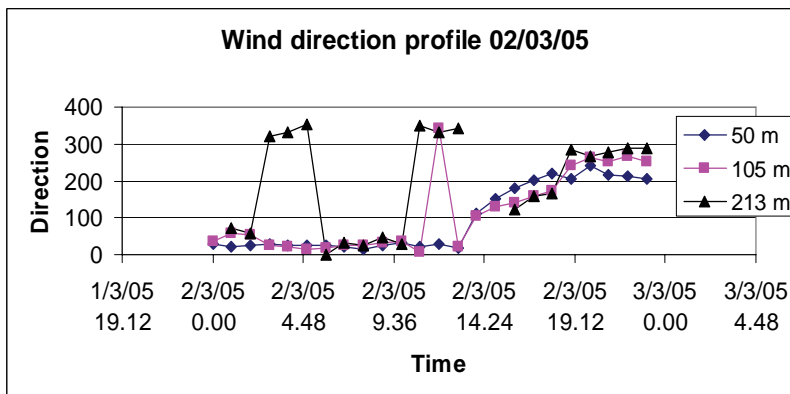


Fig. 9 – Wind direction profile

Comparing Fig. 8 and Fig. 9 it can be seen that in the early morning and at in the late afternoon (when the boundary layer height is lower) the aerosol concentration is higher when the wind (at about 200 m) comes from around 300 degrees.

3.4 Vertical aerosol profile

Fig. 10 shows an example of vertical aerosol profile concentration obtained with the LIDAR on February 17th at 06:15 pm

In the first 300 m of altitude liquid particles have been observed, while at higher altitude (from 2000 m to 3000 m) solid particles are visible. The vertical wind profile gives a SE direction and perhaps the liquid particles observed are droplets and /or hygroscopic aerosol particles at deliquescent point ; at higher altitude the wind comes from the northerly direction and the aerosol particles are solid.

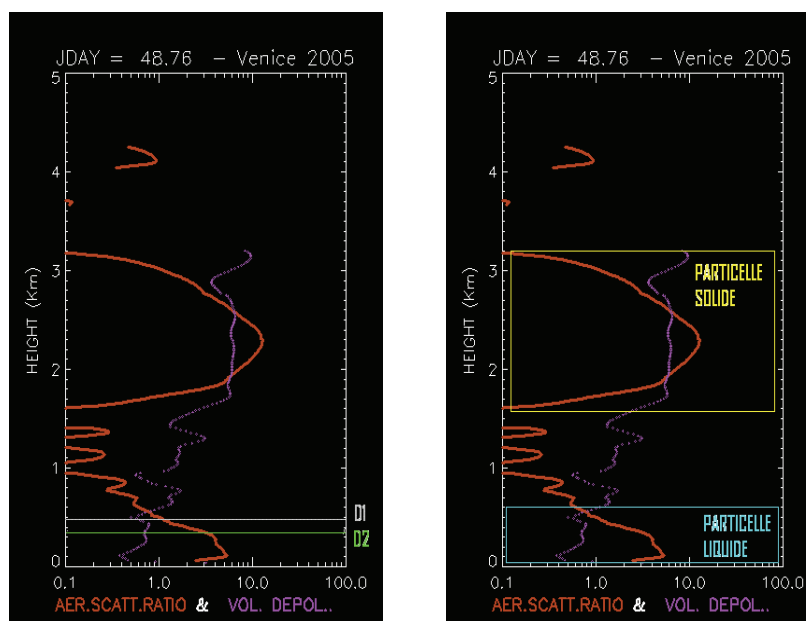


Fig. 10 – LIDAR profile

4 Conclusions

The experimental campaigns have outlined the presence of different spatial scales for the sources of pollutants:

a- Short range sources (local industrial emissions) when the wind is blowing from the westerly directions. Experimental data, for instance, evidence events in which there is transport from the more polluted areas of Porto Marghera (industrial area) and Mestre (traffic area) (e.g. March the 2nd 2005).

b- Medium range sources (from the Po Valley) with higher PM concentrations positively correlated with the Aerosol Optical Thickness (AOT) from AERONET sunphotometer. The 22nd of July 2004 shows an example.

c- Long range transport (Sahara dust) as for example July the 8th 2004.

The correlation with the meteorological parameters (vertical wind profile and temperature) is of great importance in establishing the transport of pollutants over the Venice lagoon area since the wind often change its direction with the altitude.

In the PM1 soluble aerosol fraction the dominant contribution of anions is due to ammonium sulphate and nitrate. The ratios Cl^-/Na^+ , K^+/Na^+ and SO_4^{2-}/Na^+ are much higher than in the sea water meaning anthropogenic sources for Cl, K and sulphate.

Moreover the comparison with the first campaign points out that the particle number concentration in the winter campaign is a factor of 10 higher, according to the real time measurements of mass concentration, which bears in evidence higher concentration in winter.

Acknowledgments

Authors wish to thank the Ente Zona Industriale di Porto Marghera (via delle Industrie, 19 - 30175 Porto Marghera, VE) for providing some meteorological data, Dr. G. Zibordi (JRC, Ispra) for providing Aeronet data, Dr. M. Snells and Mr. M. Morbidini (ISAC-Rome) for their help with the LIDAR measurements, Mr. G. Trivellone and M. Tercon (ISAC-Bologna) for their technical support. Authors also wish to thank Dr. F. Luccarelli (Univ. of Florence) for the PIXE analysis, Dr. R. Udisti (Univ. of Florence) for the Ion Chromatograph investigations and Mr. S. Berti (Univ. of Bologna) for the SEM observations.

References

- Giugliano M., Lonati G., Butelli P., Romele L., Tardivo R. and Grosso M., 2005. Fine particulate (PM_{2.5}-PM₁) at the urban site with different traffic exposure. *Atmos. Environ.* 39, 2421-2431
- Hinkley E.D., 1976. *Laser Monitoring of the Atmosphere*, Springer Verlag.
- Kerminen V.M., Tienila K. and Hillamo R., 2000. Chemistry of sea-salt particles in the summer Antarctic atmosphere. *Atmos. Environ.*, 34, 2817-2825.
- Prodi F., Belosi F., Ferrari S., Santachiara G. and Masia P., 2005. Size characterisation of aerosol in the Venice Lagoon. *Scientific Research and Safeguarding of Venice*, Edited by P. Campostrini, Vol. IV, pp. 207:217.
- Zhuang H., Chan C.K., Fang M. and Wexler A.S., 1999a. Size distribution of particulate sulfate, nitrate and ammonium at a coastal site in Hong Kong. *Atmos. Environ.*, 33, 4223-4233.
- Zhuang H., Chan C.K., Fang M. and Wexler A.S., 1999b. Formation of nitrate and non-sea-salt sulfate on coarse particles. *Atmos. Environ.*, 33, 843-853
- Yao X, Fang M. and Chan C.K., 2001. Experimental study of the sampling artifact of chloride depletion from collected sea salt aerosols. *Environ. Sci. Technol.*, 35, 600-605.

REAL TIME PM_{2.5} CONCENTRATION AND VERTICAL TURBULENT FLUX ON THE VENICE LAGOON

Daniele Contini¹, Antonio Donateo¹, Franco Belosi², Franco Prodi²

¹ *Istituto di Scienze dell'Atmosfera e del Clima, CNR, unità operativa di Lecce SP Lecce-Monteroni km 1.2, 73100 Lecce* ² *Istituto di Scienze dell'Atmosfera e del Clima, CNR, Via Gobetti 101, 40129 Bologna*

Riassunto

In questo lavoro si presenta uno studio della dinamica locale di aerosol, ed in particolare della frazione PM_{2.5} sull'isola di Mazzorbetto nella laguna di Venezia. I dati sono stati ottenuti in due campagne di misura (estate 2004 ed inverno 2005) utilizzando una stazione di misura basata su di un anemometro ultrasonico tridimensionale ed un rivelatore ottico veloce di PM_{2.5}. Il sistema permette di rilevare le fluttuazioni del campo di concentrazione e di velocità del vento che sono anche utilizzate per il calcolo dei flussi verticali turbolenti di massa di PM_{2.5}. Tali informazioni, correlate con i parametri meteorologici, permettono una più approfondita analisi della dinamica dell'aerosol atmosferico migliorando l'interpretazione dei dati di qualità dell'aria. Sono stati evidenziati dei "pattern" di concentrazione sia stagionali sia giornalieri con un valore medio della concentrazione diurna che è circa il 25% più basso di quello notturno (in entrambi i periodi di misura). Questo andamento giornaliero è stato correlato ad alcuni parametri meteorologici locali quali direzione del vento, umidità relativa ed altezza dello strato limite. I dati meteorologici mostrano che la circolazione tipica dalle Alpi e dal mare Adriatico trovata nel periodo estivo non si presenta, in maniera persistente, nel periodo invernale.

Abstract

In this work an analysis of the aerosol local dynamics, for the PM_{2.5} fraction, is presented. Measurements have been carried out in the Mazzorbetto Island in the Venice Lagoon using a measuring station based on a 3D-ultrasonic anemometer and a real-time PM_{2.5} optical detector. Measurements refer to two campaigns (summer 2004 and winter 2005) that are compared in this work. Measurement system allows detecting fluctuations of the concentration and velocity fields that are also used to evaluate the vertical turbulent fluxes of PM_{2.5}. The information obtained, correlated with local meteorological parameters, gives insights about local aerosol dynamics that are useful to interpret air quality data. Seasonal and daily patterns have been observed in concentration data with an average diurnal concentration that is about 25% lower than the average nocturnal value (in both measurement periods). The daily pattern has been correlated with some local meteorological parameters like wind direction, relative humidity and boundary-layer height. Meteorological measurements show that the typical circulation from Alps and Adriatic Sea that

has been found during the summer is not stably present during the winter.

1 Introduction

In this work mainly the results of the second measurements campaign, carried out in February 2005, are reported and they have been compared to the ones obtained during the first measurement campaign performed in the summer 2004. In particular some specific trends in PM_{2.5} concentration levels will be discussed in terms of their relationships with trends of the main meteorological parameters. Results indicate that concentration levels are correlated with wind directions and this also give information about the main sources of aerosol acting on the site. Seasonal and daily patterns in concentration levels are observed. Daily pattern is correlated with some meteorological parameters like wind direction, relative humidity and Boundary-Layer height. Results indicate that the stable circulation with wind coming from Alps (night) and Adriatic Sea (day) is not evident in the winter but it is present during the summer period. Vertical turbulent fluxes do not show stable trends, moreover they are mainly positive in the winter period and mainly negative during the summer.

2 Measurement set-up and post-processing procedure

The instruments platform used is the same described in [Contini et al., 2006] and it is here only briefly summarised (Fig. 1):

- A tridimensional ultrasonic anemometer, Gill R3, operating at 100 Hz.
- An Optical sensor for PM_{2.5} concentration Mie pDR-1200 (Personal Data logging Real time Aerosol Monitor) by Thermo Electron Corp., operating in active sampling at 1 Hz with a pump TECORA Bravo H-Plus. It is equipped with a cyclone (2.5 µm cut-off at the 4l/m flow rate used).
- A low response termo-igrometer ROTRONIC MP100A.
- An inclinometer, bi-axial, (model FAS-A, Microstrain).

Measuring station was placed at 9.6m above the ground using a telescopic mast. Data post-processing is based on 30 minutes averages in the streamlines reference system [McMillen, 1988]. The eddy-correlation procedure is used to estimate vertical turbulent mass momentum, energy and PM_{2.5} fluxes as described in [Donateo et al., 2006]. In the calculation of turbulent fluxes a 2s delay has been introduced to synchronize real time concentration measurements with wind speed. The necessary delay has been evaluated in laboratory tests of the pDR-1200 first-order time response τ to a step in concentration from zero up to about 36 µg/m³. The average of several repeated trials gave $\tau=1.1$ s. This value is also confirmed by the 5%-95% time response to the concentration step $\Delta t=3.2$ s that has been measured and that is related to τ as: $\tau=\Delta t/2.944$. The value of τ indicates that the instrument is essentially able to follow concentration fluctuations up to about 0.5Hz and this is usually enough to measure most of the correlation $\langle w'c' \rangle$ because the maximum of the co-spectra between vertical wind velocity fluctuations w' and concentration fluctuations c' is usually located at frequencies around 0.1Hz [Dorsey et al.,

2002; Buzorius et al., 1998; Nemitz et al., 2002]. An analysis of our data in terms of spectra and co-spectra for selected periods of both measurement campaigns (not shown) brings to the same conclusions.



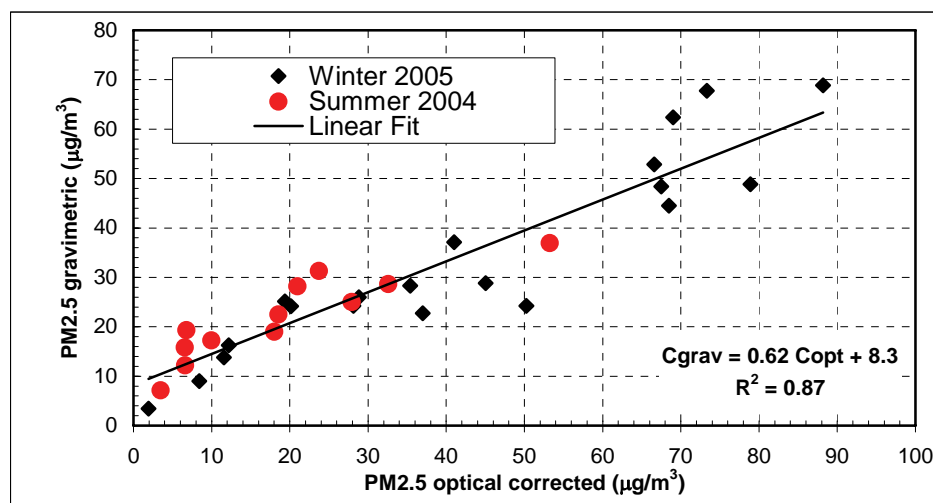
Fig. 1 - Instruments platform used on the Mazzorbetto island in the Venice lagoon.

Measured optical concentrations have been corrected with the procedure described in [Contini et al., 2006; Donateo et al., 2006] for the effect of relative humidity (RH). Corrected daily averaged concentrations have been compared with gravimetric detection of aerosol and a good correlation has been observed. Results are reported in Figure 2 and a summary is reported in Tab. 1. The determination coefficient R^2 change from 0.66 for uncorrected concentrations up to 0.87 for RH-corrected values. The corresponding Pearson correlation coefficients change from 0.81 to 0.93. This means that the use of the correction procedure improves significantly the agreement between the two different measurement methods. In the following of this paper PM_{2.5} instantaneous concentrations will be always corrected for RH effect with the mentioned procedure.

	Without Correction	With Correction	Gravimetric
Average Conc. ($\mu\text{g}/\text{m}^3$)	69.1	33.7	29.4
R^2	0.66	0.87	1
Pearson	0.81	0.93	1
Slope	0.2	0.62	1
Intercept	15.5	8.3	0

Tab. 1 - Comparison between daily concentration from integration of optical signal and gravimetric one

Fig. 2 - Scatter plot of daily gravimetric concentrations as function of RH-corrected PM2.5 concentrations.



3 Winter campaign results

Average wind speed (Fig.3) in the measurement period is 2.8 m/s at 9.6m above the ground with a maximum wind speed of about 10 m/s. This wind values are analogous to the ones found in the first measurement campaign (summer 2004). Wind direction (Fig.4) time history is compared with Sodar measurements (at 160m above the ground) showing a similar trend. The cases of large wind speed are distributed before 4/3/2005. Periods of large wind speed (over 6 m/s) are essentially the period 20-22 February and 28 February and both are in relation with wind direction from EEN and NE. On the other hand in winter campaign there is not the periodical and stable circulation with wind blowing from NE, for nocturnal period, and from SE, for daily period. This circulation was instead present in the summer period. During the winter campaign temperature was ranging between 12°C during day and -6°C during night. Relative humidity was in the range 22% - 98%. Several micrometeorological parameters are obtained from data taken in this period: momentum flux F_M , sensible heat flux F_H , turbulent kinetic energy (TKE) and friction velocity u^* that are not shown here. Maximum value of u^* and TKE is in the morning of 21/02/2005 corresponding to maximum peak value in wind speed. F_H time history show regular peak after 07/03/2005. Before this date there is an irregular pattern for this quantity with several low-flux values; basically this is a consequence of meteorological events as rain or cloudiness and snow. A summary of meteorological conditions during the measurement campaign is reported in Table 2 together with the indication of the average daily values of PM2.5 concentrations. In Fig.5 PM2.5 concentration measured during winter is reported as function of local time and in Fig.6 the PM2.5 turbulent vertical flux is reported. It has to be put in evidence that there is a great variability of PM2.5 concentrations caused by different meteorological events (rain, snow and large wind speed). Average concentration on whole period is $41.8 \mu\text{g}/\text{m}^3$ ($\pm 31.6 \mu\text{g}/\text{m}^3$), with a peak value on 30 min average equal to $144 \mu\text{g}/\text{m}^3$. This concentration is significantly higher than the one observed in the

summer period ($16.7 \pm 18 \mu\text{g}/\text{m}^3$).

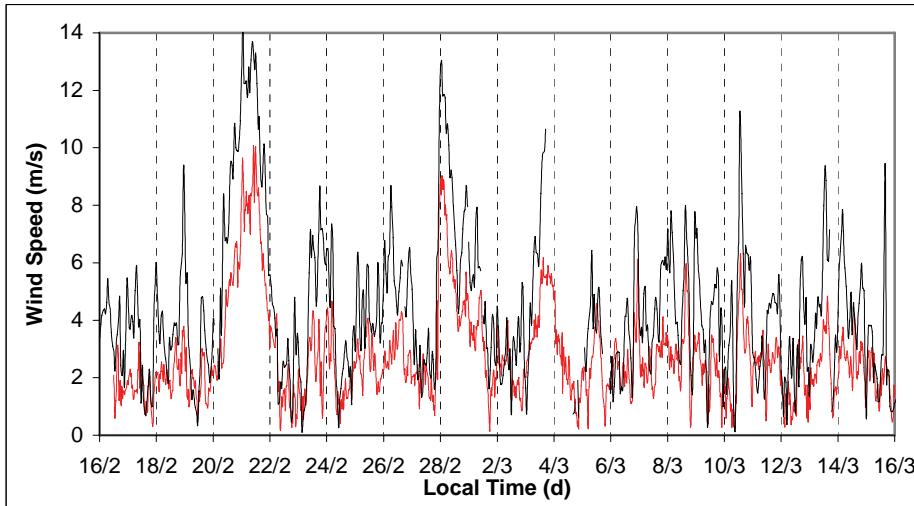


Fig. 3 – Wind speed at 9.6m (black) and Sodar data (red) obtained at 160m

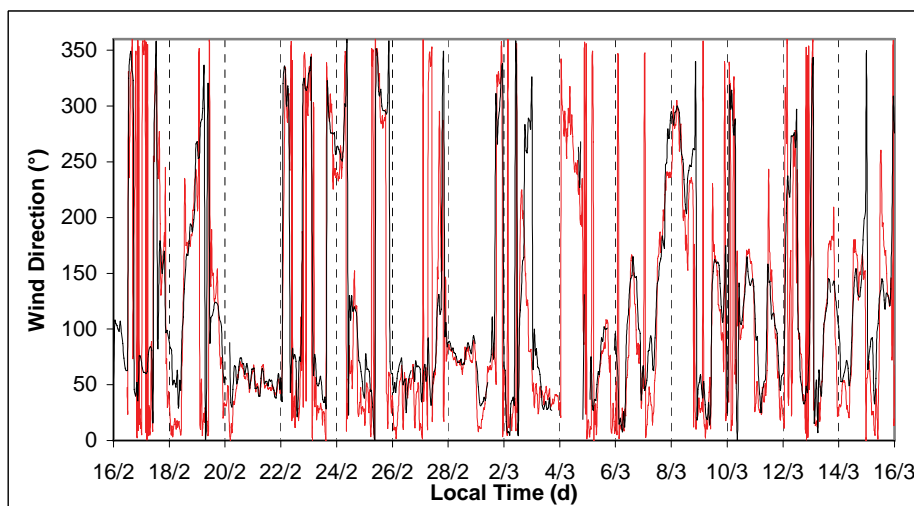


Fig. 4 – Wind direction at 9.6m (black) and Sodar data (red) obtained at 160m.

This means that a seasonal pattern is present with higher winter concentrations, as it often happens in the north of Italy (Marcazzan et al, 2001). The PM_{2.5} time-history shows several brief concentration peaks (over $100 \mu\text{g}/\text{m}^3$) and also long periods of large concentrations. In the period from 28/2 to 2/3 concentrations are instead relatively small. It has to be put in evidence that during 28/02/2005 the average wind speed is the largest one and it is also a rainy day. In 8/03/2005 a peak in PM_{2.5} daily concentration is present and the day is characterized by a moderate average wind speed and wind direction at about 1500m, obtained by radiosoundings in Udine, is prevalently from SW. Wind direction near the ground is also from S-SW sectors. High concentration value can be explained with transport from Pianura Padana (at high altitude) and also from the industrial area of Porto Marghera, as it was also shown in summer campaign (Contini et al, 2006). Vertical turbulent fluxes do not show an evident pattern even if the main activity is during the day. The fluxes are mainly

positive during the winter and mainly negative during the summer. During 08/03/2005 PM2.5 vertical turbulent flux is positive on average and, on absolute value, it is the day in which the daily turbulent flux is higher.

Fig. 5 - Fine particulate PM2.5 concentration on 30 min average

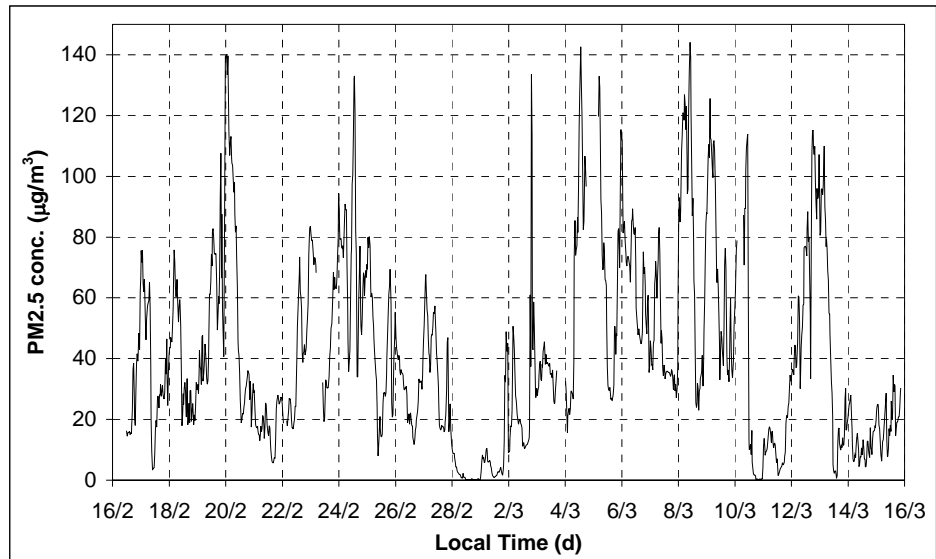
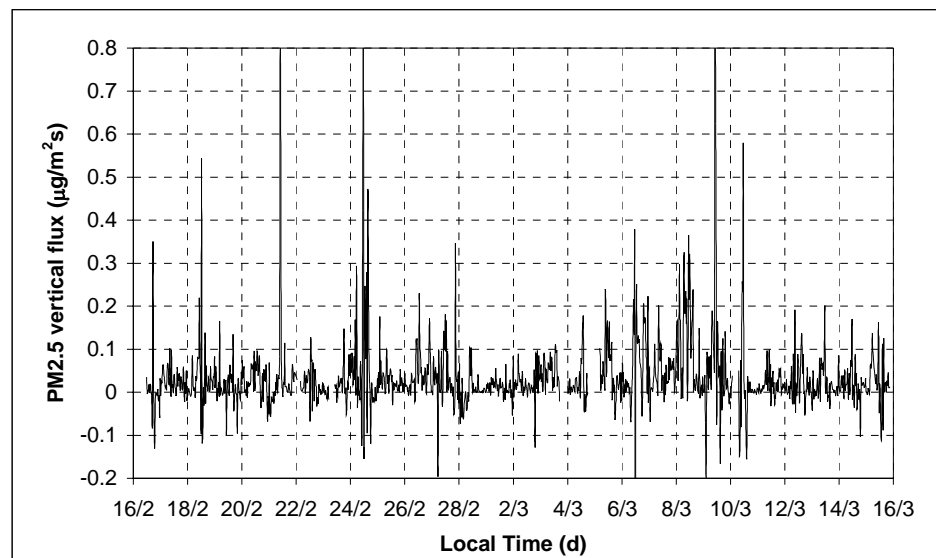


Fig. 6 - PM2.5 vertical turbulent flux



In both measurement campaigns the average PM2.5 concentration calculated in diurnal periods (from 8.00 to 20.00) is about 25% lower than the average calculated during nocturnal periods (from 20.00 to 8.00). A summary is shown in Table 3. Correlations between wind speed and direction and concentration values are studied. Results indicate that the average concentration calculated when wind speed is above 2 m/s is lower (Table 4) than the average calculated for wind speed lower than 2 m/s. This happens for both measurement campaigns, even if to a different extent in summer and winter, and it is a consequence of the increased transport and mixing that take place in high wind

speed conditions.

Day	PM2.5 Conc. ($\mu\text{g}/\text{m}^3$)	Wind Speed (m/s)	Prevalent Wind Direction	T ($^{\circ}\text{C}$)	RH (%)	Rain (mm)	Meteo Events
16/02/05	29.3	1.63	N	4.9	56.3	0	
17/02/05	37.0	1.62	N	3.6	69.1	0	
18/02/05	38.3	2.27	S - NNE	3.4	67.3	0	
19/02/05	58.8	1.80	NNE	3.0	72.8	0	
20/02/05	61.4	4.37	NE	3.0	66.9	0	Haze
21/02/05	17.9	7.32	NE	0.2	93.7	4.4	Snow
22/02/05	41.5	1.61	NE-NW	1.5	87.2	9.6	Snow
23/02/05	55.2	2.38	NNE	1.7	86.8	0	Fog
24/02/05	72.5	2.02	NE	2.3	82.6	0	Fog
25/02/05	41.4	2.53	NE-NW	3.1	78.9	0.2	Snow
26/02/05	28.8	2.90	NE	2.9	71.7	0	
27/02/05	36.0	2.42	NNE-EEN	2.6	63.0	0	
28/02/05	1.8	5.74	EEN	-0.4	39.5	0.2	
01/03/05	9.2	2.86	NNE-EEN	-2.4	45.7	0	
02/03/05	28.8	2.18	NNE	-0.7	51.2	0	
03/03/05	35.4	4.39	NE	-1.2	75.1	0	Snow
04/03/05	69.0	2.19	W	1.4	91.2	7	Fog
05/03/05	64.5	2.29	NNE	2.6	70.4	0	Fog
06/03/05	66.2	2.57	NE	2.9	70.8	0	
07/03/05	44.9	2.60	SW - NNE	2.8	55.4	0	
08/03/05	79.1	2.91	SW-W	4.3	65.5	0	
09/03/05	67.7	2.28	NNE	4.9	74.2	0	
10/03/05	32.0	2.55	SE	5.5	75.5	0	
11/03/05	12.9	2.58	NE	4.1	72.8	0	
12/03/05	68.5	1.56	NE	6.0	78.1	0	
13/03/05	39.2	2.45	NE - S	7.3	73.2	0	
14/03/05	12.4	2.63	NE - SSE	7.7	74.1	0	
15/03/05	19.4	1.95	NNE - SE	7.9	91.1	0	Fog
16/03/05	N.A.	1.29	NE	5.0	98.6	0	Fog

Tab. 2 - A daily summary of meteorological situation during winter measurement campaign, February - March 2005. N.A. means Not Available data.

The correlation with wind direction is not evident at 30 minutes average, however if the average values for each wind sector (30° wide) are calculated the results show an evident trend reported in Fig.7. Concentration values larger than the average are associated to wind blowing from SW – W sectors and this is likely a consequence of short range transport from the Venice city and from Porto Marghera, as it is also confirmed from the presence of brief concentration peaks in real-time series. However this is also compatible with long-range transport from Pianura Padana. Instead concentrations are lower than the average when wind is blowing from the Adriatic Sea between S and E.

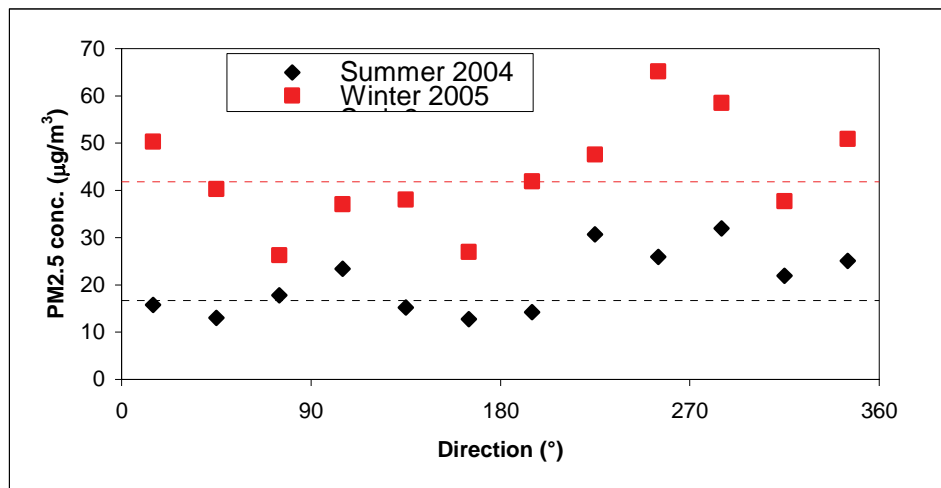
Tab. 3 - PM2.5 average concentration during night (20-8) and day (8-20) measured on Mazzorbo island.

	PM2.5 ($\mu\text{g}/\text{m}^3$)	PM2.5 ($\mu\text{g}/\text{m}^3$) (8-20)	PM2.5 ($\mu\text{g}/\text{m}^3$) (20-8)
Summer 2004	16.7	14.3	19.2
Winter 2005	41.8	36.3	47.7
All data	32.2	27.8	36.7

Tab. 4 – PM2.5 30 min average concentration as function of wind speed

	PM2.5 (all data) ($\mu\text{g}/\text{m}^3$)	PM2.5 with speed > 2 m/s ($\mu\text{g}/\text{m}^3$)	PM2.5 with speed < 2 m/s ($\mu\text{g}/\text{m}^3$)
Summer 2004	16.7	13	23.5
Winter 2005	41.8	37.6	50
All data	32.2	28.3	39.7

Fig. 7 - Correlation plot between concentration values and wind directions.



4 Aerosol (PM2.5) dynamics

The daily pattern of concentration is analyzed in terms of typical day: averaging all data registered in a specified hour of the day. In Fig. 8 results obtained are reported for the two measurements periods (summer and winter). In the figure, to put in evidence eventual trends, the analysis has been carried out using the hourly fluctuations of concentrations C_f with respect to the daily average:

$$C_f = \frac{C - \langle C \rangle_{\text{daily}}}{\langle C \rangle_{\text{daily}}} \quad (1)$$

where C is the hourly concentration and $\langle C \rangle_{\text{daily}}$ is the daily average. Results show a very similar pattern both in summer and winter even if the original concentrations are quite different. Therefore in the following parts of this paper the two patterns are considered together averaging all the data coming from the two measurement campaigns. This pattern could be due to correlation with several meteorological parameters, which shows diurnal patterns and could

influence aerosol concentrations, like: wind speed, wind direction, relative humidity and boundary-layer height. To investigate the origin of this pattern a correlation analysis with all the mentioned parameters has been carried out. Results indicate that the concentration pattern is not related to an average wind speed pattern because, even if there is on average a decrease of concentration when wind speed increases, there are several cases of high wind speed also late in the evening and during the night and the trends of the two quantities are quite different. However the concentration pattern is related to the typical daily pattern of hourly prevalent wind direction as shown in Fig.9. The Pearson correlation coefficient between the concentration and the wind direction patterns is 0.81.

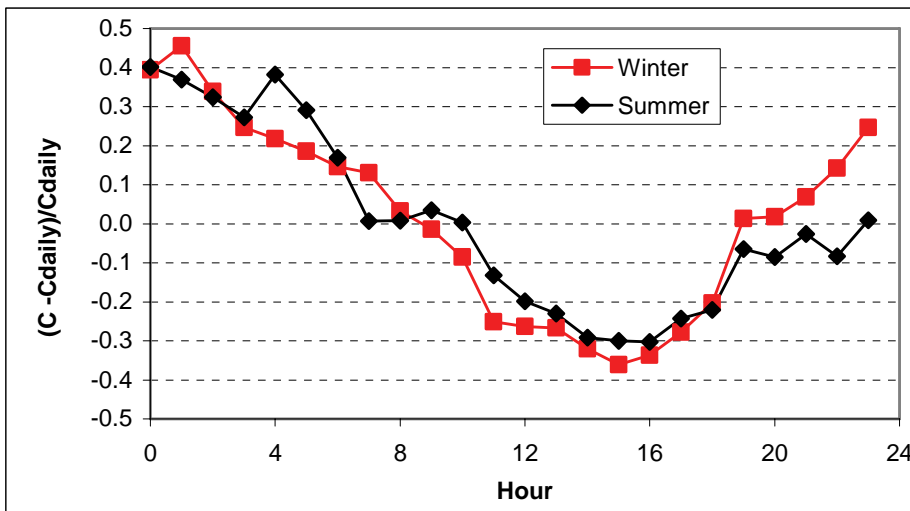


Fig. 8 – Typical daily trend for PM2.5 optical concentration measured in summer and winter campaign

This happens because the cases with wind coming from the E-SE sectors, that are associated with concentrations lower than the average (as shown in Fig. 7), are not uniformly distributed in the 24 hours but they happen mainly during the day and in the first afternoon. Also a good correlation is observed (Fig. 10) with the daily pattern of relative humidity RH calculated as:

$$RH_f = \frac{RH - \langle RH \rangle_{\text{daily}}}{\langle RH \rangle_{\text{daily}}} \quad (2)$$

Relative humidity could actually influence aerosol concentration through a direct increase of the size of hygroscopic particles and also through formation of secondary aerosol that is favoured at high values of RH and it could be an important part of PM2.5. The Pearson correlation coefficient is 0.94.

Fig. 9 – Typical daily trend for PM2.5 concentration compared with prevalent wind direction trend. Data from both measurement campaigns are analyzed together.

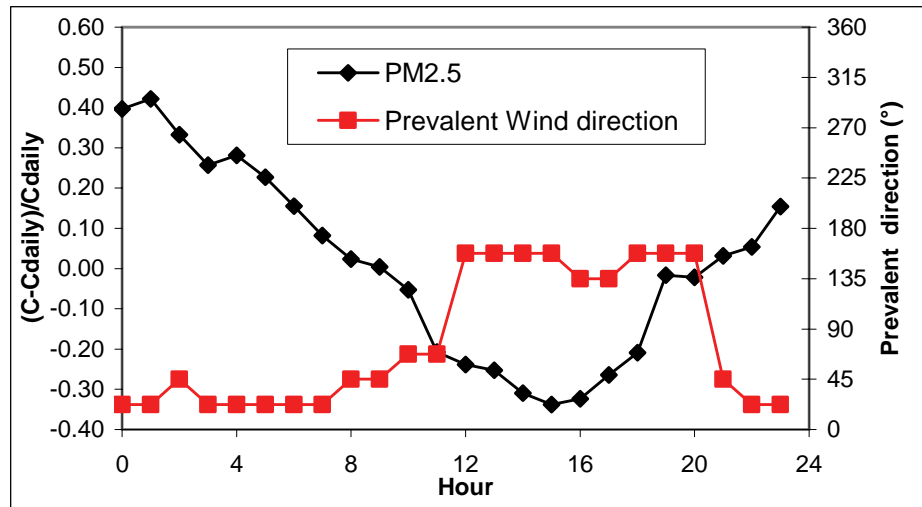
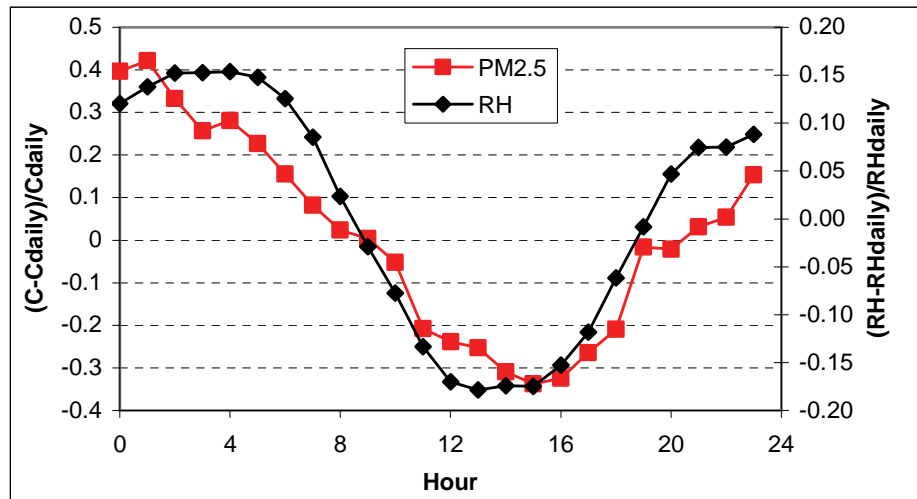


Fig. 10 – Typical daily trend for PM2.5 concentration compared with relative humidity trend. Data from both measurement campaigns are analyzed together.



5 Boundary layer height

The height of turbulent atmospheric boundary layer H is characterized by a typical diurnal cycle, increasing during daytime because of the heat flux from the surface and strongly decreasing during the night. The determination of this height is important in several applications, in particular in dispersion problems of atmospheric pollutants. We used a one-dimensional model for the calculation of time dependent boundary layer height, using one point surface data [Martano & Romanelli, 1997]. The implemented routine attempts to join together already existing models for convective boundary layer growth [Batchvarova & Gryning, 1991 et 1994], stable boundary layer (SBL) decay [Tennekes and Nieuwstadt, 1981] and surface inversion height development [Yamada, 1979]. The algorithm uses a stationary solution that allows the reduction of the problem to a direct integration in time. The routine needs wind, temperature, heat flux and momentum flux, hourly averaged, as input data. The algorithm divides the diurnal cycle in two parts: night-time and day-time, according to the sign of the sensible heat flux at the surface (negative or positive respectively). The

algorithm details can be found in [Martano & Romanelli, 1997]. The other parameter needed in the calculation routine is the potential temperature lapse rate $\gamma = \partial\theta/\partial z$ above the boundary-layer at sunrise, which is the only not surface quantity that remains to be given as model input. Two ways of estimating γ are used in this work.

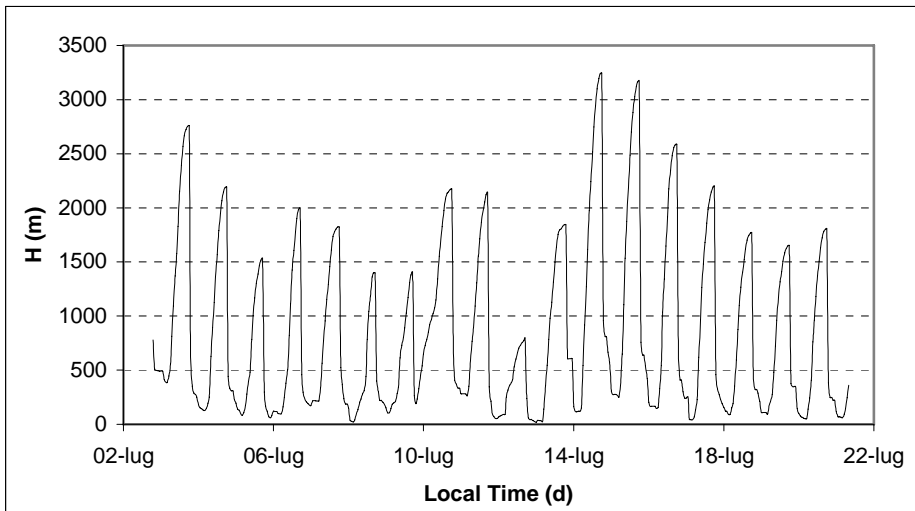


Fig. 11 - Boundary layer height during the summer measurement campaign.

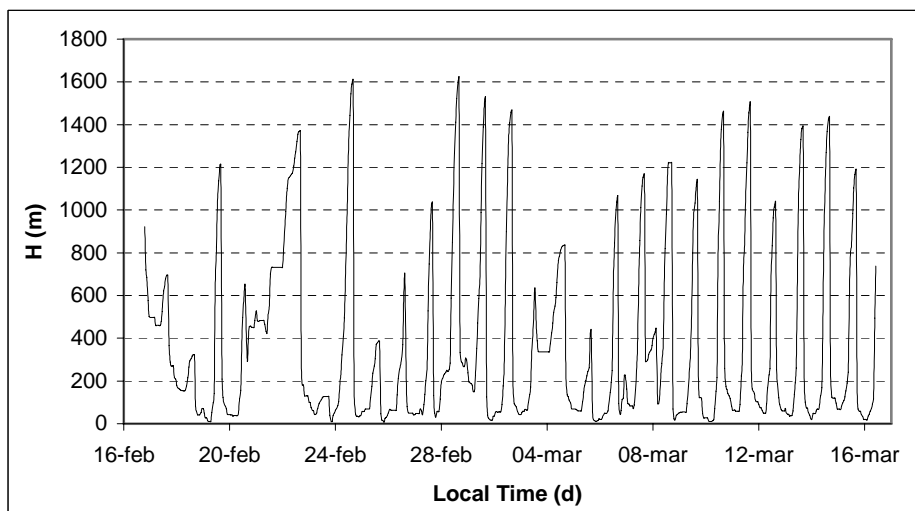


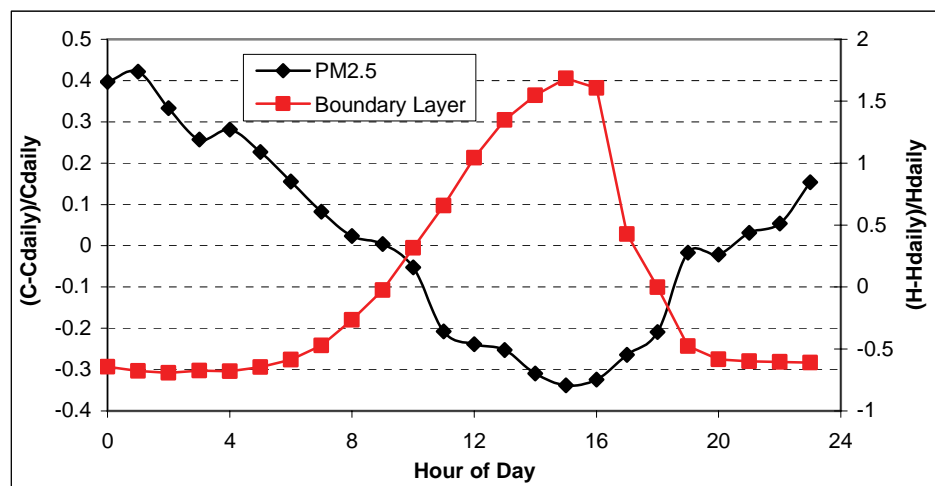
Fig. 12 - Boundary layer height during the winter measurement campaign.

During the summer campaign Sodar-Rass measurements were available from Ente Zona Industriale di Porto Marghera and the daily lapse rate was calculated from an analysis of the hourly Rass measurements at sunrise time. For the winter campaign no Rass measurements were available so that the average lapse rate of all the measurement period has been calculated by using the temperature profiles of radio soundings performed at Udine airport. From this radio soundings an average value, for whole period, of $0.003 \text{ }^\circ\text{Km}^{-1}$ has been calculated and used in the model. In Fig. 11 and Fig. 12 results for modelled boundary layer height are reported for two campaigns. Results indicate that there are several periods in which H and C are correlated (at hourly level),

especially in the summer period, but also other in which this correlation is not present and this means that the growth of the boundary-layer is not the only driving force of concentration changes. This is likely because changes in the sources and in the meteorological conditions are also present and they affect environmental concentrations. Top put in evidence the correlation between the daily concentration pattern and the evolution of the boundary layer a calculation of the typical daily pattern of the fluctuations H_f in the hourly boundary layer height has been evaluated as:

$$H_f = \frac{H - \langle H \rangle_{\text{daily}}}{\langle H \rangle_{\text{daily}}} \quad (3)$$

Fig.13 - Typical daily trend for PM2.5 concentration (black) compared with the boundary layer height trend (red). Data from both measurement campaigns are analyzed together



Results are reported in Fig.13 and they show a good correlation (Pearson coefficient 0.86) between the two patterns. The correlation coefficient increases up to 0.94 if it is calculated only from 0.00 to 15.00, so mainly during the phase of growth of the boundary-layer at the sunrise. This is actually expected because early in the morning and during most of the day the boundary-layer is actually growing from the bottom because of the convective turbulence and the pollution that was trapped near the ground during the night is mixed in a much larger volume. At sunset there is not a compression of the boundary layer but it takes place the formation of a new stable boundary layer, which again starts near the ground and it is not coupled with the residual layer above in which the turbulence tends to decrease. The newly formed boundary layer will develop during the night, trapping again part of the atmospheric pollution near the ground, and it will start again to growth at the next sunrise. Therefore the correlation is good when the nocturnal boundary layer is established and it will develop during the next day; the correlation is instead poor when the new boundary-layer is created near the ground.

Conclusions

In this paper some details of the results obtained with the micrometeorological station equipped for real-time measurements of PM_{2.5} concentrations, during the first two measuring campaigns in the Mazzorbo Island in the Venice Lagoon, are reported. Results indicate that concentration levels are influenced by sources (like Venice city and Porto Marghera) placed at short distances but also from long-range transport from Pianura Padana and in some cases from African Dust (Contini et al 2006). Correlation of concentration levels with wind direction shows that higher concentration are associated to wind blowing from the SW-W sectors and lower concentration are associated to wind coming from the Sea (SE). Results put in evidence the presence of a seasonal pattern with higher concentrations measured during the winter and also a daily pattern with diurnal (8-20) average PM_{2.5} concentration about 25% lower than nocturnal average (20-8). This pattern is highly correlated with the pattern of prevalent wind direction, relative humidity and also boundary layer height. Vertical turbulent fluxes of PM_{2.5} are essentially positive during the winter and negative during the summer. The persistent circulation with wind coming from the Alps (NE – mainly during the night) and from the Adriatic Sea (SE – mainly during the day) is present in the summer period but it is not evident during the winter with only some sporadic cases at the end of the measurement period.

Acknowledgments

Authors wish to thank Dr. A. Gambaro, Dr. L. Manodori and Mr. I. Ongaro of the University of Venice and Dr. S. Ferrari of ISAC-CNR for their help in the research. Authors also wish to thank Mr. F. Bertoldo of the Ente Zona Industriale di Porto Marghera (via delle Industrie, 19 - 30175 Porto Marghera, VE) for providing some meteorological data and also Sodar-Rass measurements.

References

- Batchvarova E. & Gryning S. 1991. Applied Model for the growth of the daytime mixed layer. *Boundary Layer Meteorology*, 56, 261-274
- Batchvarova E. & Gryning S. 1994. Applied Model for the height of the daytime mixed layer and the entrainment zone. *Boundary Layer Meteorology*, 71, 311-323
- Buzorius G., Rannik U. Makela J.M., Vesala T., Kulmala M., 1998. Vertical aerosol particle fluxes measured by eddy covariance technique using condensational particle counter. *J. Aerosol Sci.* 29, 157-171.
- Contini D., Donato A., Belosi F., Prodi F., 2006. Measurements of PM_{2.5} concentration and vertical turbulent mass fluxes in the surface layer. *Scientific Research and Safeguarding of Venice. CORILA Research programme 2004-2006. Volume IV, 2005 results.* pp. 512, ISBN 88-89405-01-5

Donateo A., D.Contini, F.Belosi, 2006. Real time measurements of PM2.5 concentrations and vertical turbulent fluxes using an optical detector. *Atmospheric Environment*, 40, 2006, pp. 1346-1360

Dorsey J.R., Nemitz E., Gallagher M.W., Fowler D., Williams P.I., Bower K.N., Beswick K.M., 2002. Direct measurements and parameterisation of aerosol flux, concentration and emission velocity above a city. *Atmospheric Environment* 36, pp. 791-800.

Marcazzan G.M., Vaccaro S., Valli G., Vecchi R. 2001. Characterisation of PM10 and PM2.5 particulate matter in the ambient of Milan (Italy). *Atmospheric Environment*, 35, 4639-4650.

Martano, P. & Romanelli, A. 1997. A routine for the calculation of the time – dependent height of the atmospheric boundary layer from surface-layer parameters. *Boundary Layer Meteorology*, 82, 105-117.

McMillen R.T., 1988. An eddy correlation technique with extended applicability to non simple terrain, *Boundary Layer Meteorology* 43, 231-245.

Nemitz, E., Gallagher, M.W., Duyzer, J.H., Fowler, D., 2002. Micrometeorological measurements of particle deposition velocities to moorland vegetation. *Quarterly Journal of the Royal Meteorological Society* 128, 2281–2300.

Tennekes, H & Nieuwstadt, F.T.M. 1981. A rate equation for the nocturnal boundary layer height. *Journal of Atmospheric Science* 38, 1418-1428.

Yamada, T. 1979. Prediction of the nocturnal surface inversion height. *Journal of Applied Meteorology*, 17, 526-531.

RESEARCH LINE 3.10

**Groundwater flows in the Venice lagoon
system**

UNDERGROUND WATER FLOW DETERMINATION IN VENICE LAGOON SYSTEM BY NATURAL ISOTOPIC MARKERS AND GEOELECTRIC TOMOGRAPHY.

UNDERGROUND WATERS MONITORING

V. Bassan¹, V. Bisaglia², E. Conchetto³, A. Mazzuccato⁴, A. Vitturi⁵, T. Abbà⁶

¹Province of Venice, Geological Survey, ²Geologist, ³Province of Venice, Geological Survey/AATO Venice Lagoon, ⁴Province of Venice, Geological Survey, ⁵Province of Venice, Civil Protection and Soil Defence, ⁶Province of Venice, Geological Survey.

Riassunto

Nell'ambito dello studio sul flusso di acque sotterranee nel sistema lagunare veneziano, la Provincia di Venezia, che si occupa del monitoraggio delle acque sotterranee, ha realizzato un campo idrogeologico nei dintorni dell'Idrovora Casetta, nel comune di Cona (VE) per svolgere un approfondimento volto alla taratura del modello tomografico e alla comprensione dei rapporti idrodinamici tra laguna, corsi d'acqua superficiali e falde, al fine anche di una corretta interpretazione dei risultati delle analisi isotopiche. È stato studiato l'assetto idrostratigrafico fino a 50 m di profondità; sono stati individuati e sottoposti a monitoraggio tre acquiferi di cui uno freatico e due in pressione. Sono state eseguite misure di livello e conducibilità elettrica ed è stato individuato il deflusso della falda freatica.

Abstract

The Province of Venice is monitoring the ISES network in the study of underground water flow in the Venice Lagoon system. It has been made a hydrogeologic field in the neighbourhood of Idrovora Casetta in Chioggia (Venice) for the calibration of the tomographic model and to better understand the relationships among lagoon, superficial water flows and groundwater layers in order to give a correct interpretation of isotopic analysis results. The stratigraphic structure of underground has been studied until 50 meters of depth. Three aquifers, one unconfined and two confined, have been characterized and monitored. Measures of level and electric conductivity have been made in the piezometers and in the channels. Water flow of unconfined aquifer has been characterized.

1 Introduction

The contribute of the Province of Venice Administration for the research derives from the realisation and the publication in 2003 of a study on saline water intrusion and subsidence of southern Venice and Padua areas (ISES Project). It has been realized with other public corporations. A monitoring network of underground water has been realized in this study: it is constituted by a several number of wells and piezometers on which measurements of piezometric level,

temperature and electric conductivity are taken twice a year. These measurements, together with geomorphological and environmental studies and stratigraphic data available on the Province Geological Survey data base, have been discussed together with the researchers interested in isotopic research, tomographic research and hydrodynamic processes. During the research the need for the realisation of a hydrogeologic field in the surrounding of Idrovora Casetta in Chioggia (Venice) emerged. It has been necessary for the calibration of the tomographic model and to better understand the relationships among lagoon, superficial water flows and aquifers in order to give a correct interpretation of isotopic analysis results. In particular the Province of Venice financed two penetration tests until 30-35 meters of depth, one borehole until 50 meters, eleven boreholes with helicoidal tip until 6 meters of depth and three hand drillings until 3 meters of depth. Two deep piezometers and fourteen superficial piezometers have been installed. All of them are fissured and topographically quoted in order to study the first three aquifers (one unconfined and two confined). The first confined aquifer, intercepted by a piezometer inserted in the hole of a destruction coring (financed by Consorzio di Bonifica Adige Bacchiglione), is monitored by a multiparametric probe measuring piezometric level, conductivity and temperature hourly.

2 ISES network monitoring

In monitoring of ISES network, measurements of the aquifer piezometric level and electric conductivity in piezometers and wells, and measurements of electric conductivity in channels have been effected twice a year.

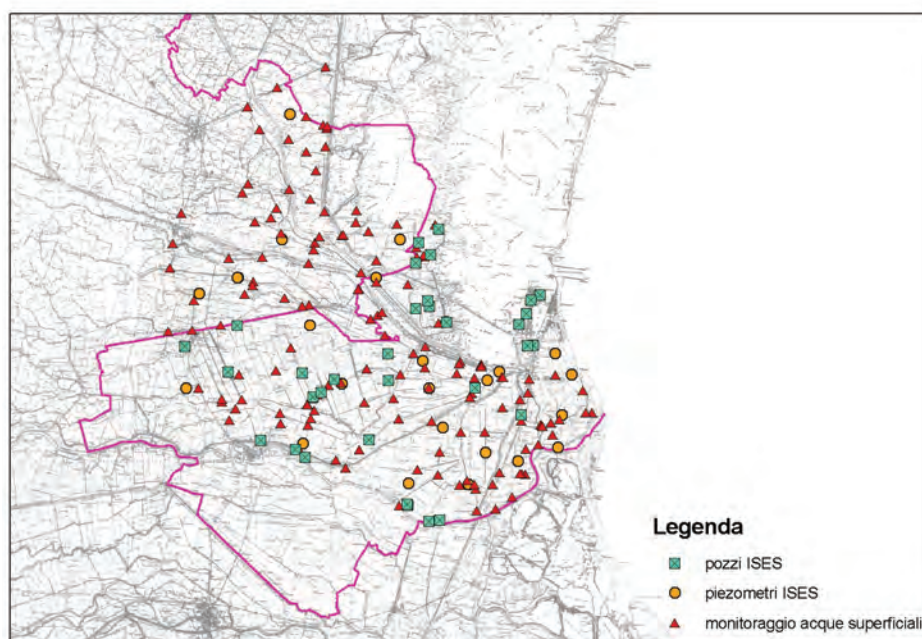


Fig. 1 – Places of monitoring.

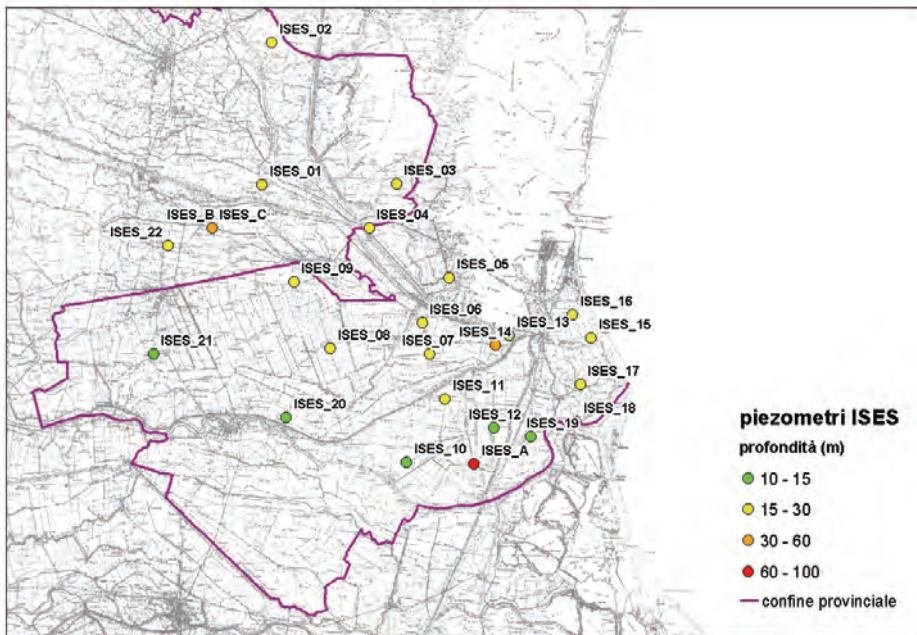


Fig. 2 – ISES piezometers

Measurements taken up to now show different types of conductivity curves trends related to depth and influenced by surrounding conditions. If we consider, for example, in two piezometers in littoral area, one on north of Brenta mouth (natural drainage area – ISES 16) and one on south of Brenta mouth (mechanical drainage area – ISES 17), trend curves appears clearly different (fig. 3).

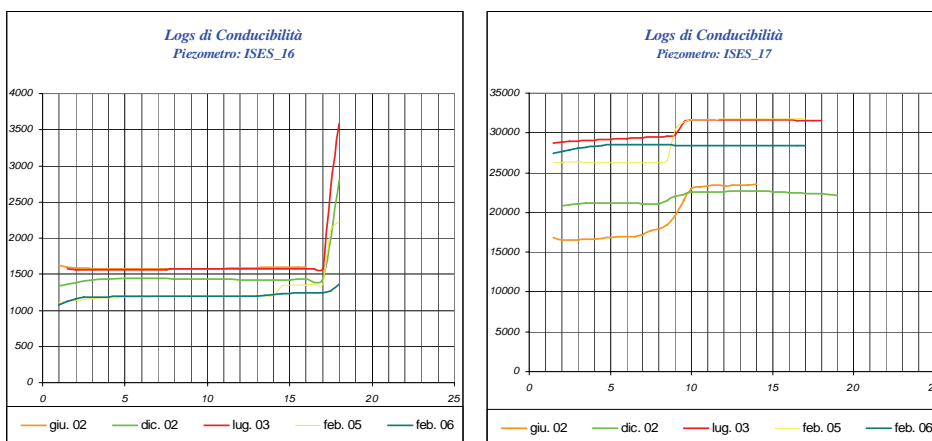


Fig. 3 – Example of conductivity curves trends related to depths

3 Investigations at Idrovora Casetta

During CORILA project investigations on underground water fluxes in venetian lagoon system, the need for further stratigraphic and hydrogeological surveys in the surrounding of Idrovora Casetta (Cona - VE), emerged (fig. 4).

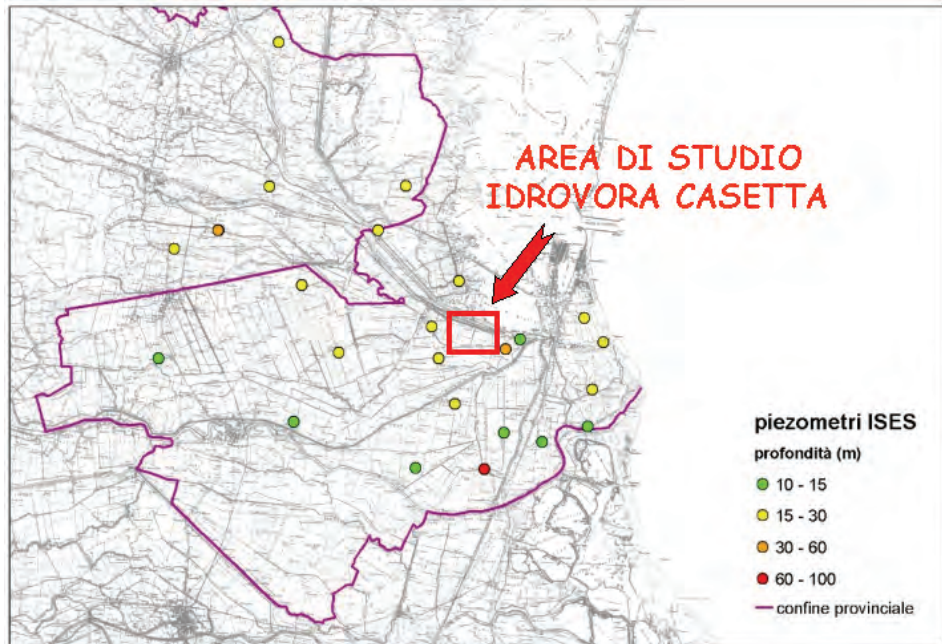


Fig. 4 – Idrovora Casetta studied area.



Fig. 5 - Idrovora Casetta studied area – geological surveys locations.

A local stratigraphic investigation has been effected in order to calibrate electric tomography, while an hydrogeological characterization has been necessary to better understand hydrodynamic relationships among the lagoon, rivers and the aquifers, to give a correct interpretation to the results of isotopic analysis.

Stratigraphic study has been done with two penetrometric tests until 30-35 meters depths and one core-boring until 50 meters depths. Eleven mechanical drilling with helicoidal tip until 6 meters depths and three hand drilling until 3 meters have been done too. In these last boreholes fourteen piezometers have been installed; they are totally fissured in order to intercept unconfined aquifer.

Concerning hydrogeological characterization, other two fissured piezometers has been located: the first one inside the 50 meters bore-hole (named CA50); the other one inside a 20 meters disruption-core bore-hole (named CA20) opportunely realized (Fig. 5).

Stratigraphic description of the cores confirmed the results given by penetrometric tests: it clearly appears the existence of three isolated aquifers although there are not considerably thick clayey levels (fig. 6).

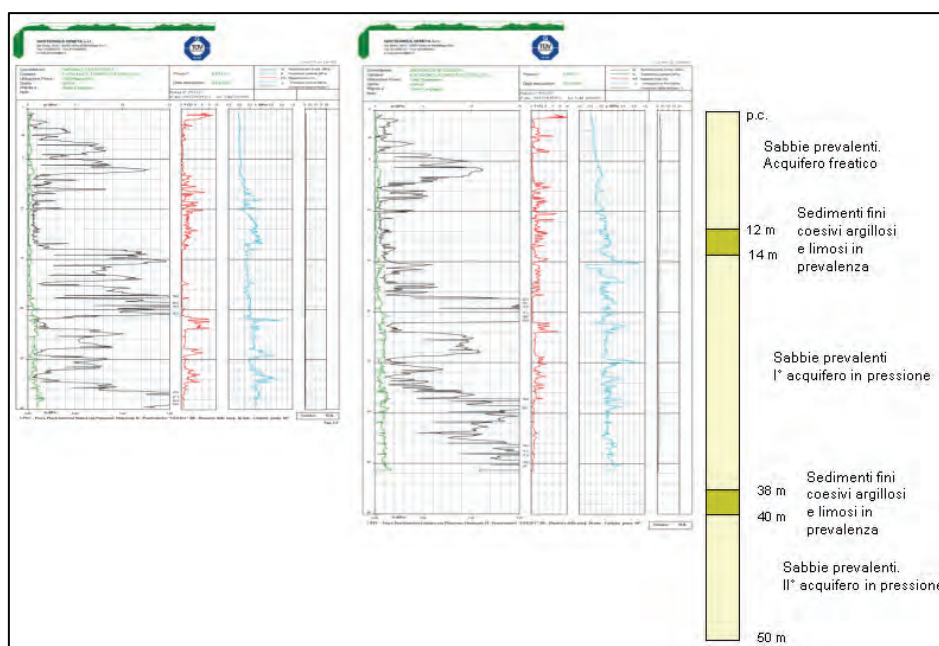


Fig. 6 – Penetrometric tests and hydrostratigraphic interpretation

In the sandy strata we can find aquifers, hydraulically isolated by the cohesive strata intercalated:

- unconfined aquifer from the surface to 12 meters depths;
- first confined aquifer from 14 to 38 m depths;
- second confined aquifer from 40 until 50 meters and further on.

Filters on piezometers are made of PVC and have been projected to intercept the aquifers described above: the micro-fissured stretch have been placed between 14 and 20 meters, for CA20 piezometer, and between 44 and 50 meters, for CA50 piezometer.

In every piezometer, both superficial and deep, measurements of aquifer level and electric conductivity have been done monthly, since they have been placed. Same measurements have been done also on even in the near channels.

All piezometers have been quoted with GPS instruments in order to quote aquifer levels to the sea level.

The first confined aquifer level rises until 20 cm above the ground level, while the second confined aquifer level, containing a discrete amount of gas, rises

until 90 cm above ground level. Conductivity is 22 mS/cm in CA20 and 5 mS/cm in CA50.

In the CA20 piezometer a multiparametric probe, measuring temperature, conductivity and water level hourly, has been installed.

The studied area is situated south of Brenta, Bacchiglione and Canal Morto rivers, where the topographic surface is about 2 or 3 meters below the sea level.

Casetta pump station, by a collector channel (Barche social canal), collects surrounding fields waters and Brentone Vecchio waters and pump them into Canal Morto.

The unconfined aquifer level results to be higher in Canal Morto nearest piezometers then in the south area, where it decreases southwards less intensively.

Flux directions seem to be the following:

- at the west of pump station the main flux direction is N-S; the degree is significant only about 200 meters from Canal Morto;
- at the east of pump station it is from NE to SW from Canal Morto; the collector channel seems to drain the aquifer.

Conductivity is very high (over 5 mS/cm) in piezometers along cross channels and in the piezometer east of pump station (similar to that of collector canal), while in the other piezometers values conductivity ranges between 2 and 5 mS/cm. We also must underline the low conductivity in central area piezometers (CA1 e CA9). (fig. 7)

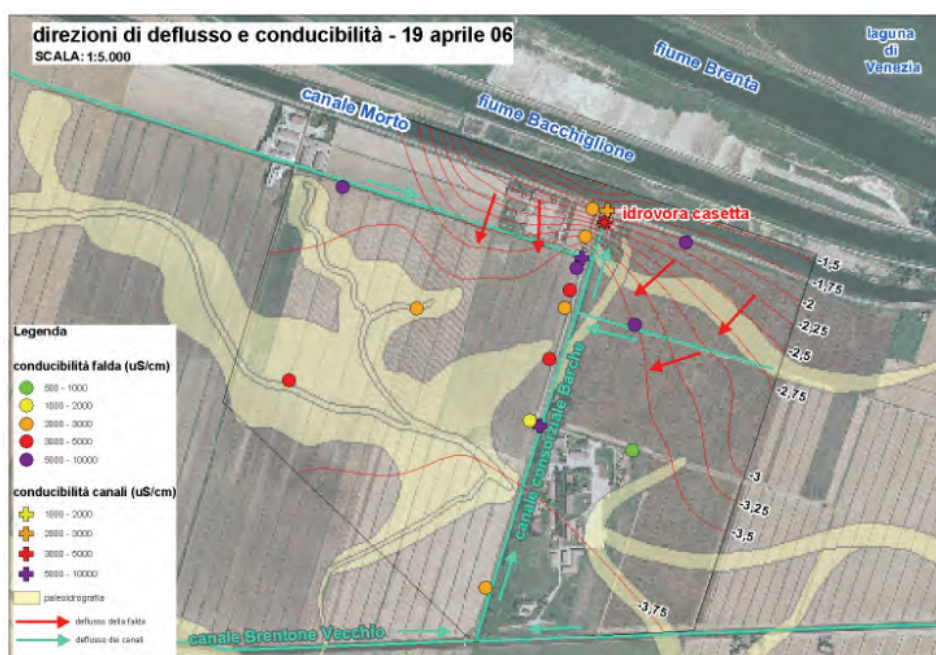


Fig. 7 – Superficial hydrography, water flux and conductivity of the unconfined aquifer.

Conclusions

In the surrounding of Idrovora Casetta, in Chioggia (Venice), it has been realized a hydrogeologic field composed by sixteen stratigraphic boreholes with piezometers inside. All of them are fissured and topographically quoted in order to study the first three local aquifers (one unconfined and two confined). In the Idrovora Casetta network, measurements of the aquifer piezometric level and electric conductivity have been effected every month. Measurements of piezometric level and electric conductivity have been made in channels too. The local stratigraphic investigation has been effected in order to calibrate electric tomography, while the hydrogeological characterization has been necessary to better understand hydrodynamic relationships among lagoon, rivers and aquifers, to give a correct interpretation of the results of isotopic analysis.

References

Dal Prà A., Gobbo L., Vitturi A., Zangheri P., 2000. Indagine Idrogeologica del territorio provinciale di Venezia. Provincia di Venezia.

Carbognin L., Tosi L., 2003. Il Progetto ISES per l'analisi dei processi di intrusione salina e subsidenza nei territori meridionali delle province di Padova e Venezia. C.N.R. - ISDGM, Città di Chioggia, Consorzio di Bonifica Adige Bacchiglione, Consorzio di Bonifica Bacchiglione Brenta, Consorzio di Bonifica Delta Po Adige, Magistrato alle Acque per la laguna di Venezia, Provincia di Padova, Provincia di Venezia.

Bondesan A., Meneghel M. et al., 2004. Geomorfologia della Provincia di Venezia. Provincia di Venezia, Magistrato alle Acque di Venezia concessionario Consorzio Venezia Nuova, Università di Padova Dipartimento di Geografia, Ministero per i Beni e le Attività Culturali Soprintendenza per i Beni Archeologici del Veneto. Esedra Editrice.

MONITORING OF THE SALINE INTRUSION WITH TIME-VARIANT GEO-ELECTRIC-TOMOGRAPHY: TEST SITE CASETTA (CHIOGGIA, ITALY)

Roberto de Franco¹, Giancarlo Biella¹, Adelmo Corsi¹, Antonio Morrone¹, Graziano Boniolo¹, Alfredo Lozej², Ginette Saracco³, Barbara Chiozzotto⁴, Marco Giada⁴, Massimo Barbetta⁶, Valentina Bassan⁵, Vittorio Bisaglia⁵, Tiziano Abba⁵, Andrea Mazzucato⁵, Christelle Claude³, Enrico Conchetto⁵, Giuseppe Gasparetto-Stori⁶, Adriano Mayer³, Federica Rizzetto⁷, Luigi Tosi⁷, Pietro Teatini⁸

¹IDPA-CNR, Milano, ²Dip. Scienze della Terra, Università degli Studi di Milano, Milano, ³CEREGE, Aix en Provence, France, ⁴Morgan Srl, Marghera (VE), ⁵Provincia di Venezia-Servizio Geologico, Venezia, ⁶Consorzio di Bonifica Adige-Bacchiglione, Padova, ⁷ISMAR-CNR, Venezia, ⁸DMSA, Università di Padova

Riassunto

Dal novembre 2005 è in funzione l'esperimento elettro-tomografico tempo variante nel sito Casetta (Chioggia) finalizzato al monitoraggio della intrusione salina; esso rimarrà in funzione fino alla fine del 2006. I test e le acquisizioni di calibrazione, effettuati nella seconda parte del 2005, hanno consentito il dimensionamento dell'apparato sperimentale che permette l'acquisizione di 10 elettro-tomogrammi al giorno, 5 dei quali con alta risoluzione, atta al monitoraggio del tetto dell'intrusione salina (2.5 m di profondità) e 5 con risoluzione idonea al monitoraggio delle unità più profonde dell'intrusione stessa (circa 40 m). In generale le tomografie identificano nella parte più superficiale una falda isolata dalle falde più profonde, come anche evidenziato dai sondaggi profondi. L'analisi dei dati acquisiti fino ad oggi consente di poter effettuare le prime correlazioni con i dati di marea, dei livelli di falda, dei livelli dei canali adiacenti e di precipitazione. In particolare si osserva una correlazione tra aumenti di resistività dei terreni superficiali fino a profondità di circa 5 m e le precipitazioni. Si osserva inoltre una correlazione della resistività con il livello del canale di Valle adiacente alla linea elettro-tomografica fino a profondità di circa 10 m. Tale correlazione è indicativa della capacità drenante e/o alimentante del canale stesso, la cui influenza è probabilmente limitata alla prima falda. Non si osserva, invece, una chiara correlazione con la marea.

Abstract

An electro-tomographic time lapse experiment, in the Casetta (Chioggia) test site, is running since November 2005; it will remain operative until the end of 2006. The test and calibration acquisitions, carried out in the second part of 2005, have concurred to the settlement of the experimental apparatus. The system allows the acquisition of 10 electro-tomograms per day, 5 of which with high resolution to sample the top of the seawater intrusion (2,5 m of depth) and 5 with a resolution suitable to the monitoring of the deeper parts of the intrusion (approximately 40 m). In general the tomograms identify a shallow phreatic

aquifer isolated from the deeper ones, as also evidenced by the deep bore holes (20 and 50 m) drilled near Casetta. The up to now acquired data allow us to carry out the first correlations with the tide and rainfall data, the levels of water tables and the levels of the adjacent channels. In particular a correlation between increases in resistivity of shallow units, up to about 5 m depth, and the rainfalls is observed. A correlation of the resistivity variations with the level of the adjacent channel (Canale di Valle) up to about 10 m depth is also observed. Such correlation is indicative of the draining or feeding behavior of the channel, whose influence probably is limited to the first aquifer. Moreover a clear correlation with the tide is not observed.

1 Introduction

The geo-electrical methods are a powerful tool to explore the subsurface hydrological features. In particular the geo-electrical time variant monitoring with the electrical tomography is capable to follow the hydrological processes involved in the coastal areas where saline intrusions are present. (bibliografia di altri case history). The present study is devoted to study the groundwater flow in the southern area of the Venice lagoon in an area test near Chioggia (Casetta). The test site is located near a pumping system of the Adige-Bacchiglione Reclamation Consortium, some 500 m far from the coast of the lagoon (fig. 1).



Fig. 1 – Electro tomographic apparatus location map.

The study area presently is at about 3 m below the sea level and the shallow terrains are mainly constituted by peat and marine fine sand with an evidence of an old river channel. Along the tomographic line four shallow borehole were drilled up to 6 m depth to control the piezometric level of the fresh water table. Near the pumping system two deeper boreholes, 50 m and 20 m depth respectively, were drilled. They have revealed the presence of two confined,

fine to medium sandy aquifers, in the depth ranges of 12-20 m and 35-45 m, separated by semi-permeable clay and sandy-clay layers (Bassan et al 2006). In the northern part, between the test area and the lagoon, there are two rivers, the Brenta and the Bacchiglione, and a reclamation channel, Canale Morto. The Casetta pumping system discharges in this channel the water pumped from the Canale di Valle (fig. 1). The preliminary geo-electrical surveys performed during the 2005 allowed the definition of the geo-electrical assessment of the study area and the setup of the experiment, in order to sample the subsurface up to about 70 m of depth (de Franco et al. 2005). In figure 2 a hydro-geological scheme is presented. In this simplified scheme of the sampled area three aquifers are hypothesised. The phreatic aquifer interacts with the local system of channels and with rainfall. This aquifer is separated from the second and third one, which are linked to the sub-regional and regional ground water system. The two confined aquifers show different hydraulic potentials, as indicated by the 50 m deep bore-hole. The saline intrusion occurs in the last two units and probably for other deeper unsampled units. The drainage and feeding system probably induces an interaction between the lagoon sea water and the superficial fresh water level.

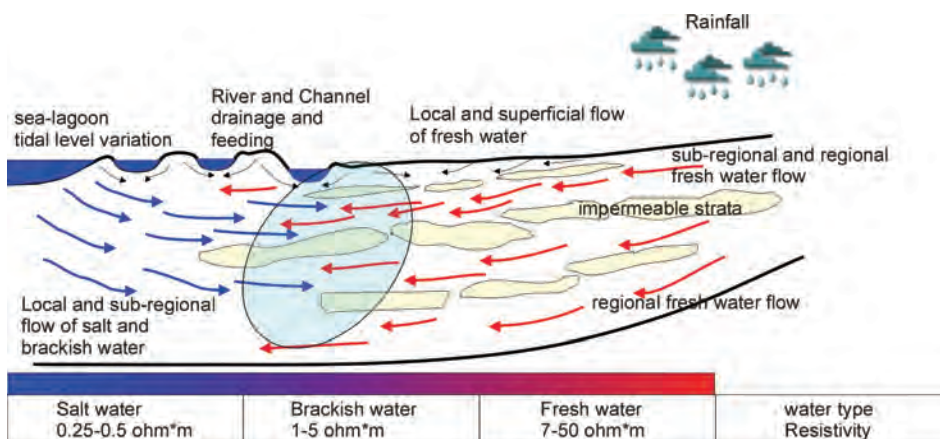


Fig. 2 – Simplified hydrogeological scheme. The ellipse indicates the investigated salt water intrusion area. In red the Fresh water (red arrows) and e sea water (blue arrows) flows are indicated.

2 The experiment

The electro tomography experiment is running in continuous acquisition mode since the beginning of November 2005. A dedicated instrument was developed and installed for the experiment along a 300 m long line (Fig. 1). The apparatus is constituted by 81 active and addressable electrodes, a unit which controls both the electrode addressing via RS-232 and the measurement cycles, an electric power unit, a laptop with an A/D PMCIA 24 bit card for current and potential measurements and a GSM modem, and a power backup system (fig 3). Each electrode is closed in an IP67 water-proof box which protects the electrical contacts between the electrode and the steel stake planted in the terrain (fig. 4). The system may be controlled in remote mode to change the acquisition parameters and to download the acquired data. The measurement cycle is sub-divided in 5 sub-cycles in which spontaneous potentials (SP), current

intensity (I) and potential (ΔV) are sequentially measured two times by inverting the polarity at the current electrodes. The electric power unit controls the maximum current injected in the terrain that in the present configuration is 350 mA. The current and potential measurements, for every sub-cycle, are acquired with a sampling rate of 22 kHz and performing the mean over 750 samples. The apparatus acquires 2 pseudo-section of the apparent resistivity every 5 hours and 30 minutes. The two tomographies allow us to sample the subsurface with different resolution using two different Wenner configurations. In this case the single measure is performed on a four-electrode base configuration with constant electrode spacing. In the two external electrode (A and B) a known current is injected and on the two internal electrodes (M and N) the voltage is measured. The tomography is obtained moving the four-electrode base configuration with a fixed spacing along the line and acquiring all the lines increasing the electrode spacing of the configuration. The first electro-tomography covers all the line with a Wenner electrode spacing variable from 5 m up to 100 m with an increasing step of 5 m (about 65-75 m of investigated depths). The second electro-tomography array samples the first northernmost 95 m of the line with a Wenner electrode spacing, starting from 2.5 m to 32.5 m with a step of 2.5m (20-25 m of investigated depths). The first one allows us to monitor the bottom of the saline intrusion and its lateral extension southward, while the second one allows to observe the variation in the top of the saline intrusion and to sample with more detail the shallow aquifer.

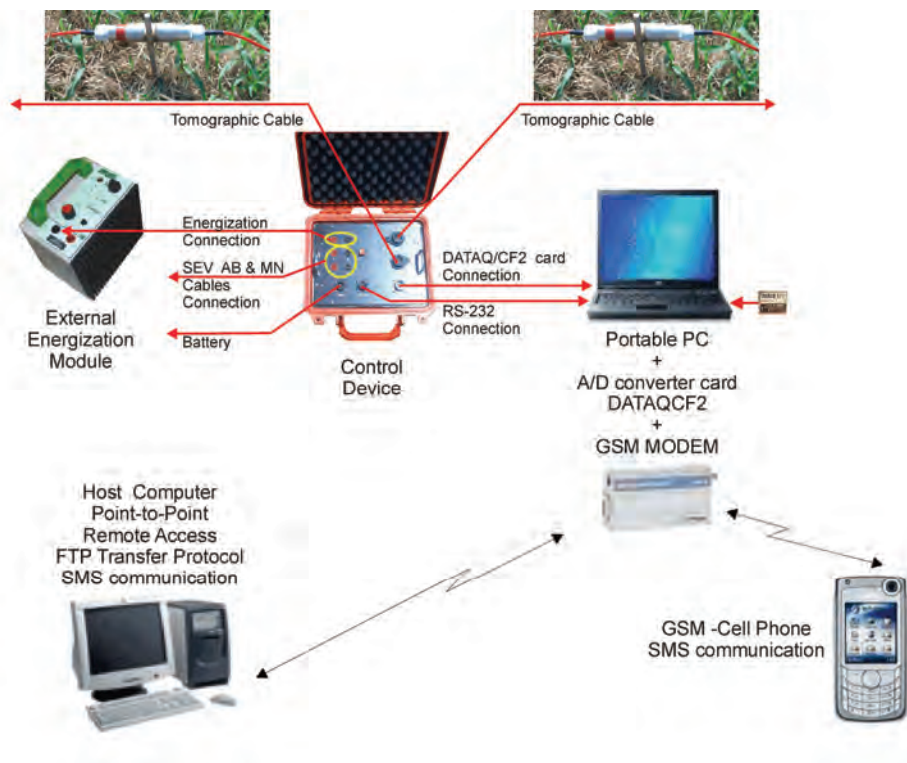


Fig. 3 – Electro – tomography instrumentation



Fig.4 – Image of the experiment (northward half line). Each box contains an electrode coupled to the terrain through a steel stake.

From the begin of the experiment 546 tomograms were acquired. The experiment include the retrieve and acquisition of other adjunctive and complementary data: the level of the first water table and the water conductivity in the boreholes along the line and in the deeper boreholes; the upload level of the Morto channel and the capture level of the Di Valle channel and their water conductivity as well as the conductivity of the Brenta and Bacchiglione rivers; temperature and rainfall at the Casetta pumping system; the tide data set of the Chioggia station. These data are integrated with the geochemical and isotopic measurements of the water of the lagoon, in the boreholes, rivers and channels (Mayer et al. 2006).

3 Preliminary data analysis

The electro-tomographic data set was transformed in two formats: the Matlab format for the data preprocessing and the Earthimager format which is suitable for the data inversion and modeling procedure. The presented preliminary data analysis covers the period from November 2005 to April 2006.

3.1 Model

The apparent resistivity pseudo-sections are inverted with a software procedure (AGI, 2004) to obtain the resistivity model. The procedure includes the solving of forward and inverse problems. In the forward problem the potential is calculated, with finite difference or finite elements, given the current source point and the 2D resistivity subsurface distribution. The non-linear inverse problem for the resistivity parameters is achieved with a damped least square approach where a weighted data misfit, objective function, is minimized. The objective function depends on the weighted difference between observed and

calculated data of current and potentials.

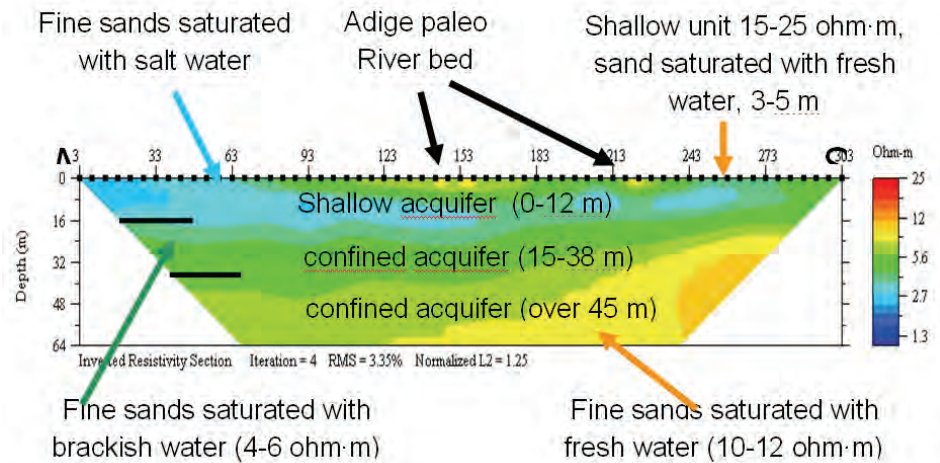


Fig. 5 – An example of resistivity model obtained with electrode spacing of 5 m

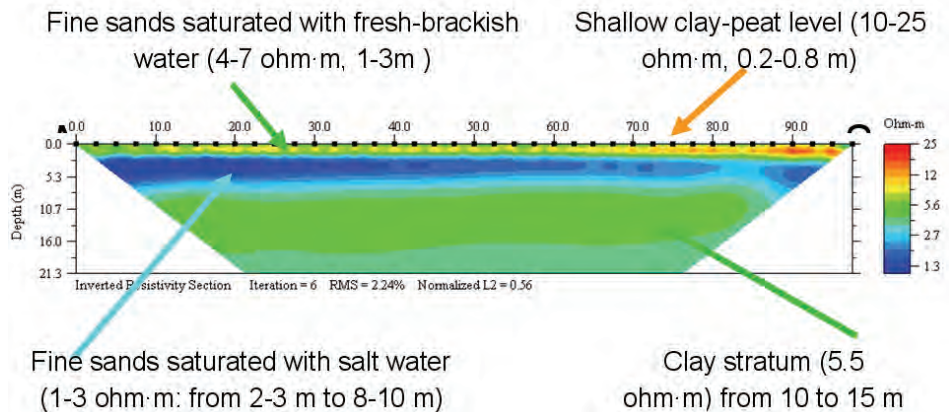


Fig. 6 - Resistivity model obtained with electrode spacing of 2.5 m.

Figures 5 and 6 show two examples of the reconstructed resistivity sections (electro-tomograms) respectively for 5 m and 2.5 m electrode configurations. The first resistivity tomogram (fig. 5) allow us to describe the main electrostratigraphic features of the investigated area up to about 60 m. Three aquifers are recognizable. The first two aquifers suffer the saline intrusion. At about 45 m depth the resistivity values greater than 10 ohm·m are interpreted as originated by fine sands saturated with fresh water. This limit constitutes the bottom of the saline intrusion. Due to the low resolution the first aquifer seems to start from the surface with an effect of averaging the resistivity values at about 3 ohm·m in the northern part. The high resolution 2.5 m resistivity tomogram (fig. 6) gives a detailed image of the first two units. The first unit show a shallow and thin clay-peat level, probably saturated with fresh water, followed by a layer of fine sands saturated with fresh/brackish water. The thickness of this layer is about 3 m. The underlying layer shows the lower resistivity values of about 1 ohm·m and extends to 12 m depth. This unit constitutes the top of the saline intrusion and it is separated from the first confined aquifer by a clay stratum between 10 and 15 m depth.

3.2 Time variant analysis of the observed resistivity and correlations with other data

The observed data (apparent resistivity pseudo-sections) are processed to analyze their time behavior. During the experiment we have some failure in the data acquisition due to the complexity of the experiment which is running in stand alone and remote mode without the presence of the operator, as it is the standard in the geo-electric tomography acquisition. The errors in the resistivity measurements mainly depends on the signal to noise ratio value of the potential measurements, being quite fixed and generally very high for the current measurements.

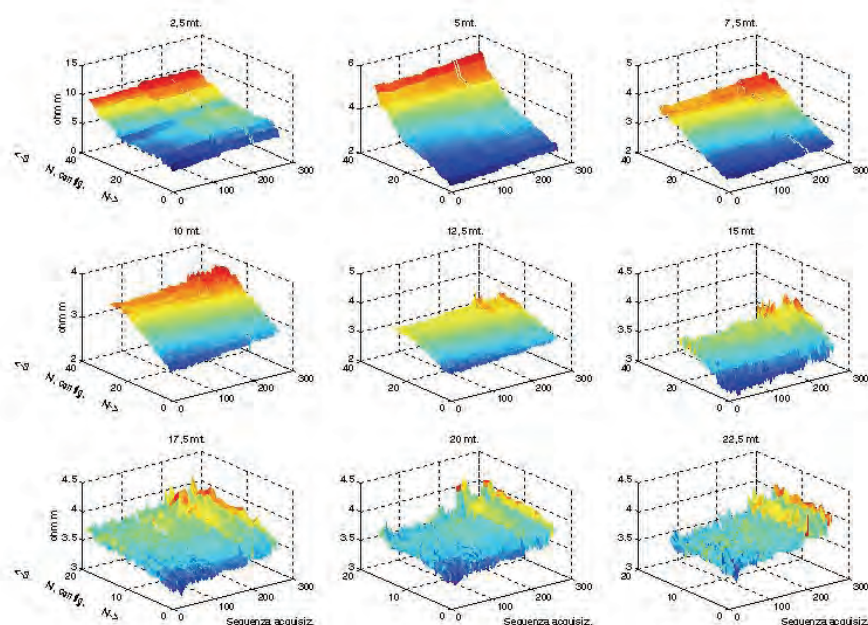


Fig. 7 – Time and spatial variation diagrams of apparent resistivity for high resolution tomography. Each plot is referred to a fixed electrode spacing.

The signal to noise ratio for the potential measurements decreases with the increasing of the electrode spacing. Therefore the resistivity relative errors are varying from of a minimum of 1% to maximum of 10%. A simple way to analyze the spatial-temporal behavior of the observed apparent resistivity values is to plot the diagram of the apparent resistivity in time (number of sequence) and for each configuration of a fixed spacing. Figure 7 shows some examples of such diagrams. In the diagram we observe a general increase in time of the apparent resistivity. The same trend is observed spatially passing from the northern configuration to those to the south. This trend is recognizable also for high electrode spacing (greater depths) but with a relatively higher variation. This is caused by a reduction in salt content due to a flow of fresh water and the relative mixing with the brackish or salt water in the investigated area. In the proposed scheme (fig. 2) this fact is interpretable as a feeding from sub-regional and regional aquifers. In the period between November 19 and 23 of 2005 a rapid decrease in the resistivity for electrode spacing greater than 7.5 m is observed as the hydraulic response of the terrain to the deeper borehole drilling

operations. In fact the drilling operation, started the November 9, 2005, probably has connected the shallow water, with high salt contents, with the two deeper aquifers characterized by a relative low salt content. If this hypothesis is correct we can perform a raw estimate of the water flow velocity of about 4-6 m/day.

The availability of the quoted complementary data allow us to inquire the correlation with rainfall, the stream level and tidal lagoon level.

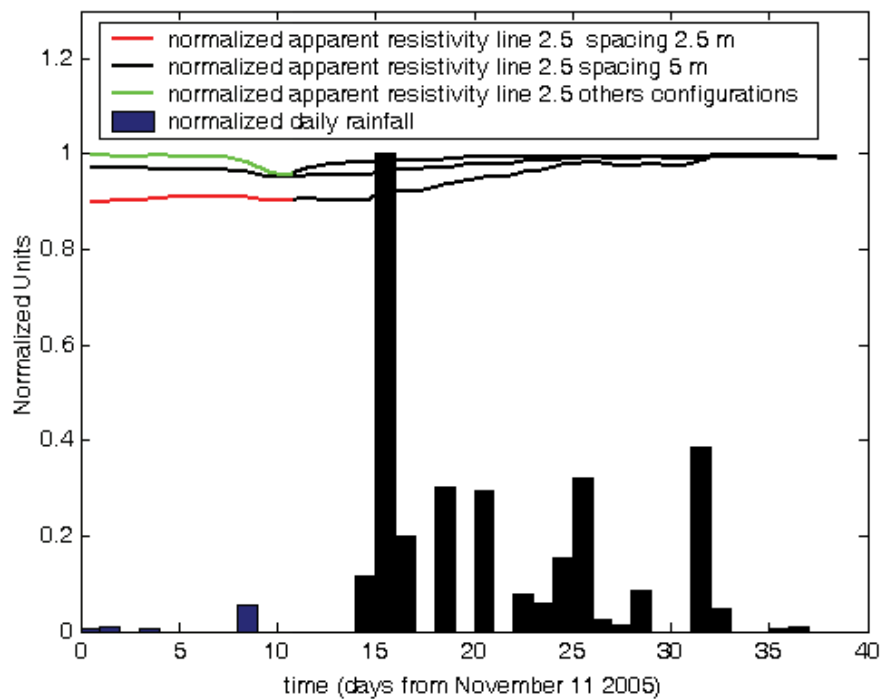


Fig. 8 – Correlation between apparent resistivity and rainfall.

In figure 8 the plot of apparent resistivity and rainfall in the November 2005 is reported. As can be observed there is a clear correlation between the highest rainfall event (centered 15 days after the Nov. 11 2005) and the increase of apparent resistivity for 2.5 m and 5 m electrode spacing. In the relative rainy period, after this event, the gradient of the apparent resistivity is higher while gradient variations are not observed for electrode spacing greater than 5 m.

The study of the correlation between the apparent resistivity and the level of the Canale di Valle indicate that there is a high negative correlation, observed for electrode spacing from 2.5 m to 7.5 m. Figure 9 is shows the correlation pseudo-section obtained calculating the correlation coefficient for each electrode configuration and the channel level every 6 hours. In particular the correlation reach the higher negative values in the northern part where seem extended to depth.

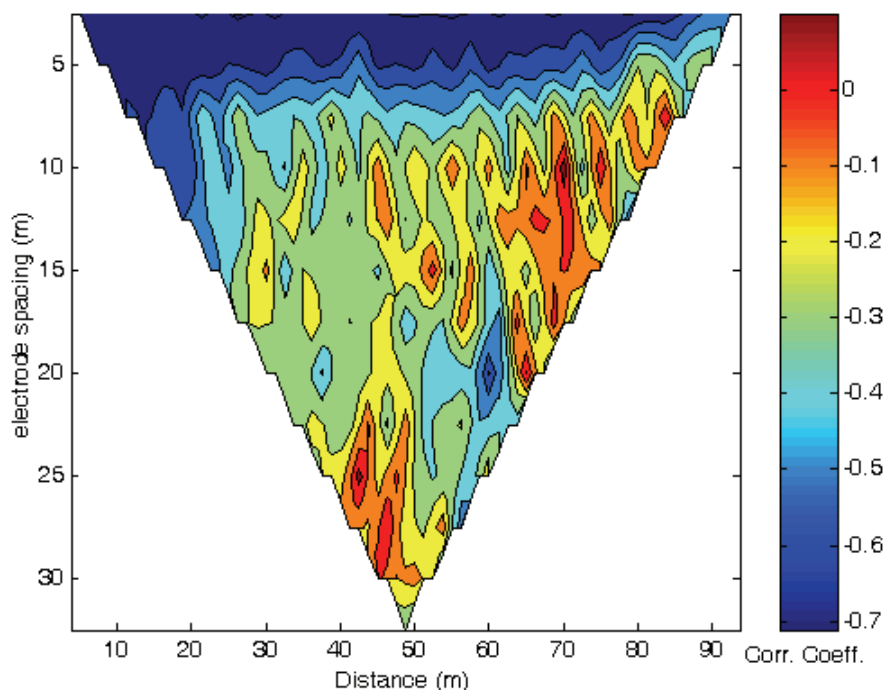


Fig. 9 – Correlation of Canale di Valle daily upload level and apparent resistivity for high resolution tomography

The last correlation analysis regards the apparent resistivity versus the tidal level. For our analysis we used the data of the canal Morto level that is the down-load level of the Casetta pumping system. The correlation between this tidal time series and that of the Chioggia station in the internal lagoon is 0.997, due to the fact that the reclamation system of the channels and rivers are connected with the lagoon; for this reason we used these tidal data. The tomographic experiment allow us to sample the variation of apparent resistivity with a period comparable with that of the tide. The analysis was performed calculating several running averages of the apparent resistivity with different electrode spacing and tide with different averaging windows. The 15 days detrended running average, for 2.5 m and 5 m of electrode spacing, gives the higher negative coefficient of -0.70 . However this result must be confirmed by a future robust analysis with longer time series of the experimental data. In figure 10 we show the detrended running averages, over a window of 32 hours, of the tidal level and apparent resistivity (for the first electrode configuration). They appears slightly negatively correlated with a correlation coefficient of -0.59 .

Integrative and detailed analyses will be carried out with more reliability when the apparent resistivity time series for longer periods and other complementary data time series will be available.

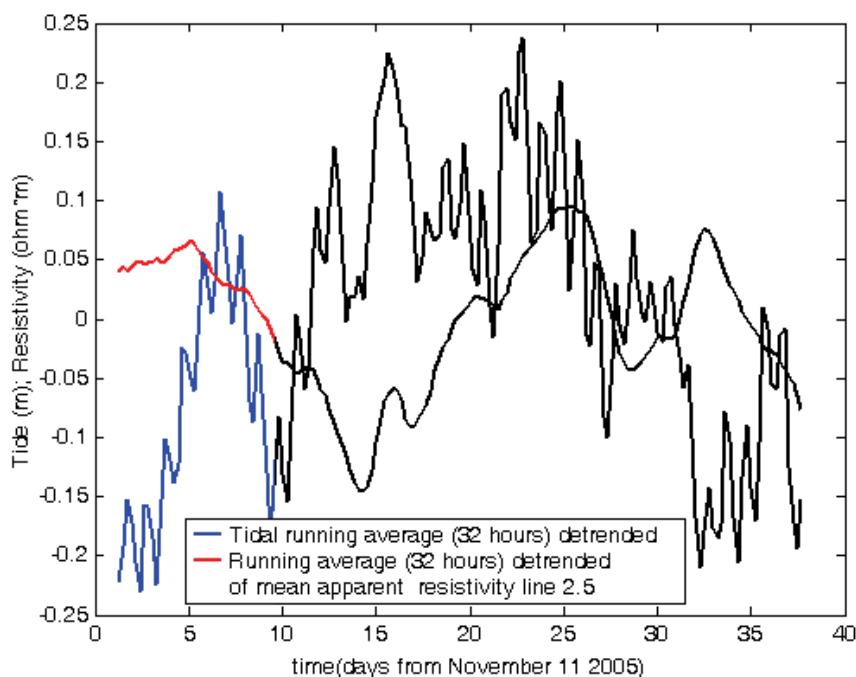


Fig. 10 – Correlation between apparent resistivity (2.5 m electrode spacing) and tidal level. Running average 32 hours.

Conclusions

We have illustrated the geoelectrical-tomographic experiment in the test site of Casetta, near Chioggia. We report the first preliminary processing results of the data acquired from the November 2005. The main results concern the electrostratigraphy of the investigated area and its lateral variation and the correlation between the observed apparent resistivity data and other complementary data: rainfall, the level of reclamation channels and the tide variations in the lagoon.

References

- Advanced Geoscience Inc., 2004. Earthimager : 2D Resistivity and IP Inversion Software. Instruction Manual. Austin, Texas, 111.
- Bassan V., Bisaglia V., Conchetto E., Mazzuccato A., Vitturi A., Abba T., 2006. Underground water flux determination in Venice lagoon system by natural isotopic markers and geoelectric tomography :Underground waters monitoring. Abstract V Riunione annuale CORILA, Venezia, 26-28, apr., 2006.
- de Franco R., Biella G., Boniolo G., Corsi A., Morrone A., Mayer A., Lozej A., Saracco G., Chiozzotto B., Giada M., Barbeta M., Bassan V., Claude C., Conchetto E., Gasparetto-Stori G., Gaspari A., Rizzetto F., Tosi L., 2005. - Studio dell'intrusione salina nella Laguna Veneta (Chioggia):misure geoelettriche per il setup dell'esperimento time-lapse. Extended Abstract 24° Convegno Gruppo Nazionale Geofisica Terra Solida, 15-17 nov. 2005, 350-352..
- Mayer A., Gattacceca J., Vallet-Coulomb C., Radakovich O., Giada M., Cucco A., Flora O., Claude C., 2006. Ground water discharge in the Venice Lagoon: isotopic data end modelling. Abstract V Riunione annuale CORILA, Venezia, 26-28, apr., 2006.

RESEARCH LINE 3.11

Ecological quality indices, biodiversity and environmental management for lagoon areas

TESTING AN INTEGRATED APPROACH BIOINDICATOR FOR THE VENETIAN LAGOON

Folco Giomi, Mariano Beltramini, Cristian Lanfrit, Diego Maruzzo, Giuseppe Fusco, Lisa Perilli, Lorenzo Zane, Micol Gennari, Ilaria Marino, Federica Barbisan, Paolo Maria Bisol

Dipartimento di Biologia, Università degli Studi di Padova

Riassunto

Nel presente contributo abbiamo testato le metodologie descritte in precedenza, al fine di sviluppare un bioindicatore affidabile per la Laguna di Venezia. Sono state analizzate la plasticità fenotipica delle emocianine, l'instabilità nello sviluppo e la variazione genetica tra campioni di *Carcinus aestuarii* raccolti in tre diversi siti nel 2005. I risultati ottenuti dai due i marcatori molecolari hanno evidenziato una differenza significativa tra siti della laguna e mare, mentre non è stato rilevata alcuna differenza a livello morfologico. L'applicazione di questa metodologia integrata è attualmente in corso in campioni raccolti nella primavera del 2006.

Abstract

With the final aim of develop a reliable biological indicator for the Venetian lagoon we test the methodologies previously elaborated and described. We analyse the hemocyanin phenotypic plasticity, the developmental instability, and the genetic variation among specimens of *Carcinus aestuarii* collected from three different localities during 2005. The results obtained by the application of both molecular markers evidence a significant difference between the lagoon sites and the sea site, while no evidence of any relationship was detected throw the analysis of developmental stability. The application of the integrated methodology is in progress, on the samples collected in spring 2006.

1 Introduction

The complex relationships between the physical environment, biological communities and human activities in the Venetian Lagoon challenge the possibility of devising an integrated ecological indicator to get a comprehensive picture of environmental quality. The integration of different methodological approaches and different investigating techniques has been proven to be effective in evaluating the impact of several environmental parameters on living organisms [Galloway et al. 2004].

On this track, the use of the crustacean decapod *Carcinus aestuarii* as bioindicator was proposed [Giomi et al. 2006]. In order to evaluate a wider spectrum of environmental perturbations, we used an interdisciplinary integrated approach, by analysing the same individuals by three different methodologies. A physiological study of respiratory proteins, a morphological analysis of developmental instability, and the genetic analyses of microsatellite

loci were combined with the aim of monitoring environmental stress at different time scales.

The arthropod respiratory protein hemocyanin, shows a considerable heterogeneity in level of the different subunits synthesis, both within and between species. This heterogeneity provides the basis for intraspecific hemocyanin polymorphisms and constitutes a mechanism of physiological adaptability [DeFur et al., 1990]. Several chemical and physical factors (e.g. salinity, dissolved oxygen, temperature) are clearly involved in subunit composition change, and it was suggested that this capability for hemocyanin modulation is strongly related to the physiological adaptation process of the whole animal [Mangum and Rainer, 1988; Mangum, 1990]. Through comparing the hemocyanin subunit patterns and measuring the differences in protein expression, it is possible to infer adaptive process toward very recent stressful events.

Developmental stability is a property of the organism developmental system reflecting its ability to resist deleterious effects of possible environmental perturbations during development. Several environmental factors have been proven to be effective in biasing the stability of embryonic and post-embryonic development in several animal taxa [Møller and Swaddle, 1997]. Measures of fluctuating asymmetry (FA), the random and non-inheritable deviation from perfect bilateral symmetry, are routinely used as indexes of developmental stability, that in its turn is correlated with the level of environmental stress that affects an organism.

Genetic diversity is a fundamental component of biodiversity and is as critical to sustainability of our natural resources as are diversity of species and ecosystems [Bagley et al. 2002]. Natural selection, genetic drift, migration and mutation determine the level of genetic diversity in any population [Hartl and Clark 1997]. The natural history of a species and the structure and dynamics of populations provide the arena in which these forces interact to drive evolutionary adaptation of populations to their environments. Thus, natural and anthropogenic environmental changes lead to changes in genetic diversity, both within and among populations, and genetic diversity measurement can provide insights into the consequences of environmental changes. For this reason, genetic approaches are very important in any bio-indicator study, because they allow both to investigate the effect of genetic diversity on biomarker response and to study the relationships between genetic polymorphism, pollution and demographic dynamics.

2 Methods

During spring 2005, some 120 specimens of *C. aestuarii* were collected in two sites of the lagoon (Fusina, Ca' Roman lagoon side) and one site on the shore (Ca' Roman sea side), representative of different environmental conditions.

Hemolymph analyses were performed individually in order to disclose by polyacrylamide gel electrophoresis, under native and dissociating conditions, the hemocyanin subunit patterns of each specimens. Western blots were

carried out using antibodies α -hemocyanin, to specifically detect the target proteins. Densitometric scan of the gels and statistical analyses were applied to measure and evaluate the difference of the mean value and the variance of each subunit.

For each specimen, 18 morphometric characters were measured (5 on the carapace, 5 on the ventral side of the thorax, 8 on the maxillipedes) for the analysis of FA. Each measure was repeated twice (during two separate sessions) for estimating measurement error.

Microsatellite loci of *C. aestuarii* were isolated from a partial genomic library enriched for the AC motif, following published protocols [Zane et al., 2002]. Seven microsatellite loci were used to analyse a total of 119 individuals from the three sampling sites of the Venice lagoon, using conditions previously described [Giomi et al. 2006]. Number of alleles, heterozygosity, departure from Hardy-Weinberg (HW) equilibrium, and linkage disequilibrium were calculated using GENEPOP ver3.1b [Raymond and Rousset, 1995]. Pattern of population differentiation was investigated by exact test of population differentiation on genic frequencies using the same software.

3 Results

By statistical comparison of the hemocyanin subunit patterns (ANOVA test on the means, followed by Bonferroni post-hoc), a significant difference in protein expression was detected. In particular, while subunit 1 resulted to be correlated with the sex of specimens, the expression of subunit V appeared to be affected by the sampling site. In details, different amount of this subunit were clearly detected among localities, and specimens collected in Ca' Roman sea side present a lower expression level in comparison with individuals from Fusina and Ca' Roman lagoon side; while samples from both lagoon sites show an equal expression level of subunits V (Fig. 1).

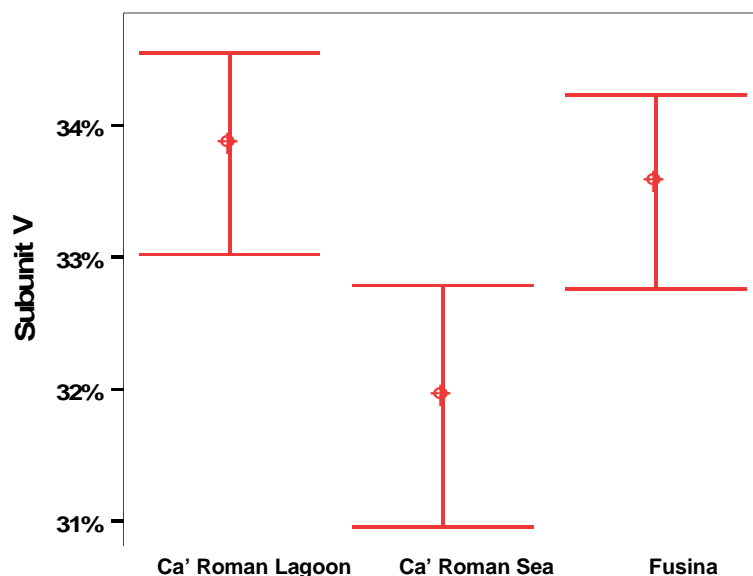


Fig 1 - Relative amount of hemocyanin subunit V among sampling sites, expressed in percentage of the total hemocyanin..

Analysis of FA, based on two-way ANOVA, followed the procedure initially proposed by Palmer [1994] and improved by Palmer and Strobeck [2003]. This showed that the method adopted for data acquisition (based on the processing of digital images, see Giomi et al. [2006]) was adequate, as FA was significantly larger than expected due to measurement error ($P < 0.0001$, ME3 descriptor of Palmer and Strobeck [2003]) for all characters and sites. However, statistical comparisons (F test) did not reveal any significant differences of FA between the sites ($P > 0.05$), either using the measures FA4a, FA10a or FA8a of Palmer and Strobeck [2003].

All 7 primer pairs reliably amplified genomic DNA extracted from single specimens (Fig 2). Number of alleles per population ranged from 3 to 39, while the observed heterozygosity ranged from 0.042 to 0.460 (Table 1). The expected heterozygosity resulted, for each locus and population, slightly higher than the observed one. Accordingly, the hypothesis of Hardy Weinberg equilibrium was rejected for locus 2 in all the three population samples, and for locus 3 and 5 in single populations (Table 1). No evidence of linkage disequilibrium was found.

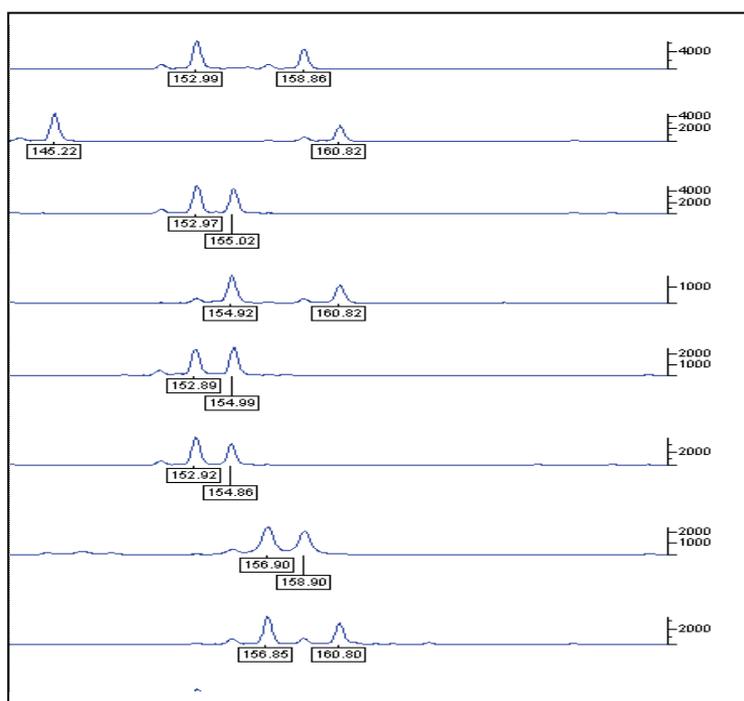


Fig 2 - Example of microsatellite genotypes in *Carcinus aestuarii*. Each line represents a single individual. Peaks indicates the alleles of each individual and their inferred size in number of base pairs.

The observed and expected heterozygosity for locus 7 resulted to be the lowest in the sample collected at Fusina, and the highest in the sample collected at Ca' Roman sea side, with the second station in the lagoon showing intermediate values (Table 1).

Exact test of genic differentiation allowed to reject the hypothesis of homogeneity between samples ($P = 0.014$). Pairwise comparison clearly indicated that this deviation from panmictic conditions is due to the sample

collected at Ca' Roman sea side, that resulted strongly different from the sample collected at Fusina ($P=0.002$) and slightly differentiated from the sample collected at Ca' Roman lagoon side ($P=0.043$).

	LOCUS	N. alleles	Het Obs	Het Exp	Fis	2N
	1	11.000	0.392	0.414	0.054	74
	2	20.000	0.432	0.468	0.077*	74
	3	20.000	0.446	0.473	0.058	74
Ca' Roman sea side	4	11.000	0.458	0.432	-0.062	72
	5	31.000	0.286	0.484	0.414*	70
	6	21.000	0.432	0.472	0.086	74
	7	4.000	0.135	0.123	-0.103	74
	Average	16.857	0.369	0.409	0.075	73.143
	1	10.000	0.383	0.385	0.005	60
	2	15.000	0.323	0.459	0.300*	62
	3	25.000	0.422	0.471	0.106	64
Ca' Roman lagoon side	4	10.000	0.411	0.440	0.068	56
	5	23.000	0.348	0.481	0.281*	46
	6	19.000	0.446	0.464	0.038	56
	7	4.000	0.091	0.087	-0.044	44
	Average	15.143	0.346	0.398	0.108	55.429
	1	11.000	0.410	0.394	-0.040	100
	2	18.000	0.378	0.462	0.184*	98
	3	24.000	0.318	0.455	0.304*	88
Fusina	4	13.000	0.460	0.423	-0.087	100
	5	39.000	0.429	0.480	0.109	98
	6	27.000	0.459	0.462	0.006	98
	7	3.000	0.042	0.041	-0.025	96
	Average	19.286	0.356	0.388	0.064	96.857

Table 1 - Results of microsatellite analysis of *C. aestuarii*. Reported is the number of alleles, the observed and expected fraction of heterozygotes, the fixation index, and sample size. Asterisks indicates lack of Hardy Weinberg equilibrium.

Conclusion

It is known that specific environmental stimuli influence the structural and functional hemocyanin phenotypes. Our results show a significant difference hemocyanin composition among sites, with a clear reduction in expression of one subunit in the sea sample.

This differential expression is mirrored by slight differences in genetic composition of the sample collected at Ca' Roman sea side with respect to the lagoon sites suggesting the existence of a complex population dynamics. In

addition, for one locus, the trend of heterozygosity clearly indicates a reduction in genetic variability towards the most internal part of the lagoon.

Thus, while the physiological and the genetic approaches spot a significant difference between sea and lagoon samples, there is no evidence of any relationship between developmental stability in *C. aestuarii* and the diversity of environmental conditions in the three sites considered.

However, conclusive comparisons between the results of the analyses of the three methodologies, not to say their full integration, will require the study, still in progress, of the materials of the field sampling carried out during spring 2006.

References

Bagley, M.J., Franson, S.E., Christ, S.A., Waits, E.R. and Toth, G.P., 2002. Genetic Diversity as an Indicator of Ecosystem Condition and Sustainability: Utility for Regional Assessments of Stream Condition in the Eastern United States. U.S. Environmental Protection Agency, Cincinnati, OH.

Conner, J.K., Hartl D.L., 2004. A primer of Ecological Genetics. Sinauer Associates, Inc. Publishers, Sunderland, Massachusetts U.S.A.

DeFur, P.L., Mangum, C.P. and Reese, J.E., 1990. Respiratory responses of the blue crab *Callinectes sapidus* to long-term hypoxia. *Biological Bulletin*, 178, 46–54.

Giomi, F., Beltramini, M., Fusco, G., Maruzzo, D., Zane, L. and Bisol, P.M. 2006. An integrated approach to biological monitoring in the Lagoon of Venice. In: Campostrini, P. (ed), Scientific Research and Safeguarding of Venice. Research Programme 2004-2006, vol.IV, 2005 results. CORILA, Venezia. XIV+511 pp.: 247-257.

Hoffmann, A.A. and Woods, R.E., 2003. Associating environmental stress with developmental stability: problems and patterns. In: Polak, M. (ed.) *Developmental instability: causes and consequences*. Oxford University Press, New York. Pp. 387-401.

Mangum, C.P. and Rainer, J.S., 1988. The relationship between subunit composition and oxygen binding of blue crab hemocyanin. *Biological Bulletin*, 174, 77–82.

Mangum, C.P., 1990. Inducible O₂ carriers in the crustaceans. In "Animal Nutrition and Transport Process: Transport, Respiration and excretion", by Truchot, J.P. and Lalou, B., Karger Basel.

Møller, A.P. and Swaddle, J.P., 1997. *Asymmetry, developmental stability, and evolution*, Oxford University Press, New York.

Palmer, A.R., 1994. Fluctuating asymmetry analyses: A primer. In: Markow T.(ed.) *Developmental Instability: Its Origins and Evolutionary Implications*. Kluwer, Dordrecht. Pp. 335-364

Palmer, A.R. and Strobeck, C., 2003. Fluctuating asymmetry analyses revisited.

In "Developmental instability: causes and consequences", by Polak, M., Oxford University Press, New York.

Raymond, M., Rousset, F., 1995. Genepop version 1.2, a population genetics software for extrat tests and ecumenicism. *Journal of Heredity*, 86: 248-249.

Zane, L., Bargelloni, L. and Patarnello, T., 2002. Strategies for microsatellite isolation: a review. *Molecular ecology* 11: 1-16.

Galloway T. S., Brown, R. J., Browne, M. A., Dissanayake, A., Lowe, D., Jones, M. B. and Depledge, M. H., 2004. Ecosystem management bioindicators: the ECOMAN project – a multi-biomarker approach to ecosystem management. *Marine Environmental Research*, 58: 233-237

PROPOSAL OF A NEW ENVIRONMENTAL QUALITY INDEX FOR THE MACROFOULING BIOCOENOSIS OF HARD SUBSTRATA IN THE LAGOON OF VENICE

Francesca Cima, Paolo Burighel, Lorian Ballarin

Dipartimento di Biologia, Università di Padova

Riassunto

È stata effettuata un'analisi dell'evoluzione temporale della comunità macrobentonica di substrato duro nel bacino meridionale della laguna di Venezia con lo scopo di sviluppare un indice di qualità ambientale poco costoso, relativamente facile da calcolare, sensibile alle varie situazioni ambientali e che, oltre ai dati biotici, tenga conto delle variazioni nel tempo di parametri chimico-fisici ritenuti altamente significativi per l'ambiente lagunare.

Abstract

We carried out an analysis of the temporal sequence of the macrofouling biocoenosis of hard substrata in the southern basin of the lagoon of Venice, with the aim of developing an environmental quality index which was cheap, easy to calculate, sensitive to many environmental conditions and considering the relationships between the biotic data and change of highly significant chemical-physical parameters as regards the lagoon environment.

1 Introduction

Fouling is the whole of phyto- and zoobenthonic sessile peopling able to settle on a hard natural or artificial substratum immersed in water. This association can not be defined from a biocoenologic point of view as an univocal and distinct entity, but varies with the change of a lot of environmental situations [Raïlkin, 2004]. In the marine environment, the organism settlement on an exposed structure depends on various aspects such as the naturally species present in the immersion place, their ability to settle and grow, the place and the period of immersion, the characteristics of the substratum, which, at least at first, may select the pioneer species, the climatic-seasonal conditions and a complex of chemical, physical and biological factors.

In the succession of the biocoenoses which colonize these substrata, it is usually possible to distinguish a temporal sequence, depending on the duration of the substratum immersion, a seasonal sequence, depending on the course of the seasons and a biotic succession or real ecological succession [Redfield and Delvy, 1952]. The temporal sequence is due to the sequence of the colonization phases and is represented by three fundamental moments: 1) already in few minutes, the virgin submerged surfaces are subjected to the deposition of a layer of organic material, constituted of polysaccharides and proteins naturally dissolved in seawater, which originate from the decomposition of animal and

vegetable organisms [Baier, 1972]; 2) the chemical composition of the surface influences the formation of the primary film mainly during the first two-three days, selecting bacterial and microalgal strains (microfouling); 3) after about one month of immersion, macroorganisms (macrofouling), are settled, represented by macroalgae and sessile invertebrates, as bryozoans, porifers, hydrozoans, anthozoans, polychaetes, molluscs, cirripeds, tunicates; on this community also grazing invertebrates, as decapods, amphipods, isopods, and predatory ones, as the wandering polychaetes, are recognizable. The settled organisms of macrofouling can show a rapid growth, as serpulids, or a slow growth, as mussels. The species with rapid growth initially assume a dominant role in the community, but they can be replaced later by species with slower growth. However, it must be taken into consideration that the above cited developmental times of the succession can be much shorter depending on the climatic circumstances.

The seasonal sequence depends on the various moments during the year in which animals and plants reproduce and settle. This is expressed in a more remarkable manner as the seasons are differentiated among them. At our latitudes, the most intense settlement occurs during the summer (from June-July to October) and in more superficial layers of the seawater column.

The biotic macrofouling succession requires changes in both structure and functions of the community, considered as the following one another of different species in conformity with a chronological order until the reaching of a state of dynamic balance named "climax". The initial stage (primary fouling) is characterized by the fortuitous aggregation of pioneer species, and is a disorder stage without biotic interactions. These organisms constitute, in turn, a biological substratum suitable for the secondary fouling, represented by mussels, which emerge only onto preexistent organisms and represent the reaching of the "climax stage" [Scheer, 1945]. Species belonging to both the primary and secondary fouling like barnacles, serpulids and tunicates can be also present.

2 The study of fouling in the lagoon of Venice and the use of bioindexes

This interest towards the fouling of the lagoon of Venice was born from demands of practical character because there was the problem of the damages caused by encrustations on submerged artificial objects as boats, harbour structures, platforms, signal buoys, fishing nets, pipes for water exchange. At the same time, from a naturalist point of view, the study of the development of macrofouling biocoenoses was of particular interest because it might represent an instrument for the evaluation of the biodiversity in the lagoon. The analysis of these communities is important because it constitutes effective means to interpret the environmental conditions since: a) the organisms studied are fixed onto the substratum and, therefore, subjected to all the variations of the chemical-physical parameters; b) the analysed substratum is available in all the lagoon and allows significant comparisons among the different parts of this ecosystem; c) the species considered have nearly always a large distribution in

both the Mediterranean and extra-Mediterranean lagoons and their ecology are quite well known.

In the lagoon of Venice, these studies acquire a critic relevance owing to they allow to reveal, in the long term, quality and quantity changes of the fouling community attributable to environmental differences and improve the comprehension of the existing interactions between the organisms of the fouling and some physical-chemical factors of seawater.

Unlike other lagoons of the Mediterranean Sea, the lagoon of Venice cannot be so distinctly subdivided in definite zones: it is very extensive and is a complex environment, formed of a mosaic of habitats and ecosystems very different between them, characteristic that makes it an environment with high biodiversity and variety. The biological indexes till now used as instruments for the monitoring of the environmental quality of the brackish lagoons, as the "Lesina bioindex" or Breber's index [Breber et al., 1998], are exclusively based on sampling involving the collection of bivalves from soft substrata and represent their bionomy which considers the zoning proposed by Frisoni et al. [1984], not completely applicable to the lagoon of Venice. Moreover, in literature, quality bioindexes carried out on the basis of monitoring hard substrata are till now absent.

The present research had its purpose to perform an evaluation of the environmental quality of the lagoon of Venice on the basis of both the biotic data and some chemical-physical parameter highly representative in the lagoon environment, like water temperature, salinity and pH. The final aim is to propose indexes of environmental quality, which are cheap to obtain, quite easy to calculate, and really applicable to the various environmental situations.

3 Observations of macrofouling ecological succession in the southern lagoon

The study was focussed on the analysis of the macrobenthonic biocoenosis of hard substrata in the southern basin of the lagoon of Venice. A condition simulating a natural one has been recreated by means of a constant immersion of wood and steel panels (20 x 15 x 0.1 cm), in two different stations of the southern lagoon (Chioggia). Station 1 (Lat. 45° 15' N, Long. 12° 15' E) was an abandoned mussel rearing along the Perognola channel, in the face of the port mouth corresponding to a zone placed far from the inhabited centre: in this site, the water was deep about 3 m and was characterized by modest wavy motion provoked prevalently by the boat transit. Station 2 (Lat. 45° 14' N, Long. 12° 17' E) was sited along the Sottomarina channel in an internal zone as regards the port mouth. The panels were anchored approximately to a mobile wharf constituted of big plastic floats. In this station, with low traffic of boats, the water presented a depth not superior to 1-1.5 m and appeared often thick turbid.

The artificial substrata remained submerged for one year (March 2004 - April 2005) and the ecological succession was followed by sampling with monthly cadence. Some important chemical-physical data were regularly collected, such as water temperature, pH, salinity, total dissolved solids, dissolved organic

carbon (Fig. 1). Biotic data were interpreted and expressed by means of the commonest biodiversity indexes for the fouling biocoenosis: species richness, biocoenosis structure, Benninghoff's covering-abundance index [Cima et al., 2005].

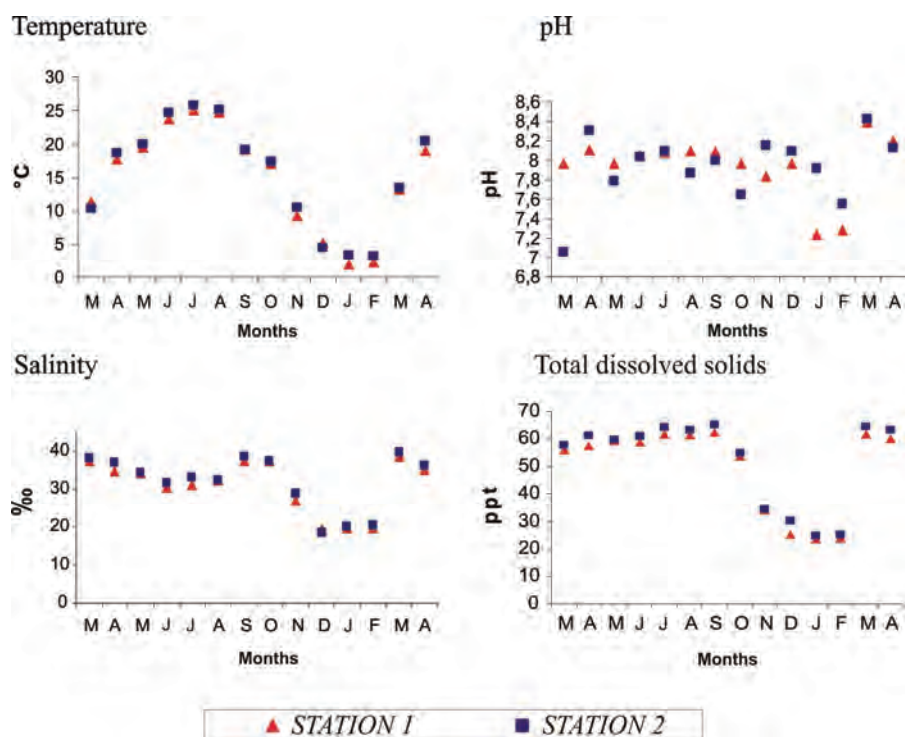


Fig. 1 – Trend of physical parameters in the two stations near Chioggia from March 2004 to April 2005.

The ecological succession began in April: in both the stations the bacterial film developed on the panels, with larger extension in the station 2. In June, the pioneer organisms dominant in the community of station 1, were 74% hydrozoans (*Tubularia crocea*) and, in the station 2, 66% chlorophyta (*Enteromorpha* sp., *Ulva* sp.). The rest of the community was represented, in both the stations, by rhodophyta (*Polysiphonia sertularioides*, *Ceramium ciliatum*), phaeophyta (*Ectocarpus siliculosus*) and amphipods (gammarids, caprellids). However, a remarkable increment of the species richness index occurred becoming from 1 to 4 in station 1 and from 1 to 6 in station 2.

In summer months, the dominant species were, in both the stations, 40% serpulids (*Hydroides dianthus*, *Serpula vermicularis*), 33% tunicates (*Botryllus schlosseri*, *Styela plicata*, *Ciona intestinalis*, *Asciidiella aspersa*), 21% cirripeds (*Balanus amphitrite*, *Balanus improvisus*), 4% bryozoans (*Bugula* sp., *Cryptosula pallasiana*), and porifers (*Aplysina aerophoba*, *Sycon ciliatum*). Among the grazing organisms, amphipods were observed above all, with vicarious species in the various months, and, with a lesser extent, isopods, decapods, wandering polychaetes, gastropods and echinoderms. The species richness remarkably increased. In July, the temperature reached its maximum values; its further increase in July-August, determined also the increase in the

species richness with the settlement of new species and confirmed the presence of species settled in the previous months: values became, in station 1, from 4 to 9 and, in station 2, from 5 to 8.

In autumn (October and November), together with significant fluctuations of salinity and temperature, the climax was reached, maintaining steady until January: the community was represented, for more than 90%, by solitary and colonial tunicates, in which botryllids (*Botryllus schlosseri* and *Botrylloides leachi*) prevailed. The fact that the climax stage was reached with the constant and massif presence of tunicates, on both wood substrata and more steel ones, represents a novelty in comparison with previous studies, where the final stage was represented by *Mytilus galloprovincialis* as a dominant species [Relini et al., 1972; Candela and Torelli, 1983; Mizzan and Moretti, 1990; Cornello and Manzoni 1998; Cornello and Occhipinti Ambrogi, 2001]: in the present research, these species resulted rare, confirming the most recent observations in the southern basin of the lagoon of Venice [Cima et al., 2004; 2005; 2006]. During the last thirty years, substantial changes would be verified in the ecological successions of the lagoon favouring the expansion of the ascidians as filtering-feeding organisms vicarious of the bivalves. Therefore, the climax of the hard substratum can be today defined with the name “*Botryllus* community”, in which colonial ascidians, like *Botryllus schlosseri*, *Botrylloides leachi* and, with less extent, bryozoans, barnacles, serpulids, chlorophyta and rhodophyta dominate.

4 Evaluation of the state of health

The analysis of the macrobenthonic biocoenosis of hard substrata in the southern basin of the lagoon of Venice through biodiversity indexes and the trend of some chemical-physical parameters became useful to develop a new environmental quality index, specific for the community of hard substrata, and represented by the following algorithm:

$$\text{Log}_{10} (R \cdot A \cdot I_{\text{pH}} \cdot I_{\text{T}} \cdot I_{\text{S}})$$

where:

R = species richness, i.e., number of species by month present onto all panels of the same type

A = area extension for each species by months (cm²)

I_{pH} = pH quality index

I_T = temperature quality index

I_S = salinity quality index.

The development of a quality index in logarithmic scale, from 1 to 10 inclusive, which allows to really evaluate the state of health of the lagoon environment assigning to it a numerical value, is very important because, besides the immediate datum, it permits to carry out a quality comparison with other zones of the lagoon and follow in the time the seasonal variations also in relation with possible anthropic impacts. The biological index or bioindex considers the species richness and the area taken up by the species together with quality values attributed to chemical-physical parameters like temperature, pH and

salinity of the seawater, which more affect the state of health of the aquatic ecosystems. Moreover, this new index is evaluated in a dynamic manner, that is considering its temporal trend in a year (Fig. 2).

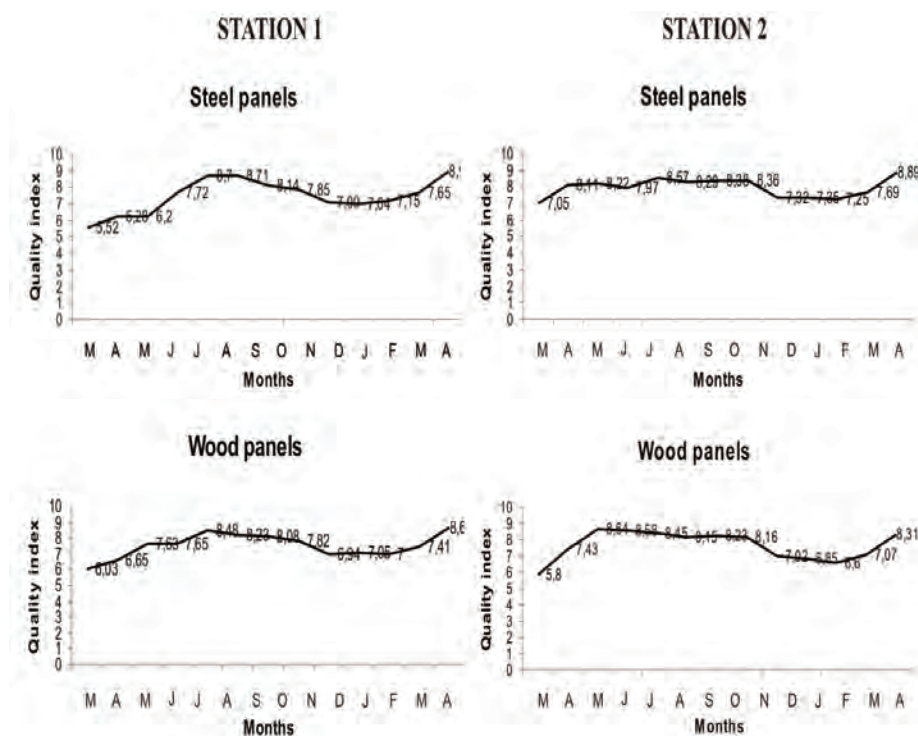


Fig. 2 – Trend of bioindex for macrofouling of hard substrata in the two stations near Chioggia from March 2004 to April 2005.

First of all, the application of this bioindex have put in evidence that the trend of the temperature during the year characterized three critic moments for the development of the macrobenthonic biocoenosis of hard substrata: the first moment, with an initial phase of fouling settlement and colonization, was observed between March and April 2004, when, in station 1, the temperature increased from 11.3 °C to 17.6 °C and, in station 2, from 10.3 °C to 18.6 °C; the second moment, between October and November, characterised by a temperature decrease of about 8 °C in station 1 and about 7 °C in station 2, took place at the same times of the reaching of the “climax” stage; the third moment, between February and March 2005, in which the temperature increased of about 11 °C in station 1 and about 10 °C in station 2, took place at the same time of beginning of a new growth cycle of the fouling community after its dismantling.

5 Conclusions

This new bioindex 1) is cheap and simple in calculating, 2) is not selective as regards the substratum, 3) is specific for the community of hard substrata, 4) is applicable in any zone of the lagoon environments together with the Breber’s index allowing to obtain quantity and quality comparisons with other lagoon zones, 5) supplies a numerical value with an immediate meaning, 6) is

evaluated in a dynamic manner, and 7) allows to follow seasonal variations also in relation with possible environmental (natural, anthropic) crisis: it registers the moment of the crisis and its effects in the time, although needing a continuous evaluation on a temporal space which must be extended further the year.

References

Baier R.E., 1972. Influence of the initial surface condition of materials on bioadhesion. Proceedings of the Third International Congress on Marine Corrosion and Fouling, October 1972, Gaithersburg, Maryland, USA, 633-639.

Breber P., Pagliani T., Sardella S. and Spada A., 1998. Una proposta di bioindice per la valutazione della qualità ambientale delle lagune. *Genio Rurale*, 61, 3-6.

Candela A. and Torelli A.R., 1983. Note sulla colonizzazione di pannelli nell'intermareale all'isola di S. Erasmo (Laguna di Venezia). *Atti del Museo Civico di Storia Naturale di Trieste*, 35, 225-234.

Cima F., Burighel P. and Ballarin L. , 2004. Biodiversity in the lagoon of Venice: a laboratory model for the study of the effects of antifouling compounds on settlement and survival of sessile species, in "Scientific Research and Safeguarding of Venice – Vol. II", by P. Campostrini Ed., Istituto Veneto di Scienze, Lettere ed Arti, Venezia, 449-456.

Cima F., Ballarin L. and Burighel P. 2005. Macrofouling ecological succession on hard substrata in the lagoon of Venice: effects of copper-containing antifouling paints, in "Scientific Research and Safeguarding of Venice – Vol. III", by P. Campostrini Ed., Istituto Veneto di Scienze, Lettere ed Arti, Venezia, 429-435.

Cima F., Burighel P. and Ballarin L. 2006. Temporal and biotic evolution of "Botryllus biocoenosis" in the presence of antifouling paints, in "Scientific Research and Safeguarding of Venice – Vol. - IV", by P. Campostrini (Ed.), CORILA, Venezia, 239-246.

Cornello M. and Manzoni A., 1998. Caratterizzazione stagionale degli insediamenti di organismi macrobentonici su substrati sperimentali nel bacino centrale della Laguna di Venezia. *Bollettino del Museo Civico di Storia Naturale di Venezia*, 49, 135-144.

Cornello M. and Occhipinti Ambrogi A., 2001. Struttura e dinamica dei popolamenti macrofouling in relazione al periodo di insediamento nel bacino centrale della laguna di Venezia. *Bollettino del Museo Civico di Storia Naturale di Venezia*, 52, 113-128.

Frisoni G., Guelorget O. and Perthuisot J.P., 1984. Diagnose écologique appliquée à la mise en valeur biologique des lagunes côtières Méditerranéennes: approche méthodologique, in "Management of Coastal Lagoon Fisheries", by J.M. Kapetsky and G. Lasserre Eds., GFCM, Studies and Reviews 61, FAO, Rome.

Mizzan L. and Moretti G., 1990. Dati sull'insediamento e sull'accrescimento del macrofouling su pannelli metallici nel porto-canale di S. Nicolò (Laguna di Venezia). *Bollettino del Museo Civico di Storia Naturale di Venezia*, 41, 55-89.

Railkin A.I., 2004. *Marine biofouling: colonization processes and defenses*. CRC Press LLC, Boca Raton.

Redfield L.W. and Delvy E.S., 1952. Temporal sequences and biotic succession. *Marine fouling and its prevention*. Wood Hole Oceanograf. Inst. Ed., Wood Hole, 42-47.

Relini G., Francescon A. and Barbaro A., 1972. Osservazioni sistematico-ecologiche sulla distribuzione dei Cirripedi toracici nella laguna Veneta. *Atti dell'Istituto Veneto di Scienze Lettere e Arti*, 130, 449-459.

Scheer B.T., 1945. The development of marine fouling communities. *Biological Bulletin*, 89, 103-121.

A PRELIMINARY CHEMICAL INDEX FOR THE ESTIMATION OF THE SEDIMENT QUALITY IN THE VENICE LAGOON: OBJECTIVES AND METHODOLOGY

Christian Micheletti¹, Stefano Ciavatta², Critto Andrea¹, Massimo Rando¹, Irene Rumonato², Roberto Pastres², Antonio Marcomini¹

¹ Dipartimento di Scienze Ambientali, Università Cà Foscari di Venezia, ² Dipartimento di Chimica Fisica, Università Cà Foscari di Venezia

Riassunto

La qualità dei sedimenti lagunari in relazione alla contaminazione da composti organici (PCB e PCDD/F) e metalli, è stata valutata attraverso la stima di un indice integrato di esposizione. L'indice chimico integra tre sub-indici che considerano: 1) la concentrazione dei contaminanti nel sedimento, 2) la concentrazione dei contaminanti negli organismi bentonici, e 3) la potenzialità dei composti organici di biomagnificare lungo la rete trofica. I sub-indici per il sedimento (1) e per gli organismi bentonici (2) sono stati calcolati utilizzando la concentrazione dei contaminanti nel sedimento e nei tessuti della vongola *Tapes philippinarum*, rilevati nell'ambito di un monitoraggio condotto dal Magistrato Alle Acque di Venezia (MAV, 2000). L'indice di biomagnificazione è stato stimato sulla base dei risultati di un modello di bioaccumulo, sviluppato, calibrato, e validato per la laguna di Venezia (Lovato et al., 2006). Il risultato degli indici è stato espresso in una scala qualitativa con classi comprese fra 1 (qualità migliore) e 5 (qualità peggiore), ricavate sulla base delle distribuzioni cumulative dei dati sito-specifici e dei percentili. L'indice relativo al sedimento è stato ottenuto applicando l'indice MPSI proposto dalla letteratura (Shin e Lam, 2001). Infine, i tre sub-indici sono stati confrontati nelle aree omogenee (aree precedentemente definite all'interno della linea di ricerca 3.11).

Abstract

A procedure to calculate an integrated exposure index is proposed, in order to estimate the quality of the lagoon sediments concerning organic (i.e. PCBs and PCDD/Fs) and inorganic compounds (i.e. metals). The chemical index integrates three sub-indices related to: 1) concentration of pollutants in sediment, 2) pollutant concentrations in benthic organisms, and 3) the potential of organic contaminants to biomagnify through the food web. In order to estimate the sub-indices for sediment and benthic organisms, experimental concentrations of pollutants in sediments and in clam (*Tapes philippinarum*) tissues (MAV, 2000) were used, while the biomagnification sub-index was estimated by applying a kinetic bioaccumulation model, recently calibrated and validated for the lagoon of Venice (Lovato et al., 2006). The indices were expressed using a qualitative scale spanning over the range 1 (best quality) - 5 (worst quality). The quality classes for the sub-indexes based on organisms

contamination were defined on the basis of the cumulative frequency distribution of the experimental data and by using the percentiles. As far as the sediment sub-index is concerned, the MPSI index (Shin e Lam, 2001) was applied. The three sub-indices were subsequently compared according to the homogeneous lagoon areas previously identified within the framework of the line 3.11 of this project.

1 Introduction

The European Water Framework Directive (WFD; 2000/60/EC) requires from Member States the integrated evaluation of river basins quality status, by taking into account different environmental quality elements. Specifically, the WFD establishes to define the ecological status of surface waters by integrating hydromorphological, physico-chemical and biological parameters, in order to develop quality indices and classify each water body. The quality evaluation for each parameter has to be expressed as the distance from a reference value and performed by comparing the value measured in the site of investigation with a reference value representing high ecological quality conditions. According to this approach five quality classes have to be defined (from high to bad).

Currently, tools able to evaluate the ecological status and trends in areas within the Venice lagoon by integrating information from different quality indices are not still been developed. Therefore, the need to implement the WFD for transitional waters and to develop transparent/clear and feasible evaluation tools for Public Authority have led to propose and define within the CORILA 2004-2007 research project a preliminary methodology for the estimation of the sediment quality in the Venice lagoon. The sediment quality index will be then integrated with ecotoxicological and ecological indices, developed by the line 3.11, in order to obtain an integrated evaluation of ecological quality.

According to the WFD and recent literature (Chapman, 1990; Canfield et al., 1994; Menzie et al., 1996; Wildhaber and Schmitt, 1996; Del Valls et al., 1998; Suter et al. 2000; Ferreira et al., 2000; Souek et al., 2000; Cherry et al, 2001; Burton et al., 2002; Grapentine et al., 2002b; Den Besten et al, 2003; Borja et al., 2004), the proposed methodology for quality evaluation is based on an integrated approach, described in the following paragraphs.

2 Objectives and methodologies

The proposed methodology for environmental quality evaluation is based on the Weight of Evidence approach, defined as “the process of combining information from multiple lines of evidence to reach a conclusion about an environmental system or stressor” (Burton et al., 2002). This approach integrated judgements on quality, quantity and concordance among results provided by different lines of evidence, experimental activities providing qualitative and/or quantitative exposure and effect information in order to support the risk characterization (US-EPA, 1998). The proposed methodology includes 3 phases: i) definition of the experimental database; ii) definition of the qualitative evaluation scale and classes for each parameter (i.e. considered pollutant) on the basis of cumulative

frequency distribution and percentiles; iii) aggregation of results obtained for each pollutant.

According to the proposed procedure, the relative quality of sediments in the Venice lagoon was estimated by means of three sub-indices: a first sub-index related to sediment contamination, a second sub-index based on pollutants concentrations in tissues of the clam *Tapes philippinarum* and a third sub-index which evaluates the potential of organic compounds to bioaccumulate through the aquatic food web.

The sediment quality sub-index was obtained by applying the Marine Sediment Pollution Index (MSPI; Shin et Lam, 2001), which was calculated on the basis of the Principal Component Analysis of the sediment contamination dataset. The sub-index related to the sediment quality was chosen because of sediments are the main source of pollutants of the lagoon, as they are a sink of organic and inorganic pollutants which were discharged in the past as well as to minor extent nowadays. Moreover, the organic and inorganic pollutants adsorbed to the sediment particles are resuspended and then transported through the lagoon, while the detritus is an important source of the diet of several organisms living in the lagoon.

The second sub-index is based on chemical concentration of metals and organic compounds in tissues of the clam *Tapes philippinarum*. This sub-index aims to evaluate the bioavailability of contaminants from sediments to the first trophic levels of the aquatic food web represented by the filter-feeder benthic organisms. The choice of the clam *Tapes philippinarum* as representative organism for the benthic community depends on three factors: i) *Tapes* is widely diffuse in the Venice lagoon and thus it is easily available for monitoring; ii) *Tapes* is tolerant to contamination and it can be found in highly contaminated areas too; iii) *Tapes* ensures a good spatial representativeness of contamination in benthic organisms. Otherwise the choice of the clam limits the evaluation of bioavailability process to a single type of diet (i.e. filter-feeders organisms) excluding detritivorous and predators organisms. In fact when different ways of feeding are considered different bioavailability measures are obtained. Consequently, a complete evaluation of bioavailability process from sediments to benthonic organisms should be carried out by analysing also crustaceans and anellidae.

The sub-index related to the potential bioaccumulation of organic pollutants through the food web was obtained by comparing pollutants concentrations in organisms at higher trophic levels (fish) with concentrations at lower trophic levels (omnivorous feed-filter macrobenthos). The chemical concentrations were estimated by applying a bioaccumulation model proposed by Arnot and Gobas (2004), which combines toxicants uptake and elimination kinetics with aquatic food web dynamics. This sub-index was selected in order to identify a potential biomagnification, and thus to verify if the sediments can be a source of pollution for the highest levels of the food web (e.g. fish). The increased pollutant concentration in fish can lead to potential risks for fish, wildlife eating fish, and finally for humans.

2.1 Definition of the experimental dataset

The definition of the experimental dataset is the first phase of the proposed procedure. The experimental database used for calculate the sediment and the bioaccumulation potential sub-indices was provided by the Venice Water Authority (MAV, 2000). Chemical concentration of metals (i.e. As, Cd, Cr, Cu, Hg, Ni, Pb, Zn) and organic compounds (i.e. PCB and PCDD/F) was determined in 95 sampling stations homogeneously distributed over the whole lagoon. In order to calculate the benthic bioaccumulation sub-index, the experimental dataset was composed by 23 sampling stations provided by the Venice Water Authority (MAV, 2000) and by 30 sampling stations collected from 1997 to 1998 by the Regione Veneto. In particular, chemical concentrations of arsenic, cadmium, chromium, lead, zinc, copper, mercury and nickel were measured in 53 sites, while the dioxin-like PCBs and PCDD/Fs congeners were analysed in 23 samples.

2.2 Definition of the qualitative classes for each pollutant

The qualitative evaluation scale used for classify the results of the three sub-indices includes 5 classes, where class 1 corresponds to the relative best condition and class 5 to the relative worst condition. For the sediment quality index, the classes were defined for the MSPI Index results, dividing the range 0-100 in 5 homogeneous classes (i.e. 0-20 = class 1; 20-40 = class 2; etc.). Concerning the sub-indices for benthic organisms (i.e. *Tapes philippinarum*) bioaccumulation, and the sub-index for the potential bioaccumulation through the food web, the quality classes were defined for each considered pollutant, on the basis of the cumulative frequency distribution of the biota pollutants concentrations. The 20th, 40th, 60th, 80th percentiles were identified as limits, i.e. the range 0-20th percentile corresponded to class 1, the range 20th-40th percentile to class 2, and so on.

2.3 Aggregation of results into sub-indices

The third phase of the proposed procedure was to calculate a single score for each sub-index in every sampling station, in order to compare the results of the three sub-indices. This phase was carried out only for the "pollutant bioaccumulation in benthic organism" and "bioaccumulation through the food web" sub-indices, because the MSPI for sediment already provided a single score in each sampling station. On the contrary, the biota sub-indices provided a score (i.e. a class between 1 and 5) for each evaluated pollutant. The single score for the sub-indices was obtained aggregating the scores of each pollutant composing the mixture by using the arithmetic average, and rounding the result to the nearest integer number.

3 Integrated evaluation

An integrated evaluation of the relative quality values obtained from the three sub-indices was then accomplished, by evaluating the concordance among results in selected homogeneous areas within the Venice lagoon. Such homogeneous areas were identified by Tagliapietra and Zanon in the CORILA

project (2005). According to the authors the lagoon does not represent an individual habitat but it consists of more interrelated environments with different physico-chemical and biological characteristics. Consequently, according to a transitional gradient based on abiotic factors (residence time, salinity, granulometry) nine typologies were defined.

The integrated evaluation was accomplished by obtaining a score for the whole homogeneous area for each sub-index. Since often for each sub-index more than 1 score in a single area was obtained (i.e. due to the presence of more than one sampling station in the same area) the scores were aggregated by using the arithmetic average, rounding the results to the nearest integer number. Finally, for each homogeneous area the results of each sub-index (sediment contamination, bioaccumulation in benthic organisms, potential bioaccumulation through the food web) were compared.

The proposed sub-indices gives information about the relative quality of an area with respect to another one (e.g. area A is better than area B with respect for instance to bioaccumulation in *Tapes philippinarum*). In order to assess an absolute risk value, i.e. the ecological quality of the investigated lagoon area, the comparison with ecotoxicological and ecological indices will be required.

References

- Arnot, J.A., and Gobas, F.A.P.C.. 2004. A food web bioaccumulation model for organic chemicals in aquatic ecosystems. *Environ. Toxicol. Chem.*, 23, 2343-2355.
- Beinat E., 1997, Case study: expert based value function models for cleaning up a polluted site, in "Value Functions for Environmental Management", by Beinat Euro, Kluwer Academic Publishers, Netherland.
- Borya A., V. Valencia, J. Franco, I. Muxica, J. Bald, M.J. Belzunce, O. Solaun, 2004. The water framework directive: water alone, or in association with sediment and biota, in determining quality standards. *Marine Pollution Bulletin*, No. 49 : pp. 8-11.
- Burton, Jr, G.A., G.E. Batley, P.M. Chapman, V.E. Forbes, E.P. Smith, T. Reynoldson, C.E. Schlegel, P.J. den Besten, A.J. Bailer, A.S. Green, R.L. Dwyer. 2002. A Weight-of-Evidence framework for assessing sediment (or other) contamination: improving certainty in the decision-making process. *Human and Ecological Risk Assessment* 8: 1675-1696.
- Canfield, T.J., N.E. Kembel, W.G. Brumbaugh, F.J. Dwyer, C.G. Ingersoll, J.F. Fairchild. 1994. Use of benthic invertebrate community structure and the sediment quality triad to evaluate metal-contaminated sediment in the upper Clark Fork river, Montana. *Environmental Toxicology and Chemistry* 13: 1999-2012.
- CE: Comunità Europea. 2000. Water Framework Directive, Direttiva 2000/60/EC, "Directive 2000/60/EC of the European Parliament and of the Council establishing a framework for the Community action in the field of water

policy".

Chapman, P.M. 1990. The Sediment Quality Triad approach to determining pollution-induced degradation. *The Science of the Total Environment* 97/98: 815-825.

Cherry, D.S., R.J. Currie, D.J. Soucek, H.A. Latimer, G.C. Trent. 2001. An integrative assessment of a watershed impacted by abandoned mined land discharges. *Environmental Pollution* 111: 377-388.

CORILA: Consorzio per la Gestione del Centro di Coordinamento delle Attività di Ricerca inerenti il Sistema Lagunare di Venezia. Programma di Ricerca 2004-2007, Rapporto di avanzamento attività scientifica 2005. Venezia.

Critto, A., Carlon, C., Marcomini, A.. 2005. Screening ecological risk assessment for the benthic community: the Venice lagoon as case study. *Environment International*, 31 (7): 1094-1100.

Del Valls T. A', J.M. Forja and A. Gómez-Parra, 1998. Integrative assessment of sediment quality in two littoral ecosystems from the gulf of Cádiz, Spain. *Environmental Toxicology and Chemistry*, No.6 (Vol.17): pp. 1073-1084.

Den Besten P.J., E. de Deckere, M.P. Babut, B. Power, T. A. Del Valls, C. Zago, A. M.P. Oen, S. Heise, 2003. Biological Effects-based Sediment Quality in Ecological Risk Assessment for European Waters. *JSS – J Soils Sediments*, No.3 (Vol.3) : pp. 144 – 162.

Ferreira J.G., 2000. Development of an estuarine quality index based on key physical and biogeochemical features. *Ocean Coastal Management*, No. 43, pp. 99-122.

Fox W.M., Connor L., Copplestone D., Johnson M.S. and Lee R.T., 2001. The organochlorine contamination history of the Mersey estuary (UK) revealed by analysis of sediment cores from salt marshes. *Marine Environmental Research*, 51, 213-227.

Grapentine, L., J. Anderson, D. Boyd, G.A. Burton, C. De Barros, G. Johnson, C. Marvin, D. Milani, S. Painter, T. Pascoe, T. Reynoldson, L. Richman, K. Solomon, P.M. Chapman. 2002b. A decision making framework for sediment assessment developed for the Great Lakes. *Human and Ecological Risk Assessment* 8: 1641-1655.

Lovato, T., Micheletti, C., Pastres, R., Marcomini, A. 2006. Verification of a POPs bioaccumulation model for the Venice Lagoon. In: *Scientific Research and Safeguarding of Venice*, Vol. IV, 2005 results, Ed. Campostrini P..

MacDonald D.D., 1994. Approach to the Assessment of Sediment Quality in Florida Coastal Waters, Tallahassee, Florida Department of Environmental Protection.

MAV-CVN, 2000. Mappatura dei fondali lagunari. Rapporto finale. Consorzio Venezia Nuova, Venezia, Italia.

Menzie, C., M.H. Henning, J. Cura, K. Finkelstein, J.H. Gentile, J. Maughan, D.

Mitchell, S. Petron, B. Potocki, S. Svirsky, P. Tyler. 1996. Special report of the Massachusetts weight-of-evidence workgroup: a weight-of-evidence approach for evaluating ecological risks. *Human and Ecological Risk Assessment* 2: 277-304.

Micheletti, C., Critto, A., Carlon, C., Marcomini, A. 2004. Ecological Risk Assessment of Persistent Toxic Substances for the Clam *Tapes philipinarum* in the Lagoon of Venice. *Environmental Toxicology and Chemistry*, 23 (6): 1575-1582.

Pastres, R., Solidoro, C., 1999. Trattamento ed analisi dei dati anche mediante un modello di qualità dell'acqua (ex art. 55 del Capitolato Speciale) - Rapporto finale. In "Interventi per l'arresto del degrado connesso alla proliferazione delle macroalghe in laguna di Venezia 1997-1998". Consorzio Interuniversitario "I.N.C.A." - Consorzio "Venezia Nuova" - Istituto Nazionale di Oceanografia e Geofisica Sperimentale, Venezia.

Shin, P.K.S., W.K.C. Lam. 2001. Development of a marine sediment pollution index. *Environmental Pollution* 113: 281-291.

Soft Inc. 2002. STATISTICA 6.0.

Souek, D.J., D.S. Cherry, R.J. Currie, H.A. Latimer, G.C. Trent. 2000. Laboratory to field validation in an integrative assessment of an acid mine drainage-impacted watershed. *Environmental Toxicology and Chemistry* 19: 1036-1043.

Suter II, G.W., R.A. Efrogmson, B.E. Sample, D.S. Jones. 2000. Ecological risk assessment for contaminated sites. Lewis, Boca Raton, Florida.

Ugo P., 2002. Personal Communication.

U.S. Environmental Protection Agency. 1989. Risk assessment Guidance superfund, Volume 1, Human Health Evaluation Manual (Part A, Chapter 5). Office of emergency and remedial response, EPA/540/1-89/002.

U.S. Environmental Protection Agency (U.S. EPA). 1998. Guidelines for Ecological Risk Assessment. Final. EPA/630/R-95/002F. Risk Assessment Forum. Washington, DC.

U.S. Environmental Protection Agency (U.S. EPA). 2003. US-EPA region 5, RCRA 2003. <http://www.epa.gov/Region5/rcra/edql.htm>.

Van den Berg M, Birnbaum L, Bosveld ATC, Brunstorom B, Cook P, Freely M, Giesy JP, Handberg A, Hasewaga R, Kennedy SW, Kubiak T, Larsen JC, van Leeuwen FXR, Liem AKD, Nolt C, Peterson RE, Poellinger L, Safe S, Schrenk D, Tillitt D, Tysklind M, Younes M, Waern F, Zacharewski T, 1998. Toxic equivalency factors (TEFs) for PCBs, PCDDs, PCDFs for humans and wildlife. *Environmental Health Perspective* 106:775-792.

Wildhaber, M.L., C.J. Schmitt. 1996. Hazard ranking of contaminated sediment based on chemical analysis, laboratory toxicity tests, and benthic community composition: prioritizing sites for remedial action. *Journal of Great Lakes Research* 22: 639-652.

RESEARCH LINE 3.12

Trophic chain and primary production in the lagoon metabolism

PICOPHYTOPLANKTON CONTRIBUTION TO PHYTOPLANKTON COMMUNITY IN THE VENICE LAGOON

Joan Coppola, Fabrizio Bernardi Aubry, Francesco Acri, Alessandra Pugnetti

C.N.R. ISMAR Istituto di Scienze Marine – Sede di Venezia, Castello 1364/A, I-30122

Riassunto

Nell'ambito delle ricerche volte a valutare il ruolo funzionale dei vari produttori primari nella Laguna di Venezia (Programma di Ricerca CORILA 2004-2006, Linea 3.12), è stata analizzata, su base stagionale, la composizione dimensionale della comunità fitoplanctonica. Particolare attenzione è stata rivolta alle variazioni spaziali e temporali della frazione picoplanctonica (0,2 – 2 μm) e del suo contributo alla biomassa fitoplanctonica totale. La frazione picofitoplanctonica è costituita principalmente da cianobatteri del tipo *Synechococcus* e da piccoli eucarioti, le frazioni micro- e nanofitoplanctoniche (> 3 μm) da diatomee e nanoflagellati. I valori medi di abbondanza (15×10^6 cells dm^{-3}) e di biomassa (2,3 $\mu\text{g C dm}^{-3}$) del picoplancton indicano che questa frazione rappresenta una componente significativa e persistente del fitoplancton della laguna di Venezia.

Abstract

In the framework of the researches aimed at evaluating the functional role of the different typologies of primary producers in the Lagoon of Venice (CORILA Research Programme 2004-2006, Line 3.12), the size distribution of the phytoplankton community has been analyzed, on a seasonally base. Emphasis has been paid on the spatial and temporal variations of autotrophic picoplankton (0.2 – 2 μm) and on its contribution to total phytoplankton biomass. Autotrophic picoplankton was mainly made up by cyanobacteria of the *Synechococcus* type and by small eucariotes, the larger fraction (> 3 μm) by diatoms and nanoflagellates. Picoplankton abundance (average: 15×10^6 cells dm^{-3}) and biomass (average: 2.3 $\mu\text{g C dm}^{-3}$) indicate that this fraction represents a significant and persistent component of the phytoplankton in the Lagoon of Venice.

1 Introduction

The size distribution within the phytoplankton community plays an essential role in determining the direction and the amount of carbon and energy fluxes in aquatic ecosystems (Bell and Kalff, 2001). In estuarine and coastal waters of the temperate zone, the marked seasonal changes in light, temperature and nutrient inputs may lead to the coexistence and, sometimes, to the seasonal alternation of smaller and larger algae and, therefore, of the structure (grazing vs. microbial) of the plankton community (Riegman *et al.*, 1993). Moreover,

there is a growing evidence of the importance of the ecological role of autotrophic picoplankton in estuarine and coastal ecosystems, (Iriarte and Purdie, 1994; Vaquer *et al.* 1996; Pinckney *et al.*, 1998; Phlips *et al.*, 1999; Murrel and Lores, 2004).

In the Lagoon of Venice the larger fraction of the phytoplankton community ($> 3 \mu\text{m}$) has been extensively studied in the last 30 years (Acri *et al.*, 2004), as it regards the taxonomic composition (Socal *et al.*, 1985; 1987, Tolomio *et al.*, 1999; Facca *et al.*, 2002) and the temporal pattern of abundance and biomass (Bianchi *et al.*, 1999; Boldrin *et al.*, 1987; Socal *et al.*, 1999; Bianchi *et al.*, 2000). The seasonal cycle of the phytoplankton has been described in the southern (Tolomio and Bullo, 2001), central (Socal *et al.*, 1999; Facca *et al.*, 2002) and northern basins (Voltolina, 1973; Bianchi *et al.*, 1999). The community is mainly made up by diatoms and nanoflagellates (chlorophyceae, cryptophyceae, prasinophyceae, crysophyceans, prymnesiophyceans) and it is characterized by the coexistence of pelagic and benthic forms. On the contrary, only few studies on the size distribution of the primary producers in Venice Lagoon have been carried out (Sorokin *et al.* 1996; Sorokin *et al.* 2002) and they highlight the relatively high contribution and the importance of the smallest size fraction (pico- and nano-phytoplankton) to the phytoplankton biomass.

The present work is part of a more extensive study on the ecological role of the different primary producers and on the carbon production and fate in the Lagoon of Venice.

In the present paper data on the contribution of autotrophic picoplankton to total phytoplankton biomass and abundance in the Lagoon of Venice, at the seasonal scale, are reported and discussed. The understanding of the interactions between environmental factors and the phytoplankton size structure, and of its temporal and spatial variations, is expected to give useful indications of the prevailing pathways of carbon transfer in the area.

2 Methods

The investigation was carried out at five sampling stations, located in the northern and central basins of the Lagoon of Venice (Fig. 1) and representative of the main characteristics of these areas (Bianchi *et al.*, 1996; 1999; Socal *et al.*, 1999).

At every station, measurements and samplings were carried out seasonally on October 2004, January, April, July and October 2005. Water and phytoplankton samples were taken at surface, using 5 dm³ Niskin bottles, at neap tide.

Trasparency was measured by Secchi disk. Temperature, salinity, dissolved oxygen and pH were recorded by an Idronaut Ocean Seven 316 multiprobe and compared with the discrete measurements performed in the laboratory (Guildline Autosal 8400 B salinometer, Dosimat for Winkler titrations and pH meter). Nutrients (N-NH₃, N-NO₂, N-NO₃, Si-SiO₄, P-PO₄) were analysed according to Grasshof *et al.*, (1983).

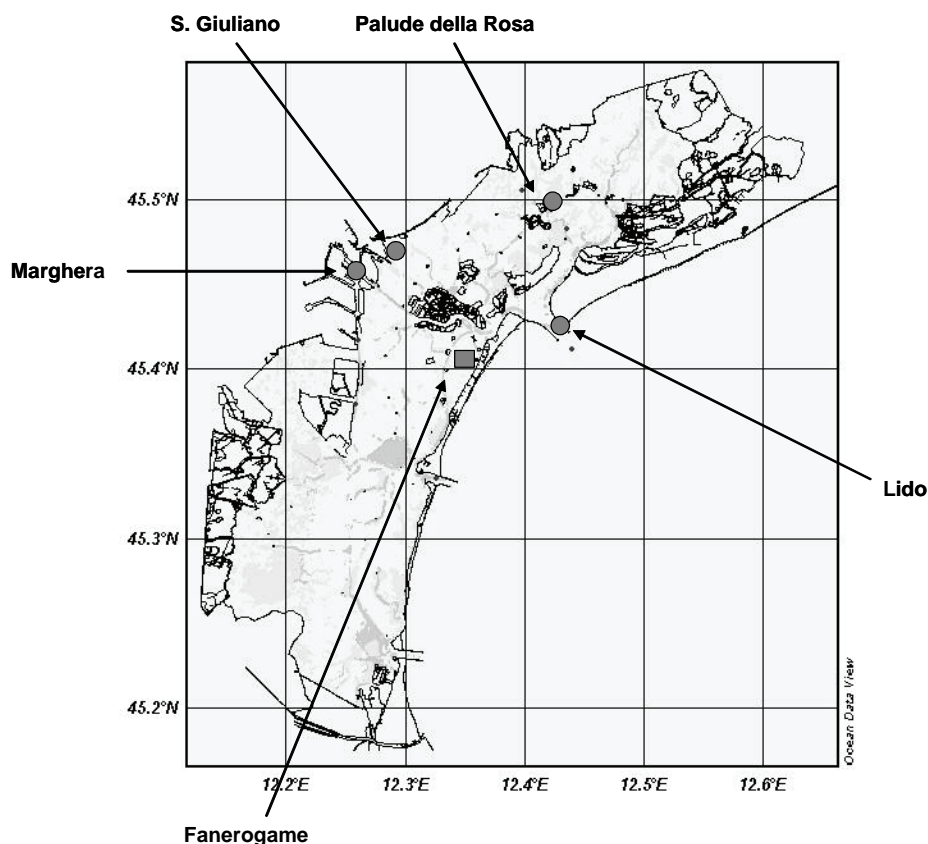


Fig. 1 – The lagoon of Venice. Location of the sampling stations

In order to estimate the autotrophic picoplankton ($0.2 - 2 \mu\text{m}$: APP) abundance, water samples were preserved with pre-filtered buffered formaldehyde and kept at 4°C . Duplicate slides were prepared from the samples by filtering 5-10 ml of water from each sample onto $0.2 \mu\text{m}$ pore size Nucleopore black membranes. The cell counts were made using a Zeiss Axiovert 35 microscope, equipped with a HBO 50 W light. A BP 450-490 exciter filter, an FT 510 chromatic beam splitter and an LP 520 barrier filter were used. At least 20 randomly selected fields, for each slide, were counted at a final X 1000 magnification. On average, about 400 cells were counted to determine abundance. Cell sizes of about 1700 randomly selected individuals were measured by Image analysis, using Image Pro Express (Media Cybernetics). Most APP cells were coccoid or rod-shaped, therefore, in order to determine their carbon biomass, cell volume was calculated by approximation to a sphere or to a rotation cylinder. For *Synechococcus*, dominant in this study, there are a number of published factors to convert biomass to carbon, ranging from 85 to $400 \text{ fg C } \mu\text{m}^{-3}$, and the actual values are supposed to be even higher (Li, 1986). We followed the indications by Tamigneaux *et al.*, (1995) for coastal area and for cells of the same size of ours. The coefficients here applied were, therefore: $0.250 \text{ fg } \mu\text{m}^{-3}$, for *Synechococcus*, and $220 \text{ fg } \mu\text{m}^{-3}$, for eukariotes.

The samples of the Utermöhl fraction of the phytoplankton community ($> 3 \mu\text{m}$ UFP) were fixed with exametilentetramine-neutralized formaldehyde to a final concentration of 4% and examined with an inverted microscope Zeiss Axiovert

35, equipped with phase contrast (model Zeiss Axiovert 35), at a final X 400 magnification. Sub-samples from 5 to 50 ml were allowed to settle for 12-48 hours and examined (Utermöhl, 1958). A variable transect number was observed until at least 200 (but often more than 500) cells were counted for each sample (Zingone et al., 1990). Species composition was defined according to Tomas (1997). The cells belonging to cryptophyceans, crysophyceans, prymnesiophyceans (except coccolithophorids), prasinophyceans and chlorophyceans, whose sizes vary between 3 and 4 μm and remained undetermined, were all included in the group "nanoflagellates". Cell size and volume of UFP were determined according to Strathmann (1967) and the phytoplankton carbon was obtained by multiplying cell or plasma volume by 0.11 for diatoms, coccolithophorids and nanoflagellates and by 0.13 for thecate dinoflagellates (Smetacek, 1975).

3 Results

At every station the abundance of UFP was lowest in January (minimum: 0.23×10^6 cells dm^{-3} , St. Lido) and highest in July (maximum: 16×10^6 cells dm^{-3} , St. Marghera). The UFP biomass varied between $3 \mu\text{g C dm}^{-3}$ and $348 \mu\text{g C dm}^{-3}$. Diatoms and nanoflagellates dominated as abundance (65% and 32% respectively), diatoms and dinoflagellates as biomass (mean contribution: 77% and 14%, respectively).

APP was dominated by cyanobacteria of the *Synechococcus* type (93% of total abundance and 88% of total biomass) and by picoeukaryotic cells. The size range of *Synechochooccus* and picoeukariotes was 0.8 -1.3 μm (mean: 1.0 μm) and 0.9 – 2.0 μm (mean: 1.2 μm), respectively.

APP abundance ranged from 2.1×10^6 cells dm^{-3} (January 2005, St. San Giuliano) to 71×10^6 cells dm^{-3} (October 2004, St. Lido). The contribution of APP to total phytoplankton abundance ranged from 47% (October 2005, St. San Giuliano) to 99% (October 2004, St. Lido). The seasonal variation of APP biomass was characterized by lowest values in winter (minimum: $0.3 \mu\text{g C dm}^{-3}$, January, St. San Giuliano) and summer peaks (maximum: $9.5 \mu\text{g C dm}^{-3}$, July, St. Lido). The APP biomass contribution to total phytoplankton biomass reached the highest value in October 2004 (St. Lido, 51%). The mean contribution of picoeukariotes to total APP biomass showed the highest value in April (21%) and the lowest in October (10%).

Considering the whole data set, the mean biomass contribution of the different fractions (pico-, nano- and microphytoplankton) to total phytoplankton biomass was 5%, 63% and 32% respectively. Nanophytoplankton dominate in October 2004 and in July 2005; microphytoplankton attained the highest values in January and in April 2005; picophytoplankton showed a relatively high contribution in October 2004 and in January and October 2005 (Fig. 2)

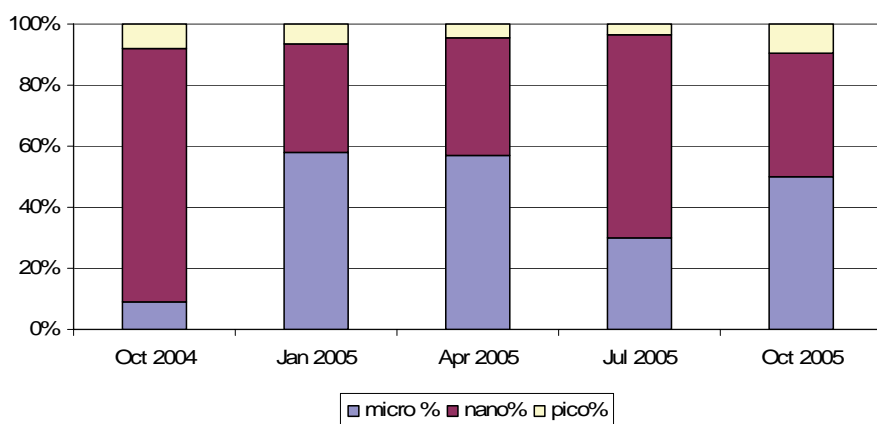


Fig. 2 – Seasonal contribution of different fractions to total phytoplankton biomass (micro = microphytoplankton; nano = nanophytoplankton; pico = picophytoplankton).

The five stations showed substantial hydrological differences (Bianchi et al., 1996; 1999; Tab. 1) mainly determined by the geographical position and trophic level.

	San Giuliano		Marghera		Lido		Palude		Fanerogame	
	Avg.	Std. Dev.	Avg.	Std. Dev.	Avg.	Std. Dev.	Avg.	Std. Dev.	Avg.	Std. Dev.
Depth	2		12		8		3		1	
Transp. (m)	0,6	0,2	1,6	0,3	2,7	1,1	1,0	0,2	1,1	0,2
Temp.(°C)	17,0	7,9	18,6	7,3	17,1	6,7	16,5	8,0	16,1	8,3
Sal.	24,1	5,7	30,3	2,5	33,4	2,2	28,7	5,4	33,5	3,8
Turb. (a.u.)	11,9	6,5	2,3	0,6	2,2	0,9	4,6	1,3	3,5	1,2
DIN (µM)	66,8	44,7	46,6	27,2	22,5	13,0	49,5	47,1	19,9	20,9
SiO ₄ (µM)	50,5	24,9	21,2	11,9	16,9	15,0	32,0	23,7	11,1	11,2
PO ₄ (µM)	1,0	0,3	1,0	0,7	0,1	0,1	0,5	0,3	0,2	0,2

Tab. 1 – Averages and standard deviations of hydrochemical data in the five stations

Quite different qualitative characteristics of the phytoplankton community could be evidenced (Fig. 3).

At St. San Giuliano the mean phytoplankton biomass was 60 µg C dm⁻³. On the average, microphytoplankton prevailed (62%), with the diatom *Cylindrotheca closterium*. Nanoplankton mean contribution was 35 % and this fraction was mainly represented by the diatoms *Skeletonema costatum* and *Thalassiosira* spp., as well as by Cryptophyceans and flagellates. The mean APP contribution was only 3% (83% cyanobacteria, 17% picoeukaryotes).

The average phytoplankton biomass at St. Palude della Rosa was much lower (15 µg C dm⁻³) and it was dominated by microphytoplankton (60%), with the diatoms *Navicula* spp. and *Cylindrotheca closterium*. Nanophytoplankton made up the 27%, with the diatoms *Amphora* spp and *Nitzschia frustulum* and

flagellates. APP contribution was considerable (13%): and cyanobacteria were clearly dominant (84%) over picoeucaryotes.

The highest mean phytoplankton biomass ($113 \mu\text{g C dm}^{-3}$) was recorded at St. Marghera. Nanophytoplankton clearly prevailed (88%) with the diatom *Skeletonema costatum* and flagellates. Microphytoplankton made up the 11% of total biomass (mostly *Gymnodinium* spp. and *Euglenophyceae* spp.). Mean APP contribution was very low (2%: 80% cyanobacteria and 20% picoeucaryotes).

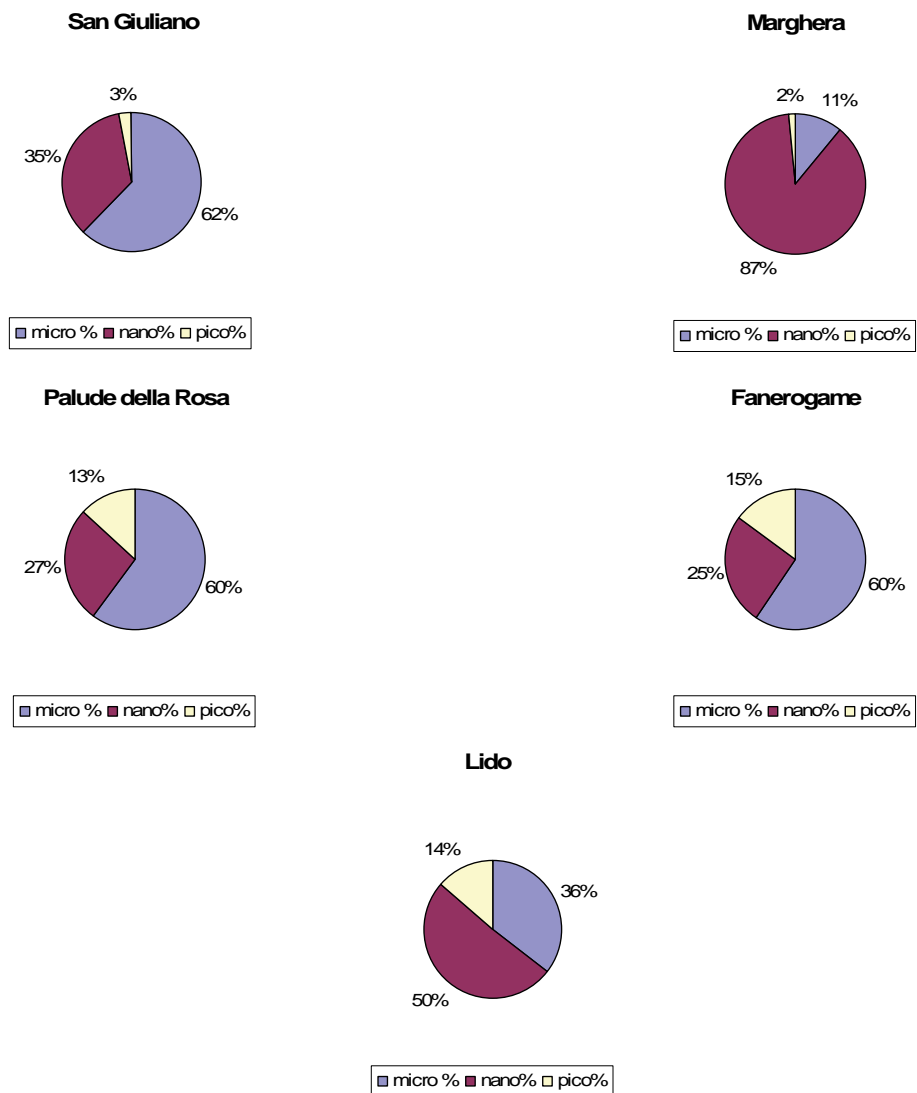


Fig. 3 – Contribution of different fractions to total phytoplankton biomass (micro = microphytoplankton; nano = nanophytoplankton; pico = picophytoplankton) at the five stations.

At St. Fanerogame, where a community of the sea grass *Nanozoostera noltii* developed, the lowest mean phytoplankton biomass was measured ($11 \mu\text{g C dm}^{-3}$). Phytoplankton was composed mostly by microphytoplankton (59%) with the diatoms *Navicula* spp., *Cylindrotheca closterium* and *Cocconeis scutellum*. Nanophytoplankton (25 %) was represented by the diatoms *Amphora* spp. and *Nitzschia frustulum* and by flagellates. Picophytoplankton contribution was considerable (15%) and was mainly due to cyanobacteria (91%).

The mean phytoplankton biomass at St. Lido was $41 \mu\text{g C dm}^{-3}$. Nanophytoplankton (*Navicula cryptocephala*, *Emiliana huxleyi* and flagellates) and microphytoplankton (*Cerataulina pelagica*, *Pseudonitzschia* spp. and *Prorocentrum minimum*) were the two dominant fractions (51 % and 36 %, respectively). Average APP contribution attained the 14 % (92 % cyanobacteria, 8 % picoeucaryotes).

4 Concluding remarks

The main aim of this study was to give a contribution to the evaluation of the importance of APP in Lagoon of Venice, where the information about this phytoplankton size class is scarce.

The APP appeared dominated by cyanobacteria of the *Synechococcus* type. The mean APP abundance and biomass at the five stations (17×10^6 cells dm^{-3} and $2.5 \mu\text{g C dm}^{-3}$) and the mean contribution to total phytoplankton biomass (5%) were lower than those reported for the central and northern basin of the Lagoon of Venice during the nineties, by Sorokin *et al.* (1996, 2002). These Authors reported, indeed, a phytoplankton biomass range between 15 and $342 \mu\text{g C dm}^{-3}$ and a picophytoplankton biomass contribution between 12% and 40%. These significant differences between past and present data are probably due to trophic changes that occurred in the Lagoon during the nineties (Facca *et al.*, 2002, and citation therein). Starting from the late nineties, a phytoplankton decrease was recorded, especially in the shallow waters of central lagoon, and it was mainly related to the increased sediment resuspension determined by bivalve catching and by macroalgae disappearance.

The spatial distribution observed in the present study indicated an increase of picophytoplankton biomass from the inner areas of the lagoon (St. San Giuliano and Marghera) to the outer ones (St. Fanerogame and Lido). The average APP contribution to total phytoplankton biomass at the stations Fanerogame and Lido was considerable and it was comparable to those reported for two offshore NW Adriatic stations by Bernardi Aubry *et al.*, (2006). Microphytoplankton and nanoplankton clearly dominate at the stations characterized by the highest total phytoplankton biomass (St. Marghera and St. San Giuliano).

At every station the seasonal variation of total phytoplankton biomass were prevalently driven by the UFP fraction. However, the APP importance was generally considerable and this fraction represented a persistent component of the phytoplankton in the Lagoon of Venice.

In estuarine and coastal waters of the temperate zone a seasonal alternation of smaller and larger algae is often reported (Riegman *et al.*, 1993). In the Lagoon of Venice a similar evidence is lacking. On the contrary, the ecosystem variability seems to lead to the coexistence of the different phytoplankton size classes and, therefore, of the structure (grazing vs. microbial) of the plankton community.

References

- Acri F., Bernardi Aubry F., Berton A., Boldrin A., Camatti E., Comaschi A., Rabitti S., Socal G., 2004. Plankton communities and nutrients in the Venice Lagoon. Comparison between current and old data. *Journal of Marine Systems*, 51: 321-329
- Bell T., Kalff J., 2001. The contribution of picophytoplankton in marine and freshwater systems of different trophic status and depth. - *Limnol Oceanogr.* 46 (5): 1243-1248.
- Bernardi Aubry F. Acri F., Bastianini M., Bianchi F., Cassin D., Pugnetti A, Socal G., 2006. Seasonal and inter annual variations of phytoplankton in the gulf of Venice (Northern Adriatic Sea). *Chemistry and Ecology*. In press.
- Bianchi, F. Socal, G. Alberighi, L. and Cioce, F. 1996. Cicli nictemerali dell'ossigeno disciolto nel bacino centrale della laguna di Venezia. *Biol. Mar. Medit.*, 3 (1), 628-630.
- Bianchi, F., Comaschi A. and Socal G. 1999. Ciclo annuale dei nutrienti, del materiale sospeso e del plancton nella laguna di Venezia. In: *Aspetti Ecologici e Naturalistici dei sistemi Lagunari e Costieri*, Arsenale Editrice, Venezia, 231-240.
- Bianchi, F. Acri, F. Alberighi, L. Bastianini, M. Boldrin, A. Cavalloni, B. Cioce, F. Comaschi, A. Rabitti, S. Socal, G. and Turchetto, M. 2000. Biological variability in the Venice lagoon. In: *Lasserre, P. and Marzollo, A. (Eds) The Venice Lagoon Ecosystem. Inputs and interactions between land and sea. Man and the biosphere series volume 25.* UNESCO and Parthenon Publishing Group. 97-125
- Boldrin, A., Rabitti S., Bianchi F., Cioce F. 1987. Dinamica della sostanza sospesa nella laguna di Venezia. *Bacino Settentrionale. Atti VII Congr. AIOL*, 165-174.
- Facca, C. Sfriso, A. and Socal, G. 2002. Phytoplankton changes and relationships with microphytobenthos and physico-chemical variables in the central part of the Venice lagoon. *Estuarine Coastal Shelf Science* 54, 5, 773-792.
- Grasshoff, K., Erhardt, M. and Kremling, K. 1983. *Methods of Seawater Analysis*, Chemie-Verlag, Weinheim.
- Iriarte A., Purdie D. A., 1994. Size distribution of chlorophyll a biomass and primary production in a temperate estuary (Southampton Water): the contribution of photosynthetic phytoplankton. – *Mar. Ecol. Progr. Ser.*, 115: 283-297.
- Li- W. K. 1986. Experimental approaches to field measurements: methods and interpretation. In: *Platt T., Li W. K. (eds) Photosynthetic picoplankton.* *Can J. Fish. Aquatic Sci.*, Department of Fisheries and Oceans, Ottawa, p 251-286.

- Murrell M.C., Lores E.M., 2004. Phytoplankton and zooplankton seasonal dynamics in a subtropical estuary: importance of cyanobacteria. - *J. Plankton Res.*, 26 (3): 371-382.
- Phlips E.J., Badylak S., Linch T.C., 1999. Blooms of picoplanktonic cyanobacterium *Synechococcus* in Florida Bay, a subtropical inner-shelf lagoon. - *Limnol. Oceanogr.*, 44 (4): 1166-1175.
- Pinckey J.L., Pearl H.W., Harrington M.B., Howe K. E., 1998. Annual cycles of phytoplankton community-structure and bloom dynamics in the Neuse River Estuary, North Carolina. - *Mar. Biol.*, 131: 371-381.
- Riegman R., Kuipers B. R., Noordeloos A.A.M., Witte H.J., 1993. Size-differential control of phytoplankton and the structure of plankton communities. - *Neth. J. Sea Res.*, 31 (3): 255-265.
- Smetacek, V., 1975: Die Sukzession sed Phytoplankton der westlichen Kieler Bucht. - PhD Thesis, Univ. Kiel.
- Socal, G. Ghetti, L. Boldrin, A. and Bianchi. F. 1985. Ciclo annuale e diversità del fitoplancton nel porto canale di Malamocco. Laguna di Venezia. *Atti Ist. veneto Sci. Lett. Arti.* 143, 15-30
- Socal, G., Bianchi, F., Comaschi, A. and Cioce, F., 1987. Spatial distribution of plankton communities along a salinity gradient in the Venice lagoon. *Archo Oceanogr. Limnol.* 21, 19-43.
- Socal, G., Bianchi, F. and Alberighi, L., 1999. Effect of thermal pollution and nutrient discharges on a spring phytoplankton bloom in the industrial area of the lagoon of Venice. *Vie et milieu* 49, 19-31.
- Sorokin Yu. I., Sorokin P.Yu., Giovanardi O. and Dalla Venezia L., 1996. Study of the ecosystem of the lagoon of Venice with emphasis on anthropogenic impact. *Marine Ecology Progress Series*, 141, 247-261.
- Sorokin P. Yu., Sorokin Yu. I., Zakuskina O. Yu. and Ravagnan G.-P., 2002. On the changing ecology of Venice lagoon. *Hydrobiologia*, 487, 1-18.
- Stratmann, R.R., 1967: Estimating the organic carbon content of phytoplankton from cell volume or plasma volume. - *Limnol. Oceanogr.*, 12: 411-418.
- Tamigeaux E., Vasquez E., Mingelbier M., Klein B., Legendre L., 1995. Environmental control of phytoplankton assemblages in nearshore waters, with special emphasis on phototrophic ultraplankton. *J. Plankton Res.* 17: 1421-1447
- Tolomio, C., Moschin, E., Moro, I. and Andreoli, C., 1999. Phytoplankton de la Lagune de Venise. I. Bassins nord et sud (avril 1988-mars 1989). *Vie et Milieu* 49, 33-44.
- Tolomio, C., Bullo, L., 2001. Prelevi giornalieri di fitoplancton in una stazione del bacino meridionale della laguna di Venezia; aprile 1993 - marzo 1994. *Boll. Museo Civ. St. nat. Venezia*, 52, 3-23.
- Tomas, C. R., 1997. *Identifying Marine Phytoplankton*. Academic Press, Arcourt Brace & Company.

Utermöhl, H., 1958: Zur Vervollkomnung der quantitativen Phytoplankten-Methodik. - *Mitt. Int. Ver. Limnol.*, 9:1-38.

Vaquier A., Troussellier M., Courties C., Bibent B., 1996: Standing stock and dynamics of picophytoplankton in the Thau Lagoon (northwest Mediterranean coast). - *Limnol. Oceanogr.*, 41 (8): 1821-1828.

Voltolina, D., 1973. A phytoplankton bloom in the lagoon of Venice. *Archo Oceanogr. Limnol.* 18, 19-37.

Zingone, A., G. Honsell, D. Marino, M. Montresor and G. Socal, 1990. Fitoplancton . - In: Innamorati M., Ferrari I., Marino D., Ribera D'Alcalà M., (Eds.) *Metodi nell'ecologia del plancton marino*. Nova Thalassia, 11: 183-198.

STUDIES ON THE SPATIAL AND TEMPORAL VARIABILITY OF MICROPHYTOBENTHOS IN THE VENICE LAGOON

Chiara Facca^{1,2}, Adriano Sfriso¹, Alessandra Pugnetti²

¹ Dipartimento di Scienze Ambientali, Università di Venezia, ² Istituto di Scienze Marine, CNR, Venezia

Riassunto

Nell'ambito delle ricerche sulla funzionalità delle comunità biologiche autotrofe nella laguna di Venezia (Programma di Ricerca CORILA 2004-2006, Linea 3.12) è stato studiato il contributo, in termini di abbondanza e produzione primaria, delle popolazioni microalgali che colonizzano i sedimenti superficiali nelle zone a basso fondale. Sono presentati i risultati di cinque campagne stagionali in aree a diverso livello di trofia e i dati relativi a due andamenti annuali in aree popolate da *Nanozostera noltii* (Horneman) Tomlinson et Posluzny. Le fluttuazioni dell'abbondanza delle diatomee non sono state direttamente influenzate dalla temperatura ed erano mediamente comprese tra 0.33 e 4.06×10^6 cells ml⁻¹. Le nanoflagellate hanno contribuito significativamente alla comunità microbentonica raggiungendo valori pari a ca. 2×10^6 cells ml⁻¹. La produzione primaria totale della comunità microbentonica, in condizioni di luce simili a quelle del fondo, è stata minima ($0.01 - 0.5 \mu\text{g C cm}^{-2} \text{ sed h}^{-1}$) a gennaio in tutte le stazioni, e massima (ca. $31.1 \mu\text{g C cm}^{-2} \text{ sed h}^{-1}$) a luglio nella Palude della Rosa.

Abstract

In the framework of a research aiming at evaluating the autotrophic community dynamics in the Venice lagoon (CORILA Research Programme 2004-2006, Line 3.12), the cell abundance and the primary production of benthic microalgae were investigated. The results obtained in five seasonal campaigns at three sampling sites, with different hydrological and trophic characteristics, and the annual trends recorded in 2 sites characterized by *Nanozostera noltii* (Horneman) Tomlinson et Posluzny coverage are presented. The diatom abundance, ranging between 0.33 and 4.06×10^6 cells ml⁻¹, was not correlated with temperature variations. The nanoflagellates, in some cases, contributed significantly to the benthic community composition, reaching up to ca. 2×10^6 cells ml⁻¹. The total community production was negligible in January ($0.01 - 0.5 \mu\text{g C cm}^{-2} \text{ sed h}^{-1}$) at each station, whereas the highest value (ca. $31.1 \mu\text{g C cm}^{-2} \text{ sed h}^{-1}$) was recorded in July in the Palude della Rosa.

1 Introduction

The importance of the benthic microalgae as primary producers in shallow ecosystems is well known and documented [MacIntyre et al., 1996]. In particular, the role of microphytobenthos can be considerable in coastal areas where macrophyte biomass is not significant. Moreover, the microphytobenthic community can be more productive than the phytoplankton one, when light irradiance is not limiting [Barranguet, 1997].

The information about the microphytobenthos in the Lagoon of Venice refers mainly to studies carried out in the central part of the Lagoon [Facca et al., 2002]: benthic microalgae distribution and variation appeared mainly determined by local sediment features that mask any seasonal pattern.

The present work is a part of a wider research, carried out in the framework of the CORILA Project 2004-2006 (Research Line 3.12), which aims at evaluating the functional importance and the role of the different primary producers in the Lagoon of Venice.

In this paper we present the data concerning the taxonomic composition and abundance of the microphytobenthos in areas of the lagoon with different hydrological and trophic characteristics and covered by different seagrass meadows. Moreover, the results of the microphytobenthos photosynthetic carbon fixation (primary production) are reported.

2 Materials and methods

The sediment samples were collected in always-submerged areas by means of a box corer. Particular attention was paid to maintain the integrity of the surface layer (1 cm). At the sites characterized by seagrasses, Lido (St. 4) and Petta di Bò (St. 5), the benthic diatom abundance and the taxonomic composition were studied monthly, from January to December 2005. At San Giuliano (St. 1), Marghera (St. 2) and Palude della Rosa (St. 3) five seasonal campaigns were carried out in order to determine the whole microphytobenthic community abundance and composition and to measure the primary production (Fig. 1). Moreover, on October 2005, at those three stations, small-scale spatial variations of benthic diatom abundance and composition were investigated by collecting sediment cores at ca. 50 cm, 100 cm, 150 cm and 200 cm far from the usual sampling site. Such samples were collected to verify the local microphytobenthos spatial distribution. The data highlighted that if the cores are collected within an area of 4-5 meters the results are not significantly affected.

A known sediment volume (in general <1 ml wet sediment) were diluted in filtered seawater, preserved with formalin and analyzed at the inverted light microscope [Totti et al., 2003]. Photosynthetic C organization (^{14}C method, Steeman-Nielsen [1952]) was measured, after resuspension of the sediments into 250 ml of filtered seawater, which simulated *in situ* conditions. The samples were incubated for 2 hours around noon, at natural sunlight and at *in situ* temperature. Light was attenuated up to the *in situ* values by means of neutral optical filters. The samples (250 ml Pyrex bottles) were inoculated with 148 kBq

$\text{NaH}^{14}\text{CO}_3$. In order to avoid any possible artifacts due to filtration, primary production was measured after acidification and stirring of duplicated 5 ml sub samples.

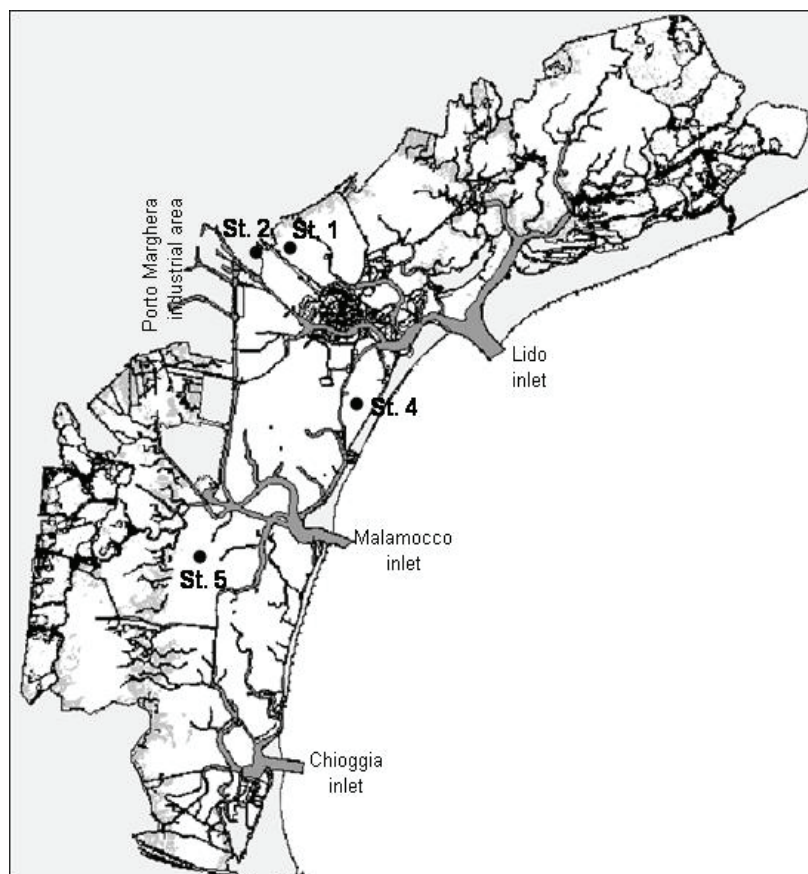


Fig. 1 – Map of the sampling sites

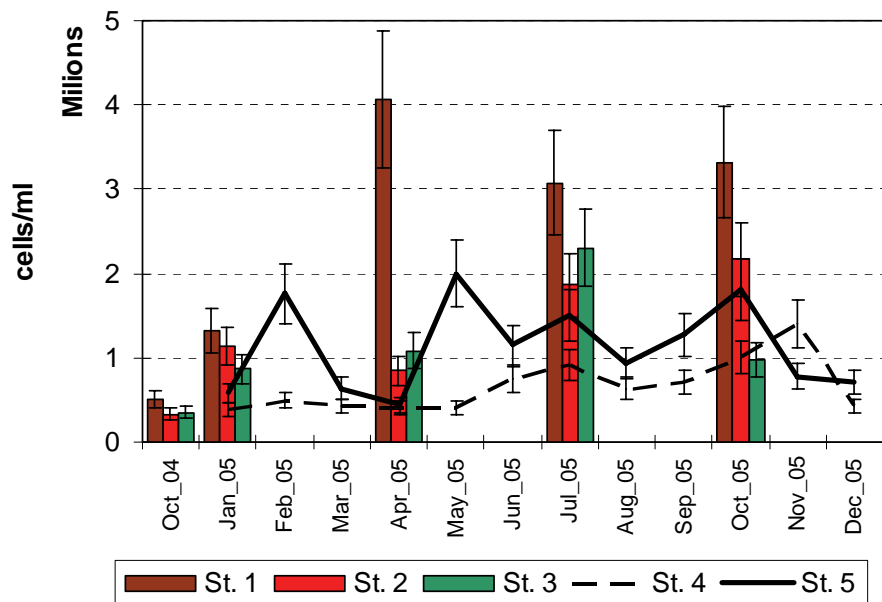
3 Results

On the whole 62 diatom taxa were identified. The highest number of species were pennate, while, among the centric taxa, only *Thalassiosira* sp. was significant.

At the *Nanozostera* sites a lot of epiphytic cells was recorded. Moreover, at St. 5, where the seagrasses coverage was high, the epiphytic cell abundance was always higher than at St. 4.

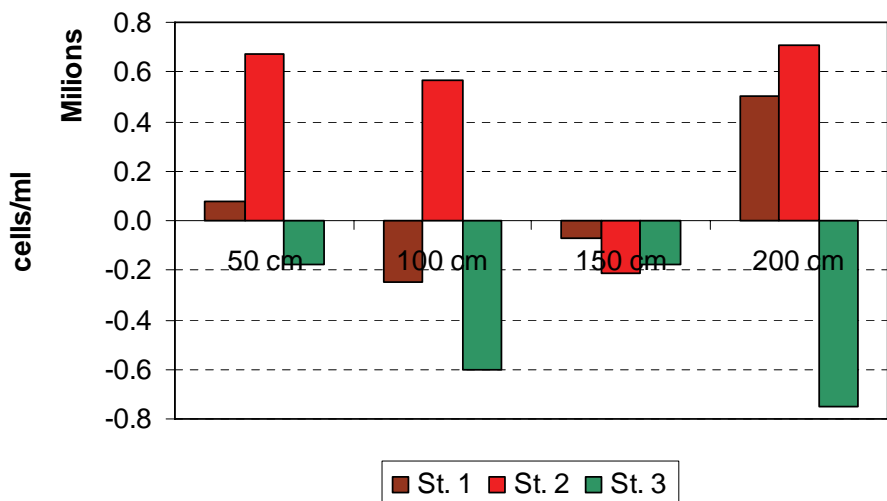
At Sts. 1, 2 and 3 nanoflagellates (cell-size < 5 μm), varied between 0.7 and 2 x 10⁶ cells ml⁻¹. They reached ca. 67% of the total microphytobenthic community, at St. 3 on October 2005. The highest diatom abundance was recorded at St. 1 on April 2005 (4 x 10⁶ cells ml⁻¹), while the lowest value occurred at St. 2 on October 2004 (ca. 0.33 x 10⁶ cells ml⁻¹). Despite of this variability, a clear seasonal trend could not be evidenced (Fig. 2).

Fig. 2 – Benthic diatom abundance. The columns represent the seasonal campaigns and the lines the monthly trends at the seagrass sites. Bars indicate the standard deviation.



The small-scale distribution of the benthic diatoms at each station was rather homogenous and the cell variation was lower than 20% (Fig. 3).

Fig. 3 – Spatial benthic diatom small-scale changes. X-axis represents the cell abundance of the usual sampling site at each station and histograms the spatial variations.



The highest primary production was recorded at Sts 1, 2 and 3 on July and at St. 4 on April; the lowest values were observed at each station on January (Tab. 1). The stations characterized by the highest mean and maximum production were Sts. 3 and 4, where the highest underwater irradiance was also measured (Tab. 2).

$\mu\text{g C cm}^{-2} \text{ sed h}^{-1}$	St. 1	St. 2	St. 3	St. 4
Oct 2004	1.9	2.2	1.8	-
Jan 2005	0.01	0.3	0.01	0.5
Apr 2005	1.0	1.1	1.9	16.1
Jul 2005	15.7	7.3	31.1	6.5
Oct 2005	2.4	1.7	4.7	8.2

Tab. 1 – Microphytobenthos primary production. Samples were incubated at a light intensity similar to that found at the bottom level of the sampling sites

%PAR	St. 1	St. 2	St. 3	St. 4
Oct 2004	1	1	20	-
Jan 2005	2	3	5	95
Apr 2005	8	2	17	45
Jul 2005	2	1	20	57
Oct 2005	1	1	26	24

Tab. 2 – Percent of PAR radiation at the bottom of sampling sites in comparison with the incident radiation recorded in air.

Concluding remarks

Microphytobenthos exhibited a quite low cell abundance, characterised by irregular changes, both on annual and on seasonal scale. The significant changes were only recorded from October 2004 to April 2005, when the cell abundance increased markedly. That observation confirms that the benthic microalgae distribution is mainly influenced by the local sediment features rather than seasonal temperature changes as it was previously observed by Facca et al. [2002] and Guarini et al., [2004 and references therein].

The main environmental factor influencing the microphytobenthos photosynthetic activity was the light availability. In particular, the peak values were recorded in the stations where the underwater light transmission, throughout the year, was the highest. The highest production found in the Venice areas ranged between 0.01 and 31.1 $\mu\text{g C cm}^{-2} \text{ sed h}^{-1}$, in agreement with Spilmont et al. [2006] who estimated values from 0 to 122 $\mu\text{g C cm}^{-2} \text{ h}^{-1}$, depending on seasonal variations and sediment features.

The main effect of the seagrass coverage was the enrichment of the microphytobenthos community, by reducing sediment re-suspension and favouring the cell settlement. Within seagrass beds, the sediment biodiversity increased also as a consequence of production of several epiphytic taxa.

References

- Barranguet C., 1997. The role of the microphytobenthic primary production in a Mediterranean mussel culture area. *Estuarine Coastal and Shelf Science*, 44, 753-765.
- Facca C., Sfriso A. and Socal G., 2002. Temporal and spatial distribution of

diatoms in the surface sediment of the Venice lagoon. *Botanica Marina*, 45,170-183.

Guarini J.M., Gros P., Blanchard G., Richard P. and Fillon A., 2004. Benthic contribution to pelagic microalgal communities in two semi-enclosed, European-type littoral ecosystems (Marennes-Oléron Bay and Aiguillon Bay, France). *Journal of Sea Research*, 52, 241– 258.

MacIntyre H.L., Geider R.J. and Miller D.C., 1996. Microphytobenthos: the ecological role of the “Secret Garden” of unvegetated, shallow-water marine habitats. I. Distribution, abundance and primary production. *Estuaries*, 19, 186-201.

Spilmont N., Davoult D. and Migné A., 2006. Benthic primary production during emersion: in situ measurements and potential primary production in the Seine Estuary (English Channel, France). *Marine Pollution Bulletin*, 53, 49-55.

Steeman-Nielsen E., 1952. The use of radioactive carbon (^{14}C) for measuring organic production in the sea. *J. Cons. Explor. Mer.*, 18, 117-140.

Totti C., De Stefano M., Facca C. and Ghirardelli L.A., 2003. Il microfitobenthos. In: Gambi M.C., Dappiano M. (eds) *Manuale di metodologie di prelievo e studio del benthos mediterraneo*. *Biologia Marina Mediterranea*, 10, 263-284.

RAPID ASSESSMENT INDEX TO ASSESS THE ECOLOGICAL STATUS OF TRANSITIONAL ENVIRONMENTS: THE LAGOON OF VENICE AS STUDY CASE

Adriano Sfriso, Chiara Facca, Marta Tibaldo

*Dipartimento di Scienze Ambientali, Università di Venezia, Calle Larga, Santa Marta
2137, 30123 Venezia*

Riassunto

La Direttiva Europea Quadro sulle Acque (2000/60/EC), entrata in vigore in Dicembre 2000, ha invitato la comunità scientifica internazionale ad avviare studi per la classificazione degli "Ambienti Costieri" in 5 categorie di "Stato Ecologico" indicate come: Pessima, Scadente, Sufficiente, Buona ed Elevata, basandosi soprattutto sulle comunità bentoniche e sulle associazioni vegetali che colonizzano questi ambienti. A questo scopo sono stati effettuati numerosi studi sia internazionali che nazionali e sono stati proposti numerosi indici più o meno complessi. Il nostro gruppo, sulla base dello studio annuale di ca. 19 stazioni localizzate nella laguna di Venezia, e di altre 13 stazioni visitate ripetutamente nella stagione estiva nella Sacca di Goro, nella laguna di Lesina e nella laguna di Orbetello propone di valutare la qualità di questi ambienti mediante l'utilizzo di un indice di qualità rapido basato principalmente sulla composizione e struttura delle associazioni di macroalghe e fanerogame marine. L'indice è la semplificazione di due indici più complessi (Rapporto R/C tra il numero di Rhodophyceae e Chlorophyceae e Punteggio Macroalgale Medio) basati sullo studio della composizione tassonomica e sulla valenza ecologica delle macroalghe presenti nei vari siti. L'indice rapido consiste in una chiave dicotomica, simile a quelle utilizzate per la classificazione tassonomica delle specie biologiche, che ci permette di arrivare rapidamente alla classificazione ecologica delle aree di studio. Le scelte sono facilitate da un manuale, attualmente in preparazione, per il facile riconoscimento delle principali associazioni di macrofite e dei taxa chiave per le varie determinazioni.

Abstract

The entering into force of the European Water Framework Directive 2000/60/EC in December 2000 provided a challenge in the international scientific community in order to promote studies for the transitional environment assessment in five classes of "Ecological Quality Status", namely: Bad, Low, Moderate, Good, High. The Directive suggested also to base the environment classification taking into account the benthic communities and the macrophyte associations which colonise those environments. For that reason several ecological indices of different complexity have been produced by international and national studies. Our research team, on the basis of 19 sites sampled

monthly for one year in the Venice lagoon and of other 13 sites sampled in summer in the lagoons of Goro, Lesina and Orbetello suggests to evaluate the ecological status of the transitional environments by using a rapid quality index based on the composition and structure of the seaweed associations and seagrass beds. That index is a simplification of two more complex indices (Rhodophyceae/Chlorophyceae ratio and Mean Macroalgal Score) based on the taxonomic composition and the ecological value of the seaweeds recorded in the lagoon sampling sites. It consists of a dichotomical key, very similar to the ones used to determine the biological taxa, which allows a rapid assessment of the study areas. The class determination is made easy from a manual, at present in preparation, for the recognition of the main macrophyte associations and some key species.

1 Introduction

Following the Directive requirements and indications, studies for the ecological assessment of transitional environments some Spanish and Greek researchers [Borja et al., 2000, 2003, 2004; Orfanidis et al., 2001, 2003; Panayotidis et al., 2004] proposed to assess the ecological quality status of estuarine environments by studying macrobenthic communities (marine Biotic Index -BI- Borja et al., 2000, 2003, 2004) and macroalgal associations (Ecological Evaluation Index -EEI- Orfanidis et al., 2001, 2003; Panayotidis et al., 2004), because the benthic organisms have a relatively long life-span, are sessile or quite sedentary. Differently to physico-chemical parameters, biological communities, which consist of different species, have a different tolerance to the environmental stress, also of short time, and can change their structure and taxonomic composition according to the environmental conditions.

The results obtained by applying BI and EEI are encouraging, however the sampling procedures and the taxonomic determinations are laborious and expansive, especially for the benthic macrofauna. As far the seaweed composition the taxa considered are very little (i.e. 36 taxa in Orfanidis et al., 2003; 60 taxa in Panayotidis et al., 2004; ca. 65 taxa in Orfanidis et al., 2001) and relative to some small lagoons in the Saronic Gulf, in eastern Macedonia, and in Trace region, located in the Northern Greece. The taxa reported in those papers are mainly species characteristic of "good" and "high" quality environments.

In the same years [Sfriso et al., 2002], and more recently [Sfriso & La Rocca, 2005, Sfriso et al., 2006a, 2006b] suggested the utilization of the "Rhodophyceae/Chlorophyceae ratio index" and the "Mean Macroalgal Score index". The first one is based on a taxonomic ratio. The rational deals with the fact that, in general, Chlorophyceae prevail in eutrophic and polluted environments whereas Rhodophyceae, on the contrary, are dominant in the presence of high environmental conditions. The second index is based on a score (0, 1, 2) assigned to each macroalgal taxon. The value 0 was associated to the macroalgae which prevail in highly polluted or stressed areas but they are everywhere present, a score 2 was associated to the species which colonise mainly the little or no polluted environments but they are missing in the areas of

bad quality, and a score 1 was assigned to the taxa which are quite indifferent to the environmental conditions. The scores of ca. 205 macroalgae living in transitional environments are reported in Sfriso et al. [2006b]. However, at present, the list is comprehensive of ca. 300 taxa. That species sorting was made by taking into account the physico-chemical characteristics (water transparency, salinity, oxygen concentrations, sediment grain-size, etc.), the trophic (nutrient concentrations) and pollution (heavy metals and organic micro-pollutant concentrations) levels of the sampling sites visited in the lagoon of Venice, Orbetello, Lesina and Goro.

However, those indices are quite laborious, time consuming and they need a certain number of taxa. They can be applied only by expertise personnel and, obviously, they are not routinely applicable.

This paper aims at presenting a rapid quality assessment index based on the previous ones, described in Sfriso et al. [2006a, b]. It consists of a dichotomical key which takes into account the main environmental characteristics of the five ecological classes (bad, low, moderate, good, high) proposed by the European normative, according to the different features of the study areas (i. e. areas with high water hydrodynamics and areas confined, areas mesotrophic or hyper-dystrophic, areas low or highly contaminated, areas hyperaline, mesoaline or hypoaline). The index is based on the presence/absence and population structure of some seagrasses and/or macrophytes and the variability of some physico-chemical parameters such as water transparency, salinity and the oxygen saturation.

2 Materials and methods

The rapid quality assessment index was drawn to obtain the immediate classification of the Mediterranean transitional environments without the need of complicate analyses or taxonomic determinations. It is low cost and does not need of expertise personnel. It is based on the observation of the structure and gross composition of macroalgal and seagrass coverage and on the valuation of some parameters such as: salinity, water transparency and the oxygen availability, which can easily attainable in field by portable instruments or by the simple observation of the environment. A manual with the main taxonomic groups, the population structure and some single key species is in preparation.

3 Results and Discussion.

The dichotomical key set up for a rapid quality assessment of transitional environments is reported in Table 1. In soft substrata, the presence/absence of seagrasses allow a rapid distinction between the "bad-low" and the "moderate-good-high" classes. The successive class separation can be obtained by taking into account the different seagrass species, the population structure and the association with some macroalgae. In hard substrates and in the "bad-low" classes of soft substrates the class distinction is based on the presence/absence and the abundance of some seaweeds. For example, the almost complete absence of seaweeds or the presence of some taxa, mainly

Chlorophyceae, but with negligible biomass allow to discriminate the “bad” class from the “low” class, where some species can blooming. In the “moderate” class the number of Rhodophyceae overcomes that of Chlorophyceae. The “good” and “high” classes are discriminated by the presence of abundant populations of some species or by many single species which grow in highly quality environments, which are characterised by low pollutant and nutrient concentrations, high water transparency, good water oxygenation and low environmental (salinity, nutrient concentration) changes.

Tab. 1 – Dichotomical key for a rapid quality assessment of transitional environments

Hard substrata: Absence or presence of some nitrophilic seaweeds, mostly Chlorophyceae.

Soft substrata: Absence of seagrasses.....1

Hard substrata: The number of Rhodophyceae is as high as that of Chlorophyceae.

Soft substrata: Presence of seagrasses.....3

1. Macrophyte are missing or quite missing. Dominance of some species of Chlorophyceae, especially Ulvaceae and Cladophoraceae. Seasonal growth of some Rhodophyceae or Ochrophyceae but with negligible biomass.

Waters very turbid and seasonally changeable but, on average, the Secchi disk is <0.5-0.8 m, due both to phytoplankton blooms or to sediment re-suspension phenomena. Presence of anoxic sediments and persistent water anoxia in spring-summer. High variability of environmental parameters such as water transparency and salinity.

Ecological status: BAD

1. Seasonal growth of some (10-30) seaweeds, but some can bloom.....2

2. Presence of a low seaweed number. Monospecific seaweed bloom can occur, especially Ulvaceae, Cladophoraceae and Gracilariaceae. Waters turbid, seasonally changeable but for long periods <1 m.

Oxygen saturation up to 300-400%, followed by macroalgal collapse and anoxia.

Ecological status: LOW

2. Presence of many seaweeds but, none of these is dominant. Seagrasses begin to be present.....3

3. Soft substrata:

Presence of *Ruppia* spp., *Nanozostera noltii* and/or *Zostera marina* patches.

Hard substrata:

Seaweed biomass composed from many Chlorophyceae and Rhodophyceae, but the number of the latter is as high.

Waters are quite transparent (1-2 m) for most of the year.

Anoxia are lacking but hypoxic conditions can occur.

Ecological status: MODERATE

3. Presence of many species with high quality score. High biomasses of laminar Ulvaceae are missing. The Rhodophyceae number is clearly prevailing on the Chlorophyceae one.

Seagrass beds well organised.....4

4. Soft substrata:

Ruppia spp., *Nanozostera noltii* and/or *Zostera marina* beds are well organised. *Cymodocea nodosa* can be present.

Many seaweeds can be associated to seagrasses populations. These latter can show high Chlorophyceae (i.e. *Chaetomorpha linum*, filamentous Ulvaceae), or more rarely Rhodophyceae (*Gracilaria* spp., *Polysiphonia* spp., etc.), biomasses.

Hard substrata:

Seaweed biomass composed by many species with high environmental score, which are sensible to the environment stress begin to be present. Dominance of some genera such as *Ceramium* spp., *Dicyota* spp. *Sargassum muticum*, etc. Presence of calcified seaweeds.

Transparent waters (2-3 m) for most of the year. Environmental parameters, such as the oxygen saturation and salinity, show only long period or seasonal changes.

Ecological status: GOOD

4. Soft substrata:

Seagrass beds very dense and well organised. *Cymodocea nodosa*, if present, is abundant. *Ruppia* spp. is negligible or missing.

Seaweeds are numerous, especially Rhodophyceae, but each taxon, rarely shows abundant biomasses. Many taxa are epiphytic species.

Hard substrata:

Presence of many taxa which are sensible to eutrophication, pollution, water turbidity or other environmental stress factors. Calcified species are numerous (*Corallina* spp., *Hydrolithon* spp., *Pneophyllum* spp. etc.).

Waters are clear (>3 m) for most of the year.

Environmental parameters, such as oxygen saturation and salinity, show low seasonal changes. Sediments are mostly sandy and well oxidised.

Ecological status: HIGH

Because of its structure, that index does not provide margin of errors but it is supported by some physico-chemical environmental observations. It was set up by considering only some species or macrophyte associations which with their presence/absence or abundance can be considered are indicators of particular conditions. We have found that the absence of seagrasses, is strictly associated to marked environmental stress factors and that observation can

rapidly discriminate the environmental ecological status between “bad-low” and “moderate-good-high” conditions. The separation between “bad” and “low” can be easily assessed by the absence or presence of blooming macroalgal species, respectively, whereas the separation of the second set of classes is relatively easy for soft bottoms by taking into account both the seaweed taxa and the structure of their populations. In the case of hard substrates, the environment classification depend on the prevalence of some macroalgal taxa and by the abundance of some species very sensible to eutrophication and pollution (Table 2).

Fig. 1 – Classification of the Venice lagoon in summer 2005. Square stations are the sites studied in the CORILA Project 2004-2006 (Research Line 3.12).



That environmental classification, based on benthic macrophytes, appears well related to the environmental conditions and the concentrations of pollutants recorded in some areas of the Venice lagoon. Seagrasses lack in the areas where pollutants are high, waters are turbid or anoxia occur. Similarly, many species which are characterized by high scores grow only in areas where pollutants are low, waters are transparent and no anoxia occur. Also the high seasonal variability of some parameters such as salinity, turbidity, oxygen saturation and the nutrient concentrations usually characterize “bad” or “low” environments. In contrast, the areas which exhibit low seasonal variations, also in the presence of low salinity values and relatively high nutrient concentrations can exhibit “good” or “high” conditions.

Conclusions

The rapid quality assessment index proposed in this paper was set up in the Venice lagoon and calibrated in the lagoons of Orbetello, Lesina and Goro. It was drawn by taking into account the ecological role of some macroalgal and seagrass taxa related mainly to bad or highly quality environments, their biomass and some environmental parameters such as water turbidity, salinity, oxygen availability and nutrient concentrations. The index is a simplification of other two indices “Rhodophyceae/Chlorophyceae ratio” and “the Mean Macroalgal Score” described by Sfriso et al. [2006a, b]. It is very easy and

rapid to apply and it does not need of expertise personnel. The environment assessment is mainly qualitative and the identification in a precise class of ecological status is immediate, also in the presence of a low number of macroalgae or even in their complete absence.

Chlorophyceae	
1	<i>Bryopsis duplex</i> De Notaris 2
2	<i>Caulerpa prolifera</i> (Forsskaal) Lamouroux 2
3	<i>Chaetomorpha linum</i> (O. F. Müller) Kützing 2
4	<i>Cladophora hutchinsiae</i> (Dillwyn) Kützing 2
5	<i>Cladophora liniformis</i> Kützing 2
6	<i>Cladophora prolifera</i> (Roth) Kützing 2
7	<i>Codium bursa</i> (Linnaeus) Agardh 2
8	<i>Flabellia petiolata</i> (Turra) Nizamuddin 2
9	<i>Halimeda tuna</i> (J. Ellis & Solander) J. V. Lamouroux 2
10	<i>Monostroma obscurum</i> (Kützing) J. Agardh 2
11	<i>Polyphysa parvula</i> (Solms-Laubach) Schnetter et Bula Meyer 2
12	<i>Valonia aegagropila</i> C. Agardh 2
Ochrophyceae	
13	<i>Cladosiphon zosterae</i> (J. Agardh) Kylin 2
14	<i>Cladostephus spongiosum</i> (Hudson) C. Agardh f. <i>verticillatum</i> (Lightfoot) Prud'homme van Reine. 2
15	<i>Cystoseira amantacea</i> (C. Agardh) Bory var. <i>amantacea</i> . 2
16	<i>Cystoseira compressa</i> (Esper) Gerloff & Nizamuddin 2
17	<i>Cystoseira corniculata</i> (Turner) Zanardini. 2
18	<i>Cystoseira schiffneri</i> Hamel f. <i>tenuiramosa</i> (Ercegovic) Giaccone. 2
19	<i>Cystoseira tamariscifolia</i> (Hudson) Papenfuss. 2
20	<i>Cutleria multifida</i> (J. E. Smith) Greville 2
21	<i>Dictyota fasciola</i> (Roth) J. V. Lamouroux var. <i>fasciola</i> . 2
22	<i>Dictyopteris polypodioides</i> (A.P. De Candolle) J.V. Lamouroux 2
23	<i>Fucus virsoides</i> J. Agardh 2
24	<i>Padina pavonica</i> (Linnaeus) Thivy 2
25	<i>Punctaria tenuissima</i> (C. Agardh) Greville 2
26	<i>Sargassum acinarium</i> (Linnaeus) Setchell. 2
27	<i>Sargassum hornschurchii</i> C. Agardh. 2
28	<i>Sphacelaria cirrosa</i> (Roth) C. Agardh 2
29	<i>Sphacelaria rigidula</i> Kützing 2
30	<i>Stictyosiphon soriferus</i> (Reinke) Rosenvinge 2
31	<i>Taonia atomaria</i> (Woodward) J. Agardh f. <i>atomaria</i> . 2
32	<i>Taonia pseudociliata</i> (J. V. Lamouroux) Nizamuddin & Godeh 2
Rhodophyceae	
33	<i>Aglaothamnion caudatum</i> (J. Agardh) Feldmann-Mazoyer 2
34	<i>Alsidium corallinum</i> C. Agardh 2
35	<i>Anotrichium furcellatum</i> (J. Agardh) Baldock 2
36	<i>Antithamnionella elegans</i> (Berthold) J. H. Price & D John var. <i>elegans</i> 2
37	<i>Centroceras clavulatum</i> (C. Agardh) Montagne 2
38	<i>Ceramium ciliatum</i> (J. Ducluzeau) var. <i>ciliatum</i> 2

Tab. 2 – Actual and past macroalgae found in the lagoons of Venice lagoon, Orbetello, Lesina and Goro with the highest score, (i.e. 2) which are indicators of high quality environments

39	<i>Ceramium ciliatum</i> (J. Ducluzeau) var. <i>robustum</i> (J. Agardh) Feldmann-Mazoyer	2
40	<i>Ceramium cimbricum</i> H.E. Petersen in Rosenvinge	2
41	<i>Ceramium circinatum</i> (Kützing) J. Agardh	2
42	<i>Ceramium codii</i> (H. Richards) Feldmann-Mazoyer	2
43	<i>Ceramium deslongchampsii</i> Chauvin ex Duby	2
44	<i>Ceramium diaphanum</i> (Lightfoot) Roth	2
45	<i>Ceramium flaccidum</i> (Kützing) Ardissonne	2
46	<i>Ceramium tenerrimum</i> (G. Martens) Okamura	2
47	<i>Champia parvula</i> (Agardh) J. Agardh.	2
48	<i>Chondracanthus acicularis</i> (Roth) Fredericq	2
49	<i>Chondracanthus teedei</i> (Roth) J.V. Lamouroux	2
50	<i>Chondria coerulescens</i> (J. Agardh) Falkenberg	2
51	<i>Chondria dasyphylla</i> (Woodward) C. Agardh	2
52	<i>Chondrophycus papillosus</i> (C. Agardh) Garbary & Harper	2
53	<i>Chylocladia verticillata</i> (Lightfoot) Bliding	2
54	<i>Corallina elongata</i> J. Ellis & Solander	2
55	<i>Corallina officinalis</i> Linnaeus	2
56	<i>Cryptonemia lomation</i> (A. Bertoloni) J. Agardh	2
57	<i>Dasya punicea</i> (Zanardini) Meneghini ex Zanardini	2
58	<i>Dohrniella neapolitana</i> Funk	2
59	<i>Gastroclonium reflexum</i> (Chauvin) Kützing	2
60	<i>Gelidium crinale</i> (Turner) Gaillon	2
61	<i>Grateloupia dichotoma</i> J. Agardh	2
62	<i>Grateloupia filicina</i> (J.V. Lamouroux) C. Agardh	2
63	<i>Griffithsia schousboei</i> Montagne	2
64	<i>Haliptilon squamatum</i> (Linnaeus) H.W.Johansen, L.M. Irvine & A.M.2 Webster	2
65	<i>Halymenia floresia</i> (Clemente) C. Agardh	2
66	<i>Heterosiphonia japonica</i> Yendo	2
67	<i>Hildenbrandia rubra</i> (Sommerfelt) Meneghini	2
68	<i>Hydrolithon cruciatum</i> (Bressan) Chanberlain	2
69	<i>Hypnea musciformis</i> (Wulfen) J. V. Lamouroux	2
70	<i>Hypnea spinella</i> (C. Agardh) Kützing	2
71	<i>Hypnea</i> cfr. <i>valentiae</i> (Turner) Montagne	2
72	<i>Janua longifurca</i> Zanardini	2
73	<i>Jania rubens</i> (Linnaeus) J.V. Lamouroux var. <i>corniculata</i> (Linnaeus)2 Yendo.	2
74	<i>Laurencia obtusa</i> (Hudson) J.V. Lamouroux	2
75	<i>Lithophyllum pustulatum</i> (J.V. Lamouroux) Foslie	2
76	<i>Lomentaria articulata</i> (Hudson) Lyngbye var. <i>articulata</i>	2
77	<i>Lomentaria ercegovicii</i> Verlaque, Boudouresque, Meinesz, Giraud &2 Marcot-Coqueugniot	2
78	<i>Lomentaria hakodatensis</i> Yendo	2
79	<i>Melobesia membranacea</i> (Esper) J. V. Lamouroux	2
80	<i>Monosporus pedicellatus</i> (J. E. Smith) Solier var. <i>pedicellatus</i>	2
81	<i>Nemalion helminthoides</i> (Vellay) Batters	2
82	<i>Nitophyllum punctatum</i> (Stackhouse) Greville	2
83	<i>Osmundea truncata</i> (Kützing) K.W. Nam & Maggs	2
84	<i>Peyssonellia dubyi</i> P. et H. Crouan	2
85	<i>Peyssonellia polymorpha</i> (Zanardini) F. Schmitz.	2
86	<i>Peyssonellia squamaria</i> (S.G. Gmelin) Decaisne.	2

87	<i>Phyllophora sicula</i> (Kützing) Guiry et L.M. Irvine	2
88	<i>Polysiphonia flocculosa</i> (C. Agardh) Endlicher	2
89	<i>Polysiphonia fucoides</i> (Hudson) Greville	2
90	<i>Pterothamnion crispum</i> (Ducluzeau) Nägeli	2
91	<i>Pterothamnion plumula</i> (J. Ellis) Nägeli	2
92	<i>Radicilingua reptans</i> (Kylin) Papenfuss	2
93	<i>Rytiphlaea tinctoria</i> (Clemente) C. Agardh	2
94	<i>Spyridia hypnoides</i> (Bory) Papenfuss	2
95	<i>Wrangelia penicillata</i> (C. Agardh) C. Agardh	2

References

- Borja A., Franco J., Pérez V., 2000. A marine biotic index to establish the ecological quality of soft-bottom benthos within European estuarine and coastal environments. *Marine Pollution Bulletin*, 12, 1100-1114.
- Borja A., Muxika I., Franco J., 2003. The application of a Marine Biotic Index to different impact sources affecting soft-bottom benthic communities along European coasts. *Marine Pollution Bulletin*, 46, 835-845.
- Borja A., Franco J., Valencia V., Bald J., Muxika I., Belzunce M. J., Solaun O., 2004. Implementation of the European water framework directive from the Basque country (northern Spain): a methodological approach. *Marine Pollution Bulletin*, 48, 209-218.
- Orfanidis S., Panayotidis P., Stamatis N., 2001. Ecological evaluation of transitional and coastal waters: A marine benthic macrophytes-based model. *Mediterranean Marine Sciences*, 2/2, 45-65
- Orfanidis S., Panayotidis P., Stamatis N., 2003. An insight to the ecological evaluation index (EEI). *Ecological Indicators*, 3, 27-33.
- Panayotidis P., Montesanto B., Orfanidis S., 2004. Use of low-budget monitoring of macroalgae to implement the European Water Framework Directive. *Journal of Applied Phycology*, 16, 49-59.
- Sfriso A., La Rocca B., Godini E., 2002. Seaweed list in three areas of the Venice lagoon characterized by different trophic levels (In Italian). *Lavori - Società Veneziana di Scienze Naturali*, 27, 85-99.
- Sfriso A., Facca C., La Rocca B., Ghetti P.F., 2006a. Set up of environmental quality indices based on seaweed taxonomic ratios for the assessment of transitional marine areas: Venice, Lesina and Goro study cases. In "Transition Waters Monitoring. Research and Institutional Monitoring. Comparison between different experiences" (In Italian). "APAT", Palazzo Labia, Venezia.
- Sfriso A., Facca C., Ghetti P. F., 2006b. Seaweeds and environmental variables to assess the ecological quality of transitional marine environments. *Biologia Marina Mediterranea* (In Italian). In press.

CARBON PARTITIONING IN THE PLANKTON COMMUNITY, PRODUCTION AND DECOMPOSITION PROCESSES IN THE LAGOON OF VENICE

A. Valeri¹, F. Aciri², F. Bernardi Aubry², D. Berto³, J. Coppola², P. Del Negro¹,
M. Giani³, C. Larato¹, A. Pugnetti²

¹ *Istituto Nazionale di Oceanografia e Geofisica Sperimentale, Trieste* ² *C.N.R. Istituto di Scienze Marine, Sede di Venezia* ³ *Istituto Centrale per la Ricerca scientifica e tecnologica Applicata al Mare, Chioggia*

Riassunto

Questo lavoro si inserisce nell'ambito delle ricerche volte allo studio dei processi di produzione e degradazione della sostanza organica nella Laguna di Venezia (Programma di Ricerca CORILA 2004-2006, Linea 3.12). Vengono presentati i risultati preliminari relativi alle attività sperimentali condotte in due campagne svolte durante l'inverno e la primavera 2005 in due delle 6 stazioni che sono state complessivamente studiate. La struttura dei popolamenti planctonici è stata analizzata sia in termini di autotrofia ed eterotrofia, sia considerando, all'interno di ogni comparto funzionale, la ripartizione del carbonio nelle classi dimensionali del pico-, nano- e micro-plancton, al fine di poter identificare i rapporti trofici prevalenti in condizioni ambientali e stagionali diverse.

Abstract

The present work is carried out in the framework of the researches aimed at evaluating the processes of production and degradation of organic matter in the Lagoon of Venice (CORILA Research Programme 2004-2006, Line 3.12).

We report some results of the experimental activity performed in two (winter and spring 2005) out of a total of five campaigns carried out in 2004 and 2005 and at 2 stations, out of the six that were examined in total. The structure of the plankton community was analyzed considering the autotrophic and heterotrophic compartments and the carbon partitioning inside the pico-, nano- and micro-plankton size classes, with the main aim of identifying the dominant trophic relationships, in different seasons and environmental conditions.

1 Introduction

The dynamics and the mechanisms that control and govern the production and the degradation of the organic carbon have important ecological implications, in terms of energy flux and trophic state of aquatic ecosystems. The fate of organic carbon is strongly influenced by the prevailing food web: when the classic grazing food chain predominates, organic matter is exported to the upper trophic levels; by contrast, when the microbial food web prevails, the recycling of the organic matter within the water column is favoured. In this

context, the size structure of the plankton community plays a central role in the carbon partitioning and destiny within the ecosystem (Fuhrman, 1992; Fenchel, 1988).

The present work was carried out in the framework of the researches aiming to assess the production and degradation dynamics of the organic matter in the Venice lagoon (CORILA Research Programme 2004-2006, Line 3.12).

We present the first results of a research focused on the evaluation of the functional role of the microbial community in relation to the degradation of the organic matter and its temporal and spatial variability. The main aim was the identification of the dominant trophic relationships in the planktonic compartment, in different seasons and environmental conditions, considering the dimensional structure of the planktonic organisms.

2 Materials and methods

Two Stations, San Giuliano (SG) and Palude della Rosa (PR), (Fig. 1) were seasonally sampled during January and April 2005.

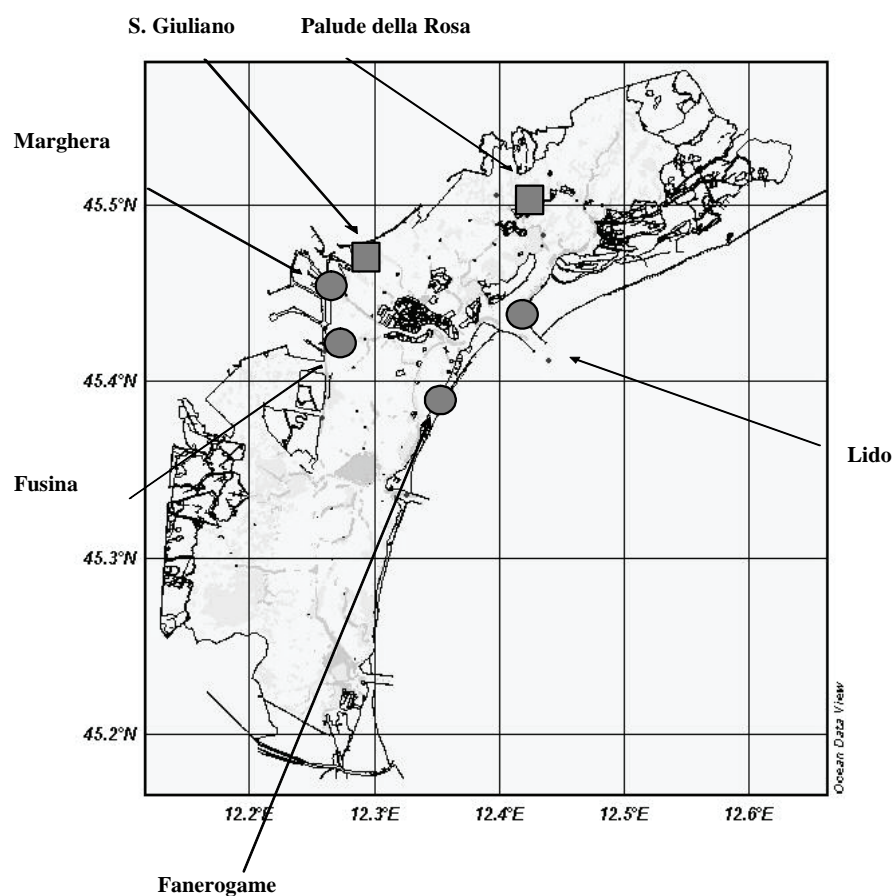


Fig. 1 – Map of sampling stations.

Surface water samples were collected using 5 l Niskin bottles, at neap tide. The following parameters have been considered: phytoplankton size structure (Utermöhl, 1958; Maugeri et al., 1990; Zingone et al., 1990), taxonomic

composition (Tomas, 1997) and photosynthetic activity (Steeman Nielsen, 1952; Richardson, 1987); bacterial abundance (Porter and Feig, 1980), bacterial C production (Smith and Azam, 1992) and exoenzymatic activities (Hoppe, 1983); dissolved (DOC) and particulated organic carbon (POC) (Sugimura and Suzuki, 1988; Nieuwenhuize et al., 1994).

To estimate autotrophic picoplankton (0.2 - 2 μm) biomass, cell volume was calculated by approximation to a sphere or to a rotation cylinder and transformed into organic carbon using the coefficients of 0.250 $\text{fg } \mu\text{m}^{-3}$, for *Synechococcus*, and 220 $\text{fg } \mu\text{m}^{-3}$, for eukariotes (Tamigneux et al., 1995). Heterotrophic picoplankton abundance was converted to carbon using a conversion factor of 20 fg C cell^{-1} (Lee and Fuhrman, 1987).

Nanoplankton (2 - 20 μm) and microplankton (> 20 μm) biomasses were estimated by measuring the linear dimension and equating shapes to standard geometric figures; the resulting volumes were transformed into organic carbon values by using the following conversion factors: nanoplankton $\text{pg C} = \mu\text{m}^3 \times 0.14$ (Edler, 1979); diatoms $\text{pg C} = \mu\text{m}^3 \times 0.11$ (Strathmann, 1967); tintinnids $\text{pg C} = \mu\text{m}^3 \times 0.053 + 444.5$ (Verity and Langdon, 1984); ciliates other than tintinnids $\text{pg C} = \mu\text{m}^3 \times 0.14$ (Putt and Stoecker, 1989); heterotrophic dinoflagellates $\text{pg C} = \mu\text{m}^3 \times 0.13$ (Edler, 1979); all the other groups $\text{pg C} = \mu\text{m}^3 \times 0.08$ (Beers and Stewart, 1970).

The bacterial exoenzymatic activities were converted to carbohydrate and protein mobilized using the conversion factor 72 $\mu\text{g C } \mu\text{mol}^{-1}$ (Hoppe, 1993).

The Bacterial Carbon Demand was estimated considering a Bacterial Growth Efficiency of 30% (e.g. Hoppe et al., 2001).

3 Results

The Stations are characterized by different hydrological features (Bianchi et al., 2003; Acri et al., 2004) mainly due to their geographical position and anthropic influence (Tab. 1).

Parameters	Station	SG		PR	
	Period	winter	spring	winter	spring
Transparency (m)		0,4	0,9	0,9	1,3
Temperature ($^{\circ}\text{C}$)		6,5	15,0	5,0	15,0
Salinity		26,7	21,6	31,0	30,4
N-NH ₃ (μM)		7,3	20,7	3,9	11,9
N-NO ₂ (μM)		1,4	3,5	1,5	1,3
N-NO ₃ (μM)		52,7	42,8	23,2	21,2
DIN (μM)		61,5	66,9	28,7	34,4
Si-SiO ₄ (μM)		32,0	58,1	8,0	19,6
P-PO ₄ (μM)		0,7	1,0	0,1	0,2

Tab. 1 - Values of the detected parameters at S. Giuliano (SG) and Palude della Rosa (PR) stations

The SG station showed the highest DOC concentration, both in winter (2078 $\mu\text{g C l}^{-1}$) and in spring (3252 $\mu\text{g C l}^{-1}$). At PR station DOC concentrations ranged between 1922 (winter) and 2236 (spring) $\mu\text{g C l}^{-1}$. The POC concentrations were around 750 $\mu\text{g C l}^{-1}$ during winter at both stations, in spring the concentrations increased up to 817 at St. SG and markedly decreased at St. PR (336 $\mu\text{g C l}^{-1}$). The living POC (live-POC) due to biomass of autotrophic and heterotrophic plankton organisms reached the highest values at St. SG (Tab. 2) and increased from winter to spring, mostly at St. PR. The heterotrophic organisms contributed from 76% to 96% to live-POC while autotrophic community was only 4-24% of living-POC. The influence of live-POC to POC was quite similar at both stations but at St. PR the percentage of live-POC was rising up in spring.

Tab. 2 – Values of living-POC (live-POC), autotrophic biomass (POC-auto) and heterotrophic biomass (POC-hetero) and relative percentage at the stations S. Giuliano (SG) and Palude della Rosa (PR).

Parameters	Station	SG		PR	
	Period	winter	spring	winter	spring
live-POC ($\mu\text{g C l}^{-1}$)		81,4	123,7	39,8	102,1
auto POC- ($\mu\text{g C l}^{-1}$)		9,9	12,7	1,7	24,9
hetero POC- ($\mu\text{g C l}^{-1}$)		71,6	111,1	38,0	77,2
live-POC/POC (%)		11	15	5	30
POC-auto/live-POC (%)		12	10	4	24
POC-hetero/ live-POC (%)		88	90	96	76

The phytoplankton size structure is shown in figures 2 and 3. At St. San Giuliano nanoplankton dominated in winter and spring; picoplankton never exceeded 8% of the total biomass and the contribution of microplankton was valuable only in winter (Fig. 2). At St. Palude della Rosa the autotrophic community was mostly composed by microplankton (Fig. 3). The picoplankton contribution was scarce (< 5%) in both seasons and nanoplankton was considerable only in winter (42%).

Primary production (PP) (Tab. 3) was very low in winter and markedly increased in spring. The highest contribution to primary production was due to the nano- and microplanktonic fractions at St. San Giuliano. At St. Palude della Rosa primary production was mainly determined by pico- and nanoplankton. In particular, in spring the relative contribution of the smallest phytoplankton to total production was higher than their share of total phytoplankton biomass.

The size structure of the heterotrophic community (Fig. 2 and 3) was quite similar at both stations. The picoplanktonic cells (bacteria) clearly prevailed, the nanoplankton and microplankton biomasses increased from winter to spring.

Bacterial carbon production (BCP) and organic carbon mobilization (OCM) (Tab. 3) were similar at both stations in winter. In spring they increased most markedly at St. San Giuliano. At St. San Giuliano BCD (Tab. 3) was low in winter and showed a clear rise in spring, while at St. Palude della Rosa was similar in both periods.

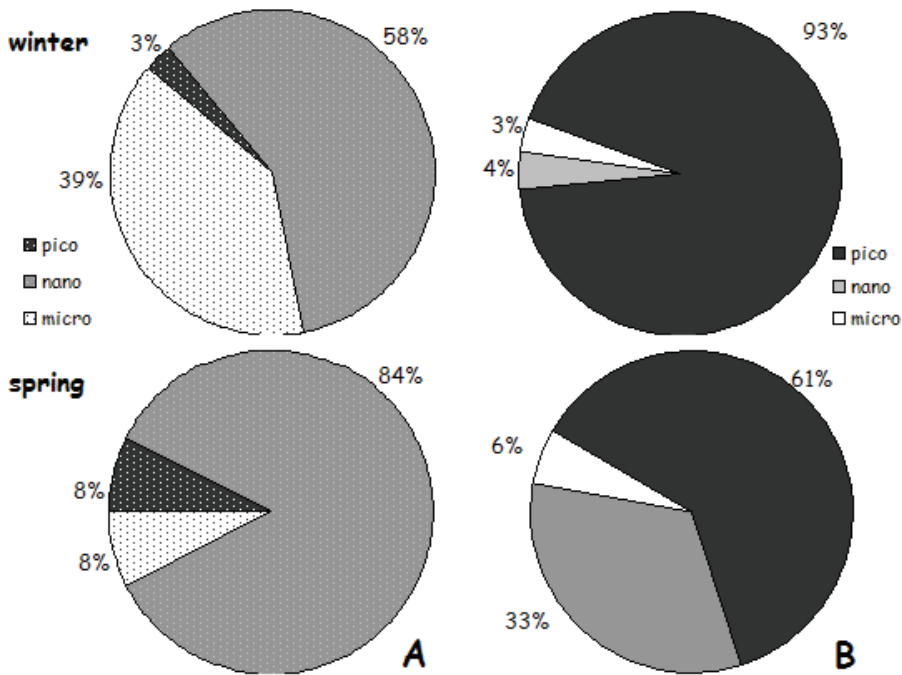


Fig 2 – Station San Giuliano: carbon concentration of the different size classes expressed as percentage. Pico = picoplankton (0.2 - 2 μ m), nano = nanoplankton (2 - 20 μ m), micro = microplankton (> 20 μ m). A=Autotrophic community, B=Heterotrophic community.

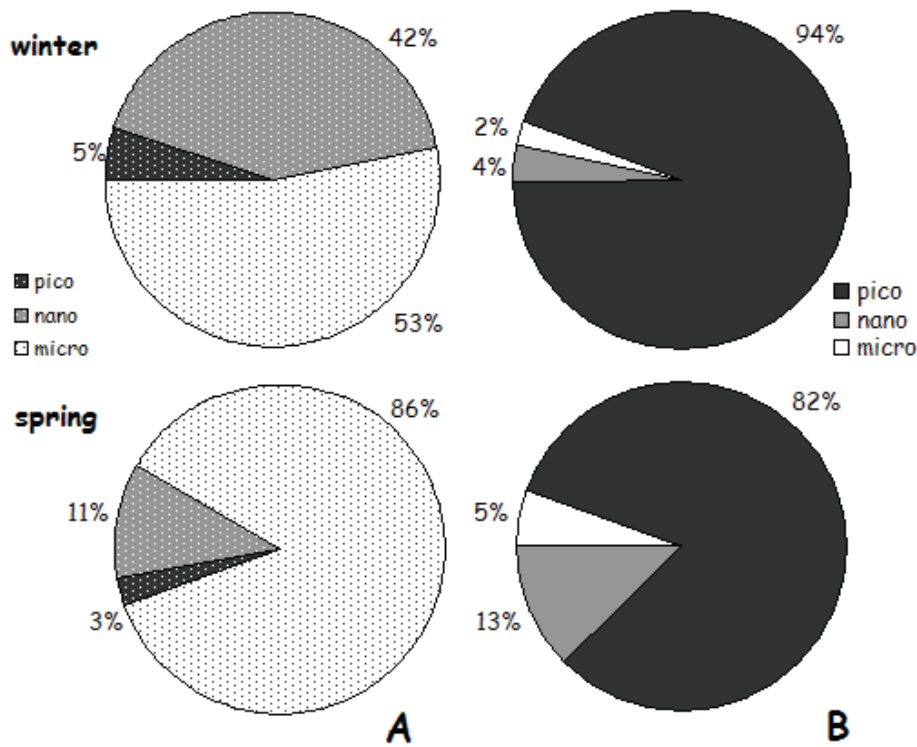


Fig. 3 – Station Palude della Rosa: carbon concentration of the different size classes expressed as percentage. Pico = picoplankton (0.2 - 2 μ m), nano = nanoplankton (2 - 20 μ m), micro = microplankton (> 20 μ m). A=Autotrophic community, B=Heterotrophic community.

Tab. 3 – PP (Primary Production), BCP (Bacterial Carbon Production), BCD (Bacterial Carbon Demand) and OCM (Organic Carbon Mobilization) at the two stations (SG = S. Giuliano, PR = Palude della Rosa) during the two campaigns.

Parameters	Station		PR	
	Period	winter	winter	spring
PP ($\mu\text{g C l}^{-1} \text{h}^{-1}$)		0,01	1,0	4,8
BCP ($\mu\text{g C l}^{-1} \text{h}^{-1}$)		2,3	3,3	4,7
BCD ($\mu\text{g C l}^{-1} \text{h}^{-1}$)		7,8	11,1	15,4
OCM ($\mu\text{g C l}^{-1} \text{h}^{-1}$)		40,0	30,8	39,8

4 Discussion and Conclusion

The information on the size structure of the autotrophic and heterotrophic community in the Lagoon of Venice is quite scarce and it refers mostly to the works by Sorokin et al. (1996, 2002, 2004). Studies on the production and degradation of organic matter in the planktonic community are scanty and sporadic as well (Degobbis et al., 1986; Bianchi et al., 2000; Sorokin et al., 1996; 2002). These studies give clues of the importance of the smallest size fractions of the plankton community in this ecosystem, for both organic carbon degradation and transfer to the upper trophic levels.

The data presented here need still to be integrated with those coming from the other study periods (summer and autumn) and from the other stations. However, they already can lead to some preliminary considerations.

At both stations, during winter and spring, the picoplankton appeared largely dominated by the heterotrophic component: bacteria represents more than 55% of the total planktonic biomass.

At St. SG, both the autotrophic and heterotrophic components were mainly represented by the smallest size fractions (pico- and nanoplankton). The phytoplankton community at St. PR, on the contrary, was characterized by a larger contribution of microplankton. The results might describe different scenarios. The smaller algae have highest photosynthetic efficiencies, PP at St. SG was higher than PP at St. PR. On the other hand, small size phytoplankton community might indicate an elevated grazing pressure on pico-nano- organisms. Actually, during spring, an increase of the heterotrophic nanoplankton, the main bacterivorous, was recorded.

As it regards primary production it should be emphasized the large range of variations that may be recorded: photosynthetic activity may span over 2 orders of magnitude (St. SG). The large range of variation of primary production in the Lagoon of Venice has been already reported by other Authors (Degobbis et al., 1986; Bianchi et al., 2000).

During winter, when primary production rates are very low, the allochthonous inputs of organic matter was probably the prevalent substrate for bacterial metabolism. Bacteria are involved more in enzymes synthesis than in growth reducing the energy transfer to the upper trophic level. The BCD was satisfied by carbon mobilized using enzymes. In spring period phytoplankton community

played an important role in organic matter production but algal exudation of high molecular weight organic molecules needed enzymatic hydrolysis as increase in glucosidases and galactosidases shown. The BCD increased and was partially satisfied by PP and partially by organic matter already available. Microbial degradation and utilization of organic substrate are more intense and increased the energy transfer to the upper trophic level sustaining the bigger size classes of the heterotrophic organisms.

Our results, suggest that in winter period the recycling of the organic matter within the water column is favoured and the microbial food web prevails while in spring period the classic grazing food chain seems to be more efficient.

References

- Acri F., Bernardi Aubry F., Berton A., Bianchi F., Boldrin A., Camatti E., Comaschi A., Rabitti S., Socal G. 2004. Plankton communities and nutrients in the Venice Lagoon. Comparison between current and old data. *Journal of Marine Systems*, 51, 321-329.
- Beers, J. R., Stewart, C. L., 1970: The ecology of the plankton off La Jolla, California, in the period April through September 1967. VI. Numerical abundance and estimated biomass of microzooplankton. *Bulletin of Scripps Institute of Oceanography*, 17, 67-87.
- Bianchi F., Acri F., Alberighi L., Bastianini M., Boldrin A., Cavalloni B., Cioce F., Comaschi A., Rabitti S., Socal G., Turchetto M. 2000. Biological variability in the Venice lagoon. In: Lasserre, P. and Marzollo, A. (Eds) *The Venice Lagoon Ecosystem. Inputs and interactions between land and sea. Man and the biosphere series volume 25.* UNESCO and Parthenon Publishing Group: 97-125.
- Bianchi F., Acri F., Bernardi Aubry F., Berton A., Boldrin A., Camatti E., Cassin D., Comaschi A. 2003. Can plankton communities be considered as bio-indicators of water quality in the Lagoon of Venice? *Marine Pollution Bulletin*, 46, 964-971.
- Degobbi D., Gilmartin M., Orio A.A. 1986. The relation of nutrient regeneration in the sediments of the Northern Adriatic to eutrophication, with special reference to the Lagoon of Venice. *The Science of the Total Environment*, 56, 201-210.
- Edler L., 1979, Recommendation on methods of marine biological studies in the Baltic Sea. *Phytoplankton and chlorophyll*, Baltic Marine Biology Publications, No 5 (Univ.Lund).
- Fenchel T., 1988. Marine plankton food chain. *Annual Review Ecological System*, 19: 19-38.
- Fuhrman J.A., 1992. Bacterioplankton role in cycling of organic matter: microbial food web. In: Falkowski, P.G. and Woodhead, A.D. (Eds) *Primary productivity and biogeochemical cycle in the sea.* Plenum Press New York NY

pp: 361-383.

Hoppe H.G., 1983. Significance of exoenzymatic activities in the ecology of brackish water: measurements by means of methylumbelliferyl substrates. *Marine Ecology Progress Series*, 11, 299-308.

Hoppe H.G., 1993. Use of Fluorogenic Model substrates for Extracellular Enzyme Activity (EEA) Measurement of Bacteria. In: *Handbook of methods in Aquatic Microbial Ecology*. Kemp P.F., Sherr B.F., Sherr E.B. and Cole J.J. (eds). Lewis Publisher.

Hoppe H.G., Gocke K., Koppe R., Begler C., 2002. Bacterial growth and primary production along a north-south transect of the Atlantic Ocean. *Nature*, 416, 168-171.

Lee S., Fuhrman J.A., 1987. Relationships between biovolume and biomass of naturally derived marine bacterioplankton. *Applied Environmental Microbiology*, 53: 1298-1303.

Maugeri T.L., Acosta Pomar M.L.C. and Bruni V., 1990. Picoplankton. *Metodi nell'ecologia del plancton marino*. Nova Thalassia, 11, 199-205.

Nieuwenhuize J., Mass E.M. and Middelburg J.J., 1994. Rapid analysis of organic carbon and nitrogen in particulate materials. *Marine Chemistry*, 45, 217-224.

Porter K.G. and Feig Y.S., 1980. The use of DAPI for identifying and counting aquatic microflora. *Limnology and Oceanography*, 25, 943-948.

Putt D., Stoecker M.D., 1989. An experimentally determined carbon: volume ratio for marine "oligotrichous" ciliates from estuarine and coastal waters. *Limnology and Oceanography*, 34(6), 1097-1103.

Richardson K. (ed), 1987. Primary production: guidelines for the measurement by ¹⁴C incorporation. ICSES, *Techniques in marine environmental sciences*, 5.

Smith D.C. and Azam F., 1992. A simple economical method for measuring bacterial protein synthesis rates in seawater using ³H-leucine. *Marine Microbial Food Webs*. 6 (2): 107-114.

Sorokin Yu. I., Sorokin P.Yu., Giovanardi O. and Dalla Venezia L., 1996. Study of the ecosystem of the lagoon of Venice with emphasis on anthropogenic impact. *Marine Ecology Progress Series*, 141, 247-261.

Sorokin P. Yu., Sorokin Yu. I., Zakuskina O. Yu. and Ravagnan G.-P., 2002. On the changing ecology of Venice lagoon. *Hydrobiologia*, 487, 1-18.

Sorokin Yu. I., Sorokin P.Yu., Boscolo R., Giovanardi O. 2004. Bloom of picocyanobacteria in the Venice Lagoon during summer-autumn 2001: ecological consequences. *Hydrobiologia*, 523, 71-85.

Steeman-Nielsen E., 1952. The use of radioactive carbon (¹⁴C) for measuring organic production in the sea. *Journal the conseil International pour l'Exploration de la Mer*, 18, 117-140

Strathmann R. R., 1967. Estimating the organic carbon content of phytoplankton from cell volume or plasma volume. *Limnology and Oceanography*, 12, 411–418.

Sugimura Y., Suzuki Y., 1988. A high-temperature catalytic oxidation method for the determination of non-volatile dissolved organic carbon in seawater by direct injection of a liquid sample. *Marine Chemistry*, 24: 105-131.

Tamigenaux E., Vasquez E., Mingelbier M., Klein B., Legendre L., 1995. Environmental control of phytoplankton assemblages in nearshore waters, with special emphasis on phototrophic ultraplankton. *Journal of Plankton Research*, 17: 1421-1447

Tomas C.R., 1997. *Identifying Marine Phytoplankton*. Academic Press, Acourt Brace & Company.

Utermöhl H., 1958. Zur Vervollkomungder quantitativen Phytoplankton-Methodik. *Mitt. Int. Verein. Limnol.*, 9, 1-38.

Verity P. G., C. Langdon, 1984. Relationships between lorica volume, carbon, nitrogen and ATP content oftintinnids in Narragansett Bay. *Journal Plankton Reserchs*, 6, 859-868.

Zingone A., Honsell G., Marino D., Montresor M. and Socal G., 1990. Fitoplancton. In: *Lint, Trieste (Ed.)*. Nova Thalassia, 11, Ministero Ambiente.

RESEARCH LINE 3.14

**Erosion and sedimentation processes in the
Venice lagoon**

TIDAL FLAT – SALT MARSHES TRANSITION IN THE VENICE LAGOON, ITALY

Andrea Defina¹, Luca Carniello¹, Luigi D'Alpaos¹

¹ *Dipartimento IMAGE, Università di Padova.*

Riassunto

Nelle lagune poco profonde, come la Laguna di Venezia, le aree di bassofondo sono caratterizzate da quote inferiori a quelle del mare mentre le barene si posizionano altimetricamente ad una quota maggiore con qualche variazione legata alle locali caratteristiche ecologiche e sedimentologiche. Le quote intermedie rispetto a queste due formazioni geomorfologiche sono decisamente poco frequenti. Ciò suggerisce che i processi che governano erosione e deposizione all'interno di questi bacini lagunari producono distintamente bassifondi o barene escludendo la possibilità di formazioni stabili a quote intermedie.

La discontinuità nella distribuzione delle quote del fondo può essere indagata attraverso l'analisi della risospensione prodotta dallo sforzo di attrito al fondo generato dalle onde da vento essendo trascurabili gli sforzi indotti dalla marea.

Lo studio di questo comportamento ha portato alla formulazione di un modello concettuale per descrivere la tendenza evolutiva riscontrata. Il modello dimostra che le aree caratterizzate da una elevazione intermedia sono intrinsecamente instabili e tendono inevitabilmente ad evolvere o come bassifondi o come barene.

L'applicazione di un modello numerico bidimensionale accoppiato in grado di descrivere contemporaneamente l'idrodinamica e la generazione e propagazione del moto ondoso ha consentito di verificare la correttezza del modello concettuale attraverso un'applicazione alla Laguna di Venezia.

I risultati delle indagini, infine, hanno portato alla formulazione di uno schema che descrive l'evoluzione a lungo termine di queste unità morfologiche.

Abstract

Shallow tidal basins like the Venice lagoon, Italy, are often characterized by extensive tidal flats and salt marshes that lie within specific ranges of elevation. Tidal flats lie just below the mean sea level, approximately between -0.6 m and -2.0 m a.m.s.l., whereas salt marshes lie at an average elevation higher than the mean sea level (i.e. between +0.1 m and +0.5 m a.m.s.l.).

Only a small fraction of the tidal basin area has elevations in the intermediate range (i.e. between -0.6 m and +0.1 m a.m.s.l.).

This occurrence suggests that the morphodynamic processes responsible for sediment deposition and erosion produce either tidal flats or salt marshes but

no landforms located in the above critical range of elevations.

A conceptual model describing this evolutionary trend has recently been proposed. The model assumes that this bimodal distribution of bottom elevations stems from the characteristics of wave induced sediment resuspension and demonstrates that areas at intermediate elevations are inherently unstable and tend to become either tidal flats or salt marshes.

In this work, the conceptual model is validated through comparison with numerical results obtained with a two dimensional wind waves – tidal model applied to the lagoon of Venice. Both the present and the 1910 bathymetries of the Venice lagoon are used in the simulations and the obtained numerical results confirm the validity of the conceptual model. A new framework to acknowledge long term evolution of shallow tidal basins, which uses the conceptual model, is finally proposed and discussed.

1 Introduction

Shallow tidal basins are often characterized by extensive tidal flats and marshes dissected by an intricate network of channels [Rinaldo et al., 1999a, 1999b; Fagherazzi, 1999; Defina, 2000; Marani et al., 2003]. Both tidal flats and salt marshes are prevalently flat landforms located in the intertidal zone. Tidal flats lie below mean sea level, and only the lowest tides expose their surface. Salt marshes have an elevation higher than the mean sea level, are flooded during high tides, and sustain a dense vegetation canopy of halophyte plants that withstand the relative infrequent flooding periods.

A typical intertidal landscape can be found in the Venice lagoon, Italy, where tidal flats and salt marshes are separated by a well defined scarp.

The distribution of elevations in the Venice lagoon shows that tidal flats have differences in elevation of few tens of centimeters, with an average elevation between -0.6 and -2.0 m above the mean sea level (m a.m.s.l.), whereas the salt marsh platform lies at an average elevation higher than +0.1 m a.m.s.l., with some variability dictated by local sedimentological and ecological conditions. Few areas are located at intermediate elevations (i.e. between -0.6 m and +0.1 m a.m.s.l.), suggesting that the processes responsible for sediment deposition and erosion produce either tidal flats or salt marshes but no landforms located in the above critical range of elevations.

Salt marshes directly form from tidal flats in locations where sedimentation is enhanced by lower tidal velocities, by higher sediment concentrations, or by the sheltering effects of spits and barrier islands [Dijkema, 1987; Allen, 2000]. Typical conceptual and numerical models of marsh formation envision a gradual transition through sediment build-up and plant colonization from sandflats and mudflats [Beefink, 1966; French and Stoddart, 1992; Fagherazzi and Furbish, 2001; D'Alpaos et al., 2006].

Conversely, in areas with consistent sediment resuspension tidal flats are dominant, since sediment deposition is balanced by erosion and the bottom elevation is constantly maintained below mean sea level [Allen and Duffy,

1998].

The role of sediment resuspension by wind waves is often decisive in shallow tidal basins, whereas tidal fluxes alone are unable to produce the bottom shear stresses necessary to mobilize tidal flat sediments [Carniello et al., 2005].

Tidal currents produce shear stresses large enough to drive morphological evolution only in the channels and in deep areas where tidal velocities are high.

However, the actual bed shear stress under the combined action of waves and currents is enhanced beyond the sum of the two singular contributions. This occurs because of the non-linear interaction between the wave and current boundary layers [Soulsby, 1995, 1997]. Therefore, even the smaller tidal currents are important in enhancing the bottom shear stress in the presence of wind waves.

A conceptual model explaining the tidal flats – salt marshes transition has recently been proposed by Fagherazzi et al. [2006]. The model shows that areas with elevations in the critical range (i.e., between -0.6 m and +0.1 m a.m.s.l. for the lagoon of Venice) are inherently unstable and tend to become either tidal flats or salt marshes.

In the present paper, the above conceptual model is validated using the results of a complete coupled wind wave – tidal model. Both models are shortly described before discussion.

2 Mathematical models

2.1 The wind waves – tidal model

Before introducing the conceptual model suggested by Fagherazzi et al. [2006] to explain the ubiquitous reduction of areas located at intermediate elevations between tidal flats and salt marshes, we briefly describe the coupled wind waves-tidal model [Carniello et al. 2005] used to validate the conceptual model.

The coupled wind waves-tidal model is composed of a hydrodynamic module and a wind wave module. The hydrodynamic module solves the two-dimensional shallow water equations modified to deal with flooding and drying processes in very irregular domains [Defina et. al., 1994; D'Alpaos and Defina, 1995].

The hydrodynamic model has been tested and validated simulating the propagation of several real tides and comparing the computed water levels and velocities with field data [D'Alpaos and Defina, 1993; 1995]. The model performs satisfactory also when wind action during stormy conditions is considered [Carniello et al., 2005].

At each time step, the hydrodynamic model yields nodal water levels which are used by the wind wave model to assess wave group celerity and bottom influence on wave propagation.

The wind wave module is based on the conservation of the wave action [Hasselmann et al., 1973], which is defined as the ratio of wave energy E to the

wave frequency σ .

For the case of shallow closed basins, the general spectral formulation of the wave action conservation equation can be simplified. In accordance with Carniello et al. [2005], we assume a monochromatic wave and neglect non linear wave-wave and wave-current interactions. We further assume that the direction of wave propagation instantaneously adjusts to the wind direction. The wave action conservation equation can thus be written as:

$$\frac{\partial E}{\partial t} + \frac{\partial}{\partial x} c_{gx} E + \frac{\partial}{\partial y} c_{gy} E = S \quad (1)$$

The first term of (1) represents the local rate of change of wave energy in time, the second and third terms represent the energy convection (c_{gx} and c_{gy} are the x and y components of the wave group celerity). The source term S on the right-hand side of (1) describes all the external contributions to wave energy and can be either positive, e.g. wind energy input, or negative, e.g. bottom friction, whitcapping, and depth-induced breaking.

Equation (1) is solved with an upwind finite volume scheme which uses the same computational grid as the hydrodynamic model. The wind wave model computes the wave energy in each computational element at each time step.

Both tidal currents and wind waves contribute to the production of bottom shear stresses. The bottom shear stress due to waves ($\tau_{b,wave}$) and the tidal current contribution ($\tau_{b,curr}$) are computed respectively as

$$\tau_{b,curr} = \rho g Y \left(\frac{|\mathbf{q}|}{k_s^2 D^{10/3}} \right) \mathbf{q} \quad (2)$$

$$\tau_{b,wave} = \frac{1}{2} f_w \rho_w u_m^2 \quad (3)$$

Here $\mathbf{q}=(q_x, q_y)$ is the flow rate per unit width, k_s is the Strickler bed roughness coefficient, and D is an equivalent water depth, u_m is the maximum horizontal orbital velocity at the bottom computed using the wave linear theory, Y the water depth and f_w the wave friction factor.

Actual bed shear stress under the combined action of waves and currents is enhanced beyond the sum of the two contributions. This occurs because of the interaction between the wave and current boundary layers. In the coupled model the empirical formulation suggested by Soulsby, [1995, 1997] is adopted.

For a more complete description of the wind wave-tidal model we refer to [Carniello et al., 2005].

2.2 The conceptual model

Based on the above wave formulation, a conceptual model to describe the critical bifurcation of tidal basins landforms in tidal flats and salt marshes has recently been proposed by Fagherazzi et al. [2006]. The model is here shortly described.

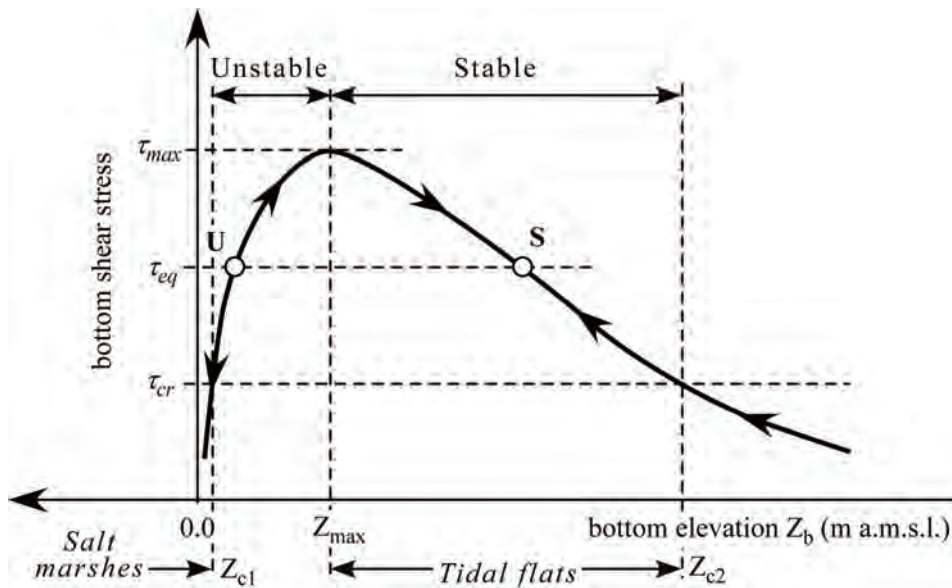


Fig. 1 – Bed shear stress distribution as a function of bottom elevation

In shallow basins waves quickly adapt to external forcing (i.e., the local rate of change of wave energy in time becomes negligible in a short period of time) and the fetch required to attain fully developed condition is short (a fetch length of 2000–3000m is required for water depths around 1m). The latter implies that energy transfer, described by the convective terms in equation (1) poorly contributes to energy balance in open areas. Therefore, as a first approximation, the conservation equation (1) can be reduced to the local equilibrium between the energy generated by the wind action (S_w) and the energy dissipated by bottom friction (S_{bf}), whitecapping (S_{wc}) and breaking (S_{brk}) (see Carniello et al., 2005 for source terms formulation):

$$S_w = S_{bf} + S_{wc} + S_{brk} \quad (4)$$

Shear stresses produced by wind waves are limited in shallow waters due to dissipative processes. However, they are also limited in deep water where the bottom is too deep to be affected by wave oscillations. Therefore, plotting the equilibrium shear stress at the bottom as a function of water depth we obtain a curve peaking at some intermediate water depth (Fig. 1). It is worth noting that the depth at which the shear stress is maximized is weakly affected by wind speed [Fagherazzi et al., 2006].

This maximum in shear stress bears important consequences for the morphological transition from tidal flats to salt marshes and for the overall redistribution of sediments in shallow coastal basins.

The model assumes that the rate of sediment erosion, E_S , is proportional to the difference between bottom shear stress (τ_b) and the critical shear stress for sediment erosion (τ_{cr}) [Fagherazzi and Furbish, 2001; Sanford and Maa, 2001]

$$E_S = E_{S0} (\tau_b / \tau_{cr} - 1)^\alpha \quad (5)$$

where E_{S0} is a suitable specific erosion and α ranges between 1 for cohesive sediments and 1.5 for loose sediments.

The model further assumes some prescribed average annual sedimentation rate, D_S , which is site dependent, but yet constant during bottom evolution.

Based on the relationship between shear stress and bottom elevation (Fig. 1), the conceptual model for the morphological development of saltmarshes from tidal flats demonstrates that starting from any initial elevation, the final, equilibrium configuration will be either a salt marsh or a tidal flat deeper than Z_{max} (Fig. 1).

When $Z_b < Z_{c2}$, bed shear stress is smaller than the critical shear stress. In this range of depths we have $E_S = 0$ and $D_S > 0$ and no equilibrium between deposition and erosion is possible. Therefore tidal flats deeper than Z_{c2} evolve toward smaller depths.

For the same reason equilibrium is not possible for $Z_b > Z_{c1}$. In this case deposition will lead to a salt marsh.

Let E_{Smax} be the rate of erosion corresponding to $\tau_b = \tau_{max}$. If deposition is greater than the maximum erosion, i.e. $D_S > E_{Smax}$, then again no equilibrium is possible and vertical accretion of tidal flat eventually will give form to an emergent salt marsh. Once the tidal flat shoals, the accretion dynamics is marginally affected by waves. The main factors determining the final salt marsh elevation are sediment supply, organic production driven by vegetation encroachment [Silvestri et al., 2005], and sediment compaction.

The most interesting range is $\tau_{cr} < \tau_b < \tau_{max}$ and $D_S < E_{Smax}$. In this case a bed shear stress exists such that $E_S = D_S$ and dynamic equilibrium is possible. We refer to this bed shear stress value as 'equilibrium bed shear stress', τ_{eq} (see Fig. 1). The equilibrium bed shear stress marks two points (points U and S) on the curve of Fig. 1. When $\tau_b < \tau_{eq}$ deposition exceeds erosion and the bottom evolves toward higher elevations. On the contrary, when $\tau_b > \tau_{eq}$ erosion exceeds deposition and the bottom evolves toward lower elevations. This behavior is marked with the arrows flowing along the curve in Fig. 1. It is clear that any point S on the right branch of the curve with $Z_{max} < Z_b < Z_{c2}$ is a stable point: any small departure from point S meets conditions that drive back the bottom elevation toward equilibrium. Any point U on the left branch of the curve with

$Z_{c1} < Z_b < Z_{max}$ is an unstable point: any small departure from point U meets conditions that drive the bottom elevation further away from equilibrium.

Therefore, a stable morphodynamic equilibrium is possible in the ranges $Z_b < Z_{c1}$ pertaining to salt marshes and $Z_{max} < Z_b < Z_{c2}$ pertaining to tidal flats.

The presence of an unstable branch in the curve of Fig. 1 (i.e., $Z_{c1} < Z_b < Z_{max}$) is a very reasonable explanation for the reduced frequency of areas at these intermediate elevations.

Fagherazzi et al. [2006] also discuss the case of depth-dependent deposition rate and show that the main conclusions are not altered.

3 Application to the lagoon of Venice

The results of a numerical simulation performed with the wind wave – tidal model are used to test the above conceptual model.

The wind wave – tidal model uses a refined mesh that reproduces the present topography of the Venice lagoon. A real meteorological event (16-17 February 2003) characterized by Bora wind blowing from North-East at an average speed of approximately 10 m/s is simulated. The recorded tidal levels are imposed at the three inlets. These tidal and meteorological conditions are representative of a typical, morphologically significant, stormy condition for the Venice lagoon. Details about the model results are reported by Carniello et al. [2005].

In the discussion we consider the hydrodynamics computed at $t=9.00$ PM of 16 February 2003 when the water level in the sea is approximately 0.2 m a.m.s.l. but the water levels in the lagoon are around 0.0 m a.m.s.l. due to phase lag.

The analysis is restricted to the central-southern part of the Venice lagoon (South of the city of Venice) where the limited marsh area and the few islands allows for the fully development of wave field over most of the domain.

The computed bottom shear stresses are plotted versus bottom elevations in Fig. 2.

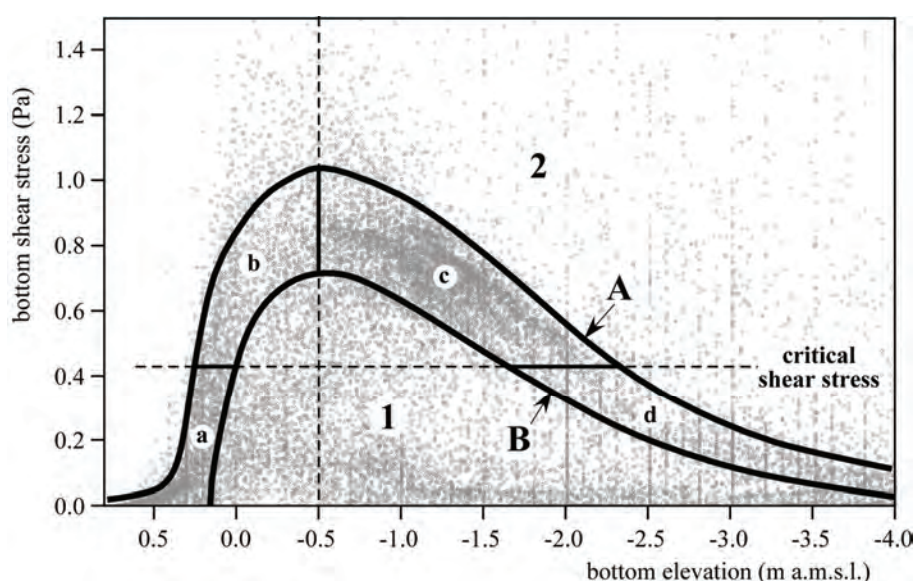


Fig. 2 – Computed bed shear stress distribution as a function of bottom elevation

According to the conceptual model most of the points should fall along the theoretical curve of Fig. 1. Although the points in Fig. 2 display a remarkable scatter, most of them are indeed clustered along a curve similar to the theoretical one.

This is even more evident when the points plotted are grouped into six regions as shown in the same Fig. 2.

Curves A and B in Fig. 2 define a strip approximately following the theoretical curve of Fig. 1. Regions a to d, within the above strip, are bounded by the critical shear stress and the bottom elevation corresponding to the maximum shear stress, Z_{max} .

We also locate the points plotted in Fig. 2 on the map of the Venice lagoon in order to discuss any correlation between the position on the plot and the geographic location.

Points belonging to region 1 have a bottom shear stress considerably lower than the one predicted by the conceptual model. This would be consistent with the theory if the limiting effects of fetch length were considered [Fagherazzi et al., 2006]. Therefore, points with shear stress and depth falling in region 1 are likely to be located leeward to spits, islands or emergent salt marshes where fetch length is considerably shorter than the one required to attain fully developed sea.

Fig. 3A shows an example of the position of all the points belonging to region 1. As expected they lie along the boundaries of the lagoon where the wave field cannot fully develop, and in sheltered areas behind islands and salt marshes where the fetch is limited. Therefore, all these points must be removed from the analysis of the conceptual model.

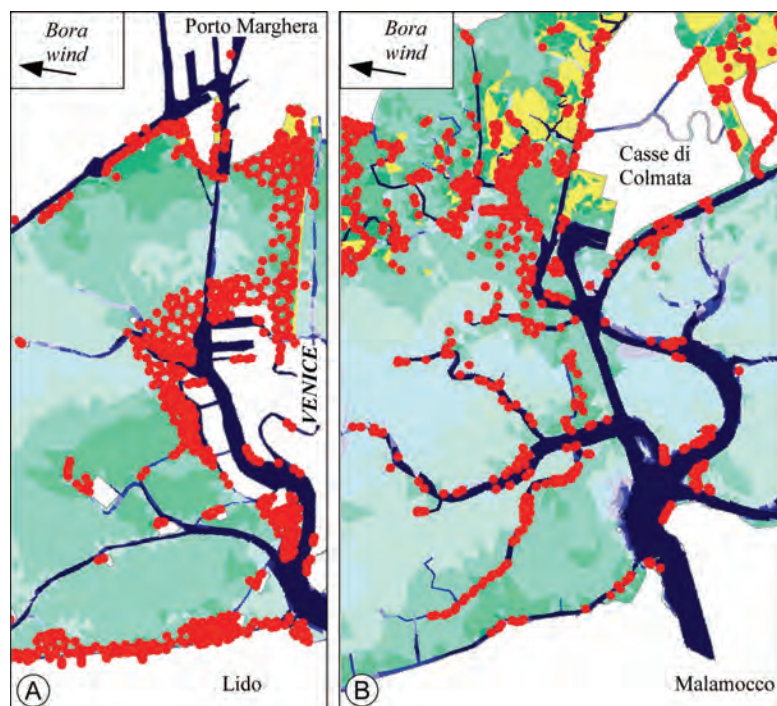


Fig. 3 – Examples of the spatial distribution of basin area following the subdivision indicated in Fig. 2: A) region 1; B) region 2; (each point marks the center of computational elements).

Region 2 comprises points with a bottom shear stress greater than the one predicted by the conceptual model. However, most of these points belong to tidal channels (see an example in Fig. 3B) where tidal flow concentrates and bed shear stress is mainly due to tidal currents rather than to wind waves. All these point are thus beyond the main assumption of the conceptual model and must be removed from the analysis.

The above results demonstrate that only points falling in the strip between curves A and B of Fig. 2 must be considered in the discussion of the conceptual model.

Points in region a are characterized by a bottom elevation higher than mean sea level. Obviously these points are uniformly distributed on salt marshes.

Points in region b belong to the unstable branch of the theoretical curve. According to the conceptual model few points should fall in this unstable region and they should mark areas in transition from tidal flats to salt marshes or vice versa. As expected points in region b are only 9.6% of the total points in the strip. Moreover most of these points are located on tidal flats close to salt marshes edges. Here, the current lagoon morphology is far from being in equilibrium as salt marshes have been reducing their extension during the last century.

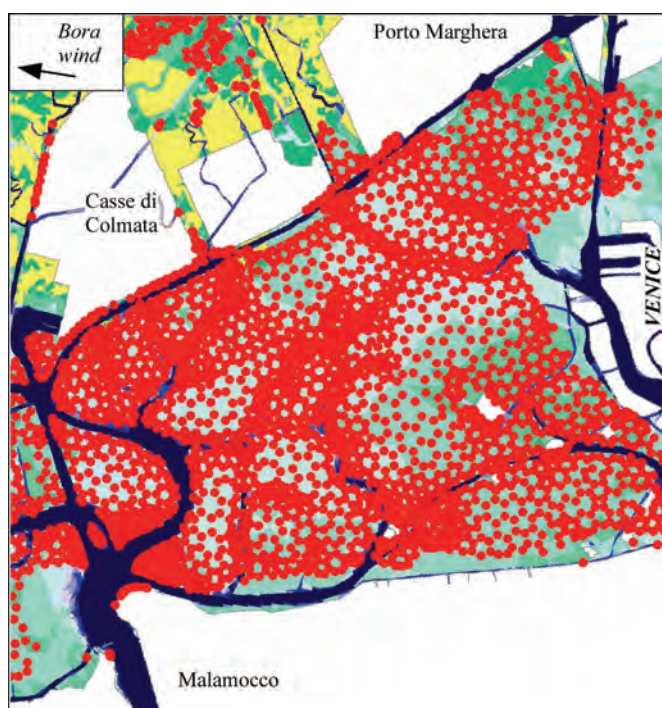


Fig. 4 – Examples of the spatial distribution of basin area following the subdivision indicated in Fig. 2: region c; (each point marks the center of computational elements).

Region c covers the stable part of the theoretical curve. Points in this region are characterized by bottom elevation lower than the curve peak and bottom shear stress higher than the critical shear stress. The conceptual model predicts that points in this region belong to stable tidal flats. Fig. 4 shows an example of the spatial distribution of these points inside the lagoon. They are uniformly

distributed on tidal flats in the central part of the lagoon; only tidal channels, salt marshes and sheltered regions are not covered by points, in agreement with the theoretical predictions. In addition, the morphological stability of region c can also be argued by the large amount of points falling in this region (more than 60% of points in the strip fall into region c). Finally, region d comprises points with a bottom elevation deeper than $-2.00\sim-2.5$ m a.m.s.l.. The conceptual model predicts no stable tidal flats in this region. Here the bottom shear stress is lower than the critical shear stress (i.e., $E_S=0$) and any deposition, however small, would rapidly infill areas deeper than $-2.00\sim-2.5$ m a.m.s.l.. Therefore, points in region d can be either unstable or located in areas beyond the validity range of the model (e.g., tidal channels). Fig. 5 shows that the few points in region d (12.1% of total points in the strip) all belong to tidal channels and must be removed from the analysis.

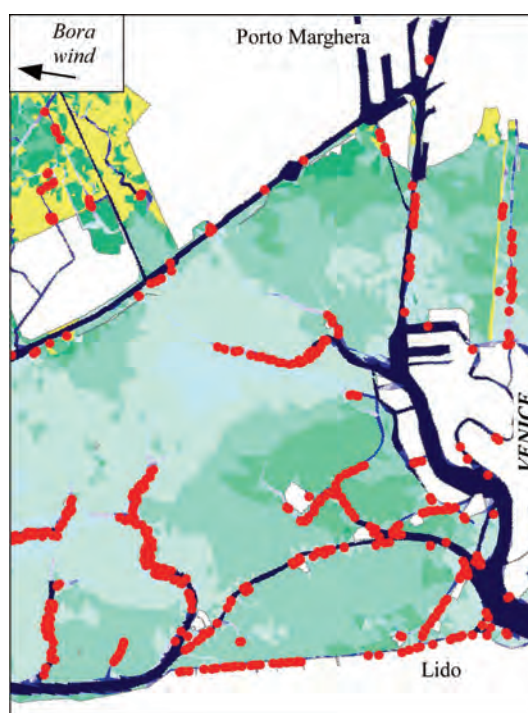


Fig. 5 – Examples of the spatial distribution of basin area following the subdivision indicated in Fig. 2: region d; (each point marks the center of computational elements).

After removing all the points in regions 1 and 2 we evaluate the bottom elevation PDF curve of the central – southern part of the Venice lagoon. The curve, plotted in Fig. 6 (upper panel), clearly shows the minimum corresponding to elevations in the unstable range thus confirming that just a small fraction of the basin is characterized with these intermediate elevations, in agreement with the conceptual model.

A second simulation performed with the wind wave – tidal model uses the topography of the Venice lagoon in 1901. Comparison between 1901 and 2000 bathymetries is shown in the lower panel of Fig. 6. Contrary to present lagoon morphology, in 1901 salt marshes covered most of the basin with a few areas occupied by tidal flats.

The same boundary conditions as in the first simulation are prescribed and the results are analyzed in the same way. After removing all points outside the strip enclosed between curves A and B of Fig. 2, the frequency area distribution curve is obtained and plotted in Fig. 6 where it is compared with the one obtained with present bathymetry.

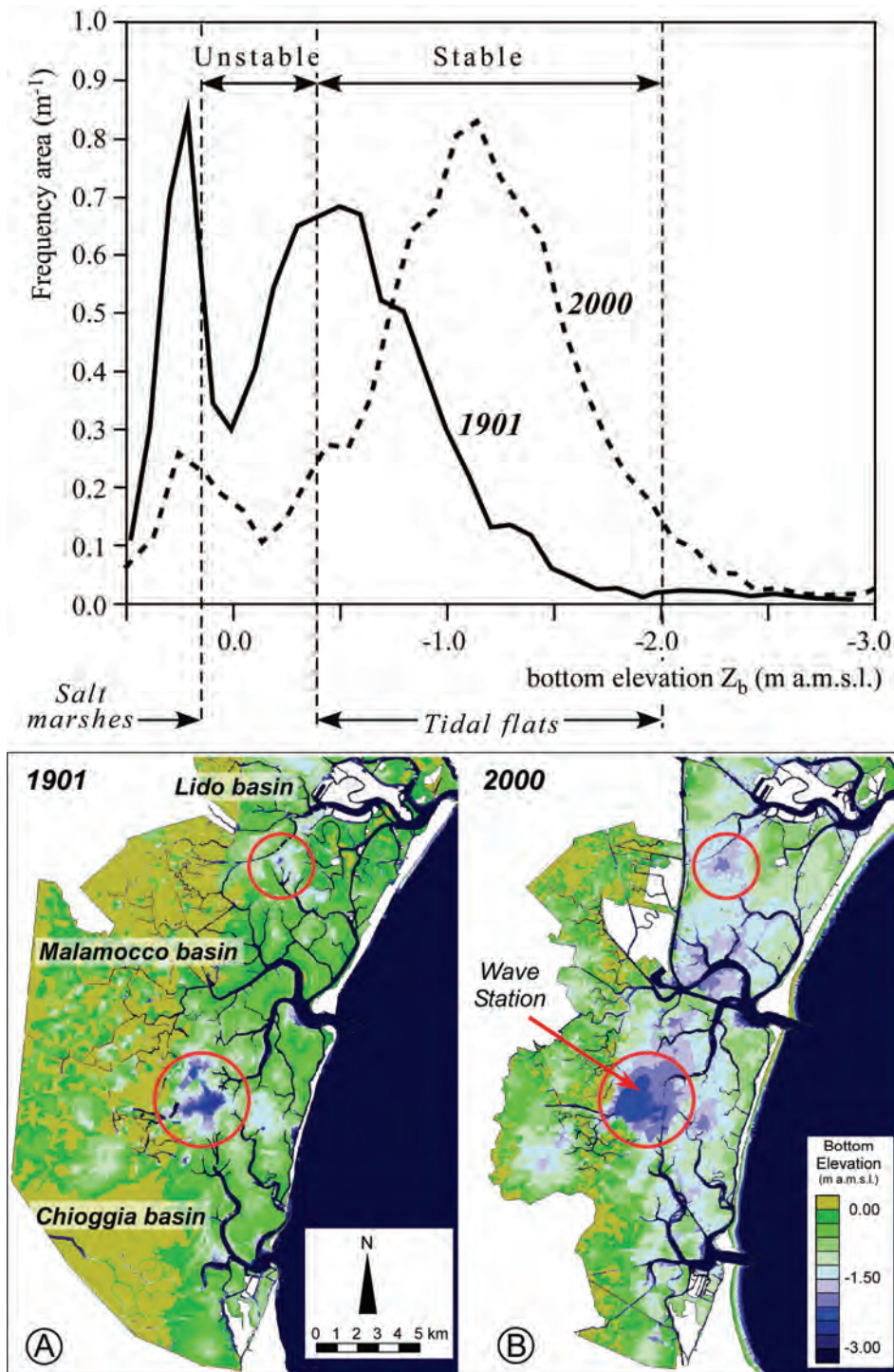


Fig. 6 – Upper panel: frequency area distributions as a function of bottom elevation for the Southern Venice lagoon (1910 and 2000 bathymetries). Lower panel: bathymetry of the Venice lagoon, Italy, in 1901 (left) and in 2000 (right). The elevation is expressed in meters above mean sea level (m a.m.s.l.)

The minimum within the unstable range of elevations is even more clear in 1901 than in 2000. The distribution peak locates near the critical elevation corresponding to the peak in the wave shear stress distribution. According to the conceptual model, this means that the ratio of deposition rate to erosion rate was larger in 1901 than at present.

Conclusions

The distribution of elevations in shallow tidal basins shows that tidal flats lie a few tens of centimeters below the mean sea level whereas salt marshes have an average elevation higher than the mean sea level. Only few areas are located at intermediate elevations, suggesting that the processes responsible for sediment deposition and erosion produce either tidal flats or salt marshes but no landforms located in the above critical range of elevations.

A conceptual model describing this evolutionary trend has recently been proposed. The model demonstrates that areas at intermediate elevations are inherently unstable and tend to become either tidal flats or salt marshes.

In this work, the above conceptual model is validated through comparison with numerical results obtained with a two dimensional wind waves – tidal model applied to the lagoon of Venice. A real tide and measured wind conditions is simulated with the model.

The plot of computed total (currents and waves) bottom shear stress versus bottom elevation shows a remarkable scatter around the theoretical behavior predicted by the conceptual model. However, analysis of spatial distribution of shear stresses demonstrates that points away from the theoretical curve (regions 1 and 2 in Fig. 2) as well as points with a bottom elevation lower than the minimum bottom elevation predicted by the conceptual model for tidal flats (region d in Fig. 2) do not meet model requirements as they are located in tidal channels or in fetch limited areas. It is further shown that all points falling along the stable branch of the curve are indeed tidal flats, while the few points (less than 10% of total) along the unstable branch are located on tidal flats close to salt marshes edges. Here, the present lagoon morphology is far from equilibrium since salt marshes are reducing their extension.

The above analysis is also supported by the bottom elevation PDF curve (Fig. 6) obtained after removing all the points that are beyond the validity range of the conceptual model. The PDF curve clearly shows the minimum corresponding to elevations between tidal flats and salt marshes.

The above conclusions are further supported by the results of the second numerical simulation which uses the 1901 bathymetry of the Venice lagoon characterized by a very different morphology with salt marsh area much larger than at present.

References

- Allen, J.R.L., 2000. Morphodynamics of Holocene saltmarshes: a review sketch from the Atlantic and Southern North Sea coasts of Europe. *Quaternary Science Reviews*, 19, 1151-1231.
- Allen, J.R.L., Duffy, M.J., 1998. Medium-term sedimentation on high intertidal mudflats and salt marshes in the Severn Estuary, SW Britain: the role of wind and tide. *Marine Geology*, 150(1-4) p. 1-27
- Beeftink, W.G., 1966. Vegetation and habitat of the salt marshes and beach plains in the south-western part of The Netherlands. *Wentia* 15, p. 83-108
- Carniello, L., A. Defina, S. Fagherazzi, and L. D'Alpaos, 2005. A combined wind wave-tidal model for the Venice lagoon, Italy. *Journal of Geophysical Research – Earth Surface.*, Vol. 110, F04007 doi: 10.1029/2004 JF000232.
- Defina, A., L. D'Alpaos, and B. Matticchio, 1994. A new set of equations for very shallow water and partially dry areas suitable to 2D numerical models, in *Proceedings of the Specialty Conference on "Modelling of Flood Propagation Over Initially Dry Areas"*, Milan (Italy) 29 June -1 July 1994, edited by P. Molinaro and L. Natale, 72-81.
- Defina, A., 2000. Two Dimensional Shallow Flow Equations for Partially Dry Areas. *Water Resources Research*, vol.36, 11, 3251-3264.
- Dijkema, K.S., 1987. Geography of salt marshes in Europe. *Zeitschrift fur Geomorphologie*, 31 p. 489-499
- D'Alpaos, L. and A. Defina, 1993. Venice lagoon hydrodynamics simulation by coupling 2D and 1D finite element models, *Proceedings of the 8th Conference on Finite Elements in Fluids. New trends and Applications*, Barcelona (Spain), 20-24 September 1993, p. 917-926.
- D'Alpaos, L. and A. Defina, 1995. Modellazione matematica del comportamento idrodinamico di zone a barena solcate da una rete di canali minori, *Rapporti e Studi, Ist. Veneto di Scienze, Lettere ed Arti*. XII, p. 353-372.
- D'Alpaos, A., Lanzoni, S., Mud, S.M., and S. Fagherazzi, 2006. Modelling the influence of hydroperiod and vegetation on the cross-sectional formation of tidal channels. *Estuarine Coastal and Shelf Sci.* In Press
- Fagherazzi, S., Bortoluzzi, A., Dietrich, W.E., Adami, A., Lanzoni, S., Marani, M., and Rinaldo, A., 1999. Tidal networks 1. Automatic network extraction and preliminary scaling features from Digital Elevation Maps. *Water Resources Research*, 35(12), p. 3891-3904
- Fagherazzi, S., and Furbish, D.J. (2001), On the shape and widening of salt marsh creeks. *Journal of Geophysical Research-Oceans*, 106(C1), p. 991-1003.
- Fagherazzi, S., D'Alpaos, L., Carniello, L. and A. Defina, 2006. Critical bifurcation of shallow microtidal landforms in tidal flats and salt marshes. *Proceedings of the National Academy of Sciences (PNAS)* vol. 103, no. 22,

8337-8341.

French, J.R., and Stoddart, D.R., 1992. Hydrodynamics of salt-marsh creek systems – implications for marsh morphological development and material exchange. *Earth Surface Processes and Landforms*, 17(3), p. 235-252.

Hasselmann, K., T.P. Barnett, E. Bouws, H. Carlson, D.E. Cartwright, K. Enke, J.A. Ewing, H. Giennapp, D.E. Hasselmann, P. Kruseman, A. Meersburg, P. Muller, D.J. Olbers, K. Richter, W. Sell, and H. Walden, 1973. Measurements of wind-wave growth and swell decay during the Joint North Sea Wave Project (JONSWAP), *Dtsch. Hydrogr. Zeit. Suppl.*, 12(A8), 1-95.

Marani, M., Belluco, E., D'Alpaos, A., Defina, A., Lanzoni, S., Rinaldo, A., 2003. On the drainage density of tidal networks. *Water Resources Research*, 39(2), 105-113.

Rinaldo, A., Fagherazzi, S., Lanzoni, S., Marani, M., Dietrich, W.E., 1999a. Tidal networks 2. Watershed delineation and comparative network morphology. *Water Resources Research*, 35(12), 3905-3917.

Rinaldo, A., Fagherazzi, S., Lanzoni, S., Marani, M., Dietrich, W.E., 1999b. Tidal networks 3. Landscape-forming discharges and studies in empirical geomorphic relationships. *Water Resources Research*, 35(12), 3919-3929.

Sanford L.P., and Maa J.P.Y., 2001. A unified erosion formulation for fine sediments. *Marine Geology* (1-2): p. 9-23.

Silvestri, S., A. Defina, and M. Marani, 2005. Tidal regime, salinity and salt marsh plant zonation. *Estuarine Coastal Shelf Sci.* 62,119-130, doi:10.1016/j.ecss.2004.08.010

Soulsby, R.L., 1995. Bed shear-stresses due to combined waves and currents. In: Stive, M.J.F., Fredsoe, J., Hamm, L., Soulsby, R.L., Teisson, C., Winterwerp, J.C. (Eds.), *Advances in Coastal Morphodynamics*. Delft Hydraulics, Delft, pp. 4-20 - 4-23.

Soulsby, R.L., 1997. *Dynamics of marine sands. A manual for practical applications*. Thomas Telford Ed. 248 pp.

MORPHODYNAMICS OF MEANDERING TIDAL CHANNELS

Valeria Garotta¹ and Giovanni Seminara¹

1 Dipartimento di Ingegneria Ambientale, Università degli Studi di Genova

Riassunto

I canali a marea in estuari e lagune hanno tipicamente un andamento meandriforme. A differenza dei meandri fluviali, i meandri dei canali a marea non sono stati oggetto di ricerche sistematiche. In particolare, i processi morfodinamici che li caratterizzano, attendono ancora di ricevere definitive interpretazioni. Risultati teorici suggeriscono che, in una sequenza di meandri a marea sinusoidali in cui il moto possa ritenersi pienamente sviluppato, le oscillazioni associate alla marea danno luogo ad oscillazioni della posizione delle barre di deposito, simmetriche rispetto all'apice della curva. Inoltre, la topografia del fondo raggiunge asintoticamente una configurazione di equilibrio morfodinamico, mediata su un ciclo di marea.

Al fine di approfondire la comprensione del processo per cui, in un canale meandriforme a marea di dimensioni finite, si forma una successione di barre di scavo e deposito, è stato realizzato un modello fisico costituito da una sequenza di cinque meandri ad andamento sinusoidale della linea d'asse, di larghezza pari a 0.4 m. Il canale era lungo 21.3 m, chiuso ad un estremo e connesso all'altro estremo con un bacino, che simulava il mare, dove veniva generata un'onda di marea. L'evoluzione del pattern di scavi e depositi indotti dalla presenza della curvatura, è stata monitorata nel corso di un lungo esperimento, durato circa 400 h, corrispondenti a circa 11 anni nel prototipo.

Le osservazioni hanno confermato le previsioni teoriche, cioè il raggiungimento di una configurazione di quasi-equilibrio del profilo medio del fondo del canale, caratterizzata da un profondo scavo in corrispondenza della bocca e dalla graduale formazione di un'area emersa all'estremità di terra. Il pattern delle barre forzate era in fase con la curvatura soltanto nel tratto interno del canale. Al contrario, nel tratto verso mare si riscontrava la formazione di depositi lungo la sponda esterna e scavi lungo la sponda interna, una configurazione che in natura sarebbe planimetricamente instabile. Si suggerisce che quest'ultimo risultato possa interpretare l'osservazione secondo cui il tratto a mare dei canali mareali ha spesso andamento quasi rettilineo.

Dai rilievi della topografia del fondo nel bacino eseguiti nel corso dell'esperimento, è stato possibile riconoscere la formazione di un 'ebb-tidal delta', le cui dimensioni sono andate crescendo con il procedere della sperimentazione.

Abstract

Tidal channels in estuaries and lagoons exhibit typically a meandering pattern. Unlike fluvial meanders, tidal meanders have not been the subject of an extensive research. In particular, their morphodynamics still awaits to be fully explored. Theoretical findings suggest that in a fully developed sequence of 'sine generated' tidal meanders, oscillations associated with the basic flow give rise to symmetric oscillations of the bar-pool pattern around the locations of maximum curvature, with no net bar migration in a tidal cycle. Moreover, bottom topography reaches eventually a state of morphodynamic equilibrium, averaged over a tidal cycle.

In order to shed further light on the process whereby the bar-pool pattern of tidal meanders establishes in a spatially confined configuration, a physical model has been constructed, consisting of a sequence of five sine generated meanders with constant width of 0.4 m. The channel was 21.3 m long, closed at one end and connected at the other end with a basin, representing the sea, where a tidal oscillation was generated. We have performed surveys of the bar-pool pattern forced by channel curvature throughout the course of a long experiment lasted about 400 h, corresponding to about 11 years in the real world.

Observations have confirmed the theoretical expectations, namely the development of a quasi equilibrium pattern of the average bed profile, showing deep scour at the inlet and the eventual formation of a shore landward. Also, the bar - pool pattern was in phase with curvature only in the inner portion of the channel. On the contrary, the seaward pattern displayed deposition at the outer bends and scour at the inner bends, a pattern which would clearly be planimetrically unstable. We suggest that the latter finding explains why the seaward portions of tidal creeks are often nearly straight.

The inlet bed topography has also been analyzed, showing the presence of an ebb-tidal delta growing throughout the experiment.

1 Introduction

Meandering channels are ubiquitous in tidal environments. Before we discuss the physical processes associated with channel curvature, let us briefly recall some recent results concerning straight tidal channels. The issue of whether tidal channels may reach an equilibrium bed profile has been tackled theoretically by *Schuttelaars and De Swart (1996, 2000)* and by *Lanzoni and Seminara (2002)*. Controlled laboratory experiments have been carried out by *Tambroni et al. (2005)*. The latter authors have shown that straight tidal channels closed at one end, do indeed evolve towards an equilibrium configuration, slightly concave seaward and convex landward, in accordance with the theoretical predictions of *Lanzoni and Seminara (2002)*. The effect of channel convergence, a feature typically observed in nature, on the morphodynamic equilibrium of the bottom profile has also been investigated.

Tidal meanders modify the lateral structure of bed topography significantly.

They display some similarities with river meanders (Marani et al., 2002), in particular they exhibit the formation of deposition (point bars) at the inner bends and scour (pools) at the outer banks. In the wide literature developed for the fluvial case, it has been clarified that these sequences of bars and pools are almost steady features, which propagate at the very slow time scale associated with the plan form evolution of the meandering pattern, migration rates being typically of the order of meters per year. Essentially, the formation of the bar-pool pattern is due to a secondary flow which affects the trajectory of sediment particles.

In a constant curvature channel, far enough from the bend entrance for the flow to be fully developed, the secondary flow is centrifugally driven. In fact, a centripetal force is required for fluid particles to follow curvilinear trajectories and this should be provided by the lateral pressure gradient: however, the former increases from the bottom to the surface, while the latter maintains a constant value along the vertical coordinate. This unbalance drives a secondary flow directed inwards close to the bed and outwards close to the free surface, with a vanishing depth average. The tangential forces associated with the secondary flow lets the trajectory of sediment particles deviate from the longitudinal direction. An equilibrium lateral bed slope is achieved when the this drag force is balanced by the (stabilizing) tangential component of gravity acting on sediment particles, which would tend to move them downhill.

A further component of secondary flow is driven by longitudinal variations of channel curvature. A shoaling effect arises whereby flow deviates towards pools: in other words, momentum is transferred from each pool to the next one, an effect which further enhances lateral bed load transport. As a result, an additional contribution to the lateral bed slope arises: the phase lag of the bar pool pattern relative to curvature depends on the meander wavenumber and on the aspect ratio of the channel. The lateral bed slope is further enhanced by the presence of suspended load.

Solari et al. (2001) and *Solari and Toffolon (2001)* have recently proposed theoretical models for flow and bed topography in a tidal meandering channel. They found that a symmetrical tidal wave gives rise, through a transient process, to an equilibrium bar-pool pattern characterized by relatively small symmetrical spatial oscillations throughout the tidal cycle. The average equilibrium topography has amplitudes of the point bar comparable with the mean flow depth.

The aim of the present experiments is two-fold:

on one hand, we wish to determine the structure of the bar-pool pattern associated with a sequence of meanders subject to the propagation of a tidal wave: the finite length of the channel will be seen to give rise to spatial variations of the pattern displaying interesting features;

on the other hand, we wish to evaluate the role of channel curvature on the cross sectionally averaged bed profile at equilibrium.

Besides its obvious geomorphic interest, the practical relevance of the problem

is related to the ability to predict bend scour in tidal settings.

The plan of the paper is as follows. A brief description of the experimental apparatus is presented in section 2. Results concerning the morphodynamic evolution of the bed topography in the channel and in the inlet region are discussed in section 3. Finally, some remarks follow in the last section.

2 Experimental Apparatus

Experiments must reproduce various ingredients of a real tidal system. The first ingredient is the mode of sediment transport. Below, we assume cohesionless sediments, an assumption suitable e.g. for the larger channels of Venice Lagoon. Moreover, we assume the size of sediments in the prototype to be in the range of fine sands, such that transport occurs both as bed load and as suspended load. The second ingredient is the geometry of tidal channels: in nature, they are typically landward convergent and meandering. The experiments discussed herein were performed on a meandering channel with constant width. The third ingredient to be reproduced is the forcing effect of the sea at the channel inlet which sets the hydrodynamic boundary condition for the tidal wave propagating through the channel. The ability of the sea to exchange sediments with the channel through the inlet is determined by the geometry of the latter. The value of the sediment concentration in the far field, which is affected by the wave climate, may also play some role. However, this cannot be readily reproduced in the laboratory and will be disregarded in the present experiments. A further ingredient is important in nature, namely the presence of tidal flats adjacent to the channel: for the time being we will ignore this feature, though it affects both the hydrodynamics of tide propagation and the sediment balance in the main channel. While it will not be too hard to model the former effect in future extensions of the present work, (see the works of *Friedrichs and Aubrey [1988]* and *Speer and Aubrey [1985]*) the exchange of sediments between the channel and the adjacent flats is crucially dependent on particle resuspension typically driven in nature by the action of wind waves, a delicate mechanism which is not easy to reproduce in the laboratory. Finally, the presence of small and large scale bed forms must also be included in the experiments as they may affect the net transport of sediments and consequently the establishment of an equilibrium morphology.

Taking into account the constraints posed by the cited requirements, experiments were carried out on a large indoor platform above which a meandering channel was built using zincked plate. The concrete platform had a weak longitudinal upslope of about 10^{-3} . The Cartesian length of the channel was 21.3 meters. Moreover the channel was 0.4 meters wide, closed at one end and connected at the other end to a rectangular basin (2.23 m wide and 6.5 m long) representing the sea. The flume was composed of a sequence of five meanders with intrinsic wavelength L_s^* of 4 meters, connected at each end to a straight reach 1 meter long. In order to simplify the drawing of the channel and the data flow between the intrinsic curvilinear coordinate system (s^*, n^*) and the Cartesian system (x^*, y^*) , we chose a pattern for the channel axis, following the law $y^*(x^*) = A^* \sin(\lambda_x^* x^*)$, with an amplitude of the sinusoidal curve A^* of 0.35

meters, and a Cartesian meander wavenumber λ_x^* taking the value 1.7 m.

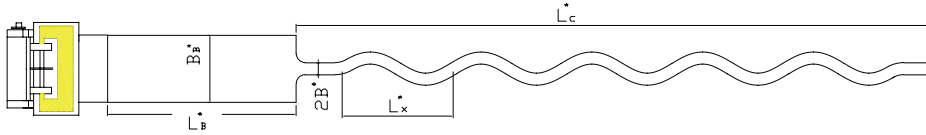


Figure 1. Sketch of the experimental apparatus and notations.

The walls of the inlet were rounded off, in order to reduce the scour depth. Figures 1 and 2 show a sketch and a picture of the model, respectively.



Figure 2. View of the physical model from the landward end

Finally, an oscillating discharge was supplied to the basin from a tank where the apparatus for tide generation was installed. The latter consisted of a cylinder set in motion by a piston held by a steel frame and controlled by an oleodynamic mechanism driven by a control system, which generated the desired law of motion. Such a law was first predicted theoretically by solving the differential equation:

$$S^* \frac{dh^*}{dt^*} = -\Omega_C(z^*) \frac{dz^*}{dt^*} + Q_{channel}^* \quad (1)$$

where S^* is the area of the free surface of the basin, h^* is the water surface elevation, Ω_C is the area of the intersection between the floating cylinder and the free surface of the basin, z^* is the elevation of the cylinder axis, t^* is time and $Q_{channel}^*$ is the flow discharge entering the basin through the channel inlet. The equation (1) was solved numerically for $z^*(t^*)$ assuming the desired law $h^*(t^*)$ for the free surface oscillation in the basin, namely:

$$h^*(t^*) = a_0^* \sin(2\pi t^* / T) \quad (2)$$

with T tidal period and a_0^* amplitude of the tidal wave.

A layer of cohesionless granular material of sufficient thickness was laid on the bottom of both the flume and the basin. The granular material was then laid on the bottom, such to have a uniform level, thick enough to prevent that the scour depth might reach the apron. Following the upslope of the concrete platform on which the channel was built, a weak slope (10^{-3}) was given to the initial bed. The granular material was chosen light enough to be entrained in suspension throughout most of the tidal cycle with the values of friction velocity typically generated in the present experiments. The final choice was to use polycarbonate grains, characterized by a density of 1.27 t/m^3 and median grain size $d_s^* = 0.15 \text{ mm}$.

The bed topography was measured at some significant stages of the experiment by a Laser sensor. In order to avoid possible artificial changes in bed topography driven by the operation of removing water, measurements were carried out with water. This has required a calibration of the instrument, in order to introduce a correction accounting for the refraction angle due to the presence of water.

Scanning of the bed topography was performed along the channel and in the basin in a sequence of cross-sections 5 cm distant from one another. The lateral step of the measuring points was 0.2 cm. In order to analyze the pattern of small-scale bed forms, a more detailed survey of bottom elevation was also carried out, the longitudinal scanning step being 1 cm. The migration of such bed forms at a given channel cross-section was monitored in time by a profile indicator, consisting of a probe which keeps at a fixed distance from the bed.

3 Experimental Results

Let us now proceed to discuss the experimental results concerning the morphodynamic evolution of the channel and of the inlet region. Concerning the channel topography, we will start analyzing the macro scale features, namely the laterally averaged bed profile and then discuss the characteristics of meso-scale bed forms, namely the bar-pool pattern. Finally the features of bed topography in the inlet region will be analyzed.

3.1 Evolution of the bed profile

Let us first outline a few significant observations on the morphodynamic evolution of the bed profile.

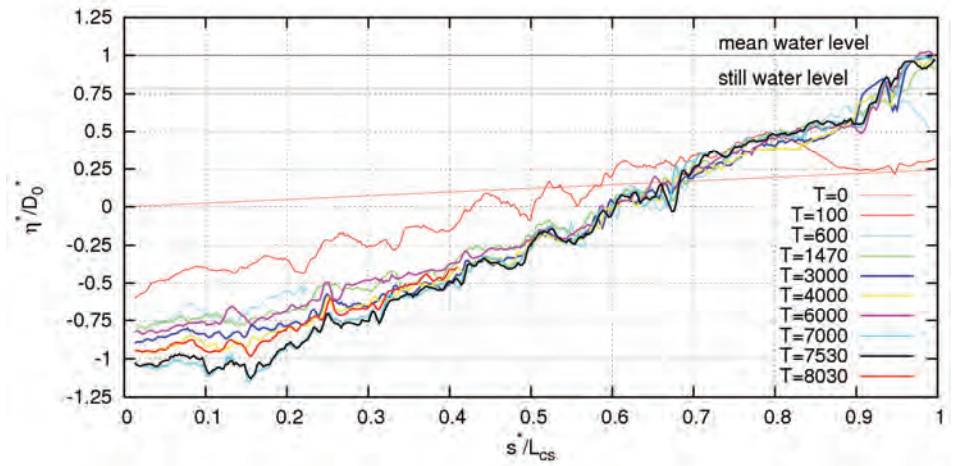
The ability of the bottom profile to reach an asymptotic equilibrium configuration was verified in the experiments of *Tambroni et al. (2005)*, carried out on a straight channel with constant width and then extended to a rectilinear convergent channel. In the present experiment, the flood dominant character of

the tidal wave in the initial stage (displayed by peak velocities higher during the flood phase than during the ebb phase, and high-water period shorter than low-water) affects the evolution of the bed profile. In fact, as a consequence of flood dominance a net sediment flux directed landward arises. Sediments are then eroded in the seaward portion of the channel, driven landward, and deposited in the inner reach. In particular, a fairly sharp front develops in the bed profile, which migrates landward. The temporal evolution of the laterally averaged bed profile is plotted in Figure 3, where D_o^* is the mean flow depth at the channel mouth at the beginning of the experiment, η^* is the local and instantaneous value of the average elevation of the bed and s^* is the landward oriented intrinsic coordinate measured along the channel axis, with origin located at the channel inlet. The bed profile evolves starting from an initial configuration characterized by a fairly weak upslope (10^{-3}). Since the very beginning of the experiment (say 100 cycles), a deep scour is observed at the channel mouth. Note that the scour depth at the channel inlet evolves throughout the experiment, finally reaching a quasi equilibrium value of the order of the initial mean flow depth D_o^* after 8000 tidal cycles. At the inner end of the channel, the sediment front, which develops quite rapidly, grows and migrates landward, reaching the channel end. Proceeding with the experiment, a wet and dry region forms and the depositional area grows until the bed elevation reaches the mean water level. Note that the bottom profile in the inner portion of the channel reaches a quite stable state after about 1500 tidal cycles: no qualitative changes are observed thereafter. On the contrary, the seaward portion of the channel displays an oscillatory behaviour. In fact, for about 4000 tidal cycles erosion occurs in this region; the survey performed after 6000 tidal cycles shows an opposite trend. At 7000 cycles, erosion is again observed in the seaward reach. The last survey at 8000 cycles displays deposition. In other words, while the bed reaches an equilibrium state in the landward portion of the channel, in the seaward reach the laterally averaged bed profile still exhibits a weak oscillatory behaviour.

The small scale oscillations displayed by the bed profile in the laboratory are associated with the presence of small-scale bed forms. Larger scale fluctuations occur on the meander scale. These oscillations of the bed profile, particularly intense in the initial stage of the experiment (say after 100 cycles), are presumably driven by the tendency of the bed topography to adapt to the spatial variations in sediment flux associated with channel curvature. In particular, the channel width being fixed, the system chooses to vary the local bed slope in order to accommodate the required sediment transport. The mechanism looks similar to that studied by *Solari and Seminara (1998)* for steady flow in a constant curvature channel: the deformation of the cross section displays scour at the outer bend and deposition at the inner bend, hence the Shields stress in the outer portion of the cross section is larger than in a straight channel with equal flow and sediment fluxes, while the opposite occurs in the inner region. The resulting increase in sediment transport can only be balanced by a reduction of bed slope in the downstream curved reach. In our case, the curvature is not constant, hence the local bed slope must experience spatial

changes on the length scale of a meander.

Figure 3. Temporal evolution of the laterally averaged bed profile along the channel

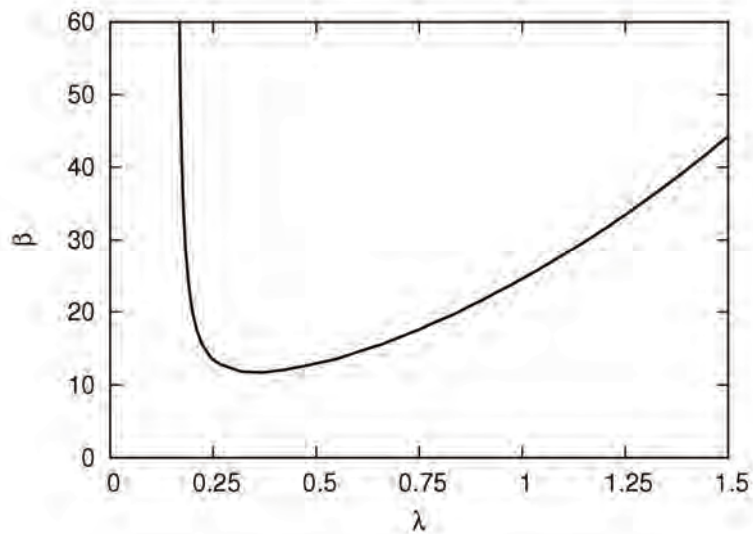


3.2 Evolution of the bar-pool pattern

We now proceed to examine the meso-scale patterns observed during the experiments. The geometry of the model and the initial water depth were not such to allow for the formation of free bars. In fact, the theoretical model developed by *Garotta et al. (2006)* (figure 4) shows that incipient formation of such bed forms occurs for values of the aspect ratio β larger than the one experienced in the initial stage of the experiment.

Moreover, if one assumes that the validity of the experimental results of *Kinoshita and Miwa (1974)* concerning the threshold curvature for suppression of alternate bar migration in steady fluvial bends, can be extended to tidal meanders, then the bend angle at the apex in our model largely exceeds the critical value for free bar suppression.

Figure 4. Marginal stability curve for alternate bars, predicted by the theoretical model of *Garotta et al. (2006)* for the values of the relevant parameters experienced in the initial stage of the experiment.



Let us now discuss the evolution of the bar-pool pattern driven by channel curvature. In the initial stage of the experiment a phase lag between scour and curvature was observed along most of the channel. This is shown in the first plot of Figure 5, which represents the bed elevation along the channel after filtering the averaged bed profile out. After 100 tidal cycles deposition has been observed at the outer bend, especially in the seaward portion of the channel. Proceeding with the experiment, the deposits located in the outer region of the bends have been partially eroded. On the other hand, the bar-pool pattern in the inner reach of the channel seems to reach a stable configuration, with scours located at the outer bend and depositions at the inner bend. On the contrary, the seaward half of the channel displays a bar-pool pattern out of phase with respect to channel curvature.

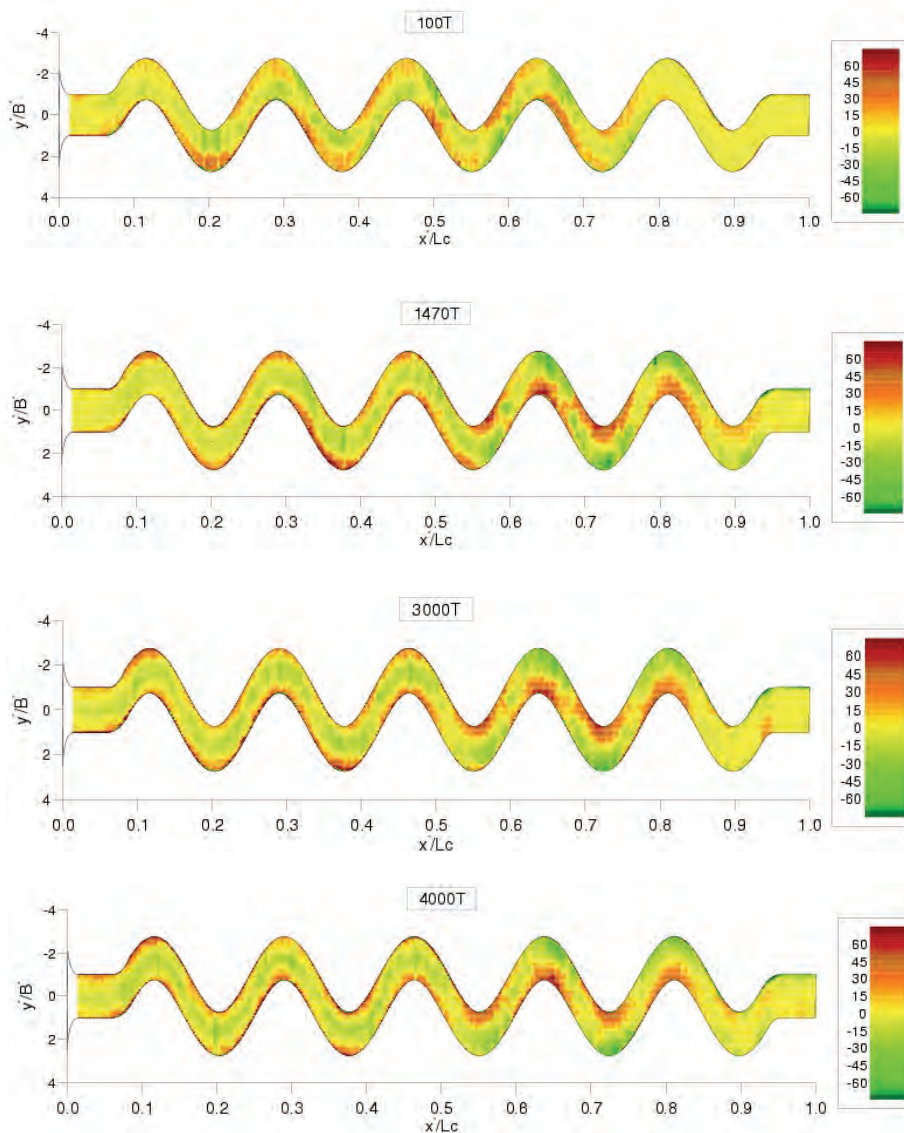


Figure 5. Evolution of bed topography showing the bar-pool pattern after 100, 1470, 3000 and 4000 tidal cycles. Note that the laterally averaged bed profile has been filtered out. Bottom elevation is expressed in mm, with positive values corresponding to depositional areas.

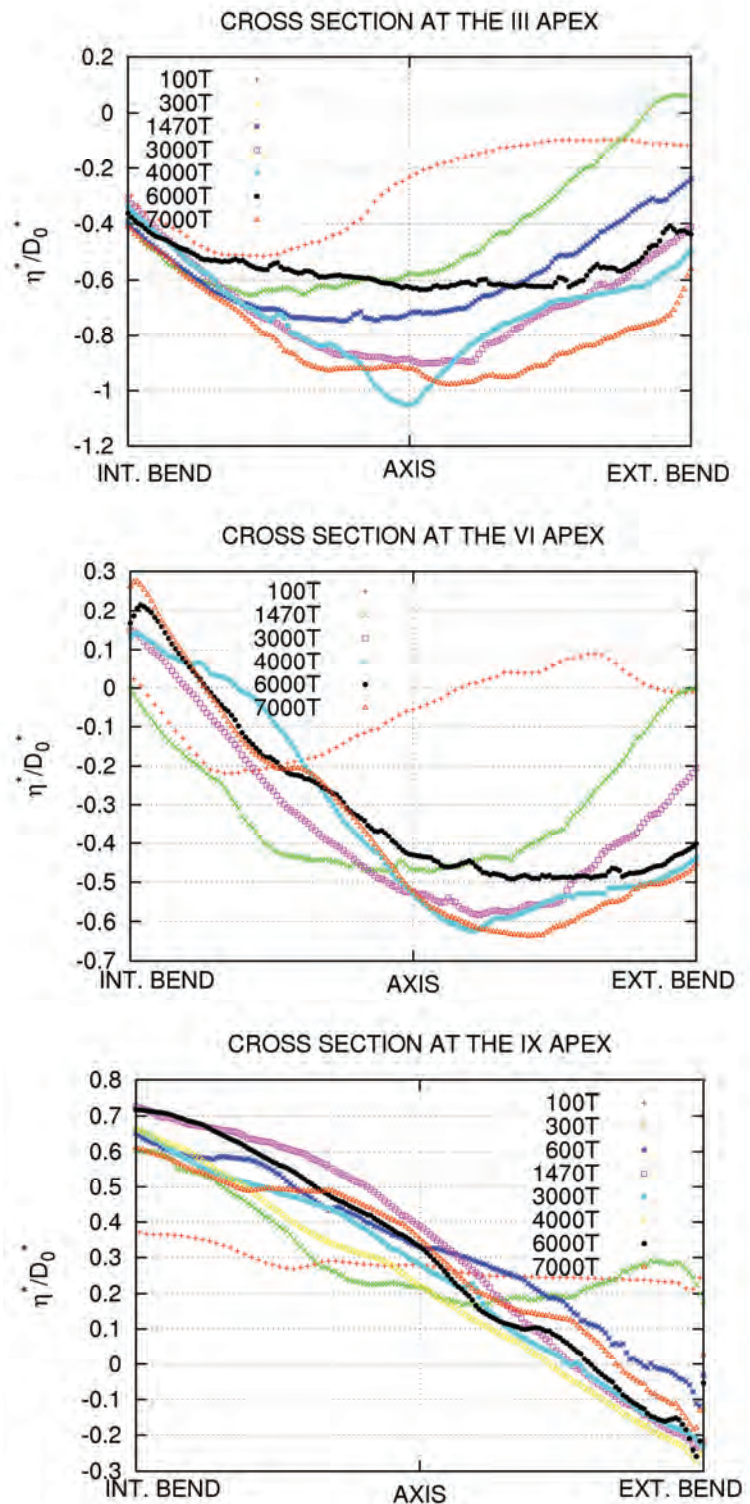


Figure 6. Temporal evolution of some channel cross-sections located at the apex of different meanders (numbering starting from the inlet). Bottom elevation is scaled by the initial flow depth.

Figure 6 shows the shape of the cross-sections located at the apexes of some meanders. In the seaward portion of the channel (see the first plot) the cross-section evolves towards a configuration typically observed in rectilinear channels, the maximum depth being located in the central region. On the contrary, the landward half of the channel shows, in the final stage of the

experiment, cross-sections with typical shapes of meandering channels, deposition being located at the inner bend and scour occurring in the outer portion. An interesting feature arises in the cross-section located at the VI apex: the bed topography changes significantly during the experiment. Starting from an initial configuration (after 100 cycles) characterized by scour at the inner bend, it evolves assuming a symmetrical shape and finally reaching a configuration typically observed in fluvial meanders (after 4000 cycles). The inner portion of the channel is characterized by a faster evolution. In fact, note that in the cross-section located at the IX apex, the bar-pool pattern is in phase with curvature after 600 tidal cycles. The final amplitude of the bar-pool pattern in the cross-sections located in the inner reach of the channel is of the order of the initial mean flow depth at the channel inlet.

The observed tendency of the bed topography in the seaward portion of the channel, namely to evolve towards a configuration typical of rectilinear reaches, is suggestive of a strong influence of the boundary condition at the inlet, which appears to force a spatial transient whereby the fully developed meander pattern develops in the inner portion of the channel. Moreover, it may provide an explanation of the observation that tidal channels in nature are rarely curved close to the inlets. In fact, our observations suggest that a meandering pattern in this region would likely be a planimetrically unstable configuration. In Figure 7 we report an aerial picture of China Camp Marsh in the San Francisco Bay (CA): note that in many creeks, the sinuous pattern is preceded by a rectilinear reach.

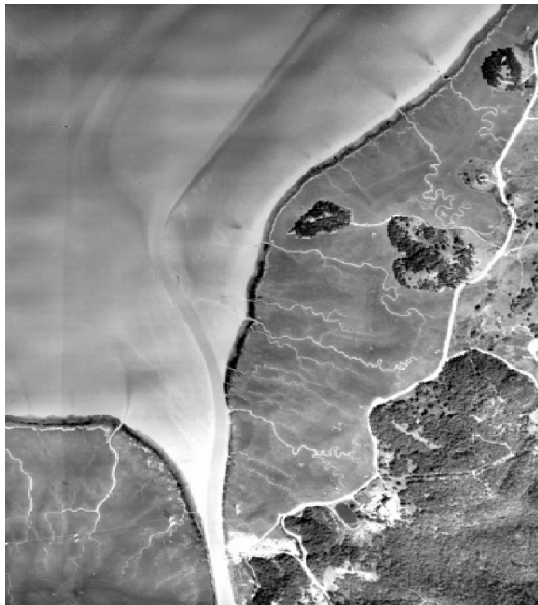


Figure 7. An aerial image of China Camp Marsh in the San Francisco Bay (CA), showing the presence of several tidal creeks displaying a quasi rectilinear pattern of the channel axis in the seaward reach.

Such a tendency may be enhanced by the fact that the aspect ratio β in this region takes very small values: in the initial stage of the experiment $\beta \approx 2$, while in the advanced stage of the morphodynamic evolution $\beta \approx 1$. These values are small, compared with those of channels furrowing tidal flats, characterized by typical values of β falling in the range 5-10. The laboratory model is much more

representative of a salt marsh channel, where β takes typical values in the range 2-5 (Marani et al., 2002). On the contrary, the inner portion of the channel is characterized by higher values of the aspect ratio, e.g. the cross-section located at $s^*/L_{cs}^* = 0.8$, where $\beta \approx 7$.

3.3 Morphodynamic evolution of the inlet region

In nature, significant portions of the inhabited coastlines are bounded by confined embayments, connected to the adjacent sea/ocean through inlets interrupting sequences of barrier islands parallel to the coast (Davis, 1996). Tidal inlets allow tidal currents to exchange water and sediments. Seaward to the inlet, the bottom topography is often characterized by the formation of a so called ebb-tidal delta, where sediments unable to re-enter the lagoon due to the asymmetric nature of the flow field, are stored. Often, the strength of the littoral currents is such to move the ebb-tidal delta alongshore some distance from the inlet.

The present laboratory work is able to reproduce the formation of an ebb-tidal delta (Figure 8).

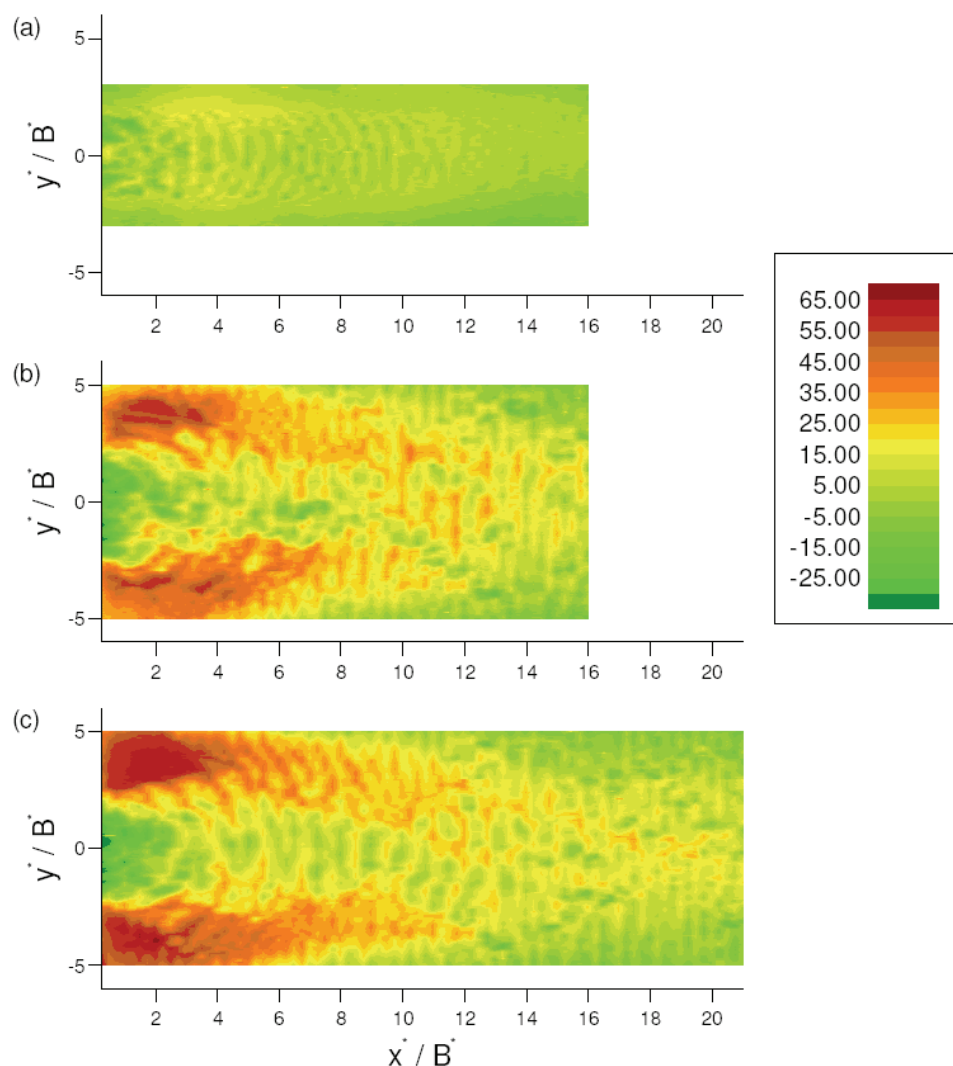


Figure 8. Evolution of the pattern of bed topography measured in the laboratory basin at different times. (a) $t^* = 100 T$. (b) $t^* = 3000 T$. (c) $t^* = 6000 T$. Bottom elevation is expressed in mm, with positive values corresponding to depositional areas.

From the very beginning of the experiment, sediments eroded close to the inlet, in the channel as well as in the sea basin, deposit in the central region of the latter, the initial width of the deposition area being approximately coincident with the channel width. Proceeding with the experiment, the extension of the ebb-tidal delta grows, both in the longitudinal and lateral directions. Scour spits are also formed in the central region of the basin: they eventually develop into a submerged channel. Along the seaward side of the barriers, i.e. along the walls of the basin adjacent to the inlet, two swash bars form, a feature typically observed in nature (see Figure 9).

The absence of a littoral current in the laboratory model does not allow the ebb-tidal delta to attain an asymmetric shape. The field measurements recently carried out by Amos et al. (2005) in the Venice Lagoon have shown the presence of an ebb-tidal delta outside the Lido inlet, inclined towards the direction of the main littoral current.

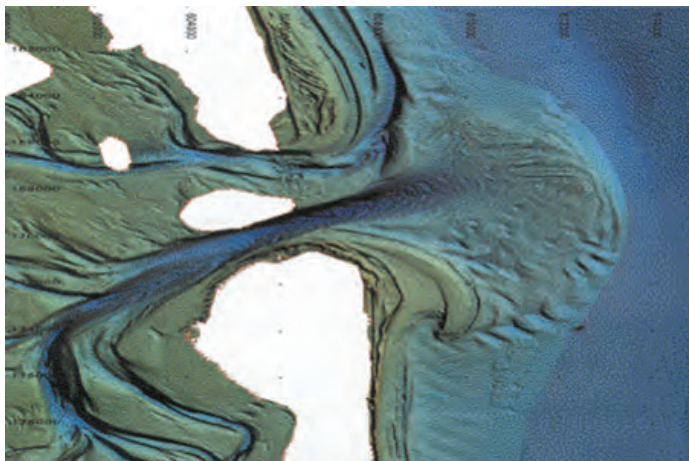


Figure 9. The Frisian Inlet in the Dutch Wadden Sea. Note the presence of an ebb-tidal delta

Conclusions

Results of the present experiment show that a tidal meandering channel closed at one end evolves towards an asymptotic equilibrium configuration, characterized by a deep scour at the channel inlet and the formation of a shoal (a wet and dry area) in the inner reach of the channel. Such a tendency is driven by the flood dominant character of the tidal wave. Note that the average bed topography in the seaward region did not actually reach exact equilibrium, displaying in the final stage of the experiment a weak oscillatory behaviour on a time scale of hundreds of cycles. Whether such a behaviour arises from some uncontrolled unsteadiness determined by the experimental setup or, more likely, to some intrinsic instability of the scour pattern at the inlet is a matter to be investigated.

The bar-pool pattern developed in the landward region is qualitatively consistent with field observations and with the theoretical results of Solari et al. (2001), with deposition occurring in the inner portion of the bend. Some quantitative comparison will be performed in the near future. However, in the

seaward portion of the channel, a tendency of bed topography to develop a symmetrical cross-section was observed, thus suggesting that the sinuous pattern in this region would be a planimetrically unstable configuration. In other words, the bed topography is strongly affected by the boundary conditions at the inlet and at the inner end. This suggests that the spatial distribution of the bar-pool pattern is not simply related to processes occurring at the meander scale hence, in order to capture the complete evolution of bed topography the whole channel length will have to be analyzed.

In the inlet region the formation of an ebb-tidal delta was observed, with size growing throughout the experiment.

The data collected in the present experiment are also intended to provide a test case for future numerical models and theoretical analyses.

In the near future we plan to carry out further experiments characterized by a lower value of the initial flow depth, i.e. by a higher aspect ratio. This may lead to the formation of free bars, thus allowing to observe a possible interaction between forced and free bars. Also, the role of convergence of meandering channels needs to be investigated, along with the effects of adjacent tidal flats.

References

- C. L. Amos, Helsby R., Umgieser G., Mazzoldi A. and Tosi L., "Sand transport in the Northern Venice Lagoon", *Scientific Research and Safeguarding of Venice, CO.RI.LA Research Programme 2001-2003, Volume III*, 2005.
- R. A. Davis, "Coasts". London: Prentice Hall, 1996.
- C.T. Friedrichs and D. G. Aubrey, "Non-linear distortion in shallow well-mixed estuaries: a synthesis", *Estuarine, Coastal and Shelf Science*, 27, 521-545, 1988.
- V. Garotta, M. Bolla Pittaluga and G. Seminara, "On the migration of tidal free bars", accepted for publication on *Physics of Fluids*.
- R. Kinoshita and H. Miwa, "River channel formation which prevents downstream translation of transverse bars", *Shin Sabo*, 94, 12-17, 1974 (in Japanese).
- S. Lanzoni and G. Seminara, "Long term evolution and morphodynamic equilibrium of tidal channels", *J. Geophys. Res.*, 107(C1), doi:10.1029/2000JC000468, 2002.
- M. Marani, S. Lanzoni, D. Zandolin, G. Seminara and A. Rinaldo, "Tidal meanders", *Water Resour. Res.* 38 (11), 2002.
- H. M Schuttelaars and H. E. De Swart, "An idealized long-term morphodynamic model of a tidal embayment", *Eur. J. Mech. B*, 15, 55-80, 1996.
- G. Seminara and L. Solari, "Finite amplitude bed deformations in totally and partially transporting wide channel bends", *Water Resour. Res.*, 34, 1585-1598, 1998.
- L. Solari, G. Seminara, S. Lanzoni, M. Marani and A. Rinaldo, "Sand bars in

tidal channels. Part 2. Tidal meanders”, *J. Fluid Mech.*, 451, 203-238, 2001.

L. Solari and M. Toffolon, “Equilibrium bottom topography in tidal meandering channels”, *Proceedings of the 2nd RCEM Symposium, Obihiro (Japan)*, 11-14 September 2001.

N. Tambroni, M. Bolla Pittaluga and G. Seminara, “Laboratory observations of the morphodynamic evolution of tidal channels and tidal inlets”, *J. Geophys. Res.*, 110, F04009, doi:10.1029/2004JF000243, 2005.

RESEARCH LINE 3.15

Solid transport and circulation of the upper layers in the inlets and the coastal zone

TIME SERIES OF SUSPENDED PARTICLE CONCENTRATION FROM THE CONVERSION OF ACOUSTIC BACKSCATTER AT THE LIDO INLET

Vedrana Kovačević¹, Valentina Defendi², Luca Zaggia², Franco Costa², Franco Arena¹,
Francesco Simonato², Andrea Mazzoldi², Miroslav Gačić¹, Carl Amos³

¹ Istituto Nazionale di Oceanografia e di Geofisica Sperimentale, Borgo Grotta Gigante 42/c, 34010 Sgonico (Trieste), Italy, ² Istituto di Scienze Marine CNR, San Polo 1364, 30125 Venezia, Italy, ³ Centre for Coastal Processes, Engineering and Management, National Oceanography Centre, Hampshire, SO14 3ZH, UK

Riassunto

Questo articolo riporta i risultati relativi a due diversi metodi di conversione dell'intensità del segnale di *backscatter* ottenuto da un Profilatore Acustico di Corrente ad Effetto Doppler (ADCP), installato sul fondo del canale di Lido, in concentrazione del particellato in sospensione. La serie temporale dell'intensità del *backscatter* dello strumento fisso è stata calibrata con i dati raccolti durante serie di misure locali. Sono state così ottenute due serie temporali della stima della concentrazione; la prima basata sui campioni d'acqua raccolti, e la seconda su stime della concentrazione fornite dalla calibrazione dei dati del *backscatter* lungo i transetti effettuati con un ADCP montato su barca. Il vantaggio del primo metodo è quello di usare la concentrazione determinata direttamente dai campioni d'acqua, ottenendo però la descrizione del profilo verticale con scarsa risoluzione spaziale. Il secondo metodo permette una risoluzione più fine, ma include i possibili effetti dei gradienti laterali nella distribuzione del particellato solido in sospensione nell'intera sezione. Nella maggioranza dei casi le differenze tra le due serie temporali risultanti sono piccole, e nell'88 % dei casi non sono maggiori del 40 %. Le differenze tra le due serie diventano importanti nei casi relativi a particolari condizioni ambientali, generalmente associate al verificarsi di fenomeni di vento particolarmente intenso da nord-est (Bora). E' ben noto che in tali condizioni il movimento ondoso genera la risospensione dei sedimenti dal fondo e causa erosione del litorale adiacente il canale di Lido. In condizioni di vento debole, differenze possono presentarsi durante le fasi di riflusso mareale con correnti superiori a 0.5 m/s. All'accuratezza della serie temporale dello strumento fisso contribuisce significativamente la stima del trasporto di sedimento in prossimità del fondo, dove, durante le recenti misure si è potuto verificare che il materiale in sospensione è costituito prevalentemente da sabbia fine e molto fine. Il lavoro futuro sarà orientato all'integrazione di questi contributi lungo tutta la colonna d'acqua, in quanto fondamentale per ottenere un bilancio complessivo tra deposizione ed erosione nella bocca di Lido.

Abstract

Two methods for conversion of the backscatter intensity provided by the

bottom-mounted Acoustic Doppler Current Profiler (ADCP) situated in Lido inlet, and related results, are outlined in this paper. The time series of the backscatter intensity from the fixed ADCP is calibrated against the in situ data collected through the extensive series of field measurements. The two time series of concentration estimates are obtained; the former is based on water samples, and the latter on concentration estimates obtained from the calibration of the backscatter measured along transects acquired by a boat-mounted ADCP. The advantage of the first method is in using the concentration determined directly from the water samples, but it describes the vertical profile with a scarce resolution. The second method provides finer vertical resolution, but includes the possible effects of the lateral gradients in the distribution of suspended particles in the investigated section. In majority of cases the differences between the two time series are low, and in 88 % of cases they are not higher than 40 %. The differences between the two become important during particular environmental conditions, in general associated to the occurrence of particularly strong north-easterly (Bora) winds. It is well known that in such circumstances the wave motion generates resuspension of the bottom sediments, and causes erosion of the littoral adjacent to the Lido inlet. For the low wind conditions, the differences may occur during the ebb tidal flow of more than 0.5 m/s. The estimates of the sediment transport close to the bottom, which is predominantly constituted by fine and very fine sand, as demonstrated by recent investigations, significantly contributes to the accuracy of the fixed instrument time series. The future work will be focused on the integration of both contributes in the water column. This is fundamental in order to obtain an overall balance between the erosion and deposition in the Lido inlet.

1 Introduction

Understanding the exchange of particulate material across the inlets of the Venice Lagoon is of fundamental importance in the study of erosion phenomena. This is of particular interest in the shallow water areas where the ecosystem is particularly sensitive, but also for the entire system of canals which ensures water exchange and permanent navigation.

The morphology of the inlets and adjacent littoral zones, which is in the process of transformation, is closely linked to the dynamics of transport and deposition. These, in turn, depend on the movement of material by both currents and wave action especially during intense storm events.

Monitoring activities, including the study of the flow of water and suspended particulate matter across the inlets, are then a primary objective, for all institutes involved in the protection of the lagoon. In particular, the balance of both sediment and dissolved organic matter across the inlets has been, and continues to be, a key element in the long-term actions for the control of the effects of these processes.

Notwithstanding the remarkable series of studies to support projects for the protection of the lagoon environment, there has yet to be, since the inception of this monitoring project, a systematical measurement of the exchange of

sediments between the lagoon and the sea. A database of sediment transport could be utilized to verify the results of bathymetric surveys and monitor the effects of morphological transformations. This lack of information was not only connected to lack of improper policies (partially owing to the transfer of responsibilities between organizations charged with monitoring the lagoon environment, as well as structural shortfalls), but was also due to the difficulty of acquiring significant data with traditional techniques in challenging conditions such as those that characterize the inlets [Thorne et al., 1994]. The speed with which the current field evolves during tidal cycles makes it very difficult, if not impossible, to sufficiently represent the details of the distribution of the suspended load in the vertical profile as well as the entire inlet by the collection of water samples. On the other hand, employing optical sensors, calibrated against suspended sediment concentration [Hoitink and Hoekstra, 2005], in fixed stations only provide point values, while their use from a moving boat for a synoptic survey of a profile or the whole section would be limited to restricted temporal windows since it requires a continued field presence of technical personnel. The research project "The Measurement of Sediment Transport between the Lagoon and Sea", begun in November 2004, is scheduled to come to an end in November 2007. It involves diverse research groups and institutions such as CNR-ISMAR, Venezia, OGS, Trieste, NOCS, Southampton, UK, ICPSM, Venezia, APAT, Venezia, and is co-funded by Comune di Venezia (the Venice municipal authority), APAT and CORILA. The extended monitoring time and the remarkable commitment dedicated to the experimental work performed are justified by the need for a series of observations representative of the average conditions of the system. This allows for the understanding of seasonal and inter-annual variability as well as marine-atmospheric conditions. The magnitude of sediment transport, particularly of the suspended load, is, indeed, strongly influenced by meteorological events. This may be the major cause of sediment movement from the bottom of the lagoon and along the littoral zone.

The method utilized for the study is essentially based on the conversion of the backscatter signal recorded by the acoustic Doppler current profilers (ADCP) which have been employed to continuously measure the velocity and direction of the current at depth in the inlet [Gačić et al., 2002; Gačić et al., 2005; Zaggia et al., 2004]. Backscatter intensity is calibrated through an extensive series of field measurements. The experimental operations include: the collection of water samples and the acquisition of physical-chemical properties along the vertical profiles of the water column by CTD casts. In addition, velocity and direction of the current as well as acoustic backscatter are measured using an ADCP mounted to a boat moving along transects perpendicular to the flow in the same section of the inlet. The profiles are utilized to calibrate the fixed instrument positioned at the bottom of the section and for the study of the distribution of the suspended sediment load across the entire section.

Preliminary flux calculations, obtained by combining the time series of the flow and of the concentration of suspended particulate matter from the conversion of backscatter of the bottom deployed ADCP have demonstrated the importance

of intense atmospheric events in the balance of transported suspended material from the sea currents across the inlets [Zaggia and Ferla, 2005]. A further investigation of this problem has been postponed to the final phase of the study, in order to allow time for the addition of the data needed to update estimates of the flow as a function of the index velocity recorded by the fixed ADCP [Simpson and Bland, 2000; Gačič et al., 2002]. In the course of the second year of activity major changes in the morphology of the inlets occurred during the work involved in the protection of the lagoon against flooding. These might have affected the velocity field in the monitoring section. It is thus believed that it is appropriate to update the relationship between velocity index and flow in the corresponding period in order to calculate a more accurate time series of suspended sediment load.

In this contribution, progress made from the experimental research at the close of the second year of project activity is described. Since there is sufficient information available in this phase, it has been possible to carry out a comparison between two different methods for obtaining the time series of suspended sediment concentration. These include: the calibration of acoustic backscatter signal with respect to water samples, and the estimates of concentration measured by backscatter transects taken from boat-mounted ADCPs. Because of intrinsic limitations of the acoustic methods the measurements must be integrated with experimental data supplied by other equipment. These are currently being employed for the evaluation of transport in the area close to the bottom. This activity was carried out in a preliminary test in September 2005, and then repeated in much greater detail in September 2006. Thanks to favorable weather conditions the results of the September 2006 campaign enabled us to obtain an estimate of transport to the bottom as a function of current intensity [Amos, personal communication]. Information on bed load movement will also be used, along with other data acquired, to produce a time series of transport to the bottom of the investigated section permitting an integration of the estimate of suspended transport obtained using the fixed ADCP.

In regard to the timetable of research, we can summarize the situation seen at the end of the second year as reported in Tab.1.

ADCP Mobile November 2004 – November 2006					
Campaign type	Planned field campaigns	Actual field campaigns	ADCP Transects	CTD Profiles	Samples
Monthly	32	24	560	310	805
Seasonal	12	8	257	198	528
Events	18 (ca.)	8	50	27	72
Total			867	535	1405
Fixed ADCP: June 2004 – June 2006					
Time series of flow:	from 2001				
Time series of concentration:	from 2004 (18075 hourly data)				

Tab. 1 - State of the advancement of experimental research planned at the end of the second year of activity.

It is important to note that eight monthly campaigns, eight seasonal campaigns and around ten measurements corresponding to meteorological events have yet to be carried out in the course of the third year of activities.

2 Methodological Approach

The backscatter intensity recorded from the fixed ADCP situated in the Lido Inlet has been utilized to obtain the concentration of suspended particulate matter. The procedure to calibrate the backscatter is carried out in two ways: the measurement of suspended sediment concentration in water samples collected at different depths in the section during the field campaign; and through estimates of concentration obtained by calibrating the boat-mounted ADCP data in transects with respect to bottle samples.

From every transect acquired with the mobile instruments, it is possible to extract, after calibration with the Sediview software [Land and Jones, 2001; Gartner, 2004], the average vertical profiles of concentration (in a strip about 30m wide) with respect to the fixed ADCP position. (Fig.1).

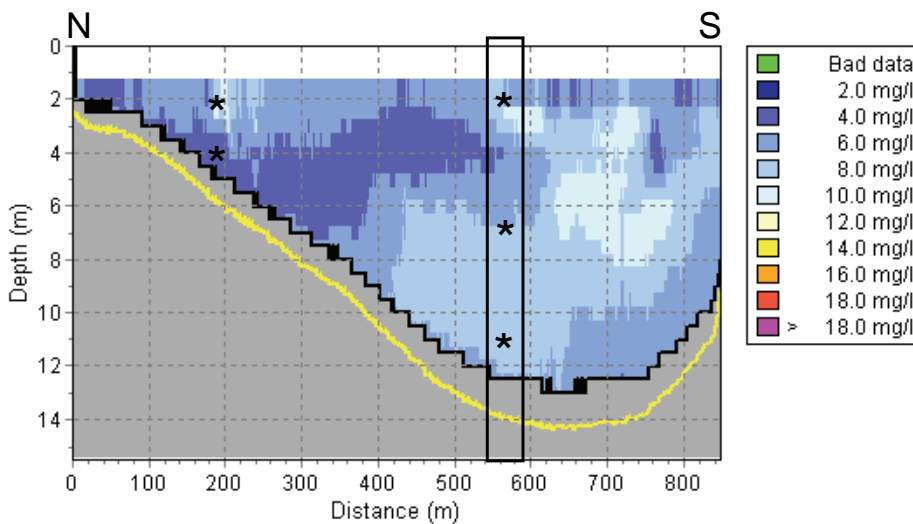


Fig.1 - Example of the distribution of the concentration of the suspended particulate matter along the section at the Lido Inlet. The rectangle indicates the average intervals of 30 ensembles (around 30-40m in width) utilized to estimate an average concentration profile based on the calibration of the fixed instrument deployed below, whereas the asterisks denote the usual depth of water sample collection. N and S denote the northern and southern inlet flank, respectively.

Since the vertical resolution of the mobile ADCP acquisition is 0.5m (depth cell size), the vertical resolution obtained allows for the calibration of the whole column recorded from the fixed ADCP (depth cell size 1m) except for the blank areas at the surface and bottom (around 1 and 2m respectively, Fig. 1), in which the instrument is unable to measure due to intrinsic limitations of the technology.

When water samples were utilized for the calibration of the acoustic backscatter signal of the fixed ADCP, only the three depths, designated by asterisk in Figure 1, were measured. However, this has the advantage of the direct measurement of suspended sediment were used instead of an estimate of concentration. From the two distinct calibrations we obtained two time series of the average vertical concentration which are comparatively analyzed and discussed herein.

Asterisks within the rectangle denote the usual depth of water sample collection at the fixed ADCP position. Locations of the additional sampling points used for calibration of boat mounted ADCP are also indicated. Northern and Southern endpoints of the transects are identified (N and S).

3 Time series of the suspended particle concentration: October 12th, 2005 - January 31st , 2006

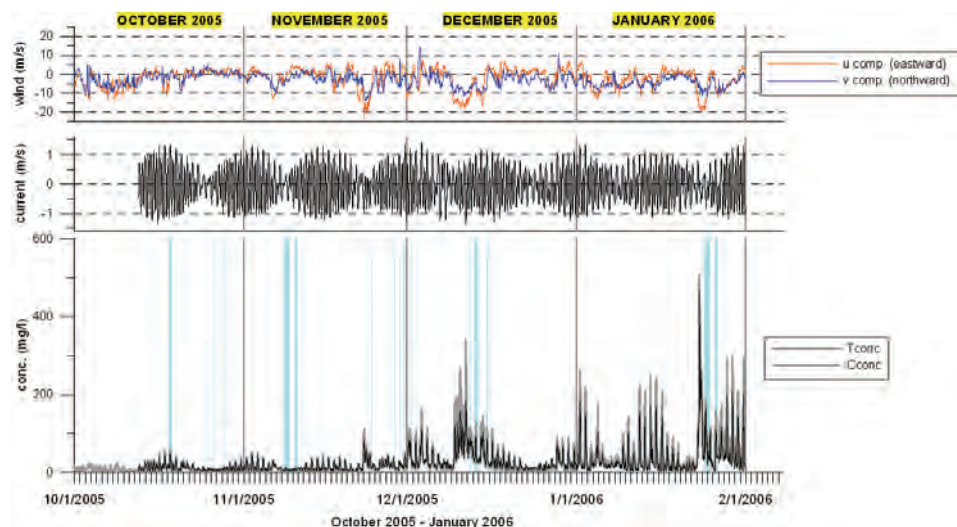
The analysis presented in this section include the data collected from the period between October 12th, 2005 and January 31st, 2006, during which a series of field measurements took place in order to calibrate the fixed ADCP at the Lido Inlet. The period under consideration is relative to the last operation of data recovery from the fixed ADCP.

The two hourly series of concentration data were obtained from the calibration of the acoustic backscatter acquired from the fixed instrument. This was calibrated with respect to water sample concentrations (Cconc) and the estimated concentrations (Tconc) extracted from the transects measured by means of a boat-mounted ADCP. They are reported in Figure 2 together with the hourly wind data recorded at the National Research Council's marine research platform, and the hourly depth averaged current data measured by the fixed ADCP and projected along the axis of the inlet channel.

The wind is represented by the two vector components u (easterly) and v (northerly). Based on the convention adopted here, when both u and v are negative, a Bora wind is present; whereas, when u is negative and v is positive there is a Sirocco wind present. We can note from the graph (upper panel in Fig. 2) that during the period under examination there are various rather intense Bora events, in some cases prolonged over time. Bora seems to have a major influence as compared to Sirocco events which are, in the analyzed period, less frequent and important for the resuspension of sediments, in particular along the north bank of the section.

The time series of the current velocity (central panel in Fig.2) shows that the hydrodynamics of the section, where maximum current speed sometimes reaches values of 1.4 m/s, is principally governed by the tides. The water samples collected during the field surveys performed by CNR-ISMAR and OGS were, therefore, used not only for the direct calibration of the acoustic backscatter signal from the fixed ADCP but also for the calibration of the boat-mounted ADCP.

Fig. 2 - Hourly time series of the two components of the wind (above), the axial current (along the axis of major variance) measured by the fixed ADCP (middle) and the concentrations of particulate suspended matter, Tconc and Cconc (below). The vertical lines indicate the field surveys carried out during the period from October 12th, 2005 to January 31st 2006.



The average concentration profiles in correspondence to the vertical profile of the fixed instrument were extracted from the calibrated transects. In the calibration phase, seasonal variations of water temperature and salinity were taken into consideration because of the influence of water density on the propagation of the acoustic signal emitted from the instrument.

In Tab. 2 we report the principal statistical parameters relative to the two concentration series, Tconc and Cconc, and the difference between them (Tconc-Cconc). It can be noted that the variability ranges of Tconc (2.4 – 508.0 mg/l) and Cconc (3.3 – 467.2 mg/l), as well as their respective means and medians are rather similar.

	Tconc	Cconc	Tconc-Cconc
Number of data	2672	2672	2672
Min (mg/l)	2.4	3.3	-4.9
Max (mg/l)	508.0	467.2	156.2
Mean (mg/l)	29.6	25.2	4.4
Median (mg/l)	14.2	14.6	-1
Number of data ≤ 50 mg/l	2269	2367	2617
percentile_08 (mg/l)	37.6	32.8	7.4
percentile_09 (mg/l)	74.5	56.3	18.0
RMS (mg/l)			14.8

Tab. 2 - Basic statistics relative to the two hourly concentration series, Tconc and Cconc, for the period from October 12th, 2005 to January 31st, 2006. The eighth and ninth percentiles (percentile_08 and percentile_09) indicate the value limits in which one can find, respectively, 80% and 90% of the data. RMS is the root mean square of the difference (Tconc-Cconc) between the two series

The dispersion diagram in Figure 3 presents, instead, the comparison between the two time series, Tconc and Cconc.

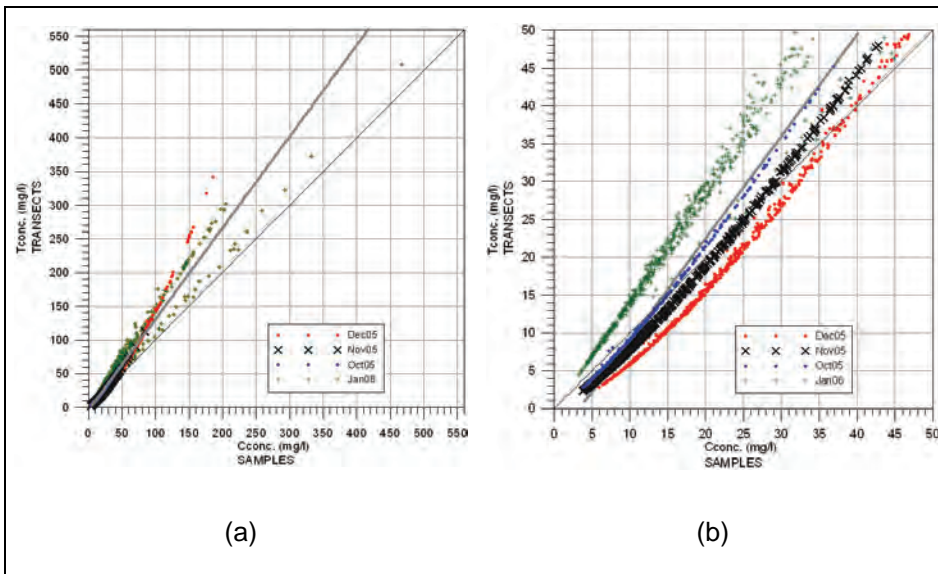


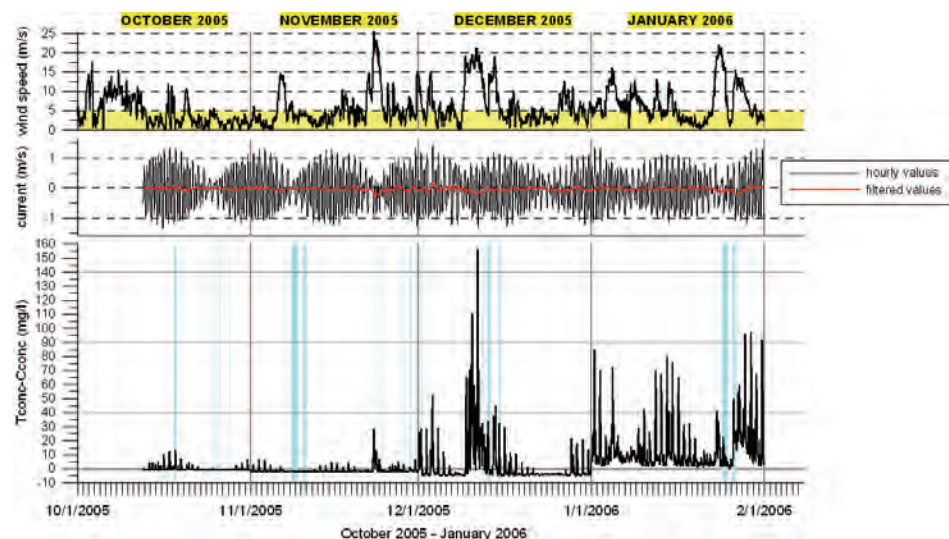
Fig. 3 - Comparison between the two series of the suspended particle concentration (a) for all the value intervals and (b) for the values less than 50 mg/l. The thin line represents the theoretical curve $y=x$, while the thicker line is the best-fit curve.

The diagram shows that values greater than 150 mg/l are relatively rare and mainly seen in December 2005 and January 2006 (Fig. 3a). The trend of the

values in the upper part of the graph, though linear, moves away from both the theoretical line and the best-fit line, which more clearly represents the lower values with a tendency for Cconc to be underestimated with respect to Tconc (Figure 3a). For values less than 50 mg/l, which comprises 84% of the examined data, it can be observed that the dispersion around the best fit line is principally due to the January values, characterized by particular environmental conditions. For the other three periods under consideration, the relationships are much closer to each other and the theoretical line (Fig. 3b). Moreover, Tconc underestimates Cconc in the low concentration range (1-15 mg/l), while for intermediate concentrations (15-35 mg/l) it is impossible to identify a trend as there are some cases in which one of the two series over- or underestimates the other (Fig. 3b). The January 2006 data shift away from this trend, so the calibration was performed in two parts, applying different coefficients to the two periods obtained. The former (January 1-22 and 27-31, 2006) was calibrated using the data acquired during the monthly campaign on January 26th, while the latter (January 23-25, 2006) with respect to the measurements taken during the seasonal survey of 24-25 January. The acquisitions of the seasonal campaign were carried out during an intense Bora wind event (Fig. 2), which significantly influenced the quantity and distribution of the particulate suspended sediments. For this reason, we used the two separate calibrations, to account for the diverse environmental conditions experienced in the field. A more in-depth study of the effect of intense meteorological events on resuspension along the investigated section should be performed in the final phase of the project. This will allow for the thorough examination of the behavior of the section under study in January 2006.

The time series of the differences (Tconc-Cconc) is presented in Figure 4, where only the velocity of the wind is reported (upper panel) to stress the effect of wind intensity. As regards the axial current (central panel), hourly values are shown which highlight tidal movement. In addition, the values averaged over 25 hours are shown to filter the effect of the tide. In the majority of the cases, the differences are low. In general, variations only become significant during strong meteorological events with high intensity of wind (upper panel in Fig. 4).

Fig. 4 - Hourly time series of wind velocity (above), the hourly and low-pass filtered axial current (along the axis of major variance) measured by the fixed ADCP (middle) and the differences (Tconc-Cconc) between the concentrations of the two series obtained from the calibrated acoustic backscatter acquired by the fixed ADCP (lower panel). The vertical lines indicate the field surveys carried out during the period from October 12th, 2005 to January 31st 2006



In these conditions, the wind influences wave heights and, therefore, sediment resuspension, especially in the shallowest areas of the section. In particular, it is noted that Bora events often coincide with the flood tide (negative axial current) as seen, for example, in Figure 2.

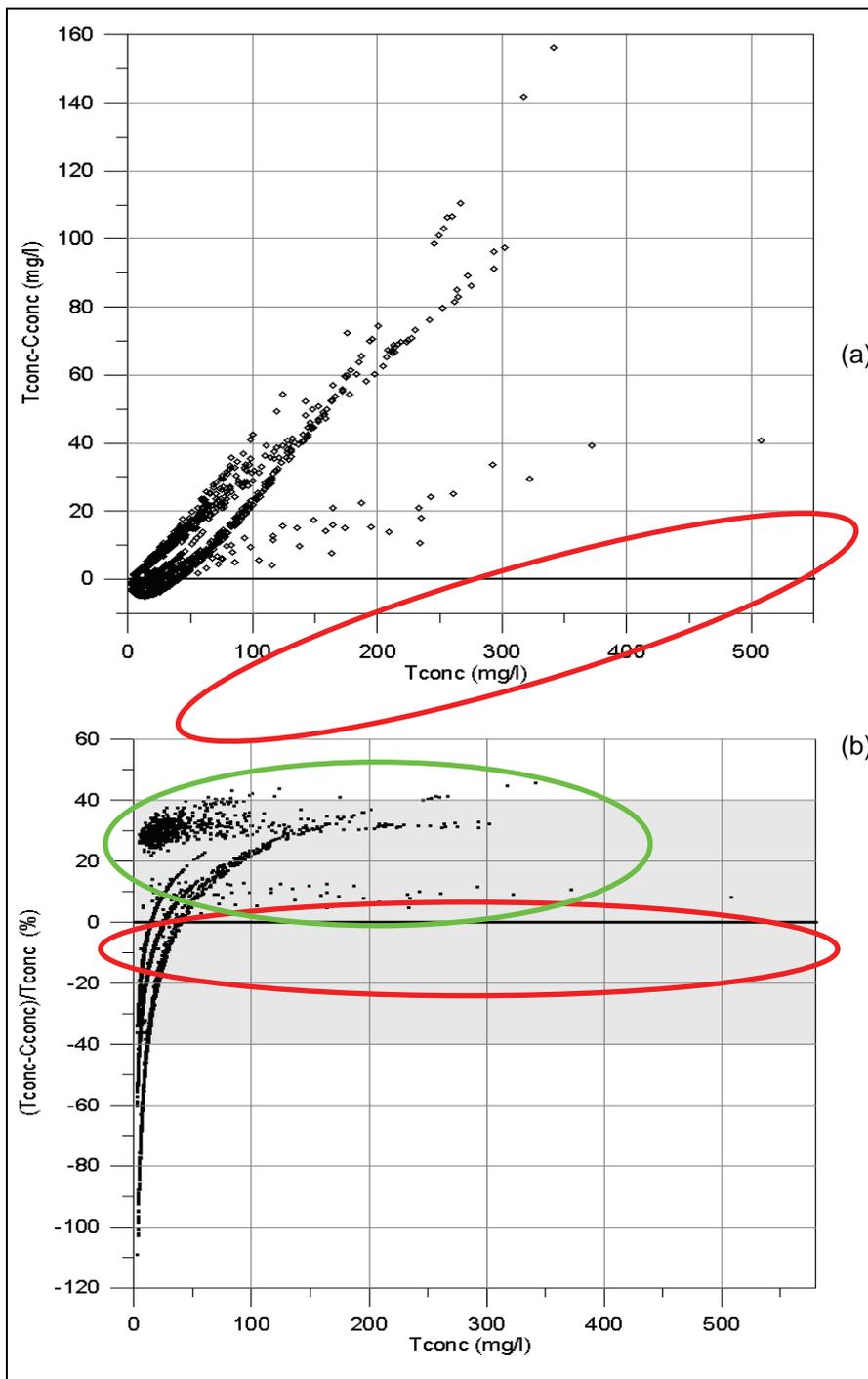


Fig. 5 - Differences between the two concentrations series, Tconc and Cconc, with respect to Tconc; (a) absolute values and (b) percentage differences. The grey band indicates the -40 to +40% interval.

The distribution of the differences between the two series is illustrated in Figure 5 in both absolute and percentage value.

The sign of the difference, likewise to Figure 4, is negative when the Cconc overestimates Tconc, but positive when Cconc underestimates Tconc.

One can see that, in the majority of cases, the differences are positive and when the concentration increases this divergence is amplified (Fig. 5a). The differences (Tconc-Cconc) range from -5 to 156 mg/l, while the root mean square is 11 mg/l as indicated in Tab. 2. In some cases the deviation is higher than 100%, however, in 88% of the cases the difference is contained between -40 % and +40 % (Fig. 5b). The values indicated in red in Figures 5a and 5b correspond to the data from January 23-25 2006, during which period a Bora event with hourly speed values higher than 20 m/s (see Fig. 4) took place. The cloud of points highlighted in green represents data from January 2006 with the exception of the Bora event (Fig. 5b).

In 75% of the cases the differences are not higher than 5 mg/l in absolute value (Fig. 6). In fact, in only 55 of the 2672 cases a difference is higher than 50 mg/l with a maximum value of 156 mg/l in December 2006 (Fig. 4).

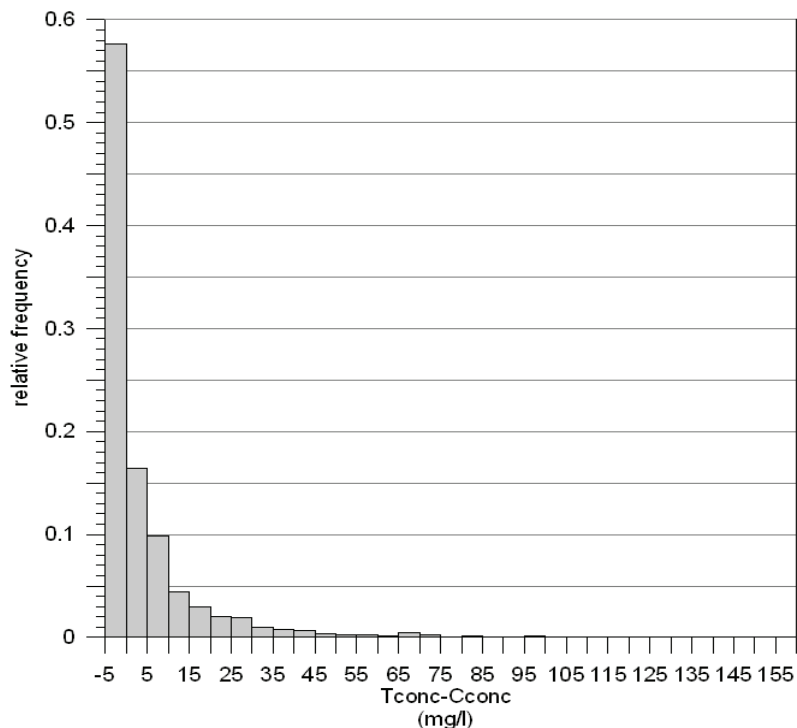


Fig. 6 - Distribution of the relative differences between the two concentration series, Tconc and Cconc.

Figure 7 shows the relation of the hourly average concentration series (Tconc) with wind (speed and direction) and water current conditions.

In conditions of weak wind (speed < 5m/s), the concentrations increase when the intensity of the ebb current becomes higher (Fig. 7a). When the velocity of the wind becomes significant, it is observed, instead, that the increase of the concentration can be independent of the current (Fig. 7a). This is due to the

resuspension of sediment from the motion of waves on shallow areas and on the beaches in the vicinity of the Lido Inlet.

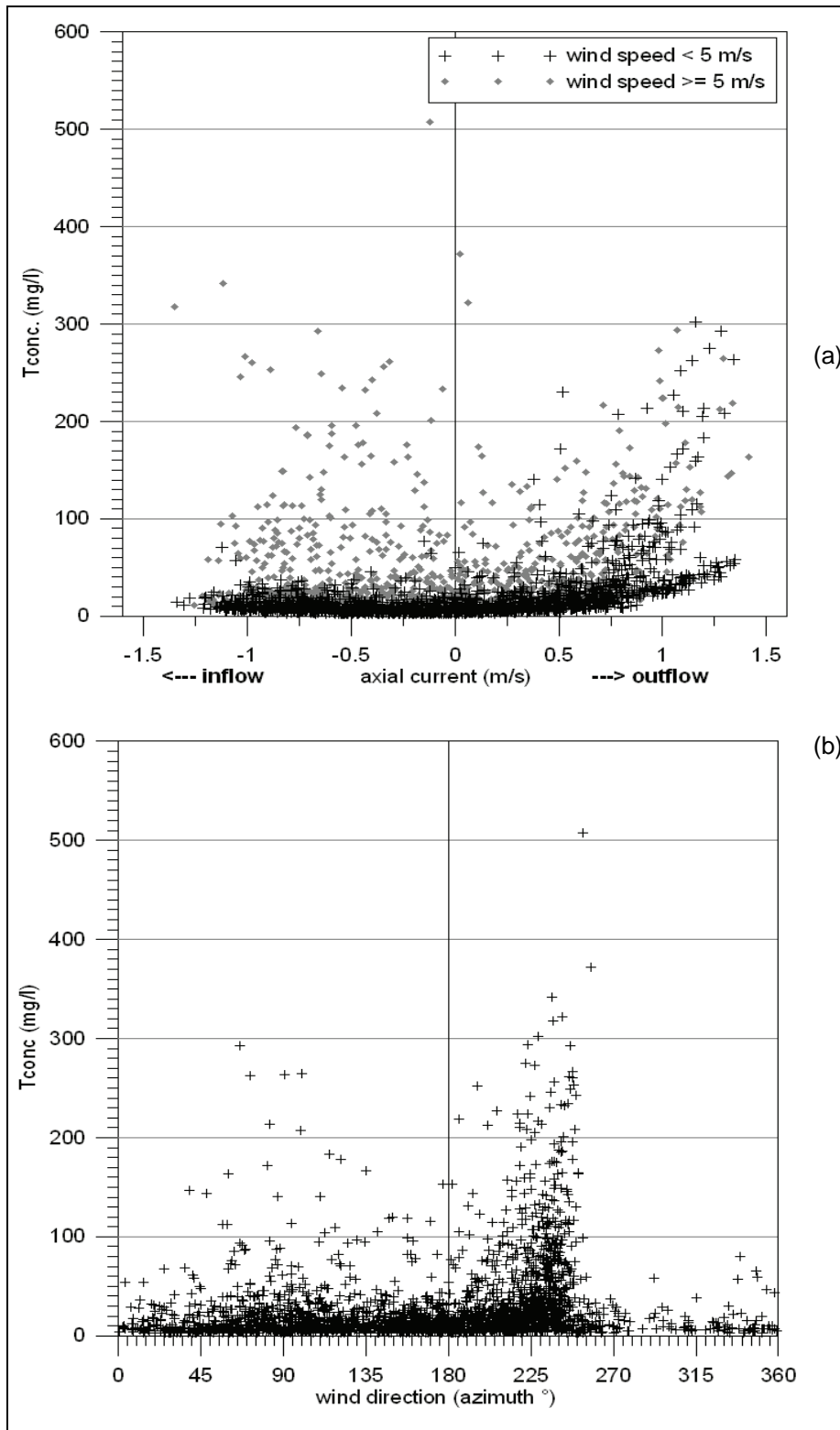


Fig. 7 - Series of the concentration of Tconc in relation to (a) axial water current and wind velocity and (b) wind direction.

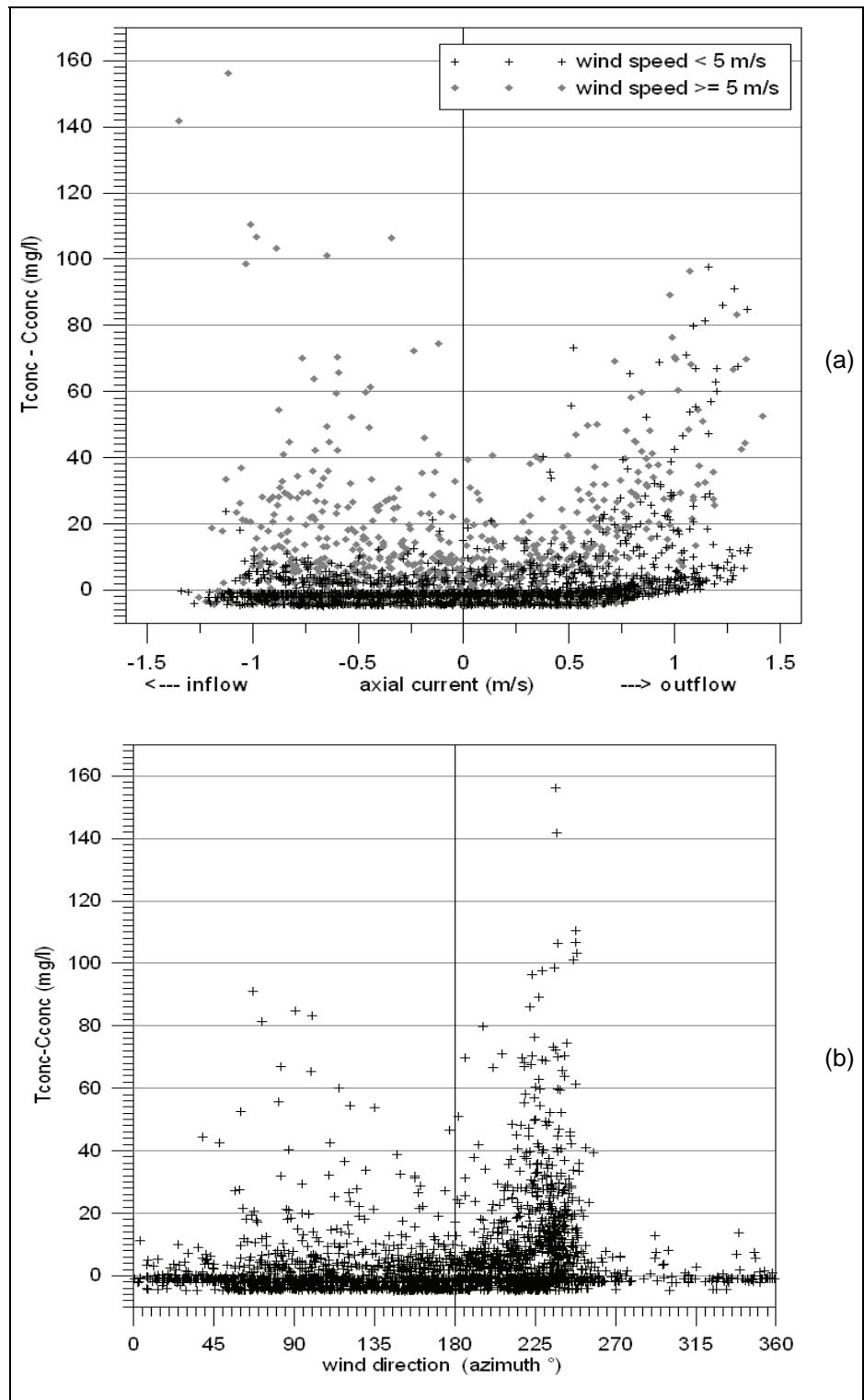


Fig. 8 - Difference between the two concentration series, T_{conc} and C_{conc} , in relation to (a) axial water current and wind velocity and (b) wind direction.

As regards current direction, the concentration increase is higher during flood phases (incoming current) combined with a sustained wind (Fig. 7a). Figure 7b shows that the winds from the NE-ENE quadrant (Bora winds), indicated by an azimuth value around 240° (the direction of the wind vector, clockwise with

respect to the north), have a major influence on the concentration of suspended particle concentration which increases because of waves resuspension and erosion.

In a similar way, we can examine the trend of the differences between T_{conc} and C_{conc} (Fig. 8).

The larger disparities are found when flood tide combines with sustained winds (Fig. 8a), specifically if the wind originates from the Bora quadrant (Fig. 8b). In these cases, the section comprising the bottom-mounted ADCP is characterized by a strong asymmetry in the spatial distribution of the sediment. In particular, the suspended load increases in correspondence to the most shallow edge of the section along the north breakwater. This is not only due to local sediment resuspension but also is affected by the transport of fine sand to neighboring beaches, particularly those of Cavallino.

Conclusion

The results obtained for the period from October 2005 to January, 2006, and described in the previous section, permit the formation of some conclusions on the two types of calibrations of acoustic backscatter signal registered by the fixed ADCP at the Lido Inlet. The two calibrations, although utilized for the same procedure, emphasize different aspects. In the case of water samples, the time series of suspended sediment concentration results from the calibration of the fixed ADCP backscatter using direct measurements. These measurements are taken at three depths, corresponding to the vertical profile of the fixed instrument and are representative of the range of values along this profile. On the contrary, concentration data provided by the boat-mounted ADCP comes from a calibration based on a wider spectrum of values which reflects concentration intervals along the entire monitoring section. Differences in the distribution of the amount and size of suspended sediments can lead to different calibration results. Therefore, data acquired with the boat mounted instrument during Bora events, when the northern part of the section is characterized by a major presence of sand in suspension, possibly affects the calibration. This may give rise to the observed differences.

Based on the findings noted above, it can be affirmed that, on one hand, the C_{conc} series is representative of the average vertical concentration of the fixed ADCP and, thus, of the central part of the section. On the other hand, using transects of the boat-mounted ADCP can produce a continuous series of measurements which reflects the distribution of suspended load in the whole experimental area. This aspect has been shown previously and will be further investigated in the last phase of the study.

The reliability of the time series derived from the calibration of the fixed ADCP also depends on the estimates of sediment transport at the bottom. Based on the results of the experimental work already conducted, the transport seems to involve fine and very fine –sand that constitutes an important part of the total solid load, particularly in conditions in which suspended transport is low. This

knowledge is fundamental to construct a balance between the processes of deposition and erosion in the Lido Inlet.

The factors affecting the variability of the distribution of the concentration of suspended particles include the natural phenomena of resuspension and advection (due to currents and waves), as well as exceptional meteorological events. In addition, construction activities, especially those concerned with the protection of Venice from flood waters have an impact on the morphology of the inlets and nearby lagoon area. The complexity of this dynamic environment requires frequent monitoring and precise evaluation of the acoustic response to the diverse environmental conditions. The information which is currently available constitutes the reference base to reduce the uncertainty in estimating the continuous series of suspended particle concentrations. This uncertainty, for the period under examination, is 40%, or less, in 88% of the cases.

Another important aspect for the research will be the comparison between vertical profiles of sand concentration, estimated from models (SHYFEM and SedTrans), and the Rouse profiles obtained from experimental measurements on bedload. This comparison should also allow the assessment of the reliability of the model as a complementary tool for an estimate of long-term net transport of sand in the Lido Inlet. In this framework, a development of modeling tools for the simulation of particle mobilization in the entire lagoon domain, including shallow-water areas, where wave resuspension is critical, is fundamental for the improvement of the accuracy of the estimates of sediment transport at the inlets.

References

Gačič, M., Kovačević, V., Mazzoldi, A., Paduan, J., Arena, F., Mancero Mosquera, I., Gelsi, G. and Arcari G., 2002. Measuring Water Exchanges between the Venetian Lagoon and the Open Sea. EOS, Transactions, Am. Geophysical Union, 83 (20), 217-222.

Gačič, M., Mazzoldi, A., Kovačević, V., Cosoli, S., Mancero Mosquera, I., Arena, F., Cardin, V., 2005. Water Fluxes in Venice Lagoon Inlets and Coastal Circulation. In: P. Campostrini (ed.), *Scientific Research and Safeguarding of Venice. Research Program 2001-2003, Vol III, 2003 Results*. Venice, 311-321.

Gartner, J.W., 2004. Estimating suspended solids concentrations from backscatter intensity measured by acoustic Doppler current profiler in San Francisco Bay, California. *Marine Geology*, 211, 169–187.

Hoitink, A.J.F. and Hoekstra, P., 2005. Observations of suspended sediment from ADCP and OBS measurements in a mud-dominated environment. *Coastal Engineering*, 52, 103– 118.

Land, J.M., Jones, P.D., 2001. Acoustic measurement of sediment flux in rivers and near-shore waters. *Proceedings of the 7th Federal Interagency Sedimentation Conference*, March 25–29, 2001, Reno, NV, pp. III 127–134.

Simpson, M.R., and Bland, R., 2000. *Methods for Accurate Estimation of Net*

Discharge in a Tidal Channel. *IEEE Journal of Oceanic Engineering*, 25 (4), 437-445.

Thorne, P.D., Hardcastle, P.J., Flatt, D. and Humphery, J.D., 1994. On the Use of Acoustics for Measuring Shallow Water Suspended Sediment Processes. *IEEE Journal of Oceanic Engineering*, 19 (1), 48-57.

Zaggia, L., Mazzoldi, A., Gačič, M., and Costa, F., 2004. The measurement of water exchanges at the Venice lagoon inlets. *Proc. of the 37th Congress C.I.E.S.M.*, Barcelona, Spain, 7-11 June, 153.

Zaggia, L. and Ferla, M., 2005. Studies on Water and Suspended Sediment Transport at the Venice Lagoon Inlets. In: *Ocean Waves Measurement and Analysis. Proc. of the Fifth International Symposium WAVES 2005*, Madrid, Spain, 3 – 7 July, Paper n. 96, 1-10.

RESEARCH LINE 3.16

**Characteristics of the lagoon underground
layer**

PRELIMINARY RESULTS OF THE HIGH RESOLUTION SEISMIC SURVEYS IN THE VENICE LAGOON

Giuliano Brancolini¹, Luigi Tosi², Luca Baradello¹, Antonio Bratus¹, Federica Donda¹,
Federica Rizzetto², Massimo Zecchin¹

¹ Dipartimento di Geofisica della Litosfera - Istituto Nazionale di Oceanografia e di Geofisica Sperimentale – OGS, Borgo Grotta Gigante 42/c, 34010 Sgonico (TS)

² Istituto di Scienze Marine – Consiglio Nazionale delle Ricerche, San Polo 1364, 30125 Venezia

Riassunto

La ricerca 3.16 Co.Ri.La. “*Applicazione di metodologie sismiche innovative ad altissima risoluzione sui bassi fondali per lo studio del sottosuolo lagunare veneziano*”. è, in parte, la prosecuzione a maggior risoluzione ed estesa ai bassifondi lagunari, degli studi eseguiti nell’ambito del progetto di cartografia geologica italiana CARG (APAT, Regione del Veneto), condotti da ISMAR-CNR di Venezia e da OGS.

Gli obiettivi della ricerca sono sostanzialmente due:

- 1) implementare un sistema di prospezione sismica ad altissima risoluzione, adatto per rilievi sui bassifondi;
- 2) effettuare una serie di rilievi per integrare la conoscenza dell’evoluzione recente (ultimi 10.000 anni) della laguna di Venezia.

Nel corso dei primi due anni di attività è stata acquistata un’imbarcazione idonea a navigare in acque particolarmente basse (fino a 50 cm), è stato implementato ed installato sulla nuova imbarcazione un sistema di acquisizione sismica e sono stati eseguiti diversi rilievi in aree particolarmente significative: la bocca di porto di Lido con il relativo settore marino, la bocca di porto di Chioggia, i bassifondi della laguna meridionale e lungo le aste fluviali del Brenta e del Sile. Il rilievo nell’area lagunare è ancora incompleto e verrà portato a termine entro il 2006.

I dati fin qui acquisiti hanno permesso di rilevare gli elementi più significativi dell’evoluzione geologica tardo-pleistocenica ed olocenica dell’area di studio:

Area marina: sono stati riconosciuti e caratterizzati il sistema trasgressivo alla base dell’Olocene (TST) ed il successivo sistema di stazionamento alto (HST) progrediente verso mare.

Bocche di porto: individuano un ambiente altamente dinamico, come dimostrato dalla presenza di fosse di erosione attive e dalla elevata asimmetria nella distribuzione dei sedimenti olocenici.

Area lagunare: caratterizzata da notevole variabilità laterale nell’assetto dei

sedimenti, prodotto prevalentemente dalla migrazione laterale dei canali tidali.

Abstract

The research line Co.Ri.La. 3.16 “*Application of innovative high resolution seismic methodologies to the shallows for the study of the subsoli in the Venice lagoon*” is the natural prosecution of the studies carried out by ISMAR-CNR and OGS in the frame of the geological mapping project (CARG) sponsored by APAT and Regione del Veneto. The main objectives of the research are:

i) implementation of an high resolution seismic system suitable for shallow water surveys, ii) acquisition of a high resolution seismic data set in order to integrate the knowledge of the recent (last 10.000 years) evolution of the Venice lagoon.

The products of the first two years of activities have been: i) acquisition of a new boat adapted for steaming in very shallow (less than 50 cm) water, ii) implementation and installation on the boat of a single channel high resolution seismic system, iii) acquisition of seismic data in area of particular interest for the recent evolution of the lagoon: the mudflat in the southern lagoon, the Lido and Chioggia inlets, the shelf off the Lido inlet, the southern boundary between the lagoon and the mainland and along the Brenta and Sile rivers. Field activities are still underway and will be completed during 2006, but the already available data, clearly outline the geological evolution of the Holocene and late Pleistocene of the study area:

The shelf area, well characterized by the Trasgressive System Tract (TST) at the base of the Holocene, and the overlying Highstand System Tract (HST), prograding toward the open sea,

The inlets, an highly dynamic environment, as testified by the active erosional deeps and by the high asymmetry of the Holocene deposits

The lagoon, characterized by the lateral variability of the deposits, mainly produced by the tidal channels migration

1 Introduction

In the next future, global changes will deeply influence the environment; the most sensitive area are the coasts, where small variations in the sea level, will have relevant impacts in human settlements and activities. In this context, the Venice lagoon is a critical area, because is a fragile environment, subject to intense antropic activities. The detailed comprehension of the rule and the interactions between the processes that led to the formation of the lagoon, is the first, indispensable step for any initiative aimed to the preservation of the lagoon.

The main processes, responsible for the settlement and evolution of the lagoon are:

- The eustatic sea level rise followed the last glacial maximum

- The sediment supply from the rivers
- The sediment exchange with the open sea through the inlets
- The human interventions that, since historical time, altered the setting of the lagoon and the surrounding area.

The sediments in the Venice lagoon keep the record of all these processes. The basic tools for knowledge of the subsoil are i) coring and ii) reflection seismic surveys.

These latter in particular are widely used to reconstruct the geometries, the distribution and the depositional characteristics of the sedimentary units, as far to correlate and extrapolate coring data. Up now however, due to logistic limits, all the seismic surveys in the Venice lagoon have been carried in the channels. That is a major limit because the channels are not representative of the recent deposits and because they represent only a minor portion of the entire lagoon. The target of the research line 3.16 was the implementation and the experimentation of an instrumented boat, able to collect high resolution seismic data in very shallow (up to 50 cm) waters. The new seismic data, calibrated with the available coring data and integrated with previous surveys, carried in the frame of the CARG project (plates Venezia and Chioggia-Cavallino), allowed the identification and the mapping of the main elements that characterize the architecture of the Venice lagoon:

- The transgressive sedimentary unit, overlying the late Pleistocene unconformity, deposited between 10.000 and 6.000 years B.P. This unit is the product of the marine incursion that followed the last glacial maximum.
- The highstand unit, between 6.000 years B.P and the present, consists of prograding deposits on the shelf and tidal channel deposits and mudflats in the lagoon.
- The historical unit that belongs to the last 600 year, testify the subsidence and a new marine incursion in the lagoon as a consequence of the diversion of the main rivers and the ground water exploitation in the mainland.

2 Development of the seismic acquisition system

The acquisition of the boat (Fig. 1), qualified for shallow water seismology, was made on the basis of an accurate market survey. The evaluation of different boats has been made based on the draught, the turbulence and the facilities for the installation of the seismic gears. Afterwards, different types of seismic sources have been considered. Based on the bandwidth, the repeatability of the signature and the portability of the hardware, a boomer system has been acquired and adapted to operate in water depth less than 1m (Fig. 2). The signature of the source has been measured during a field test and shows an amplitude spectra almost flat between 200 and 9.000 Hz (Fig. 3).

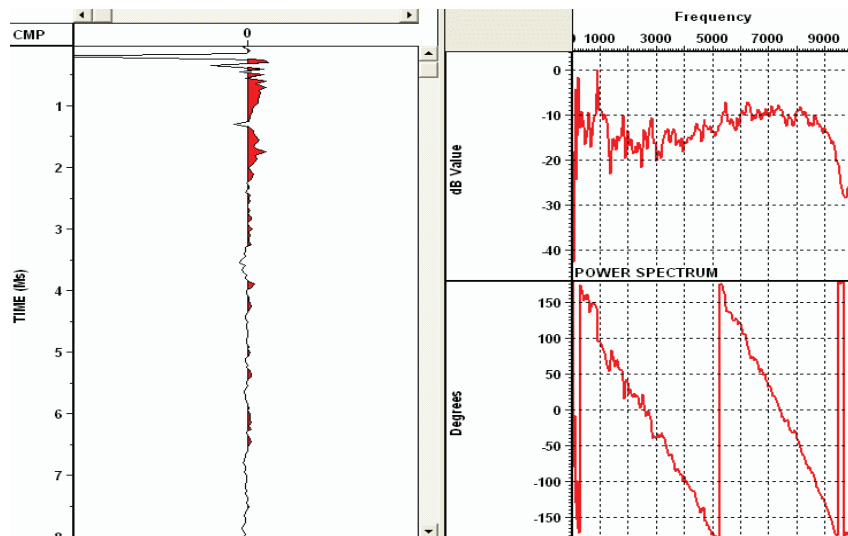
Figure 1 – The new boat “Aretusa” that has been implemented for shallows acquisition



Figure 2 – The boomer with the floating supports.



Figure 3 – The field signature of the boomer



The hydrophone configuration has been chosen after various field tests on single hydrofones and on arrays. The single hydrophone guarantees the best resolution, but is characterized by a very low Signal/Noise ratio. The array improves the S/N ratio but, particularly for shallow targets, it reduces the resolution of the signals because the different travel times along the array, produce a phase shift in the incoming signals (Fig. 4). As a rule of thumb, the length of the array (L) should be expressed by the formula below:

$$L \ll \sqrt{X^2 + 2r\lambda} - X$$

Where: X is the near offset, L is the array length, r is the travel time for the near offset hydrophone and λ the wavelength of the signal.

The array we chose was made by 8 in-line hydrophones for a total length of 270 cm. In order to reduce the filtering effect of the array, we adopted an acquisition geometry with the same offset for the array and the source. This geometry minimize the differences in the travel times along the array and therefore reduce the shifts between the incoming signals.

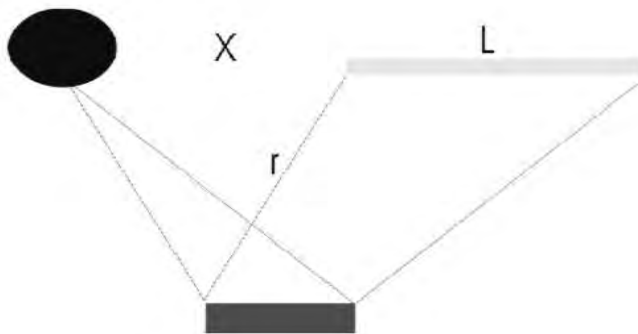


Figure 4 – Geometry for seismic acquisition with source and receiver in line.

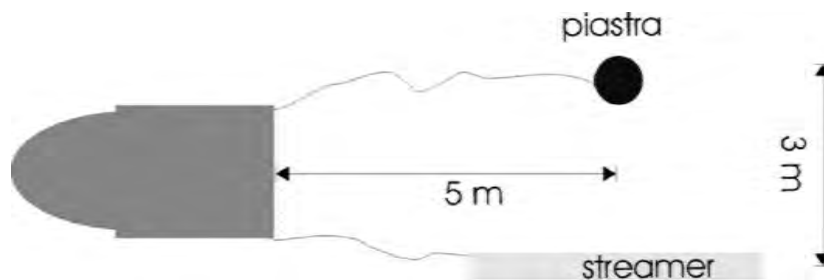


Figure 5 – The adopted geometry.

3 Seismic acquisition

Three field surveys in the lagoon area have been carried by the new CORILA boat “ARETUSA”, while the surveys along the rivers and on the shelf area and the inlets, by the CNR boat “LITUS”. The seismic data have been recorded in SEG-Y format and GPS coordinates have been stored in the header of each single trace.

The survey areas (Fig. 6) are significant for specific topics in the evolution and

setting of the lagoon and have been chosen also considering the previous surveys realized in the frame of the CARG project.

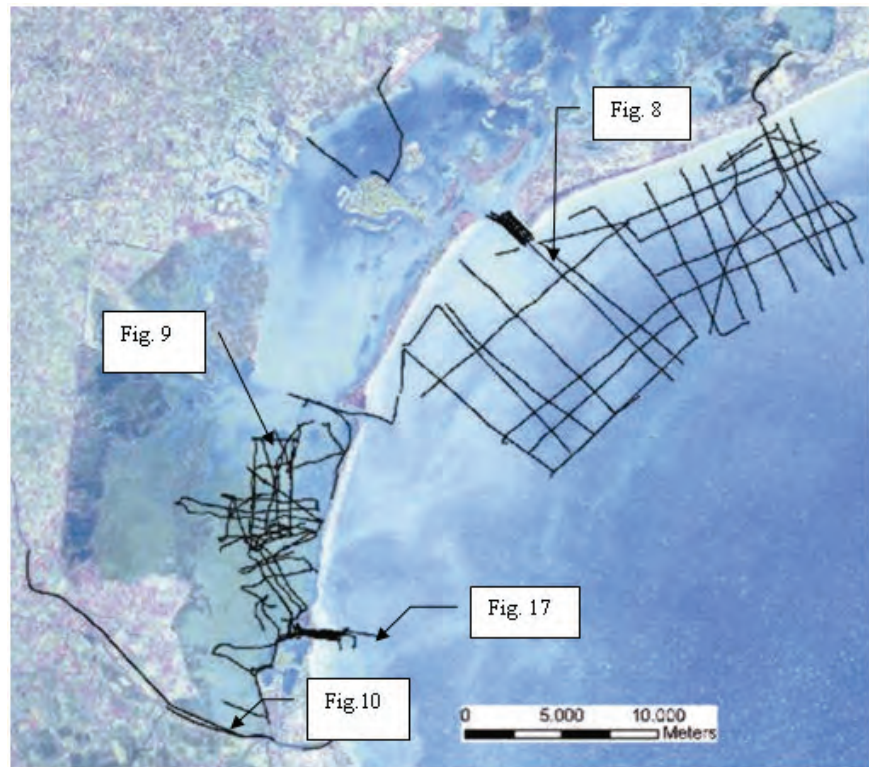


Figure 6 – Position map of the high resolution seismic survey recorded in the frame of the research line 3.16

Area 1: Lido and Chioggia inlets. In this area, two high density surveys have been carried (Fig. 7), that produced a 3D reconstruction of the inlets. The two areas are characterized by a strong hydraulic regime produced by tide flow and by the building of the dams. The Lido inlet is particularly important because in that area will be made the first installation of the MOSE project.

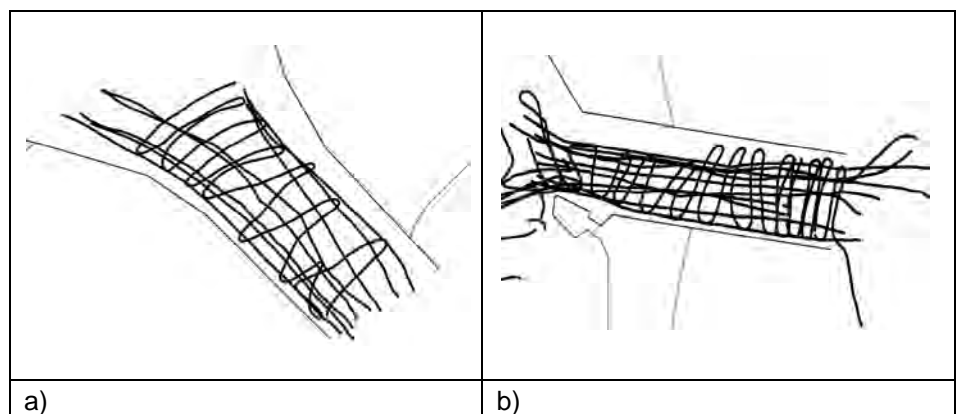


Figure 7 – Position of the seismic lines in the Lido (a) and Chioggia (b) inlets.

Area 2: The shelf area off the Lido inlet. It includes the ebb tidal delta and the Sile delta. In Fig. 8 a seismic profile from the ebb tidal delta.

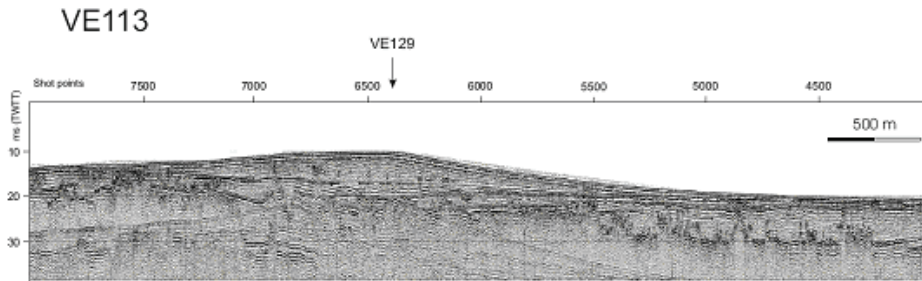


Figure 8 – Seismic profile Ve 113 across the ebb tidal delta of the Lido inlet

Area 3: The lagoon. The seismic surveys have been mainly carried in the southern portion of the lagoon, where the holocene sediments are much thicker than in the other sectors. For the first time, the very shallow water area (less than 1m) of the mud flats have been surveyed (Fig. 9).

Area 4: The Brenta and Sile rivers. Two lines have been recorded along these rivers that are important to link the lagoon area with the mainland (Fig. 10).

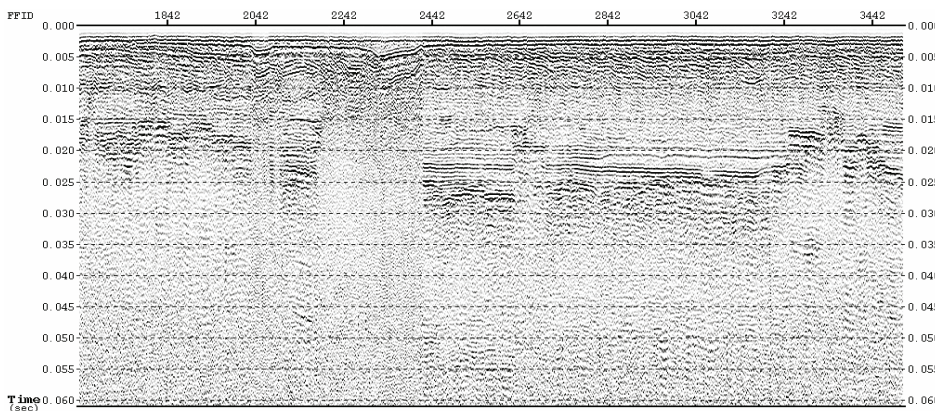


Figure 9 – Example of seismic section from very shallow water

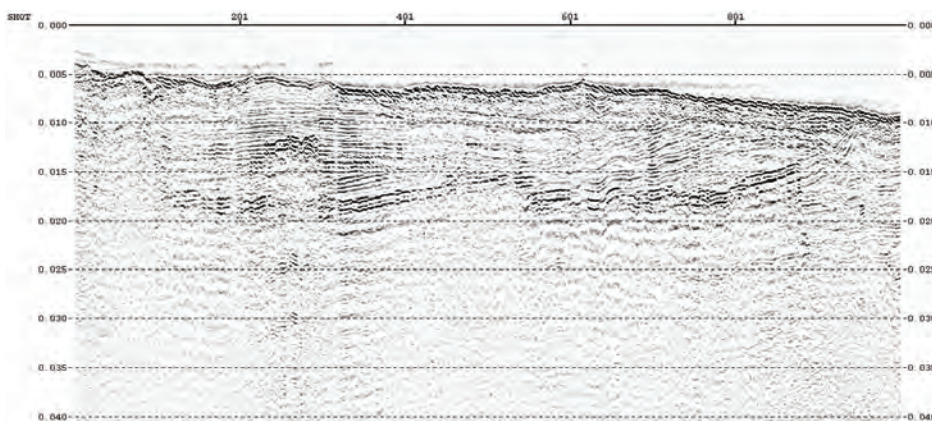


Figure 10 – Example of seismic line from the Brenta river

4 Seismic processing

The processing sequence is illustrated in Fig. 11; the main steps are:

Gain recovery: The energy and therefore the amplitude of the seismic signal, decay with the distance from the source. The main reasons are:

- spherical divergence, that depends on the square of the travel time;
- internal friction that may be considered linear with time.

The correction for the amplitude decay (C) applied to the data, in function of the time (t) was:

$$C = t + 20 \text{ Log}_{10} t$$

After the amplitude recovery, seismic data have been filtered to eliminate the low frequency noise (normally below 200 Hz). Based on the filter tests, an Ormsby filter 300-7.000 Hz has been applied. Then the data have been equalized by a balance window of 10 ms. Figure illustrate a portion of section VE-255 without any processing, while in Fig. 12b the same section has been compensated for amplitude decay, filtered and equalized.

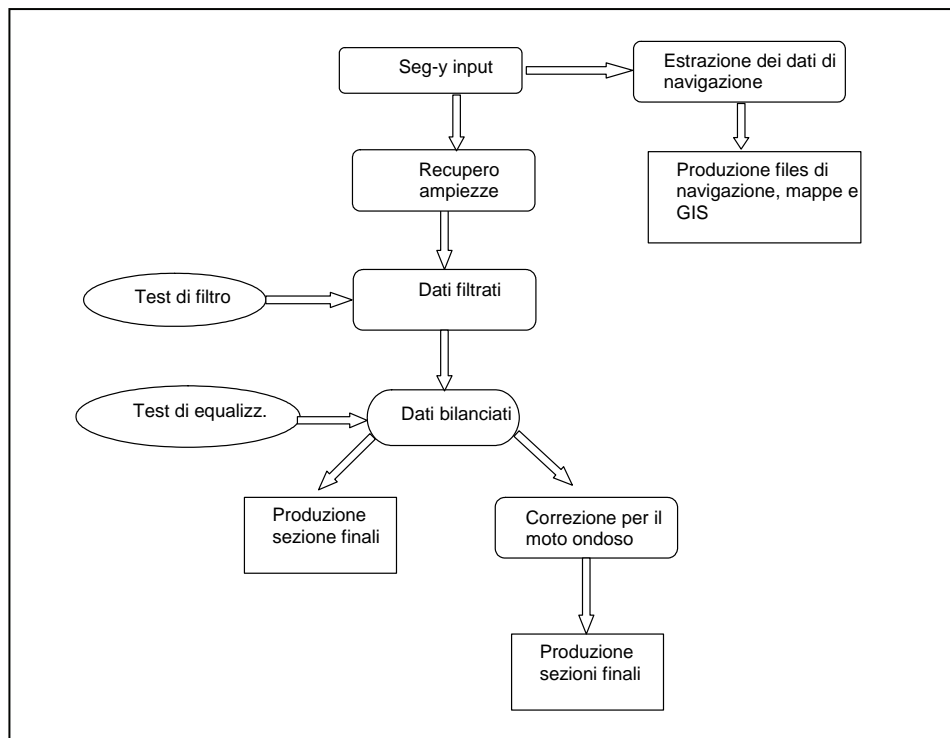


Figure 11 – Processing sequence

Wave motion correction: some seismic sections, particularly in the offshore area, are affected by strong wave motion that produce a worsening in the data quality. To eliminate this effect we adapted a techniques very similar to the one normally applied for compensate on land seismic for residual statics. This technique is based on the cross-correlation, inside a designed window, of each seismic trace with a pilot trace obtained from the data itself. When the procedure works correctly the shift of the cross correlation corresponds to the

shift induced by the waves.

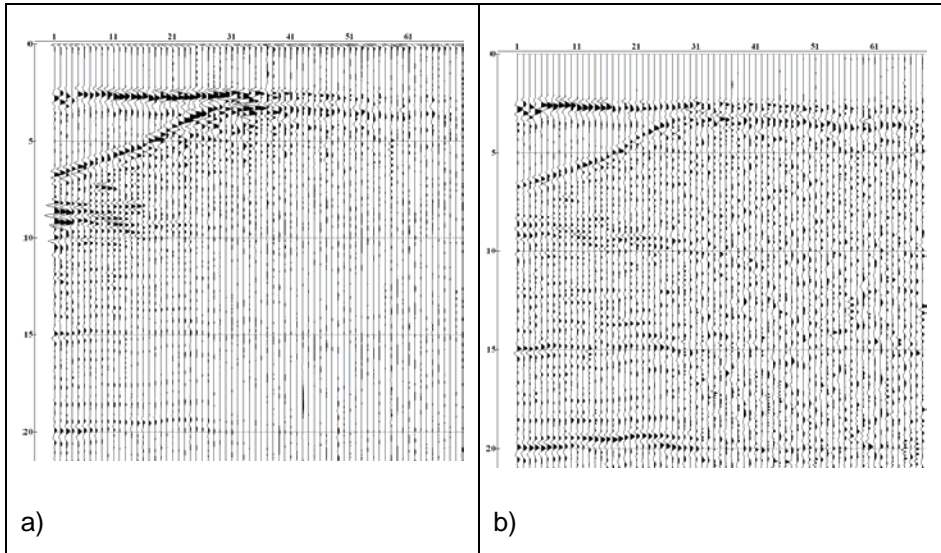


Figure 12- a) Line VE- 255 raw data; b) Line Ve- 255, gain recovery, filter and balance

In our case the pilot trace was obtained by the weighted (50-100-50) stack of three adjacent traces, the length of the designed window was 12 ms and included the sea bottom. In Fig. 13a and 13b an example of seismic section affected by wave motion and the same section corrected according to the above mentioned procedure.

All the seismic data, their position and the most usefull stratigraphic informations have been included in a GIS system

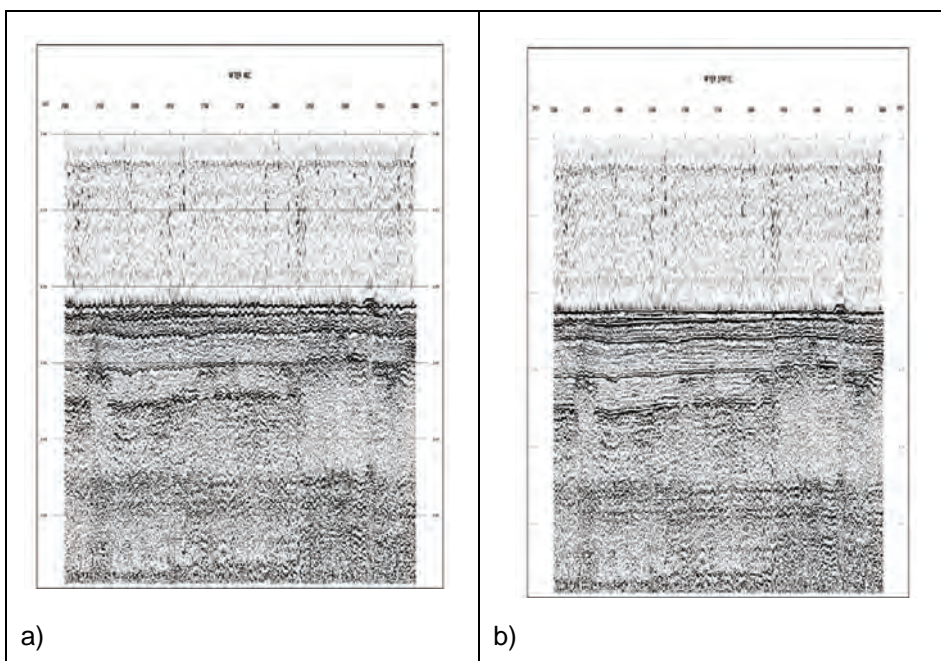


Figure 13 – a) Seismic section from the shelf area affected by wave motion, b) corrected for the wave motion.

5 Preliminary interpretation of the seismic data

The deposits investigated in the frame of the research line 3.16 belong to two well distinct geological epochs:

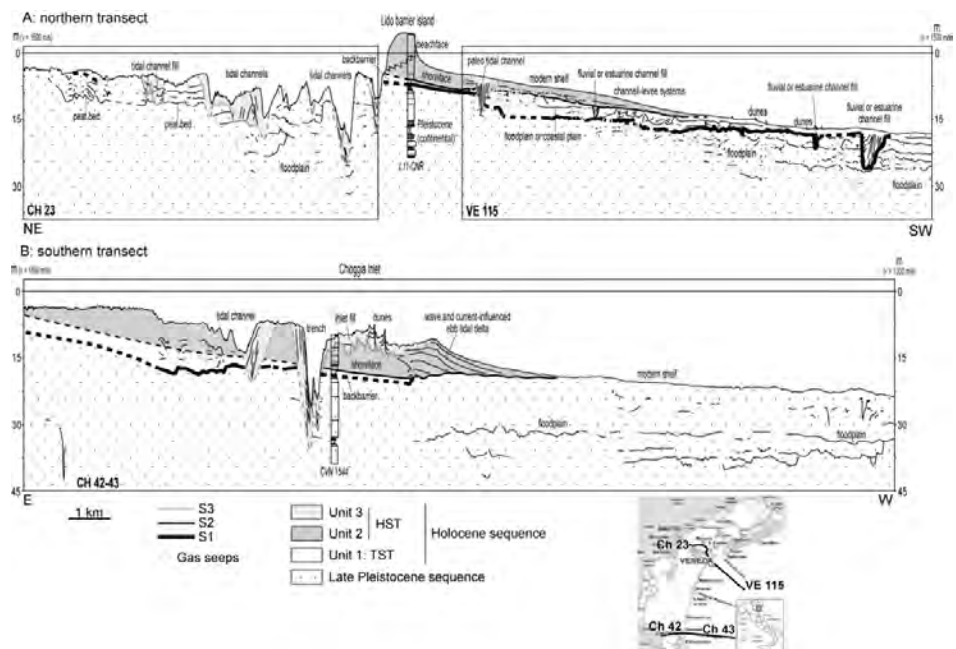
- The late Pleistocene
- The Holocene

5.1 The late Pleistocene sequence

The Pleistocene succession is bounded at the top by an unconformity (S1) that records conditions of sub aerial exposure (Fig. 14). Pleistocene deposits investigated by the new survey, should be totally referred to the late Pleistocene. Late Pleistocene seismic reflectors are mostly sub-horizontal, but erosional and channelized facies are common (Fig. 14). An overall aggradational stacking pattern characterizes the succession, as evidenced by the vertical stack of sub-horizontal seismic reflectors and channels (Zecchin et al., in press). Locally a transparent and homogeneous seismic facies has been recognized (Fig. 15) that has tentatively attributed to the presence of lacustrine deposits.

From multidisciplinary studies (e.g. Tosi et al., 2006a, 2006b) it is known that the upper Pleistocene sequence, accumulated since the last Tyrrhenian marine transgression, until the end of the Last Glacial Maximum, consists only of continental deposits.

Figure 14 – Line drawings showing the architecture and the interpreted sequence-stratigraphic organization of the late Pleistocene and Holocene sequences in the northern (a) and southern (b) locations of the study area (modified from Zecchin et al., in press).



5.2 The Holocene sequence

In the Venice Lagoon area the Holocene sequence has various thickness, larger in the southern lagoon (20-22 m) and reduced to at least 1-2 m toward

the inner lagoon margin and offshore in the Adriatic Sea (Tosi et al., 2006a, 2006b). The new seismic survey outlines three seismic units inside the Holocene sequence that have been named Unit 1, Unit 2, and Unit 3 (Zecchin et al., in press). These units are bounded by stratal surfaces: S1, S2, and S3 (Zecchin et al., in press) (Fig. 14).

Based on distribution, geometries and correlation with the stratigraphy of the lagoon, Unit 1 has been attributed to the transgressive system tract (TST) at the base of the Holocene and S2 and S3 to the overlying highstand system tract (HST) (Zecchin et al., in press).

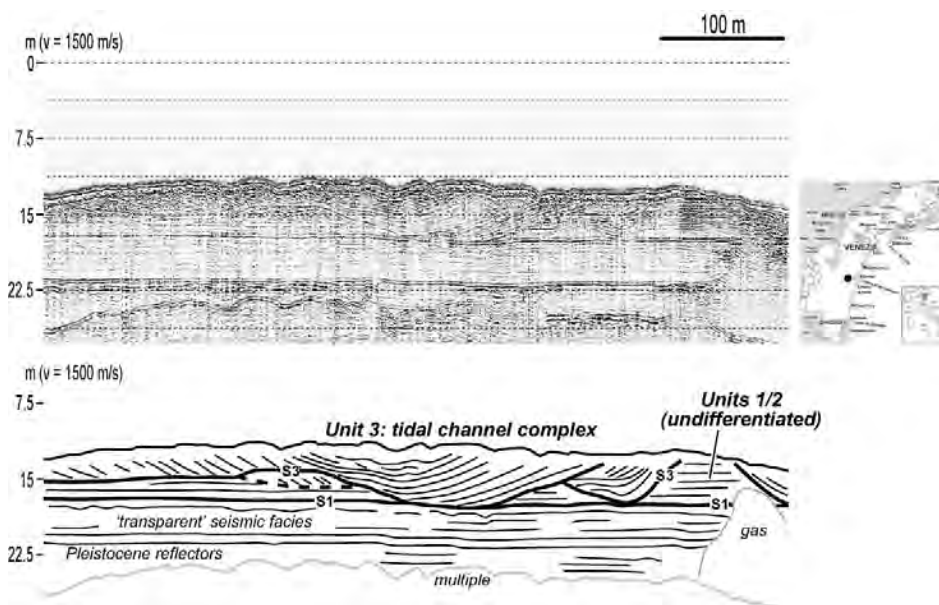


Figure 15 – Late Pleistocene and Holocene sequences in the Venice lagoon, near the Malamocco inlet. Late Pleistocene deposits show sub-horizontal reflectors and a continuous interval characterized by a more transparent seismic facies, placed immediately below the S1 surface and inferred as a possible lacustrine deposit (modified from Zecchin et al., in press)

5.2.1 Key stratal surfaces

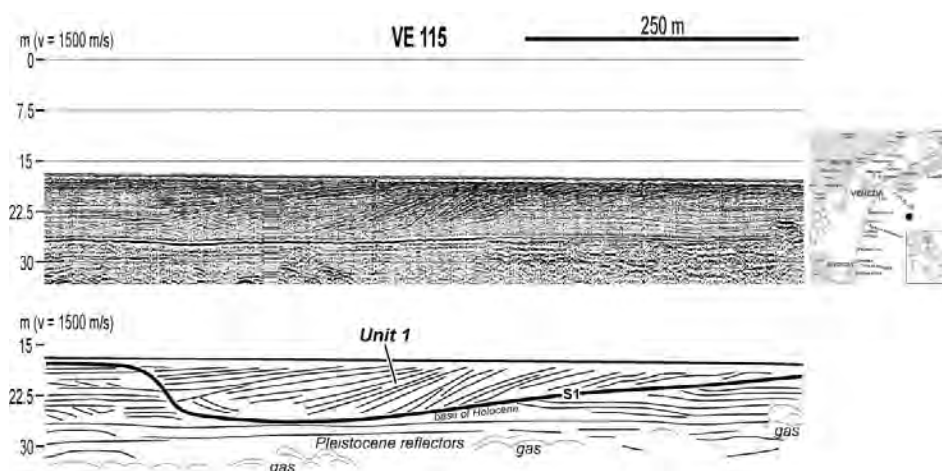
Unit 1

The lower part of the Holocene succession, between S1 and S2 surfaces, is composed of channelized deposits separated by sectors showing sub-horizontal and hummocky reflectors. Sub-horizontal reflectors onlap onto the S1 surface in the landward direction (Fig. 14). Major channelized deposits, up to 8 m thick, show lateral accretion and well defined clinoforms (Fig. 16). These deposits testify an overall aggradational stacking pattern. Locally (e.g. off the Chioggia inlet) Unit 1 is absent, and S1/S2 surfaces are coincident (Fig.14b).

In the proximal area, below the lagoon, sub-horizontal reflectors above the S1 surface are dominant. Core data demonstrate that they consist of thin coastal plain strata draping the S1 surface and passing upward into muddy deposits accumulated in a less restricted lagoonal environment (Tosi et al., 2006a, 2006b). In the lagoonal area, the boundary between Unit 1 and Unit 2 is not easily distinguishable, moreover, both units have been totally removed from the deeper tidal channels (Fig. 15).

The recognized structures of channelized deposits in the northern offshore area may be the result of point bar migration and the development of channel-levee systems (Zecchin et al., in press). Both seismic and core data indicate that similar features are absent landward, in the correspondence of the modern lagoon-barrier system. In the absence of core data from the shelf area, we hypothesize that the observed channelized units may be fluvial channel deposits separated by floodplain areas and locally entrenched in the late Pleistocene strata, or more probably estuarine fills, resulting from the drowning of previous fluvial valleys, and distributary channel deposits (the channel-levee systems) (Zecchin et al., in press). The latter hypothesis was already suggested by Trincardi et al. (1994) in the northern Adriatic shelf.

Figure 16 – Large channelized deposit showing a lateral accretion and located off the Lido barrier island. This feature is interpretable as the consequence of the migration of a point bar in a fluvial channel or in an estuary. In both hypothesis, this deposit is interpreted as the lower part of the Holocene sequence (Unit 1) (from Zecchin et al., in press).



Unit 2

This unit is bounded at the base by the S2 surface and it is well distinguishable from Unit 1 only in the northern offshore area and in the correspondence of the Lido barrier island (Fig. 14a). In the south, off the Chioggia inlet, only Unit 2 is recognizable (Fig. 14b and 17). Both units are present landward in the lagoon, where they show sub-horizontal to irregular reflectors (Fig. 14a and b), but their distinction is not easy due to the uncertain recognition of the S2 surface.

Seaward, Unit 2 consists of a sandy to muddy, aggrading and prograding wedge that is up to 10 m thick in the correspondence of the Lido littoral (Figs. 14a and 17). This wedge is alongshore elongated and is recognizable up to 6.5 km seaward from the modern shoreline. Clinofolds display a sigmoidal shape, have tangential bases, and downlap onto the S2 surface. They are inclined from 0.4° (off the Chioggia inlet) to 0.06° in distal locations. The direction of progradation is to the south-east. Core data from the Lido littoral and the Chioggia inlet confirm the regressive character of Unit 2 (evidence of an overall coarsening- and shallowing-upward succession above the S2 surface). A fining-upward trend in the lower part of the unit and a more marked coarsening-upward trend in the upper part are recognizable in cores from other locations in the barrier island (Tosi et al., 2006a, 2006b). Core data illustrate that low-

energy mud flat, tidal flat, and brackish marsh sub-environments are common in the Holocene lagoon (e.g. Bonardi et al., 2006).

Seismic profiles indicate that the regressive wedge of Unit 2, located between the lagoon inlets, is a shoreface-shelf system, prograding south-eastward (Zecchin et al., in press). In the correspondence of the inlet outer side (e.g. off the Chioggia inlet), the wedges are interpreted as ebb tidal deltas influenced by waves and alongshore currents (Zecchin et al., in press) (Fig. 17). Ebb tidal deltas, in fact, interact laterally with the shoreface-shelf-system. The fan shape of these ebb tidal deltas is also evidenced by bathymetric maps (Amos et al., 2005).

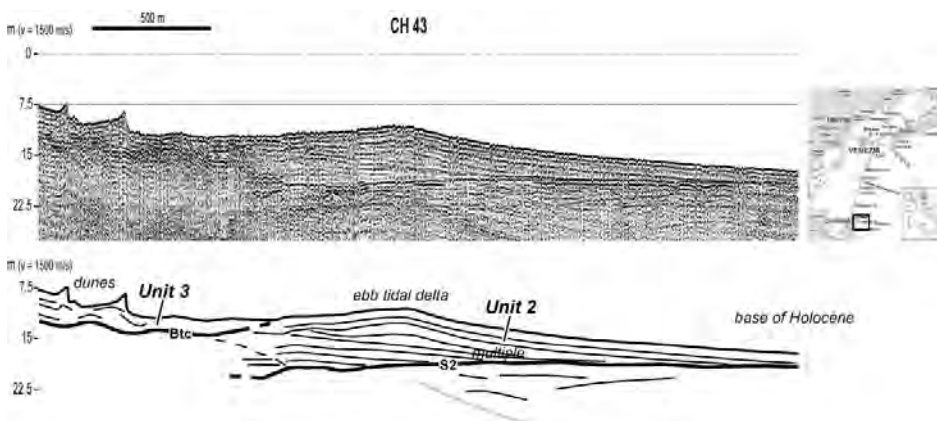


Figure 17 – Ebb tidal delta forming part of Unit 2 located immediately off the Chioggia inlet. In this case, the transgressive deposits of Unit 1 are absent and the S2 surface reworks the S1 surface and coincides with the boundary of the Holocene sequence (from Zecchin et al., in press).

Unit 3

Active, partially filled tidal channels are characteristic of the Venice Lagoon. They are entrenched in the lagoonal mud-flat and may cut the Pleistocene-Holocene boundary (the S1 surface) (Figs. 15). Channels are deeper near the inlets (Fig. 14). In some cases, channels have been over deepened by dredging activities. Lateral accretion and scour and fill features were commonly recognized (cf. McClennen et al., 1997) (Fig. 15). Buried channelized deposits showing lateral accretion were found below the modern lagoonal floor, between the Malamocco and Chioggia inlets. A V-shaped channelized deposit, which is entrenched in both units 1 and 2, is present off the Lido littoral (Fig. 14).

Inlets are highly dynamic, especially after human interventions carried out during the last centuries that have enhanced current velocity and tidal prism (Carbognin, 1992; Carbognin et al., 2000). Erosional trenches are present at the inner end of both the Chioggia (30 m deep) and Malamocco (50 m deep) inlets (Fig. 14). The base of inlet is recognizable as an irregular reflector, whereas inlet deposits consist of accreting macroforms and dunes. These deposits are relatively thick (up to 7.5 m) in the northern part of the Lido inlet, whereas the southern part is subjected to prevailing erosion. The opposite situation is recognizable in the Chioggia inlet (Zecchin et al., 2006).

References

Amos, C. L., Helsby, R., Ungiesser, G., Mazzoldi, A., Tosi, L., 2005, Sand transport in northern Venice Lagoon, in Campostrini, P., ed., *Scientific research and safeguarding of Venice: Co.Ri.La. Research Program 2001-2003*, v. 3, p. 369-383.

Bonardi, M., Tosi, L., Rizzetto, F., Brancolini, G., and Baradello, L., 2006, Effects of climate changes on the late Pleistocene and Holocene sediments of the Venice Lagoon, Italy: *Journal of Coastal Research, Special Issue 39*, p. 279-284.

Carbognin, L., 1992, *Evoluzione naturale e antropica della Laguna di Venezia: Memorie Descrittive della Carta Geologica d'Italia*, v. 42, p. 123-134.

Carbognin, L., Cecconi, G., and Ardone, V., 2000, Interventions to safeguard the environment of the Venice Lagoon (Italy) against the effects of land elevation loss, in *Land Subsidence* (Eds L. Carbognin, G. Gambolati and A.I. Johnson), *Proc. Sixth Int. Symp. Land Subsidence, Ravenna (Italy)*, La Garangola, Padova (Italy), 1, 309-324.

McClennen, C.E., Ammerman, A.J., and Schock, S.G., 1997, Framework stratigraphy for the Lagoon of Venice, Italy: revealed new seismic-reflection profiles and cores: *Journal of Coastal Research*, v. 13, p. 745-759.

Tosi, L., Rizzetto, F., Bonardi, M., Donnici, S., Serandrei Barbero, R., and Toffoletto, F., 2006a, *Note illustrative della Carta Geologica d'Italia alla scala 1:50.000. Foglio 128 – Venezia, SystemCart, Roma* (in press).

Tosi, L., Rizzetto, F., Bonardi, M., Donnici, S., Serandrei Barbero, R., and Toffoletto, F., 2006b, *Note illustrative della Carta Geologica d'Italia alla scala 1:50.000. Foglio 148-149 – Chioggia-Malamocco, SystemCart, Roma* (in press).

Trincardi, F., Correggiari, A., and Roveri, M., 1994, Late Quaternary transgressive erosion and deposits in a modern epicontinental shelf: the Adriatic Semienclosed Basin: *Geo-Marine Letters*, v. 14, p. 41-51.

Zecchin, M., Brancolini, G., Donda, F., Rizzetto, F., Tosi, L., 2006. Preliminary results of the high resolution seismic surveys in the Venice lagoon: *Co.Ri.La. Research Program 2004-2006, 5th Annual Meeting, Venice (Italy)*, 26-28 April 2006, 3.16 research line.

Zecchin, M., Baradello, L., Brancolini, G., Donda, F., Rizzetto, F., Tosi, L., *Sequence stratigraphy based on high-resolution seismic profiles in the late Pleistocene and Holocene deposits of the Venice area: Sedimentology*, in press.

PRELIMINARY STUDY OF GEOMORPHOLOGICAL FEATURES DISCOVERED IN TIDAL FLATS OF THE VENICE LAGOON BY VHR SEISMIC SURVEYS

Luigi Tosi¹, Giuliano Brancolini², Luca Baradello², Federica Donda², Federica Rizzetto¹, Massimo Zecchin²

¹*Istituto di Scienze Marine - Consiglio Nazionale delle Ricerche, San Polo 1364, 30125, Venice, Italy,* ²*Istituto Nazionale di Oceanografia e Geofisica Sperimentale, Borgo Grotta Gigante 42/C, 34010, Sgonico, Trieste, Italy*

Riassunto

In questo studio sono stati elaborati i dati sedimentologici, stratigrafici, batimetrici e cartografici disponibili pregressi e una serie di nuovi rilievi sismici ad altissima risoluzione eseguiti sui bassi fondali lagunari. I dati raccolti hanno consentito di individuare le strutture geomorfologiche a scala regionale mentre quelli di nuova acquisizione hanno fornito una serie di dettagli locali delle stesse strutture.

In particolare, i nuovi dati sismici hanno permesso di individuare per la prima volta la presenza di elementi geomorfologici nei bassifondi lagunari ed in alcuni casi di caratterizzare la loro evoluzione spazio-temporale.

Abstract

Available sedimentological, stratigraphic and bathymetric data, historical maps and a number of new Very High Resolution Seismic (VHRS) surveys acquired in the lagoon shallows were processed. Collected data allowed the characterization of the geomorphological setting at regional scale, whereas new VHRS data locally provided details of feature extent.

In particular the new VHRS surveys pointed out, for the first time, the occurrence and, in some cases, the evolution of buried and surface morphological features found in the lagoon shallows.

1 Introduction

In order to provide new geological knowledge on the Venetian lagoon subsoil, within the Co.Ri.La. subproject 3.16 "Application of innovative high resolution seismic methodologies to the shallows for the study of the subsoil in the Venice Lagoon", a Very High Resolution Seismic (VHRS) system has been implemented to investigate in very shallow waters, i.e. less than 1 m depth, and a number of surveys were carried out in the southern portion of the lagoon.

VHRS profiles acquired in the south lagoon area allowed excellent images of the subsoil architecture down to 30 m b.s.l and the identification of geomorphological features never been found in previous studies.

In addition, this study allowed a detailed characterization of the Late

Pleistocene and Holocene depositional setting and results provides a tool for next research projects regarding the effects of climate changes and the human impact on lagoon sedimentary processes.

This paper pointed out preliminary investigation results and more accurate description and detailed interpretation of the various geomorphological features will be available within the final work scheduled for the next year.

2 Material and methods

Collected and new data were used to carry out this study. A large amount of information, derived from several boreholes made along the Venetian littoral and in the lagoon basin, were collected and used for the regional geomorphological setting characterization. Available information include sedimentological, stratigraphic, geotechnical, mineralogical, ¹⁴C datings, textural, and bathymetric data, satellite images and historical maps [Bonardi and Tosi 1997; Bonardi and Tosi 2000a,b; Bonardi et al., 1997; Bonardi et al., 2004; Bonardi et al., 2005; Bonardi et al., 2006; Brancolini et al., 2005; Rizzetto et al., 2002; Rizzetto et al., 2003; Rizzetto et al., 2005; Tosi 1993; Tosi 1994a,b,c (1994); Tosi et al. 2006a,b; Zecchin et al., 2006]. Collected data were verified, selected and homogenized. In particular bathymetric data were processed to obtain the digital elevation model of the bottom lagoon morphology of sites under investigation.

New VHRS surveys were acquired through the ARETUSA, the new boat of the Co.Ri.La. Subproject 3.16, ad hoc implemented for surveys in lagoon shallows. Seismic data were processed [Brancolini et al., this volume] and a detailed line-drawing of the various seismic reflectors were done. Finally seismic data were calibrated and validated by available collected data from core lithostratigraphy and sedimentological and radiocarbon analyses.

3 Results

The integrated analysis of the collected and new data provided several blow up figures of features occurring in the regional geomorphological setting. In some cases, images of the space-time evolution of morphological structures were pointed out.

The investigated depth subsoil is down to 30 m b.s.l. and concerns the Late Pleistocene and Holocene deposits (the last 30,000 years). Different depositional environments were revealed and, in particular, alluvial, marine, littoral, lagoon, and deltaic facies were recognized.

The first step of this work was the integration of data from space and in situ for recognizing geomorphological features at regional scale. The merge of LANDSAT TM and bathymetric data allow the correlation between geomorphological features, such as old lagoon channels, paleoriver beds, ancient beach ridges partially outcropping in the southern catchment and lagoon basin. Fig. 1 shows DEM of the lagoon bottom, which has revealed a series of paleobeach ridges with NE-SW direction. VHRS pointed out their prograding architecture toward the present coastline [Brancolini et al., this

volume] and 14C data allow their dating to 5,000-3,000 years B.P. [Rizzetto et al., 2002, 2003; Tosi 1994a,b,c; Tosi et al. 2006a,b]. These features are correlated with similar ones found in the SW part of the complex system of ancient beach ridges and sand dunes identified by satellite images south of the lagoon basin, between Adige and Brenta rivers.

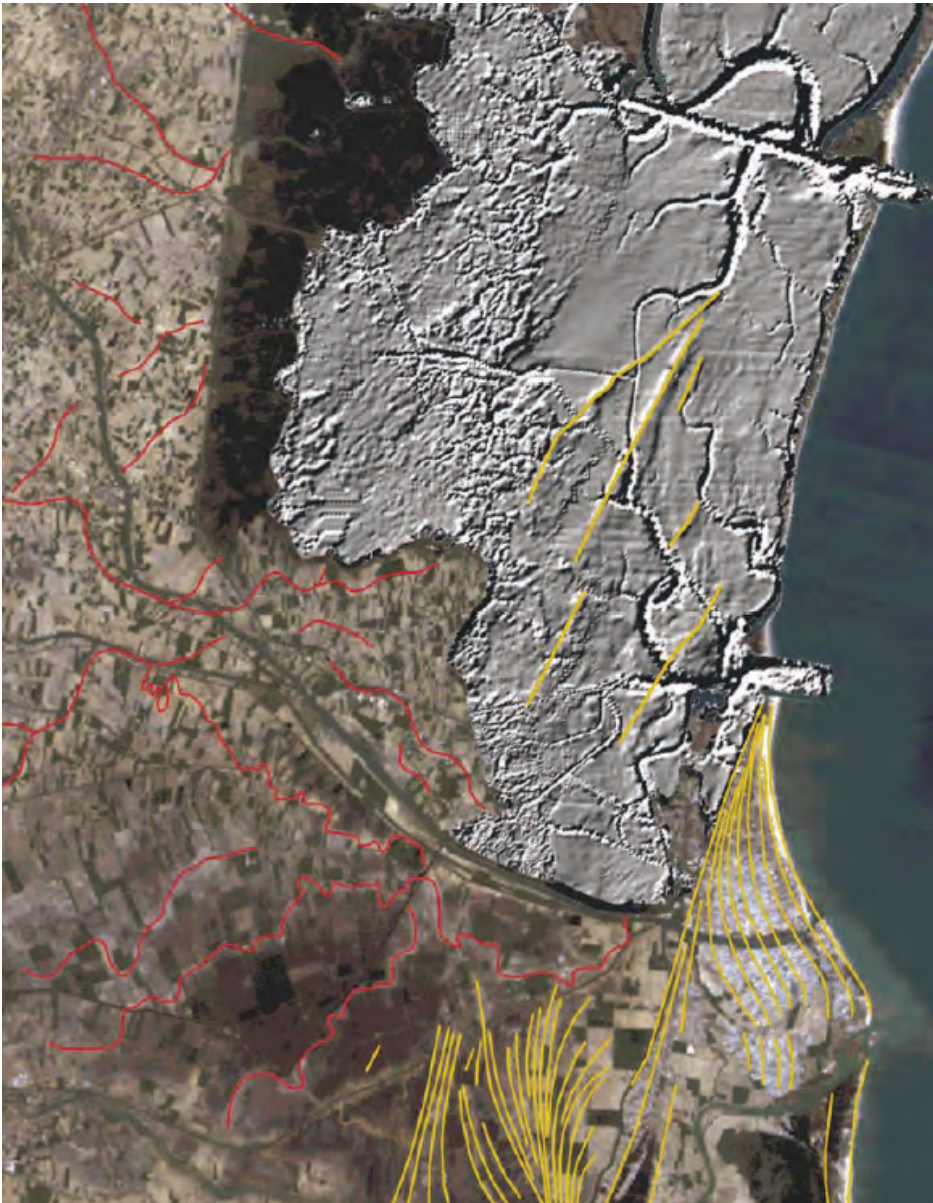


Fig. 1 – DEM of the lagoon bottom merged to LANDSAT TM image of the southern catchment. Yellow lines point out ancient beach features and red lines paleorivers and paleochannels.

The eastern evidences of this littoral system are related to the Adige, Brenta, and Bacchiglione river mouth evolution occurred over the last 2,000 years.

A number of filled channels with ancient direction fluxes toward the lagoon basin were found in the mainland-lagoon border. The integrated analysis of all available information allows to distinguish the origin of some of these, i.e. their belonging to the Brenta, Bacchiglione, Adige fluvial systems.

The new VHRS survey is the unique tool allowing detailed subsoil images in lagoon shallows and tidal flats. Seismic sections pointed out details of the depositional architecture previously never been revealed.

Following, some selected geomorphological features discovered in the south lagoon basin by VHRS survey, as examples of preliminary study concerning this topic, are reported.

Their locations are shown in Fig. 2.

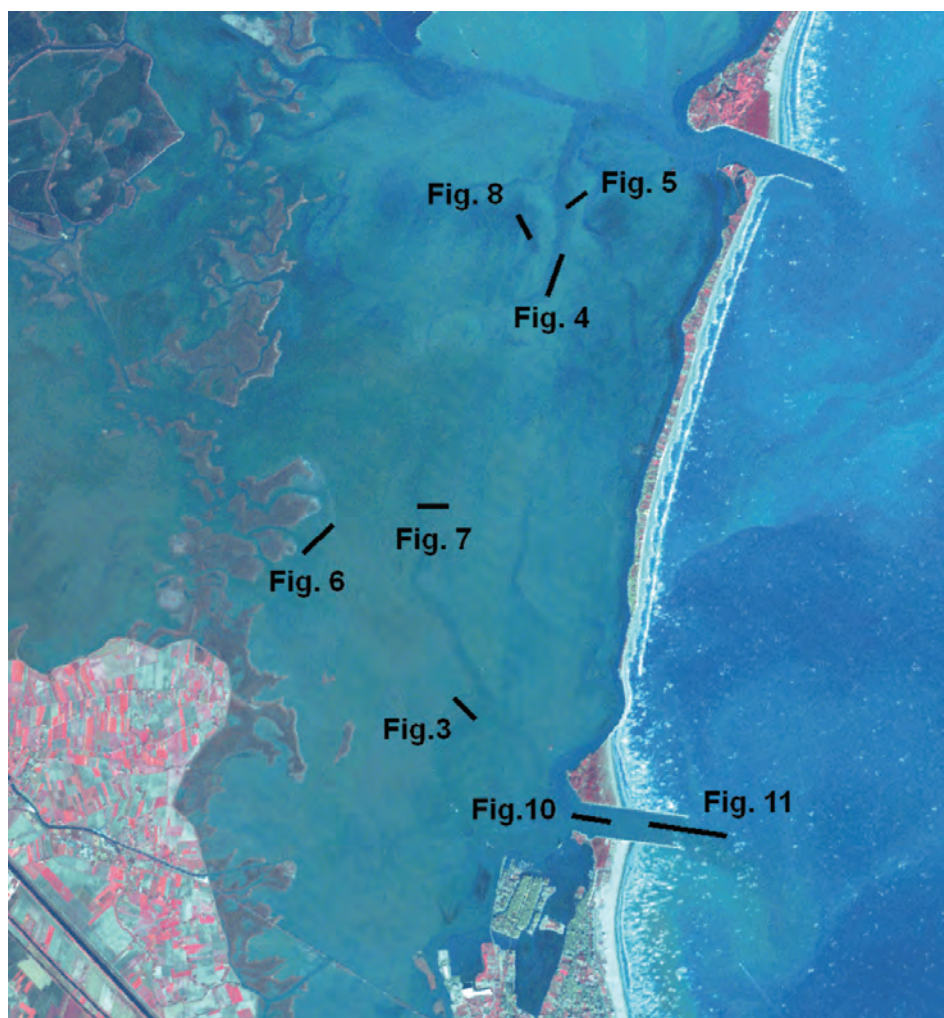


Fig. 2 – Location map of the selected geomorphological features.

An example of a Holocene tidal channel complex system is given in Fig. 3. Line drawing and interpretation point out vertical and horizontal evolution of the tidal channel from its origin to the present setting. The active tidal channel, partially filled, and the lagoon mudflat show sub-horizontal reflectors.

An additional example of lagoon channel architecture is given in Fig. 4. Sigmoidal foresets indicate the evolution of a sand bar system and the north direction migration of the ancient channel. The morphology of the present active channel is characterized by truncation and erosion of the previously deposited layers.

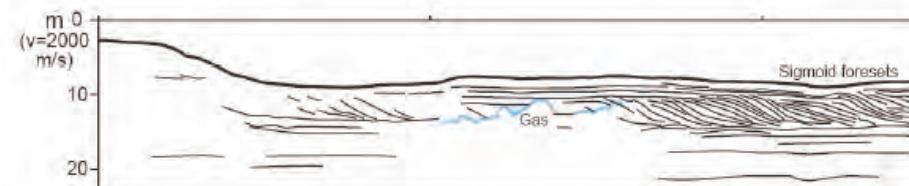
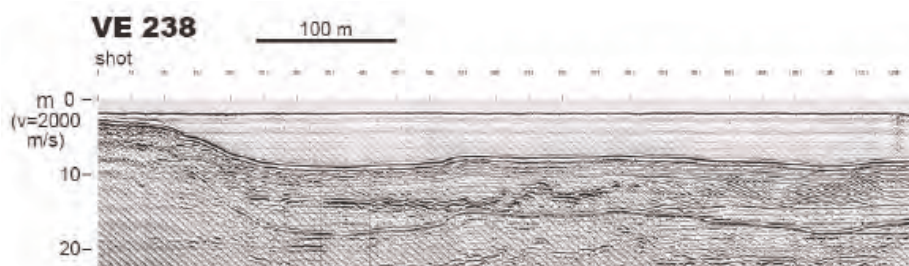
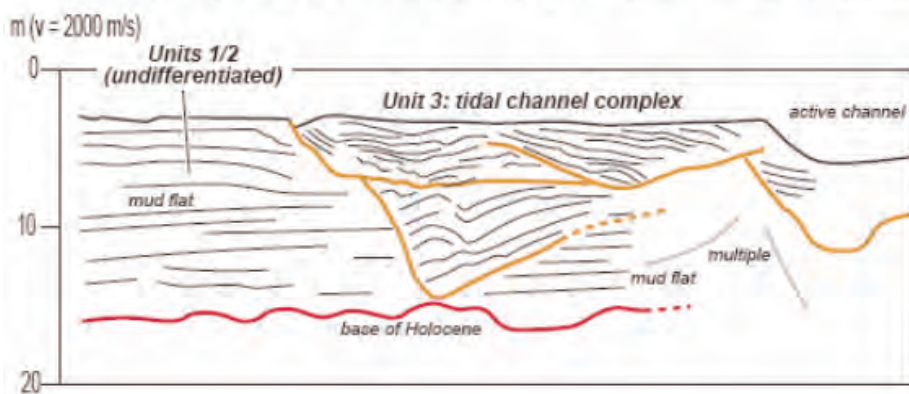
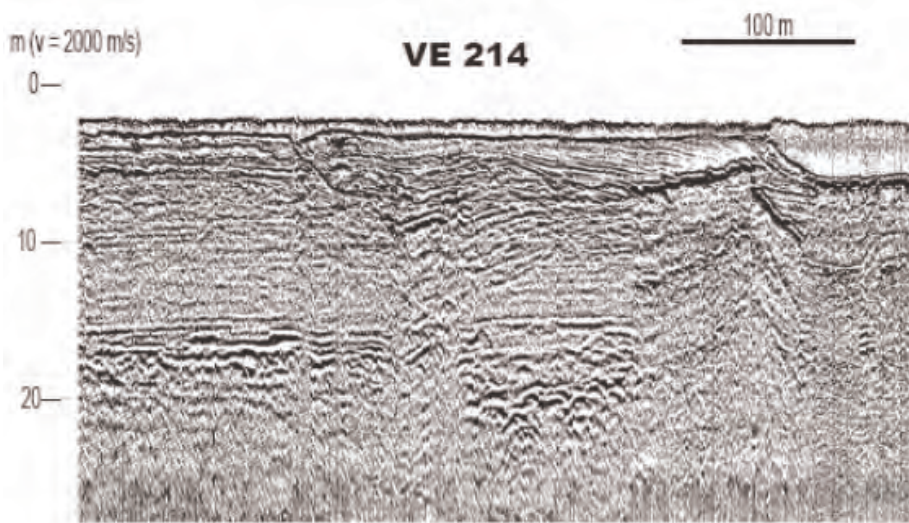


Fig. 3 – Example of Holocene complex tidal channel system evolution.

Fig. 4 – Section of active lagoon channel.

Fig. 5 reports another example of architecture of an active channel. In this section, a like island shape (i.e. the morphological high) divides the channel in two sectors. Lateral accretion process, which partially filled an ancient channel, is recognizable on the left sector. On the right sector, the active channel is migrating to NE direction. This is evidenced by the lateral migrating bar (probably a meander) occurring on its left side and by the erosion of the previous accretion features (foreset truncation) on the right side.

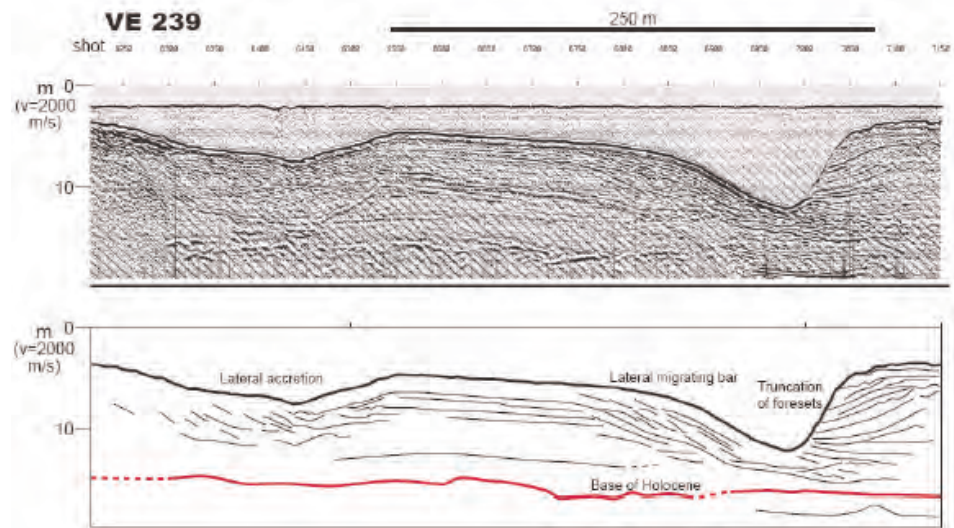


Fig. 5 – Example of subsoil architecture and morphology of an active lagoon channel.

Inactive Holocene channelized deposits and channel-levee systems developed in a delta-plain are recognizable in Fig. 6, whereas a large buried Pleistocene channelized deposit, showing a lateral accretion, in Fig. 7. The latter is related to an ancient branch of the Brenta River system.

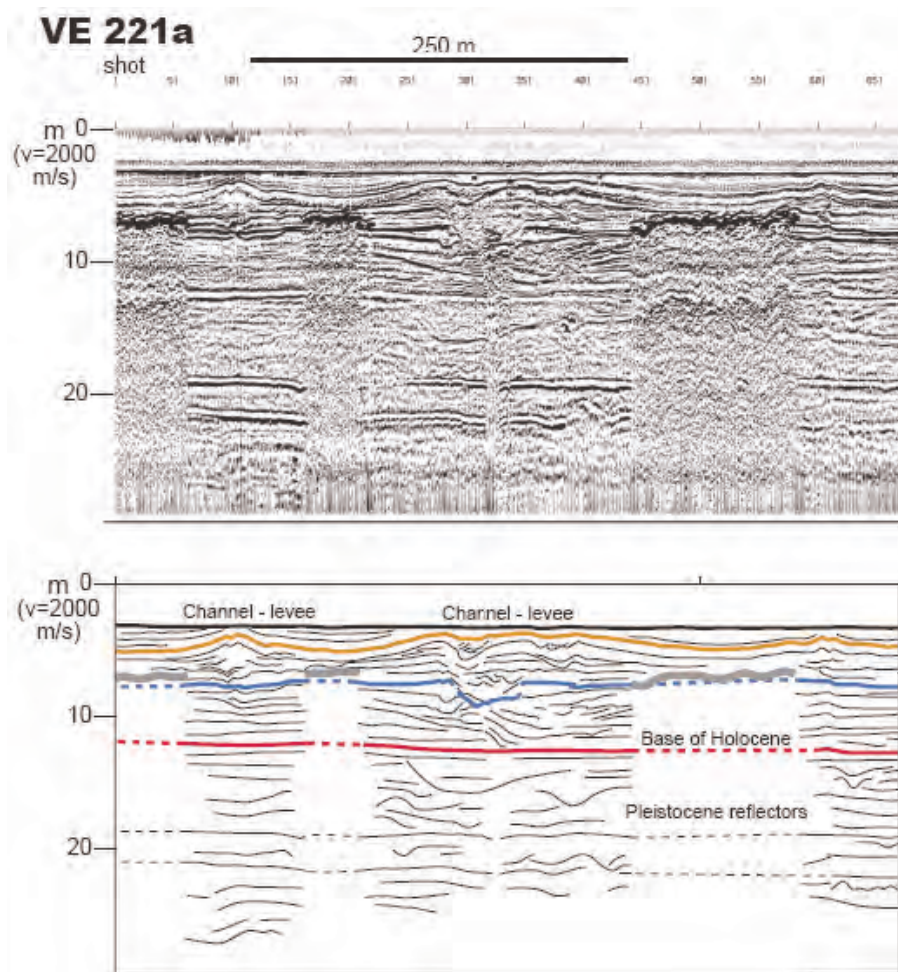


Fig. 6 – Example of inactive Holocene channel-levee system architecture.

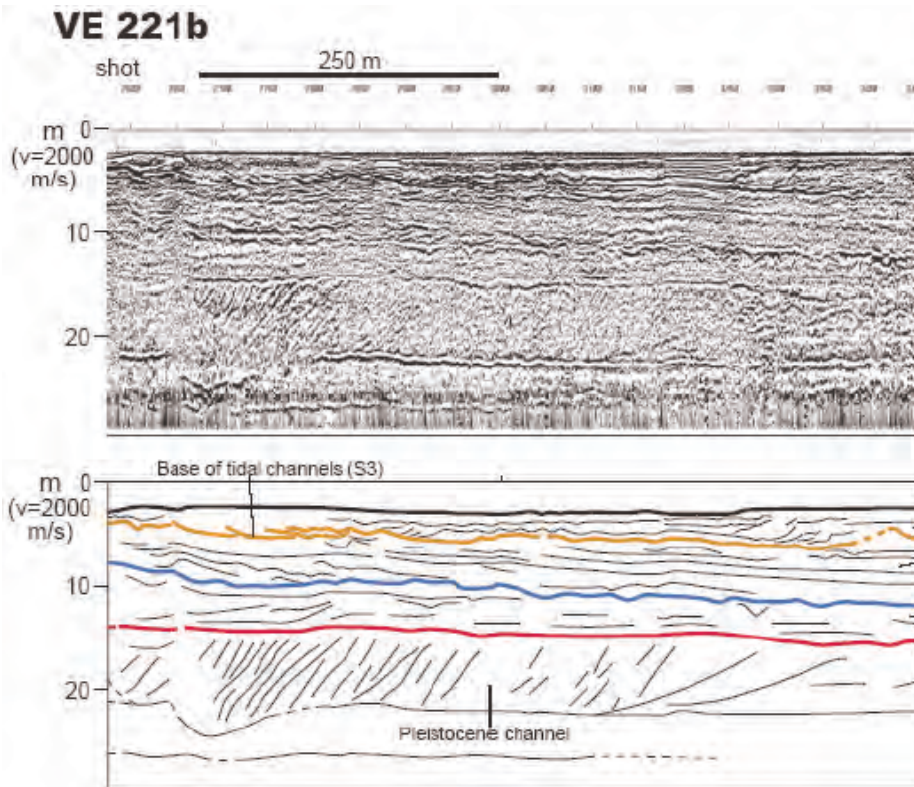


Fig. 7 – Lateral accretion in a buried channel of the Pleistocene Brenta river system.

The complexity of the Holocene lagoon environment is shown in Fig. 8. A number of tidal buried channelized deposits were found below the modern lagoon floor.

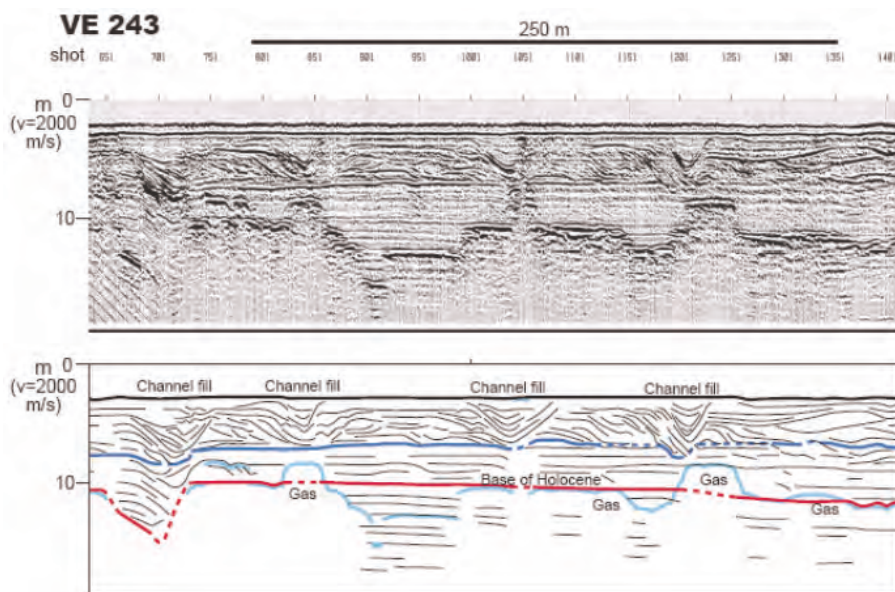


Fig. 8 – Example of inactive Holocene channel fill system showing the complexity of the past lagoon environment.

Investigations in the Chioggia inlet have shown the occurrence of sedimentary processes, both deposition and erosion, highly dynamic.

Bathymetric data processing provides spectacular figures of the inlet sea

bottom (Fig. 9).



Fig. 9 – Morphology of the Chioggia inlet. Trench and dune features occur in left and right side respectively.

A 30 m deep erosional trench, due to the hydrodynamic flux confluence of some tidal channels, occurs toward the lagoon side of the inlet. The VHRS survey revealed that the trench is characterized by accretion and erosion of the west and east side walls respectively (Fig. 10).

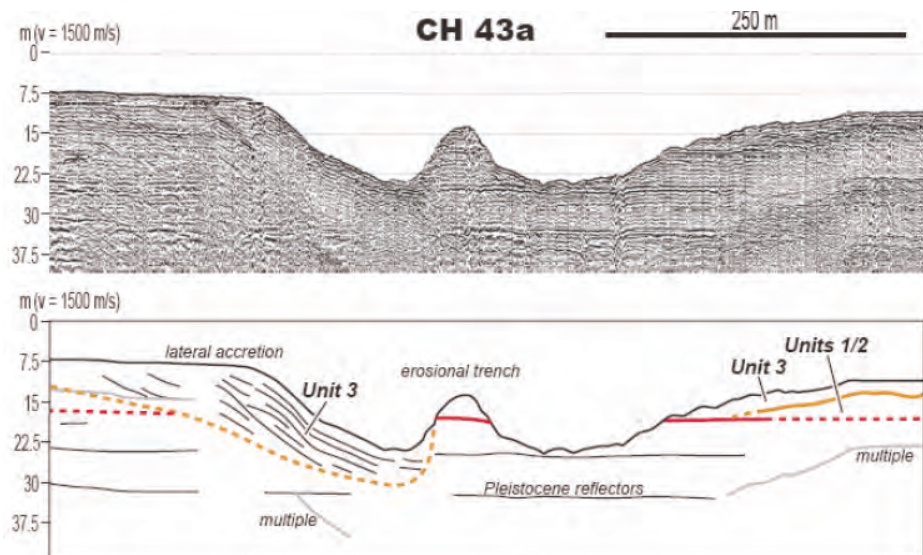


Figura 10 – Erosional trench located in the Chioggia inlet.

Furthermore, in the seaward side of the inlet dune features with accreting deposit architecture were found (Fig. 11).

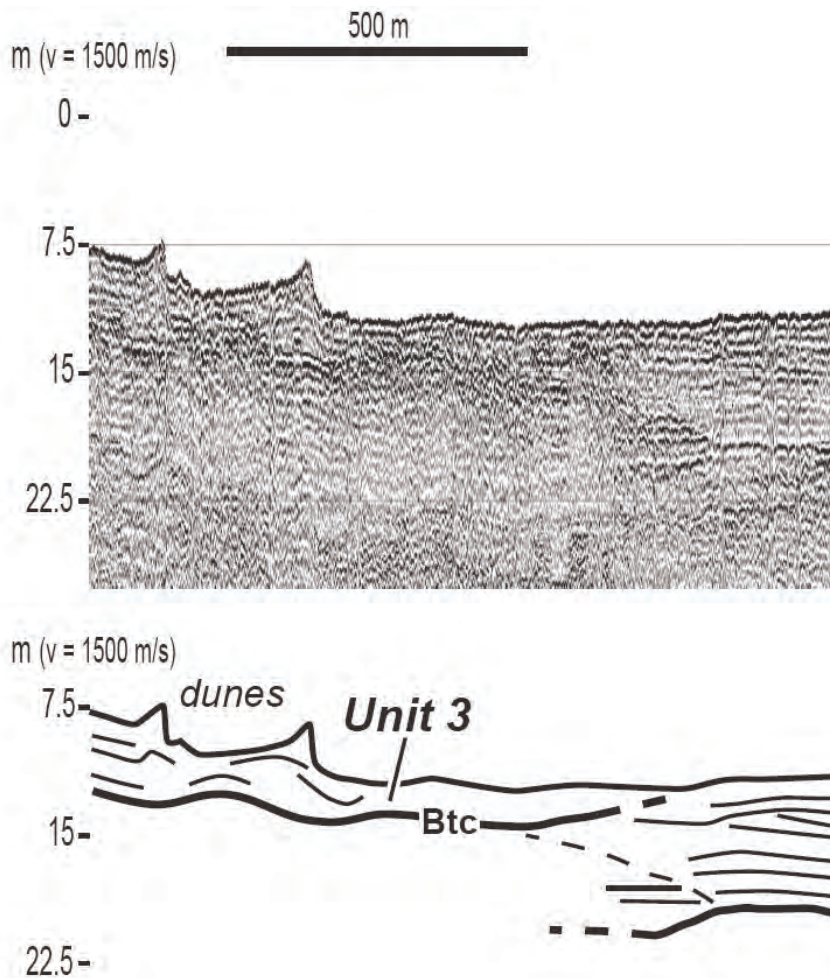


Fig. 11 – Dune features revealed by VHRS in the Chioggia inlet.

4 Conclusive remarks

Geomorphological features were discovered in the Venice Lagoon shallows by the VHRS system recently implemented for this purpose.

Preliminary investigation pointed out the presence of paleoriver beds, ancient tidal channels and beach ridges occurring in lagoon shallows and mud flats.

The integrated analysis of new VHRS and collected data, i.e. radiochronology and sedimentology, allows to attribute these features to the Late Pleistocene and Holocene deposits and their correlation with the evolution of the south lagoon basin.

Acknowledgments

This study was performed in the frame of the Co.Ri.La. 2004-2006 Research Programme - Subproject 3.16 "New very high resolution seismic methods in shallows to study the Venice lagoon subsoil". CH43 seismic line was made available by CARG Project (APAT-Regione Veneto) and bathymetric data by

Sistema Informativo of Venice Water Authority.

References

Bonardi M. and Tosi L., 1997. Evidence of climatic variations in Upper Pleistocene and Holocene sediments from the Lagoon of Venice (Italy) and the Yellow Sea (China). *World Resource Review*, 9(1): 101-112.

Bonardi M. and Tosi L., 2000a. Studio mineralogico dei sedimenti sabbiosi tardo-pleistocenici ed olocenici del litorale veneziano. Istituto Veneto di Scienze Lettere ed Arti, *La Ricerca Scientifica Per Venezia, Il Progetto Sistema Lagunare Veneziano Modellistica del Sistema Lagunare, Studio di Impatto Ambientale*, 2(2): 961-966.

Bonardi M. and Tosi L., 2000b. Studio sedimentologico di un livello di argilla sovraconsolidata sottostante il litorale veneziano. Istituto Veneto di Scienze Lettere ed Arti, *La Ricerca Scientifica Per Venezia, Il Progetto Sistema Lagunare Veneziano, Modellistica del Sistema Lagunare, Studio di Impatto Ambientale*, 2(2): 952-960.

Bonardi M., Tosi L. and Rizzetto F., 2004. Mineralogical characterization of the Venice Lagoon top sediments. In: Campostrini P. (ed.) - *Scientific Research and Safeguarding of Venice. Co.Ri.La. Research Program 2001-2003. La Garangola, Padova*, 2: 145-155.

Bonardi M., Breda A., Bonsembiante N., Tosi L. and Rizzetto F., 2005. Spatial variation of surficial sediment characteristics of the Lagoon of Venice, Italy. In: *Scientific Research and Safeguarding of Venice. Co.Ri.La. Research Program 2001-2003. Ed. P. Campostrini, Vol. III*, 131-144.

Bonardi M., Percival J. and Tosi L., 1997. The compositional Relation of Selected Clay Sediments to Late Pleistocene-Holocene Depositional Environments from Italy and China. *Clay for our future*, Edited by H.Kodama, A.R. Mermuth, J.K.Torrance, pp. 767-774, Ottawa, Canada, 1999.

Bonardi M., Tosi L., Rizzetto F., Brancolini G. and Baradello L., 2006. Effects of climate changes on the Late Pleistocene and Holocene sediments of the Venice Lagoon, Italy. *Journal of Coastal Research*, SI 39, 279-284.

Brancolini G., Tosi L., Rizzetto F., F., Donda F. and Baradello L., 2005. The unconformity at the Pleistocene-Holocene boundary in the Venice coastal area (Italy). *Geitalia 2005, Spoleto*, 21-23 settembre 2005, *Epitome*, 1: 253.

Rizzetto F., Tosi L., Bonardi M., Gatti P., Fornasiero A., Gambolati G., Putti M. and Teatini P., 2002. Geomorphological evolution of a part of the southern catchment of the Venice Lagoon (Italy): the Zennare Basin. In: Campostrini P. (ed) - *Scientific research and safeguarding of Venice. Co.Ri.La. Research Program 2001 Results*, Istituto Veneto di Scienze Lettere ed Arti, La Garangola, Padova: 217-228.

Rizzetto F., Tosi L., Carbognin L., Bonardi M. and Teatini P., 2003. Geomorphological setting and related hydrogeological implications of the

coastal plain south of the Venice Lagoon (Italy). In: Servat E., Najem W., Leduc C. & Shakeel A. (eds) - Hydrology of Mediterranean and Semiarid Regions. IAHS Publication, 278: 463-470.

Rizzetto F., Tosi L., Bonardi M., Serandrei Barbero R., Donnici S. and Toffoletto F., 2005. The Geological Map of Italy: Map Sheets 128 "Venezia" and 148-149 "Chioggia-Malamocco". *Geitalia 2005*, Quinto Forum Italiano di Scienze della Terra, Spoleto, 21-23 settembre 2005, Epitome, 1: 70-71.

Tosi L., 1993. Caratteristiche geotecniche del sottosuolo del litorale veneziano. Consiglio Nazionale delle Ricerche - Istituto per lo Studio della Dinamica delle Grandi Masse, Venezia, Rapporto Tecnico 171: 34 pp.

Tosi L., 1994a. Rapporto e prime interpretazioni sulle analisi paleontologiche condotte su campioni tardo-quadernari del sottosuolo del litorale veneziano. Consiglio Nazionale delle Ricerche-Istituto per lo Studio della Dinamica delle Grandi Masse, Venezia, Rapporto Tecnico 182: 52 pp.

Tosi L., 1994b. I sedimenti tardo-quadernari dell'area litorale veneziana: analisi delle caratteristiche fisico-meccaniche. *Geologia Tecnica ed Ambientale*, 2: 47-60.

Tosi L., 1994c. L'evoluzione paleoambientale tardo-quadernaria del litorale veneziano nelle attuali conoscenze. *Il Quadernario*, 7(2): 589-596.

Tosi L., Rizzetto F., Bonardi M., Donnici S., Serandrei Barbero R. and Toffoletto F. 2006a. Note illustrative della Carta Geologica d'Italia alla scala 1:50.000. Foglio 128 - Venezia. APAT, Dipartimento Difesa del Suolo, Servizio Geologico d'Italia, Casa Editrice SystemCart, Roma, 164pp.

Tosi L., Rizzetto F., Bonardi M., Donnici S., Serandrei Barbero R. and Toffoletto F., 2006b. Note illustrative della Carta Geologica d'Italia alla scala 1:50.000. Foglio 148-149 - Chioggia-Malamocco. APAT, Dipartimento Difesa del Suolo, Servizio Geologico d'Italia, Casa Editrice SystemCart, Roma, 162 pp.

Zecchin M., Brancolini G., Donda F., Tosi L., Rizzetto F. and Baradello L., 2006. Sedimentary features and seismic stratigraphy of the Late Pleistocene and Holocene deposits in the Venice Lagoon. *Proceedings of Adria 2006 - International Geological Congress on the Adriatic Area*, Urbino, June 19th-20th, 2006, 120-121.

RESEARCH LINE 3.17

Transport phenomena in the hydrological cycle: model of substances release in lagoon

MATHEMATICAL MODELLING OF LOW-VELOCITY FLOWS IN WETLANDS

Anna Chiara Bixio¹, Martino Cerni¹

¹ *Dipartimento di Ingegneria Idraulica Marittima Ambientale e Geotecnica, Università di Padova*

Riassunto

Le caratteristiche idrauliche dell'area umida di Ca' di Mezzo di Codevigo sono state studiate mediante simulazioni con un modello idrodinamico bidimensionale agli elementi finiti, utilizzando anche un modello di trasporto per la valutazione dei tempi di residenza e dell'efficienza idraulica. Il modello idrodinamico risolve il sistema di equazioni di De Saint Venant costituito dalle equazioni di conservazione della massa e della quantità di moto lungo le due direzioni piane, ed utilizza la formulazione di Manning per il computo della resistenza al moto offerta dal fondo e dalla vegetazione. I dati sperimentali ed i risultati numerici ottenuti forniscono valori di velocità compresi tra pochi millimetri e qualche centimetro al secondo, evidenziando così il carattere assai lento del moto all'interno dell'area umida. Per tali motivi è stato sviluppato un diverso approccio modellistico, specifico per moti in ambienti vegetati in regime laminare o di transizione. Le equazioni di De Saint Venant sono state semplificate e modificate trascurando i termini convettivi dell'accelerazione ed esprimendo la resistenza al moto tramite la formula di Darcy-Weisbach opportunamente trasformata per rappresentare l'effetto della vegetazione e la dipendenza lineare dalla velocità delle dissipazioni di energia propria dei moti laminari. Il modello è stato preliminarmente implementato e testato su bacini semplici di forma rettangolare. Si è verificata l'influenza di diverse distribuzioni e densità della vegetazione sul campo di velocità calcolato, sui tempi di residenza e sull'efficienza idraulica. I risultati sono stati poi confrontati con quelli prodotti, per le medesime geometrie e condizioni, dal precedente modello.

Abstract

The hydraulic behaviour of the Ca' di Mezzo di Codevigo constructed wetland has been investigated by using a hydrodynamic two-dimensional finite element model, together with a water quality transport model for residence time distribution function evaluation. The hydrodynamic model is based on the solution of the classical Saint Venant equations, with the Manning's friction formula to take into account the resistance due to the bottom and the vegetation. Numerical results are in good agreement with available experimental data, and put in evidence that water flow in the wetland is characterized by low velocities, varying between some millimetres and some centimetres per second. Preferential flow paths are present due to topographic and vegetative heterogeneous distributions.

For this reason a new model has been developed, specifically formulated for low-velocity flows in vegetated environments. The Saint Venant equations have been opportunely simplified and modified neglecting the acceleration terms and introducing a Darcy-Weisbach formulation for friction losses computation, with the friction coefficient depending on vegetation characteristics and flow regime.

The model has been developed and tested on simple rectangular basins. The influence of various vegetation distributions on the velocity field, residence time distribution and hydraulic efficiency have been investigated. Numerical results have been compared with the ones computed by the first model for the same geometries and conditions.

1 Introduction

The Ca' di Mezzo di Codevigo wetland was constructed some years ago by the Land Reclamation Consortium Adige Bacchiglione to reduce by means of phytoremediation processes the amount of nutrients and suspended solids driven by the Altipiano channel into the Venice lagoon (Bixio, 2000).

Some experimental researches were performed in the wetland during year 2004 (Bixio et al., 2005), in order to obtain a complete geometrical and topographical description of the area and to investigate the hydraulic behaviour of the system in terms of velocity field, partition of discharge between the different wetland compartments, water retention time and dispersion. These experimental information, together with water level and discharge data at the inlet and the outlet of the wetland, are here utilized to support hydrodynamic modelling of the wetland.

In the first part of this paper we present the application to the Ca' di Mezzo wetland of a two-dimensional hydrodynamic finite element model based on the solution of the classical De Saint Venant equations, coupled with a water quality transport model. The two models are employed to examine the hydrodynamic properties of the wetland, i.e. the water depth and velocity field and the residence time distribution function.

Since both experimental data and numerical results put in evidence the very low character of the flow inside the system due to vegetative drag, we developed a new model approach for the study of low flows in vegetated environments, based on the solution of a simplified form of the De Saint Venant equations, with a Darcy-Weisbach formulation for vegetative resistance. The second part of the paper is thus devoted to new model illustration, and to presentation of a first set of applications to simple basins with the aim of studying the influence of vegetation distribution on wetlands performance.

2 Mathematical modelling of the Ca' di Mezzo wetland

The hydraulic behaviour of the Ca' di Mezzo wetland was investigated by using the hydrodynamic model RMA2 (Donnell et al., 2003) and the transport model RMA4 (Letter at al., 2003), widely used in recent literature for the study of various wetland systems (Barrett, 1998; Koskiahho, 2003).

RMA2 is a two-dimensional depth averaged finite element model, based on the

solution of the De Saint Venant system of equations written as:

$$\frac{\partial h}{\partial t} + h \left(\frac{\partial u}{\partial x} + \frac{\partial v}{\partial y} \right) + u \frac{\partial h}{\partial x} + v \frac{\partial h}{\partial y} = 0 \quad (1)$$

$$h \frac{\partial u}{\partial t} + hu \frac{\partial u}{\partial x} + hv \frac{\partial u}{\partial y} - \frac{h}{\rho} \left[E_{xx} \frac{\partial^2 u}{\partial x^2} + E_{xy} \frac{\partial^2 u}{\partial y^2} \right] +$$

$$+ gh \left[\frac{\partial z}{\partial x} + \frac{\partial h}{\partial x} \right] + \frac{gun^2}{h^{1/6}} (u^2 + v^2)^{0.5} = 0 \quad (2)$$

$$h \frac{\partial v}{\partial t} + hu \frac{\partial v}{\partial x} + hv \frac{\partial v}{\partial y} - \frac{h}{\rho} \left[E_{yx} \frac{\partial^2 v}{\partial x^2} + E_{yy} \frac{\partial^2 v}{\partial y^2} \right] +$$

$$+ gh \left[\frac{\partial z}{\partial y} + \frac{\partial h}{\partial y} \right] + \frac{gvn^2}{h^{1/6}} (u^2 + v^2)^{0.5} = 0 \quad (3)$$

where h [m] is water depth, t is time [s], u and v [m s^{-1}] are velocities in the x and y Cartesian coordinates in a horizontal plane, E [Pa s] is the eddy viscosity coefficient, ρ [kg m^{-3}] is fluid density, g [m s^{-2}] gravitational acceleration, z [m] is bottom elevation above a datum and n [$\text{s m}^{-1/3}$] is the Manning's roughness coefficient.

The assumptions made in deriving these equations limit RMA2 to solving subcritical flows with hydrostatic pressure distribution.

RMA4 is a finite element water quality transport model, designed to simulate the depth-averaged advection-diffusion process in aquatic environments. It utilizes the hydrodynamics from RMA2, and is based on the solution of the following transport equation:

$$h \left(\frac{\partial c}{\partial t} + u \frac{\partial c}{\partial x} + v \frac{\partial c}{\partial y} - \frac{\partial}{\partial x} D_x \frac{\partial c}{\partial x} - \frac{\partial}{\partial y} D_y \frac{\partial c}{\partial y} \right) +$$

$$+ h \left(-\sigma + kc + \frac{R(c)}{h} \right) = 0 \quad (4)$$

where c [kg m^{-3}] is concentration of pollutant for a given constituent, D_x and D_y [$\text{m}^2 \text{s}^{-1}$] are turbulent mixing (dispersion) coefficients in x and y directions, k [s^{-1}] is the first order decay constant of pollutant, σ [$\text{kg m}^{-3} \text{s}^{-1}$] represents source/sink term and $R(c)$ [$\text{kg m}^2 \text{s}^{-1}$] the rainfall/evaporation rate.

For model application, a finite element mesh formed by 18544 nodes and 8955 triangles (Fig. 1) was determined on the basis of a 3800 points topographical survey (Bixio et al., 2005).

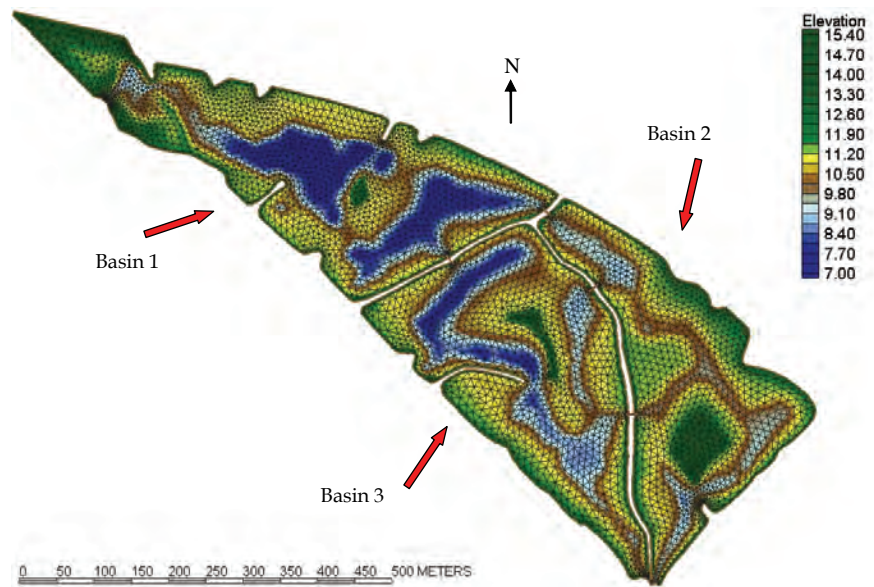


Fig. 1 – Ca' di Mezzo wetland: the finite element mesh and bottom elevations (meters above mean sea level+ 10).

Three different kinds of vegetative conditions of the area were identified for mesh zonation (Fig. 2): higher vegetation density, lower vegetation density and bare soil. Bare soil with no vegetation is typical of the main channels of the wetland, due to deep water levels (1 - 1.5 m) which prevent Phragmites growth.

Different Manning's roughness coefficients and eddy viscosity values were then defined for each mesh material through calibration, utilizing the available experimental fields of velocities (Bixio et al., 2005).



Fig. 2 – Ca' di Mezzo wetland: mesh materials definition.

Boundary conditions for hydrodynamic model simulations, consisting into discharges at the wetland entrance and water levels at the outlet, were derived thanks to the automatic network managed by the Land Reclamation Consortium Adige Bacchiglione.

The following values of Manning's n were derived for the different mesh materials: $n = 3 \text{ s m}^{-1/3}$ for densely vegetated zones, $n = 1 \text{ s m}^{-1/3}$ for sparse vegetation areas, $n = 0.025 \text{ s m}^{-1/3}$ for bare soil channels. These values are in very good agreement with results of other experimental and theoretical studies, such as Guardo & Tommasello, 1996; Kadlec & Knight, 1996; Barrett, 1998; Somes et al., 1999; Tsihrintzis & Madiedo, 2000; Koskiaho, 2003.

Eddy viscosity values were found to vary in the range 50 - 100 Pa s.

Numerical results obtained for typical operating conditions of the wetland, with 300 l/s flowing into the system and an outlet water level equal to 10.20 m are reported in Figure 3.

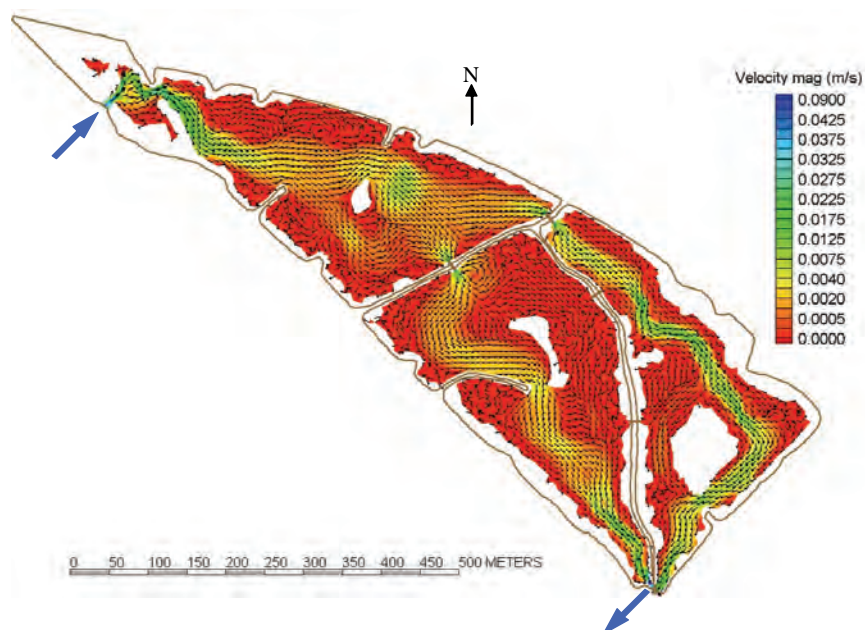


Fig. 3 – Flow patterns at a typical flood situation in the Ca' di Mezzo wetland (flowing discharge $Q=300 \text{ l s}^{-1}$ and outlet depth 10.20 m. Tone value of shading expresses flow velocity (m s^{-1}).

As evidenced also by experimental data, the model confirms that flow is concentrated in the main channels of the wetland, characterized by absence of emergent vegetation, with velocities ranging between 1 and 10 cm/s; in the lateral zones velocity values are generally on the order of some millimetres per second due to additional vegetative drag. The largest zone characterized by very low velocity values is located in basin 3, between the central isle and the internal levee which divides basins 2 and 3. Additional model simulations put in evidence that this low velocity zone could be reduced in size by opening the actually closed culverts between basins 2 and 3.

The water level and velocity fields as calculated by RMA2 model were then used as input for the RMA4 model, with the aim of evaluating the residence time distribution inside the wetland (Kadlec and Knight, 1996) and the hydraulic

efficiency of the system (Thackston et al., 1987; Persson et al., 1999).

A first set of simulations was performed to calibrate the dispersion coefficient D of the transport model, reproducing the experimental conditions of the tracer tests realized during may 2004 (Bixio et al., 2005). The dispersion coefficient, here supposed to be isotropic, was found to vary between 0.1 and 0.7 m^2s^{-1} .

Further simulations, with dispersion coefficients set to 0.01, 0.1, 0.5 and 0.7, allowed the evaluation of the residence time distribution curves (Fig. 4) and, by statistical analysis, of the hydraulic efficiency of the system as suggested by Thackston et al. (1987) and Persson et al. (1999).

Thackston et al. (1987) defined the “effective volume ratio” of a wetland system as the ratio between the water volume V effectively involved by water motion and the total available wetland volume V_{tot} , that is the ratio between the mean (effective) residence time τ and the nominal residence time t_n of the system ($t_n = V_{tot}/Q$, where Q is flowing discharge):

$$\eta = \frac{V_{eff}}{V_{tot}} = \frac{\tau}{t_n} \quad (5)$$

In ideal conditions characterized by full utilizing of the available volume for treatment processes, without dead zones excluded by flow, we have $\eta = 1$.

Persson et al. (1999) multiplied the effective volume ratio by a term describing the degree of mixing of the system, physically due to the existence of preferential flow paths and lower velocity zones, obtaining the following expression for hydraulic efficiency:

$$\lambda = \eta(1 - \sigma_\theta^2) \cong \frac{t_p}{t_n} \quad (6)$$

In which σ_θ^2 and t_p represent respectively the dimensionless variance and the peak time of the residence time distribution function (Kadlec and Knight, 1996).

Figure 4 and Table 1 summarize the results of the transport model.

We can observe that the nominal theoretical residence time of the wetland is 8.7 days, while the effective residence time varies between 7.8 and 8.5 days depending on the value of the diffusion coefficient. Effective volume ratio assumes high values, in the range 0.90-0.97, which means substantial absence of dead zones and quite fully use of available water volume for phytoremediation processes.

The dimensionless variance of the system varies between 0.33 (for $D=0.7 \text{ m}^2 \text{ s}^{-1}$) and 0.147 ($D=0.01 \text{ m}^2 \text{ s}^{-1}$); consequently, the hydraulic efficiency as defined by Persson et al. (1999) ranges between 0.60 and 0.80.

These results suggest that the concentration of flow in the main channels of the

wetland and the establishment of lower flow conditions in the channel banks, physically due to topographical and vegetative heterogeneities, diminish the global hydraulic efficiency of the system.

However, it's remarkable that the presence of both unvegetated deep channels and densely vegetated channel banks has noticeable values from the ecological point of view, promoting the safeguarding of different habitats and biodiversity, favouring water oxygenation and bacterial removals in deep waters and enhancing filtration and sedimentation processes through dense vegetation (ANPA, 2002).

	$D=0.7 \text{ m}^2 \text{ s}^{-1}$	$D=0.5 \text{ m}^2 \text{ s}^{-1}$	$D=0.1 \text{ m}^2 \text{ s}^{-1}$	$D=0.01 \text{ m}^2 \text{ s}^{-1}$
t_n (days)	8.70	8.70	8.70	8.70
t_p (days)	4.35	4.77	6.19	6.08
τ (days)	7.85	8.03	8.45	8.13
σ_{θ}^2	0.330	0.297	0.180	0.147
η	0.90	0.92	0.97	0.93
λ	0.60	0.65	0.80	0.80

Tab. 1 – Statistical analysis of calculated residence time distribution .

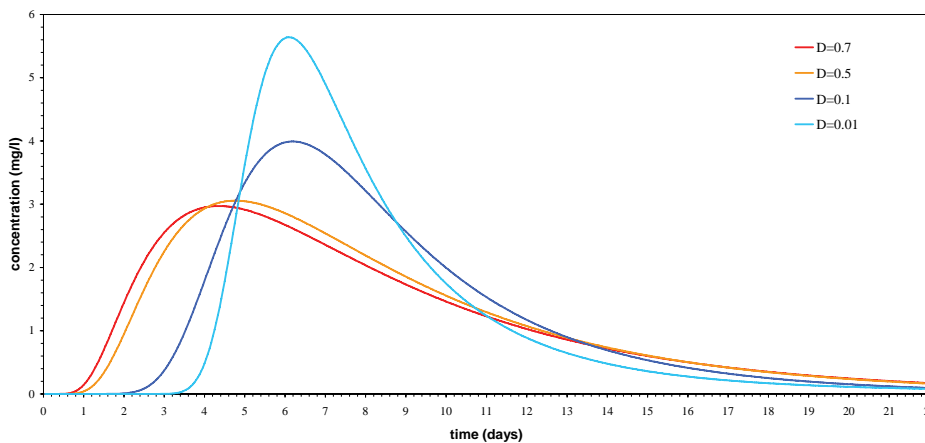


Fig. 4 – Results of the transport model: concentration vs. time curves at the wetland outlet for different values of diffusion coefficient.

3 A new approach for modelling low velocity flows in vegetated environments

Both experimental measurements and hydrodynamic model calculations evidence the very low character of the flow inside the wetland. Reynolds number based on stem diameter $Re_D = ud / \nu$ (Nepf, 1999) vary between about 10 and 100 in vegetated areas, indicating that flow develops prevalently in the laminar or transitional regime. Turbulent flow conditions are restricted to the main channels of the wetland.

For these reasons, a new 2-D finite element hydrodynamic model has been developed in MATLAB environment, following the ideas of Worman and Kronnas (2005). A Darcy-Weisbach formulation is implemented to express bottom and vegetation resistance to flow, and the friction coefficient f is expressed as function of vegetation characteristics.

The De Saint Venant system of equations (1), (2) and (3) can be written as:

$$\frac{\partial h}{\partial t} + \nabla(\mathbf{V}h) = 0 \quad (7)$$

$$\frac{\partial \mathbf{V}}{\partial t} + \mathbf{V} \cdot \nabla \mathbf{V} + g \nabla(h + z) = -\frac{f}{8R_H} \mathbf{V}|\mathbf{V}| \quad (8)$$

where V is flow velocity [m/s], bold face type denote a vector quantity, h [m] is water depth, z [m] is bottom elevation above a datum, f [-] is the Darcy-Weisbach friction factor, R_H [m] is hydraulic radius, t is time and $\nabla = (\partial/\partial x, \partial/\partial y)$ is the Nabla operator in the two horizontal dimensions x and y .

Commonly, water flow in wetlands can be assumed to be stationary, and velocity head is very small in relation to water depth. Under these assumptions, equations (7) and (8) simplify to:

$$\nabla(\mathbf{V}h) = 0 \quad (9)$$

$$g \nabla(h + z) = -\frac{f}{8R_H} \mathbf{V}|\mathbf{V}| \quad (10)$$

Generally, the friction factor can be expressed as a function of Reynolds number $Re = VR_H / \nu$ and relative roughness ε/h , where ε represents length scale of microtopography of the bed and characteristic dimensions of vegetation. Since power functions have been applied to wetland flows (Kadlec and Knight, 1996; Bolster and Saiers, 2002), the friction factor is here written as:

$$f = \alpha \left(\frac{\varepsilon}{h} \right)^m Re^{-n} \quad (11)$$

where α [-] is a constant and the exponents m and n depend on water flow regime. For a laminar flow $n = 1$, whereas n approaches zero as the flow becomes turbulent. For a porous medium flow, like in a dense vegetation, $m = -2$.

Substituting (11) in (10) and combining with (9), assuming $n = 1$ and $m = -2$, we obtain:

$$\nabla \left[\frac{h}{F} \nabla (h + z) \right] = 0 \quad (12)$$

$$F = \frac{\alpha \varepsilon^{-2} \nu}{2g} \quad (13)$$

If vegetation is schematized as an array of cylinders of diameter d and spacing s_x and s_y along the x and y directions, the coefficient F can be shown to be $F = 5\nu/g s_x s_y$.

Some recent literature studies present model-based investigations on wetland efficiency. Persson and Wittgren (1999) investigated with a two-dimensional hydrodynamic model the effects of basin shape and configuration on wetland performance, considering thirteen different ponds characterized by the same area and absence of vegetation. Koskiaho (2003) studied with RMA2 and RMA4 models the hydrodynamics and the efficiency of two different wetlands, and examined possible performance improvements to be reached by different design options.

Since our new finite element model is specifically designed for vegetated environments, expressing friction as a function of vegetation characteristics, we utilized it for the analysis of the effects of vegetation on flow field, and consequently on hydraulic efficiency. We considered some simple basins of rectangular shape with different length to width ratios, and performed a series of numerical simulations varying vegetation diameter and density and vegetative cover and distribution (Jenkins and Greenway, 2005). Two different vegetation distributions were basically considered: fringing vegetation, distributed lengthwise in the basin parallel to flow direction, and banded vegetation, distributed orthogonally to flow direction.

A particle tracking procedure was then implemented to calculate residence time distribution functions for the different configurations.

The results of the new model were finally compared with the ones calculated by RMA2 for the same configurations and conditions. Manning's n for RMA2 simulations was calculated following Petryik and Bosmajan (1975):

$$n = n_0 + \sqrt{a \cdot C_D \cdot d / 2g R_H^{2/3}},$$

where n_0 represents bottom roughness, C_D [-] is drag coefficient, d [m] is plant diameter and a [stems m^{-2}] is plant density.

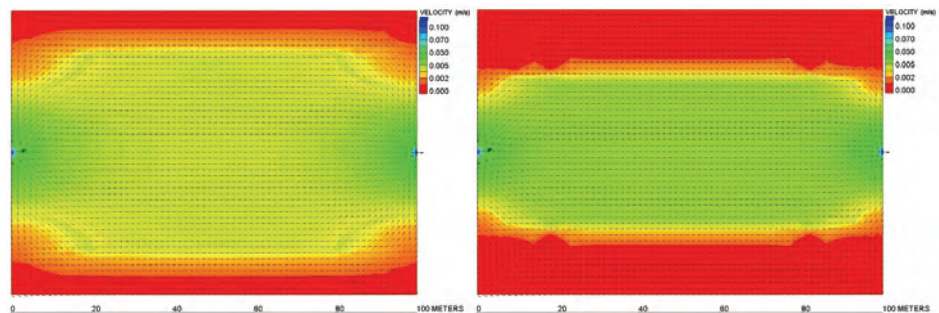
Figure 5 reports as an example the comparison between the flow fields calculated by the new model in a basin 70 m wide and 100 m long, with an incoming discharge of $0.1 \text{ m}^3 \text{ s}^{-1}$ and a fixed outlet stage of 0.5 m, for two different vegetation distributions, i.e. fringing vegetation covering respectively about 23 % and 50% of basin area. We can observe that fringing vegetation produce preferential flow paths through the central non vegetated region of the

basin, and lower velocities within the vegetated zones, with consequent reduction of wetland efficiency. These phenomena increase with the widening of vegetative cover.

Figure 6 illustrates the different impact on the velocity field of fringing and banded vegetation distribution, evidencing that banded vegetation configuration avoids short-circuiting and promotes lower velocities and higher residence times, increasing hydraulic efficiency.

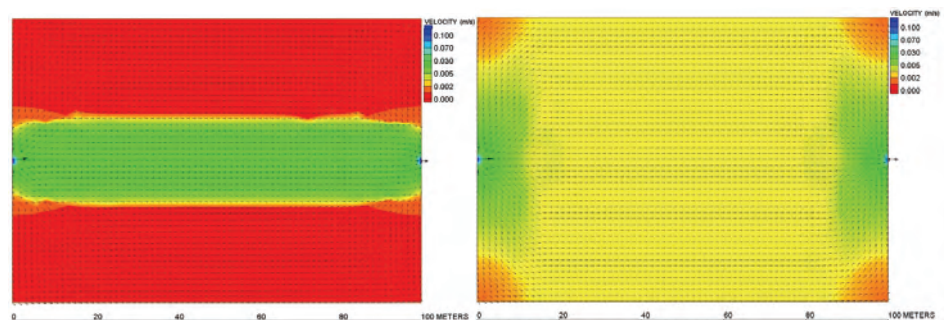
We calculated for the basin of Figures 5 and 6 a nominal residence time of 9.7 hours, and an effective (mean) residence time equal to 9 hours for non vegetated conditions. When fringing vegetation is present in the lateral zones, mean residence time shifts down to 7.3 hours (vegetation cover 23%), 5.3 hours (vegetation cover 50%) and 3 hours (vegetation cover 74%). Banded vegetation covering 74% of basin area increases mean residence time to 9.6 hours.

Fig. 5 – Simulation results (new model) for the following vegetation characteristics: $d = 0.01$ m; $a = 100$ stems/m²; vegetation cover 22.9% (on the left) and 51.4 % (on the right).



Numerical results of the new model and calculations of RMA2 are in good agreement for the test cases considered in this research. It is remarkable that the new model calculates higher velocity differences between vegetated and non vegetated regions, enhancing the short circuiting phenomena. This is mainly due to the different mathematical formulations of the two models. Anyway, some experimental field or laboratory measurements should allow the verification of the friction coefficient formulation on which the new model is based, ascertaining the dependence of coefficient F on vegetation characteristics.

Fig. 6 – Simulation results (new model) for the following vegetation characteristics: $d = 0.01$ m; $a = 100$ stems/m²; vegetation cover 74.3%; fringing (on the left) and banded (on the right) distribution.



Conclusions

The two-dimensional hydrodynamic model RMA2 together with experimental measurements has enabled inspection of flow directions, flow velocities and water levels inside the Ca' di Mezzo wetland system. RMA2 output has been coupled with a water quality transport model, allowing the reproduction of tracer tests and evaluation of hydraulic efficiency. Simulation results show that in ordinary functioning conditions flow concentrates in the main channels, non vegetated, with velocities varying between 1 and 10 cm/s, while lateral vegetated zones experiment sensibly lower velocities, in the range of 1-5 mm/s. This determines the reduction of the global hydraulic efficiency of the wetland, even if it must be carefully kept into account the high ecological value of alternating deep non vegetated zones to low densely vegetated areas.

The very low values of flow velocities in the vegetated zones of the wetland have suggested the need of the development of a new hydrodynamic model, specifically designed for laminar to transitional flows through emergent vegetation. The model has been used for simulating hydrodynamics of simple test basins with different vegetation distribution, in order to assess the influence of vegetation features (diameter, spacing, spatial distribution) on wetlands performance. Numerical results evidence that wetland hydraulic efficiency can be enhanced by a banded distribution of vegetation, while fringing vegetation tend to favour short circuiting phenomena. The model requires experimental verification in order to clarify the friction factor dependence on vegetation characteristics.

References

- ANPA, Linee guida per la ricostruzione di aree umide per il trattamento di acque superficiali. Manuali e linee guida 9/2002.
- K.R. Barrett, "Two-dimensional flow and transport modeling for hydraulic design and analysis of treatment wetlands", *Proceedings of the 1998 International Water Resources Engineering Conference*, (1998), pp. 520–525.
- V. Bixio, "Water quality improvements in the drainage networks flowing in the Venetian Lagoon". *International workshop on development and management of flood plans and wetlands*. IWF 2000, Beijing, 107-116.
- V. Bixio, A. C. Bixio, M. Cerni, A. Marion, M. Zaramella, "Experimental researches on the hydraulic behaviour of the Ca' di Mezzo in Codevigo wetland", In *Proceedings of annual meeting of CORILA*, vol. V, Venice, 2005.
- C. H. Bolster and J. E. Saiers, Development and evaluation of a mathematical model for surface water flow within Shark River Slough of the Florida Everglades, *Journal of Hydrology*, 259 (2002), 221-235.
- B.P. Donnell, J.V. Letter, W.H. McAnally et al., "Users Guide for RMA2 Version 4.5," US Army, Engineer Research and Development Center, Water Experiment

Station, Coastal and Hydraulics Laboratory, (2003).

M. Guardo and R. Tomasello, "Hydrodynamic simulation of a constructed wetland in Florida", *Water Res. Bull*, 31 (4) (1995), pp. 687-701

J.F. Holland, J.F. Martin, T. Granata, V. Bouchard, M. Quigley, L. Brown, "Effects of wetlands depth and flow rate on residence time distribution characteristics", *Ecological Engineering* (2004), 23 (3), pp. 189-203.

R.H. Kadlec, "Detention and mixing in free water wetlands", *Ecological Engineering* (1994), 3 (4), pp. 345-380.

R.H. Kadlec, R.L. Knight, "Treatment wetlands", CRC Press-Lewis Publishers New York, (1996).

G. Jenkins and M. Greenway, "The hydraulic efficiency of fringing vegetation in constructed wetlands". *Ecol. Eng.* (2005) 25, 61-72.

J. Koskiaho, "Flow velocity retardation and sediment retention in two constructed wetland-ponds", *Ecological Engineering* (2003), 19 (5), pp. 325-337.

J.V. Letter, B.P. Donnell et al., "Users Guide for RMA4 Version 4.5", US Army, Engineer Research and Development Center, Water Experiment Station, Coastal and Hydraulics Laboratory, (2003).

H. M. Nepf, "Drag, turbulence and diffusion in flow through emergent vegetation", *WRR* 35(2), 479-489, 1999.

J. Persson, N.L.G. Somes, T.H.F. Wong, "Hydraulic efficiency of constructed wetlands and ponds", *Journal of Water, Science and Technology* (1999), 40 (3), pp. 291-300.

J. Persson, H. B. Wittgren, "How hydrological and hydraulic conditions affect performance of ponds", *Ecological Engineering* (2003), 21 (4-5), pp. 259-269.

S. Petryk and G. Bosmajian, "Analysis of flow through vegetation", *Journal of the Hydraulics Division, ASCE*, 101, 871-884, 1975

N.L.G. Somes, W.A. Bishop, T.H.F. Wong, "Numerical simulations of wetland hydrodynamics", *Environment International* (1999), 25 (6-7), pp. 773-779.

E.L. Thackston, F.D. Shields, P.R. Schroeder, "Residence time distributions of shallow basins", *Journal of Environmental Engineering* (1987), 113 (6), pp. 1319-1332.

V.A. Tsihrintzis, E.E. Madiedo, "Hydraulic resistance determination in marsh wetlands", *Water Resources Management* (2000), 14 (4), pp. 285-309.

T.M. Werner, R.H. Kadlec, "Wetland residence time distribution modeling", *Ecological Engineering* (2000), 15 (1-2), pp. 77-90.

A. Worman and V. Kronnas, "Effect of pond shape and vegetation heterogeneity on flow and treatment performance of constructed wetlands", *Journal of Hydrology*, 301 (2005) 123-138.

RESEARCH LINE 3.18

**Residence times and hydrodynamical
dispersion in the Venice lagoon**

LONG TERM NET EXCHANGE OF SAND THROUGH VENICE INLETS: PART II

Nicoletta Tambroni¹, Giovanni Seminara¹

¹ *Dipartimento di Ingegneria Ambientale, Università di Genova*

Riassunto

Nel caso in cui una laguna abbia più di un'apertura possono scaturire interazioni tra le bocche per cui l'idrodinamica ed il trasporto di sedimenti in ognuna di esse sia dipendente anche dalle caratteristiche delle altre. Nel seguente lavoro si riferisce di uno studio recente [Tambroni & Seminara, 2006] in cui tale effetto è stato studiato modellando la laguna di Venezia come un singolo bacino collegato al mare attraverso tre canali rettilinei. I risultati suggeriscono che le caratteristiche generali della dipendenza temporale dello scambio netto di sabbie e la stima del volume totale di sabbie perse ogni anno dalla laguna di Venezia non sono significativamente alterate dalle interazioni tra le bocche. Tuttavia in queste valutazioni si è trascurato un importante meccanismo, ovvero la capacità del moto ondoso di caricare di sedimenti le correnti mareali entranti in laguna oltre la loro capacità di trasporto, ciò nel corso di eventi intensi in cui il frangimento delle onde induce forte risospensione. Nel presente lavoro si propone una stima del ruolo di tale meccanismo schematizzando il moto nella fase di flusso come piano ed irrotazionale, e risolvendo l'equazione di avvezione-diffusione per la concentrazione di sabbia nella regione di mare prossima alle bocche. I risultati dimostrano che l'eccesso di sabbie risospese dal moto ondoso, trasportato dalle correnti mareali in fase di flusso, non riesce a raggiungere la laguna interna bensì sedimenta nella regione esterna prossima alle bocche.

Abstract

In the presence of multiple inlets, interactions may occur whereby hydrodynamics and sediment transport in each inlet may also be affected by variations occurring at the other inlets. Here, we report a recent investigation [Tambroni & Seminara, 2006] of the above effects, modelling Venice Lagoon as a single basin connected to the sea through three straight rectangular channels. Results suggest that the general features of the temporal dependence of the net sand exchange and the total volume of the yearly loss of sand from Venice Lagoon are not significantly altered by inlet interactions. Hence, in the absence of an excess supply from the sea, the yearly loss of sand through Venice inlets is still an order of magnitude smaller than the total sediment loss usually claimed. We also show that, at least in the short term, this estimate is only slightly affected by the sand supply from wave resuspension in the far field whose effect is simply to store sediments in the near inlet region. This is done by modelling the flood flow in the near inlet region as a two-dimensional irrotational plane flow and coupling the hydrodynamics with the transport of

suspended sediments, evaluated through the solution of an advection-diffusion equation for sand concentration.

1 Introduction

The hydrodynamics of tidal inlets is a major subject of research widely explored in the literature. An estimate of the average inlet velocity was obtained, using simple concepts of steady-flow hydraulics, as early as 1928 by Brown. More recently, numerical models have provided more detailed pictures using 1-D, 2-D or 3-D approaches. Though feasible, these numerical models are computationally demanding to allow for 'long-term' predictions. Tambroni & Seminara [2005] have recently revisited an analytical formulation of Marchi [1990] for inlet hydrodynamics, essentially based on the 1-D model proposed by Bruun [1978], in order to estimate the net exchange of sand associated with the sequence of tidal events recorded in the period 1994-1998. Each of the three Venice inlets was modelled as a straight rectangular channel which connects the open sea with a closed basin representing the portion of the lagoon drained by the inlet. However, in the presence of multiple inlets, interactions may occur whereby hydrodynamics and sediment transport in each inlet may also be affected by variations occurring at the other inlets. In this paper we investigate the above effects modelling Venice lagoon as a single basin connected to the sea through three straight rectangular channels. Results suggest that, as a result of the presence of the other inlets, the net volume of sand exchanged at Malamocco increases while it decreases at Lido. However, the general features of the temporal dependence of the net sand exchange and the total volume of the yearly loss of sand from Venice Lagoon are not significantly altered. Note that, in the above estimate, we restrict our attention on the transport of sand and we assume that sediment transport equals the transport capacity of the stream during both the flood and the ebb phases. This is, needless to say, a strong assumption, as it essentially ignores the role of boundary conditions. In fact:

- on one hand, the ebb currents may carry sediments much finer than sand, i.e. particles resuspended in the inner lagoon and unable to settle in the channel network (wash load in "fluvial terms");
- on the other hand, sand resuspended in the surf zone during storm events can overload the flood currents beyond transport capacity.

In the second part of our paper we estimate to what extent the latter mechanism is able to affect the net exchange of sand through the inlets. We show that an excess supply of sand overloading the flood currents, is unable to enter the lagoon: it rather settles in the region close to the inlet and in the inlet itself, encouraging siltation. This is shown by modelling the flood flow in the near inlet region as a two-dimensional (2-D) irrotational plane flow, a simple scheme substantiated by our recent and less recent experimental observations [Blondeaux et al. 1982; Tambroni et al., 2005]. The latter assumption simplifies the treatment considerably and allows us to couple the hydrodynamics with the transport of suspended sediments, evaluated through the solution of an

advection-diffusion equation for sand concentration. We find that a very small fraction of the sand overload reaches the inlet.

The procedure employed in the rest of the paper is as follows. Chapter 2 is devoted to the description of a simple model which is able to account for the effects of inlet interactions. In chapter 3 we investigate the effect of the excess supply of sediment driven to the inlet by the nearly irrotational flood currents overloaded in the far field by storm events. Finally, chapter 4 concludes the paper with some discussion.

2 Effects of inlet interactions

Let us model the lagoon as a single basin with surface area S , connected to the sea through three straight rectangular inlets.

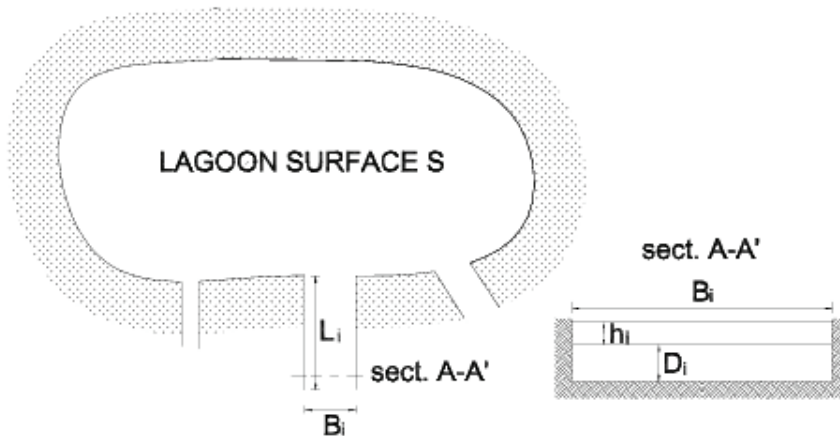


Fig. 1 – Sketch of the system sea – inlet channels-lagoon and notations.

INLET	L_i [m]	D_i [m]	B_i [m]	C_i [/]
Lido	4500	8.9	900	16
Malamocco	3000	14.4	500	15.4
Chioggia	2000	8.5	570	13

Tab. 1 – Geometrical parameters characteristic of the Venice inlets and flow conductance coefficients employed for the computations.

The formulation of inlet hydrodynamics does not differ substantially from the one already discussed in the companion paper [Tambroni & Seminara , 2005]. The main difference is that, in this case, all the inlets discharge into the same basin hence the free surface elevation h_2 at the inner boundary of each inlet takes the same value. Assuming the free surface in the basin to be effectively horizontal and following a 1-D approach similar to that reported in Tambroni & Seminara [2005], we end up with three differential equations governing the flow

velocity U_i at each inlet:

$$\frac{dU_i}{dt} + g \frac{h_2 - h_1}{L_i} + \frac{U_i |U_i|^2}{C_i^2 D_i} = 0. \quad (1)$$

where h_1 is the tidal forcing, g is gravity and D_i , C_i and L_i are depth, flow conductance and length of the i^{th} inlet, respectively.

In order to find a solution for U_i , the three equations (1) ($i=1,2,3$) must be coupled to a further equation imposing continuity, which may be written in the form:

$$\sum_{i=1}^3 U_i D_i B_i = S \frac{dh_2}{dt} \quad (2)$$

with B_i inlet width.

We then assume a simple harmonic forcing tide with amplitude $a_0 = 0.5$ m to fix h_1 and solve the system of equations (1) and (2) numerically.

The maximum flow velocity at Malamocco is plotted in Figure 2a as a function of the local mean flow depth, for given values of the mean flow depths at Chioggia and Lido (8.5 m and 8.9 m, respectively). The curve obtained for an isolated inlet is also reported in Figure 2a for comparison. Figures 2b and 2c show the same plots for Lido and Chioggia, respectively. Results may be summarized as follows:

1. at Malamocco the peak value of U_{max} is roughly the same whether or not we take into account the presence of the other inlets; in the case of multiple inlets the peak value of U_{max} decreases at Lido while it increases at Chioggia;
2. if the effect of multiple inlets is taken into account the peak value of U_{max} at each inlet is associated with a value of the inlet depth D_c larger than in the single inlet approach;
3. moreover, the branch of the curve with $D > D_c$ decays much faster as the flow depth increases.

Furthermore, the threshold conditions relative to a static equilibrium limit, defined by the inability of tidal currents to transport (either in suspension or as bed load) the sediments available in the bed, can be obtained by stipulating that the maximum current speed must not exceed the critical speed for sediment motion defined by Shields criterion. The latter conditions are plotted in Figure 2 for a realistic range of sediment sizes, suggesting that, also when accounting for the effect of inlet interactions, the present configuration of each of Venice inlets is quite far from static equilibrium, which would require flow depths much larger than the present ones.

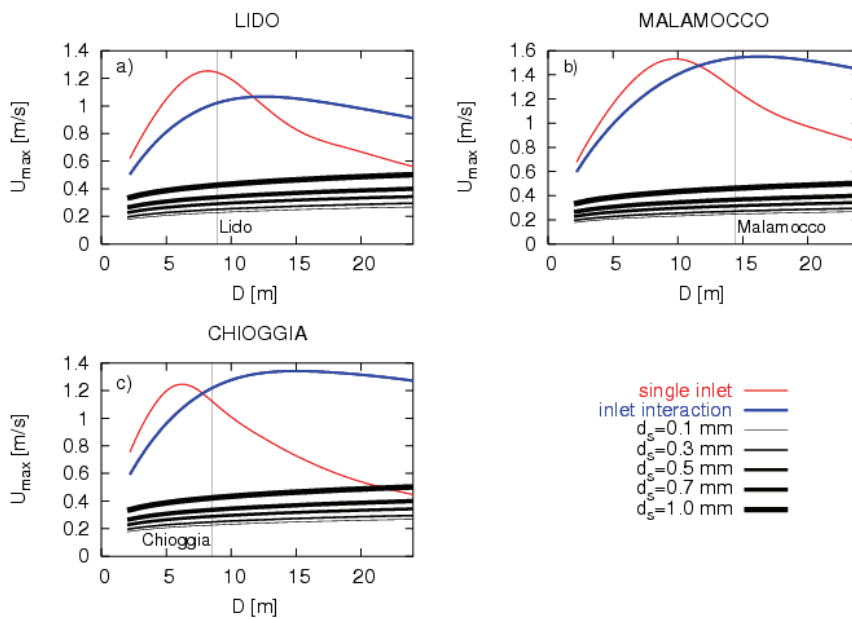


Fig. 2– Maximum velocity at Lido (a), Malamocco (b) and Chioggia (c) are plotted versus inlet depth. The red line describes the case where inlets have been modelled as independent. The blue line in (a) accounts for the effects of Chioggia and Malamocco on Lido inlet assuming the flow depth at Chioggia and Malamocco to be fixed and equal to the one presently observed; similarly for (b) and (c). Also plotted is the critical speed for sediment motion for sizes in the range 0.1 - 1 mm.

Finally, it is of some interest to compare the results obtained by the two approaches discussed above with some field data. Figure 3 compares the temporal dependence of the cross-sectionally averaged flow velocity predicted at each of Venice inlets using the single inlet model with that obtained by the interactive inlets approach. It turns out that both models predict roughly the same results at Chioggia, while slightly larger differences emerge at Malamocco and Lido. Both predictions are in fairly good agreement with field observations at each inlet for an M2 dominated event although, at Malamocco, the measured speeds appear to be better reproduced by the single inlet model.

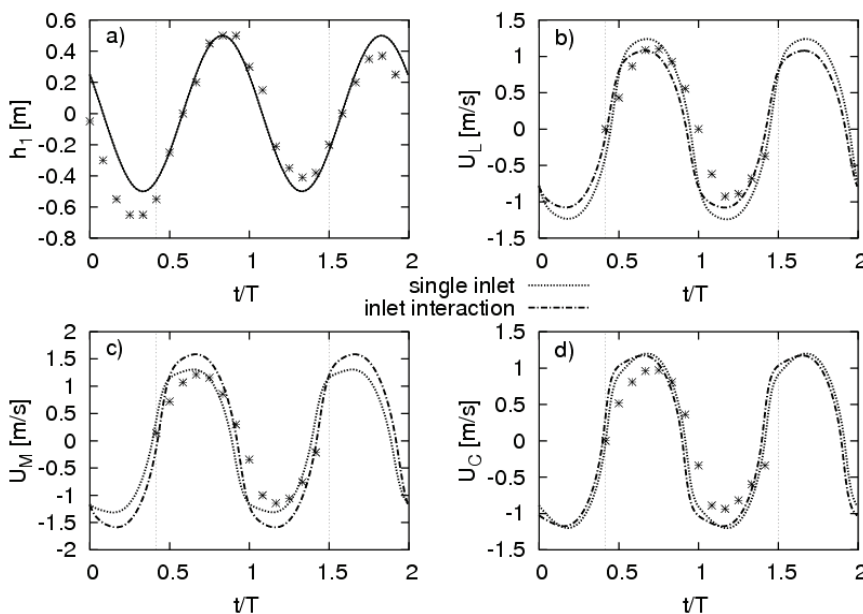


Fig. 3 – Comparison between the temporal evolution of the cross-sectionally averaged flow velocities observed at Lido (b), Malamocco (c) and Chioggia (d) inlets during an event occurred in September 1970 [Di Paola et al., 1979] (dots) and the velocity distributions calculated under a pure M2 forcing tidal oscillation with amplitude $a_0 = 0.5$ m (a) using the present model (dash dotted line) and the single inlet approach (dotted line) which neglects inlet interaction.

The second exercise we performed, was to assume for the forcing function the sequence of tidal oscillations recorded in the years from 1994 to 1998 by the CNR gauge station located in the sea region adjacent to Venice Lagoon, and evaluate, following the approach discussed above, the sequence of tidal currents which have determined the exchange of sands through the inlets. Once inlet hydrodynamics is known, the total sediment flux transported as both bed load and suspended load is evaluated at each instant of time throughout the tidal cycle using Engelund and Hansen's [1967] predictor. Time integration of the total load finally provides the sought estimate of the temporal evolution of the volume of sand exchanged through each inlet. Note that we restrict our attention to the sediments available in the near inlet region (i.e. fine sands with sizes in the range 0.1 - 0.3 mm). The temporal evolution of the net volume of sand exchanged through each inlet in the period 1994 - 1998 is plotted in Figure 4. The same calculations, performed using the single inlet model, are reported in Figure 5.

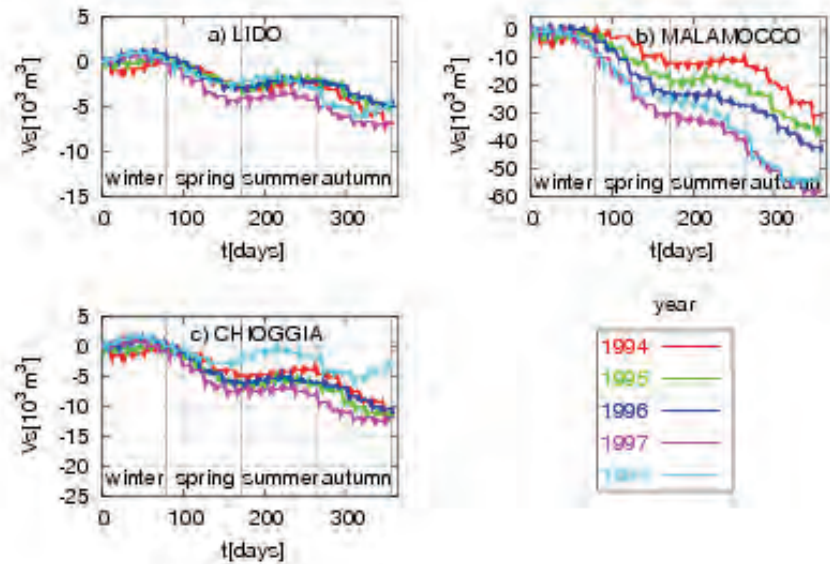


Fig. 4 – Temporal evolution of the net volume of sand exchanged through a) Lido, b) Malamocco, c) Chioggia inlets in the years 1994 – 1998 accounting for the effect of inlet interactions.

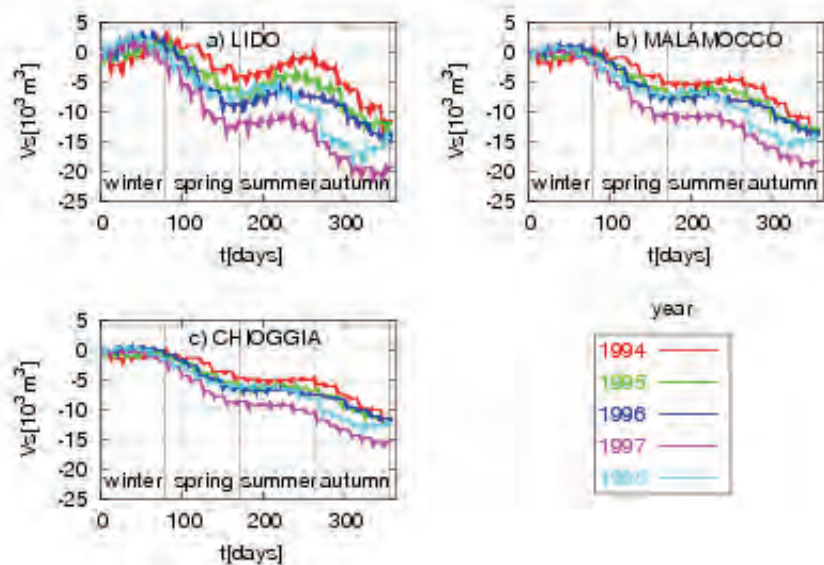


Fig. 5 – Temporal evolution of the net volume of sand exchanged through a) Lido, b) Malamocco, c) Chioggia inlets in the years 1994 – 1998 neglecting the effect of inlet interactions.

A comparison between Figure 4 and Figure 5 suggests that, accounting for the presence of the other inlets through the present simple approach, it is found that the net volume of sand exchanged at Malamocco increases while it decreases at Lido. However, the general features of the temporal dependence of the net sand exchange and the total volume of the yearly loss of sand from Venice Lagoon are not significantly altered by the effect of inlet interaction. In particular in both cases the yearly loss of sand from Venice Lagoon is about an order of magnitude smaller than the overall loss of sediments usually claimed [Magistrato alle Acque di Venezia - Consorzio Venezia Nuova, 2002]: a result clearly suggesting that the major contribution to the yearly sediment loss from Venice Lagoon is unlikely associated with an exchange of the sand available in the bed close to the inlets, amenable to transport either as bed load or as suspended load. However, before the latter conclusion can be firmly reached, we need to check whether an excess supply of sand resuspended in the surf zone may significantly modify the picture.

3 An analysis of the effect of sand supply in the far field

We now attempt to estimate to what extent the availability of sand resuspended in the surf zone, i.e. in the far field, may modify the supply of sand to the inlet in the flood phase. To this aim we model the flood flow as an irrotational plane flow: this assumption simplifies the treatment considerably and has received some support from laboratory observations on mobile bed physical models of tidal inlets [Tambroni et al., 2005] which confirm earlier observations performed on fixed bed models [Blondeaux et al., 1982].

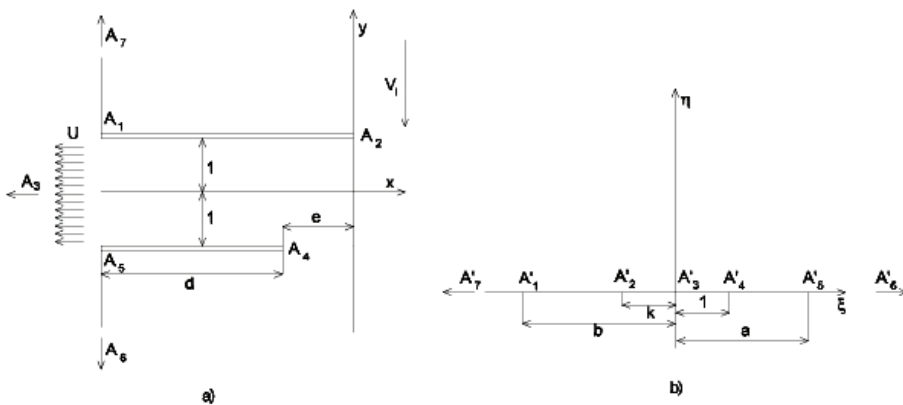


Fig. 6 – Sketch of the physical domain and of the domain transformed according to (3) for the Malamocco inlet.

Let us represent the boundary of Venice inlets as shown in Figure 6, which specifically refers to Malamocco. Using Cartesian dimensionless coordinates x and y , scaled by half the inlet width, the flow region consists of the half plane ($x>0, -\infty<y<\infty$) and the strip ($-\infty<x<0, -1<y<1$). Following Blondeaux et al. [1982], we then use the Scharwz - Christoffel conformal transformation to transform the physical plane into a half plane. Let us denote by $z (= x + i y)$ the complex variable describing the physical plane; moreover, let $\zeta (= \xi + i \eta)$ denote the complex variable describing the transformed region (Figure 6). Applying the

Scharwz - Christoffel transformation Blondeaux et al. [1982] were able to transform the flow region of the physical plane z into the upper half plane ζ through the relationship:

$$z = -\frac{2\sqrt{ab}}{\pi k} i\sqrt{(\zeta - a)(\zeta + b)} + \frac{2}{\pi} \operatorname{ar\,cosh} \frac{2ab + (a - b)\zeta}{\zeta(a + b)} \quad (3)$$

where a , b and k are the parameters describing the transformation, depending on the inlet geometry. With the notations of Figure 6 the value of the relevant parameters describing the Malamocco inlet are: $e = 1.83$, $d = 5.44$, $a = 3.65$, $b = 9.4$, $k = 3.87$. We now assume that the flood flow in the physical plane is driven by a given temporal dependence of the flow discharge $Q(t)$ at $x \rightarrow -\infty$ along with a littoral current of speed (V_l , $V_l > 0$) uniformly distributed in the far field. In the transformed plane, the flow corresponds to a sink of intensity $Q(t)$ (with $Q(t) < 0$) superimposed on a uniform flow parallel to the ξ axis, with velocity V_l , whose complex potential W_P is readily written in the form:

$$W_P = \frac{Q}{\pi} \ln \zeta + V_l \zeta \quad (4)$$

In the physical plane, the complex velocity v^* associated with the latter form of the complex potential in the transformed plane, is obtained as follows:

$$\frac{dW_P}{d\zeta} = \frac{dW_P}{dz} \frac{dz}{d\zeta} = v^* \frac{dz}{d\zeta} \Rightarrow v^* = \frac{V_l + \frac{Q}{\pi\zeta}}{dz/d\zeta}, \quad (5)$$

with the quantity $dz/d\zeta$ readily calculated by differentiating the transformation (3). Using the latter procedure we end up with an expression for the complex velocity of the form $v^*[\zeta(z)] = U(z) - i V(z)$. Calculations were performed assuming constant depth equal to the average inlet depth, using for Q the values obtained from the 1-D model forced by a pure M_2 tide and assuming for V_l a typical value for the intensity of the littoral current along the Venice coast where it ranges about 0.1 m/s. In Figure 7 we have plotted the velocity distributions at various times during the flood phase of the tidal cycle. Figure 7 shows that the spatial scale of the region where the presence of the inlet is felt is of the order of few inlet widths. Moreover, it is not surprising that, within the framework of the present irrotational scheme, the velocity peaks at the edges of the inlet jetties due to the presence of geometrical discontinuities. Needless to say, the scheme fails in the immediate neighborhood of the edges where flow separation occurs.

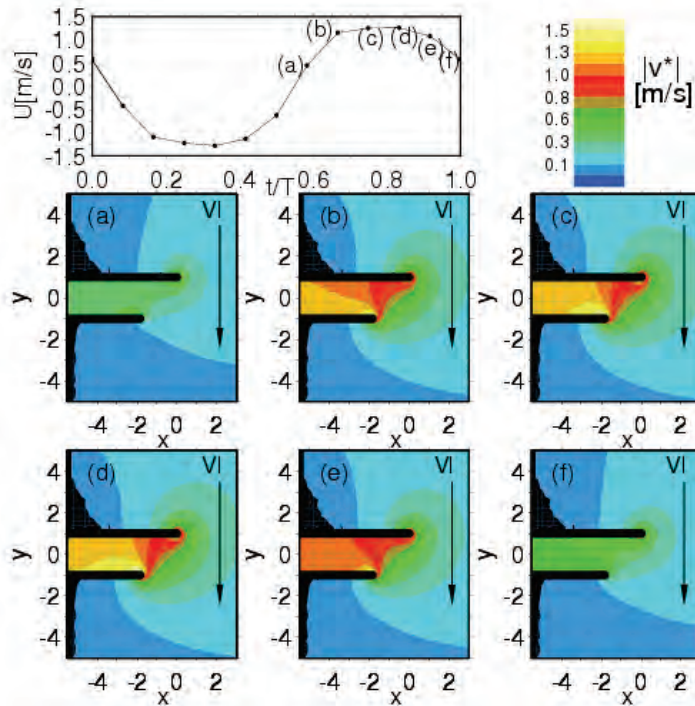


Fig. 7 – The velocity distribution in the sea region close to Malamocco inlet is plotted assuming an M2 tidal forcing with $a_0 = 0.5$ m and a uniform littoral current in the far field with intensity $VI = 0.1$ m/s.

Having determined the structure of the flow field in the near inlet region, we can proceed to attempt estimating the concentration distribution built up in response to far field conditions as well as advection, settling and turbulent diffusion: our aim is to ascertain to what extent our previous assumption, namely that sediment transport through the inlet is determined by the transport capacity of the stream, may be violated in the flood phase due to a deficit or excess of sediment supply from the far field.

Let us then write the advection - diffusion equation for the mean volumetric concentration of suspended sediment c in the Cartesian coordinates x, y, z , where x and y coincide with the horizontal coordinates represented in Figure 6 and z is a vertical coordinate. Hence we write:

$$\begin{aligned} \frac{\partial c}{\partial t} + v_x \frac{\partial c}{\partial x} + v_y \frac{\partial c}{\partial y} + v_z \frac{\partial c}{\partial z} - w_s \frac{\partial c}{\partial z} = \frac{\partial}{\partial x} \left(D_{T_x} \frac{\partial c}{\partial x} \right) + \\ + \frac{\partial}{\partial y} \left(D_{T_y} \frac{\partial c}{\partial y} \right) + \frac{\partial}{\partial z} \left(D_{T_z} \frac{\partial c}{\partial z} \right). \end{aligned} \quad (6)$$

In (6) v_x, v_y, v_z are the components of the 3-D mean velocity vector. The vertical component of flow velocity v_z is much smaller than the horizontal speed of the fluid velocity and is also negligible compared with the settling speed w_s of sand particles. The horizontal component v_x, v_y can be evaluated from the knowledge of the plane irrotational velocity field determined above by noting that the flow can be taken as a slowly varying sequence of locally and instantaneously uniform near horizontal flows characterized by depth averaged velocity equal to the plane irrotational velocity. We then write:

$$(v_x, v_y) = (U, V)F\left(\frac{z}{z_0}\right), \quad F\left(\frac{z}{z_0}\right) = \frac{D_0 \ln(z/z_0)}{\int_{z_0}^{D_0} \ln(z/z_0) dz}, \quad (7)$$

having denoted by z_0 the reference elevation for the no slip condition, a quantity which can be expressed in terms of the mean flow conductance C_0 as follows:

$$z_0 = D_0 \exp(-kC_0 - 1). \quad (8)$$

Further simplification of (6) can be achieved noting that the horizontal turbulent diffusion is negligible compared with the vertical turbulent diffusion. In conclusion, the advection diffusion equation may be reduced to the simpler approximate form:

$$\frac{\partial c}{\partial t} + UF\left(\frac{z}{z_0}\right)\frac{\partial c}{\partial x} + VF\left(\frac{z}{z_0}\right)\frac{\partial c}{\partial y} - w_s \frac{\partial c}{\partial z} = \frac{\partial}{\partial z} \left(D_{T_z} \frac{\partial c}{\partial z} \right). \quad (9)$$

The latter equation can be solved once a closure relationship for the vertical diffusivity and appropriate boundary conditions are adopted. In the present work, given the slowly varying character of the concentration field we will assume that

$$D_{T_x} = ku_* z \left(1 - \frac{z}{D_0} \right). \quad (10)$$

The boundary conditions associated with (9) impose:

1. no flux at the free surface, hence:

$$[q \cdot n]_{z=D_0} = \left[w_s c + D_{T_z} \frac{\partial c}{\partial z} \right]_{z=D_0} = 0; \quad (11)$$

2. gradient boundary condition at the bed:

$$[q \cdot n]_{z=z_a} = w_s (c_e - c), \quad (12)$$

where c_e is the equilibrium concentration at the reference elevation z_a . We employ van Rijn's [1984] formula to estimate the reference concentration at the bed, assuming the latter to be plane or dune covered depending on whether or not the local and instantaneous value of the Shields stress satisfies van Rijn's [1984] criterion. Finally, we assume a significant wave height of 3 m, assign the concentration at the breaking line using Bijker's [1968] approach, which

accounts for the simultaneous presence of waves and currents, and solve the equation (9) numerically for each inlet of Venice Lagoon using an explicit finite difference scheme. In the Figures 8a, b, c we have plotted the concentration distributions driven by a pure M_2 forcing tide of amplitude $a_0 = 0.5$ m at Lido, Malamocco and Chioggia inlets respectively, at the peak of the flood phase. Results suggest that, at Malamocco and Chioggia, the concentration distribution induced by wave breaking is able to overload the current above transport capacity only close to the breaker region, i.e. outside the inlets. In other words most of the sediment overload settles outside the inlets. At Lido, part of the sediments resuspended by waves in the near inlet region is able to enter the inlet (see Figure 8d), a result which agrees with field observations suggesting the presence of large deposits of sand along the inner side of the northern jetty. Hence, the dominant effect of sand resuspension by the action of breaking waves during storms is simply to store sediments in the near inlet region.

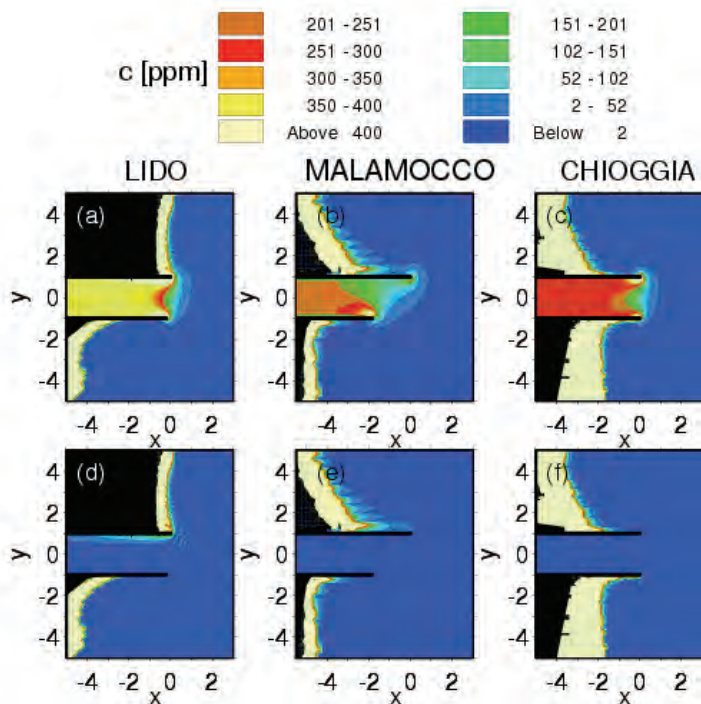


Fig. 8 – Top: depth averaged sediment concentration field in the sea region close to Lido (a), Malamocco (b) and Chioggia (c) inlets at the peak of the flood phase driven by a pure M_2 forcing tide of amplitude $a_0 = 0.5$ m and a uniform littoral current with intensity $V_l = 0.1$ m/s. Bottom: depth averaged sediment concentration in excess with respect to the local equilibrium value at Lido (d), Malamocco (e) and Chioggia (f). Values expressed in ppm.

Conclusions

The present work allows us to reach some preliminary conclusions. Firstly the temporal dependence of the average cross-sectional velocity predicted using the multiple inlet model for each of Venice inlets under a pure M_2 forcing tide ($a_0 = 0.5$ m), shows very small differences when compared with that obtained using a single inlet approach. However, the assumption that the free surface keeps horizontal and displays the same instantaneous elevation in all the basins is a strong one: in fact, though the free surface elevation is definitely continuous through the basins, each of Venice inlets has its own 'drainage basin' and the

average free surface elevation of different basins may reasonably be slightly different. Secondly, our calculations show that, in the absence of an excess supply of sand from the sea, a net yearly export of sands averaging approximately some tens of thousands cubic meters would be experienced by the lagoon. Such an estimate is only slightly affected by the effect of inlet interactions and provides an upper bound for the actual export of sand. In fact, our third conclusion is that the excess supply of sediment driven by the nearly irrotational flood currents overloaded in the far field by storm events, is mostly deposited near or inside the inlets. On the contrary, the amount of sand exchanged between the lagoon and the sea is not significantly affected by the sediment supply in the far field: the stream can only transport through the channel the amount of sand which it is able to entrain as bed load and suspended load with its hydrodynamic characteristics. Enhancing the sediment supply from the sea by modifying the inlet shape would drive inlet siltation, a process already observed at Lido: in fact, due to the pronounced progradation of the northern coast, this inlet is more prone to deposition than Malamocco, which, being located farther from the shoreline, is less exposed to the sediment supply from the sea. Our last conclusion is that counteracting the morphological degradation of Venice Lagoon will mainly require to stop the production of wash load, arising from the collapse of banks of salt marshes as well as by sediment resuspension in the shoals, possibly favored by boat-wake wash. This is a major task, already partly undertaken by Magistrato alle Acque di Venezia, which might be helped by the controlled reintroduction of fluvial sediments in the lagoon. Needless to say, detailed measurements as well as better theoretical understanding of wind driven sediment resuspension in the inner lagoon will be needed in order to support our qualitative estimate of the export of wash load.

References

- Bijker E. W., 1968, Littoral drift as function of waves and current, XI Coastal Eng. Conf. Proc. ASCE, 415-435.
- Blondeaux P., De Bernardinis B. and Seminara G., 1982, Correnti di marea in prossimità di imboccature e loro influenza sul ricambio lagunare, Atti XVIII Conv. Idraulica e Costruzioni Idrauliche, Bologna, 21-23 Sept.
- Brown E. I., 1928, Inlets on sandy coast, Proceedings of the American Society of Civil Engineers, 54, 1, 505-523.
- Bruun P., 1978, Stability of tidal inlets: theory and engineering, Elsevier scientific Publishing Co., New York.
- Di Paola L., Ghetti A., Bartorelli U., Lippe E., D'Alpaos L. and Di Silvio G., 1979, Le correnti di marea nella Laguna di Venezia, Hydraulic Institute, University of Padua, Padua.
- Engelund F. and Hansen E., 1967, A monograph on sediment transport in alluvial streams, Danish Tech. Press, Copenhagen.
- Magistrato alle Acque di Venezia – Consorzio Venezia Nuova, 2002,

Valutazione degli effetti delle nuove configurazioni sulla gestione delle opere mobili, VEN340-STUDIOB.5.58, Venice.

Marchi E., 1990, Sulla stabilità delle bocche lagunari a marea, *Rend. Fis. Acc. Lincei*, 137-150.

O'Brien M. P., 1931, Estuary tidal prism related to entrance areas, *Civil Engineering*, vol. 1, n. 8, 738-739.

Tambroni N., Bolla Pittaluga M. and Seminara G., 2005, Laboratory observations of the morphodynamic evolution of tidal channels and tidal inlets, *J. Geophys. Res.*, 110, F04009, doi:10.1029/2004JF000243.

Tambroni N , and Seminara G., 2005, Long term net exchange of sands through Venice inlets, *Scientific Research and Safeguarding of Venice, Research Programme 2001-2003, Volume III*.

van de Kreeke J., 1990, Stability analysis of a two-inlet bay system, *Coastal Eng.*, 14, 481-497.

van Rijn L. C., 1984, Sediment transport part II: suspended load transport, *J. Hydraul. Eng., ASCE*, 110(1), 1616-1641.

AREA 4

Data management

RESEARCH LINE 4.2

Modeling, analysis and environmental data visualization

SPATIAL ON LINE ANALYTICAL PROCESSING FOR ENVIRONMENTAL DATA

Sandro Bimonte, Anne Tchounikine, Taher Ahmed, Maryvonne Miquel, Robert Laurini

LIRIS INSA de Lyon, Bâtiment B. Pascal, 7 Avenue Capelle, 69621 Villeurbanne, France

Riassunto

La maggior parte delle applicazioni OLAP si concentra su dimensioni testuali e misure numeriche. Comunque circa l'80% dei dati presenta delle informazioni spaziali. Conseguentemente queste informazioni devono e possono essere utilizzate nel processo di analisi decisionale in modo effettivo e concreto. Ciò conduce alla definizione del concetto di Spatial On Line Analytical Processing (SOLAP). In questo lavoro sono proposti due modelli formali e un prototipo chiamato GéOlap che permette la definizione e l'analisi di dati multidimensionali integrando la dimensione spaziale. Questo approccio multidimensionale è stato applicato ai dati sull'inquinamento della campagna Drain nella laguna di Venezia.

Abstract

Most of OLAP and data warehousing applications focus on textual dimensions and numeric measures. However about 80% of data integrates spatial information. It is obvious that those meaningful data are worth being integrated in decision making process as a first class knowledge thus leading to the concept of Spatial On Line Analytical Processing. We propose formal models and a prototype named GéOlap that allows the design and the analysis of multidimensional data integrating spatial dimension. This multidimensional approach has been applied on pollution data from the DRAIN campaign in Venice lagoon.

1 Introduction

Data warehousing and OLAP technologies are efficient practices in order to manage, analyse and explore historised data. These technologies can advantageously be used for the analysis of the pollution data from Venice Lagoon, but need to be adapted in order to take into account the quality of the data and to exploit the spatial information associated to the data. In this paper, we first present the main principles of data warehousing and OLAP technologies. Then, we propose a spatial OLAP interface and we describe its use on pollution data.

2 Data warehouses and OLAP

Data warehousing in addition to OLAP (On Line Analytical Processing) technologies intend to be an innovative support for business intelligence and knowledge discovery. It has now become a leading topic in the commercial

world as well as in the research community. The main motivation is to take benefits from the enormous amount of data relying in distributed and heterogeneous databases in order to enhance data analysis and decision making (Kimball, 1996).

2.1 Definition and usage

A data warehouse is a subject-oriented, integrated, non-volatile and time-variant collection of data stored in a single site repository and collected from multiple sources (Inmon, 1996). Information in the data warehouse is organized around major subjects and is modeled in order to allow pre-computation and fast access to summarized data in support of management's decisions. OLAP tools refer to analysis techniques used to explore the data warehouse.

Data warehouse models are called multidimensional models or hypercubes. They are designed to represent measurable facts or *indicators* and the various *dimensions* that characterize the facts. As an example in a retail area, typical facts are the price and the amount of a purchase; dimensions are Product, Location, Time and Customer. A dimension is usually organized in *hierarchy*, for example the Location dimension can be aggregated in City, State, and Country, allowing analysis at different levels of details.

2.2 Architecture

OLAP architectures are based on a multi-tier architecture (Figure 1). The first tier is a warehouse server, often implemented using a relational DBMS. Data of interest must be extracted from operational legacy databases, cleaned and transformed by ETL (Extraction, Transformation, and Loading) tools before being loaded into the warehouse. This critical and important step aims to consolidate heterogeneous schema and to reduce data in order to comply it with the data warehouse model. Then the warehouse should definitely contain high quality, historical and homogeneous data.

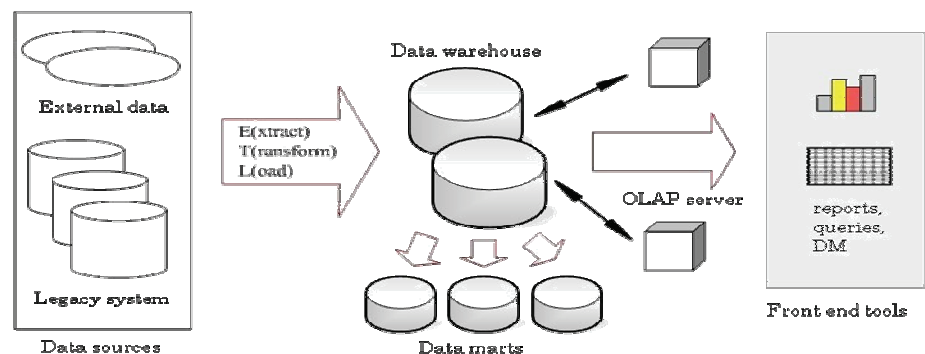


Fig. 1 – OLAP multi-tier architecture.

The second (but optional) tier is a data mart that handles data sourced from the data warehouse, reduced for a selected subject. The main advantage of data marts is to isolate data of interest for a smaller scope, thus permitting the focus on optimization needs for this data and increase security control.

The third level is the OLAP server. It calculates and optimizes the hypercube

(Figure 2), i.e. the set of fact values for all combinations of instances of dimensions (also called *members*). In order to optimize accesses to the data, query results are pre-calculated in the form of aggregates. OLAP operators enable the materialization of various views of the hypercube, allowing interactive queries and analysis of the data. Common OLAP operators include roll-up, drill-down, slice and dice, rotate.

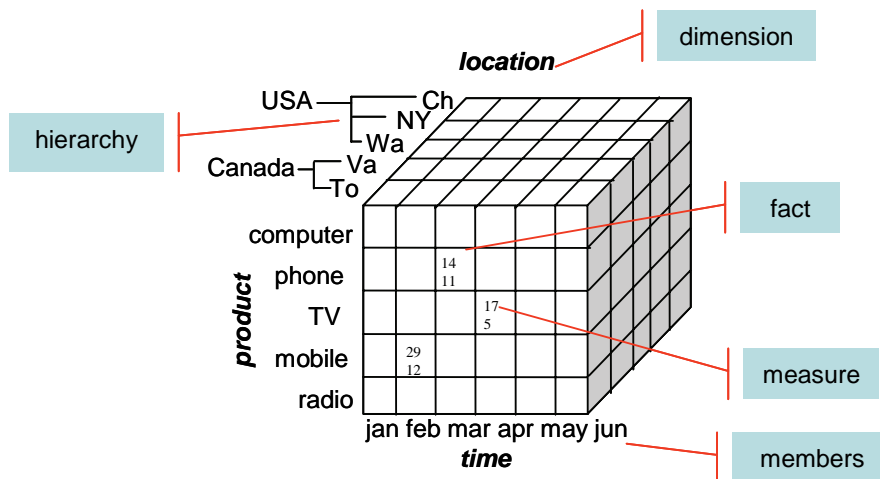


Fig. 2 – A hypercube.

The fourth level is an OLAP client, and provides a user interface with reporting tools, analysis tools and/or data mining tools. Software solutions exist for a traditional use. When the studied data and analysis processes are more complex, then a specific interface must be designed.

In conclusion, data warehousing process intends to provide:

- ~ a guarantee for the quality and comparability of data
- ~ a fast access to summarized data
- ~ an interactive and user-friendly navigation through data at different levels of detail.

3 Spatial OLAP

Most of OLAP applications focus on textual dimensions and numeric measures. As previously said about 80% of data integrates spatial information. It is obvious that those meaningful data are worth being integrated in decision making process as a first class knowledge thus leading to Spatial On Line Analytical Processing (SOLAP) concepts. SOLAP is defined as a visual platform especially built to support rapid and easy spatio-temporal analysis and exploration of data following a multidimensional approach including aggregation levels available in cartographic displays as well as in tabular and diagram displays (Rivest and al., 2001).

3.1 Spatial dimension

A straightforward way to integrate spatial information in a multidimensional decisional application is to use it as an analysis axis i.e. as a dimension. Spatial

data in OLAP dimensions brings to the definition of *spatial non geometric* dimension (i.e. text only members), *spatial geometric* dimension (i.e. members with a cartographic representation) or *mixed spatial* dimension (i.e. combine cartographic and textual members). An example of a multidimensional model including a spatial dimension is shown fig. 3. This spatial hypercube authorizes queries such as "what is the average and maximum pollution per months and per pollutants in FIUME DESE location?".

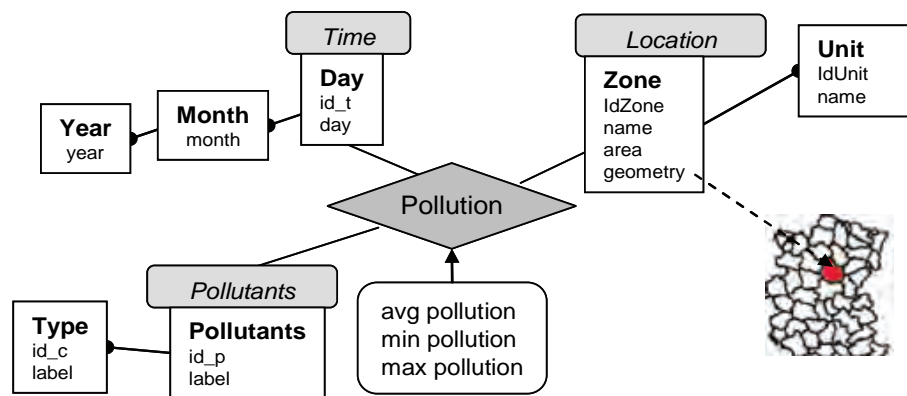


Fig. 3 –Example of a spatial dimension.

Some of the theoretical issues while integrating spatial dimensions are:

- ~ Design and storage:
 - o provide models in order to integrate geometric information,
 - o provide spatial indexes in order to optimize queries,
 - o take into account the continuous nature of the spatial information.
- ~ Visualization:
 - o display spatial members at different levels of granularity,
 - o provide relevant visual display for measure(s) and non spatial dimension(s) with cartographic means.
- ~ Algebra:
 - o integrate spatial OLAP operators into OLAP queries.

3.2 Spatial measure

When the studied subject of the decision process is the spatial information itself, then the concept of spatial measures must be introduced. Spatial measure can be analyzed through non spatial and/or spatial dimensions. An example of a multidimensional model including a spatial measure is shown fig. 4. This spatial hypercube authorizes queries such as "Which are the locations where pollutant FERRO monthly exceeded 0.5 ?"

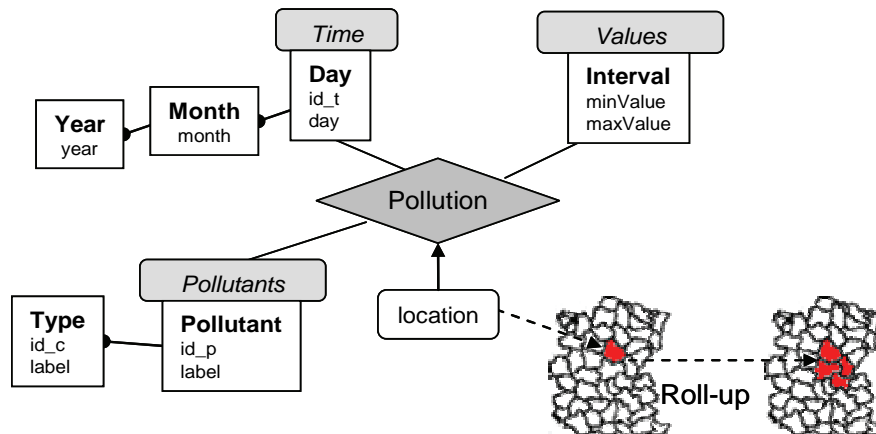


Fig. 4 – Example of a spatial measure.

Some of the theoretical issues in modeling spatial dimensions rely in:

- Pre-aggregation at computational time with un-classical and time-consuming aggregation operators (fusion of geometric data),
- Visualization of (multiple) cartographic cells into cross tabs,
- Design and integration of the descriptive and metric attributes of the spatial measure that can be useful to the decision process.

4 Contribution and on-going work

We provide formal models that allow the definition of spatial dimension and/or spatial measure taking all spatial, metric and descriptive attributes of the geographic information into account. These models also permit to simulate the spatio-temporal continuity during navigation thanks to on-the-fly interpolation of the data. The theoretical fundamentals of the models are detailed in (Bimonte and al., 2005) and (Ahmed and al., 2005). These concepts are partially implemented in a prototype named GéOlap that provides navigation through spatial hypercubes.

4.1 GéOlap

We have defined a tool named GéOlap which is a dynamic and integrated interface that allows the user to connect to and then to navigate through a spatio-temporal hypercube containing one or several spatial dimensions (Fig. 5).

Each hierarchical level of the spatial dimension is represented by a cartographic layer. The result of a navigation OLAP query is a new on-the-fly calculated layer that represents the members of the spatial dimension at the required granularity and the measures with graphic means (value, density, color, histograms...). The user interface allows navigation in a same and synchronized way using different frames presenting the tree structure of measures and dimensions, cross tabs, diagram representation and/or cartographic display. All of these frames provide a toolbar offering classical OLAP operators (*roll-up*, *drill-down*, *pivot*, ...).

In the cartographic display, roll-up and drill-down operators are applied on

graphically selected geometric objects. An automatic focus on the region of interest is also proposed.

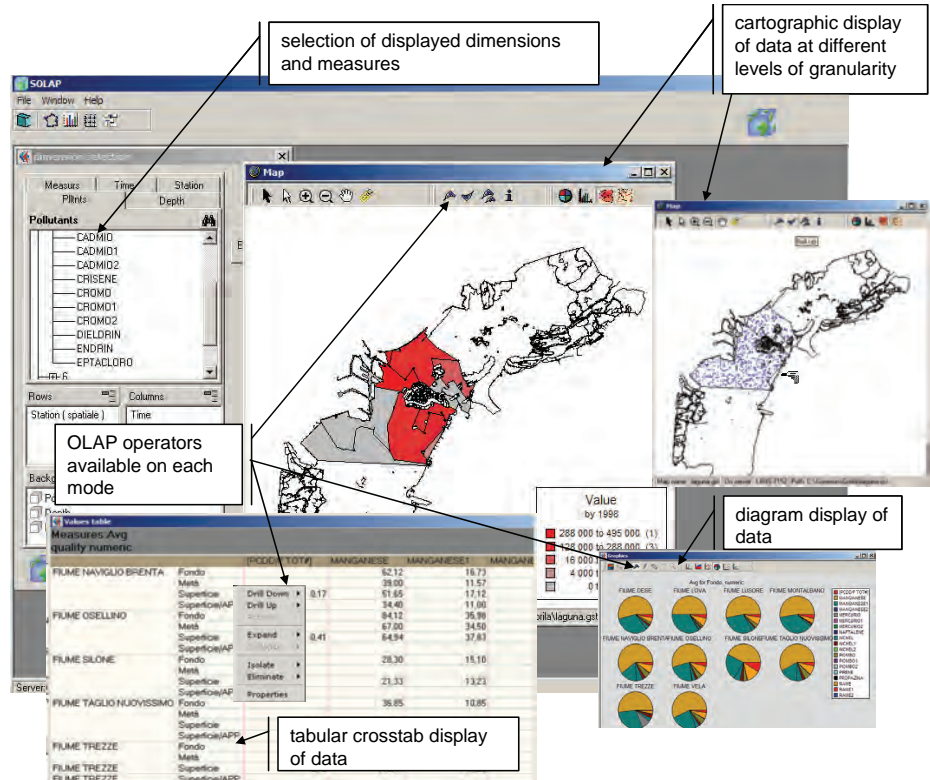


Fig. 5 – GéOlap interface: navigation through a spatial dimension.

4.2 Application

This multidimensional approach has been applied on the pollution data from the DRAIN campaign. We used 8 source files containing pollution measurements for 10 different locations, 2826 timestamps (3 years, 28 months, 207 days) and 100 pollutants. The files contain 294425 measures and raise several problems concerning the quality of the data (heterogeneity in types and values, multiple redundant or contradictory inputs, missing data and sparsity).

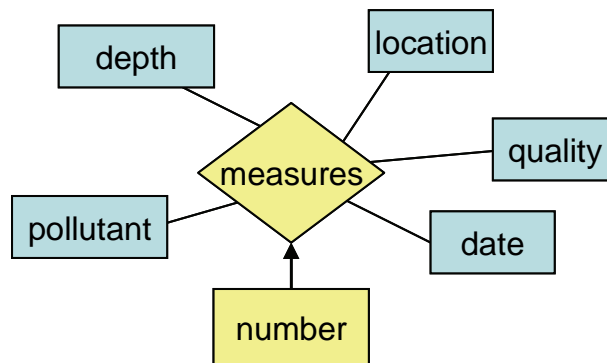


Fig. 6 – The conceptual model for the quality hypercube.

We first migrate the data and populate a relational data base. Then we design two multidimensional cubes, the first one controls and reports the quality of the data captured (fig. 6) and the second one allows the user to analyze and explore the chemical measures according to the date of the campaign, localization of sensors and chemical element. Some of the results are shown figure 7 obtained with the GéOlap navigation interface.

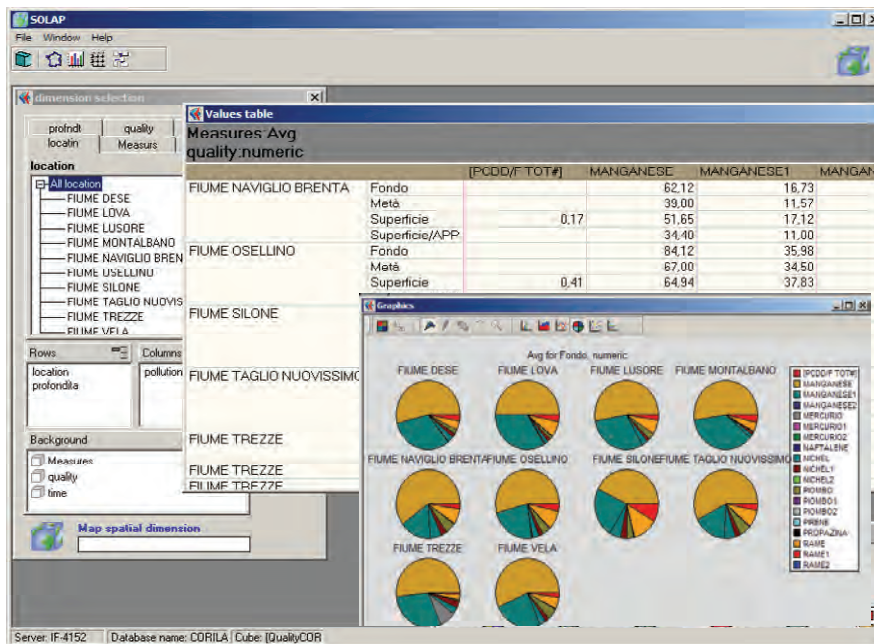


Fig. 7 – GéOlap interface: navigation through a numeric dimension

Conclusion

GéOlap is a proposal for spatio-temporal data analysis tool. Applied to pollution data from the DRAIN campaign, this environment allows exploring both the data and the quality of data. However this approach can be used on other use-case where interactive exploration of the data is needed. We are now working on a new version of GéOlap allowing a SOLAP navigation with a Web access to the data.

References

Ahmed, T. O., and Miquel, M. Multidimensional structures dedicated to continuous spatiotemporal phenomena. In Database: Enterprise, Skills and Innovation, 22nd British National Conference on Databases, BNCOD 22, Sunderland, UK, July 5-7, 2005, Proceedings (2005), M. Jackson, D. Nelson, and S. Stirk, Eds., vol. 3567 of Lecture Notes in Computer Science, Springer, pp. 29-40.

Bimonte, S., Tchounikine, A., and Miquel, M. Towards a spatial multidimensional model. In DOLAP 2005, ACM 8th International Workshop on

Data Warehousing and OLAP, Bremen, Germany, November 4-5, 2005, Proceedings (2005), I.-Y. Song and J. Trujillo, Eds., ACM, pp. 39-46.

Inmon, W. H. The data warehouse and data mining. *Commun. ACM* 39, 11 (1996), 49-50.

Kimball, R. *The Data Warehouse Toolkit*. John Wiley, 1996. and other books.

Rivest, S., Bédard, Y., and Marchand, P. Towards better support for spatial decision-making: Defining the characteristics of Spatial On-Line Analytical Processing (SOLAP). *Geomatica*, the journal of the Canadian Institute of Geomatics 55, 2001 (2001), 539-555.